frontiers | Research Topics

Applications of omics in plant-microbiome interactions

Edited by
Long Yang, Yi Wang and Xuewen Wang

Published in
Frontiers in Plant Science

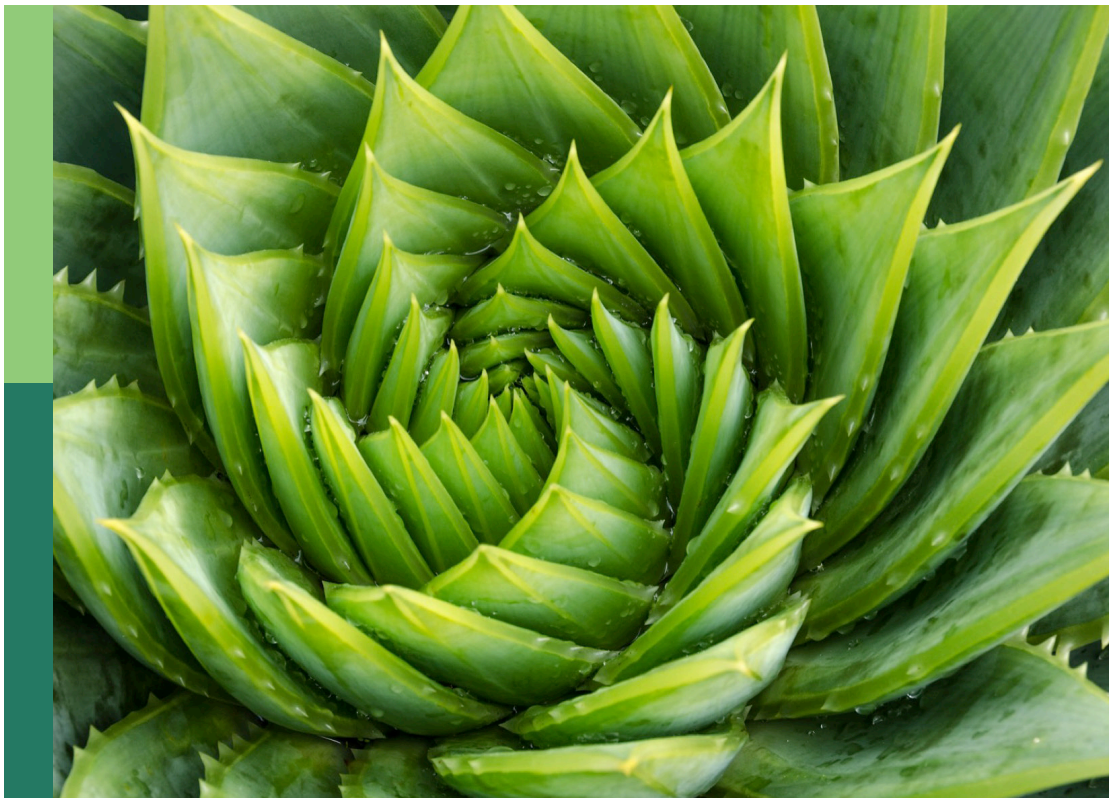

ISSN 1664-8714
ISBN 978-2-8325-4723-6
DOI 10.3389/978-2-8325-4723-6

About Frontiers

Frontiers is more than just an open access publisher of scholarly articles: it is a pioneering approach to the world of academia, radically improving the way scholarly research is managed. The grand vision of Frontiers is a world where all people have an equal opportunity to seek, share and generate knowledge. Frontiers provides immediate and permanent online open access to all its publications, but this alone is not enough to realize our grand goals.

Frontiers journal series

The Frontiers journal series is a multi-tier and interdisciplinary set of open-access, online journals, promising a paradigm shift from the current review, selection and dissemination processes in academic publishing. All Frontiers journals are driven by researchers for researchers; therefore, they constitute a service to the scholarly community. At the same time, the *Frontiers journal series* operates on a revolutionary invention, the tiered publishing system, initially addressing specific communities of scholars, and gradually climbing up to broader public understanding, thus serving the interests of the lay society, too.

Dedication to quality

Each Frontiers article is a landmark of the highest quality, thanks to genuinely collaborative interactions between authors and review editors, who include some of the world's best academicians. Research must be certified by peers before entering a stream of knowledge that may eventually reach the public - and shape society; therefore, Frontiers only applies the most rigorous and unbiased reviews. Frontiers revolutionizes research publishing by freely delivering the most outstanding research, evaluated with no bias from both the academic and social point of view. By applying the most advanced information technologies, Frontiers is catapulting scholarly publishing into a new generation.

What are Frontiers Research Topics?

Frontiers Research Topics are very popular trademarks of the *Frontiers journals series*: they are collections of at least ten articles, all centered on a particular subject. With their unique mix of varied contributions from Original Research to Review Articles, Frontiers Research Topics unify the most influential researchers, the latest key findings and historical advances in a hot research area.

Find out more on how to host your own Frontiers Research Topic or contribute to one as an author by contacting the Frontiers editorial office: frontiersin.org/about/contact

Applications of omics in plant-microbiome interactions

Topic editors

Long Yang — Shandong Agricultural University, China

Yi Wang — Southwest University, China

Xuewen Wang — University of North Texas Health Science Center, United States

Citation

Yang, L., Wang, Y., Wang, X., eds. (2024). *Applications of omics in plant-microbiome interactions*. Lausanne: Frontiers Media SA. doi: 10.3389/978-2-8325-4723-6

Table of contents

frontiers | Frontiers in Plant Science

TYPE Original Research
PUBLISHED 20 February 2023
DOI 10.3389/fpls.2023.1107690

OPEN ACCESS

EDITED BY
Long Yang,
Shandong Agricultural University, China

REVIEWED BY
Krishan K. Verma,
Guangxi Academy of Agricultural Sciences, China
Yinghui Mu,
South China Agricultural University, China

*CORRESPONDENCE
Hua Xie
774350762@qq.com

SPECIALTY SECTION
This article was submitted to Plant Symbiotic Interactions, a section of the journal Frontiers in Plant Science

RECEIVED 25 November 2022
ACCEPTED 07 February 2023
PUBLISHED 20 February 2023

CITATION
Gao J and Xie H (2023) Daylily intercropping: Effects on soil nutrients, enzyme activities, and microbial community structure.
Front. Plant Sci. 14:1107690.
doi: 10.3389/fpls.2023.1107690

Daylily intercropping: Effects on soil nutrients, enzyme activities, and microbial community structure

Jingxia Gao and Hua Xie*

Ningxia Academy of Agriculture and Forestry Sciences, Yinchuan, Ningxia, China

The daylily (*Hemerocallis citrina Baroni*)/other crop intercropping system can be a specific and efficient cropping pattern in a horticultural field. Intercropping systems contribute to the optimization of land use, fostering sustainable and efficient agriculture. In the present study, high-throughput sequencing was employed to explore the diversity in the root-soil microbial community in the intercropping of four daylily intercropping systems [watermelon (*Citrullus lanatus*)/daylily (WD), cabbage (*Brassica pekinensis*)/daylily (CD), kale (*Brassica oleracea*)/daylily (KD), watermelon/cabbage/kale/daylily (MI)], and determine the physicochemical traits and enzymatic activities of the soil. The results revealed that the contents of available potassium (2.03%-35.71%), available phosphorus (3.85%-62.56%), available nitrogen (12.90%-39.52%), and organic matter (19.08%-34.53%), and the urease (9.89%-31.02%) and sucrase (23.63%-50.60%) activities, and daylily yield (7.43%- 30.46%) in different intercropping soil systems were significantly higher compared to those in the daylily monocropping systems (CK). The bacterial Shannon index increased significantly in the CD and KD compared to the CK. In addition, the fungi Shannon index was also increased significantly in the MI, while the Shannon indices of the other intercropping modes were not significantly altered. Different intercropping systems also caused dramatic architectural and compositional alterations in the soil microbial community. A prominently higher relative richness of *Bacteroidetes* was noted in MI compared to that in CK, while *Acidobacteria* in WD and CD and *Chloroflexi* in WD were pronouncedly less abundant compared to those in CK. Furthermore, the association between soil bacteria taxa and soil characteristic parameters was stronger than that between fungi and soil. In conclusion, the present study demonstrated that the intercropping of daylily with other crops could significantly improve the nutrient levels of the soil and optimize the soil bacterial microflora composition and diversity.

KEYWORDS

daylily, soil nutrients, enzymatic activity, microbial diversity, intercropping, yield

1 Introduction

Daylily (*Hemerocallis citrina* Baroni.), common names Citron daylily and long yellow daylily, is a species of herbaceous perennial plant in the family Asphodelaceae, which is native to central and northern China, the Korea Peninsula, and Japan (Hou et al., 2017). Citron dayliy is now cultivated widely in Asia as ornamental plant and vegetable plant because of its beautiful flower, pleasant flavor, and beneficial secondary metabolites (Lin et al., 2013). In addition, daylily flowers has been used to treat various diseases including inflammation, insomnia, and depression (Yang et al., 2017). Due to the low cost of field management of day lily, one-time planting can benefit many years, and it has great economic benefits, so the cultivation area and output are constantly expanding. Growing demand for yields and the limited arable land have resulted in daylily production with high cropping intensity and monocultures over long periods (Zhu et al., 2018). Previous researches reported that continuous cropping obstacles often appear after a few years of continuous cropping (Xiong et al., 2015). Even with a good field management regime, crops under a continuous cropping system may still be affected by slower growth and development, lower yield and quality, and increased disease incidence (Li et al., 2016; Gao et al., 2019; Zeng et al., 2020).

Soil microorganisms are crucial for agricultural production as these contribute to maintaining soil quality and sustaining nutrient cycling (Sun et al., 2015; Beckers et al., 2017). The interaction between soil properties and the soil bacterial microflora affects the plant pathogens in certain cases, thereby influencing the health of plants (Wei et al., 2015). Therefore, management strategies related to the soil bacterial microflora have become an imperative research direction in the field of sustainable agriculture (Zhang et al., 2019). Intercropping refers to the concurrent cultivation of 2 crops in proximity. Intercropping, in addition to affecting crop yield, may also cause functional and architectural alterations in the soil microbiota (Duchene et al., 2017; Yu et al., 2018). In the intercropping systems, the soil microorganisms, enzymes, and nutrients may interact in various ways, which could either enhance or compromise the bacterial quantity and the enzymatic action, thereby facilitating or challenging the soil micro-ecotope improvement (Zhou et al., 2019). Soil microorganisms are crucial for facilitating various chemical, biological, and physical events in the soil, including the formation of the soil architecture, nutrient cycling, toxin aggregation/removal, organic matter turnover, and soil-borne pathogen inhibition (Bever et al., 2012; Blagodatskaya and Kuzyakov, 2013). Therefore, to elucidate the effects of intercropping on the soil microbiota architecture and diversity, enzyme activities, and nutrient levels, further research is warranted. Such research would be crucial for determining the energy output and nutrient status of the soil microorganisms in agroecosystems.

While the intercropping-induced alterations in soil microbial traits have been explored in a few studies (Jin et al., 2020), the alterations in the soil microbiota due to intercropping with other crops have not been studied in detail in the context of daylily. The diverse intercropping patterns exert different kinds of effects on the microbial characteristics and physicochemical traits of the soil. Therefore, in the present study, the bacterial and fungal microflora alterations occurring in the intercropping systems comprising daylily with various other crops were assessed. It was hypothesized that intercropping would greatly impact the soil physicochemical traits, enhance the microbiota diversity and enzyme activities, and alter the architecture of the soil microbiota. The main objectives of the present study were as follows: (1) investigating the effects of daylily intercropping with various other crops on the soil physicochemical properties, soil enzyme activities, and daylily yield; (2) comparing the differences in the bacterial and fungal diversity and the soil microflora composition between monocropping and intercropping; and (3) determining the associations of soil bacterial microflora with the enzymatic activities and physicochemical traits of the soil.

2 Materials and methods

2.1 Experimental design and sampling

The experiment was conducted at the Modern Agricultural Plantation of the Ningxia Academy of Agriculture and Forestry, Yinchuan, Ningxia, China (38°28'48" N, 106°13'31" E; altitude 1100 m). The field soil was sand-loam, and a 3-year continuous daylily cropping was implemented for the plantation. The climate of the temperate continental was semi-arid kind with the average yearly temperature (8.5°C), precipitation (200 mm), potential precipitation (2250 mm), and sunshine (2850 h), respectively. The frost-free season lasted for 185 days.

Watermelon (*Citrullus lanatus*), cabbage (*Brassica pekinensis*), and kale (*Brassica oleracea*) were intercropped with daylily. The experimental design included the following 5 treatments: (1) watermelon–daylily intercropping (WD); (2) cabbage–daylily intercropping (CD); (3) kale–daylily intercropping (KD); (4) row mixed intercropping in which watermelon, cabbage, and kale were alternately intercropped with daylily (MI); (5) monoculture of daylily (CK). A completely randomized design was adopted for field experimentation, with 3 plots (each with a surface area of 120 m^2) per treatment. Daylily was planted on April 16, 2020, and later, on May 20, 2020, watermelon, cabbage, and kale were intercropped with daylily. The planting densities of different treatments are presented in Figure S1. Drip irrigation was used for all crops, and the entire cultivation was managed conventionally.

The soil near the roots of daylily were collected from 15 test plots using an auger on August 30, 2020. After the random collection of 5 soil sub-samples (10–20 cm depth) from each experimental plot, all samples were integrated into a whole soil sample. Prior to laboratory transfer, this whole soil sample was sieved through a 2-mm mesh for complete homogenization and elimination of stones, roots, and plant residues. Each sample was divided into 2 aliquots, one of which was stored at an ambient temperature for use in the chemical assay while the other was cryopreserved at −80°C for later use in the biological analysis. The soil samples for chemical analysis were cryopreserved at −20°C after a week of air-drying treatment.

2.2 Soil properties and enzyme activities

Soil pH was determined using a pH meter (PHS-25, Shanghai, China) at a constant soil/water ratio of 1:2.5. The available nitrogen (AN) concentration in the soil samples was determined using the DigiPREP TKN System (KJELTEC 8400, Foss, Denmark). A UV–Vis spectrophotometer (UH5300, North Points Ruili) was utilized for assessing the available phosphorus (AP) concentration in the soil. The available potassium (AK) in the soil was quantified using an inductively coupled plasma (ICP) spectrometer (Spectro Analytical Instruments, Kleve, Germany). The $K_2Cr_2O_7$-H_2SO_4 oxidation approach was adopted to assess the organic matter (OM) content in the soil.

Soil enzymes associated with nitrogen, phosphorus, and carbon degradation, including peroxidase (POD), sucrase (SC), and urease (UE), were evaluated for their activity. The soil UE activity was determined as described by Bao (2000) (Bao, 2000) using urea as the substrate. The spectrophotometric approach was adopted for the soil POD quantification in a 96-well microplate, using L-3,4-dihydroxyphenylalanine (L-DOPA) as the substrate (Bach et al., 2013). The soil SC activity was evaluated by determining the glucose discharge from an 8% sucrose solution following 24 h of incubation at 37°C (Chen et al., 2010).

2.3 Soil DNA extraction, PCR amplification, and sequencing

The total genomic DNA was extracted from the soil samples using sterile cotton swabs and the FastDNA spin kit for soil (MP, USA) according to the provided protocol. The extracted genomic DNA was amplified and sequenced by the Gene Denovo company. Li and Wu's report (2018) was referred to for designing the specific primers ITS4–2409R and ITS3_KYO2F for the ITS2 zone amplification of the ITS rRNA gene, and the specific primers 341F and 806R for the V3-V4 zone amplification of the 16S rRNA gene (Li and Wu, 2018). In order to sequence the purified amplicons, paired-end sequencing (HiSeq 2500, PE250) was performed on the Illumina platform following standard operations.

Quality filtration and sequence fusion were conducted on the raw fastqfiles of 50 microbial samples using FASTP version 0.18.0 and FLSAH version 1.2.11, thereby deriving Tags. The next step was to filter out the low-quality tags following the Tags Quality Control process of QIIME Ver. 1.9.1, which generated high-quality Clean Tags (Edgar, 2013). The chimeras of the tags were recognized and deleted *via* the UCHIME algorithm by exploiting the reference database, thereby generating valid Clean Tags (Edgar et al., 2011). Finally, using UPARSE version 9.2.64, the Clean Tags were assigned to the identical Operational Taxonomic Units (OTUs) in the similarity setting of tingil (Edgar, 2013). In this process, for every OUT, the tag sequence with the maximum richness was selected as the typical sequence, and for every typical sequence, the classification information was annotated *via* the Mothur algorithm in the Silva database (Quast et al., 2013).

2.4 Statistical analyses

The "Vegan" R software version 2.5–6 was employed for estimating the alpha- and beta-diversities (Bray–Curtis dissimilarity). SPSS 25.0 (IBM, USA) was used for conducting the one-way analysis of variance (ANOVA) and the least significant difference (LSD) approach ($p < 0.05$) to determine whether the differences in the inter-sample diversities based on the alpha index were statistically significant. The distribution trends of the soil microorganism communities in different treatments were assessed using the 'labdsv' package for the principal coordinates analysis (PCoA). Analysis of similarities (ANOSIM) and permutational multivariate analysis of variance (ADONIS) with 999 permutations were used for determining the significant inter-sample group differences in the beta diversity using Bray–Curtis distance matrices. The taxonomic traits of the microbial species characterizing the inter-treatment differences (https://www.cloudtutu.com) were elucidated through the linear discriminant analysis effect size (LEfSe) assay. In order to simplify the LEfSe process, only the OTUs with a relative richness of >0.01% were selected through OTU table filtration screened. The taxa with significant differential inter-group richness levels were recognized using the factorial Kruskal–Wallis sum-rank test ($\alpha = 0.05$). Thereafter, the effect size was computed for every discriminative trait based on the logarithmic LDA score (threshold = 2.0). The associations of the environmental parameters with the microbial communities were explored using the "vegan" R software for redundancy analysis (RDA) and the Mantel test. Using the same"vegan" package, the associations of the OTUs with the physicochemical properties and enzymatic activities were visualized through RDA.

3 Results

3.1 Effects of intercropping on the soil physicochemical properties and enzyme activities

Among all treatments, prominently higher levels of AN, AK, AP, and OM (LSD, $p < 0.05$, Table 1) were noted in the intercropping soil systems (WD, CD, KD, and MI) compared to that in the monocropping system (CK). The nutrient levels were higher in WD compared to CK by 12.90% for AN, 15.8% for AP, 35.71% for AK, and 30.95% for OM. The nutrient levels were higher in CD compared to CK by 39.52% for AN, 62.56% for AP, 26.47% for AK, and 34.53% for OM. The nutrient levels were higher in KD compared to CK by 17.21% for AN, 35.90% for AP, 14.90% for AK, and 20.46% for OM. The nutrient levels were higher in MI compared to CK by 31.73% for AN, 3.85% for AP, 2.03% for AK, and 19.08% for OM (Table 1). Among the different intercropping soil systems, CD presented the highest concentrations of soil AN, AP, and OM, while WD presented the highest soil AK concentration (Table 1). The WD, CD, and KD systems were less different from CK in terms of soil pH while presenting significantly

TABLE 1 Chemical properties and enzymatic activities of soil.

	WD	CD	KD	MI	CK	*P*-values	significant
pH	7.90 ± 0.01b	7.91 ± 0.01b	7.90 ± 0.02b	7.95 ± 0.02a	7.91 ± 0.01b	0.004	**
OM (g/kg)	20.86 ± 0.93ab	21.43 ± 1.79a	19.19 ± 0.77b	18.97 ± 1.11b	15.93 ± 0.45c	0.001	**
AN (mg/kg)	70.00 ± 1.01c	86.5 ± 1.49a	72.67 ± 1.53c	81.67 ± 1.52b	62.00 ± 1.05d	0	**
AP (mg/kg)	156.33 ± 0.77a	211.33 ± 0.42c	176.67 ± 0.63b	135.00 ± 0.43d	130.00 ± 0.35e	0	**
AK (mg/kg)	79.70 ± 0.58c	75.78 ± 2.89a	68.85 ± 3.06b	59.92 ± 1.01d	58.73 ± 1.02e	0	**
UE (U/g)	73.80 ± 0.25c	70.14 ± 0.59d	83.63 ± 0.53a	80.08 ± 0.58b	63.83 ± 2.08e	0	**
POD (U/g)	42.24 ± 0.47a	37.97 ± 0.59d	39.45 ± 0.55c	41.81 ± 0.19a	40.71 ± 0.16b	0	**
SC (U/g)	241.45 ± 1.55c	293.29 ± 1.38a	257.91 ± 1.91b	294.12 ± 1.29a	195.3 ± 1.41d	0	**
Yield (kg/ha)	21,553 ± 113a	18,637 ± 125c	17,749 ± 131d	19,553 ± 113b	16,521 ± 182e	0	**

Values are presented as mean ± standard error (n = 3). Different lowercase letters indicate statistically significant differences (P < 0.05) by Tukey's test between different treatments. **, indicates a significant difference at the P < 0.01 level. AN, available nitrogen; AP, available phosphorus; AK, available potassium; OM, organic matter. UE, urease; POD, peroxidase; SC, sucrase. WD, watermelon-daylily intercropping; CD, cabbage-daylily intercropping; KD, kale-daylily intercropping; MI, row mixed intercropping, watermelon, cabbage, and kale were alternately intercropped with daylily; CK, monoculture daylily.

increased MI (Table 1). Similarly, soil enzyme activities differed significantly. The UE and SC activities were significantly higher in the intercropping soil systems (WD, CD, KD, and MI) compared to the monocropping soil system (CK) (Table 1). The POD activity was significantly higher in WD and MI compared to CK, while it was significantly lower in CD and KD (Table 1). For yield, the yield of daylily in all intercropping soil systems was higher than that in monocropping systems, with WD having the highest yield (30.46%), followed by MI (18.35%), CD (12.81%) and KD (7.43%) (Table 1).

3.2 Effects of intercropping on microbial community diversity and community structure

Approximately 1,665,552 superior-quality V3-V4 sequences and 1,501,148 superior-quality ITS2 sequences were yielded in total in the raw-read sequencing process. The mean read lengths for bacteria and fungi were 456 bp and 357 bp, respectively. The sequences of all samples were clustered into 93,898 bacterial OTUs and 8,372 fungal OTUs, using an identity threshold of 97%. The flat trend of the rarefaction curve (Figure S2) suggested that the desired overall coverage of OTUs was provided by deep sequencing. Figure 1 depicts the calculated alpha diversity (α-diversity) indices of the bacterial and fungal communities for the different intercropping modes based on the Shannon index metric, which incorporates both the abundance and evenness of the microbiota. In the case of the bacterial microflora, the Shannon diversity values were in the following order: KD > CD > MI >WD > CK; in comparison to CK, the Shannon diversity values of CD and KD were pronouncedly higher (LSD, $p < 0.05$, Figure 1A), while no significant differences ($p > 0.05$, Figure 1A) were observed among WD, MI, and CK. In the case of the fungal microflora, the Shannon diversity values were in the following order: MI > CD > KD > WD > CK; in comparison to CK, the Shannon index of MI was pronouncedly higher ($p < 0.05$, Figure 1B), while no significant differences were observed among CD, KD, WD, and CK ($p > 0.05$, Figure 1B). The microbiota differences among the different treatments were assessed using the Bray-Curtis distance-based principal coordinate analysis (PCoA). In the case of bacterial microbiota, a sharp separation was observable among CD, WD, KD, MI and CK, while KD and MI were partially overlapped (Figure 1C); as demonstrated by the PCoA outcomes, the first 2 axes explained 36.3% and 26.05%, respectively, of the overall variation in the bacterial microflora. In the case of fungal microbiota, a distinct separation was observed among KD, WD, MI, and CK, while CD was overlapped with both KD and WD (Figure 1D); the PCoA outcomes revealed that the first 2 axes explained 25.31% and 16.91%, respectively, of the overall variation in the fungal microflora. The results of ANOSIM and ADONIS also indicated significant differences in the bacterial and fungal microbiota in the soil between a minimum of two treatments (Table S1). The Venn diagrams verified that the variation in the microflora among different soil intercropping systems was due to the alterations in the composition of several unique and shared OTUs. Among all the OTUs identified in this study, the bacteria shared across all intercropping soil systems had 2679 OTUs, the WD had 463 unique OTUs, the CD had 481 unique OTUs, the KD had 470 unique OTUs, the MI had 579 unique OTUs, the CK had 527 unique OTUs (Figure 1E). Among all the OTUs identified in this study, the fungi shared across all intercropping soil systems had 160 OTUs, the WD had 69 unique OTUs, the CD had 54 unique OTUs, the KD had 63 unique OTUs, the MI had 89 unique OTUs, the CK had 80 unique OTUs (Figure 1F).

3.3 Effects of intercropping on the composition of soil microbiota

Figure 2 depicts the outcomes of the sequence analyses conducted at the genus and phylum levels. In the case of bacteria, the richest phylum was *Proteobacteria* (35.93%), followed by

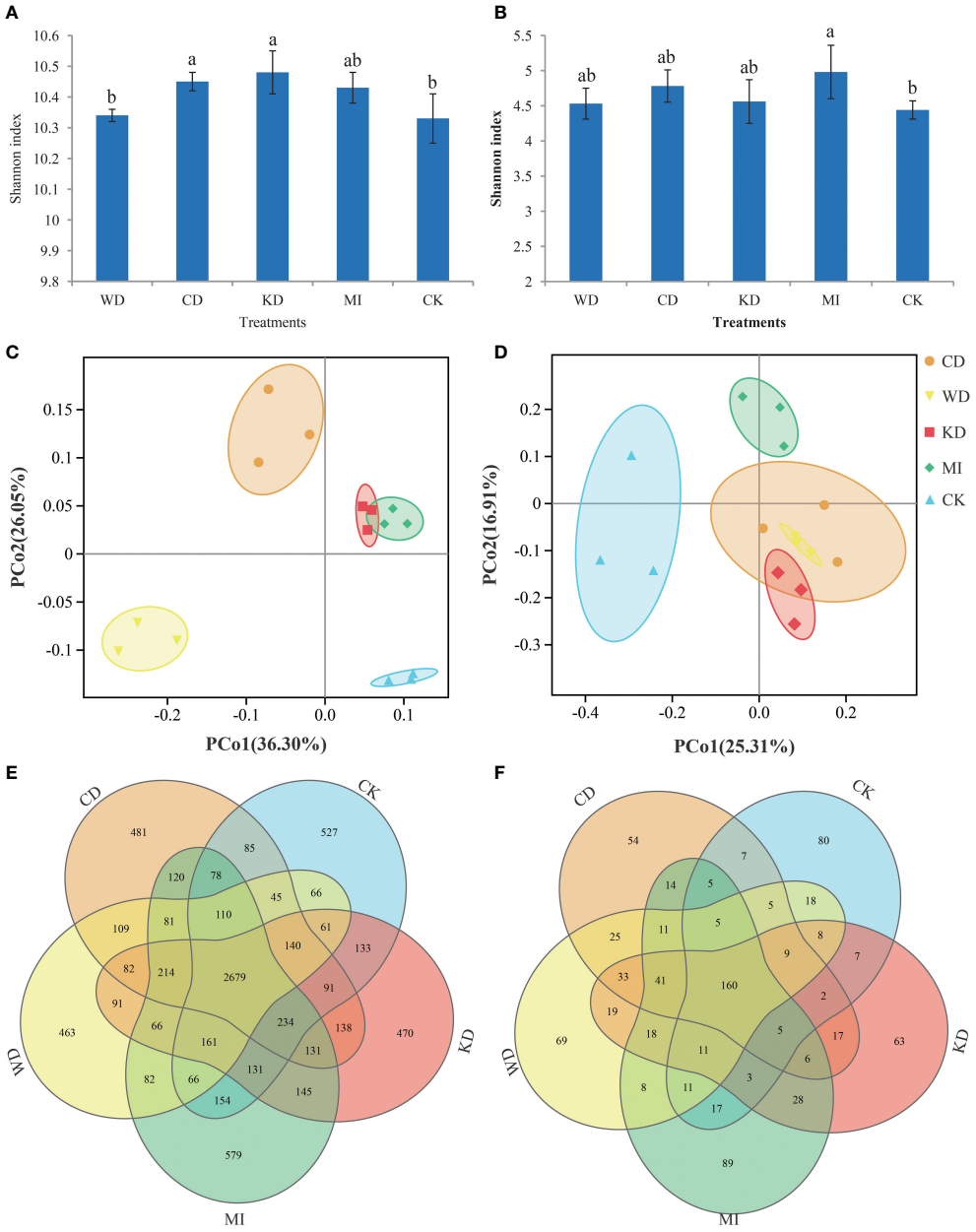

FIGURE 1
Microbial community diversity in different intercropping modes. Shannon index diversity of bacteria **(A)** and fungi **(B)** communities under different treatments. A lowercase letter on each box represents a least significant difference (LSD; $p < 0.05$) between treatments. Principal coordinate analysis (PCoA) plots based on the Bray-Curtis distance demonstrating the separation between soil bacteria **(C)** and fungi **(D)** communities of different treatments. The Venn diagram shows the numbers of bacteria **(E)** and fungi **(F)** operational taxonomic units (OTUs) that are shared or unshared by different treatments. WD, watermelon-daylily intercropping; CD, cabbage-daylily intercropping; KD, kale-daylily intercropping; MI, row mixed intercropping, watermelon, cabbage, and kale were alternately intercropped with daylily; CK, monoculture daylily.

Gemmatimonadetes (16.51%) and *Acidobacteria* (12.99%), respectively. Among the dominant taxa, the abundances of *Proteobacteria*, *Gemmatimonadetes*, *Planctomycetes*, *Actinobacteria*, *Patescibacteria*, and *Firmicutes* did not change significantly in the intercropping soil systems (CD, WD, KD, and MI) compared to their abundances in the monocropping soil system (CK) (Table S2, Figure 2A). *Rokubacteria* in KD and *Acidobacteria* in WD and CD were significantly less abundant compared to CK. A significantly greater abundance of *Chloroflexi* in WD and *Bacteroidetes* in MI was observed compared to CK (Table S2, Figure 2A). The richest genera in the different intercropped soils were *Sphingomonas* (3.94%), *Lysobacter* (3.33%), RB41 (2.51%), Subgroup_10 (1.49%), *Lactobacillus* (1.34%), MND1 (1.33%), SWB02 (1.29%), *Dongia* (0.90%), SM1A02 (0.80%), and *Arenimonas* (0.67%) (Figure 2C, Table S2). *Sphingomonas*, MND1, SWB02, *Dongia*, and *Arenimonas* were not significantly altered in the intercropping systems (WD, CD, KD, and MI) compared to the monocropping system (CK) (Table S2). A significantly greater abundance of Lysobacter in CD, KD, and MI and that of Lactobacillus in WD was observed compared to CK.

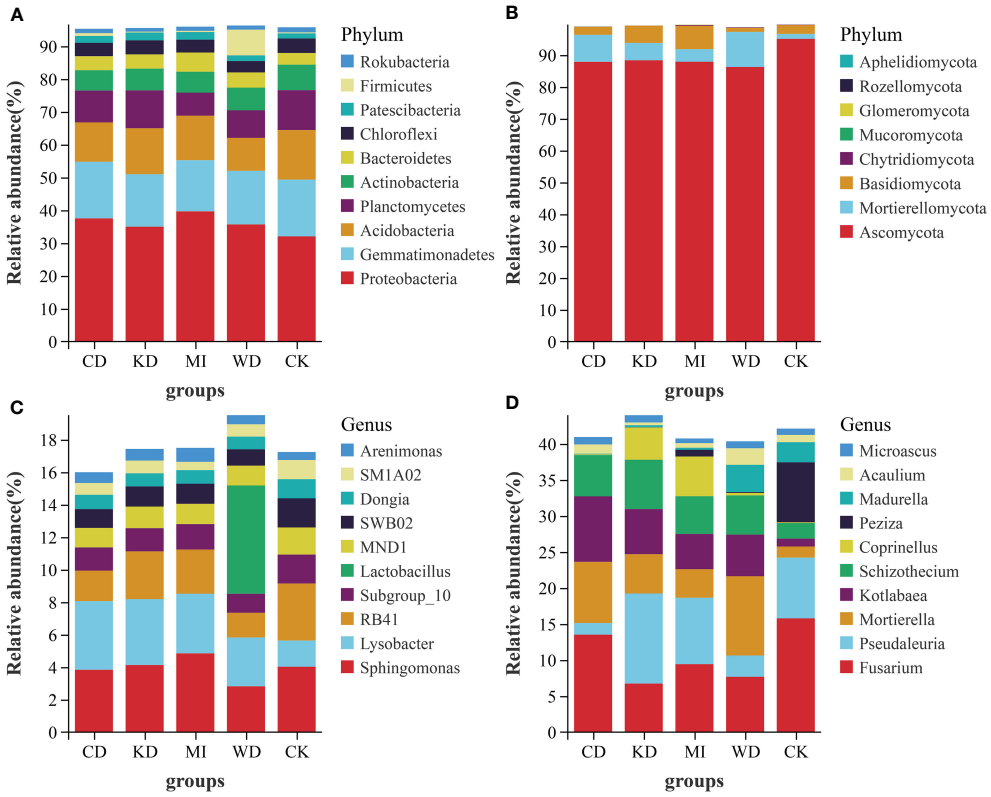

FIGURE 2
Relative abundance at phylum and genus level of soil microbial community of intercropping systems (top 10 shown). **(A)** bacteria phylum level; **(B)** fungi phylum level; **(C)** bacteria genus level; **(D)** fungi genus level. WD, watermelon-daylily intercropping; CD, cabbage-daylily intercropping; KD, kale-daylily intercropping; MI, row mixed intercropping, watermelon, cabbage, and kale were alternately intercropped with daylily; CK, monoculture daylily.

RB41 in WD and CD, Subgroup_10 in WD, and SM1A02 in MI were significantly less abundant compared to CK (Table S2).

In the case of fungi, the richest phylum was *Ascomycota* (89.05%), followed by *Mortierellomycota* (6.11%) and *Basidiomycota* (3.88%). Among the dominant taxa, the abundances of *Ascomycota*, *Chytridiomycota*, *Glomeromycota*, *Rozellomycota*, and *Aphelidiomycota* did not change significantly in the 4 investigated intercropping systems compared to those in the monocropping soil system (CK) (Table S3, Figure 2B). A significantly greater abundance of *Mortierellomycota* in WD and CD, *Basidiomycota* in KD and MI, and *Mucoromycota* in CD was observed compared to CK (Table S3, Figure 2B). The richest genera in the different intercropping soil systems were *Fusarium* (10.65%), *Pseudaleuria* (6.92%), *Mortierella* (6.11%), *Kotlabaea* (5.42%), *Schizothecium* (5.06%), *Coprinellus* (2.11%), *Peziza* (1.88%), *Madurella* (1.46%), *Acaulium* (1.13%), and *Microascus* (0.92%) (Figure 2D, Table S3). *Kotlabaea* and *Schizothecium* were prominently richer, while *Fusarium* and *Peziza* were pronouncedly less abundant in the 4 investigated intercropping systems compared to their abundances in the monocropping soil system (CK); the differences in the abundance of *Microascus* were not significant between the two kinds of systems (Table S3). Significantly greater abundances of *Mortierella* in WD, CD, and KD, *Pseudaleuria* in KD, *Coprinellus* in KD and MI, and *Madurella* and *Acaulium* in WD were observed compared to CK. Significantly lower abundances of *Pseudaleuria* in WD and CD and *Madurella* in CD, KD, and MI were observed compared to CK (Table S3).

Further, the effects of the different intercropping patterns on soil microbial community composition were determined using the linear discriminant analysis effect size analysis (LEfSe). LEfSe results revealed seventy-seven bacterial taxa that differed significantly in terms of relative richness among the different intercropped soil systems. As depicted in Figure 3A, 12 bacterial taxa in WD, 18 bacterial taxa in CD, 13 bacterial taxa in KD, 11 bacterial taxa in MI, and 23 bacterial taxa in CK were identified as biomarkers. As revealed by LEfSe, 60 fungal taxa differed significantly in terms of relative richness among the different intercropped soil systems. Among the identified biomarkers were one fungal taxon in WD, 4 fungal taxa in CD, 15 fungal taxa in KD, 26 fungal taxa in MI, and 14 fungal taxa in CK (Figure 3B).

3.4 Relationships between the soil properties and the soil microbial communities

Redundancy analysis (RDA) revealed a relationship between the microbial community structure, soil properties (soil chemistry and

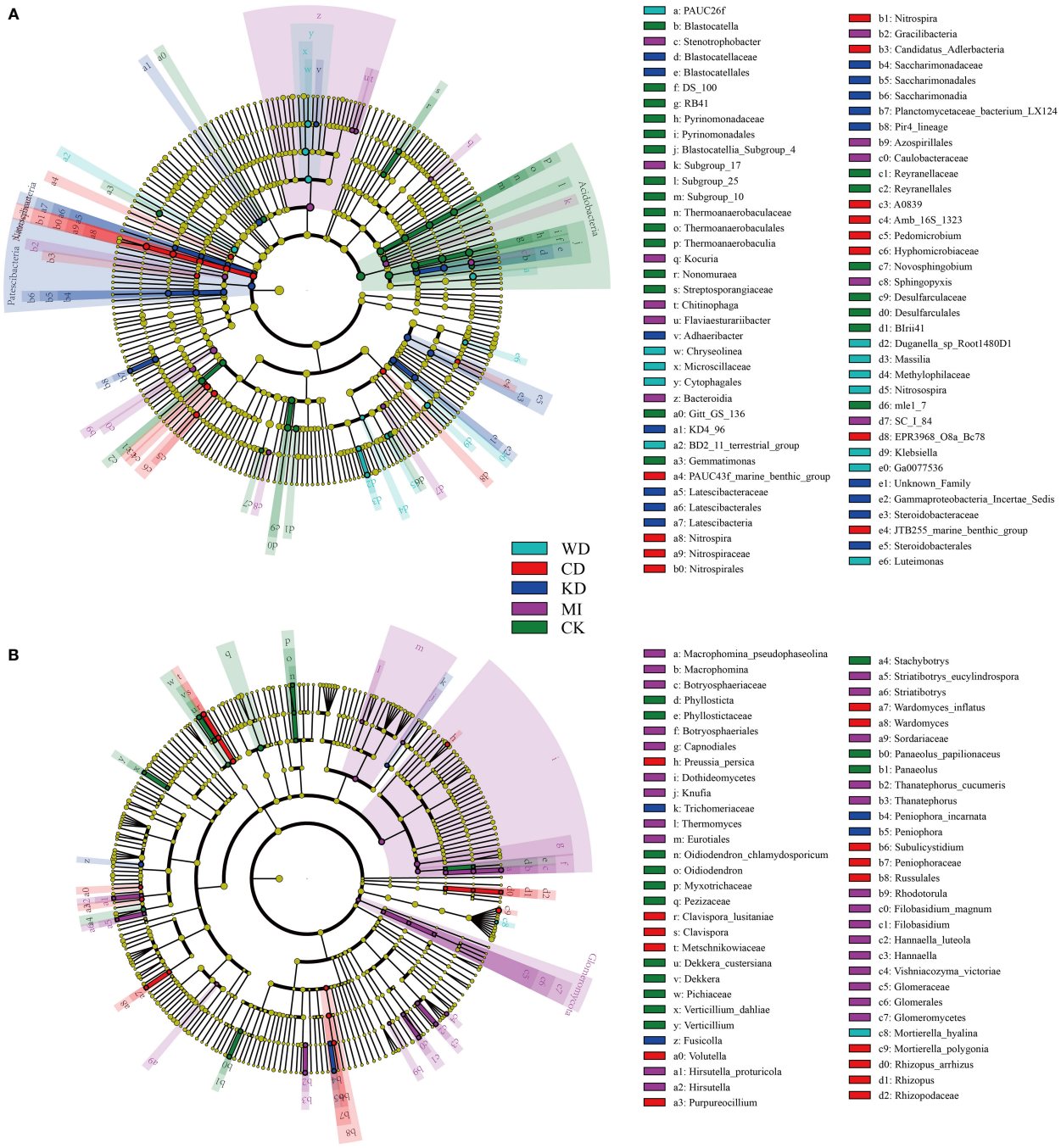

FIGURE 3
Linear discriminant analysis effect size (LEfSe) taxonomic cladogram identified significantly discriminant bacteria **(A)** and fungi **(B)** taxa (LDA > 2) associated with soils of different intercropping modes. WD, watermelon-daylily intercropping; CD, cabbage-daylily intercropping; KD, kale-daylily intercropping; MI, row mixed intercropping, watermelon, cabbage, and kale were alternately intercropped with daylily; CK, monoculture daylily.

enzymatic activity) and daylily yield. In the case of bacteria, AK, AP, AN, and OM were closely associated with WD and CD; UE, pH, and SC were closely related to KD and MI; POD was closely related to CK; Yield was closely related to WD and CD, and was also affected by AK, AP, AN and OM (Figure 4A). The ANOVA-like permutation test revealed that OM, UE, SC, AN, AK, Yield, and AP were significantly associated with the bacterial communities (Table S4, p-value < 0.01), while pH and POD did not exhibit a significant association (Table S4, p-value > 0.05). In the case of fungi, AP, AK, and OM were closely related to WD, CD, and KD; AN, UE, and pH were closely related to MI; POD and SC were closely related to CK; Yield was closely related to WD, CD and KD, and was also affected by AK, AP, AN and OM (Figure 4B). The ANOVA-like permutation test revealed that AP, AK, and SC were significantly

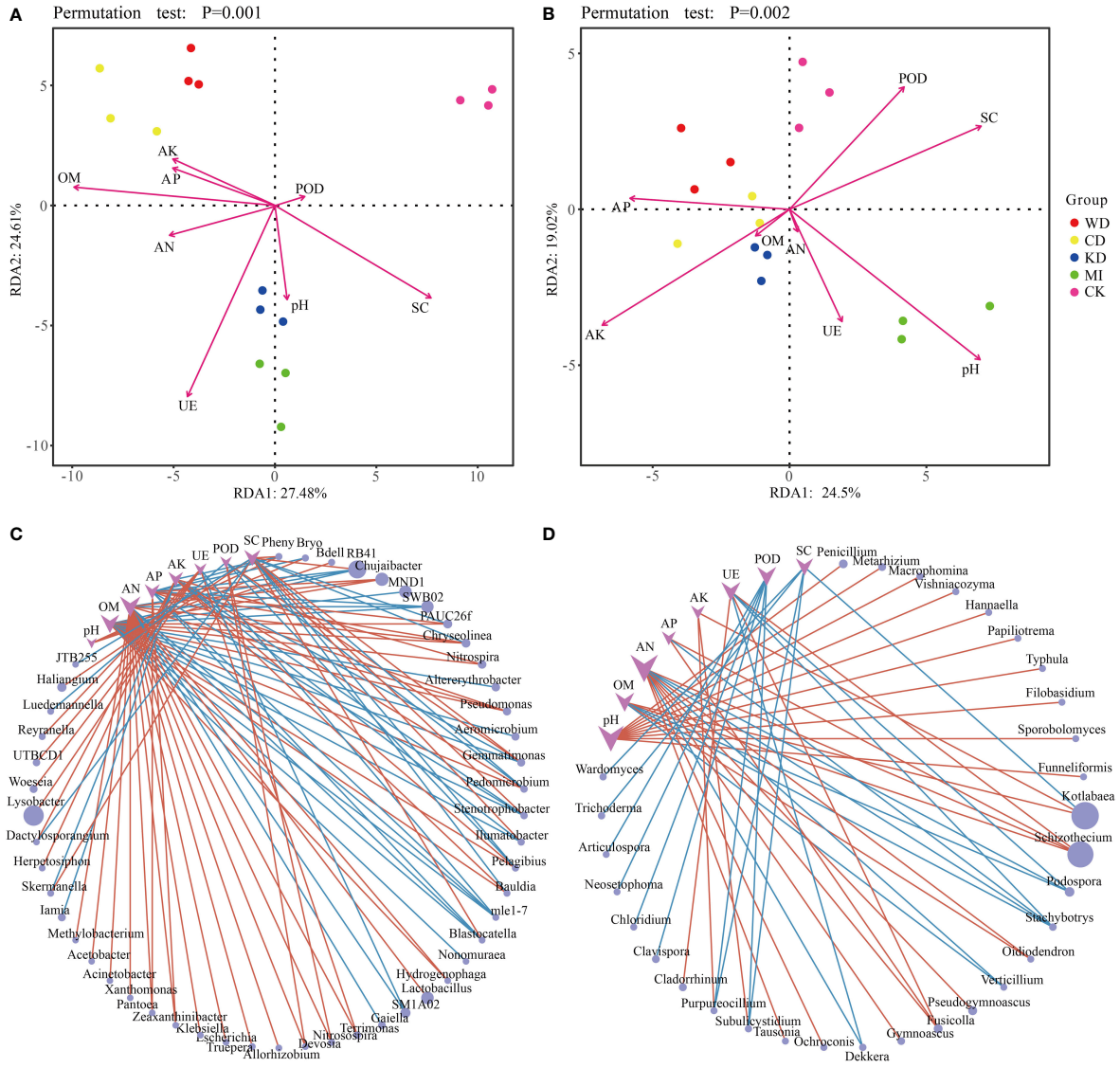

FIGURE 4
Statistical correlation of soil properties with the microbiome. Redundancy analysis (RDA) based on bacteria **(A)** and fungi **(B)** community composition of intercropping systems. Network analysis reflected the co-occurrence relationship between bacteria **(C)** and fungi **(D)** taxa and soil parameters. Purple vee nodes represent soil parameters. Grey ellipse nodes represent microbial members. Direct connections between nodes indicate strong correlations (Pearson correlation coefficient, $|r| \geq 0.5$; $P < 0.05$). The color of the edges represents positive correlation (pink) or negative correlation (blue). The sizes of vee nodes are proportional to the interconnected degree. The sizes of ellipse nodes are proportional to the relative abundance. AN, available nitrogen; AP, available phosphorus; AK, available potassium; OM, organic matter. UE, urease; POD, peroxidase; SC, sucrase. WD, watermelon-daylily intercropping; CD, cabbage-daylily intercropping; KD, kale-daylily intercropping; MI, row mixed intercropping, watermelon, cabbage, and kale were alternately intercropped with daylily; CK, monoculture daylily.

associated with the fungal communities (Table S4, p-value < 0.05), while pH, OM, AN, UE, POD, and Yield did not exhibit a significant association (Table S4, p-value > 0.05).

The co-occurrence patterns between the microbiome and soil properties were investigated using network analysis. As depicted in Figures 4C, D, overall, the module was more densely connected in the case of bacteria (average degree = 1.72) compared to fungi (average degree = 1.28). Several microbial taxa were associated significantly with various soil parameters, particularly AN, which exhibited high connectivity. For instance, Blastocatella was linked positively to SC and negatively to AN, AP, and OM, Gemmatimonas was associated positively with SC and POD and negatively with OM and AK (Figure 4C), Fusicolla was associated positively with AN, AP, and UE, and Stachybotrys was associated negatively with OM, AN, AP, and UE (Figure 4D).

4 Discussion

Intercropping is considered to be an environmentally friendly system that can improve crop yield as well as water and nutrient-use efficiency (Gaiser et al., 2004; Li et al., 2014; Cong et al., 2015; Dai et al., 2019). One of the greatest superiorities of intercropping is a further efficient utilization of lands and positive inter-crop interplays, which

facilitates the survival, fitness, and growth of crops (Hauggaard-Nielsen and Jensen, 2005). Intercropping systems are reported to improve the carbon and nitrogen concentrations, physicochemical traits, bulk density, and pH of the soil (Bedoussac and Justes, 2009; Liu et al., 2014; Li and Wu, 2018; Cuartero et al., 2022). The present study also verified that the levels of nutrients (AP, AN, AK, and OM) in the soil and daylily yields were prominently higher in all intercropping systems compared to the monocropping system, suggesting that concurrent growth of 2 or more crops could contribute to elevating the levels of soil nutrients (Table 1). The soil nutrient contents and daylily yields of the different intercropping soil systems (WD, CD, KD, and MI) were significantly different, indicating the existence of crop competition for soil nutrients. For instance, a pronouncedly lower nitrogen concentration in WD was noted compared to that in CD, KD, and MI (Table 1). This could be related to the development of watermelon, as substantial nitrogen is necessary for promoting photosynthesis and, ultimately, the watermelon vine growth, thereby affecting the watermelon quality (Gulut, 2021). The contents of AK and AP were significantly increased in the intercropped soils, which may be attributed to the increased richness of the soil nutrient cycling-associated microorganic taxa, such as phosphate- and potassium-solubilizing bacteria and rhizobia (Palm, 1995). This increase in yield could be due to higher nitrogen disposal from the rhizosphere of intercropping systems, which should be higher in soils with low N fertilization addition (Yu et al., 2018). This fact has previously been observed in other intercrop relationships, such as cowpea-maize (Latati et al., 2014).

Soil enzymatic activity is a vital parameter indicating how organic matter is degraded, and the nutrients are cycled in the soil (Nannipieri et al., 2012; Hussain et al., 2021). Soil enzymatic activity is reportedly impacted by the physicochemical traits and microbial communities of the soil (Gu et al., 2009). In the present study, the intercropping soil systems (WD, CD, KD, and MI) presented the highest UE and SC activities compared to the CK. Bai et al. (2022) also reported that the sucrase activity of the soil in the intercropping forests was higher than that in the monocropping walnut and tea forests. Zhou et al. (2011) reported elevation in the soil urease activity in the cucumber–garlic/onion intercropping system, with this effect persisting a few growing seasons compared to the cucumber monocropping system. Sucrase hydrolyzes sucrose and, therefore, reflects the convertibility of the soil organic carbon, while urease impacts the metabolism of soil nitrogen through urea hydrolyzation (Cantarella et al., 2018). Peroxidase activity is considered a crucial predictor of the dynamics of soil organic matter (Tian and Shi, 2014). In the present study, the intercropping soil systems (WD, CD, KD, and MI) presented weakened POD activity as the availability of inorganic nitrogen increased (Table 1), which is consistent with the results reported by Bai et al. (2022). It appears that different intercropping patterns of different crops play a pivotal role in the aggregation, decomposition, and conversion of the soil organic carbon, and are, therefore, capable of offering sufficient energy to the soil microbes.

Soil microorganic diversity is strongly associated with the stability of the soil ecotope and soil nutrient conversion, and intercropping facilitates the management of diverse agroecosystem services through the upgradation of soil quality (Cong et al., 2015). It is noteworthy that the composition of soil microbiota is linked remarkably to the alterations in the soil chemical traits (Lauber et al., 2008; Campbell et al., 2010). In the present work, intercropping systems presented improved microbial diversity and nutrient content in the soil (Figures 1A, B; Table 1), suggesting that besides enhancing the quality of the continuous cropping soil, intercropping also facilitates enhancing the stability of the facility ecosystem. The potential factors that influence the soil microbiota include the soil types, plant varieties, and root exudates (Wieland et al., 2001; Broeckling et al., 2008; Lauber et al., 2008; Lauber et al., 2009). Significant alterations in the composition of the soil microorganic taxa were noted among the monocropping and intercropping systems in the present study (Figures 2C, D). For instance, both unique OTUs and marker taxa in the different intercropping soil systems (WD, CD, KD, and MI) were altered compared to CK (Figure 1E, F; Figure 3). The prevailing taxonomic groups identified in the investigated soils were *Proteobacteria*, *Actinobacteria*, *Acidobacteria*, *Firmicutes*, *Gemmatimonadetes*, *Planctomycetes*, *Chloroflexi*, and *Bacteroidetes*, all of which are ordinary soil inhabitants (Zhou et al., 2018), and the same result was also observed in this study. As implied by a higher relative richness of *Bacteroidetes* in MI and the lower richness of *Acidobacteria* in WD and CD and that of *Chloroflexi* in WD, compared to CK (Table S2), the richness of the prevailing taxa in the soil is alterable through changes in both planting patterns and crop species, as since these taxa are adaptable to a novel microenvironment (Zhang et al., 2018; Gong et al., 2019; Zhi-dan et al., 2019).

Further, the different intercropping modes led to alterations in the soil physicochemical traits and enzymatic activities, prompting the enrichment of a particular subset of functional bacteria and fungi in the soil, which manifested as elevated diversities of both microbial types in the intercropped soil compared to the tea monoculture (Bai et al., 2022). Previous reports have indicated that *Bacteroidetes* are linked to the cycling of N and P in soil (Lidbury et al., 2021). A few plant-beneficial microbes recognized in previous studies, such as *Bacillus*, *Pseudomonas*, *Sphingomonas*, and *Streptomyces* (Bhattacharyya and Jha, 2012; Asaf et al., 2020), were reported to be capable of lowering the proportion of harmful fungi in the soil (Negawo and Beyene, 2017) through the inhibition of fungal growth and facilitating plant growth (Tejera-Hernández et al., 2011; Sivasakthi et al., 2014). In the present study, the richness of *Pseudomonas* exhibited a significant positive association with AP, AN, and OM (Figure 4C). In addition, the richness of *Chujaibacter*, a bacteria implicated in nitrification (a process of N cycling) (Semenov et al., 2020), was linked positively to the levels of AP, AN, and OM in the soil (Figure 4C). Improvement in the uptake of nitrogen and phosphorus in the presence of *Oidiodendron* has been reported previously (Vohník et al., 2005). In the present study, the richness of *Oidiodendron* exhibited a significant positive association with OM and AN (Figure 4D). In addition, the different intercropping soil systems (WD, CD, KD, and MI) presented the enrichment of a few bacterial genera related to potassium and phosphorus solubilization. Examples of these bacterial genera include *Pseudomonas*, *Arthrobacter*, *Sphingomonas*, *Bacillus*, and *Burkholderia* (data not presented), which have been previously acknowledged to possess functions such as facilitation of plant growth, solubilization of

phosphorus, fixation of nitrogen, organic compound degradation and bioconversion, and stimulation of growth (Rodríguez and Fraga, 1999; Sharma et al., 2013; Panhwar et al., 2014; Chen et al., 2016; Sadauskas et al., 2020; Tapia-García et al., 2020; Yang et al., 2020). Similarly, the potassium-solubilizing activities of *Bacillus* and *Burkholderia* have also been reported previously (Basak and Biswas, 2008; Zhang and Kong, 2014). These results indicated that intercropping impacts the soil nutrient levels, microbiota composition, and enzymatic activity favorably and that microorganisms have crucial roles to play in nutrient cycling.

5 Conclusion

Intercropping of daylily with other crops could increase the concentrations of organic matter, nitrogen, potassium, and phosphorus in the soil and daylily yield, thereby facilitating the improvement of soil nutrient status greatly. Meanwhile, the different intercropping modes also caused great alterations in the architecture and diversity of the microbial communities in the soil. In addition, the microbial taxa in the soil were closely related to soil characteristic parameters. In conclusion, besides significantly optimizing the microbiota architecture in the soil, the intercropping system also led to an enhanced relative abundance of the beneficial taxa of bacteria and fungi associated primarily with disease prevention and nutrient cycling. Further long-term analysis of these intercropping systems will be needed to reinforce findings on the positive interaction between daylily and other crops microbiota and their functions, and to study more in depth which intercropping pattern would be the most beneficial for the farmer and contribute to the development of sustainable agriculture.

Data availability statement

The data presented in the study are deposited in the CNCB repository (https://ngdc.cncb.ac.cn/databases), accession number PRJCA010600.

Author contributions

JG performed the statistical analysis and wrote the first draft of the manuscript. HX contributed to conception and design of the study. All authors contributed to manuscript revision, read, and approved the submitted version.

Funding

This study was supported by the Autonomous Region Agricultural Science and Technology Independent Innovation Special Scientific and Technological Innovation (NKYG-20-05) and Ningxia Liupan Mountain Area agricultural characteristic industry quality and efficiency technology integration and demonstration project (2022YFD1602500).

Conflict of interest

The authors declare that the research was conducted in the absence of any commercial or financial relationships that could be construed as a potential conflict of interest.

Publisher's note

Supplementary material

The Supplementary Material for this article can be found online at: https://www.frontiersin.org/articles/10.3389/fpls.2023.1107690/full#supplementary-material

References

Asaf, S., Numan, M., Khan, A. L., and Al-Harrasi, A. (2020). Sphingomonas: from diversity and genomics to functional role in environmental remediation and plant growth. *Crit. Rev. Biotechnol.* 40 (2), 138–152. doi: 10.1080/07388551.2019.1709793

Bach, C. E., Warnock, D. D., Horn, D. J. V., Weintraub, M. N., Sinsabaugh, R. L., Allison, S. D., et al. (2013). Measuring phenol oxidase and peroxidase activities with pyrogallol, l-DOPA, and ABTS: Effect of assay conditions and soil type. *Soil Biol. Biochem.* 67, 183–191. doi: 10.1016/j.soilbio.2013.08.022

Bai, Y.-C., Li, B.-X., Xu, C.-Y., Raza, M., Wang, Q., Wang, Q.-Z., et al. (2022). Intercropping walnut and tea: Effects on soil nutrients, enzyme activity, and microbial communities. *Front. Microbiol.* 13. doi: 10.3389/fmicb.2022.852342

Bao, S. D. (2000). *Soil and agricultural chemistry analysis* (Beijing: Agriculture Publication).

Basak, B. B., and Biswas, D. R. (2008). Influence of potassium solubilizing microorganism (Bacillus mucilaginosus) and waste mica on potassium uptake dynamics by sudan grass (Sorghum vulgare pers.) grown under two alfisols. *Plant Soil* 317 (1-2), 235–255. doi: 10.1007/s11104-008-9805-z

Beckers, B., Beeck, M. O. D., Weyens, N., Boerjan, W., and Vangronsveld, J. (2017). Structural variability and niche differentiation in the rhizosphere and endosphere bacterial microbiome of field-grown poplar trees. *Microbiome* 5 (1), 25. doi: 10.1186/s40168-017-0241-2

Bedoussac, L., and Justes, E. (2009). The efficiency of a durum wheat-winter pea intercrop to improve yield and wheat grain protein concentration depends on n availability during early growth. *Plant Soil* 330 (1-2), 19–35. doi: 10.1007/s11104-009-0082-2

Bever, J. D., Platt, T. G., and Morton, E. R. (2012). Microbial population and community dynamics on plant roots and their feedbacks on plant communities. *Annu. Rev. Microbiol.* 66, 265–283. doi: 10.1146/annurev-micro-092611-150107

Bhattacharyya, P. N., and Jha, D. K. (2012). Plant growth-promoting rhizobacteria (PGPR): emergence in agriculture. *World J. Microbiol. Biotechnol.* 28 (4), 1327–1350. doi: 10.1007/s11274-011-0979-9

Blagodatskaya, E., and Kuzyakov, Y. (2013). Active microorganisms in soil: Critical review of estimation criteria and approaches. *Soil Biol. Biochem.* 67, 192–211. doi: 10.1016/j.soilbio.2013.08.024

Broeckling, C. D., Broz, A. K., Bergelson, J., Manter, D. K., and Vivanco, J. M. (2008). Root exudates regulate soil fungal community composition and diversity. *Appl. Environ. Microbiol.* 74 (3), 738–744. doi: 10.1128/AEM.02188-07

Campbell, B. J., Hanson, T. E., Polson, S. W., Mack, M. C., and Schuur, E. A. G. (2010). The effect of nutrient deposition on bacterial communities in Arctic tundra soil. *Environ. Microbiol.* 12 (7), 1842–1854. doi: 10.1111/j.1462-2920.2010.02189.x

Cantarella, H., Otto, R., and Soares, J. R. (2018). Agronomic efficiency of NBPT as a urease inhibitor: A review. *J. Adv. Res.* 13, 19–27. doi: 10.1016/j.jare.2018.05.008

Chen, C., Huang, Q., Zhang, J., Wang, J., Lu, M., Qin, C., et al. (2016). Microbial communities of an arable soil treated for 8 years with organic and inorganic fertilizers. *Biol. Fertil. Soils* 52, 455–467. doi: 10.1007/s00374-016-1089-5

Chen, F.-S., Zeng, D.-H., Fahey, T. J., and Liao, P.-F. (2010). Organic carbon in soil physical fractions under different-aged plantations of Mongolian pine in semi-arid region of northeast China. *Appl. Soil Ecol.* 44 (1), 42–48. doi: 10.1016/j.apsoil.2009.09.003

Cong, W.-F., Hoffland, E., Li, L., Six, J., Sun, J.-H., Bao, X.-G., et al. (2015). Intercropping enhances soil carbon and nitrogen. *Glob. Chang. Biol.* 21 (4), 1715–1726. doi: 10.1111/gcb.12738

Cuartero, J., Pascual, J. A., Vivo, J.-M., Ozbolat, O., Sanchez-Navarro, V., Egea-Cortines, M., et al. (2022). A first-year melon/cowpea intercropping system improves soil nutrients and changes the soil microbial community. *Agricult. Ecosyst. Environ.* 328, 107856. doi: 10.1016/j.agee.2022.107856

Dai, J., Qiu, W., Wang, N., Wang, T., Nakanishi, H., and Zuo, Y. (2019). From Leguminosae/Gramineae intercropping systems to see benefits of intercropping on iron nutrition. *Front. Plant Sci.* 10. doi: 10.3389/fpls.2019.00605

Duchene, O., Vian, J.-F., and Celette, F. (2017). Intercropping with legume for agroecological cropping systems: Complementarity and facilitation processes and the importance of soil microorganisms. a review. *Agricult. Ecosyst. Environ.* 240, 148–161. doi: 10.1016/j.agee.2017.02.019

Edgar, R. C. (2013). UPARSE: highly accurate OTU sequences from microbial amplicon reads. *Nat. Methods* 10 (10), 996–998. doi: 10.1038/nmeth.2604

Edgar, R. C., Haas, B. J., Clemente, J. C., Quince, C., and Knight, R. (2011). UCHIME improves sensitivity and speed of chimera detection. *Bioinformatics* 27 (16), 2194–2200. doi: 10.1093/bioinformatics/btr381

Gaiser, T., Barros, I. D., Lange, F.-M., and Williams, J. R. (2004). Water use efficiency of a maize/cowpea intercrop on a highly acidic tropical soil as affected by liming and fertilizer application. *Plant Soil* 263, 165–171. doi: 10.1023/B:PLSO.0000047733.98854.9f

Gao, Z., Ha, M., Hu, Y., Li, Z., Liu, C., Wang, X., et al. (2019). Effects of continuous cropping of sweet potato on the fungal community structure in rhizospheric soil. *Front. Microbiol.* 10. doi: 10.3389/fmicb.2019.02269

Gong, X., Liu, C., Li, J., Luo, Y., Yang, Q., Zhang, W., et al. (2019). Responses of rhizosphere soil properties, enzyme activities and microbial diversity to intercropping patterns on the loess plateau of China. *Soil Tillage Res.* 195, 104355. doi: 10.1016/j.still.2019.104355

Gu, Y., Wang, P., and Kong, C. H. (2009). Urease, invertase, dehydrogenase and polyphenoloxidase activities in paddy soil influenced by allelopathic rice variety. *Eur. J. Soil Biol.* 45 (5-6), 436–441. doi: 10.1016/j.ejsobi.2009.06.003

Gulut, K. Y. (2021). Nitrogen and boron nutrition in grafted watermelon I: Impact on pomological attributes, yield and fruit quality. *PloS One* 16 (5), e0252396. doi: 10.1371/journal.pone.0252396

Hauggaard-Nielsen, H., and Jensen, E. S. (2005). Facilitative root interactions in intercrops. *Plant Soil* 274 (1-2), 237–250. doi: 10.1007/s11104-004-1305-1

Hou, F., Li, S., Wang, J., Kang, X., Weng, Y., and Xing, G. (2017). Identification and validation of reference genes for quantitative real-time PCR studies in long yellow daylily, hemerocallis citrina borani. *PloS One* 12 (3), e0174933. doi: 10.1371/journal.pone.0174933

Hussain, S., Shafiq, I., Skalicky, M., Brestic, M., Rastogi, A., Mumtaz, M., et al. (2021). Titanium application increases phosphorus uptake through changes in auxin content and root architecture in soybean (Glycine max l.). *Front. Plant Sci.* 12. doi: 10.3389/fpls.2021.743618

Jin, P., Ren, B., Wang, X. C., Jin, X., and Shi, X. (2020). Mechanism of microbial metabolic responses and ecological system conversion under different nitrogen conditions in sewers. *Water Res.* 186, 116312. doi: 10.1016/j.watres.2020.116312

Latati, M., Blavet, D., Alkama, N., Laoufi, H., Drevon, J. J., Gérard, F., et al. (2014). The intercropping cowpea-maize improves soil phosphorus availability and maize yields in an alkaline soil. *Plant Soil* 385, 181–191. doi: 10.1007/s11104-014-2214-6

Lauber, C. L., Hamady, M., Knight, R., and Fierer, N. (2009). Pyrosequencing-based assessment of soil pH as a predictor of soil bacterial community structure at the continental scale. *Appl. Environ. Microbiol.* 75 (15), 5111–5120. doi: 10.1128/AEM.00335-09

Lauber, C. L., Strickland, M. S., Bradford, M. A., and Fierer, N. (2008). The influence of soil properties on the structure of bacterial and fungal communities across land-use types. *Soil Biol. Biochem.* 40 (9), 2407–2415. doi: 10.1016/j.soilbio.2008.05.021

Li, X., Lewis, E. E., Liu, Q., Li, H., Bai, C., and Wang, Y. (2016). Effects of long-term continuous cropping on soil nematode community and soil condition associated with replant problem in strawberry habitat. *Sci. Rep.* 6, 30466. doi: 10.1038/srep30466

Li, L., Tilman, D., Lambers, H., and Zhang, F.-S. (2014). Plant diversity and overyielding: insights from belowground facilitation of intercropping in agriculture. *New Phytol.* 203 (1), 63–69. doi: 10.1111/nph.12778

Li, S., and Wu, F. (2018). Diversity and Co-occurrence patterns of soil bacterial and fungal communities in seven intercropping systems. *Front. Microbiol.* 9 1521. doi: 10.3389/fmicb.2018.01521

Lidbury, I. D. E. A., Borsetto, C., Murphy, A. R. J., Bottrill, A., Jones, A. M. E., Bending, G. D., et al. (2021). Niche-adaptation in plant-associated bacteroidetes favours specialisation in organic phosphorus mineralisation. *ISME J.* 15 (4), 1040–1055. doi: 10.1038/s41396-020-00829-2

Lin, S.-H., Chang, H.-C., Chen, P.-J., Hsieh, C.-L., Su, K.-P., and Sheen, L.-Y. (2013). The antidepressant-like effect of ethanol extract of daylily flowers (Jin zhen hua) in rats. *J. Tradit. Complement. Med.* 3 (1), 53–61. doi: 10.4103/2225-4110.106548

Liu, T., Cheng, Z., Meng, H., Ahmad, I., and Zhao, H. (2014). Growth, yield and quality of spring tomato and physicochemical properties of medium in a tomato/garlic intercropping system under plastic tunnel organic medium cultivation. *Scientia Hortic.* 170, 159–168. doi: 10.1016/j.scienta.2014.02.039

Nannipieri, P., Giagnoni, L., Renella, G., Puglisi, E., Ceccanti, B., Masciandaro, G., et al. (2012). Soil enzymology: Classical and molecular approaches. *Biol. Fertility Soils* 48 (7), 743–762. doi: 10.1007/s00374-012-0723-0

Negawo, W. J., and Beyene, D. N. (2017). The role of coffee based agroforestry system tree diversity conservation in eastern Uganda. *J. Landscape Ecol.* 10 (2). doi: 10.1515/jlecol-2017-0001

Palm, C. A. (1995). Contribution of agroforestry trees to nutrient requirements of intercropped plants. *Agroforestry Syst.* 30, 105–124. doi: 10.1007/BF00708916

Panhwar, Q. A., Naher, U. A., Jusop, S., Othman, R., Latif, M. A., and Ismail, M. R. (2014). Biochemical and molecular characterization of potential phosphate-solubilizing bacteria in acid sulfate soils and their beneficial effects on rice growth. *PloS One* 9 (10), e97241. doi: 10.1371/journal.pone.0097241

Quast, C., Pruesse, E., Yilmaz, P., Gerken, J., Schweer, T., Yarza, P., et al. (2013). The SILVA ribosomal RNA gene database project: improved data processing and web-based tools. *Nucleic Acids Res.* 41 (Database issue), D590–D596. doi: 10.1093/nar/gks1219

Rodríguez, H., and Fraga, R. (1999). Phosphate solubilizing bacteria and their role in plant growth promotion. *Biotechnol. Adv.* 17, 319–339. doi: 10.1016/S0734-9750(99)00014-2

Sadauskas, M., Statkeviciute, R., Vaitekunas, J., and Meškys, R. (2020). Bioconversion of biologically active indole derivatives with indole-3-Acetic acid-degrading enzymes from caballeronia glathei DSM50014. *Biomolecules* 10 (4). doi: 10.3390/biom10040663

Semenov, M. V., Krasnov, G. S., Semenov, V. M., and Bruggen, A. H. C. V. (2020). Long-term fertilization rather than plant species shapes rhizosphere and bulk soil prokaryotic communities in agroecosystems. *Appl. Soil Ecol.* 154, 103641. doi: 10.1016/j.apsoil.2020.103641

Sharma, S. B., Sayyed, R. Z., Trivedi, M. H., and Gobi, T. A. (2013). Phosphate solubilizing microbes: Sustainable approach for managing phosphorus deficiency in agricultural soils. *SpringerPlus* 2, 587. doi: 10.1186/2193-1801-2-587

Sivasakthi, S., Usharani, G., and Saranraj, P. (2014). Biocontrol potentiality of plant growth promoting bacteria (PGPR) - pseudomonas fluorescens and bacillus subtilis: A review. *Afr. J. Agric. Res.* 9 (16), 1265–1277. doi: 10.5897/AJAR2013.7914

Sun, L., Gao, J., TingHuang, R. A., Kendall, J., Shen, Q., and Zhang, R. (2015). Parental material and cultivation determine soil bacterial community structure and fertility. *FEMS Microbiol. Ecol.* 91 (1), 1–10. doi: 10.1093/femsec/fiu010

Tapia-García, E. Y., Arroyo-Herrera, I., Rojas-Rojas, F. U., Ibarra, J. A., Vásquez-Murrieta, M. S., Martínez-Aguilar, L., et al. (2020). Paraburkholderia lycopersici sp. nov., a nitrogen-fixing species isolated from rhizoplane of lycopersicon esculentum mill. var. saladette in Mexico. *Syst. Appl. Microbiol.* 43 (6), 126133. doi: 10.1016/j.syapm.2020.126133

Tejera-Hernández, B., Rojas-Badía, M. M., and Heydrich-Pérez, M. (2011). Potencialidades del género bacillus en la promoción del crecimiento vegetal y el control biológico de hongos fitopatógenos. *Rev. CENIC Cienc. Biológicas* 42 (3), 131–138.

Tian, L., and Shi, W. (2014). Soil peroxidase regulates organic matter decomposition through improving the accessibility of reducing sugars and amino acids. *Biol. Fertility Soils* 50 (5), 785–794. doi: 10.1007/s00374-014-0903-1

Vohník, M., Albrechtová, J., and Vosátka, M. (2005). The inoculation with oidiodendron maius and phialocephala fortinii alters phosphorus and nitrogen uptake, foliar C:N ratio and root biomass distribution in rhododendron cv. azurro. *Symbiosis* 40, 87–96.

Wei, Z., Yang, T., Friman, V.-P., Xu, Y., Shen, Q., and Jousset, A. (2015). Trophic network architecture of root-associated bacterial communities determines pathogen invasion and plant health. *Nat. Commun.* 6, 8413. doi: 10.1038/ncomms9413

Wieland, G., Neumann, R., and Backhaus, H. (2001). Variation of microbial communities in soil, rhizosphere, and rhizoplane in response to crop species, soil type, and crop development. *Appl. Environ. Microbiol.* 67 (12), 5849–5854. doi: 10.1128/AEM.67.12.5849-5854.2001

Xiong, W., Li, Z., Liu, H., Xue, C., Zhang, R., Wu, H., et al. (2015). The effect of long-term continuous cropping of black pepper on soil bacterial communities as determined by 454 pyrosequencing. *PloS One* 10 (8), e0136946. doi: 10.1371/journal.pone.0136946

Yang, A., Akhtar, S. S., Fu, Q., Naveed, M., Iqbal, S., Roitsch, T., et al. (2020). Burkholderia phytofirmans PsJN stimulate growth and yield of quinoa under salinity stress. *Plants (Basel)* 9 (6). doi: 10.3390/plants9060672

Yang, R.-F., Geng, L.-L., Lu, H.-Q., and Fan, X.-D. (2017). Ultrasound-synergized electrostatic field extraction of total flavonoids from hemerocallis citrina baroni. *Ultrason Sonochem* 34, 571–579. doi: 10.1016/j.ultsonch.2016.06.037

Yu, Z., Liu, J., Li, Y., Jin, J., Liu, X., and Wang, G. (2018). Impact of land use, fertilization and seasonal variation on the abundance and diversity of nirS-type denitrifying bacterial communities in a mollisol in northeast China. *Eur. J. Soil Biol.* 85, 4–11. doi: 10.1016/j.ejsobi.2017.12.001

Yu, L., Tang, Y., Wang, Z., Gou, Y., and Wang, J. (2018). Nitrogen-cycling genes and rhizosphere microbial community with reduced nitrogen application in maize/soybean strip intercropping. *Nutrient Cycling Agroecosyst.* 113 (1), 35–49. doi: 10.1007/s10705-018-9960-4

Zeng, J., Liu, J., Lu, C., Ou, X., Luo, K., Li, C., et al. (2020). Intercropping with turmeric or ginger reduce the continuous cropping obstacles that affect pogostemon cablin (Patchouli). *Front. Microbiol.* 11. doi: 10.3389/fmicb.2020.579719

Zhang, C., and Kong, F. (2014). Isolation and identification of potassium-solubilizing bacteria from tobacco rhizospheric soil and their effect on tobacco plants. *Appl. Soil Ecol.* 82, 18–25. doi: 10.1016/j.apsoil.2014.05.002

Zhang, M.-M., Wang, N., Hu, Y.-B., and Sun, G.-Y. (2018). Changes in soil physicochemical properties and soil bacterial community in mulberry (Morus alba l.)/alfalfa (Medicago sativa l.) intercropping system. *Microbiologyopen* 7 (2), e00555. doi: 10.1002/mbo3.555

Zhang, M., Wang, N., Zhang, J., Hu, Y., Cai, D., Guo, J., et al. (2019). Soil physicochemical properties and the rhizosphere soil fungal community in a mulberry (Morus alba L.)/Alfalfa (Medicago sativa l.) intercropping system. *Forests* 10 (2), 167. doi: 10.3390/f10020167

Zhi-dan, F., Wei-guo, L., Li, Z., Ping, C., Wen-yu, Y., Qing, D., et al. (2019). Effects of maize-soybean relay intercropping on crop nutrient uptake and soil bacterial community. *J. Integr. Agric.* 18 (9), 2006–2018. doi: 10.1016/s2095-3119(18)62114-8

Zhou, Q., Chen, J., Xing, Y., Xie, X., and Wang, L. (2019). Influence of intercropping Chinese milk vetch on the soil microbial community in rhizosphere of rape. *Plant Soil* 440 (1-2), 85–96. doi: 10.1007/s11104-019-04040-x

Zhou, X., Wang, Z., Jia, H., Li, L., and Wu, F. (2018). Continuously monocropped Jerusalem artichoke changed soil bacterial community composition and ammonia-oxidizing and denitrifying bacteria abundances. *Front. Microbiol.* 9. doi: 10.3389/fmicb.2018.00705

Zhou, X., Yu, G., and Wu, F. (2011). Effects of intercropping cucumber with onion or garlic on soil enzyme activities, microbial communities and cucumber yield. *Eur. J. Soil Biol.* 47 (5), 279–287. doi: 10.1016/j.ejsobi.2011.07.001

Zhu, S., Wang, Y., Xu, X., Liu, T., Wu, D., Zheng, X., et al. (2018). Potential use of high-throughput sequencing of soil microbial communities for estimating the adverse effects of continuous cropping on ramie (Boehmeria nivea l. *Gaud) PloS One* 13 (5), e0197095. doi: 10.1371/journal.pone.0197095

frontiers | Frontiers in Plant Science

TYPE Original Research
PUBLISHED 06 March 2023
DOI 10.3389/fpls.2023.1124139

OPEN ACCESS

EDITED BY
Long Yang,
Shandong Agricultural University, China

REVIEWED BY
Mengya Song,
Swedish University of Agricultural Sciences, Sweden
Roxana Vidican,
University of Agricultural Sciences and Veterinary Medicine of Cluj-Napoca, Romania

*CORRESPONDENCE
Danwei Ma
danwei10ma@126.com

SPECIALTY SECTION
This article was submitted to Plant Symbiotic Interactions, a section of the journal Frontiers in Plant Science

RECEIVED 14 December 2022
ACCEPTED 13 February 2023
PUBLISHED 06 March 2023

CITATION
Zhou X, Xiao Y, Ma D, Xie Y, Wang Y, Zhang H and Wang Y (2023) The competitive strategies of poisonous weeds *Elsholtzia densa* Benth. on the Qinghai Tibet Plateau: Allelopathy and improving soil environment.
Front. Plant Sci. 14:1124139.
doi: 10.3389/fpls.2023.1124139

The competitive strategies of poisonous weeds *Elsholtzia densa* Benth. on the Qinghai Tibet Plateau: Allelopathy and improving soil environment

Xijie Zhou, Yunxing Xiao, Danwei Ma*, Yusi Xie, Yu Wang, Hong Zhang and Yanan Wang

College of Life Science, Sichuan Normal University, Chengdu, China

Introduction: The competitive strategies of plants play a crucial role in their growth. Allelopathy is one of the weapons that plants use to improve their competitive advantage.

Methods: In order to explore the competitive strategy of a poisonous weed *Elsholtzia densa* Benth. (*E. densa*) on the Qinghai-Tibet Plateau (QTP), the effects of decomposing substances of *E. densa* on growth, root border cells (RBCs) characteristics of highland crop highland barley (*Hordeum vulgare* L.), and soil environment were determined.

Results: The decomposing allelopathic effect of *E. densa* on the germination and seedling growth of highland barley mainly occurred in the early stage of decomposing. The allelopathic effects were mainly on seed germination and root growth of highland barley. After treatment with its decomposing solution, the RBC's mucilage layer of highland barley thickened, and the RBC's activity decreased or even apoptosis compared with the control. However, only the above-ground part of the treatment group showed a significant difference. The effects of *E. densa* decomposed substances on the soil environment were evaluated from soil physicochemical properties and bacterial community. The results showed that soil bacteria varied greatly in the early stage of decomposion under different concentrations of *E. densa*. In addition, *E. densa* decomposing substances increased the soil nutrient content, extracellular enzyme activities, and bacterial community diversity. In the process of decomposition, the bacterial community structure changed constantly, but Actinobacteriota was always the dominant phylum.

Discussion: These results indicated that *E. densa* might adopt the following two strategies to help it gain an advantage in the competition: 1. Release allelochemicals that interfere with the defense function of surrounding plants and directly inhibit the growth and development of surrounding plants. 2. By changing the physical and chemical properties of soil and extracellular enzyme activity, residual plant decomposition can stimulate soil microbial activity,

improve soil nutrition status, and create a more suitable soil environment for growth.

KEYWORDS

Elsholtzia densa Benth., competitive strategies, allelopathy, root border cells, soil environment

1 Introduction

As one of the most sensitive regions in the world to climate change, the Qinghai-Tibet Plateau (QTP) has great ecological fragility (Peng et al., 2012). In recent decades, a combination of adverse factors has led to serious land degradation on the QTP, resulting in a sharp decline in biodiversity and productivity (Geissler et al., 2019). Land degradation also changes the organization of plant communities, and poisonous weeds that are more tolerant to harsh environments take advantage of this opportunity to expand (Peng et al., 2020), gradually replacing native crops as new dominant species. At the same time, soil resources, microbial communities, and the spatial pattern of other groups changed dramatically (Dong et al., 2020).

Previous reports have shown that poisonous weeds compete with surrounding plants for natural resources such as light, water, and nutrients (Mushtaq et al., 2019) and release allelochemicals into the soil, like the "Novel weapon" hypothesis of invasive plants, directly inhibiting the growth of other plants in the habitat. They also disrupt the interaction between underground beneficial microbes and surrounding plants, thereby indirectly interfering with the growth and development of surrounding plants (Kalisz et al., 2020; Qu et al., 2021).

Allelochemicals can be released into the environment through various ways, such as volatilization, rain and fog leaching, root secretion, and decomposition of plant residues or litters (Hickman et al., 2021; Nikolaeva et al., 2021). After the allelochemicals enter the environment, they interact with the environment through retention, transformation, and migration, eventually leading to the increase or decrease of allelopathy (Xiao et al., 2017). Compared with hydrophilic allelochemicals, lipophilic allelochemicals may stay longer and continuously affect the surrounding plants through soil retention (Whitehead et al., 2018).

During evolution and in response to external stresses, including allelochemicals, root tips that were originally exposed directly to soil generated and released root border cells (RBCs) (Ropitaux et al., 2020). The RBCs and the mucus secreted by the plant themselves form a protective sheath of the root tip, which builds a biological, chemical, and physical barrier between the plant-root-external environment. The RBCs can attract and capture soil organisms and microorganisms, adsorb and neutralize the soil's toxic substances and regulate the rhizosphere environment (Carreras et al., 2020). Therefore, the allelochemicals entering the soil must break through the biological defense line constructed by the RBCs to affect the growth and development of the root system.

In the microenvironment comprising plant root-soil-microbe interactions, the soil microbes are the bridge connecting plants to soil and plants to plants. They can decompose complex components in the soil to form small molecular substances, helping the plant roots to absorb nutrients and improve stress resistance (Zhang et al., 2020). However, the allelochemicals released by plants disrupt the balance between the surrounding plants and soil and establish new microbial communities mutually beneficial to themselves (Li et al., 2022). Soil bacteria influence potential soil functions (nutrient cycling and climate regulation) more than soil fungi in a highly cold environment (Wang et al., 2021).

The plant community affected by poisonous weeds will gradually change from perennial herbs (gramineaceae and sedge family) to annual herbs and eventually form a single dominant community of poisonous weeds. During the evolution process, soil moisture and fertility decreased gradually, and community species composition and the carbon water cycle in the ecosystem were seriously affected (Qin et al., 2022). *Elsholtzia densa* Benth. (*E. densa*) is a dominant poisonous weed widely distributed in the QTP (Duan et al., 2019), which is a serious hazard to the farmland ecosystem of the QTP (Shang et al., 2018; Xiao et al., 2021). As an annual herb, *E. densa* produces manydead twigs and withered leavesyearly, and its decomposition inevitably releases allelochemicals into the soil continuously. Therefore, we have two hypotheses: 1) *E. densa* might interfere with the defense function of surrounding plants and directly inhibits the growth and development of surrounding plants by releasing allelochemicals; 2) *E. densa* may change the soil environment by residual plant decomposition.

In order to verify the above hypothesis, this study used the highland barley (*Hordeum vulgare* L.), a gramineous crop with strong adaptability to the high cold environment of the QTP (Li et al., 2020), as the receptor. The seeds, seedlings, and RBCs of highland barley were treated with different decomposing parts of the decomposing solution. These results were used to evaluate the allelopathic potential of *E. densa* decomposing solution and its effect on defense indexes of RBCs. In addition, different contents of *E. densa* residue were mixed in the soil and divided into short and long time stages of decomposition. Under decomposition time and

residue concentration, two variables were studied: the change law of nutrient content, extracellular enzyme activity, and bacterial diversity of decomposition soil.

2 Materials and methods

2.1 Materials and sources

The plants of *E. densa* and soil are collected at an altitude of 3470 m from Axi Township (102°55.944′ E, 33°41.023′ N), Hongyuan County, Aba Tibetan, and Qiang Autonomous Prefecture, Sichuan Province, China. The collected *E. densa* plants were at the maturity stage. The entire plant was divided into roots and aerial parts, dried in the shade under natural conditions, and cut into small sections of about 2 cm. In order to avoid interference, soil without *E. densa* growth in the area was selected for the test. We scooped up the topsoil (depth 0-20 cm) with a sampling shovel and placed it in a sealed bag. The soil samples were returned to the laboratory and sieved into 1 mm for use. The highland barley seeds were purchased from Daofu County, Garze Tibetan Autonomous Prefecture.

2.2 Allelopathic effect and cytotoxicity experiments of decomposing solution

2.2.1 Preparation of decomposing solution

The root decomposing solution (RD) and the above-ground decomposing solution (AD) were prepared according to the biomass of *E. densa* residues. RD = 25 groot: 500 g soil: 1 L water, AD = 50 g of aerial parts of *E. densa*: 500 g soil: 1 L water. The above components were evenly stirred and sealed at room temperature to decompose away from light. The decomposition process was divided into short-term 30 days (d) and long-term 60 d, during which the mixture was stirred once every 7 d, and each treatment was repeated 3 times. At the end of decomposition, clean gauze was used to remove the coarse substances in the decomposition solution, and the vacuum pump was used to extract the remaining filtrate under the filter paper. Then the filtrate volume after extraction was fixed to 1 L to obtain raw RD (25 mg/mL) and raw AD (50 mg/mL), respectively. During the experimental treatment, both were diluted with distilled water to obtain different concentrations of treatment solutions. The RD concentrations were 5, 10, 15, 20, and 25 mg/mL, and the AD concentrations were 10, 20, 30, 40, and 50 mg/mL.

2.2.2 Seed germination test

The highland barley seeds with full grains and no pest damage were sterilized with 0.5% $KMnO_4$ solution for 15 minutes (min) and then rinsed repeatedly with distilled water. After soaking in a 25°C incubator for 4 hours (h), the seeds were spread evenly in a germination box (12 cm × 12 cm × 9 cm) padded with two layers of filter paper, with 60 seeds per box. 15 mL of different concentrations of RD and AD were added to the germination box, and 15 mL of distilled water was used as the control. The number of germinated seeds and rooting was counted every day in a 25°C incubator for 7 d. The temperature in the incubator was set to 25°C/20°C, the illumination period to 12 h/12 h (light/dark), and the illumination to 2000 lx. The germinated germ reached half the length of the seed as germination, and the radicle reached half the length of the seed as rooted. Next, we calculated the following parameters (Sun et al., 2021):

$$GR = \frac{GN}{SN} \times 100\,\%$$

$$GI = \Sigma\left(\frac{G_t}{D_t}\right)$$

$$RR = \frac{RN}{SN} \times 100\,\%$$

where *GR* is the germination rate, *GN* is the number of germinated seeds, *SN* is the total number of seeds, *GI* is the germination index, *Gt* is the germination number on day *t*, *Dt* is the corresponding germination day, *RR* is the rooting rate, and *RN* is the number of rooted seeds.

2.2.3 Seedling growth test

The highland barley seeds were disinfected according to the steps in 2.2.2 and then immersed in the incubator at 25°C for 12 h. The seeds, after soaking, were transferred to a porcelain plate covered with wet double sterile gauze and continued to promote germination without light for 24 h. After the seeds were exposed to the white root tips, the full seeds with the same radicle lengthwere selected and inserted into a small pot covered with 3 cm perlite (diameter 10 cm, height 6 cm, 300 g perlite). Then we added 50 mL 1/4 MS nutrient solution and poured the nutrient solution every 1 day. The small flower pots were cultured in a light incubator for 4 days with a light intensity of 4500 lx, a light cycle of 12 h/12 h (light/dark), and a diurnal temperature of 25°C. After the first true leaves of the highland barley seedlings grow, 20 mL of different concentrations of RD and AD were added and distilled, using water as a control. Each treatment was repeated three times. After adding the decomposing solution, the seedlings were cultured for 7 d. After the cultivation, the seedlings werewashed with distilled and dried with filter paper. The plant height and root length of the highland barley seedlings were measured. After defoliating at 105°C and drying to constant weight at 85°C, the dry weight of the seedlings and roots wasmeasured (Sun et al., 2021).

2.2.4 Toxicity test of a decomposing solution to RBCs

The radicles of the highland barley seeds with exposed white root tips are inserted into a culture flask (volume 200 mL, diameter 9 cm, height 8.5 cm) containing 0.8% pure agar medium and cultured upside down. When the root length reaches 40 mm (at this time, the number of RBCs reaches the peak, and the activity is high), 10 root tips with a length of about 5 mm are randomly

selected and placed in 100 μL of 25 mg/mL RD and 50 mg/mL AD treatment solutions vortexed for 30 seconds (s). Then we rinsed the root tip twice with 50 μL of the treatment solution to prepare a cell suspension (200 μL), which was mixed and placed in an incubator at 25°C for 30 min in the dark. Each treatment was repeated six times.

Referring to Singh's method, 20 μL of cell suspension was added to a centrifuge tube (0.5 mL capacity), and 8 μL of AO/EB mixed dye solution was added dropwise and stained for 2 min. The cell viability and morphology were observed under a LEICA DM300 fluorescence microscope, where the orange ones are dead cells, and the green ones are living cells (Singh et al., 2021). Each treatment was repeated five times. Then we calculated the cell viability:

$$\text{RBCs survival rate} = \text{number of viable cells}/\text{total number of cells} \times 100\,\%$$

Referring to the method of Ropitaux, 8 μL of the cell suspension was taken, and 8 μL of Indian ink was added. After being stained for 10 min, the cells were observed with a Nikon ECLIPSE 55i microscope at x40 in a bright field, and pictures were captured to measure the thickness of the mucilage layer (Ropitaux et al., 2020). Each treatment measured 10 cells, and each cell measured 6 different locations.

2.3 Determination of soil properties

2.3.1 Experimental treatment

We pulverized the dried plants of *E. densa* with a crusher and prepared the decomposed soil according to the residue content of *E. densa* in 0, 0.02, 0.04 g/g, and 0.08 g/g, and added an appropriate amount of distilled water to keep the soil moist. In order to have sufficient samples to repeat the test, the total amount of soil in each treatment group was 300 g. Each treatment was repeated three times, and the soil samples were collected on 20 d, 40 d, and 60 d, respectively, some of which were tested for soil nutrients and enzyme activities, while the others were stored in a -80°C refrigerator to determine bacterial diversity.

2.3.2 Soil nutrient determination

The determination method was slightly modified by referring to Pan et al. (Pan et al., 2016; Geng et al., 2017; Li et al., 2021). The soil's pH was measured based on the electrode potential method (air-dried soil: distilled water = 1:2.5). The soil organic matter (SOM) was determined by the potassium dichromate volumetric method. In contrast, the total phosphorus (TP) and the available phosphorus (AP) were determined using the sodium hydroxide alkali fusion-molybdenum antimony anti-colorimetric method. The absorbance values at 585 nm, 700 nm, and 882 nm were measured using a SpectraMax M2 microplate reader (Molecular Devices, USA). Both the total potassium (TK) and available potassium (AK) were measured using a Z-2000 Zeeman atomic absorption spectrophotometer and the ammonium acetate extraction-flame photometer method. The total nitrogen (TN) and available nitrogen (AN) were determined by an automatic Kjeldahl analyzer (FOSS, KJELTECTM 2300).

2.3.3 Soil enzyme activity determination

The determination method was slightly modified by referring to Xie et al. (Chen et al., 2020; Xie et al., 2020). The urease activity was determined by the sodium phenolate colorimetric method, and the invertase and cellulase activities were determined by the 3,5-dinitrosalicylic acid colorimetric method. The polyphenol oxidase activity was determined by the colorimetric method for measuring pyrogallol, while the acid phosphatase activity was measured using the Solarbio soil acid phosphatase (S-ACP) activity assay kit.

2.3.4 High throughput sequencing of bacteria

The genomic DNA of the soil samples was extracted using the DNA extraction kit to detect the DNA concentration and purity. By employing the diluted genomic DNA as a template, the V3-V4 region of the bacterial 16S DNA was amplified by PCR using specific primers with Barcode and the Takara Ex Taq high-fidelity enzyme (Takara, Japan). The primer sequences were the 343 F (5'-TACGGRAGGCAGCAG-3') and 798 R (5'-AGGGTATCTA ATCCT-3'). After performing electrophoresis detection on the PCR product and purifying it using magnetic beads as a template for two rounds of PCR amplification, the second-round PCR products were electrophoresed again and purified with magnetic beads for Qubit quantification. An equal number of samples were mixed according to the PCR product concentration, and the high-throughput sequencing analysis of the soil bacteria 16S rDNA was performed using the Illumina platform Miseq high-throughput sequencing technology (Xu et al., 2019).

2.4 Statistical analysis

According to the results of various bioassay indicators, we calculate the allelopathic response index (*RI*) as follows (Williamson and Richardson, 1988):

$$RI = 1 - \frac{C}{T} (T \geq C)$$

$$RI = \frac{T}{C} - 1 (T < C)$$

where T is the treatment value, and C is the control value. $RI > 0$ refers to promotion, and $RI < 0$ to inhibition, where the absolute value is proportional to the intensity of the allelopathy. The integrated allelopathic sensitivity index formula (*SI*) is the arithmetic mean of *RI*.

Regarding the one-way analysis of variance (ANOVA), Tukey's test for multiple comparisons (*LSD*) and Pearson's correlation analysis are performed using the SPSS software (IBM, SPSS Version 20.0), with a confidence level of 95%. The redundancy analysis (Canoco 5.0) studies the correlation between soil factors and dominant bacterial phyla. The bioinformatics analysis uses the Vsearch (version 2.4.2) software to classify the high-quality sequence valid tags obtained from quality control according to 97% similarity to out and selected the most abundant sequence in

10.3389/fpls.2023.1124139

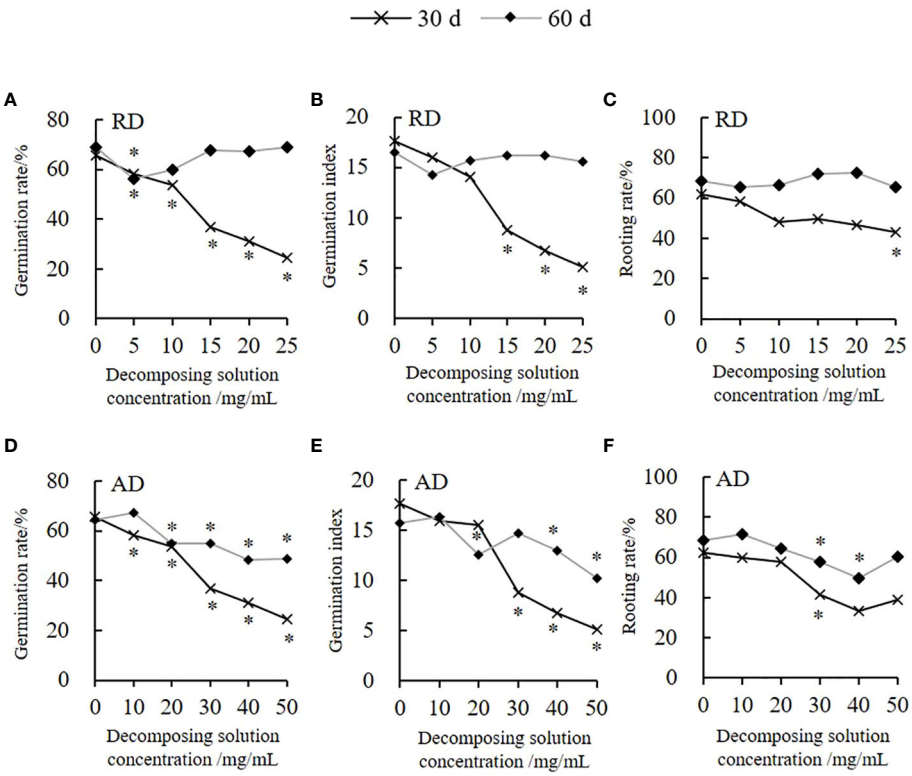

FIGURE 1
Variation trend of the highland barley seed germination and rooting under *E. densa* decomposing solution treatment. The decomposing part is marked on the upper right side of the Y-axis. "*" indicates the significant difference at the level of 0.05 between different concentrations of decomposing solution. "*" for 30 d and 60 d are marked below and above the broken line, respectively. **(A, D)** *GR*, **(B, E)** *GI*, **(C, F)** *RR*.

each OTU as the representative OUT sequence. The Chao1 index (S) size estimates the total number of soil bacterial species. Data in the chart are mean ± standard deviation (SD).

3 Results

3.1 Allelopathic potential of decomposing solution of *E. densa*

The decomposing solution of *Elsholtzia densa* Benth. (*E. densa*) has a specific allelopathic inhibitory effect on the germination of the highland barley seeds (Figure 1). Among them, the decomposing solution for 30 days (d) presents the greatest inductive effect. The germination rate (*GR*) and germination index (*GI*) decrease as the decomposing concentration increases; both are lower than the control. Moreover, the decomposing solution has a delayed germination effect. With the prolongation of the decomposing time, the effect of the decomposing solution of *E. densa* on the germination of highland barley seeds weakens. Under the action of 25 mg/mL root decomposing solution (RD) for 30 d, the *GR* of the highland barley is the lowest. Except for 5 mg/mL, there are no significant differences in *GR* and *GI* between RD for 60 d of other treatments and the control ($P > 0.05$) (Figures 1A, B). According to the integrated allelopathic sensitivity index (*SI*), the decomposing solution with the shortest decomposing time has the strongest effect of the decomposing solution. The allelopathic effect of RD and the above-ground decomposing solution (AD) for 30 d is 2.56 times and 2.09 times the decomposing solution of the decomposed 60 d, and the *SI* of AD is 2.06 times the RD. The effect of the decomposing solution of *E. densa* on the rooting of highland barley has a time effect (Figure 1). The decomposing solution for 30 d has the greatest effect on the rooting of highland barley, and the rooting rate (*RR*) gradually decreases as the decomposing solution's concentration increases. Under the action of 25 mg/mL RD and 50 mg/mL AD for 30 d, the *RR* of the highland barley is 69.13% and 62.42% of the control group, respectively. There is no significant effect on the *RR* of the highland barley, while the AD presents an increasing-declining-increasing trend as the concentration increases. Furthermore, we find that as the decomposition time prolongs, the inhibitory effect of the decomposing solution on the rooting of the highland barley seeds weakens or even turns into a promoting effect. The allelopathic effects of the RD and AD for 30 d are 4.75 and 1.97 times the decomposing solution for 60 d, respectively, and the *SI* of the AD is 1.52 times that of the RD.

Figure 2 illustrates the effect of the decomposing solution of *E. densa* on the growth of highland barley seedlings. RD has no significant effect on the plant height and root length of the highland barley seedlings ($P > 0.05$). Under the AD action, the highland barley plant height increases in a time-dependent and concentration-dependent manner, while the root length shows a concentration-dependent decrease. In the 50 mg/mL treatment

10.3389/fpls.2023.1124139

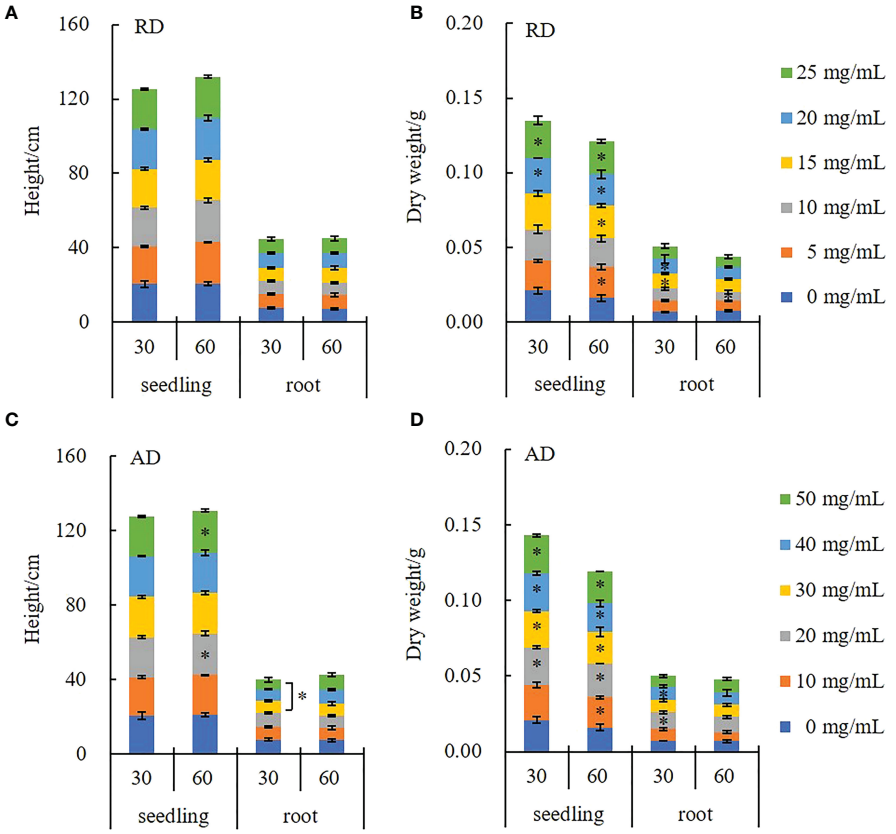

FIGURE 2
Changes in the growth indexes of highland barley seedlings under the action of *E. densa* decomposing solution. "*" indicates the significant difference at the level of 0.05 between different concentrations of decomposing solution. **(A, C)** height, **(B, D)** dry weight.

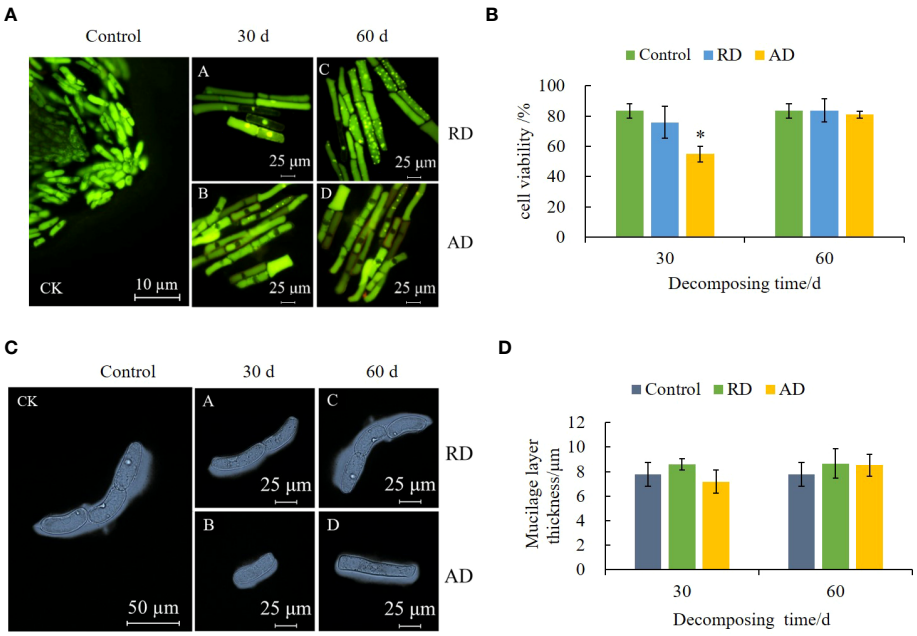

FIGURE 3
Effects of *E. densa* decomposing solution on cell activity and mucilage layer thickness of RBCs of highland barley. "*" indicates a significant difference at the 0.05 level. **(A)** the fluorescence micrograph under the action of the decomposing solution, green represents living cells, and orange-red represents cells that show the characteristics of cell death. **(B)** the activity of RBCs. **(C)** the micrograph of the RBCs and their mucilage layer of highland barley under the action of the decomposing solution. **(D)** the variation trend of the thickness of the mucilage layer of RBCs.

group, the plant height of the decomposing solution for 30 d and 60 d increased by 3.88% and 8.73%, respectively. However, the root length of the 50 mg/mL AD treatment is only 67.87% of that of the control (Figure 2C). The effect of the decomposing solution on dry weight has a promoting effect with a time-concentration dual effect. Among them, the highland barley seedlings treated with 50 mg/mL AD for 60 d are dried, with the weight being 1.3 times the control group (Figure 2D).

The above study demonstrates that the negative effects of the decomposing process of the stumps of *E. densa* on highland barley are mainly manifested in the effects on seed germination and root growth.

3.2 Changes in the characteristics of RBCs of highland barley under the action of a decomposing solution of *E. densa*

After AO/EB staining, the root border cells (RBCs) in the control group showed green fluorescence, with a clear cell outline, evident nuclear structure, and bright green fluorescence spots. After treatment with the decomposing solution, the cells' nuclei are pyknotic, present some apoptosis (Figure 3A), and the overall cell viability decreases (Figure 3B). The cytotoxicity of the short-term decomposing solution is higher. Compared with the control, the cell viability treated by AD for 30 d decreased by 28.56%. At the same time, the decomposing solution treatment induced the thickening of the mucilage layer of the RBCs (Figure 3C), but there was no significant difference from the control ($P > 0.05$) (Figure 3D).

3.3 Effects of the decomposing process of *E. densa* on soil properties and bacterial community

The *E. densa* decomposition significantly increases the soil's pH ($P < 0.05$), with the 0.08 g/g treatment group presenting the largest pH increase after 20 d of decomposition. Over time, the growth amplitudes decrease, but all are higher than the pH of the control group (Figure 4A).

In addition to having a minor effect on the soil organic matter (SOM) and total potassium (TK) content ($P > 0.05$) (Figures 4B, E), other nutrients are changed to varying degrees during the decomposing process of *E. densa*. Compared with the control, the soiltotal phosphorus (TP) (Figure 4C) and available phosphorus (AP) (Figure 4D) contents increase, and the changes are the largest

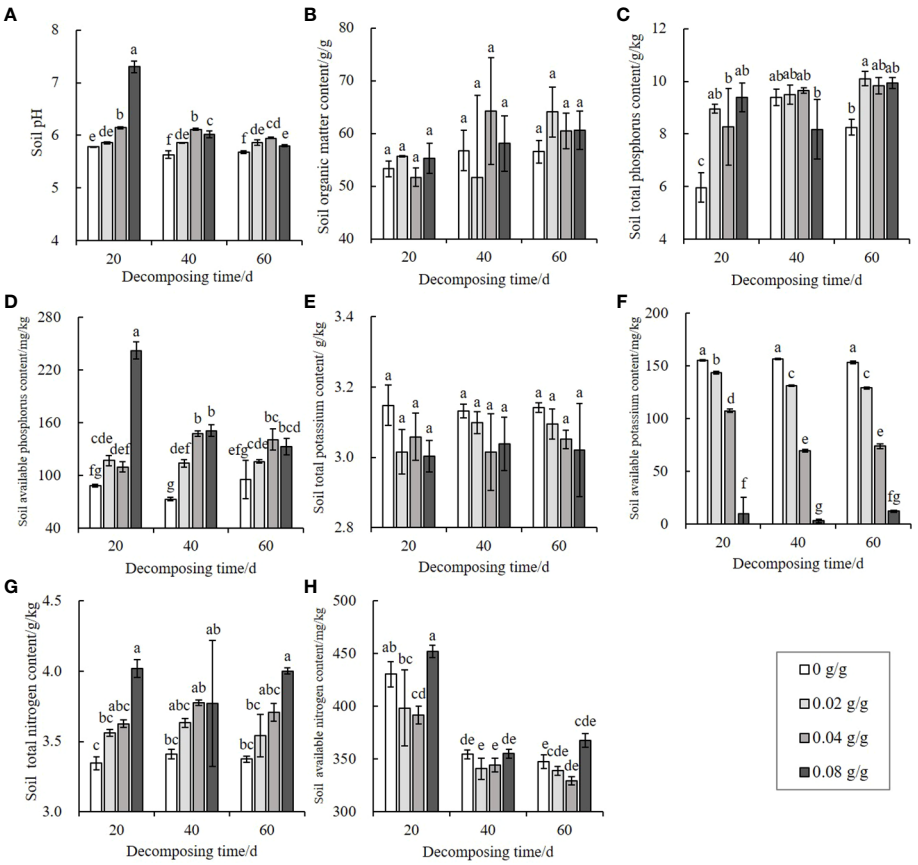

FIGURE 4
Effects of decomposing *E. densa* on soil pH and nutrients. The color in the column from light to dark indicates that the content of residues of *E. densa* increases. Different decomposition days or concentrations are treated as separate groups. Different lowercase letters indicate the difference significant at the 0.05% level, the same below. **(A)** soil pH, **(B–H)** the content of SOM, TP, AP, TK, AK, TN, and AN on the soil.

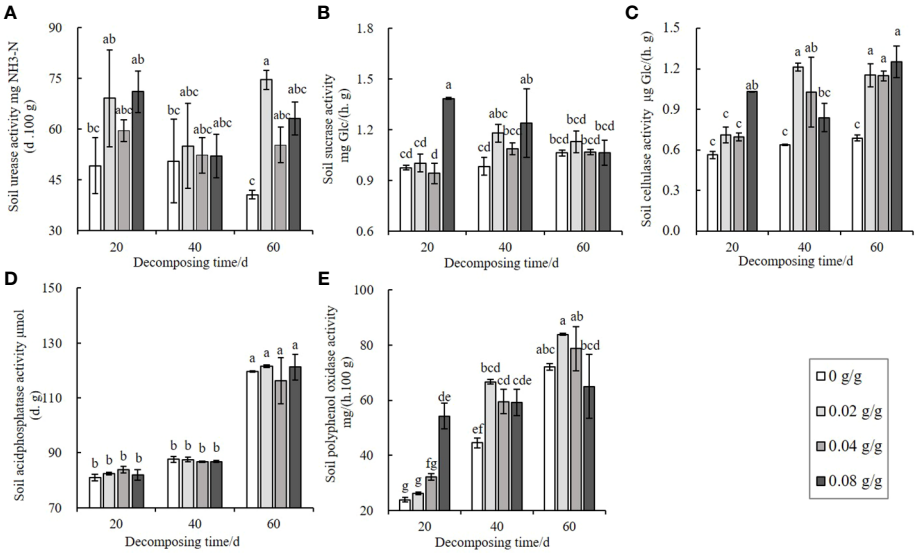

FIGURE 5
Effects of decomposing of *E. densa* on soil enzyme activities. **(A–E)** the activities of soil urease, soil invertase, soil cellulase, soil acid phosphatase, and soil polyphenol oxidase. Different lowercase letters indicate the difference significant at the 0.05 level.

when decomposing for 20 d. The difference from the control decreases as the decay time increases but is still higher than the control. The available potassium (AK) content of the treatment group is lower than the control and dose-dependent. The AK content of the 0.08 g/g treatment for 40 d is only 1.92% of the control (Figure 4F). The soil total nitrogen (TN) content increases significantly with the increase of the treatment dose ($P < 0.05$), and the maximum treatment dose (0.08 g/g) of decomposing for 20 d has the highest soil TN content, 1.20 times the control (Figure 4G). The soil available nitrogen (AN) content first decreases and then increases with the increase of the treatment dose, and decreases with the prolongation of the decomposing time (Figure 4H).

The decomposing process of *E. densa* increases the activity of extracellular enzymes in soil. The urease activity shows an increasing-decreasing trend with the increase of the treatment dose and reaches a peak at 0.02 g/g (Figure 5A). The decomposition time has a minor effect on the urease activity. The changes in sucrase, cellulase, and polyphenol oxidase activities are the same, showing an increasing-decreasing trend with the increase of the treatment dose at 40 d and 60 d, and the activities of the three soil extracellular enzymes increase in a dose-dependent manner at 20 d of decomposing. The activities of sucrase (Figure 5B) and polyphenol oxidase (Figure 5E) increase the most in the 0.08 g/g treatment group at 20 d. In comparison, the cellulase increases the most at 0.02 g/g at 40 d (Figure 5C). The acid phosphatase activity of the 60 d treatment group is significantly higher than the decomposing 20 d and 40 d treatment groups. However, there is no significant difference with the control (Figure 5D), indicating that the changes in soil acid phosphatase activity are irrelevant to the decomposition of *E. densa*.

The α-diversity index of soil bacteria increases with the prolongation of the decomposing time of *E. densa* (Table 1). In different decomposing times, the PD value shows an increasing-decreasing trend with the increase of the residue content of *E. densa* in the soil. Except for the 0.08 g/g treatment decomposed for 20 d, the PD values of the other treatments are higher than the control. The number of observed species shows a decreasing-increasing trend with the prolongation of decomposing time. Among them, the 0.08 g/g treatment group at 20 d has the lowest observed species (1727) and reaches the highest (2485) at 60 d. Shannon-Weiner index and Chao 1 index of the 0.08 g/g treatment at 20 d are lower than the control group. In contrast, the other treatments are higher than the control, indicating that the decomposing process of *E. densa* increases the level of bacterial community diversity. Except that the 20 d decomposing treatment group has a more significant difference within the group, the β-diversity of soil bacteria in the 40 d and 60 d is similar (Figure 6).

A total of 30 bacterial phyla are detected in the decomposed soil of *E. densa*. During the decomposing process of *E. densa*, the six phyla Proteobacteria, Actinobacteria, Bacteroidetes, Firmicutes, Gemmatimonadetes, and Acidobacteria accounted for the highest proportion (Figure 7). The relative abundances of Proteobacteria, Bacteroidetes, Acidobacteria, and Gemmatimonadetes in the decomposed soil increase significantly with the prolongation of the decomposing time. In contrast, the relative abundances of Actinobacteria and Firmicutes decrease significantly. At 20 d and 40 d of decomposition, the relative abundance of Proteobacteria shows a decreasing-increasing trend with the increase of residue content in the soil, while at 60 d of decomposition, it increases first and then decreases with the increase of residue content of *E. densa*, but still higher than the control. With the increased residue content of *E. densa*, the relative abundance of Bacteroidetes increased-decreased. The relative abundance of Firmicutes decreased, and the relative abundance of Acidobacteriaincreased. The relative abundance of Bacteroidetes and Gemmatimonadetes increased with the prolongation of decomposing time.

10.3389/fpls.2023.1124139

TABLE 1 Bacterial α-diversity analysis in the decomposed soil of *E. densa*.

Time /d	Residue content g/g	Phylogenetic diversity	Chao 1 index	Observed species	Shannon-Weiner index
20	0	88.54 ± 4.26^{ab}	3069.75 ± 132.91^{ab}	2369.27 ± 120.39^{ab}	9.31 ± 0.17^{ab}
20	0.02	90.29 ± 3.6^{a}	3031.77 ± 219.18^{ab}	2385.2 ± 123.18^{ab}	9.44 ± 0.08^{a}
20	0.04	90.63 ± 3.27^{ab}	3210.79 ± 48.66^{ab}	2441.8 ± 62.02^{ab}	9.51 ± 0.14^{ab}
20	0.08	67.57 ± 0.55^{b}	2604.23 ± 22.75^{b}	1727 ± 31.42^{b}	7.87 ± 0.08^{b}
40	0	84.45 ± 1.7^{ab}	2996.29 ± 122.86^{ab}	2262.67 ± 7.74^{ab}	9.05 ± 0.07^{ab}
40	0.02	85.89 ± 3.87^{ab}	3144.62 ± 81.79^{ab}	2293.6 ± 117.67^{ab}	9.09 ± 0.27^{ab}
40	0.04	88.36 ± 0.99^{ab}	3309.81 ± 121.09^{a}	2404 ± 60.85^{ab}	9.43 ± 0.11^{ab}
40	0.08	86.47 ± 3.02^{ab}	3164.17 ± 110.98^{ab}	2344.77 ± 75.83^{ab}	9.38 ± 0.08^{a}
60	0	88.98 ± 0.78^{ab}	2965.78 ± 21.75^{ab}	2395.77 ± 7.62^{ab}	9.62 ± 0.07^{a}
60	0.02	91.76 ± 2.15^{a}	3212.95 ± 10.65^{a}	2479.3 ± 47.52^{a}	9.54 ± 0.16^{a}
60	0.04	92.53 ± 1.46^{ab}	3230.53 ± 18.3^{a}	2485.95 ± 30.33^{ab}	9.53 ± 0.11^{ab}
60	0.08	86.34 ± 1^{ab}	3189.56 ± 29.53^{a}	2349.4 ± 24.8^{ab}	9.42 ± 0.04^{ab}

Residue content is the content of E. densa residue per gram of soil. 3 replicates per sample. Different lowercase letters indicate the difference significant at the 0.05 level.

The RDA redundancy analysis (Figure 8) highlights that the soil chemical properties during the decomposing process of *E. densa* explain 51.56% of the bacterial community variability, and the two ranking axes explain 75.12% of the variability. Bacteroidetes and Proteobacteria are significantly positively correlated with urease, cellulase, sucrase, TN, AN, AP, and pH. Bacteroidetes and Proteobacteria were negatively correlated with acid phosphatase, AK, and TK. The Actinobacteria are positively correlated with acid phosphatase, polyphenol oxidase, AK, TK, and SOM, while significantly negatively correlated with urease, cellulase, sucrase, TN, AN, AP, and pH. The Firmicutes have a significant positive correlation with AK and TK and a negative correlation with other environmental factors.

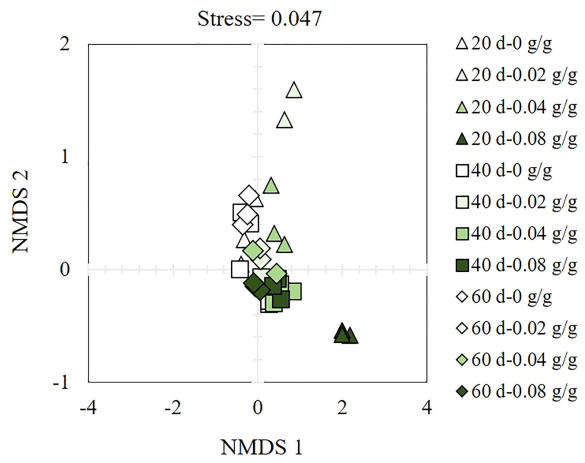

FIGURE 6
Bacterial β-diversity analysis in the decomposed soil of *E. densa*. The legend reads, "Decomposition time- the content of residues of *E. densa*", "△" indicates the 20 d treatment group, "□" is the 40 d treatment group, and "◇" is the 60 d treatment group. The green in the graph from light to dark indicates that the content of residues of *E. densa* increases.

4 Discussion

4.1 The decomposition of *E. densa* has a strong allelopathic effect on the growth of highland barley

In ecosystems, the organization and dynamics of plant communities are controlled by biological processes such as resource competition, promotion, and allelopathy (Zeng, 2008). The active allelochemicals are contained in the organs of many higher plants and play an essential role in plant interactions. During the decomposition of plant residues, allelochemicals are passively released to affect the growth of surrounding plants (Sarheed et al., 2020). Allelochemicals adversely affect the seed germination and growth of neighboring plants by affecting some physiological processes in plants, such as cell division, photosynthesis, respiration, enzyme activity, and cell membrane permeability (Thiébaut et al., 2018; Mushtaq et al., 2019).It can even affect plant community structure and cause the evolution of the ecosystem (Badalamenti et al., 2016). The decomposing solution of the poisonous weed on the QTP, *Steura chamaejasme*, had allelopathic effects on the plant height and biomass of *Onobrychis viciifolia* seedlings. The allelopathy of RD was greater than that of AD. Besides, it also affected the leaf area, leaf cell conductivity, and chlorophyll content of the recipient plants (Zhou et al., 2009). Seed germination is the most sensitive growth stage for plants to external stress (Huang et al., 2020). Our study highlights that decomposing the stubble of the poisonous weed *E. densa* has an apparent inhibitory effect on the seed germination and young root growth of highland barley and exhibits concentration-dependent and

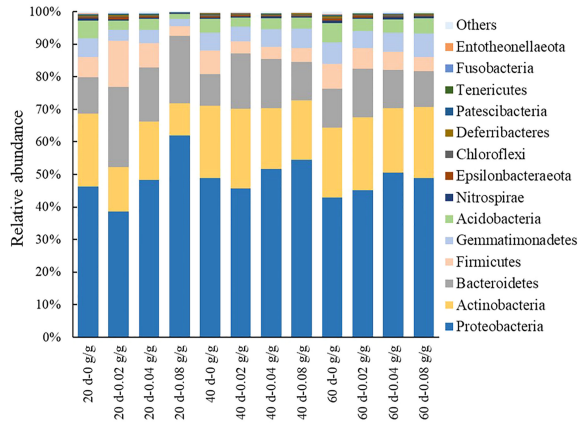

FIGURE 7
Relative abundance of bacteria at the phyla taxonomic level in the decomposed soil of *E. densa*.

delayed effects. Different from *Steura chamaejasme*, the allelopathic inhibitory effect of AD was greater than that of RD made by *E. densa*' stubble. However, this negative effect is mainly reflected in the early decomposition stage, as in the late decomposition stage, the decomposing solution of *E. densa* has a significant promoting effect on the biomass accumulation of highland barley, manifested in the increase of dry weight, especially the dry weight of roots. It should be noted that the allelopathy of *Allium senescens*, a companion species of grassland, was treated with the water extract of *Steura chamaejasme*, the allelopathy of the water extract of *Steura chamaejasme* root was smaller than that of stem and leaf (Liu et al., 2022). Combined with the results of this study, it can be found that the strength and direction of allelopathy are not only related to the site of decomposition and the type of the recipient plant but also related to the stage of decomposition.

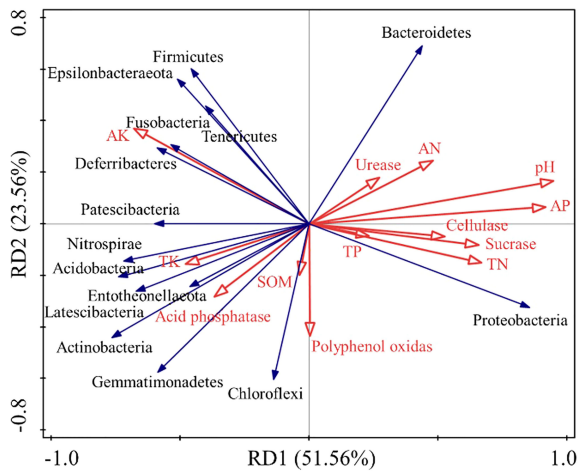

FIGURE 8
Correlation redundancy analysis between soil bacterial diversity and chemical properties during the decomposing process of *E. densa*. The red arrows represent different environmental factors, and the blue arrows represent different bacteria.

4.2 The decomposition of *E. densa* interferes with the defense function of highland barley RBCs

RBCs and their secretions form a protective structure, the root extracellular trap (RET), the first line of defense for plants to defend against microorganisms, heavy metals, and other harmful substances invading the root system (Ropitaux et al., 2020). When plants are under allelopathic stress, their RBCs rapidly increase the thickness of the mucilage layer to resist harmful allelochemicals (Ma et al., 2020). To a certain extent, changes in the thickness of the mucilage layer can represent the intensity of external stress. Our study shows that under the action of the decomposed substance of *E. densa*, the activity at the RBCs of the highland barley is reduced, the characteristics of apoptosis are observed, and the thickened mucilage layer is removed. These effects are similar to the decomposing solution effects on seed germination and root length. The shorter the decomposing time, the stronger the cytotoxicity of the decomposing solution. The cytotoxicity of the decomposing solution in the later stage of decomposing weakens or even disappears, and the cytotoxicity of AD is greater than RD. Combined with the experimental phenomenon that root growth is inhibited, it can be speculated that the decomposed substance of *E. densa* interfered with the defense function of RBCs, broke through the biological defense line, and affected the division and elongation activities of root tip cells to block root growth.

4.3 The decomposition of *E. densa* changed the soil living environment

E. densa is an annual aromatic herb, and the stems and leaves, especially the leaves, contain many volatile substances (Chauhan et al., 2018). The main chemical components in the volatile oil of *E. densa* are α-bisabolol, elements, β-selinene, thymol, and carvacrol, which have antiviral and antibacterial effects (Zhou et al., 2019). Presently, the most reported allelochemical in nature is phenolic compounds, terpenoids, and compounds containing nitrogen atoms (benzoxazines). Under natural conditions, allelopathy is not the effect of a single component but the result of the synergistic action of various allelochemicals (Scavo and Mauromicale, 2021). Allelochemicals produced by the decomposition of plant residues will be chemically transformed into polymers or degraded into small molecules under natural conditions and then lose their allelopathic activity, which is generally considered the self-detoxification function of soil (Rawat et al., 2019). This function is closely related to environmental factors such as soil colloid buffer, soil nutrient content, and soil microflora (Li et al., 2015; El-Darier et al., 2018). Therefore, the main effector allelochemicals of *E.densa* may be released in the early stage of decay but gradually aggregated or decomposed by microorganisms in soil with the prolongation of decay time. The allelopathic effect of *E. densa* residues during decomposition is brief, mainly occurring in the early stage of decomposition. In the later stage of decomposition, with the allelopathic effect of *E. densa* allelochemical weakened, the nutrient

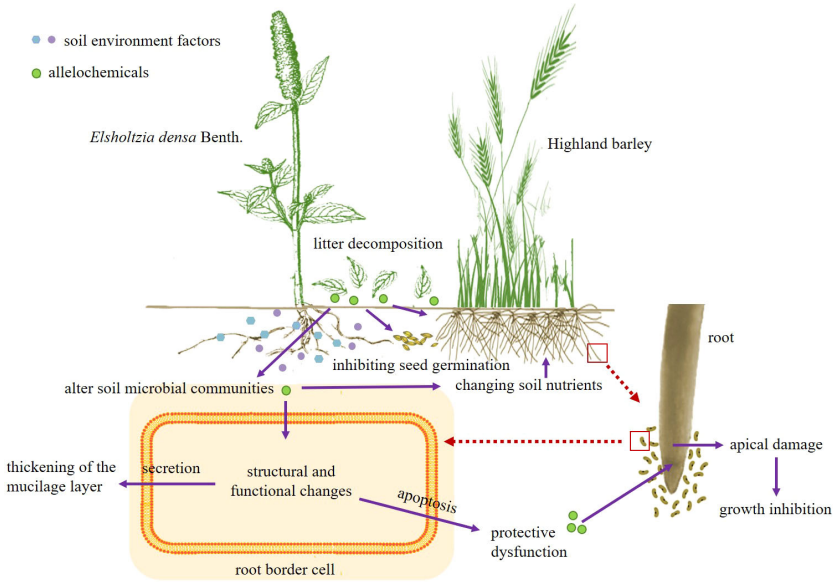

FIGURE 9
Competitive strategies of *E. densa*.

elements in the residues were decomposed and released continuously, which promoted the growth of highland barley, such as promoting rooting and increasing dry weight. In the next step, it is necessary to analyze further and verify the main effecting allelochemicals and detect the content changes of the main effecting allelochemical in different decomposition stages for further exploration.

The interaction of plants-microorganisms-soil is the key to realizing plant community exchanges, changing biological diversity, and ecosystem functions (Mueller et al., 2020). As the core driving force of nutrient cycling and energy transformation (Shao et al., 2019), soil microbial communities are extremely sensitive to changes in the external environment, and their quantity and structural composition are affected by the soil environment and the dominant plant groups in the habitat (Yang et al., 2021). Most soil bacteria do not thrive in acidic environments (Li et al., 2022). However, the decomposition of *E. densa* residues increased soil pH, which effectively improved the living environment of soil bacteria and increased the α- diversity of the bacterial community. Meanwhile, the decomposition of *E. densa* stubble changed the bacterial community structure. The β-diversity analysis shows that the bacterial community changes the most in the early 20 d of decomposing, and there is little difference in other decomposing periods. These results are consistent with the results that the decomposition of *E. densa* can inhibit highland barley, mainly in the early stage of decomposition.

Soil properties and pH are stubble factors in determining the distribution of poisonous plants (Li et al., 2014). Actinobacteria were always in a dominant position in the decomposing process of *E. densa*. It can accelerate the decomposition of animal (Araujo et al., 2020) and plant residues in the soil and increase the TN content in the soil with Bacteroidetes (Krishna et al., 2020). In addition, Bacteroidetes also have a phosphorus enrichment effect (Hou et al., 2021), which synergized with Actinobacteria with a phosphorus-dissolving effect (Omotayo et al., 2021) to increase the content of AP in soil. Proteobacteria with increasing relative abundance during decomposition have nitrogen fixation and can adapt to various complex environments (Hou et al., 2019). The larger the proportion of Proteobacteria and Bacteroidetes in soil, the higher the soil fertility (Lu et al., 2020). In the late stage of decomposition, soil pH decreases, and the relative abundance of oligotrophic bacteria, Acidobacteria, which are suitable for growth in an acidic environment, increase and participate in the decomposition of organic matter and the balance of the micro-ecological environment (Wu et al., 2021). The relative abundance of Firmicutes continues to decrease, indicating that the carbon utilization rate continues to decline in the later decomposition stage (Uksa et al., 2017). This corresponds to an increase in the relative abundance of Acidobacteria. Acidobacteria plays an important role in the degradation of plant residues and cellulose (Wang et al., 2016). Acidobacteria and Gemmatimonadetes are more advantageous in an environment with lower water content (Gao et al., 2019). Under the influence of such a complex and constantly changing bacterial influence network, there is no significant change in SOM.

Many hypotheses are used to explain the high competitiveness of invasive plants, such as the rapid growth and reproduction (Ni et al., 2018), high allelopathy, strong adaptability to the heterogeneous environment, and resource assimilation capacity (Gruntman et al., 2013; Wang et al., 2017). Studies have shown that the dominant population of poisonous weeds on the QTP is caused not only by directly suppressing and crowding out other plants through allelopathy but also by changing soil physical and chemical properties and soil microbial community composition by releasing allelochemical (He et al., 2015). Furthermore, the poisonous weed *E. densa* may have a similar ability. Soil enzymes are mainly derived from soil microbial activities, plant root

exudates, and enzymes released during the decomposition of animal and plant residues, which play an essential role in soil material cycling and energy transformation (Wu et al., 2020). In our study, hydrolase activities such as urease, sucrase, cellulase, and acid phosphatase which are closely related to soil nitrogen, carbon, and phosphorus cycling (Wang et al., 2020) and redox-related polyphenol oxidase activities (Chen et al., 2020), are increased, indicating that the decomposition of the stubble of *E. densa* can release related enzymes to promote the synthesis of humus components in the soil and the flow and circulation of nutrient elements. We also observe no significant change in TK content but a significant decrease in the AK content. This may be related to the great demand for quick-acting potassium in the decomposition of *E. densa*. According to the resource allocation theory, soil microorganisms may also invest in abundant elements to produce extracellular enzymes to exploit relatively limited elements (Zhou et al., 2020).

Decomposition of *E. densa* stumps stimulates soil microbial activities by changing soil properties and extracellular enzyme activities. It jointly promotes the conversion of soil macromolecules into small molecules and eventually leads to a significant increase in soil phosphorus and nitrogen content. Our hypothesis is further confirmed in the correlation redundancy analysis between soil bacterial diversity and chemical properties. Thus, *E. densa*, which can expand despite land degradation on the QTP, may have adopted similar competitive strategies as invasive plants: takes advantage of the strong allelopathy and resource assimilation ability to transform the surrounding environment to expand its competitive advantage constantly.

5 Conclusions

Our study found that the decomposing solution of *E. densa* had allelopathic effects on the germination and seedling growth of highland barley and interfered with the defense function of the RBCs of highland barley. This effect was related to the time and part of decomposition. The soil environment changed in the decomposition process of *E. densa*. In the early stage of decomposition, soil bacteria varied greatly under different concentrations of *E. densa* residues. In addition, the decomposition process of *E. densa* increased the soil nutrient content, extracellular enzyme activities, and bacterial community diversity. The results showed that the decomposition of *E. densa* residues could stimulate soil microbial activity and promote the flow and circulation of nutrient elements by changing soil properties and extracellular enzyme activities. Therefore, we believe that the competitive strategies adopted by *E. densa* in the farmland ecosystem on the QTP are as follows (Figure 9): 1. The release of allelochemicals interferes with the defense function of surrounding plants and directly inhibits the growth and development of surrounding plants. 2. By changing the physical and chemical properties of soil and extracellular enzyme activity, residual plant decomposition can stimulate soil microbial activity, improve soil nutrition status, and create a more suitable soil environment for growth.

Data availability statement

The data presented in the study are deposited in the NCBI repository, accession number PRJNA914485.

Author contributions

All authors contributed to the article and approved the submitted version. XZ and YXX: Experiments, analysis and interpretation of data, writing and reviseing the manuscript. DM: Analysis and interpretation of data, writing and reviseing the manuscript. YSX: Experiments, analysis and interpretation of data. YW: analysis and interpretation of data. HZ: Experiments. YNW: analysis and interpretation of data.

Funding

This research was funded by Technology department of Sichuan Province (Project No.2020YJ0335) and The fourth national survey of traditional Chinese medicine resources (Project No.2019PC006) and fundamentally applied research project in Science.

Acknowledgments

The authors would like to express their gratitude to EditSprings (https://www.editsprings.cn) for the expert linguistic services provided. In addition, parts of this article were previously published in prepreprint.

Conflict of interest

The authors declare that the research was conducted in the absence of any commercial or financial relationships that could be construed as a potential conflict of interest.

Publisher's note

References

Araujo, R., Gupta, V. V. S. R., Reith, F., Bissett, A., Mele, P., and Franco, C. M. M. (2020). Biogeography and emerging significance of actinobacteria in Australia and northern Antarctica soils. *Soil Biol. Biochem.* 146, 107805. doi: 10.1016/j.soilbio.2020.107805

Badalamenti, E., Gristina, L., Laudicina, V. A., Novara, A. L., Pasta, S., and Mantia, L. T. (2016). The impact of *carpobrotus cfr. acinaciformis* (L.) L. bolus on soil nutrients, microbial communities structure and native plant communities in mediterranean ecosystems. *Plant Soil* 409, 19–34. doi: 10.1007/s11104-016-2924-z

Carreras, A., Bernard, S., Durambur, G., Gügi, B., Loutelier, C., Pawlak, B., et al. (2020). In vitro characterization of root extracellular trap and exudates of three sahelian woody plant species. *Planta* 251, 19. doi: 10.1007/s00425-019-03302-3

Chauhan, A., Venkatesha, K. T., Padalia, R. C., Singh, V. R., Verma, R. S., and Chanotiya, C. S. (2018). Essential oil composition of leaves and inflorescences of *Elsholtzia densa* benth. from western himalaya. *J. Essential Oil Res.* 31, 217–222. doi: 10.1080/10412905.2018.1545706

Chen, X., Zhang, Q., Zeng, S. M., Chen, Y., and Huang, X. J. (2020). Rhizosphere soil affects pear fruit quality under rain-shelter cultivation. *Can. J. Plant Sci.* 100, 683–691. doi: 10.1139/CJPS-2018-0249

Dong, S., Shang, Z., Gao, J., and Boone, R. B. (2020). Enhancing sustainability of grassland ecosystems through ecological restoration and grazing management in an era of climate change on Qinghai-Tibetan plateau. *Agriculture Ecosyst. Environ.* 287, 106684. doi: 10.1016/j.agee.2019.106684

Duan, Z., Quan, X., Qiao, Y., Li, X., Pei, H., and He, G. (2019). Distribution characteristics and implication of *n*-alkanes in soils and plants in alpine meadow. *Russian J. Ecol.* 50, 20–26. doi: 10.1134/s1067413619010120

El-Darier, S. M., Abdelaziz, H. A., and Zein El-Dien, M. H. (2018). Effect of soil type on the allelotoxic activity of *Medicago sativa* L. residues in *Vicia faba* L. agroecosystems. *J. Taibah Univ. Sci.* 8, 84–89. doi: 10.1016/j.jtusci.2014.01.001

Gao, J., Luo, Y., Wei, Y., Huang, Y., Zhang, H., He, W., et al. (2019). Effect of aridity and dune type on rhizosphere soil bacterial communities of *Caragana microphylla* in desert regions of northern China. *PloS One* 14, e0224195. doi: 10.1371/journal.pone.0224195

Geissler, K., Fiedler, S., Ni, J., Herzschuh, U., and Jeltsch, F. (2019). Combined effects of grazing and climate warming drive shrub dominance on the Tibetan plateau. *Rangeland J.* 41, 425–439. doi: 10.1071/rj19027

Geng, Y., Baumann, F., Song, C., Zhang, M., Shi, Y., Kühn, P., et al. (2017). Increasing temperature reduces the coupling between available nitrogen and phosphorus in soils of Chinese grasslands. *Sci. Rep.* 7, 43524. doi: 10.1038/srep43524

Gruntman, M., Pehl, A. K., Joshi, S., and Tielbörger, K. (2013). Competitive dominance of the invasive plant *Impatiens glandulifera*: using competitive effect and response with a vigorous neighbour. *Biol. Invasions* 16, 141–151. doi: 10.1007/s10530-013-0509-9

He, W., Guo, L., Fan, P., Guo, B., Fu, Y., and Wei, Y. (2015). Allelopathly and the rhizospere bacterial community structure of *Oxytropis ochrocephala*. *Acta Pedologica Sin.* 24, 21–29. doi: 10.11686/cyxb2014504

Hickman, D. T., Rasmussen, A., Ritz, K., Birkett, M. A., and Neve, P. (2021). Review: allelochemicals as multi-kingdom plant defence compounds: towards an integrated approach. *Pest Manage. Sci.* 77, 1121–1131. doi: 10.1002/ps.6076

Hou, X., Han, H., Tigabu, M., Cai, L., Meng, F., Liu, A., et al. (2019). Changes in soil physico-chemical properties following vegetation restoration mediate bacterial community composition and diversity in Changting, China. *Ecol. Eng.* 138, 171–179. doi: 10.1016/j.ecoleng.2019.07.031

Hou, J., Xu, X., Yu, H., Xi, B., and Tan, W. (2021). Comparing the long-term responses of soil microbial structures and diversities to polyethylene microplastics in different aggregate fractions. *Environ. Int.* 149, 106398. doi: 10.1016/j.envint.2021.106398

Huang, W., Reddy, G. V. P., Shi, P., Huang, J., Hu, H., and Hu, T. (2020). Allelopathic effects of *Cinnamomum septentrionale* leaf litter on *Eucalyptus grandis* saplings. *Global Ecol. Conserv.* 21, e00872. doi: 10.1016/j.gecco.2019.e00872

Kalisz, S., Kivlin, S. N., and Bialic-Murphy, L. (2020). Allelopathy is pervasive in invasive plants. *Biol. Invasions* 23, 367–371. doi: 10.1007/s10530-020-02383-6

Krishna, M., Gupta, S., Delgado-Baquerizo, M., Morriën, E., Garkoti, S. C., Chaturvedi, R., et al. (2020). Successional trajectory of bacterial communities in soil are shaped by plant-driven changes during secondary succession. *Sci. Rep.* 10, 9864. doi: 10.1038/s41598-020-66638-x

Li, Y., Dong, S., Liu, S., Wang, X., Wen, L., and Wu, Y. (2014). The interaction between poisonous plants and soil quality in response to grassland degradation in the alpine region of the Qinghai-Tibetan plateau. *Plant Ecol.* 215, 809–819. doi: 10.1007/s11258-014-0333-z

Li, Y., Feng, Y., Chen, Y., and Tian, Y. (2015). Soil microbes alleviate allelopathy of invasive plants. *Sci. Bull.* 60, 1083–1091. doi: 10.1007/s11434-015-0819-7

Li, Z., Lhundrup, N., Guo, G., Dol, K., Chen, P., Gao, L., et al. (2020). Characterization of genetic diversity and genome-wide association mapping of three agronomic traits in Qingke barley (*Hordeum vulgare* l.) in the Qinghai-Tibet plateau. *Front. Genet.* 11. doi: 10.3389/fgene.2020.00638

Li, H., Wang, H., Jia, B., Li, D., Fang, Q., and Li, R. (2021). Irrigation has a higher impact on soil bacterial abundance, diversity and composition than nitrogen fertilization. *Sci. Rep.* 11, 16901. doi: 10.1038/s41598-021-96234-6

Li, S., Xie, D., Ge, X., Dong, W., and Luan, J. (2022). Altered diversity and functioning of soil and root-associated microbiomes by an invasive native plant. *Plant Soil* 473, 235–249. doi: 10.1007/s11104-022-05338-z

Liu, G., Liu, L., Guo, J., Su, H., Lan, Q., and Liu, G. (2022). The allelopathic effect of aqueous extracts of *Stellera chamejasme* on seed germination and seedling growth of *Allium senescens*. *Acta Agrestia Sin.* 30, 2391–2398. doi: 10.11733/j.issn.1007-0435.2022.09.019

Lu, Y., Zhao, Y., and Zhang, Y. (2020). Research on the distribution characteristics of soil bacteria communities under the influence of two main sand-fixing plants in minqin desert area of gansu province. *Ecol. Environ. Sci.* 29, 717–724. doi: 10.16258/j.cnki.1674-5906.2020.04.010

Ma, J., Feng, X., Yang, X., Cao, Y., Zhao, W., and Sun, L. (2020). The leaf extract of crofton weed (*Eupatorium adenophorum*) inhibits primary root growth by inducing cell death in maize root border cells. *Plant Diversity* 42, 174–180. doi: 10.1016/j.pld.2020.02.001

Mueller, L. O., Borstein, S. R., Tague, E. D., Dearth, S. P., Castro, H. F., Campagna, S. R., et al. (2020). Populations of *Populus angustifolia* have evolved distinct metabolic profiles that influence their surrounding soil. *Plant Soil* 448, 399–411. doi: 10.1007/s11104-019-04405-2

Mushtaq, W., Ain, Q., Siddiqui, M. B., and Hakeem, K. R. (2019). Cytotoxic allelochemicals induce ultrastructural modifications in *Cassia tora* L. and mitotic changes in *Allium cepa* L.: a weed versus weed allelopathy approach. *Protoplasma* 256, 857–871. doi: 10.1007/s00709-018-01343-1

Ni, M., Liu, Y., Chu, C., Xu, H., and Fang, S. (2018). Fast seedling root growth leads to competitive superiority of invasive plants. *Biol. Invasions* 20, 1821–1832. doi: 10.1007/s10530-018-1664-9

Nikolaeva, A. A., Golosova, E. V., and Shelepova, O. V. (2021). Allelopathic activity of *Acer negundo* L. leaf litter as a vector of invasion species into plant communities. *Bio Web Conferences* 38, 00088. doi: 10.1051/bioconf/20213800088

Omotayo, O. P., Igiehon, O. N., and Babalola, O. O. (2021). Metagenomic study of the community structure and functional potentials in maize rhizosphere microbiome: elucidation of mechanisms behind the improvement in plants under normal and stress conditions. *Sustainability* 13, 8079. doi: 10.3390/su13148079

Pan, Y., Zhang, H., Li, X., and Xie, Y. (2016). Effects of sedimentation on soil physical and chemical properties and vegetation characteristics in sand dunes at the southern Dongting lake region, China. *Sci. Rep.* 6, 36300. doi: 10.1038/srep36300

Peng, J., Liu, Z., Liu, Y., Wu, J., and Han, Y. (2012). Trend analysis of vegetation dynamics in Qinghai–Tibet plateau using hurst exponent. *Ecol. Indic.* 14, 28–39. doi: 10.1016/j.ecolind.2011.08.011

Peng, F., Xue, X., Li, C., Lai, C., Sun, J., Tsubo, M., et al. (2020). Plant community of alpine steppe shows stronger association with soil properties than alpine meadow alongside degradation. *Sci. Total Environ.* 733, 139048. doi: 10.1016/j.scitotenv.2020.139048

Qin, R., Wei, J., Ma, L., Zhang, Z., She, Y., Su, H., et al. (2022). Effects of *Pedicularis kansuensis* expansion on plant community characteristics and soil nutrients in an alpine grassland. *Plants (Basel)* 11, 1673. doi: 10.3390/plants11131673

Qu, T., Du, X., Peng, Y., Guo, W., Zhao, C., and Losapio, G. (2021). Invasive species allelopathy decreases plant growth and soil microbial activity. *PloS One* 16, e0246685. doi: 10.1371/journal.pone.0246685

Rawat, L. S., Maikhuri, R. K., Bahuguna, Y. M., Maletha, A., Phondani, P. C., Jha, N. K., et al. (2019). Interference of *Eupatorium adenophorum* (Spr.) and its allelopathic effect on growth and yield attributes of traditional food crops in Indian Himalayan region. *Ecol. Res.* 34, 587–599. doi: 10.1111/1440-1703.12042

Ropitaux, M., Bernard, S., Schapman, D., Follet-Gueye, M., Vicré, M., Boulogne, I., et al. (2020). Root border cells and mucilage secretions of soybean, *Glycine max* (Merr) L.: characterization and role in interactions with the oomycete *Phytophthora parasitica*. *Cells* 9, 2215. doi: 10.3390/cells9102215

Sarheed, M. M., Rajabi, F., Kunert, M., Boland, W., Wetters, S., Miadowitz, K., et al. (2020). Cellular base of mint allelopathy: menthone affects plant microtubules. *Front. Plant Sci.* 11, 546345. doi: 10.3389/fpls.2020.546345

Scavo, A., and Mauromicale, G. (2021). Crop allelopathy for sustainable weed management in agroecosystems: knowing the present with a view to the future. *Agronomy* 11, 2104. doi: 10.3390/agronomy11112104

Shang, Z., Dong, Q., Shi, J., Zhou, H., Dong, S., Shao, X., et al. (2018). Research progress in recent ten years of ecological restoration for 'Black soil land' degraded on Tibetan plateau-concurrently discuss of ecological restoration in sangjiangyuan region. *Acta Agrestia Sin.* 26, 1–21. doi: 10.11733/j.issn.1007-0435.2018.01.001

Shao, K., Bai, C, Cai, J., Hu, Y., Gong, Y., Chao, J., et al. (2019). Illumina sequencing revealed soil microbial communities in a Chinese alpine grassland. *Geomicrobiology J.* 36, 204–211. doi: 10.1080/01490451.2018.1534902

Singh, S. P., Mishra, A., Shyanti, R. K., Singh, R. P., and Acharya, A. (2021). Silver nanoparticles synthesized using *Carica papaya* leaf extract (AgNPs-PLE) causes cell

cycle arrest and apoptosis in human prostate (DU145) cancer cells. *Biol. Trace Element Res.* 199, 1316–1331. doi: 10.1007/s12011-020-02255-z

Sun, Y., Xu, J., Miao, X., Lin, X., Liu, W., and Ren, H. (2021). Effects of exogenous silicon on maize seed germination and seedling growth. *Sci. Rep.* 11, 1014. doi: 10.1038/s41598-020-79723-y

Thiébaut, G., Thouvenot, L., and Rodríguez-Pérez, H. (2018). Allelopathic effect of the invasive *Ludwigia hexapetala* on growth of three macrophyte species. *Front. Plant Sci.* 9, 01835. doi: 10.3389/fpls.2018.01835

Uksa, M., Buegger, F., Gschwendtner, S., Lueders, T., Kublik, S., Kautz, T., et al. (2017). Bacteria utilising plant-derived carbon in the rhizosphere of *Triticum aestivum* change in different depths of an arable soil: spatial distribution of rhizosphere bacteria. *Environ. Microbiol. Rep.* 9, 729–741. doi: 10.1111/1758-2229.12588

Wang, G., Liu, J., Yu, Z., Wang, X., Jin, J., and Liu, X. (2016). Research progress of *Acidobacteria* ecology in soils. *Biotechnol. Bull.* 32, 14–20. doi: 10.13560/j.cnki.biotech.bull.1985.2016.02.002

Wang, Y., Müller-Schärer, H., Van Kleunen, M., Cai, A., Zhang, P., Yan, R., et al. (2017). Invasive alien plants benefit more from clonal integration in heterogeneous environments than natives. *New Phytol.* 216, 1072–1078. doi: 10.1111/nph.14820

Wang, J., Wang, X., Liu, G., Zhang, C., and Wang, G. (2021). Bacterial richness is negatively related to potential soil multifunctionality in a degraded alpine meadow. *Ecol. Indic.* 121, 106996. doi: 10.1016/j.ecolind.2020.106996

Wang, N., Zhang, M., Zhao, N., Feng, F., and Zhao, M. (2020). Season-dependence of soil extracellular enzyme activities in a *Pinus koraiensis* forest on Changbai Mountain. *J. Forestry Res.* 32, 1713–1722. doi: 10.1007/s11676-020-01213-8

Whitehead, J., Wittemann, M., and Cronberg, N. (2018). Allelopathy in bryophytes - a review. *Lindbergia* 41, 01097. doi: 10.25227/linbg.01097

Williamson, G. B., and Richardson, D. (1988). Bioassays for allelopathy: Measuring treatment responses with independent controls. *J. Chem. ecology(USA)* 14, 181–187. doi: 10.1007/BF01022540

Wu, J., Wang, H., Li, G., Ma, W., Wu, J., Gong, Y., et al. (2020). Vegetation degradation impacts soil nutrients and enzyme activities in wet meadow on the Qinghai-Tibet plateau. *Scientifc Rep.* 10, 21271. doi: 10.1038/s41598-020-78182-9

Wu, X., Yang, J., Ruan, H., Wang, S., Yang, Y., Naeem, I., et al. (2021). The diversity and co-occurrence network of soil bacterial and fungal communities and their implications for a new indicator of grassland degradation. *Ecol. Indic.* 129, 107989. doi: 10.1016/j.ecolind.2021.107989

Xiao, Y., Wang, Y., Ma, D., Zhou, X., Wu, Y., Xie, Y., et al. (2021). Effects of invasion of *Elsholtzia densa* benth. on soil properties and soil bacterial diversity in alpine meadow of Qinghai-Tibet plateau. *Southwest China J. Agric. Sci.* 34, 584–590. doi: 10.16213/j.cnki.scjas.2021.3.018

Xiao, Z., Xu, Z., Gu, Z., Lv, J. F., and Shamsi, I. H. (2017). Vertical leaching of allelochemicals affecting their bioactivity and the microbial community of soil. *Agric. Food Chem.* 65, 7847–7853. doi: 10.1021/acs.jafc.7b01581

Xie, L., Ge, Z., Li, Y., Li, S., Tan, L., and Li, X. (2020). Effects of waterlogging and increased salinity on microbial communities and extracellular enzyme activity in native and exotic marsh vegetation soils. *Soil Sci. Soc. America J.* 84, 82–98. doi: 10.1002/saj2.20006

Xu, L., Han, Y., Yi, M., Yi, H., Guo, E., and Zhang, A. (2019). Shift of millet rhizosphere bacterial community during the maturation of parent soil revealed by 16S rDNA high-throughput sequencing. *Appl. Soil Ecol.* 135, 157–165. doi: 10.1016/j.apsoil.2018.12.004

Yang, X., Wang, X., Xiao, S., Liu, Z., Zhou, X., Du, G., et al. (2021). Dominant plants affect litter decomposition mainly through modifications of the soil microbial community. *Soil Biol. Biochem.* 161, 108399. doi: 10.1016/j.soilbio.2021.108399

Zeng, R. (2008). Allelopathy in Chinese ancient and modern agriculture. *Allelopathy Sustain. Agric. Forestry*, 39–59. doi: 10.1007/978-0-387-77337-7_3

Zhang, B., Hong, J., Zhang, Q., Jin, D., and Gao, C. (2020). Contrast in soil microbial metabolic functional diversity to fertilization and crop rotation under rhizosphere and non-rhizosphere in the coal gangue landfill reclamation area of loess hills. *PLoS One* 15, e0229341. doi: 10.1371/journal.pone.0229341

Zhou, S., Huang, Z., Wang, H., Liu, Y., and Hu, H. (2009). Allelopathic effect of *Steura chamaejasme* decomposing in soil on *Onobrychis viciifolia*. *Pratacultural Sci.* 26, 91–94.

Zhou, Y., Liao, F., Weng, J., Mo, Q., Xu, R., Zhang, Y., et al. (2019). Composition and acaricidal activity of essential oil from *Elsholtzia densa* benth against *Sarcoptes scabiei* mites in vitro. *Veterinární Medicína* 64, 178–183. doi: 10.17221/20/2018-vetmed

Zhou, L., Liu, S., Shen, H., Zhao, M., Xu, L., Xing, A., et al. (2020). Soil extracellular enzyme activity and stoichiometry in China's forests. *Funct. Ecol.* 34, 1461–1471. doi: 10.1111/1365-2435.13555

frontiers | Frontiers in Plant Science

TYPE Original Research
PUBLISHED 08 March 2023
DOI 10.3389/fpls.2023.1136439

OPEN ACCESS

EDITED BY
Long Yang,
Shandong Agricultural University, China

REVIEWED BY
Giuseppe Di Miceli,
University of Palermo, Italy
Bo Zhou,
China Agricultural University, China

*CORRESPONDENCE
Na Xiao
201608156@hhstu.edu.cn
Yuan Li
liy681@snnu.edu.cn

SPECIALTY SECTION
This article was submitted to Plant Symbiotic Interactions, a section of the journal Frontiers in Plant Science

RECEIVED 03 January 2023
ACCEPTED 13 February 2023
PUBLISHED 08 March 2023

CITATION
Zhang M, Xiao N, Yang H, Li Y, Gao F, Li J and Zhang Z (2023) The layout measures of micro-sprinkler irrigation under plastic film regulate tomato soil bacterial community and root system. *Front. Plant Sci.* 14:1136439. doi: 10.3389/fpls.2023.1136439

The layout measures of micro-sprinkler irrigation under plastic film regulate tomato soil bacterial community and root system

Mingzhi Zhang[1,2], Na Xiao[1]*, Haijian Yang[1], Yuan Li[3]*, Fangrong Gao[4], Jianbin Li[5] and Zhenxing Zhang[6,7]

[1]Faculty of Engineering, Huanghe Science and Technology University, Zhengzhou, China, [2]Institute of Water Resources and Rural Water Conservancy, Henan Provincial Water Conservancy Research Institute, Zhengzhou, China, [3]Vegetable station, Northwest Land and Resources Research Center, Shaanxi Normal University, Xi'an, China, [4]Hydraulic Research Laboratory, Yellow River Hydrologic Survey Planning and Design Co.,Ltd., Zhengzhou, China, [5]Agricultural Technology Extension Center of Xi'an City, Xi'an, Shaanxi, China, [6]Key Laboratory of Vegetation Ecology, Ministry of Education, Northeast Normal University, Changchun, China, [7]State Environmental Protection Key Laboratory of Wetland Ecology and Vegetation Restoration, School of Environment, Northeast Normal University, Changchun, China

Introduction: The change in rhizosphere soil bacterial community and root system under new water-saving device is not clear.

Methods: A completely randomized experimental design was used to explore the effects of different micropore group spacing (L1: 30 cm micropore group spacing, L2: 50 cm micropore group spacing) and capillary arrangement density (C1: one pipe for one row, C2: one pipe for two rows, C3: one pipe for three rows) on tomato rhizosphere soil bacteria community, roots and tomato yield under MSPF. The bacteria in tomato rhizosphere soil were sequenced by 16S rRNA gene amplicon metagenomic sequencing technology, the interaction of bacterial community, root system and yield in tomato rhizosphere soil was quantitatively described based on regression analysis.

Results: Results showed that L1 was not only beneficial to the development of tomato root morphology, but also promoted the ACE index of tomato soil bacterial community structure and the abundance of nitrogen and phosphorus metabolism functional genes. The yield and crop water use efficiency (WUE) of spring tomato and autumn tomato in L1 were about 14.15% and 11.27%, 12.64% and 10.35% higher than those in L2. With the decrease of capillary arrangement density, the diversity of bacterial community structure in tomato rhizosphere soil decreased, and the abundance of nitrogen and phosphorus metabolism functional genes of soil bacteria also decreased. The small abundance of soil bacterial functional genes limited the absorption of soil nutrients by tomato roots and roots morphological development. The yield and crop water use efficiency of spring and autumn tomato in C2 were significantly higher than those in C3 about 34.76% and 15.23%, 31.94% and 13.91%, respectively. The positive

interaction between soil bacterial community and root morphological development of tomato was promoted by the capillary layout measures of MSPF.

Discussion: The L1C2 treatment had a stable bacterial community structure and good root morphological development, which positively promoted the increase of tomato yield. The interaction between soil microorganisms and roots of tomato was regulated by optimizing the layout measures of MSPF to provide data support for water-saving and yield-increasing of tomato in Northwest China.

KEYWORDS

rhizosphere soil, soil bacteria, root system, yield, positive interaction

1 Introduction

Soil microorganisms are the main components of terrestrial ecosystems, which plays a key role in the decomposition of organic matter, nutrient cycling and the degradation of harmful substances, and also play an important role in facility planting agricultural ecosystems (Zhu et al., 2019; Ma et al., 2023). Soil bacteria are the main component of soil microorganisms (Wang et al., 2017), which have high diversity, high abundance and complete functions (Li and Ma, 2018; Xu et al., 2022; Zhu et al., 2022). Soil bacteria are mainly involved in the formation of humus and the mineralization of organic matter, which is essential for regulating soil enzyme activity, soil nutrient cycle and crop root morphological development (Özbolat et al., 2023; Zheng et al., 2023). Previous studies have found that soil bacterial diversity and heterogeneity are often used to characterize soil fertility and predict ecological environment risks (Guo et al., 2018). Soil bacteria are significantly affected by physical and chemical properties such as soil water, heat and nutrients, plant growth, and other microorganisms (Huang et al., 2018; Zhang et al., 2018). Therefore, the study of soil bacterial community is of great significance for measuring regional soil productive potential and sustainable development.

Facility Planting agriculture has the characteristics of fast crop growth and high demand for soil water and fertilizer (Nie et al., 2022; Zhao et al., 2022). Measuring the level of soil water and fertilizer has become a hot topic in current research. The nutrients needed for plant growth mainly come from the soil, in which the mineralization of soil nutrients by microorganisms and the absorption of nutrients by plant roots are important links in the nutrient cycle (Jafari et al., 2018; Morio et al., 2022). Previous studies have found that soil nitrogen-fixing bacteria can convert nitrogen in the air into nitrogen sources, promote plant root morphological development to support plant needs, and thus reduce plant nutritional stress (Wang J. et al., 2022). Plant roots can make the plant-soil feedback direction develop in a positive direction. In response to soil drought, plant fine roots can grow into aggregates and open microsites, where oxygen stimulates microbial activity and N release. Root exudates and litter produced by root growth provide energy sources for the growth of soil microorganisms (Veresoglou et al., 2022; Xiao et al., 2023). Therefore, it is urgent to explore the relationship between soil microorganisms and plant roots for the efficient utilization of land resources.

Redistribution of soil moisture, heat and air is closely related to field irrigation management, which directly or indirectly affects the development of soil microbial community and plant root morphological development (Feng et al., 2023; Vera et al., 2023). In order to improve the stability of soil microbial community structure in plant root zone and promote root morphological development, researchers have proposed methods such as microbial inoculation and growth regulator addition (Lewis et al., 2020; Zhou et al., 2023). However, there are many problems in the implementation of the above methods, such as high investment cost and environmental pollution (Boddington and Dodd, 1999; Zhao et al., 2017). At the same time, other researchers have found that it is feasible to optimize soil microbial communities and root morphological development in crop root zones by adjusting crop irrigation management methods, such as changes in field layout measures of tomato drip irrigation that can change soil microbial communities and yield (Sun et al., 2021; Wang et al., 2017). Proper field layout of drip irrigation pipe can promote the morphological development of tomato root system (Wang et al., 2020a; Li et al., 2023). The arrangement of drip irrigation under plastic film indirectly affects the morphological development of crop root system and soil microbial community (Wang et al., 2016; Ye et al., 2016). Therefore, exploring the effects of irrigation management measures on crop soil microorganisms and crop roots has guiding significance for elucidating the relationship between soil microbial community and root system in facility planting agriculture and guiding the water-saving, yield-increasing and quality-improving of facility planting agricultural crops.

At present, the mechanism of the change of crop soil bacterial community and root system regulated by the new water-saving technology of facility planting agriculture under MSPF (Zhang et al., 2020a) is not clear. At the same time, the interaction relationship between soil bacterial community-root system-yield of tomato in greenhouse under MSPF lacks qualitative and quantitative description. Therefore, in this study, greenhouse tomato was used as the research object to explore the response of rhizosphere soil

bacteria community, root system and yield of greenhouse tomato under MSPF to the different micropore group spacing and capillary arrangement density of micro-sprinkler pipe. The purpose of this paper is to adjust the interaction between tomato roots system and soil microorganisms by optimizing the layout measures of MSPF through greenhouse experiment and mathematical analysis, and to provide data support for the prediction of soil production potential of facility planting agriculture and the water-saving and yield-increasing of tomato.

2 Materials and methods

2.1 Experimental site and management

The experiment was carried out in the greenhouse of Xi 'an Modern Agricultural Science and Technology Exhibition Center (108°52'E, 34°03'N) in Shaanxi Province from March 23, 2019 to January 30, 2020. The tested tomato variety was 'Jingfan 401' (Jingyan Yinong Seed Industry Technology Co., Ltd., Beijing·China). The tomato adopts the ridge planting structure mode, in which the row spacing is 50.00 cm and the plant spacing is 40.00 cm. The length of the experimental plot is 3.40 m, and the spacing between the plots is 4.00 m. The planting, irrigation and harvest time of spring tomato and autumn tomato are shown in Figure 1. Meteorological data and irrigation record of tomato growth period are shown in Figure 2.

In this experiment, the irrigation amount was controlled on the basis of the cumulative evaporation from a 20-cm diameter standard pan (Epan, DY.AM3, Weifang Dayu Hydrology Technology Co., Ltd., Shandong, China) following Zhang (Zhang et al., 2020a). The evaporation amount was measured at 08:00 am every 5 d. The irrigation amount was evaluated after the measurement. The irrigation quota was calculated according to Formula (1), and the irrigation times and amounts were recorded (see Figure 2).

$$W = A \times E_{pan} \times k_{cp} \quad (1)$$

E_{pan} represents the evaporation within the interval of two irrigation, based on the cumulative evaporation from a 20 cm diameter pan (mm); A represents the capillary control area (mm) and k_{cp} represents the crop- pan coefficient. In this paper, adopting adequate irrigation mode, the crop-pan coefficient of is 1.0 (Zhang et al., 2020a).

2.2 Experimental design

In this experiment, two factors of micropore group spacing and capillary arrangement density were set.

Micropore group spacing (L, see Figure 3) sets 2 levels (30, 50 cm). The capillary arrangement density (C, see Figure 4) sets 3 levels ((one pipe for one row, one row of tomatoes irrigated by one pipe, C1), (one pipe for two rows, two rows of tomatoes irrigated by one pipe, C2), (one pipe for three rows, three rows of tomatoes irrigated by one pipe, C3)).

This study consisted of 6 treatments (Table 1), each treatment was repeated 3 times, a total of 18 experimental plots. The irrigation water in this experiment comes from the groundwater in the region. The head of the water source is connected in series with a 120-mesh sieve filter. The principle of diversion is used to ensure that the working pressure of the control system is constant, and the complete random test is used to arrange the test fields. Each experimental field was irrigated separately and controlled by a spherical valve.

2.3 Measurements and computational methods

2.3.1 Collection and determination of soil bacterial

1) Soil samples were collected from rhizosphere soil of spring tomato and autumn tomato after 72 days of planting. The soil shaking method was used to extract (Taking tomato plants as the center, the cylindrical soil with tomato roots at a radius of 20 cm and a depth of 5-25 cm was excavated, and the loose soil combined with tomato roots was shaken off. The soil closely combined with tomato roots in greenhouse was gently brushed with a soft brush after sterilization as the rhizosphere soil of tomato in greenhouse). Three rhizosphere soil samples were randomly taken from each experimental plot, and the samples were transported to the

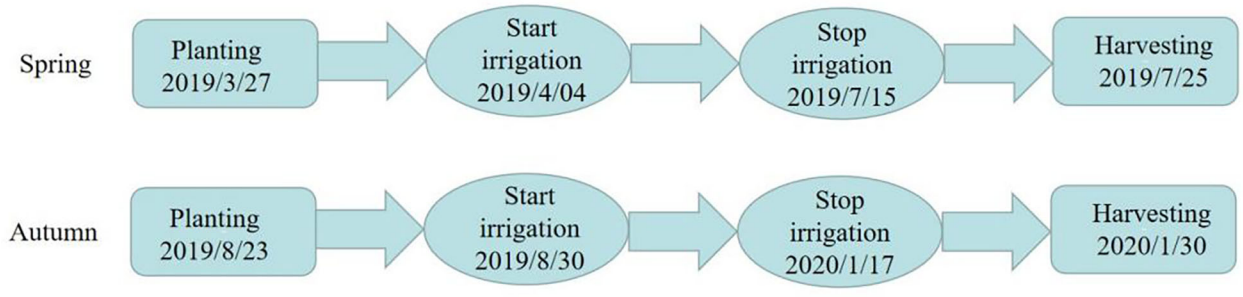

FIGURE 1
The planting, irrigation and harvesting time of tomato.

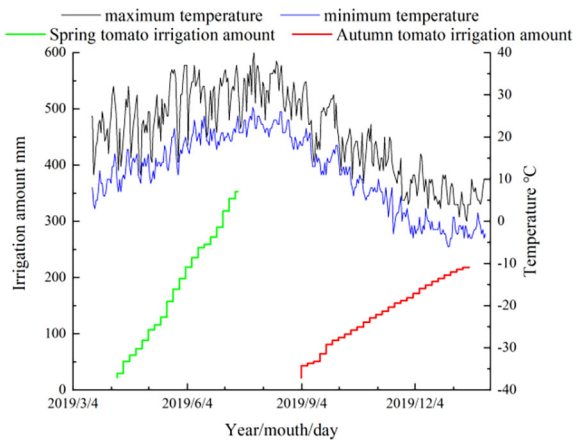

FIGURE 2
Meteorological data and irrigation record of tomato growth period. Diameter of micropore is d=0.8mm; The internal spacing of the micropores group was l =0.4cm; The Angle of micropores is =68°; The micropore group spacing is L.

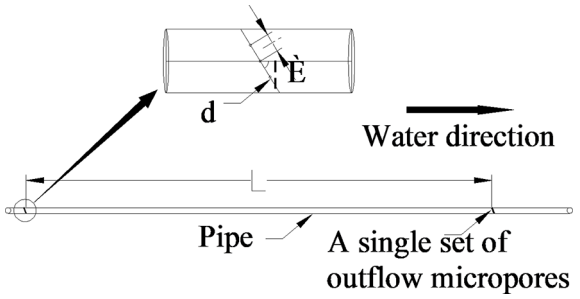

FIGURE 3
Micropores group (inside) spacing structure parameters (Zhang et al., 2020b). Diameter of micropore is d=0.8mm; The internal spacing of the micropores group was l =0.4cm; The Angle of micropores is =68°; The micropore group spacing is L.

laboratory on ice. The samples were brought back to the room and the fresh soil plant residues were removed. Three soil samples in the plot were fully stirred and evenly mixed as soil samples for sequencing in the experimental plot. The soil samples were collected and quickly frozen in liquid nitrogen. The soil samples were stored in a -80°C refrigerator and sent to Shanghai Meiji Biomedical Technology Co., Ltd. (Shanghai, China) to determine soil bacterial community. The main analysis steps of soil bacterial community determination are divided into three parts:

A. DNA extraction and PCR amplification

Total DNA was extracted from tomato rhizosphere soil using the E.Z.N.A.Â ® soil kit (Omega Bio-tek, Norcross, GA, USA), which reliably and quickly separates high-quality genomic DNA from various soil samples (up to 1 g of soil can be processed in 60 min). After the quality of DNA extraction was detected by 1% agarose gel electrophoresis, the V3-V4 variable region was amplified by PCR with 338 F (5 ‘ -ACTCCTACGGGAGGGAGCAGCAG-3 ‘) and 806 R (5 ‘ -GGACTACHVGGGTWTCTAAT-3 ‘) primers. The amplification procedure was: 95 °C pre-denaturation 3 min, 27 cycles (95 °C denaturation 30 s, 55 °C annealing 30 s, 72 °C extension 30 s). Finally, extension at 72 °C for 10 min (PCR instrument: ABI GeneAmp ® 9700).

B. Illumina Miseq sequencing

The bacterial 16S rDNA V3-V4 region was selected, and the NA samples were sequenced using the Illumina Miseq PE300 high-throughput sequencing platform (Shanghai Meiji Biomedical Technology Co., Ltd.). The bacterial 16 S rDNA V3-V4 amplification primers were 338 F (5 ‘ -ACTCCTACGGGGAGGCAGCAG-3 ‘) and 806 R (5 ‘ -GGACTACNNGGGTATCTAAT-3 ‘). The PCR products were recovered using 2% agarose gel, purified and eluted for detection. PCR reaction system (total system was 25 μL): 12.5 μL KAPA 2G Robust Hot Start Ready Mix, 1 μL Forward Primer (5 μmol/L), 1 μL Reverse Primer (5 μmol/L), 5 μL DNA (the total amount of DNA added was 30 ng), and finally 5.5 μL dd H_2O was added to make up to 25 μL. Reaction parameters: 95 °C for 5 min; 95 °C denaturation 45 s, 55 °C annealing 50 s, 72 °C extension 45 s, 28 cycles; 72 °C for 10 min. The original sequence was uploaded to the figshare database (https://figshare.com/articles/dataset/The_Layout_Measures_of_Micro-sprinkler_Irrigation_under_Plastic_Film_Regulate_Tomato_Soil_Bacterial_Community_and_Root_System/21818610).

C. Sequencing data processing

The original data obtained by Miseq sequencing were optimized after splicing and quality control. After distinguishing the samples, OTU (Operational taxonomic unit) cluster analysis and species

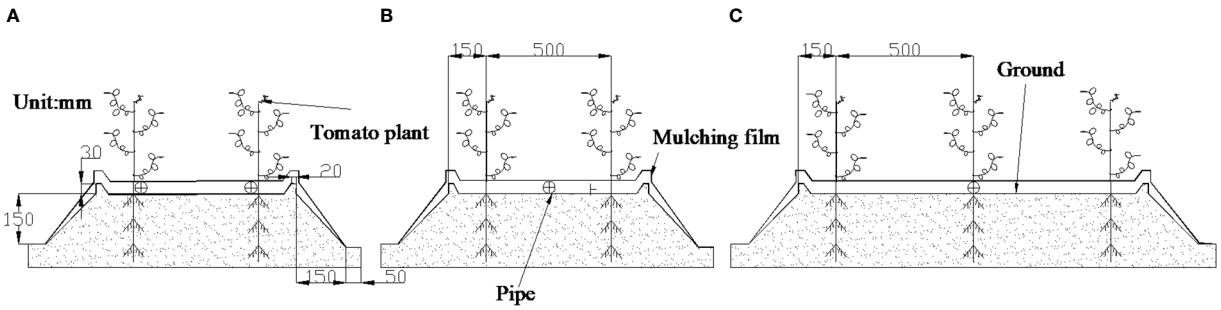

FIGURE 4
Capillary arrangement. (Zhang et al., 2020b). **(A)** represents one pipe for one row; **(B)** represents one pipe for two rows; **(C)** represents one pipe for three rows.

TABLE 1 Experimental design.

No.	Treatment	Micropore group spacing	Capillary arrangement density	Polt		Tomato growth period irrigation quota mm	
				Spring	Autumn	Spring	Autumn
1	L1C1	30	one pipe for one row	6	6	353.03	218.19
				1	1		
				13	13		
2	L1C2	30	one pipe for two rows	11	11		
				2	2		
				7	7		
3	L1C3	30	one pipe for three rows	16	16		
				10	10		
				5	5		
4	L2C1	50	one pipe for one row	3	3		
				17	17		
				15	15		
5	L2C2	50	one pipe for two rows	18	18		
				9	9		
				4	4		
6	L2C3	50	one pipe for three rows	8	8		
				12	12		
				14	14		

L represents the micropore group spacing, C represents the capillary arrangement density, and one pipe for two rows represents two rows of tomatoes irrigated by one pipe.

taxonomy analysis were performed. The OUT similarity was set to 97%. The OTU was subjected to diversity index analysis and statistical analysis of community structure at each classification level, and then a series of in-depth statistical and visual analysis such as multivariate analysis and difference significance test of sample community composition and phylogenetic information were completed. The ACE index of soil bacterial (ACE), CHAO index of soil bacterial (CHAO), COVERAGE index of soil bacterial (COVERAGE), SHANNON index of soil bacterial (SHANNON), SIMPSON index of soil bacterial (SIMPSON), SOBS index of soil bacterial (SOBS), Species Veen diagram analysis and species composition analysis can be obtained by direct analysis of Shanghai Meiji Biological Cloud platform (https://login.majorbio.com/login).

2) Based on the results of soil bacterial community determination, and referring to the Kyoto Encyclopedia of Genes and Genomes and related references (Wang et al., 2020b), the functional genes related to soil bacterial nitrogen fixation, nitrification, denitrification and phosphorus metabolism functional gene abundance were obtained. The functional genes related to soil bacterial nitrogen metabolism are the sum of the abundance of soil bacterial nitrogen fixation, nitrification and denitrification functional genes.

2.3.2 Root system

Three tomato plants were randomly selected from each plot to dig a soil volume with a depth of about 0.4 m and a diameter of 0.2 m centered on the plant at 76 and 78 days after planting spring tomato and autumn tomato, respectively. The samples were placed in a 150 mesh sieve to rinse the roots. The roots were scanned by Epson Perfection V700 scanner to obtain the TIF diagram. Finally, the TIF diagram was processed by WinRHIZO Pro software to obtain the total root length, total number of root tips and bifurcation number of greenhouse tomatoes. The root activity of tomato was determined by triphenyltetrazolium chloride method (Li et al., 2020).

2.3.3 Yield and water use efficiency

Four tomato plants were randomly selected, and the mature fruit mass of four tomatoes was weighed by electronic scale with precision of 0.01 g, and the yield per hectare was converted.

Time-domain reflectometry soil moisture sensor (TRIME-PICO-IPH, IMKO, Inc., Ettlingen, Germany) was used to measure the soil volume moisture content at different layers of soil (0–10, 10–20, 20–30, 30–40, 40–50, 50–60, 60–70, and 70–80 cm, respectively). It was measured once before and after each growth period. Water consumption (ET_a)and crop water use

efficiency (WUE) were calculated formulas (2) and (3), respectively (Zhang et al., 2020a):

$$ET_a = I \pm 1000 \times H \times (\theta_{t1} - \theta_{t2}) \quad (2)$$

represents crop water consumption during growth period (mm); I represents the irrigation quota of crop growth period (mm); H represents the depth of the wetting layer with plan (H = 0.8 m); θ_{t1} and θ_{t2} represent 80-cm average soil volumetric water contents at times $t1$ and $t2$ cm^3/cm^3), respectively.

$$WUE = 1000 * \frac{Y}{ET_a} \quad (3)$$

Y indicates crop grain yield (t/hm^2).

2.4 Data analysis

The interaction of bacterial community, root system and yield in tomato rhizosphere soil was quantitatively described based on regression analysis. The significant difference was analyzed by F test of SPSS22.0 (IBM Crop., Armonk, New York, NY, USA), and the significant level was set to $P<0.05$. The picture was drawn by OriginPro2019 (Origin Lab Corporation, Northampton, MA, USA). Excel 2016 (Microsoft Excel, Microsoft, Washington, USA) was used for regression analysis.

2.5 Abbreviations

The abbreviations of this article are explained in Table 2.

3 Results

3.1 Effects of different treatments on soil bacterial community of greenhouse tomato

3.1.1 Diversity of soil bacterial community structure

It can be seen from the dilution curve of Figure 5 that the amount of sequencing data in each treatment is sufficient. It can be seen from Table 3 that the micropore group spacing (L) had a significant effect on the ACE index of soil bacterial (ACE), CHAO index of soil bacterial (CHAO), SHANNON index of soil bacterial (SHANNON) and SOBS index of soil bacterial (SOBS) of spring tomato and autumn tomato. The relative contribution of L to ACE,

TABLE 2 Abbreviations.

No	Abbreviations	Full name
1	L	Micropores group spacing
2	C	Capillary arrangement density
3	ACE	Ace index of soil bacterial
4	CHAO	Chao index of soil bacterial
5	COVERAGE	Coverage index of soil bacterial
6	SHANNON	Shannon index of soil bacterial
7	SIMPSON	Simpson index of soil bacterial
8	SOBS	Sobs index of soil bacterial
9	NFFA	Soil bacterial nitrogen fixation functional gene abundance
10	NFA	Soil bacterial nitrification functional gene abundance
11	DFA	Soil bacterial denitrification functional gene abundance
12	GAN	Soil bacterial nitrogen metabolism functional gene abundance
13	GAP	Soil bacterial phosphorus metabolism functional gene abundance
14	RL	Total root length
15	RS	Total root surface area
16	RV	Total root volume
17	RT	Total number of root tips
18	RB	Total root bifurcation number
19	RA	Root activity
20	Y	Yield
21	WUE	Water use efficiency

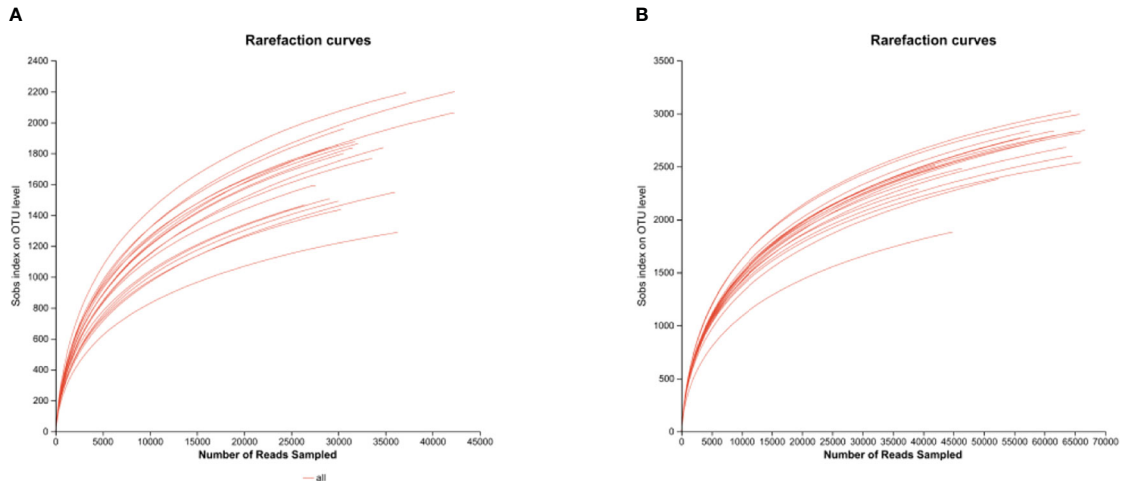

FIGURE 5
Bacterial dilution curve of tomato rhizosphere soil. **(A)** Spring **(B)** Autumn.

TABLE 3 Diversity of soil bacterial community structure.

	Treatment	ACE	CHAO	COVERAGE	SHANNON	SIMPSON	SOBS
Spring	L1C1	2406.8 ± 29.04ab	2383.97 ± 33.63ab	0.9826 ± 0.00105a	5.92 ± 0.13a	0.0078 ± 0.00094b	1855.67 ± 22.48ab
	L1C2	2652.77 ± 27.34a	2621.97 ± 27.11a	0.9834 ± 0.0032a	5.8 ± 0.42a	0.0162 ± 0.01155ab	2070.33 ± 115.28a
	L1C3	2031.45 ± 74.45cd	2057.69 ± 99.6cd	0.983 ± 0.00138a	5.28 ± 0.15b	0.0219 ± 0.0038a	1528.33 ± 54.72cd
	L2C1	2512.34 ± 256.48ab	2498.21 ± 291.71ab	0.9829 ± 0.00182a	5.7 ± 0.13ab	0.0133 ± 0.0026ab	1950 ± 218.06ab
	L2C2	2283.43 ± 194.19bc	2268.15 ± 165.33bc	0.9844 ± 0.00154a	5.3 ± 0.14b	0.0222 ± 0.00321a	1716.67 ± 150.93bc
	L2C3	1837.32 ± 154.57d	1816.54 ± 173.38d	0.9859 ± 0.00377a	5.28 ± 0.3b	0.0183 ± 0.00758ab	1395.67 ± 94.21d
Autumn	L1C1	3511.24 ± 65.45a	3482.2 ± 55.93a	0.9888 ± 0.00123a	6.38 ± 0.09a	0.0047 ± 0.00069a	2881.67 ± 96.02a
	L1C2	3548.28 ± 52.62a	3531.84 ± 57.54a	0.988 ± 0.00111a	6.26 ± 0.18a	0.0068 ± 0.00219a	2894.67 ± 109.55ab
	L1C3	3228.32 ± 93.53ab	3199.86 ± 122.29ab	0.9858 ± 0.00326a	6.24 ± 0.09a	0.0051 ± 0.00022a	2524 ± 148.93bc
	L2C1	3358.6 ± 137ab	3345.88 ± 126.55a	0.9886 ± 0.00222a	6.19 ± 0.02a	0.0063 ± 0.00056a	2737.33 ± 124.56ab
	L2C2	3218.74 ± 240.75ab	3214.89 ± 253.78ab	0.9876 ± 0.00269a	6.17 ± 0.13a	0.0064 ± 0.00205a	2588.33 ± 139.69abc
	L2C3	2931.81 ± 462.44b	2887.25 ± 474.53b	0.985 ± 0.00224a	6.05 ± 0.38a	0.0069 ± 0.00374a	2261.33 ± 371.27c
F-value	L	10.405** (30.20)	9.687** (28.80)	0.361ns (1.50)	7.665* (24.20)	1.453ns (5.70)	11.738** (32.80)
	C	20.102** (62.60)	18.300** (60.40)	0.539ns (4.30)	7.195* (37.50)	4.714* (28.30)	25.949** (68.40)
	D	250.944** (91.30)	225.566** (90.40)	55.017** (47.80)	87.795** (78.50)	48.827** (67.00)	277.107** (92.00)
	L*C	2.262ns (15.90)	2.235ns (15.70)	0.143ns (1.20)	0.654ns (5.20)	0.825ns (6.40)	2.697ns (18.30)
	L*D	0.700* (2.80)	0.507* (2.10)	1.431ns (5.60)	0.344ns (1.40)	0.282ns (1.20)	0.922ns (40.00)
	C*D	1.165ns (8.90)	0.643ns (5.10)	3.615* (23.20)	2.486ns (17.20)	3.410* (22.10)	0.209ns (1.70)
	L*C*D	0.453ns (3.60)	0.394ns (3.20)	0.397ns (3.20)	1.463ns (10.90)	1.410ns (10.50)	0.601ns (4.80)

The L represents the micropore group spacing, the C represents the capillary arrangement density, the D represents the different planting seasons of tomato, the data are all average ± standard deviation in the table, the bracketed number is the factor relative contribution%, the same below. The ACE represents ACE index of soil bacterial, CHAO represents CHAO index of soil bacterial, COVERAGE represents COVERAGE index of soil bacterial, SHANNON represents SHANNON index of soil bacterial, SIMPSON represents SIMPSON index of soil bacterial, SOBS represents SOBS index of soil bacterial.
Different letters in the same line meant significant difference at 0.05 level, *: P<0.05, **: P<0.01, ns: P>0.05.

CHAO, SHANNON, and SOBS of tomato was 30.20%, 28.80%, 24.20% and 32.80%, respectively. The capillary arrangement density (C) had a significant effect on the ACE, CHAO, SHANNON, SIMPSON index of soil bacterial (SIMPSON) and SOBS of spring tomato and autumn tomato. The relative contribution of C to ACE, CHAO, SHANNON, SIMPSON and SOBS of tomato was 62.60%, 60.40%, 37.50%, 28.30% and 38.4%, respectively. The different planting seasons (D) had a significant effect on the ACE, CHAO,

COVERAGE index of soil bacterial (COVERAGE), SHANNON, SIMPSON and SOBS of spring tomato and autumn tomato. The relative contribution of D to ACE, CHAO, COVERAGE, SHANNON, SIMPSON and SOBS of tomato was 62.60%, 60.40%, 37.50%, 28.30% and 38.4%, respectively.

Compared with L2, the ACE, CHAO, SHANNON, and SOBS of spring tomato and autumn tomato treated with L1 were higher. With the decrease of C, the ACE, CHAO, SHANNON, SIMPSON and SOBS of soil bacterial with spring tomato and autumn tomato showed a decreasing trend. The diversity of soil bacterial community structure in spring tomato was lower than that in autumn tomato.

3.1.2 Soil bacterial community structure species composition

As can be seen from Figure 6, there are 1304 and 2145 identical OTUs in the soil bacteria of spring tomato and autumn tomato in the six treatments, accounting for 30.77% and 37.21% of the total OTUs. Single factor significant analysis showed that the total number of soil bacteria in spring tomato and autumn tomato treated with L1C2 was the highest at the OTUs classification level (3271 and 4407). Compared with L2, the total number of soil bacteria in spring tomato and autumn tomato treated with L1 increased by 13.50% and 6.16% at the OTUs classification level. With the decrease of C, the total number of soil bacteria in spring tomato and autumn tomato decreased at the OTUs classification level. Compared with C3, the total number of soil bacteria in C2 spring tomato and autumn tomato increased by about 30.68% and 16.21% at the OTUs classification level.

From Figure 7, it can be seen that the dominant bacterial populations in spring tomato soil at the genus level of soil bacteria mainly include *Bacillus* (10.71%-23.68%), *Streptomyces* (1.44%-3.17%), *Sphingomonas* (1.40%-3.21%); the soil of autumn tomato mainly includes *Sphingomonas* (6.07%-10.68%), *Bacillus* (2.55%-6.85%) and *Gemmatimonas* (1.75%-2.65%). *Bacillus* is a common genus of spring tomato and autumn tomato soil. With the decrease of C, the abundance of *Bacillus* in spring and autumn tomato increased first and then decreased. Compared with L2, the abundance of *Bacillus* with spring and autumnin L1 treatment increased by 23.50% and 76.17% at genus level.

3.2 Soil bacterial nitrogen metabolism functional gene abundance and soil bacterial phosphorus metabolism functional gene abundance

From Table 4, it can be seen that the L has a significant effect on the soil bacterial nitrogen metabolism functional gene abundance (GAN) and soil bacterial phosphorus metabolism functional gene abundance (GAP). The contribution of L to the GAN and GAP in tomato were 18.90%, 21.80%, respectively. The C had a significant effect on the soil bacterial nitrogen fixation functional gene abundance (NFFA), soil bacterial nitrification functional gene abundance (NFA), soil bacterial nitrification functional gene abundance (DFA), GAN and GAP. The relative contribution of capillary arrangement density to the NFFA, NFA, GAN and GAP in tomato soil were 72.60%, 63.20%, 30.90%, 60.90% and 48.20%, respectively. The D had a significant effect on the NFFA, NFA, DFA, GAN and GAP. The relative contribution of D to the NFFA, NFA, DFA, GAN and GAP in tomato soil were 96.60%, 96.70%, 86.70%, 95.30% and 93.30%, respectively. The GAN and GAP in L1C2 treatment were not significantly lower than that in L1C1 and L2C1, but significantly higher than that in L1C3, L2C2 and L2C3 treatments, indicating that L1C2 treatment had higher nitrogen and phosphorus metabolism functional gene

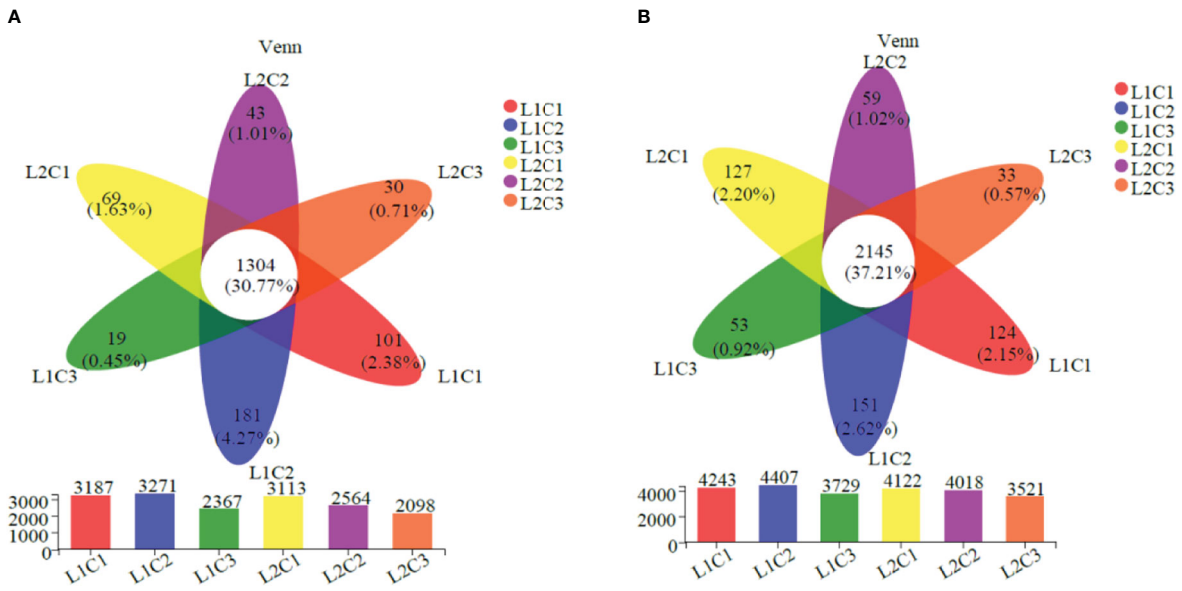

FIGURE 6
OTUs classification of soil bacteria. **(A)** Spring **(B)** Autumn.

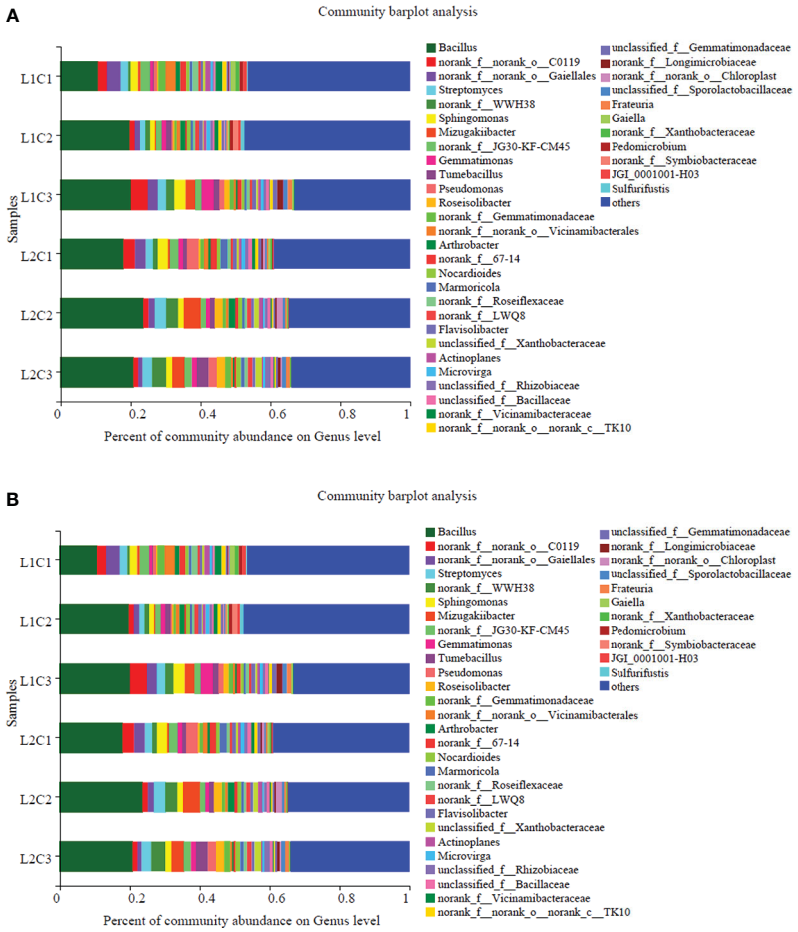

FIGURE 7
Taxonomic level of soil bacteria. **(A)** Spring **(B)** Autumn.

TABLE 4 Comparative analysis functional genes related to N and P metabolism of soil bacteria.

	Treatment	NFFA	NFA	DFA	GAN	GAP
Spring	L1C1	7968 ± 1184.68a	4146.33 ± 397.81a	10190 ± 734.72bc	22304.33 ± 2125.17a	164247 ± 4734.48a
	L1C2	6377.33 ± 1372.51ab	4053 ± 218.09ab	10862.67 ± 280.9ab	21293 ± 2111.14a	151945.67 ± 6087.11a
	L1C3	3936 ± 145.14c	3527.33 ± 276.1bc	9354 ± 193.45c	16817.33 ± 443.6b	113045.67 ± 5058.62c
	L2C1	5288.67 ± 1201.81bc	4360.67 ± 276.8a	11608.67 ± 658.01a	21258 ± 4228.28a	152421.67 ± 15321.09a
	L2C2	3671.67 ± 101.19c	3374.33 ± 377.31c	9761.67 ± 307.11bc	16807.67 ± 1167.53b	137102 ± 6061.43b
	L2C3	3722.67 ± 248.09c	3343 ± 340.74c	9295.67 ± 1164.67c	16361.33 ± 1054.67b	112817.67 ± 5730.07c
Autumn	L1C1	21089 ± 969.35a	10654.67 ± 589.55a	22881.33 ± 835.97a	54625 ± 1747.79a	397943.33 ± 19602.93a
	L1C2	19958.33 ± 1954.3ab	9289 ± 965.06ab	20197 ± 2016.25a	49444.33 ± 3855.53ab	371200.33 ± 16870.22a
	L1C3	16616 ± 1842.29b	8918 ± 508.66b	18578.33 ± 4332.23a	44112.33 ± 5241.44b	333575 ± 70090.14ab
	L2C1	20697.33 ± 1091.38a	8839.67 ± 1253.06b	21807.33 ± 3075.77a	51344.33 ± 3767.77ab	357470.33 ± 9445.11a
	L2C2	19851 ± 3432.89ab	9644.67 ± 300.9ab	20517.67 ± 4273.95a	50013.33 ± 7947.17ab	337817 ± 73672ab
	L2C3	11662 ± 1285.12a	6339 ± 444.66c	16598 ± 3757.27a	34599 ± 5110.82c	260776.33 ± 45050.68b
F-value	L	13.273** (35.60)	16.422** (40.60)	0.270ns (1.10)	5.578* (18.90)	6.685* (21.80)

(Continued)

TABLE 4 Continued

	Treatment	NFFA	NFA	DFA	GAN	GAP
	C	31.828** (72.60)	20.601** (63.20)	5.375* (30.90)	18.660** (60.90)	11.158** (48.20)
	D	676.695** (96.60)	712.845** (96.70)	156.417** (86.70)	481.999** (95.30)	334.246** (93.30)
	L*C	0.544ns (4.30)	3.341* (21.80)	0.188ns (1.50)	0.577ns (4.60)	0.118ns (1.00)
	L*D	0.002ns (0.01)	8.589** (26.40)	0.396ns (1.60)	0.654ns (2.70)	3.183ns (11.70)
	C*D	8.023** (40.10)	6.266** (34.30)	1.348ns (10.10)	4.509* (27.30)	0.881ns (6.80)
	L*C*D	5.616** (31.9)	7.953** (39.90)	0.593ns (4.70)	2.513ns (17.30)	0.549ns (4.40)

The L represents the micropore group spacing, the C represents the capillary arrangement density, the D represents the different planting seasons of tomato, the data are all average ± standard deviation in the table, the bracketed number is the factor relative contribution%, the same below. The NFFA represents the soil bacterial nitrogen fixation functional gene abundance, the NFA represents the soil bacterial nitrification functional gene abundance, the DFA represents the soil bacterial denitrification functional gene abundance, the GAN represents the soil bacterial nitrogen metabolism functional gene abundance, GAP represents the soil bacterial phosphorus metabolism functional gene abundance.
Different letters in the same line meant significant difference at 0.05 level, *: P<0.05, **: P<0.01, ns: P>0.05.

abundance, which could promote soil nitrogen and phosphorus cycle transformation.

Compared with L2, the NFFA, NFA, soil bacterial denitrification functional gene abundance (DFA), GAN and GAP in spring tomato and autumn tomato soil treated with L1 increased by 44.14% and 10.44%, 5.85% and 16.27%, -0.85% and 4.64%, 11.00% and 8.99%, 6.69% and 15.34%, respectively. With the decrease of C, the NFFA, NFA, DFA, GAN and GAP in spring tomato and autumn tomato soil increased first and then decreased. The NFFA, NFA, DFA, GAN and GAP in C2 of spring tomato and autumn tomato soil was significantly higher than that in C3 about 31.21% and 40.78%, 8.11% and 24.10%, 10.59% and 15.74%, 14.83% and 26.36%, 27.97% and 19.29%, respectively. The abundance of soil bacterial nitrogen metabolism and phosphorus metabolism functional genes in spring tomato was lower than that in autumn tomato.

TABLE 5 Root morphology of tomato in greenhouse.

	Treatment	RL cm/plant	RS cm^2/plant	RV cm^3/plant	RT	RB	RA mg/g/h
Spring	L1C1	363.63 ± 28.95ab	119.5 ± 25.65a	3.3 ± 1.36a	831.11 ± 131.75a	1774.44 ± 591.7ab	2.31 ± 0.25ab
	L1C2	369.43 ± 16.2a	121.18 ± 24.56a	3.42 ± 1.38a	838 ± 56.99a	1984.44 ± 485.65a	2.53 ± 0.61a
	L1C3	325.4 ± 47.93ab	98.44 ± 17.29ab	2.42 ± 0.55a	706.89 ± 158.88b	1312.33 ± 479.37bc	2.05 ± 0.37b
	L2C1	359.26 ± 53.15ab	117.46 ± 26.01ab	3.27 ± 1.33a	816.89 ± 220.85a	1761.56 ± 641.17ab	2.29 ± 0.54ab
	L2C2	353.89 ± 49.96ab	116.31 ± 20.29ab	3.27 ± 1a	807.67 ± 111.26ab	1649.67 ± 495.41abc	2.2 ± 0.49ab
	L2C3	318.3 ± 53.25b	95.89 ± 18.27b	2.3 ± 0.61b	663.89 ± 158.1b	1162.89 ± 350.5c	1.87 ± 0.35b
Autumn	L1C1	317.31 ± 35.94a	96.4 ± 12.28ab	2.48 ± 0.94ab	824.56 ± 102.27a	1503.33 ± 443.89a	1.41 ± 0.25a
	L1C2	322.82 ± 39.36a	102.63 ± 16.34a	2.82 ± 0.89a	809.89 ± 125.52a	1454 ± 379.42ab	1.45 ± 0.56a
	L1C3	294.9 ± 39.84ab	83.53 ± 19.84b	1.87 ± 0.55b	684.67 ± 106.29ab	1216.22 ± 260.74ab	1.16 ± 0.22a
	L2C1	310.01 ± 23.53ab	89.07 ± 12.09ab	2.24 ± 0.81ab	822.33 ± 168.11a	1334.44 ± 326.83ab	1.35 ± 0.21a
	L2C2	315.53 ± 45.3a	94.49 ± 23.15ab	2.55 ± 0.89ab	764.78 ± 176.69ab	1388.89 ± 293.34ab	1.31 ± 0.22a
	L2C3	271.91 ± 47.29b	80.39 ± 18.3b	1.82 ± 0.49b	664.89 ± 103.06b	1132.22 ± 273.35b	1.14 ± 0.26a
F-value	L	3.803* (11.80)	1.476ns (1.50)	0.62ns (0.60)	3.899** (12.60)	2.632ns (2.70)	3.837* (11.90)
	C	9.183** (16.10)	9.447** (16.40)	9.232** (16.10)	10.999** (18.60)	10.196** (17.50)	7.280** (13.20)
	D	28.645** (23.00)	27.968** (22.60)	14.637** (13.20)	4.327* (10.30)	10.349** (9.70)	147.428** (60.60)
	L*C	0.122ns (0.20)	0.075ns (0.20)	0.041ns (0.10)	0.109ns (0.20)	0.154ns (0.30)	0.589ns (1.00)
	L*D	0.048ns (0.10)	0.157ns (0.20)	0.055ns (0.10)	0.016ns (0.01)	0.127ns (0.10)	0.459ns (0.50)
	C*D	0.114ns (0.20)	0.624ns (1.30)	0.446ns0.90)	0.146ns0.30)	1.539ns0.31)	0.435ns (0.90)
	L*C*D	0.189ns (0.40)	0.031ns (0.10)	0.046ns (0.10)	0.043ns (0.10)	0.539ns (0.11)	0.274ns (0.60)

The L represents the micropore group spacing, the C represents the capillary arrangement density, the D represents the different planting seasons of tomato, the data are all average ± standard deviation in the table, the bracketed number is the factor relative contribution%, the same below. The RL represents the total root length, the RS represents the total root surface area, the RV represents the total root volume, the RT represents the total number of root tips, the RB represents the total root bifurcation number, the RA represents the root activity.
Different letters in the same line meant significant difference at 0.05 level, *: P<0.05, **: P<0.01, ns: P>0.05.

3.3 Effects of different treatments on tomato roots in greenhouse

It can be seen from Table 5 that the L had significant effects on total root length (RL), total number of root tips (RT) and root activity (RA) of tomato, in which the relative contributions of L to RL, RT and RA of tomato are 11.80%, 12.60% and 11.90%, respectively. The C had a significant effect on RL, total root surface area (RS), total root volume (RV), RT, total root bifurcation number (RB) and RA of tomato ($P \leq 0.05$). The relative contribution of C to RL, RS, RV, RT, RB and RA of tomato was 16.10%, 16.40%, 16.10%, 18.60%, 17.50% and 13.20%, respectively. The D had a significant effect on RL, RS, RV, RT, RB and RA of spring tomato and autumn tomato ($P \leq 0.05$). The relative contribution of D to RL, RS, RV, RT, RB and RA of tomato was 23.00%, 22.60%, 13.20%, 10.30%, 9.70% and 13.20%, respectively.

Compared with L2, the RL, RS, RV, RT, RB and RA of spring tomato and autumn tomato in L1 increased by 2.62% and 4.19%, 2.87% and 7.05%, 3.45% and 8.49%, 3.83% and 2.98%, 10.87% and 8.25%, 8.31% and 5.94%, respectively. With the decrease of C, the RL, RS, RV, RT, RB and RA of spring tomato and autumn tomato increased first and then decreased. The RL, RS, RV, RT, RB and RA of spring tomato and autumn tomato in C2 treatment were about 1.06% and 1.76%, 1.22% and 6.28%, 1.76% and 14.07%, 0.14% and 4.39%, 2.77% and 0.18%, 2.67% and 1.04% higher than those in C1 treatment. It was also higher than C3 treatment by about 12.37% and 12.62%, 22.21% and 20.25%, 41.73% and 45.63%, 20.05% and 16.68%, 46.82% and 21.05%, 20.42% and 20.23%, respectively. The root morphological development of spring tomato was better than that of autumn tomato.

3.4 Effects of different treatments on yield and water use efficiency of greenhouse tomato

It can be seen from Figure 8 that the L and C have significant effects on yield (Y) and water use efficiency (WUE) of spring and autumn tomatoes. Compared with L2, the Y and WUE of spring tomato and autumn tomato in L1 treatment increased by 14.15% and 11.27%, 12.64% and 10.35%, respectively. With the decrease of C, the Y and WUE of spring tomato and autumn tomato showed an increasing trend. The Y and WUE of C2 spring tomato and autumn tomato were significantly higher than those of C3 by about 34.76% and 15.23%, 31.94% and 13.91%, respectively.

3.5 Correlation of tomato soil bacterial community, root system and yield

Based on Pearson's two-tailed test, the indexes with better correlation among soil bacterial community, root system, and yield were screened out. Correlation analysis (Figure 9) showed that ACE, GAN, GAP RL, RT and RA were positively correlated with tomato yield, indicating that there was a positive interaction between soil bacterial community and root system. A stable bacterial community and good root morphological development positively promoted the increase of tomato yield. It was also found that the ACE, GAN and GAP had the highest positive correlation with the RT in the root index (0.758 and 0.870, 0.704 and 0.875, 0.756 and 0.853). In order to further quantitatively describe how the soil bacterial community affects tomato roots and thus affects tomato yield, we selected RT, which has the highest correlation with ACE, GAN and GAP, as a bridge. The

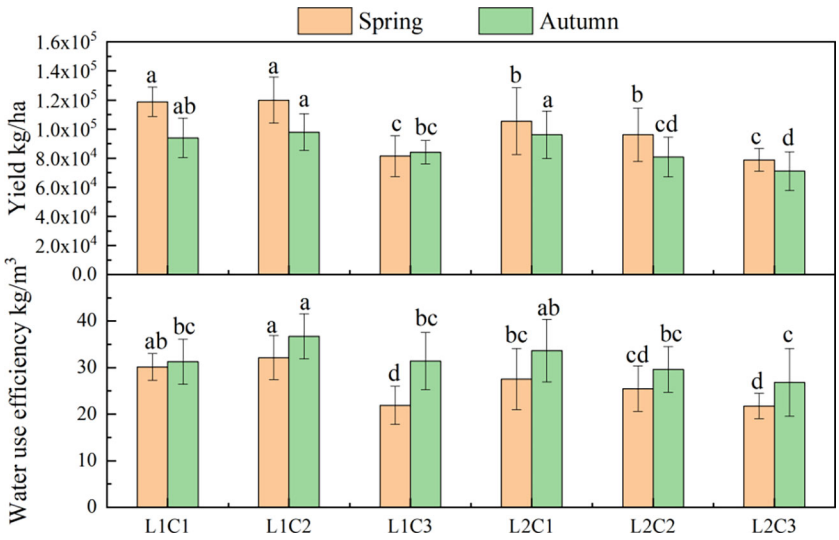

FIGURE 8
Yield and water use efficiency of tomato. The data are all average±standard deviation in the figure, different letters in the same column meanS significant difference at 0.05 level, the same as blow.

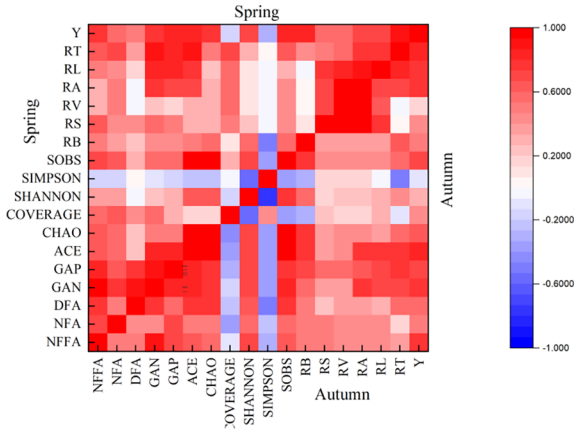

FIGURE 9
Correlation between tomato soil bacterial community, root system and yield. Spring represents the correlation between the indicators of spring tomato; Autumn represents the correlation between the indicators of autumn tomato. The NFFA represents the soil bacterial nitrogen fixation functional gene abundance, the NFA represents the soil bacterial nitrification functional gene abundance, the DFA represents the soil bacterial denitrification functional gene abundance, the GAN represents the soil bacterial nitrogen metabolism functional gene abundance, GAP represents the soil bacterial phosphorus metabolism functional gene abundance. The ACE represents ACE index of soil bacterial, CHAO represents CHAO index of soil bacterial, COVERAGE represents COVERAGE index of soil bacterial, SHANNON represents SHANNON index of soil bacterial, SIMPSON represents SIMPSON index of soil bacterial, SOBS represents SOBS index of soil bacterial. The RL represents the total root length, the RS represents the total root surface area, the RV represents the total root volume, the RT represents the total number of root tips, the RB represents the total root bifurcation number, the RA represents the root activity. The Y represents the yield.

relationship between ACE, GAN, GAP and RT, and the relationship between RT and yield were quantitatively described by regression analysis, respectively. The analysis results are shown in Figure 9.

From Figure 10, it can be seen that the ACE and RT showed a quadratic parabolic curve relationship, in which the determination coefficient R^2>0.6015, indicating that the ACE in the regression model can explain 60.15% of the change of tomato RT. The GAN and GAP also showed a quadratic parabolic curve relationship with the RT of tomato. The determination coefficient R^2 of the regression equation between the GAN and the RT of tomato was higher than that of the determination coefficient R^2 of the regression equation between the GAP and the RT of tomato, indicating that the GAN had a greater impact on the RT of tomato. The relationship between the RT of tomato and the yield was a quadratic parabolic curve, and the coefficient of determination R^2>0.6461, indicating that the RT of tomato in the regression model could explain 64.61% of the change in yield of tomato. The RT of tomato could be used to estimate the yield, and the tomato production potential in this area could be indirectly evaluated by soil bacterial community.

4 Discussion

4.1 The layout measures regulate the soil bacterial community of greenhouse tomato

Previous studies have shown that under drought stress, plants will reduce the supply of carbon sources for soil bacteria, and sustainably reduce the diversity and richness of bacterial community structure (de Vries et al., 2018; Zeng et al., 2019). It was found that the diversity of bacterial community structure in tomato soil treated with L1 was higher than that of L2. It may be due to the high soil volumetric water content and strong soil aeration in the tillage layer with a micropore group spacing of 30 cm. The average soil volumetric water content in the 0-40 cm soil layer of spring tomato and autumn tomato irrigated by L1 treatment was about 2.18% and 3.61% higher than that of L2, and the soil water filling porosity was only 0.92 and 0.93 times that of L2. The higher water vapor environment of the soil can reduce the limitation of drought stress and hypoxia stress on soil bacterial community (Hartmann and Six, 2022; Tang et al., 2022). This conclusion is consistent with the study of Qu (Qu et al., 2022) and Alekhina (Alekhina et al., 2001) that drought stress reduces the diversity of soil bacterial community structure. The L1 had higher soil GAN of tomato than L2. It may be due to the fact that the L1 has higher soil volume moisture content and strong soil ventilation, increase root exudates and root nitrogenase activity and increase the process of above-ground carbon assimilation of tomato. Further increase the transport of carbohydrates to the underground part of tomato (root), higher root morphological development can provide more living substrates for soil bacteria (Pathania et al., 2020; Tiziani et al., 2022; Wang et al., 2023). At the same time, the rhizobia in tomato soil were greatly affected by soil moisture, which easily affected the identification and infection of host plants, and finally promoted the abundance of functional genes of soil bacterial nitrogen metabolism under L1 treatment irrigation (Mantovani et al., 2014).

The C can change the composition of microbial community by changing the wet/dry conditions of soil, thus changing the mineralization rate of soil nutrients and affecting the absorption capacity of crop roots to nutrients (Wang Z. et al., 2022; Wang et al., 2021). This study found that the diversity of bacterial community structure in tomato rhizosphere soil of C2 treatment

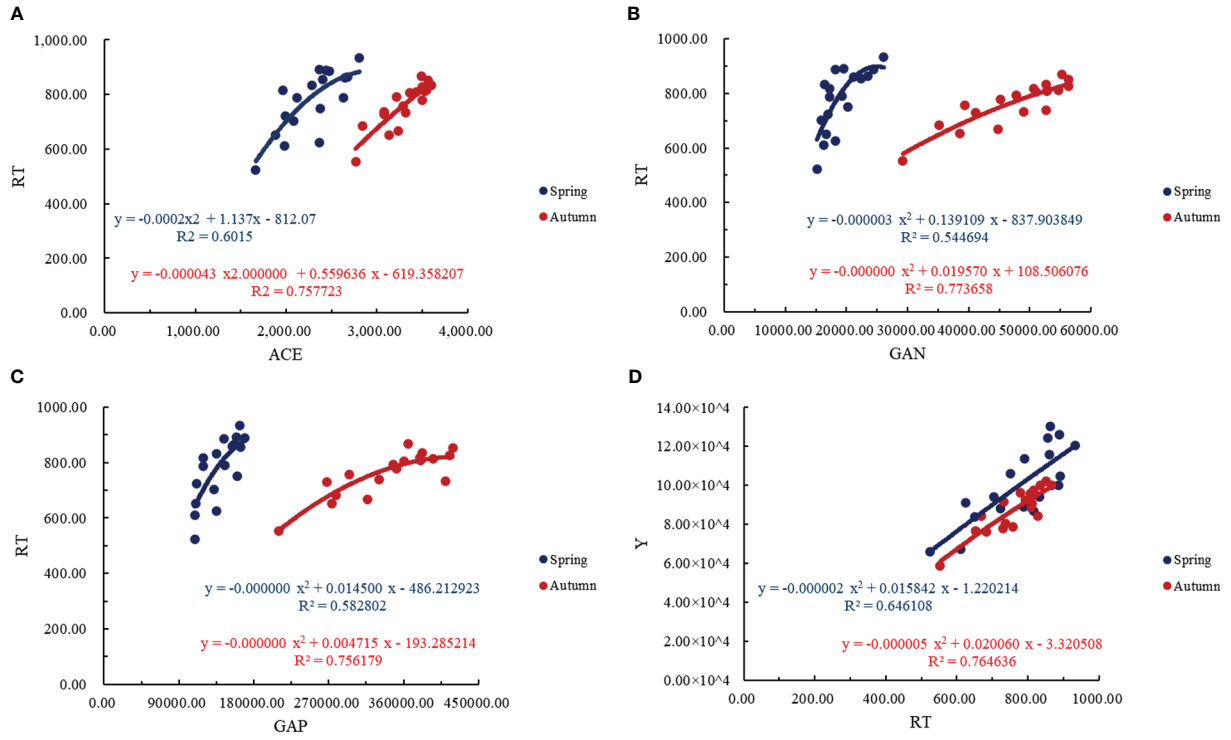

FIGURE 10
Quantitative analysis of tomato soil bacterial community, root system and yield in greenhouse. **(A)** represents the regression analysis of ACE index of soil bacterial and total number of root tips, **(B)** represents the regression analysis of soil bacterial nitrogen metabolism functional gene abundance and total number of root tips, **(C)** represents the regression analysis of soil bacterial phosphorus metabolism functional gene abundance and total number of root tips, **(D)** represents the regression analysis of yield and total number of root tips. The ACE represents ACE index of soil bacterial, the GAN represents the soil bacterial nitrogen metabolism functional gene abundance, GAP represents the soil bacterial phosphorus metabolism functional gene abundance, the RT represents the total number of root tips, the Y represents the yield.

was significantly higher than that of C3 treatment. It may be because the soil water availability per unit irrigated plough layer of C2 treatment is significantly higher than that of C3 by 6.67% and 6.69%, respectively. Stress effects of lower soil moisture increase on soil microorganisms (Alekhina et al., 2001). At the same time, the irrigation control area of C3 is larger, the irrigation amount in the plot is larger, and the local soil moisture experience is longer and higher, which is easy to increase the effect of low oxygen stress on soil microorganisms. The uneven distribution of soil moisture per unit area of C3 promotes the soil organisms in the rhizosphere of tomato under low water and low oxygen stress. Because of the existence of the filtration mechanism of the living environment, some bacteria in the soil are eliminated (Xu et al., 2020; Yang et al., 2020). The conclusion of this study is consistent with the conclusion of Wang (Wang, 2017) that the capillary density of one tube and two rows of drip irrigation promotes the diversity of microbial community structure in greenhouse tomato rhizosphere soil, and it is also consistent with the conclusion that the excessive number of dry-wet cycles of Jiao (Jiao et al., 2022) reduces the diversity of soil bacterial structure. The study also found that the abundance of nitrogen and phosphorus metabolism functional genes in C2 treated tomato rhizosphere soil was significantly higher than that in C3. It may be due to the decrease of soil litter concentration and carbon decomposition under C3, the substrate concentration of soil nitrogen and phosphorus bacteria decreased, and then decreased the abundance of nitrogen and phosphorus metabolism genes of soil bacteria (Jin et al., 2013; Zhang J. et al., 2022; Ullah et al., 2023).

4.2 The layout measures regulate the root system of greenhouse tomato

The effect of C change of MSPF on soil wetted body is similar to that of dripper spacing change (Chen et al., 2010; Zhang M. et al., 2022). There is a phenomenon that wetting fronts intersect between two adjacent groups of micropores on the pipe. The larger the distance is, the smaller the ratio of horizontal migration distance to vertical migration distance of soil moisture wetting front is, which is not conducive to the overall deep migration of soil moisture between two groups of micropores on the capillary. The volumetric water content and irrigation uniformity of plough layer per unit area will decrease (Ould Mohamed El-Hafedh et al., 2001; Sun and Wang, 2007; Del Vigo et al., 2020). The average soil volumetric water content in 0-40 cm soil layer of spring tomato and autumn tomato in L1 was 2.18% and 3.61% higher than that in L2. The higher soil volumetric water content in the plough layer was beneficial to the development of crop root morphology (Abdelhafeez et al., 1975; Silveira et al., 2020). This may be one of the reasons why the

root morphological development and root activity of spring tomato and autumn tomato under L1 were higher than those under L2. The conclusion of this study is consistent with Zhang (Zhang S. et al., 2022) who found that the uniformity of soil nutrient distribution of drip irrigation 30 cm dripper spacing is higher than that of 50 cm dripper spacing, which is conducive to the development of apple root morphology.

This study found that too high or too low capillary density was not conducive to tomato root morphological development. It may be due to the increase of the outflow cross section per unit area in the test area when the C is too high (C1), which is easy to be saturated in shallow soil, form water accumulation layer on the surface, restrict the exchange of soil air and external gas, produce hypoxia stress and restrict root growth (Aixia et al., 2022; Junhao et al., 2022). When the C was too low (C3), the outflow cross section per unit area in the experimental plot decreased, the soil moisture distribution per unit area was uneven, the deep leakage increased, which led to the decrease of soil moisture in tomato tillage layer. The average soil volumetric water content in the cultivated layer (0-40 cm) of spring tomato and autumn tomato treated with C2 was significantly higher than that of C3 by about 6.67% and 6.69%, respectively. Drought stress limits root morphological development (Enciso et al., 2007; Samoy-Pascual et al., 2022; Fan et al., 2023). The conclusion of this study is consistent with the conclusion of Liu's (Liu et al., 2019) study that too high or too low drip pipe spacing is not conducive to the development of alfalfa root morphology under drip irrigation.

4.3 Layout measures to regulate bacterial community and root interaction in tomato soil

Previous studies have found that the difference in soil water distribution caused by irrigation can significantly affect soil bacterial community, crop root morphological development, and increase or decrease soil carbon, nitrogen and phosphorus metabolic activity (Wang et al., 2021; Wang J. et al., 2022). It was found that there was a significant positive correlation between the diversity of bacterial community structure soil, the abundance of soil nitrogen and phosphorus metabolic genes in tomato rhizosphere and the RA, RL and RT of tomato roots. It may be that the RA, RL and RT determine the distribution and structure of tomato root system in soil. The high values of these indexes can improve the ability of plant roots to obtain soil moisture and nutrients, to colonize roots and enhance and enhance the strength of root-microorganism interaction. On the contrary, the diversity and abundance of soil bacterial community structure are high, which is conducive to the mineralization of soil organic matter, more soil nutrients are absorbed and utilized by plants, and the development of tomato root morphology is promoted (Leng et al., 2022; Andrade et al., 2023). It is consistent with the conclusion that Wang (Wang et al., 2017) drip irrigation crop root length is positively correlated with soil bacterial community structure diversity and yield, which is consistent with the conclusion that Nazir (Nazir et al., 2021) drip irrigation rape root activity, length and yield are positively correlated.

Previous studies have found that there is an interactive relationship between tomato root morphological development and soil microorganisms (Wang J. et al., 2022). In this study, the root morphological development of L1C2 treatment is better, which may be one of the reasons why the soil bacterial community of L1C2 treatment is superior to the other five treatments. In addition, we found that the RT was the key factor of tomato soil bacteria and tomato root interaction and played an important role in enhancing the positive interaction between soil bacteria and roots (Figure 10). The L1C2 significantly increased the RT of tomato, thus promoting the benign interaction between bacteria and roots in tomato soil. The effect of the layout measures of MSPF on the interaction between soil bacteria community and roots in tomato will inevitably affect the tomato yield. In this study, we found that the RT and ACE had the greatest influence on tomato yield under the regulation of MSPF. It may be that the layout measures of MSPF directly affects the RT and soil bacteria, and indirectly affects the interaction between tomato root system and soil bacteria through soil moisture, and regulates tomato yield directly or indirectly. In this study, the soil moisture distribution in the root zone of tomato treated with L1C2 was uniform, and the RT and ACE were significantly increased, which promoted the tomato yield under L1C2 better than other treatments.

5 Conclusion

By exploring the layout measures of MSPF to regulate the soil bacterial community and root morphological development of tomato in greenhouse, it was found that the diversity and abundance of soil bacterial community structure of spring tomato and autumn tomato in L1 were higher than those of L2. Among them, the total number of OTUs classification of soil bacteria in spring tomato and autumn tomato with L1 was higher than that of L2 by about 13.50% and 6.16%, respectively, and the ACE in spring tomato and autumn tomato with L1 was higher than that of L2 about 6.90% and 8.19%, respectively. The GAN and GAP in spring tomato and autumn tomato soil with L1 was higher than that of L2 about 11.00% and 8.99%, 6.69% and 15.34%, respectively. As a result, the yield and water use efficiency of spring tomato and autumn tomato treated with L1 were higher than those of L2 by about 14.15% and 11.27%, 12.64% and 10.35%, respectively. With the decrease of C, the diversity of soil bacterial community structure decreased significantly. Among them, the ACE and total number of OTUs classification of soil bacteria with C2 was significantly higher than that of C3 about 27.59% and 9.85%, 30.68% and 16.21%, respectively. The GAN and GAP decreased with the decrease of C. For example, the GAN and GAP in soil of spring tomato and autumn tomato with C2 was significantly higher than that of C3 about 14.83% and 26.36%, 27.97% and 19.29%, respectively. Lower soil bacterial community structure diversity and soil bacterial nitrogen and phosphorus metabolism functional gene abundance reduced greenhouse tomato soil nitrogen and phosphorus cycle. As a result, the yield and water use efficiency of spring and

autumn tomatoes with C2 were significantly higher than those of C3 by 34.76% and 15.23%, 31.94% and 13.91%, respectively. Pearson two-tailed test and regression analysis showed that there was a positive interaction between soil bacterial community and root morphological development. The relationship between soil bacterial community and RT was a quadratic curve, and the relationship between RT and yield was also quadratic curve, indicating that the RT of tomato could be used to estimate the yield, and the tomato production potential in this area could be indirectly evaluated by soil bacterial community. This study provides a reference for regulating tomato root system and soil microbial interaction and increasing tomato yield by optimizing the layout measures of MSPF.

Data availability statement

The data presented in the study are deposited in the figshare repository, https://figshare.com/articles/dataset/The_Layout_Measures_of_Micro-sprinkler_Irrigation_under_Plastic_Film_Regulate_Tomato_Soil_Bacterial_Community_and_Root_System/21818610.

Author contributions

MZ wrote and revised the manuscript. YL participated in the experiments. NX, HY, FG, and JL collected the materials and analyzed the data. YL, ZZ and MZ conceived and designed the research. All authors contributed to the article and approved the submitted version.

Funding

This work is supported jointly by Natural Science Foundation of China (No. 41807041), Ninth batch of key disciplines in Henan Province—Mechanical Design, Manufacturing and Automation (JG [2018] No.119), Key Research and Development Program of Shaanxi (No. 2022NY-191), Funda-mental Research Funds for the Central Universities (GK202103129), and the Program of Introducing Talents of Discipline to Universities (B16011).

Conflict of interest

Author FG was employed by Yellow River Hydrologic Survey Planning and Design Co.,Ltd. Author JL was employed by Agricultural Technology Extension Center of Xi'an City.

The remaining authors declare that the research was conducted in the absence of any commercial or financial relationships that could be construed as a potential conflict of interest.

Publisher's note

References

Abdelhafeez, A. T., Harssema, H., and Verkerk, K. (1975). Effects of air temperature, soil temperature and soil moisture on growth and development of tomato itself and grafted on its own and egg-plant rootstock. *Scientia Hortic.* 3, 65–73. doi: 10.1016/0304-4238(75)90035-7

Aixia, R., Weifeng, Z., Anwar, S., Wen, L., Pengcheng, D., Ruixuan, H., et al. (2022). Effects of tillage and seasonal variation of rainfall on soil water content and root growth distribution of winter wheat under rainfed conditions of the loess plateau, China. *Agric. Water Manage.* 268, 107533. doi: 10.1016/j.agwat.2022.107533

Alekhina, L. K., Dobrovol'Skaya, T. G., Pochatkova, T. N., and Zvyagintsev, D. G. (2001). Evaluation of bacterial diversity in soil microcosms at different moisture contents. *Microbiology* 70, 731–737. doi: 10.1023/A:1013100218465

Andrade, G. V. S., Rodrigues, F. A., Nadal, M. C., Da Silva Dambroz, C. M., Martins, A. D., Rodrigues, V. A., et al. (2023). Plant-endophytic bacteria interactions associated with root and leaf microbiomes of cattleya walkeriana and their effect on plant growth. *Scientia Hortic.* 309, 111656. doi: 10.1016/j.scienta.2022.111656

Boddington, C. L., and Dodd, J. C. (1999). Evidence that differences in phosphate metabolism in mycorrhizas formed by species of glomus and gigaspora might be related to their life-cycle strategies. *New Phytol.* 142, 531–538. doi: 10.1046/j.1469-8137.1999.00422.x

Chen, R., Wang, Q., and Yang, Y. (2010). Numerical analysis of layout parameters and reasonable design of grape drip irrigation system for stony soil in xinjiang uighur autonomous region. *Trans. Chin. Soc. Agric. Eng. (Transactions CSAE)* 26, 40–46. doi: 10.3969/j.issn.1002-6819.2010.12.007

Del Vigo, Á., Zubelzu, S., and Juana, L. (2020). Numerical routine for soil water dynamics from trickle irrigation. *Appl. Math. Model.* 83, 371–385. doi: 10.1016/j.apm.2020.01.058

de Vries, F. T., Griffiths, R. I., Bailey, M., Craig, H., Girlanda, M., Gweon, H. S., et al. (2018). Soil bacterial networks are less stable under drought than fungal networks. *Nat. Commun.* 9, 3033–3033. doi: 10.1038/s41467-018-05516-7

Enciso, J., Jifon, J., and Wiedenfeld, B. (2007). Subsurface drip irrigation of onions: Effects of drip tape emitter spacing on yield and quality. *Agric. Water Manage.* 92, 126–130. doi: 10.1016/j.agwat.2007.05.017

Fan, J., Wu, X., Yu, Y., Zuo, Q., Shi, J., Halpern, M., et al. (2023). Characterizing root-water-uptake of wheat under elevated CO2 concentration. *Agric. Water Manage.* 275, 108005. doi: 10.1016/j.agwat.2022.108005

Feng, S., Ding, W., Shi, C., Zhu, X., Hu, T., and Ru, Z. (2023). Optimizing the spatial distribution of roots by supplemental irrigation to improve grain yield and water use efficiency of wheat in the north China plain. *Agric. Water Manage.* 275, 107989. doi: 10.1016/j.agwat.2022.107989

Guo, Y., Chen, X., Wu, Y., Zhang, L., Cheng, J., Wei, G., et al. (2018). Natural revegetation of a semiarid habitat alters taxonomic and functional diversity of soil microbial communities. *Sci. Total Environ.* 635, 598–606. doi: 10.1016/j.scitotenv.2018.04.171

Hartmann, M., and Six, J. (2022). Soil structure and microbiome functions in agroecosystems. *Nat. Rev. Earth Environment.* 4, 4–18. doi: 10.1038/s43017-022-00366-w

Huang, Y., Huang, M., Chai, L., and Zhao, Y. (2018). Drivers of the spatial patterns of soil microbial communities in arid and semi-arid regions. *Ecol. Environ. Sci.* 27, 191–198. doi: CNKI:SUN:TRYJ.0.2018-01-026

Jafari, M., Yari, M., Ghabooli, M., Sepehri, M., Ghasemi, E., and Jonker, A. (2018). Inoculation and co-inoculation of alfalfa seedlings with root growth promoting microorganisms (piriformospora indica , glomus intraradices and sinorhizobium meliloti) affect molecular structures, nutrient profiles and availability of hay for ruminants. *Anim. Nutr.* 4, 90–99. doi: 10.1016/j.aninu.2017.08.008

Jiao, P., Xiao, H., Li, Z., Yang, L., and And Zheng, P. (2022). Drying-rewetting cycles reduce bacterial diversity and carbon loss in soil on the loess plateau of China. *Pedosphere* 9, 1262–1273. doi: 10.1016/j.pedsph.2022.09.002

Jin, V. L., Haney, R. L., Fay, P. A., and Polley, H. W. (2013). Soil type and moisture regime control microbial c and n mineralization in grassland soils more than

atmospheric CO2-induced changes in litter quality. *Soil Biol. Biochem.* 58, 172–180. doi: 10.1016/j.soilbio.2012.11.024

Junhao, C., Pengpeng, C., Xiaodong, G., Qifang, Z., Yunjie, F., Xiaobo, G., et al. (2022). Effects of plastic film residue and emitter flow rate on soil water infiltration and redistribution under different initial moisture content and dry bulk density. *Sci. Total Environ.* 807, 151381. doi: 10.1016/j.scitotenv.2021.151381

Leng, Z., Wu, Y., Li, J., Nie, Z., Jia, H., Yan, C., et al. (2022). Phenolic root exudates enhance avicennia marina tolerance to cadmium under the mediation of functional bacteria in mangrove sediments. *Mar. pollut. Bull.* 185, 114227. doi: 10.1016/j.marpolbul.2022.114227

Lewis, W. H., Tahon, G., Geesink, P., Sousa, D. Z., and Ettema, T. J. G. (2020). Innovations to culturing the uncultured microbial majority. *Nat. Rev. Microbiol* 19 (4), 225–240.

Li, D., and Ma, K. (2018). PICRUSt-based predicted metagenomic analysis of treeline soil bacteria on mount Dongling, Beijing. *Acta Ecologica Sin.* 38, 2180–2186. doi: 10.5846/stxb201703130423

Li, Y., Niu, W., Zhang, M., Wang, J., and Zhang, Z. (2020). Artificial soil aeration increases soil bacterial diversity and tomato root performance under greenhouse conditions. *Land Degradation Dev.* 31, 1443–1461. doi: 10.1002/ldr.3560

Li, X., Yang, J., Jia, H., Lv, Q., Sha, R., Yao, D., et al. (2023). Impact of fruit tree hole storage brick treatment on the growth of grape seedlings and water transport in the root zone under root restriction and subsurface drip irrigation. *Scientia Hortic.* 308, 111552. doi: 10.1016/j.scienta.2022.111552

Liu, Y., Jiao, X., Chen, J., and Wang, S. F. (2019). Effect of drip-line distance of shallow buried drip irrigation on the growth of alfalfa. *J. Water Resour. Water Eng.* 30, 255–260. doi: CNKI:SUN:XBSZ.0.2019-05-038

Ma, W., Du, W., Gu, K., Xu, M., Yin, Y., Sun, Y., et al. (2023). Elevated CO_2 exacerbates effects of TiO2 nanoparticles on rice (Oryza sativa l.) leaf transcriptome and soil bacteria. *Sci. Total Environ.* 857, 159689.

Mantovani, D., Veste, M., Boldt-Burisch, K., Fritsch, S., Koning, L. A., and Freese, D. (2014). Carbon allocation, nodulation, and biological nitrogen fixation of black locust (Robinia pseudoacacia l.) under soil water limitation. *Ann. For. Res.* 58, 1–16. doi: 10.15287/afr.2015.420

Morio, K. A., Sternowski, R. H., and Brogden, K. A. (2022). Dataset of endodontic microorganisms killed at 265 nm wavelength by an ultraviolet c light emitting diode in root canals of extracted, instrumented teeth. *Data Brief* 40, 107750. doi: 10.1016/j.dib.2021.107750

Nazir, F., Fariduddin, Q., Hussain, A., and Khan, T. A. (2021). Brassinosteroid and hydrogen peroxide improve photosynthetic machinery, stomatal movement, root morphology and cell viability and reduce Cu- triggered oxidative burst in tomato. *Ecotoxicology Environ. Saf.* 207, 111081. doi: 10.1016/j.ecoenv.2020.111081

Nie, K., Bai, Q., Chen, C., Zhang, M., and Li, Y. (2022). DMPP and polymer-coated urea promoted growth and increased yield of greenhouse tomatoes. *Horticulturae* 8, 472. doi: 10.3390/horticulturae8060472

Ould Mohamed El-Hafedh, A. V., Daghari, H., and Maalej, M. (2001). Analysis of several discharge rate–spacing–duration combinations in drip irrigation system. *Agric. Water Manage.* 52, 33–52. doi: 10.1016/S0378-3774(01)00126-3

Özbolat, O., Sánchez-Navarro, V., Zornoza, R., Egea-Cortines, M., Cuartero, J., Ros, M., et al. (2023). Long-term adoption of reduced tillage and green manure improves soil physicochemical properties and increases the abundance of beneficial bacteria in a Mediterranean rainfed almond orchard. *Geoderma* 429, 116218. doi: 10.1016/j.geoderma.2022.116218

Pathania, P., Bhatia, R., and Khatri, M. (2020). Cross-competence and affectivity of maize rhizosphere bacteria bacillus sp. MT7 in tomato rhizosphere. *Scientia Hortic.* 272, 109480. doi: 10.1016/j.scienta.2020.109480

Qu, Z. M., Haojie, F., Qi, C., Yanli, L., and Chengliang, L. (2022). Effects of controlled release potassium chloride application on rhizosphere bacterial community and metabolites under reduced irrigation volume. *Appl. Soil Ecol.* 180, 104617.

Samoy-Pascual, K., Lampayan, R. M., Remocal, A. T., Orge, R. F., Tokida, T., and Mizoguchi, M. (2022). Optimizing the lateral dripline spacing of drip-irrigated aerobic rice to increase water productivity and profitability under the water-limited condition. *Field Crops Res.* 287, 108669. doi: 10.1016/j.fcr.2022.108669

Silveira, L. K., Pavão, G. C., Dos Santos Dias, C. T., Quaggio, J. A., and Pires, R. C. D. M. (2020). Deficit irrigation effect on fruit yield, quality and water use efficiency: A long-term study on pêra-IAC sweet orange. *Agric. Water Manage.* 231, 106019. doi: 10.1016/j.agwat.2020.106019

Sun, A., Jiao, X., Chen, Q., Wu, A., Zheng, Y., Lin, Y., et al. (2021). Microbial communities in crop phyllosphere and root endosphere are more resistant than soil microbiota to fertilization. *Soil Biol. Biochem.* 153, 108113. doi: 10.1016/j.soilbio.2020.108113

Sun, H., and Wang, Q. (2007). Research for soil water movement from drip irrigation iterference infiltration. *J. Soil Water Conserv.*, 115–118.

Tang, Y., Winterfeldt, S., Brangarí, A. C., Hicks, L. C., and Rousk, J. (2022). Higher resistance and resilience of bacterial growth to drought in grasslands with historically lower precipitation. *Soil Biol. Biochem.* 177, 108889.

Tiziani, R., Miras-Moreno, B., Malacrinò, A., Vescio, R., Lucini, L., Mimmo, T., et al. (2022). Drought, heat, and their combination impact the root exudation patterns and rhizosphere microbiome in maize roots. *Environ. Exp. Bot.* 203, 105071. doi: 10.1016/j.envexpbot.2022.105071

Ullah, M. R., Carrillo, Y., and Dijkstra, F. A. (2023). Relative contributions of fungi and bacteria to litter decomposition under low and high soil moisture in an Australian grassland. *Appl. Soil Ecol.* 182, 104737. doi: 10.1016/j.apsoil.2022.104737

Vera, A., Bastida, F., Patiño-García, M., and Moreno, J. L. (2023). The effects of boron-enriched water irrigation on soil microbial community are dependent on crop species. *Appl. Soil Ecol.* 181, 104677. doi: 10.1016/j.apsoil.2022.104677

Veresoglou, S. D., Li, G. C., Chen, J., and Johnson, D. (2022). Direction of plant–soil feedback determines plant responses to drought. *Global Change Biol.* 28, 3995–3997. doi: 10.1111/gcb.16204

Wang, J. (2017). *Effect of mulched drip irrigation on crop root-zone soil microenvironment and crop growth in plastic greenhouse* (Northwest A&F University). http://cdmd.cnki.com.cn/Article/CDMD-10712-1017064536.htm.

Wang, J., Du, Y., Niu, W., Han, J., Li, Y., and Yang, P. (2022). Drip irrigation mode affects tomato yield by regulating root–soil–microbe interactions. *Agric. Water Manage.* 260, 107188. doi: 10.1016/j.agwat.2021.107188

Wang, J., Li, Y., and Niu, W. (2020a). Deficit alternate drip irrigation increased root-Soil-Plant interaction, tomato yield, and quality. *Int. J. Environ. Res. Public Health* 17, 781. doi: 10.3390/ijerph17030781

Wang, J., Li, Y., and Niu, W. (2021). Effect of alternating drip irrigation on soil gas emissions, microbial community composition, and root–soil interactions. *Agric. Water Manage.* 256, 107123. doi: 10.1016/j.agwat.2021.107123

Wang, Z., Li, X., Wang, J., Qi, S., Dai, Z., and Du, D. (2022). Effect of nitrogen-fixing bacteria on resource investment of the root system in an invasive clonal plant under low nutritional environment. *Flora* 297, 152166. doi: 10.1016/j.flora.2022.152166

Wang, X., Luo, J. F., Liu, R., Liu, X., and Jiang, J. (2023). Gibberellins regulate root growth by antagonizing the jasmonate pathway in tomato plants in response to potassium deficiency. *Scientia Hortic.* 309, 111693. doi: 10.1016/j.scienta.2022.111693

Wang, J., Niu, W., and Li, Y. (2020b). Nitrogen and phosphorus absorption and yield of tomato increased by regulating the bacterial community under greenhouse conditions via the alternate drip irrigation method. *Agronomy* 10, 315. doi: 10.3390/agronomy10030315

Wang, J., Niu, W., Xu, J., and Li, Y. (2016). Effects of drip irrigation under plastic film on muskmelon soil environment and yield in greenhouse. *Trans. Chin. Soc. Agric. Eng. (Transactions CSAE)* 32 (6), 232–241. doi: 10.11975/j.issn.1002-6819.2016.06.032

Wang, J., Niu, W., Zhang, M., and Li, Y. (2017). Effect of alternate partial root-zone drip irrigation on soil bacterial communities and tomato yield. *Appl. Soil Ecol.* 119, 250–259. doi: 10.1016/j.apsoil.2017.06.032

Xiao, W., Zhang, Q., Zhao, S., Chen, D., Gao, N., Huang, M., et al. (2023). Citric acid secretion from rice roots contributes to reduction and immobilization of Cr(VI) by driving microbial sulfur and iron cycle in paddy soil. *Sci. Total Environ.* 854, 158832. doi: 10.1016/j.scitotenv.2022.158832

Xu, H., Qu, Q., Li, G., Liu, G., Geissen, V., Ritsema, C. J., et al. (2022). Impact of nitrogen addition on plant-soil-enzyme c–N–P stoichiometry and microbial nutrient limitation. *Soil Biol. Biochem.* 170, 108714. doi: 10.1016/j.soilbio.2022.108714

Xu, X., Wang, N., Lipson, D., Sinsabaugh, R., Schimel, J., He, L., et al. (2020). Microbial macroecology: In search of mechanisms governing microbial biogeographic patterns. *Global Ecol. Biogeography* 29, 1870–1886. doi: 10.1111/geb.13162

Yang, Y., Liang, C., Wang, Y., Cheng, H., An, S., and Chang, S. X. (2020). Soil extracellular enzyme stoichiometry reflects the shift from p- to n-limitation of microorganisms with grassland restoration. *Soil Biol. Biochem.* 149, 107928. doi: 10.1016/j.soilbio.2020.107928

Ye, D., Q, R., Zhang, M., and And Li, H. (2016). Study of saving-irrigation regulated the soil microbial Characteristics, Soil enzyme activities and soil nutrient in the winter wheat field. *Acta Agriculturae Boreali-Sinica* 31, 224–231. doi: 10.7668/hbnxb.2016.01.036

Zeng, Q., An, S., Liu, Y., Wang, H., and Wang, Y. (2019). Biogeography and the driving factors affecting forest soil bacteria in an arid area. *Sci. Total Environ.* 680, 124–131. doi: 10.1016/j.scitotenv.2019.04.184

Zhang, S., Hu, T., Chen, S., Li, H., and Zhang, J. (2022). Effects of drip technical parameters and fertilization cycle on spatial and temporal distribution of nitrate nitrogenin apple root-zone soil. *Agric. Res. Arid Areas* 40, 79–87. doi: 10.7606/j.issn.1000-7601.2022.03.10

Zhang, M., Li, Y., Liu, J., Wang, J., Zhang, Z., and Xiao, N. (2022). Changes of soil water and heat transport and yield of tomato (Solanum lycopersicum) in greenhouses with micro-sprinkler irrigation under plastic film. *Agron. (Basel)* 12, 664. doi: 10.3390/agronomy12030664

Zhang, M., Lu, Z., Bai, Q., Zhang, Y., Qiu, X., Qin, H., et al. (2020a). Effect of microsprinkler irrigation under plastic film on photosynthesis and fruit yield of greenhouse tomato. *J. Sensors* 2020, 1–14. doi: 10.1155/2020/8849419

Zhang, M., Niu, W., Bai, Q., Li, Y., Wang, J., Wang, Z., et al. (2020b). Improvement of quality and yield of greenhouse tomato (Solanum lycopersicum l.) plants by micro-sprinkler irrigation under plastic film. *Appl. Ecol. Environ. Res.* 18, 6905–6926. doi: 10.15666/aeer/1805_69056926

Zhang, J., Zhang, B., Liu, Y., Guo, Y., Shi, P., and Wei, G. (2018). Distinct large-scale biogeographic patterns of fungal communities in bulk soil and soybean rhizosphere in China. *Sci. Total Environ.* 644, 791–800. doi: 10.1016/j.scitotenv.2018.07.016

Zhang, J., Zhou, J., Lambers, H., Li, Y., Li, Y., Qin, G., et al. (2022). Nitrogen and phosphorus addition exerted different influences on litter and soil carbon release in a tropical forest. *Sci. Total Environ.* 832, 155049. doi: 10.1016/j.scitotenv.2022.155049

Zhao, M., Li, C., Zhang, C., Han, B., Wang, X., Zhang, J., et al. (2022). Typical microplastics in field and facility agriculture dynamically affect available cadmium in different soil types through physicochemical dynamics of carbon, iron and microbes. *J. Hazardous Materials* 440, 129726. doi: 10.1016/j.jhazmat.2022.129726

Zhao, Q., Xing, Y., Sun, Y., Lin, X., Zhu, F. F., Long, Y. Z., et al. (2017). Effects of different soil conditioner application on coffee seedlings growth and soil enzyme activities in acidic continuous cropping soil. *Chin. J. Trop. Crops* 38, 1868–1873. doi: 10.3969/j.issn.1000-2561.2017.10.016

Zheng, W., Wu, Q., Rao, C., Chen, X., Wang, E., Liang, X., et al. (2023). Characteristics and interactions of soil bacteria, phytocommunity and soil properties in rocky desertification ecosystems of southwest China. *CATENA* 220, 106731. doi: 10.1016/j.catena.2022.106731

Zhou, Y., Ma, J., Yang, J., Lv, Z., Song, Z., and Han, H. (2023). Soybean rhizosphere microorganisms alleviate Mo nanomaterials induced stress by improving soil microbial community structure. *Chemosphere* 310, 136784. doi: 10.1016/j.chemosphere.2022.136784

Zhu, X., Gong, W., Li, W., Bai, X., and Zhang, C. (2022). Reclamation of waste coal gangue activated by stenotrophomonas maltophilia for mine soil improvement: Solubilizing behavior of bacteria on nutrient elements. *J. Environ. Manage.* 320, 115865. doi: 10.1016/j.jenvman.2022.115865

Zhu, X., Shen, C., Chen, G., Zhang, W., Li, B., and And Wang, G. (2019). Advancement in research on bacterial chemotaxis in soil. *Acta Pedologica Sin.* 56, 259–275.

frontiers | Frontiers in Plant Science

TYPE Original Research
PUBLISHED 23 March 2023
DOI 10.3389/fpls.2023.1161469

OPEN ACCESS

EDITED BY
Xuewen Wang,
University of North Texas Health Science Center, United States

REVIEWED BY
Yadong Cheng,
Chinese Academy of Agricultural Sciences (CAAS), China
Weiren Wu,
Fujian Agriculture and Forestry University, China

*CORRESPONDENCE
Shiping Zhu
zhushiping@cric.cn

SPECIALTY SECTION
This article was submitted to Plant Symbiotic Interactions, a section of the journal Frontiers in Plant Science

RECEIVED 08 February 2023
ACCEPTED 10 March 2023
PUBLISHED 23 March 2023

CITATION
Zhang M, Li X, Wang X, Feng J and Zhu S (2023) Potassium fulvic acid alleviates salt stress of citrus by regulating rhizosphere microbial community, osmotic substances and enzyme activities.
Front. Plant Sci. 14:1161469.
doi: 10.3389/fpls.2023.1161469

Potassium fulvic acid alleviates salt stress of citrus by regulating rhizosphere microbial community, osmotic substances and enzyme activities

Manman Zhang[1,2], Xiaoya Li[1,2], Xiaoli Wang[1,2], Jipeng Feng[1,2] and Shiping Zhu[1,2]*

[1]Citrus Research Institute, Southwest University, Chongqing, China, [2]National Citrus Engineering Research Center, Beibei, Chongqing, China

Salt stress damage to plants has been becoming a global concern for agriculture. The application of potassium fulvic acid (PFA) is a promising strategy to alleviate the damage to plants and improve soil quality. However, the study of PFA on plant growth and rhizosphere microbial community remains limited. In this study, microcosmic experiments were conducted to verify the effect of PFA on citrus. Trifoliate orange (*Poncirus trifoliata*), the most important citrus rootstock, was used to evaluate the effect of PFA on salt damage. The results showed that PFA significantly increased the contents of chlorophyll a, chlorophyll b and carotenoid by 30.09%, 17.55% and 27.43%, and effectively avoided the yellowing and scorching of leaves under salt stress. Based on the results of two-way ANOVA, the mitigation of salt stress on trifoliate seedlings primarily attributed to the enhancement of protective enzyme activities, K^+/Na^+ ratio and the contents of soluble sugar, soluble protein and proline. Moreover, PFA enhanced neutral protease (S-NPT), sucrase (S-SC) and urease (S-UE) of rhizosphere soil and improved soil nutrition status. The abundance of *Bacillus*, a kind of rhizosphere beneficial bacteria, was improved by PFA under salt stress, which was mainly associated with the increased activities of S-NPT, S-SC and S-UE. Overall, the application of PFA showed great potential for the alleviation of salt damage on citrus.

KEYWORDS

potassium fulvic acid, microbial community, salt stress, citrus rootstock, distance-based redundancy analysis

Introduction

Soil salinity, mainly caused by chaotic fertilization, poor irrigation and anthropogenic pollution, has seriously affected more than 6% of the world's lands (Hassani et al., 2020; Mukhopadhyay et al., 2020). High salinity affects the growth and production of crops by preventing absorbing water and various nutrition elements from

the soil (Mukhopadhyay et al., 2020; Sun et al., 2022; Zied et al., 2022). Citrus belongs to sweet-soil plant that is extremely sensitive to salt (Mokrani et al., 2020; Wei et al., 2020). Trifoliate orange (*Poncirus trifoliata*) is a widely used rootstock in citrus industry, which is sensitive to salt stress (Wei et al., 2021). Cl^- and Na^+ are the major elements for citrus salt stress, and excessive Cl^- and Na^+ can break the potential balance and increase the permeability of plasma membrane (Lin et al., 2015; Bankaji et al., 2019; Sun et al., 2022). Under salt stress, many adverse symptoms occur, such as chlorosis, scorching of leaf tip, early leaf falling and even trees dying (Wu et al., 2010; Navarro et al., 2014; Syvertsen and Garcia-Sanchez, 2014). Therefore, it is urgent to explore an effective, ecological and economic method to alleviate salt damage in citrus industry.

Fulvic acid (FA) is a short-chain molecular structure substance derived from natural humic acid, with high physiological activity and loading capacity (Islam et al., 2020; Brazien et al., 2021). FA can interact with oxides, hydroxides, metal ions, organic matter and minerals in the environment, effectively improve the availability of soil nutrients, reduce soil salinity, and promote plant growth (Brazien et al., 2021; Liu et al., 2022). Anjum et al. (2011) found that FA could enhance the activities of various antioxidant enzymes and protect plants from oxidative damage. The pre-treatment of FA improved salt tolerance of soybean (*Glycine max* L.) by maintaining ion balance (Dinler et al, 2016). In addition, Elrys et al. (2020) reported that under salt stress FA could promote the growth of wheat by reducing the level of active oxygen species and improving the antioxidant defense system. Potassium fulvic acid (PFA) is formed with FA by chelating K^+ and rich in exchangeable K (Qiao et al., 2022). Compared with FA, PFA has superior advantages in composition, performance, price and physiological activity (He et al., 2022; Qiao et al., 2022; Wang et al., 2022). Although PFA is widely used in improving soil properties and crop production, it is rarely used as a salt hazard mitigation agent in plant under salt stress.

Soil microorganism directly or indirectly interacts with the roots of plant to influence the growth and health (Berendsen et al., 2012; Bai et al., 2015). Simultaneously, roots affect the functions and structures of soil microbial community through the root exudates and the metabolic activities of the marginal cells (Bai et al., 2015; Hartmann et al., 2015; Fu et al., 2017). Recently, it has been proved that the interaction between soil microorganisms and plant roots mainly depends on the rhizosphere microorganisms, which play key roles in response to biotic and abiotic stresses (Qu et al., 2020; Liu et al., 2021). For example, rhizosphere beneficial bacteria (i.e., *Pseudomonas*, *Rhizobium*, *Bacillus*, *Pantoea*, *Berkholderia*, *Microbacterium*, *Achromobacter* and *Methylbacillus*) significantly improved the tolerance of hosts to salt stress (Grover et al., 2011). Rhizosphere growth-promoting bacteria (PGPR) can alleviate the damage of salt stress on plants through selective absorption of Na^+, K^+ and Ca^{2+}, and maintaining a high K^+/Na^+ ratio (Rojas-Tapias et al., 2012; Han et al., 2014). Ashraf et al. (2004) reported that the extracellular polysaccharide secreted by PGPR strains can not only bind cations, but also promote the formation of biofilm on the root surface, thus limiting the inflow of Na^+ into the body of plants. Consequently, the response of plant rhizosphere microbial community to the alleviation of salt damage on citrus should be considered.

In this study, the effect of PFA on the growth of trifoliate seedlings under salt stress was investigated with microcosmic experiments. We hypothesized that PFA could alleviate salt damage on citrus by regulating rhizosphere microbial community and enhancing the physicochemical properties and nutrient status of soil. The main objectives of this study were to: (i) investigate the effect of PFA on the growth and the characteristics of biochemistry and physiology of citrus under salt stress; (ii) evaluate the effect of PFA on the physicochemical properties and nutrient status of rhizosphere soil; (iii) illustrate the effect of PFA on microbial community of citrus root and rhizosphere soil; and (i) explore the correlations between properties, enzyme activities of rhizosphere soil and dominant microorganisms. We expected that the new insights from our study would contribute to further application of PFA for the alleviation of salt damage on citrus.

Material and methods

Microcosmic experiment design and sample collection

The mineral PFA was purchased from Stanley Agricultural Group Co., Ltd (Linyi City, Shandong Province, China). The soil sample (0-20 cm in depth) was collected from a citrus orchard located in Chongqing City, China (29.76°N, 106.38°E). The soil samples were air-dried, ground and screened with a sieve (aperture of 2 mm). The visibly similar citrus rootstock trifoliate orange (*Poncirus trifoliata*) seedlings (5 days after germination) grown under the same conditions were transferred to a plastic pot filled with the soil (250 g, with one seedling in each pot). The seedlings were treated as follows 30 days after transplanting: treated firstly with PFA solution (100 mg/L, 20 mL) for three times at an interval of one week, and then with NaCl solution (100 mM, 20 mL) for three times at an interval of one week (PFA+SS); treated with PFA solution as mentioned above, and then with equal amount of water (PFA); treated with equal amount of water in the first three weeks, and then with NaCl solution (100 mM, 20 mL) (SS); treated with only water during the whole process (CK). Each treatment contained a total of 45 seedlings and they were used for three biological repeats. The experiments were conducted in a greenhouse with temperature (25 ± 2°C) and humidity (50%-60%). The rhizosphere soil, fresh roots and leaves of the seedlings were collected 7 days after treatment.

Growth and characteristics analysis of citrus

The plant height, root length, and fresh/dry biomass of the seedlings were measured. The contents of chlorophyll a, chlorophyll b and carotenoid were determined by using spectrophotometry (Shang et al., 2021). The root vigor and the contents of soluble protein, soluble sugar, proline and malondialdehyde (MDA) in

fresh roots and leaves of the seedlings were analyzed using the corresponding test kits (Nanjing Boyan Biotechnology Co., Ltd., Nanjing City, Jiangsu Province, China). In addition, the activities of peroxidase (POD), catalase (CAT) and superoxide dismutase (SOD) of the seedling roots and leaves were measured using different enzyme-linked immunosorbent assay (ELISA) kits (Nanjing Boyan Biotechnology Co., Ltd., Nanjing City, Jiangsu Province, China), respectively. Based on the digestion systems of concentrated HNO_3 and $HClO_4$ (4:1, v/v), the concentrations of Na^+ and K^+ in the roots and leaves of the seedlings were determined with a flame atomic absorption spectrophotometer (Sun et al., 2022).

Physicochemical properties and enzyme activities analysis of the rhizosphere soil

The values of electrical conductivity (EC) and pH of the rhizosphere soil samples were all determined at a water/soil mass ratio of 5:1. The contents of ammonium nitrogen (AN) and nitrate nitrogen (NN) in rhizosphere soil samples were detected using Skalar Continuous Flow Analyzer 5000 (Skalar Analytical BV, Breda, Netherlands). The available phosphorus (AP) contents of soil samples were estimated using the ammonium acetate-flame photometer method (Yin et al., 2022). In addition, the potassium dichromate heating oxidation-volumetric method was used for the determination of organic matter (OM). The activities of the soil catalase (S-CAT), neutral protease (S-NPT), sucrase (S-SC) and urease (S-UE) were determined using enzyme activity test kits (Nanjing Boyan Biotechnology Co., Ltd., Nanjing City, Jiangsu Province, China), according to the manufacturer's instructions.

DNA extraction, PCR amplification, and 16S rRNA gene amplicon sequencing of root and rhizosphere soil samples

The FastDNA Spin Kit for Soil (MP Biomedicals, CA, United States) was used to extract the genomic DNA from the entire roots and rhizosphere soils. Following the manufacturer's instructions, 50 μL of DNA was extracted from root (250 mg) and rhizosphere soil (300 mg), and then stored at -20°C for further analysis. The universal primers 799F/1193R and ITS1F/ITS2R were used to amplified the V5-V7 regions of the 16S rRNA genes and ITS region 1 of the nuclear ribosomal coding cistron of the extracted DNA, respectively. The PCR amplification were performed according to Zheng et al. (2021) and Shang et al. (2021). After PCR amplification, the bands were excised and purified with 2% agarose gel using a PCR Purification Kit. The purified PCR products from all samples were collected, and paired-end sequencing was performed on the Illumina MiSeq sequencing platform (Shanghai Majorbio Bio-pharm Technology Co., Ltd., Shanghai City, China).

Amplicon sequence processing and bioinformatics analysis

Restricting the data to similarity of ≥97%, operational taxonomic unit (OTU) clustering of non-repetitive sequences was obtained using UPARSE (version 7.0.1090). The α-diversity (Chao 1 index) was calculated using *Mothur* software. To visualize the variations in microbial compositions, the principal components analysis (PCoA) of the treatments were applied using *QIIME* and *R* software (v. 3.5.3). The distance-based redundancy analysis (db-RDA) screened the environmental factors on the Majorbio i-Sanger Cloud Platform (Shanghai Majorbio Bio-pharm Technology Co., Ltd., Shanghai City, China, https://cloud.majorbio.com). Sequence data have been deposited in the NCBI Sequence Read Archive under BioProject number PRJNA935538.

Statistical analysis

Statistical analysis and figure creations was conducted using *SPSS Statistics 20.0* (Chicago, USA) and *Origin 8.5* (Northampton, USA), respectively. The significances between two different treatments were analyzed by Student's t test. Two-way ANOVA analyses were conducted to analyze the significance of interactions between PFA and SS. Data in the tables are expressed as means ± standard error (n = 3).

Results

Effect of PFA on the growth and root vigor of citrus seedlings

The plant height, root length, fresh biomass and dry biomass of the seedlings are shown in Figure S1. Although PFA had no significant effect on plant height, root length, fresh biomass, dry biomass of the seedlings (Figure S1), PFA significantly increased the contents of chlorophyll a, chlorophyll b and carotenoid by 30.09%, 17.55% and 27.43%, respectively (Figures 1A–C). In addition, PFA+SS significantly elevated the chlorophyll a, chlorophyll b and carotenoid of leaves and the root vigor, compared to SS treatment (Figures 1A–D). Two-way ANOVA revealed a significant positive interaction of PFA × SS treatment on root vigor of the seedlings (Figure 1D), indicating that PFA had a greater promoting effect on root vigor under salt stress, which was conducive to the root growth under salt stress. Under salt stress, the leaves of trifoliate seedlings gradually appeared yellow and scorched, but PFA+SS significantly alleviated the harm of salt stress to the seedlings (Figures 1E, F).

10.3389/fpls.2023.1161469

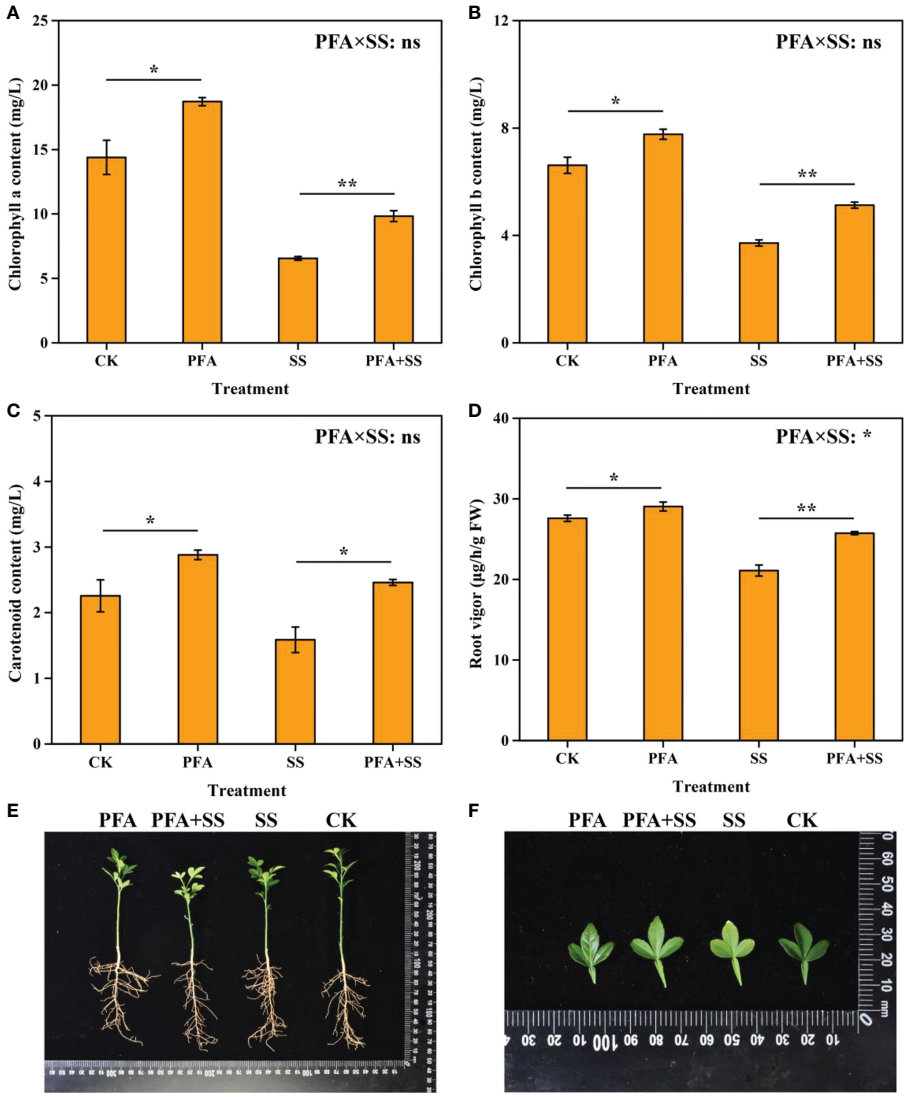

FIGURE 1
The contents of chlorophyll a **(A)**, chlorophyll b **(B)**, carotenoid **(C)** and root vigor **(D)**, plant growth **(E)**, leaves **(F)** of the seedlings. CK, the seedlings without PFA and salt stress; PFA, the seedlings amended with PFA and without salt stress; SS, the seedlings with salt stress; PFA+SS, the seedlings amended with both PFA and salt stress. PFA × SS, interaction between PFA and SS. The error bars represent the standard error (n = 3). "ns", "*", and "**" mean not significant, $p < 0.05$ and $p < 0.01$ according to Student's t test and two-way ANOVA, respectively.

Effect of PFA on the biochemical and physiological characteristics of the seedlings

Protective enzyme activities

The activities of protective enzymes in the seedlings were affected by PFA (Figures 2A–C). PFA and PFA+SS treatments enhanced the activities of SOD and CAT in the seedling leaves compared to CK and SS treatments, respectively (Figures 2A, B). Two-way ANOVA revealed highly significant positive effects of PFA × SS treatment interaction on the activities of SOD and CAT in leaves, showing the greater promoting effects of PFA under salt stress, which means that PFA can effectively alleviate the damage of citrus caused by SS. Moreover, the activities of POD in root and leaf samples were significantly increased with the addition of PFA under salt stress or without salt stress (Figure 2C). However, the results of two-way ANOVA demonstrated that there was no significant PFA × SS treatment interaction on the POD activities.

Accumulation of K^+ and Na^+

The contents of K^+ and Na^+ in the roots and leaves are displayed in Figure 2. PFA and PFA+SS treatments generally increased the contents of K^+ in the leaves, but there was no significant difference in the root samples (Figure 2D). SS and PFA +SS treatments enhanced the accumulation of Na^+ in the roots, and PFA+SS conspicuously decreased Na^+ content in the leaves, compared to SS treatment (Figure 2E). Two-way ANOVA

10.3389/fpls.2023.1161469

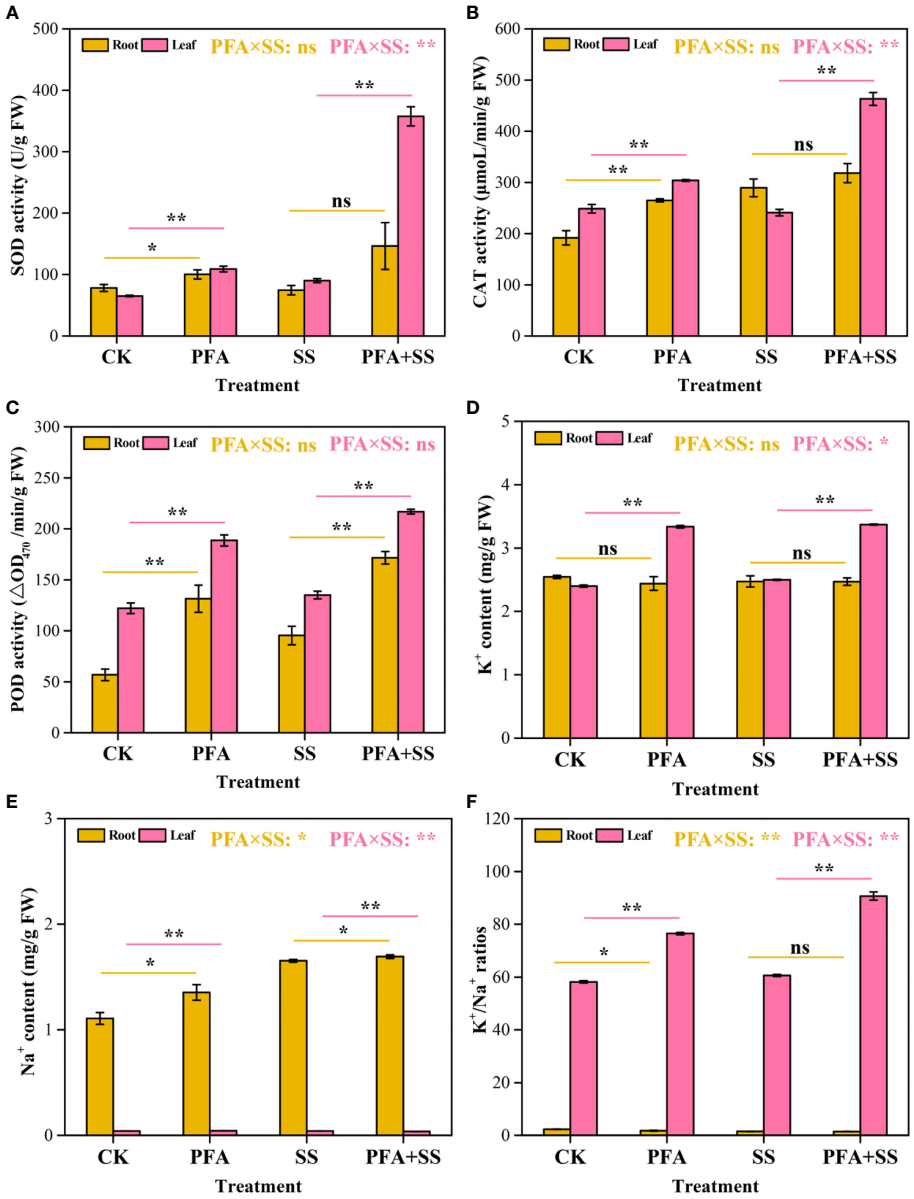

FIGURE 2
The activities of SOD **(A)**, CAT **(B)**, POD **(C)** and K^+ content **(D)**, Na^+ content **(E)**, K^+/Na^+ ratios **(F)** in the seedlings. CK, the seedlings without PFA and salt stress; PFA, the seedlings amended with PFA and without salt stress; SS, the seedlings with salt stress; PFA+SS, the seedlings amended with both PFA and salt stress. PFA × SS, interaction between PFA and SS. The error bars represent the standard error (n = 3). "ns", "*", and "**" mean not significant, $p < 0.05$ and $p < 0.01$ according to Student's t test and two-way ANOVA, respectively.

revealed a significant negative effect of PFA × SS treatment interaction on the Na^+ contents in the leaves of the seedlings, which showed that PFA reduced the accumulation of Na^+ under salt stress. And decreased content of Na^+ mitigated the harmful effects of salt on the seedlings. In root samples, the K^+/Na^+ ratios were dramatically decreased with the treatments of PFA, compared to CK treatment. However, PFA and PFA+SS treatments increased the K^+/Na^+ ratios in the leaves by 31.46% and 49.72%, compared to CK and SS treatments, respectively (Figure 2F). Especially, PFA × SS treatment interaction showed a significant positive effect on the K^+/Na^+ ratio in the leaves, which was beneficial to alleviate salt stress on citrus.

Soluble sugar, soluble protein, proline and MDA contents

PFA affected the contents of osmoregulation substances (Figure 3). PFA treatment significantly increased soluble sugar contents in the roots by 39.34% compared to CK treatment, but there was no significant effect of PFA on the contents in root samples under salt stress (Figure 3A). In addition, the contents of soluble sugar in the leaves exhibited an extremely significant increase under PFA+SS treatment. The soluble protein contents were increased by 45.28% and 20.41% in the roots and leaves with PFA+SS treatment, compared to SS treatment (Figure 3B). However, PFA treatment showed no significant improvement

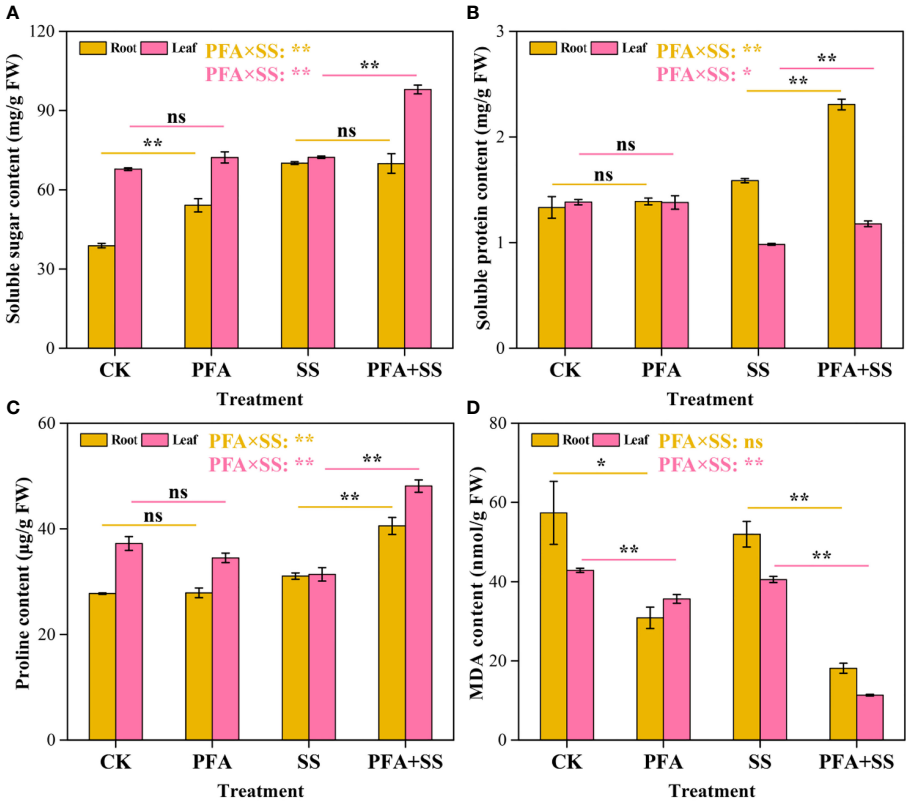

FIGURE 3
The contents of soluble sugar **(A)**, soluble protein **(B)**, proline **(C)** and MDA **(D)** in the seedlings. CK, the seedlings without PFA and salt stress; PFA, the seedlings amended with PFA and without salt stress; SS, the seedlings with salt stress; PFA+SS, the seedlings amended with both PFA and salt stress. PFA × SS, interaction between PFA and SS. The error bars represent the standard error (n = 3). "ns", "*", and "**" mean not significant, $p < 0.05$ and $p < 0.01$ according to Student's t test and two-way ANOVA, respectively.

effect on the soluble protein contents of the seedlings. For the proline contents, there were no significant differences between CK and PFA treatments in root and leaf samples, but PFA+SS treatment significantly promoted the synthesis of proline in the seedlings compared to SS treatment (Figure 3C). Moreover, two-way ANOVA indicated that PFA × SS treatment interaction had highly significant positive influences on the soluble sugar, soluble protein and proline contents in leaves, which were beneficial to the growth of plants, indicating that PFA had greater promoting effects of them under salt stress. Compared to CK treatment, the contents of MDA in the root and leave samples decreased under PFA treatments (Figure 3D). Notably, PFA+SS treatment significantly decreased MDA contents in the roots and leaves by 65.10% and 71.96%, compared to SS treatment, respectively (Figure 3D). Two-way ANOVA also showed that PFA × SS treatment interaction had a highly significant negative influence on the content of MDA in leaves, of which excessive accumulation was harmful to plants, indicating that PFA has a better inhibition effect on MDA under stress.

Effect of PFA on the physicochemical properties and enzyme activities of rhizosphere soil

The effect of PFA on rhizosphere soil physicochemical properties is provided in Table 1. PFA showed no significant effect on the pH values of the soil samples, but there were significant effects of PFA and PFA+SS treatments on the soil EC values. PFA treatment significantly decreased the soil EC value by 47.78%, compared to CK, and the results of two-way ANOVA also demonstrated a highly significant PFA × SS treatment interaction on the EC values of soil. Furthermore, PFA treatment significantly promoted soil OM contents by 37.75%. Specifically, PFA amendment significantly improved soil AN content from 5.05 mg/kg to 6.73 mg/kg, but significantly decreased soil NN content by 38.46%. The contents of OM and AN were not significantly affected by PFA under salt stress, but PFA+SS treatment significantly increased the NN contents compared to SS treatment. As for the effect on

TABLE 1 Effect of PFA on the rhizosphere soil properties of the seedlings.

Soil properties	Treatment				Significance
	CK	PFA[a]	SS	PFA+SS[b]	PFA×SS[c]
pH	8.22 ± 0.01	8.20 ± 0.00 ns	8.13 ± 0.05	8.08 ± 0.02 ns	ns
EC (μS/cm)	642.5 ± 15.08	335.5 ± 18.21**	675.25 ± 10.05	617.75 ± 8.18**	**
OM ($g.kg^{-1}$)	6.49 ± 0.08	8.94 ± 0.53**	8.11 ± 0.90	10.69 ± 1.05ns	ns
AN ($mg.kg^{-1}$)	5.05 ± 0.21	6.73 ± 0.26**	4.95 ± 0.28	4.97 ± 0.19ns	**
NN ($mg.kg^{-1}$)	0.39 ± 0.01	0.24 ± 0.01**	0.36 ± 0.01	0.57 ± 0.01**	**
AP ($mg.kg^{-1}$)	2.35 ± 0.09	7.78 ± 0.54**	6.18 ± 0.23	6.71 ± 0.34ns	**

EC, Electrical conductivity; OM, Organic matter; AN, Ammonium nitrogen; NN, Nitrate nitrogen and AP, Available phosphorus. CK, the seedlings without PFA and salt stress; PFA, the seedlings amended with PFA and without salt stress; SS, the seedlings with salt stress; PFA+SS, the seedlings amended with both PFA and salt stress. PFA × SS, interaction between PFA and SS. [a] "ns" and "**" mean not significant, and $p < 0.01$ between CK and PFA treatments according to Student's t test; [b] "ns" and "**" mean not significant, and $p < 0.01$ between SS and PFA+SS treatments according to Student's t test; [c] "ns" and "**" mean not significant interaction of PFA × SS treatment, and $p < 0.01$ according to two-way ANOVA.

AP content of rhizosphere soil, PFA+SS treatment showed no significant effects on soil AP content compared to SS treatment, but PFA treatment significantly increased soil AP content by 231.06%. Two-way ANOVA revealed a highly significant positive effect of PFA× SS treatment interaction on the NN contents of soil, suggesting that PFA had greater promoting effects on them under stress.

The effect of PFA on the enzymatic activities of the citrus rhizosphere soil is presented in Table 2. There was no significant effect of PFA treatment on S-CAT activity, but PFA+SS treatment remarkably increased S-CAT by 28.74%, compared to SS treatment. In addition, SS treatment decreased S-NPT activity from 41.30 $\mu g \cdot h^{-1} \cdot g^{-1}$ to 26.16 $\mu g \cdot h^{-1} \cdot g^{-1}$, but PFA and PFA+SS treatments dramatically promoted S-NPT activity by 23.22% and 159.10%, compared to CK and SS treatments, respectively. Similarly, the results of two-way ANOVA showed that PFA × SS treatment interaction had a highly significant positive effect on the activities of S-NPT, indicating a better promotion of PFA on S-NPT activities under salt stress. The activities of S-SC were dramatically higher by 69.95% under PFA amendment. In addition, the significant differences of S-UE activities were observed between CK and PFA treatments, SS and PFA+SS treatments. The significant PFA × SS treatment interaction also affected the activities of S-SC and S-UE positively.

Effect of PFA on the microbial diversity and community of root and rhizosphere soil

Based on the 16S rRNA gene and ITS amplicon sequencing, a total of 223,572 and 813,072 clean reads were obtained, respectively. The Venn diagram revealed that 452 and 172 bacterial OTUs, 238 and 73 fungal OTUs were shared among the all treatments in the roots and rhizosphere soils (Figure S2). In addition, 48–184, 69–104, 62–121 and 31–98 unique microbial OTUs were observed for CK, FPA, SS and FPA+SS treatments, respectively. PFA treatment significantly decreased the bacterial Chao1 index in the rhizosphere soil samples (Figure S3A), but the PFA and salt stress showed no significant effects on the fungal Chao1 indexes of rhizosphere soil and root samples of trifoliate seedling (Figures S3C, D). PCoA on the OTU level showed that the soil bacterial and fungal communities in the different treatments were entirely distributed in different quadrants (Figures 4A, C). However, the bacterial communities of root samples in the CK were similar to that in the PFA, SS, and PFA+SS treatments (Figure 4B). The PC1 and PC2 axis totally explained 25.41%–45.84% of the variation (Figure 4D), indicating the shifts in the composition of root fungal communities under different treatments.

The microbiota of root and rhizosphere soil samples at the phylum level are shown in Figures 5A, B, S4A, B. For the rhizosphere soil samples, the dominant bacterial phyla (relative

TABLE 2 Effect of PFA on the rhizosphere soil enzyme activities of the seedlings.

Soil enzyme activities	Treatment				Significance
	CK	PFA[a]	SS	PFA+SS[b]	PFA×SS[c]
S-CAT ($\mu mol \cdot h^{-1} \cdot g^{-1}$)	228.70 ± 13.00	231.08 ± 16.14ns	164.31 ± 6.88	211.54 ± 19.53**	*
S-NPT ($\mu g \cdot h^{-1} \cdot g^{-1}$)	41.30 ± 2.70	50.89 ± 2.12**	26.16 ± 4.40	67.78 ± 6.41**	**
S-SC ($mg \cdot d^{-1} \cdot g^{-1}$)	2.13 ± 0.38	3.62 ± 0.41**	2.15 ± 0.26	5.50 ± 0.16**	**
S-UE ($\mu g \cdot d^{-1} \cdot g^{-1}$)	42.92 ± 2.33	47.22 ± 1.32*	36.69 ± 2.29	63.11 ± 8.59**	**

S-CAT: soil catalase, S-NPT: soil neutral protease, S-SC: soil sucrase, S-UE: soil urease. CK: the seedlings without PFA and salt stress; PFA: the seedlings amended with PFA and without salt stress; SS: the seedlings with salt stress; PFA+SS: the seedlings amended with both PFA and salt stress. PFA × SS: interaction between PFA and SS. [a] "ns", "*", and "**" mean not significant, $p < 0.05$ and $p < 0.01$ between CK and PFA treatments according to Student's t test; [b] "ns", "*", and "**" mean not significant, $p < 0.05$ and $p < 0.01$ between SS and PFA+SS treatments according to Student's t test; [c] "ns", "*", and "**" mean not significant interaction of PFA × SS treatment, $p < 0.05$ and $p < 0.01$ according to two-way ANOVA.

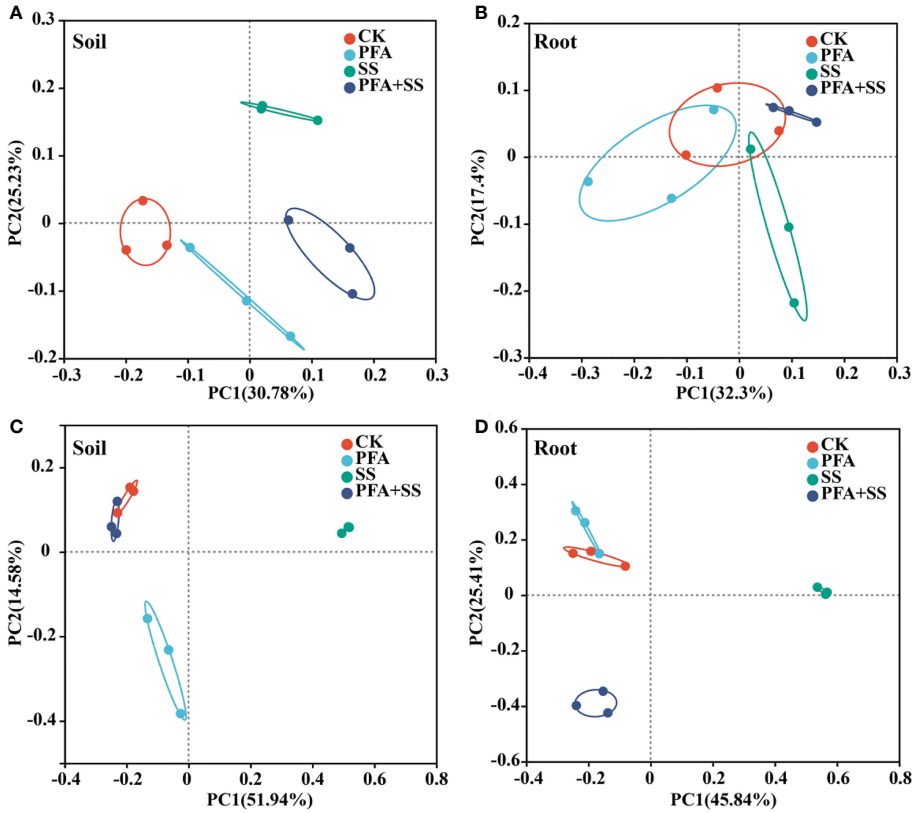

FIGURE 4
Principal components analysis (PCoA) based on the microbial community of the seedlings at the OTU level. **(A)** Bacterial community for the rhizosphere soil sample; **(B)** bacterial community for the root sample; **(C)** fungal community for the rhizosphere soil sample; **(D)** fungal community for the root sample. CK, the seedlings without PFA and salt stress; PFA, the seedlings amended with PFA and without salt stress; SS, the seedlings with salt stress; PFA+SS, the seedlings amended with both PFA and salt stress.

abundance >10%) in all treatments were Proteobacteria (47.36%–60.75%), Firmicutes (16.25%–32.32%) and Actinobacteria (9.50%–18.40%) (Figure 5A), while only Proteobacteria (>94.67%) was the most dominant in root samples (Figure 5B). The predominant fungal phylum of rhizosphere soil and root samples were Basidiomycota (27.26%–74.89%) and Ascomycota (14.86%–46.67%) in all treatments (CK, PFA, SS and PFA+SS) (Figures S4A, B). Moreover, the comparative response of bacterial and fungal communities between SS and PFA+SS in the roots and rhizosphere soils was observed at genus level (Figures 5C, D, S4C, D). Comparing with SS, PFA+SS treatment significantly enhanced the relative abundances of *Bacillus* and decreased *Sphingomonas* abundances (Figures 5C, D). The PFA and salt stress treatments significantly influenced a total of 7 fungal genera abundances in the rhizosphere soil and root samples, in which the two most dominant genera (*Rhizoctonia* and *Ceratobasidium*) were increased by PFA+SS (Figures S4C, D).

Correlations between rhizosphere soil properties, enzyme activities and dominant microorganisms of the seedlings

The db-RDA was carried out to evaluate the correlations between properties, enzyme activities of soil and dominant microbial communities (Figures 6A, B). Of the soil properties indicators, soil AP content was mostly affected by the soil bacterial communities, followed by OM, NN and AN (Figure 6A). In addition, soil AN content was negatively with NN content. As for the enzyme activities of rhizosphere soil samples, S-NPT was positively correlated with S-SC, S-UE and S-CAT. Especially, SS treatment had the most significant effect on the S-NPT, S-SC and S-UE activities. The soil EC value was significantly correlated with the relative abundances of 7 bacterial genera and 3 fungal genera, respectively (Figures 6C, D). *Bacillus* and *Fictibacillus* abundances were significantly positively correlated with S-NPT, S-SC and S-UE (Figure 6C). Moreover, AP was significantly correlated with 4 fungal genera, including *Preussia*, *Chaetomium*, *Acremonium* and *Albifimbria* (Figure 6D). *Fusarium* had significantly positive correlation with soil EC, but negative with soil pH and S-CAT. The relative abundances of *Cupriavidus*, *Lysobacter*, *Microvirga*, *Pseudarthrobacter*, *Ascobolus* had no significant correlation with physicochemical properties and enzyme activities of rhizosphere soil samples.

Discussion

Recently, large numbers of evidences have showed that PFA serves as a promising strategy to alleviate the damage to plants

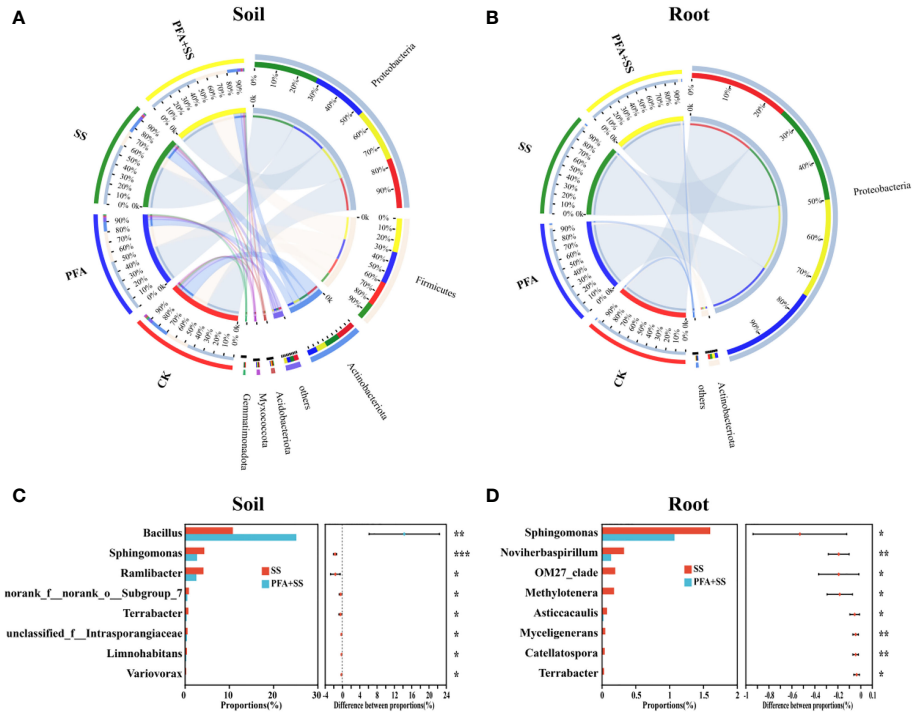

FIGURE 5
The relative abundance and composition of bacterial communities in the rhizosphere soil **(A)** and root **(B)** samples at the phylum level, the significance comparisons of bacterial communities in the rhizosphere soil **(C)** and root **(D)** samples at the genus level. CK, the seedlings without PFA and salt stress; PFA, the seedlings amended with PFA and without salt stress; SS, the seedlings with salt stress; PFA+SS, the seedlings amended with both PFA and salt stress. *p<0.05, **p<0.01, and ***p<0.001.

caused by various abiotic stresses (Elrys et al., 2020; Qiao et al., 2022; Wang et al., 2022). In this study, we found that PFA avoided yellowing and scorching of leaves and significantly increased the contents of chlorophyll a, chlorophyll b and carotenoid of the seedlings (Figure 1), but PFA × SS treatment interaction showed no significant effect, indicating that PFA can effectively promote the growth status of citrus with or without salt stress.

The protective enzyme systems of plant play important roles in response to environmental stress (Abdelaal et al., 2019; Unoki et al., 2020). As important members of the plant protective enzyme systems, the activities of CAT, SOD and POD were used to evaluate the resistance of citrus to salt stress in this study. Excessive accumulation of O_2^- in plants can provoke oxidative stress, which cause toxicity and show symptoms (Shang et al., 2021). However, SOD and POD of plants can convert O_2^- into H_2O_2, and then, CAT effectively remove H_2O_2 to reduce oxidative damage to the cell membrane systems (Abdelaal et al., 2019; Che et al., 2020; Shang et al., 2021). In this study, PFA+SS treatment significantly enhanced the activities of CAT, SOD and POD in the leaves of citrus compared to SS treatment, and two-way ANOVA revealed highly significant positive effects of PFA × SS treatment interaction on the activities of SOD and CAT in leaves (Figures 2A–C), indicating that PFA had greater promoting effects of them and alleviated the oxidative damage caused by saline stress *via* the protective enzyme system (Figures 1E, F). Additionally, the accumulation of reactive oxygen species (ROS) in plants dramatically increased the MDA content caused by membrane lipid peroxidation (Li et al., 2017; Sun et al., 2022). The increased contents of osmoregulation substances, such as soluble sugar, soluble protein and proline, effectively removed ROS, reducing the content of MDA in plants, and thus relieved the damage of salt stress to plants (Wang et al., 2013; Dien et al., 2019; Kucerova et al., 2019; Lin et al., 2019; Gurrieri et al., 2020; Sun et al., 2022). The relief of symptoms in leaves induced by PFA (Figures 1E, F) might be related to the highly significant positive PFA × SS treatment interactions on the contents of soluble sugar, soluble protein and proline (Figures 3A–C) and the highly significant negative PFA × SS treatment interaction on MDA contents (Figure 3D), which caused the significantly increased contents of soluble sugar, soluble protein, proline and the decreased content of MDA under salt stress.

Properties and nutrient contents of soil directly affect plant growth and productivity (Ma et al., 2021). The high EC value of soil reflects the over-concentration of soluble salt, which is not conducive to plant growth (Sun et al., 2022; Yin et al., 2022). In this study, PFA treatment significantly reduced the EC value of salt-stressed soil (Table 1), indicating the alleviation of salt damage under PFA+SS treatment. Furthermore, PFA directly provides nutrients and also improves soil nutrient availability for the plants. In this study, PFA improved physicochemical properties of the soil under salt stress, such as OM, NN and AP (Table 1), which is in agreement with the report of Kumar Sootahar et al. (2019) and Sun et al. (2022).

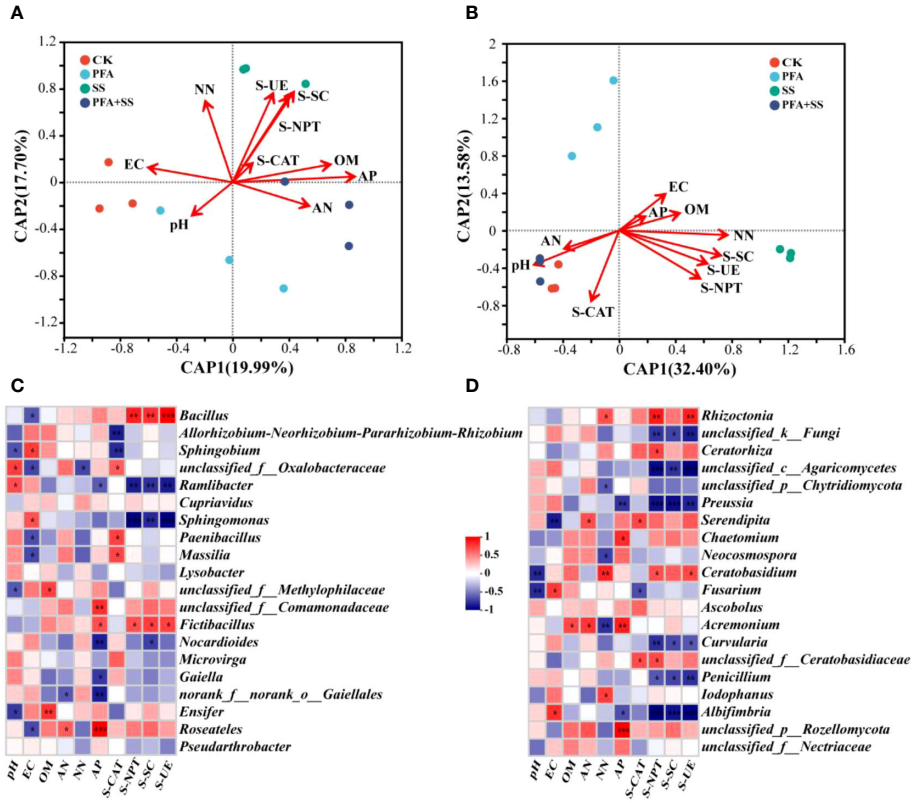

FIGURE 6
The db-RDA of bacterial **(A)**, fungal **(B)** communities and properties, enzyme activities in the rhizosphere soil of the seedlings, and correlation heat maps of properties, enzyme activities and the relative abundances of top 20 dominant genera of bacteria **(C)**, fungi **(D)** in the rhizosphere soil samples. CK, the seedlings without PFA and salt stress; PFA, the seedlings amended with PFA and without salt stress; SS, the seedlings with salt stress; PFA+SS, the seedlings amended with both PFA and salt stress. EC, Electrical conductivity; OM, Organic matter; AN, Ammonium nitrogen; NN, Nitrate nitrogen and AP, Available phosphorus. S-CAT, soil catalase; S-NPT, soil neutral protease; S-SC, soil sucrase; S-UE, soil urease. *p<0.05, **p<0.01, and ***p<0.001.

Soil enzyme is an important driving force of soil nutrient metabolism, and its activity can directly reflect the intensity and direction of soil nutrient conversion and the biochemical process of soil (Fei et al., 2019; Aponte et al., 2020). S-CAT, an important indicator of soil micro-ecological environment, is related to soil respiration intensity and soil microbial activity, which can effectively prevent the toxicity of hydrogen peroxide (Aponte et al., 2020; Shang et al., 2021). In this study, PFA+SS treatment significantly enhanced the activity of S-CAT compared to SS treatment (Table 2), which was consistent with the report by Zhu et al. (2021). Additionally, S-UE can promote the hydrolysis of urea to ammonia and the supply of nitrogen nutrition for plants (Lee et al., 2021). S-SC can catalyze the hydrolysis of oligosaccharides in soil to glucose, fructose and other monosaccharides available to plants, and participate in the soil organic carbon cycle (Farooq et al., 2021). S-NPT is mainly involved in the conversion of amino acids, proteins and other organic compounds containing protein nitrogen in the soil, and the hydrolysate is one of the nitrogen sources of plants (Manyun et al., 2018). In this study, PFA+SS treatment significantly increased the activities of S-UE, S-SC and S-NPT compared to SS treatment (Table 1), which might be attributed to the increased abundance of beneficial rhizosphere microorganisms. In our study, two-way ANOVA revealed highly significant positive PFA × SS treatment interactions on the enzyme activities (S-UE, S-SC, S-NPT) and physicochemical property (NN) of soil, indicating the better improvement of soil nutrient status with PFA under salt stress. Overall, PFA significantly improved the soil nutrient status under salt stress, such as NN, S-UE and S-NPT of rhizosphere soil.

Rhizosphere microbes play key roles in maintaining soil quality and affecting the host plant growth (Shang et al., 2021; Zheng et al., 2021; Sun et al., 2022). Compared to CK, PFA treatment decreased the bacterial Chao 1 index in the rhizosphere soil samples, suggesting that PFA affected the bacterial diversity, however, PFA had positive influence on the bacterial activity under salt stress (Figure S3). PCoA showed that PFA obviously shifted the rhizosphere microbial community composition of citrus (Figure 4). Qiao et al. (2022) also reported that the bacterial and fungal community were affected by potassium humate and PFA. Consequently, the rhizosphere microbial community affected by PFA was beneficial to the alleviation of salt damage to the seedlings.

The dominant bacterial phylum in the root and rhizosphere soil samples of the seedling was Proteobacteria (Figures 5A, B), which is easier to survive in the environments rich in multiple nutrients (Trivedi et al., 2013). The bacteria in Actinobacteria can enhance host nutrition acquisition and protect plant against various abiotic stresses (Shi et al., 2019), which was also found to widely exist in the

rhizosphere soil of the seedlings (Figure 5A). At the genus level, PFA+SS treatment enhanced the relative abundances of *Bacillus* (Figure 5C), which had positive correlations with S-NPT, S-SC and S-UE, but negatively correlated with EC value (Figure 6C). *Bacillus*, a kind of rhizosphere beneficial bacteria, plays important roles in improvement of soil, promotion of plant growth, resistance against disease and enhancement of plant tolerance to salt (Miljaković et al., 2020; Shang et al, 2021). The changes of soil nutrient status can directly affect the morphological structure and function of rhizosphere microbial community, and the feedback effect also gradually affects the nutrient status and quality of soil (Sun et al., 2022; Yin et al., 2022). Therefore, the correlations between nutrient status and dominant microorganisms of the rhizosphere soil were evaluated in this study (Figure 6). These results suggested the evolutions of microbial community affected by PFA was closely related to the changes of soil nutrient status (OM, AN, NN, S-UE, S-SC and S-NPT), as supported by some studies (Zheng et al., 2021; Sun et al., 2022; Yin et al., 2022).

Conclusion

PFA can effectively alleviate salt damage to citrus on yellowing and scorching of leaves. It showed obvious promotion effects on the physiological status of the seedlings and physicochemical properties and enzymatic activities of rhizosphere soil under salt stress. PFA improved the evolution of bacterial and fungal communities in root and rhizosphere soil of trifoliate seedlings, and significantly enhanced the relative abundances of *Bacillus*, a kind of rhizosphere beneficial microbes, under salt stress. Moreover, AP, S-SC and S-NPT affected by PFA were the most critical environmental factors influencing the compositions of microbial genera. Thus, PFA can be used as a potential conditioner to alleviate salt damage to citrus rootstocks.

Data availability statement

The raw data has been deposited in the NCBI Sequence Read Archive under BioProject with the number PRJNA935538.

Author contributions

MZ and SZ designed the experiments, analyzed the data and wrote the manuscript. MZ, XL, XW and JF performed the laboratory measurements. MZ and SZ discussed the results and provide critical idea in greenhouse experiment. All authors contributed to the article and approved the submitted version.

Funding

This work was supported by China Agriculture Research System (CARS-Citrus), the National Key Research and Development Program of China (2018YFD1000101), and the "Double World-classes" Development Plan of Southwest University.

Conflict of interest

The authors declare that the research was conducted in the absence of any commercial or financial relationships that could be construed as a potential conflict of interest.

Publisher's note

Supplementary material

The Supplementary Material for this article can be found online at: https://www.frontiersin.org/articles/10.3389/fpls.2023.1161469/full#supplementary-material

References

Abdelaal, K. A., Elmaghraby, L. M., Elansary, H., Hafez, Y. M., Ibrahim, E. I., Elbanna, M., et al. (2019). Treatment of sweet pepper with stress tolerance-inducing compounds alleviates salinity stress oxidative damage by mediating the physio-biochemical activities and antioxidant systems. *Agronomy* 10 (1), 26. doi: 10.3390/agronomy10010026

Anjum, N. A., Ahmad, I., Válega, M., Pacheco, M., Figueira, E., Duarte, A. C., et al. (2011). Salt marsh macrophyte *Phragmites australis* strategies assessment for its dominance in mercury-contaminated coastal lagoon (Ria de aveiro, Portugal). *Environ. Sci. Pollut. R.* 19 (7), 2879–2888. doi: 10.1007/s11356-012-0794-3

Aponte, H., Meli, P., Butler, B., Paolini, J., and Kuzyakov, Y. (2020). Meta-analysis of heavy metal effects on soil enzyme activities. *Sci. Total Environ.* 737, 139744. doi: 10.1016/j.scitotenv.2020.139744

Ashraf, M., Hasnain, S., Berge, O., and Mahmood, T. (2004). Inoculating wheat seedlings with exopolysaccharide-producing bacteria restricts sodium uptake and stimulates plant growth under salt stress. *Biol. Fert. Soils* 40 (3), 157–162. doi: 10.1007/s00374-004-0766-y

Bai, Y., Muller, D. B., Srinivas, G., Garrido-Oter, R., Potthoff, E., and Rott, M. (2015). Functional overlap of the *Arabidopsis* leaf and root microbiota. *Nature* 528, 364–369. doi: 10.1038/nature16192

Bankaji, I., Sleimi, N., Vives-Peris, V., Gómez-Cadenas, A., and Pérez-Clemente, R. M. (2019). Identification and expression of the *Cucurbita* WRYK transcription factors in response to water deficit and salt stress. *Sci. Hortic.* 256, 108562. doi: 10.1016/j.scienta.2019.108562

Berendsen, R. L., Pieterse, C., and Bakker, P. (2012). The rhizosphere microbiome and plant health. *Trends Plant Sci.* 17, 478–486. doi: 10.1016/j.tplants.2012.04.001

Brazien, Z., Paltanaviius, V., and Aviienyt, D. (2021). The influence of fulvic acid on spring cereals and sugar beets seed germination and plant productivity. *Environ. Res.* 195, 110824. doi: 10.1016/j.envres.2021.110824

Che, Y., Zhang, N., Zhu, X., Li, S., and Si, H. (2020). Enhanced tolerance of the transgenic potato plants overexpressing Cu/Zn superoxide dismutase to low temperature. *Sci. Hortic.* 261, 108949. doi: 10.1016/j.scienta.2019.108949

Dien, D. C., Mochizuki, T., and Yamakawa, T. (2019). Effect of various drought stresses and subsequent recovery on proline, total soluble sugar and starch metabolisms in rice (*Oryza sativa* l.) varieties. *Plant Prod. Sci.* 22 (4), 530–545. doi: 10.1080/1343943X.2019.1647787

Dinler, B. S., Gunduzer, E., and Tekinay, T. (2016). Pre-treatment of fulvic acid plays a stimulant role in protection of soybean (*Glycine max* L.) leaves against heat and salt stress. *Acta Biologica Cracoviensia S Botanica* 58 (1), 29–41. doi: 10.1515/abcsb-2016-0002

Elrys, A. S., Abdo, A., Abdel-Hamed, M. W., and Desoky, E. (2020). Integrative application of licorice root extract or lipoic acid with fulvic acid improves wheat production and defenses under salt stress conditions. *Ecotox. Environ. Safe.* 190, 110144. doi: 10.1016/j.ecoenv.2019.110144

Farooq, T. H., Kumar, U., Mo, J., Shakoor, A., Wang, J., Rashid, M. H. U., et al. (2021). Intercropping of peanut–tea enhances soil enzymatic activity and soil nutrient status at different soil profiles in subtropical southern China. *Plants* 10, 881. doi: 10.3390/plants10050881

Fei, Y., Huang, S., Zhang, H., and Tong, Y. (2019). Response of soil enzyme activities and bacterial communities to the accumulation of microplastics in an acid cropped soil. *Sci. Total Environ.* 707, 135634. doi: 10.1016/j.scitotenv.2019.135634

Fu, L., Penton, C. R., Ruan, Y., Shen, Z., Xue, C., and Li, R. (2017). Inducing the rhizosphere microbiome by biofertilizer application to suppress banana fusarium wilt disease. *Soil Biol. Biochem.* 104, 39–48. doi: 10.1016/j.soilbio.2016.10.008

Grover, M., Ali, S. Z., Sandhya, V., Rasul, A., and Venkateswarlu, B. (2011). Role of microorganisms in adaptation of agriculture crops to abiotic stresses. *World J. Microbiol. Biotechnol.* 27, 1231–1240. doi: 10.1007/s11274-010-0572-7

Gurrieri, L., Merico, M., Trost, P., Forlani, G., and Sparla, F. (2020). Impact of drought on soluble sugars and free proline content in selected *Arabidopsis* mutants. *Biology* 9, 367. doi: 10.3390/biology9110367

Han, Q., Lü, X., Bai, J., Qiao, Y., Paré, P., Wang, S., et al. (2014). Beneficial soil bacterium *Bacillus subtilis* (GB03) augments salt tolerance of white clover. *Front. Plant Sci.* 5, 525. doi: 10.3389/fpls.2014.00525

Hartmann, M., Frey, B., Mayer, J., Mader, P., and Widmer, F. (2015). Distinct soil microbial diversity under long-term organic and conventional farming. *ISME J.* 9, 1177–1194. doi: 10.1038/ismej.2014.210

Hassani, A., Azapagic, A., and Shokri, N. (2020). Predicting long-term dynamics of soil salinity and sodicity on a global scale. *P. Natl. Acad. Sci. U.S.A.* 117 (52), 33017–33027. doi: 10.1073/PNAS.2013771117

He, X., Zhang, H., Li, J., Yang, F., Dai, W., Xiang, C., et al. (2022). The positive effects of humic/fulvic acid fertilizers on the quality of lemon fruits. *Agron. J.* 12 (8), 1919. doi: 10.3390/agronomy12081919

Islam, M. A., Morton, D. W., Johnson, B. B., and Angove, M. J. (2020). Adsorption of humic and fulvic acids onto a range of adsorbents in aqueous systems and their effect on the adsorption of other species: A review. *Sep. Purif. Technol.* 247, 116949. doi: 10.1016/j.seppur.2020.116949

Kucerova, K., Henselova, M., Slovakova, L., and Hensel, K. (2019). Effects of plasma activated water on wheat: Fermination, growth parameters, photosynthetic pigments, soluble protein content, and antioxidant enzymes activity. *Plasma Process Polym.* 16 (3), e1800131.1–e1800131.14. doi: 10.1002/ppap.201800131

Kumar Sootahar, M., Zeng, X., Su, S., Wang, Y., Bai, L., Zhang, Y., et al. (2019). The effect of fulvic acids derived from different materials on changing properties of albic black soil in the northeast plain of China. *Molecules* 24 (8), 1535. doi: 10.3390/molecules24081535

Lee, J. K., Park, H. J., Cha, S. J., Kwon, S. J., and Park, J. H. (2021). Effect of pyroligneous acid on soil urease, amidase, and nitrogen use efficiency by Chinese cabbage (*Brassica campestris* var. pekinensis). *Environ. Pollut.* 291, 118132. doi: 10.1016/j.envpol.2021.118132

Li, H., Lei, P., Pang, X., Li, S., Xu, H., Xu, Z., et al. (2017). Enhanced tolerance to salt stress in canola (*Brassica napus* L.) seedlings inoculated with the halotolerant enterobacter cloacae HSNJ4. *Appl. Soil Ecol.* 119, 26–34. doi: 10.1016/j.apsoil.2017.05.033

Lin, Q., Xie, Y., Guan, W., Duan, Y., Wang, Z., and Sun, C. (2019). Combined transcriptomic and proteomic analysis of cold stress induced sugar accumulation and heat shock proteins expression during postharvest potato tuber storage. *Food Chem.* 297, 124991. doi: 10.1016/j.foodchem.2019.124991

Lin, X., Xie, Z., Zheng, J., Liu, Q., Bei, Q., and Zhu, J. (2015). Effects of biochar application on greenhouse gas emissions, carbon sequestration and crop growth in coastal saline soil. *Eur. J. Soil Sci.* 66, 329–338. doi: 10.1111/ejss.12225

Liu, X., Yang, J., Tao, J., and Yao, R. (2022). Integrated application of inorganic fertilizer with fulvic acid for improving soil nutrient supply and nutrient use efficiency of winter wheat in a salt-affected soil. *Appl. Soil Ecol.* 170, 104255. doi: 10.1016/j.apsoil.2021.104255

Liu, Q., Zhao, X., Liu, Y., Xie, S., Xing, Y., Dao, J., et al. (2021). Response of sugarcane rhizosphere bacterial community to drought stress. *Front. Microbiol.* 12, 716196. doi: 10.3389/fmicb.2021.716196

Ma, D., Yin, L., Ju, W., Li, X., and Wang, S. (2021). Meta-analysis of green manure effects on soil properties and crop yield in northern China. *Field Crop Res.* 266 (25), 108146. doi: 10.1016/j.fcr.2021.108146

Manyun, Z., Jun, W., Hosseini, B. S., Ying, T., and Xu, Z. (2018). Evaluating the effects of phytoremediation with biochar additions on soil nitrogen mineralization enzymes and fungi. *Environ. Sci. Pollut. Res.* 25, 23106–23116. doi: 10.1007/s11356-018-2425-0

Miljaković, D., Marinković, J., and Balešević-Tubić, S. (2020). The significance of bacillus spp. in disease suppression and growth promotion of field and vegetable crops. *Microorganisms* 8 (7), 1037. doi: 10.3390/microorganisms8071037

Mokrani, S., Nabti, E., and Cruz, C. (2020). Current advances in plant growth promoting bacteria alleviating salt stress for sustainable agriculture. *Appl. Sci.* 10 (20), 1–27. doi: 10.3390/app10207025

Mukhopadhyay, R., Sarkar, B., Hanuman, S., Parbodh, C., and Nanthi, S. (2020). Soil salinity under climate change: challenges for sustainable agriculture and food security. *J. Environ. Manage.* 280, 111736. doi: 10.1016/j.jenvman.2020.111736

Navarro, J. M., Pérez-Tornero, O., and Asunción, M. (2014). Alleviation of salt stress in citrus seedlings inoculated with arbuscular mycorrhizal fungi depends on the rootstock salt tolerance. *J. Plant Physiol.* 171 (1), 76–85. doi: 10.1016/j.jplph.2013.06.006

Qiao, J. A., Zhang, Y., Wang, Q., Li, M., Sun, H., Liu, N., et al. (2022). Effects of potassium fulvic acid and potassium humate on microbial biodiversity in bulk soil and rhizosphere soil of *Panax ginseng*. *Microbiol. Res.* 254, 126914. doi: 10.1016/j.micres.2021.126914

Qu, Q., Zhang, Z., Peijnenburg, W. J. G. M., Liu, W., Lu, T., Hu, B., et al. (2020). Rhizosphere microbiome assembly and its impact on plant growth. *J. Agric. Food Chem.* 68 (18), 5024–5038. doi: 10.1021/acs.jafc.0c00073

Rojas-Tapias, D., Moreno-Galvan, A., Pardo-Diaz, S., Obando, M., Rivera, D., and Bonilla, R. (2012). Effect of inoculation with plant growth-promoting bacteria (PGPB) on amelioration of saline stress in maize (Zea mays). *Appl. Soil Ecol.* 61, 264–272. doi: 10.1016/j.apsoil.2012.01.006

Shang, X., Cai, X., Zhou, Y., Han, X., Zhang, C. S., Ilyas, N., et al. (2021). *Pseudomonas* inoculation stimulates endophytic *Azospira* population and induces systemic resistance to bacterial wilt. *Front. Plant Sci.* 12, 738611. doi: 10.3389/fpls.2021.738611

Shi, S., Lei, T., Nasir, F., Bahadur, A., and Tian, C. (2019). Response of microbial communities and enzyme activities to amendments in saline-alkaline soils. *Appl. Soil Ecol.* 135, 16–24. doi: 10.1016/j.apsoil.2018.11.003

Sun, R., Zheng, H., Yin, S., Zhang, X., You, X., Wu, H., et al. (2022). Comparative study of pyrochar and hydrochar on peanut seedling growth in a coastal salt-affected soil of yellow river delta, China. *Sci. Total Environ.* 833, 155183. doi: 10.1016/j.scitotenv.2022.155183

Syvertsen, J. P., and Garcia-Sanchez, F. (2014). Multiple abiotic stresses occurring with salinity stress in citrus. *Environ. Exp. Bot.* 103, 128–137. doi: 10.1016/j.envexpbot.2013.09.015

Trivedi, P., Anderson, I. C., and Singh, B. K. (2013). Microbial modulators of soil carbon storage: integrating genomic and metabolic knowledge for global prediction. *Trends Microbiol.* 21, 641–651. doi: 10.1016/j.tim.2013.09.005

Unoki, T., Akiyama, M., and Kumagai, Y. (2020). Nrf2 activation and its coordination with the protective defense systems in response to electrophilic stress. *Int. J. Mol. Sci.* 21 (2), 545. doi: 10.3390/ijms21020545

Wang, Y., Liu, H., Lin, W., Jahan, M. S., Wang, J., Sun, J., et al. (2022). Foliar application of a mixture of putrescine, melatonin, proline, and potassium fulvic acid alleviates high temperature stress of cucumber plants grown in the greenhouse. *Technol. Hortic.* 2, 6. doi: 10.48130/TIH-2022-0006

Wang, Y., Luo, Z., Du, R., Liu, Y., Ying, T., and Mao, L. (2013). Effect of nitric oxide on antioxidative response and proline metabolism in banana during cold storage. *J. Agric. Food Chem.* 61, 8880–8887. doi: 10.1021/jf401447y

Wei, T., Guo, D., and Liu, J. (2021). PtrMYB3, a R2R3-MYB transcription factor from *Poncirus trifoliata*, negatively regulates salt tolerance and hydrogen peroxide scavenging. *Antioxidants* 10 (9), 1388. doi: 10.3390/antiox10091388

Wei, T., Wang, Y., and Liu, J. H. (2020). Comparative transcriptome analysis reveals synergistic and disparate defense pathways in the leaves and roots of trifoliate orange (*Poncirus trifoliata*) autotetraploids with enhanced salt tolerance. *Hortic. Res.* 7, 88. doi: 10.1038/s41438-020-0311-7

Wu, Q. S., Zou, Y. N., Liu, W., Ye, X. F., and Zhao, L. J. (2010). Alleviation of salt stress in citrus seedlings inoculated with mycorrhiza: Changes in leaf antioxidant defense systems. *Plant Soil Environ.* 56 (10), 470–475. doi: 10.1007/s11104-009-9988-y

Yin, S., Zhang, X., Suo, F., You, X., Yuan, Y., Cheng, Y., et al. (2022). Effect of biochar and hydrochar from cow manure and reed straw on lettuce growth in an acidified soil. *Chemosphere* 298, 134191. doi: 10.1016/j.chemosphere.2022.134191

Zheng, Y., Han, X., Zhao, D., Wei, K., and Zhang, C. S. (2021). Exploring biocontrol agents from microbial keystone taxa associated to suppressive soil: A new attempt for a biocontrol strategy. *Front. Plant Sci.* 12, 655673. doi: 10.3389/fpls.2021.655673

Zhu, Y., Guo, B., Liu, C., Lin, Y., Fu, Q., Li, N., et al. (2021). Soil fertility, enzyme activity, and microbial community structure diversity among different soil textures under different land use types in coastal saline soil. *J. Soils Sediments* 21, 2240–2252. doi: 10.1007/s11368-021-02916-z

Zied, H.-A., Tesfay, A., Dong-Gill, K., Salem, B., Jaehyun, L., Wahida, G., et al. (2022). Soil salinity and its associated effects on soil microorganisms, greenhouse gas emissions, crop yield, biodiversity and desertification: A review. *Sci. Total Environ.* 843, 156946. doi: 10.1016/j.scitotenv.2022.156946

frontiers | Frontiers in Plant Science

TYPE Original Research
PUBLISHED 30 March 2023
DOI 10.3389/fpls.2023.1143878

OPEN ACCESS

EDITED BY
Long Yang,
Shandong Agricultural University, China

REVIEWED BY
Janne J. Koskimäki,
University of Oulu, Finland
Huihui Zhang,
Northeast Forestry University, China

*CORRESPONDENCE
Changjun Ding
changjund@126.com

†These authors have contributed equally to this work

SPECIALTY SECTION
This article was submitted to Plant Symbiotic Interactions, a section of the journal Frontiers in Plant Science

RECEIVED 13 January 2023
ACCEPTED 20 March 2023
PUBLISHED 30 March 2023

CITATION
Liu J, Zhang W, Liu Y, Zhu W, Yuan Z, Su X and Ding C (2023) Differences in phyllosphere microbiomes among different *Populus* spp. in the same habitat. *Front. Plant Sci.* 14:1143878. doi: 10.3389/fpls.2023.1143878

Differences in phyllosphere microbiomes among different *Populus* spp. in the same habitat

Jiaying Liu[1,2†], Weixi Zhang[2,3†], Yuting Liu[1], Wenxu Zhu[1,2,4], Zhengsai Yuan[2,3], Xiaohua Su[2,3] and Changjun Ding[2,3*]

[1]College of Forestry, Shenyang Agriculture University, Shenyang, China, [2]State Key Laboratory of Tree Genetics and Breeding, Research Institute of Forestry, Chinese Academy of Forestry, Beijing, China, [3]Key Laboratory of Tree Breeding and Cultivation of State Forestry Administration, Research Institute of Forestry, Chinese Academy of Forestry, Beijing, China, [4]Research Station of Liaohe-River Plain Forest Ecosystem, Chinese Forest Ecosystem Research Network (CFERN), College of Forestry, Shenyang Agricultural University, Tieling, China

Introduction: The above-ground parts of terrestrial plants are collectively known as the phyllosphere. The surface of the leaf blade is a unique and extensive habitat for microbial communities. Phyllosphere bacteria are the second most closely associated microbial group with plants after fungi and viruses, and are the most abundant, occupying a dominant position in the phyllosphere microbial community. Host species are a major factor influencing the community diversity and structure of phyllosphere microorganisms.

Methods: In this study, six Populus spp. were selected for study under the same site conditions and their phyllosphere bacterial community DNA fragments were paired-end sequenced using 16S ribosomal RNA (rRNA) gene amplicon sequencing. Based on the distribution of the amplicon sequence variants (ASVs), we assessed the alpha-diversity level of each sample and further measured the differences in species abundance composition among the samples, and predicted the metabolic function of the community based on the gene sequencing results.

Results: The results revealed that different Populus spp. under the same stand conditions resulted in different phyllosphere bacterial communities. The bacterial community structure was mainly affected by the carbon and soluble sugar content of the leaves, and the leaf nitrogen, phosphorus and carbon/nitrogen were the main factors affecting the relative abundance of phyllosphere bacteria.

Discussion: Previous studies have shown that a large proportion of the variation in the composition of phyllosphere microbial communities was explained by the hosts themselves. In contrast, leaf-borne nutrients were an available resource for bacteria living on the leaf surface, thus influencing the community structure of phyllosphere bacteria. These were similar to the conclusions obtained in this study. This study provides theoretical support for the study of the composition and structure of phyllosphere bacterial communities in woody plants and the factors influencing them.

KEYWORDS

phyllosphere microorganism, microbiomes, *Populus* spp., phyllosphere microbial community, phyllosphere

Introduction

Microorganisms are an important part of the ecosystem and play an important role in its stability. Their survival and reproduction affect the healthy growth of the plants. The plants are one of the most important habitats for microorganisms, and both the underground roots and above-ground branches and leaves are colonized by a large number of microorganisms, with the above-ground environment formed by the branches and leaves called the phyllosphere (Ruinen, 1956; Vorholt, 2012; Vacher et al., 2017). For a long time, research on phyllosphere microbial communities has lagged far behind that on rhizosphere microbial communities (Lindow and Brandl, 2003; Miura et al., 2019). Compared to soil and rhizosphere, phyllosphere microorganisms are less diverse but still play a key role (Xu et al., 2022). In general, the phyllosphere refers mainly to the environment in which the leaf is formed, and the microorganisms that colonize the leaf are called phyllosphere microorganisms (Lindow and Brandl, 2003; Vorholt, 2012). The phyllosphere contains both the leaf surface and the internal leaf environment, and accordingly, phyllosphere microorganisms also include epiphytic bacteria on the leaf surface and endophytic bacteria in the leaf interior (Peñuelas and Terradas, 2014; Tkacz et al., 2020; Gong and Xin, 2021).

The total surface area of the above-ground portion of plants worldwide is estimated to be about 10^9 km^2 (mostly leaf surface) (Vorholt, 2012), an area about twice the size of the Earth, making it one of the largest microhabitats on the planet (Vorholt, 2012). Also, in the phyllosphere grows a large number of microorganisms, including bacteria, yeasts, filamentous fungi, archaea and algae (Lindow and Brandl, 2003; Berlec, 2012). Bacteria are the most abundant group closely associated with plants (Bringel and Couée, 2015; Bao et al., 2020), with an average of 10^6 ~10^7 bacterial cells per square centimeter of leaf surface, occupying a major position in the phyllosphere microbial community (Vorholt, 2012). Also, several studies show that bacteria can have very intimate interactions with plants that involve intracellular colonization and even endosymbiosis (Hardoim et al., 2015; Koskimäki et al., 2015). Much of the research on phyllosphere microbes has been focused on phyllosphere bacteria (Dickinson et al., 1975; Bodenhausen et al., 2013).

Phyllosphere microorganisms are normally attached to the surface of leaves and form complex parasitic, mutualistic relationships with host plants and other microorganisms, but most phyllosphere microorganisms are in a symbiotic relationship with their host plants (Kishore et al., 2005). Phyllosphere microorganisms are complexly diverse, with different species having different microbial communities (Leveau, 2015). It has been shown that the presence of phyllosphere microorganisms is the result of a combination of colony competition, climatic selection and host selection. The composition of phyllosphere microorganisms can vary across plants, and factors associated with the population structure of phyllosphere microorganisms include plant phenotypic traits, leaf height and position, and leaf age (Hunter et al., 2010). Environmental factors, plant genotypes and the shape of plant species all affect the community composition of phyllosphere microorganisms to varying degrees. Vokou et al. (2012); Redford et al. (2010) and Vogel et al. (2020) suggest that plant species are a major factor influencing the composition and diversity of phyllosphere microorganism communities, and that different plant species have corresponding phyllosphere microorganism communities. In contrast, Laforest-Lapointe et al. (2016) explored the different drivers influencing the composition of phyllosphere bacterial communities in trees and found that host species accounted for 27% of the factors influencing the composition of phyllosphere bacteria. Existing studies have shown that host species are a major factor influencing the community diversity and structure of phyllosphere microorganisms. The main factor of host species is related to differences in the physicochemical properties of plant leaves (Whipps et al., 2008). Different plant leaf characteristics such as stomata, trichomes, leaf thickness, nutrient content (carbon, phosphorus and soluble sugar content) and water content all influence the colonisation of phyllosphere microorganisms (Bunster et al., 1989; Yadav et al., 2005; Beattie, 2011; Kembel and Mueller, 2014; Kembel et al., 2014).

A study of the model plant *Arabidopsis thaliana* using genome wide association study (GWAS) found that different species of *A. thaliana* phyllosphere microorganisms have different community composition (Horton et al., 2014). In addition, different species of the same plant species exhibited different phyllosphere microorganisms' communities among themselves. This has been confirmed by many scholarly studies on common cash crops such as *Solanum tuberosum*, *Capsicum frutescens* var. *grossum*, *Lycopersicon esculentum*, and *Gossypium* spp. (Adams and Kloepper, 2002; Sessitsch et al., 2002; Rasche et al., 2006a; Rasche et al., 2006b; Correa et al., 2007; Hunter et al., 2015). Hunter et al. (2010) also found that different varieties of *Lactuca sativa* had different phyllosphere bacterial communities, and that differences in bacterial community structure were related to the characteristics of the leaves themselves, such as leaf morphology and soluble carbohydrates, calcium and phenolic compounds. *Populus* spp. are the model species of choice for woody plant research because of its compact genome composition, species richness, wide distribution, ease of genetic transformation and ease of asexual reproduction (Bradshaw et al., 2000; Taylor, 2002; Beckers et al., 2016; Beckers et al., 2017; Brunner et al., 2004). The poplar germplasm conservation trial forest in Tongzhou, Beijing has six species of *Populus* spp. planted in 2015 under the same stand conditions. High-throughput sequencing analysis has become one of the most commonly used methods for analyzing the composition of phyllosphere microbial communities (Rastogi et al., 2012), increasing the extent of our knowledge of the composition of phyllosphere microbial communities. Based on this, we hypothesized: do different *Populus* spp. under the same stand conditions also have different phyllosphere bacterial communities? Are the differences in bacterial community composition and structure related to the properties of the leaves themselves, such as carbon, nitrogen, phosphorus and non-structural carbohydrates in the leaves?

Method and materials

Plant environmental factor analysis of different samples

The sampling site of this experiment was the International Seed Technology Park in Beixindian Village, Yujiawu Township,

Tongzhou District, Beijing (116°40'46″E, 39°42'59″N). The location has a temperate continental monsoon climate, which is influenced by both winter and summer winds, resulting in a windy and arid climate in spring, more rain and higher temperatures in summer, crisp climate in autumn and cold weather in winter. The average annual temperature can reach 11.3°C, and the average precipitation is about 620mm. the terrain is flat. The poplar germplasm conservation test forest in Tongzhou, Beijing, was planted in March 2015. The test species were *Populus* × *euramaricana* 'Bofeng 3 hao' (YA), *P. deltoides* 'Shanghaiguan' × *P. deltides* 'Harvard' (YB), *P. nigra* 'N46' (YC), *P. nigra* 'N102' (YD), *P.* × *euramericana* 'Guariento' (YE), and *P. alba* × *P. glandulosa* '84k' (YF). Each species was planted in a 30×30 m sample plot.

Sample collection and processing

In August 2022, three 10 × 10 m sample plots were set up in each sample area, and five poplars of similar growth were selected in each sample plot according to the five-point sampling method. Plant samples were collected from the middle tip of the canopy in three directions (120°), and mixed into one replicate in each sample plot. Each leaf sample was cut with a pair of sterilized scissors and placed in a sterile sampling bag placed on an ice box. In order to standardize conditions as much as possible, only green, healthy, whole leaves were selected. A total of 18 samples (3 replicates × 6 tree species) were collected (Supplementary Figure 1). Plants were planted in each plot with the density of 2 m × 2 m. All plant samples were collected on the same day and transported to the laboratory for subsequent analysis.

In each leaf replicate, 30 g of leaf samples were placed in a 1000 mL sterile conical flask and then filled with 500 mL of sterile PBS buffer (pH 7.4, 1 × phosphate buffer). To wash the microbial cells from the leaves, sonication was performed in an ultrasonic clearing bath at a frequency of 40 kHz for 6 min, with oscillation at 200 r/min for 20 min at 30°C, followed by sonication (frequency 40 kHz) for 3 min. The microbial cells were separated from the leaves by filtering the cell suspension through a sterile nylon membrane of 0.22 μm × 50 mm. The membrane samples were stored at -80°C.

Afterwards, the plant leaves were repeatedly rinsed with sterile distilled water and the surface dried with phosphate-free filter paper. After baking at 105°C for 30 min, with drying at 65°C for more than 48 h until the samples were of constant weight. The petioles and veins were cut off, ground and passed through a 100-mesh sieve for the determination of physicochemical properties.

Leaves chemical properties determination

Dried plant samples of 3.5-4.2 mg were weighed and sealed in a tin container and then the carbon and nitrogen contents of the leaves were determined by the elemental analyzer (Elementar Vario EL III Germany). Phosphorus of leaves was determined by the molybdenum antimony anti-colorimetric method (Li et al., 2019). The content of soluble sugars and starch in the leaves was determined by the anthrone colorimetric method (Du et al., 2020).

DNA extraction and high-throughput sequencing

All DNA was extracted using the Fast®DNA SPIN kit (MP Biomedicals, Santa Ana, CA, USA) according to the manufacturer's instructions. The amount and quality of DNA was measured by NanoDrop NC2000 spectrophotometer (Thermo Fisher Scientific, Waltham, MA, USA) and agarose gel electrophoresis for extracted DNA. The library was constructed using Illumina's TruSeq Nano DNA LT Library Prep Kit. The end repair process starts by using the End Repair Mix2 in the kit to excise the base protruding from the 5' end of the DNA, fill in the missing base at the 3' end, and add a phosphate group to the 5' end. A separate A-base is then added to the 3' end of the DNA to prevent self-association of the DNA fragment. PCR amplification of the bacterial 16S rRNA genes V3–V4 region was performed using the forward primer 338F (5'–ACTCCTACGGGAGGCAGCA–3') and the reverse primer 806R (5'–GGACTACHVGGGTWTCTAAT–3') (Claesson et al., 2009). Sample-specific 7-bp barcodes were incorporated into the primers for multiplex sequencing. The PCR components contained: 5 × reaction buffer 5 μL, 5 × GC buffer 5 μL, dNTP (2.5 mM) 2 μL, Forwardprimer (10 uM) 1 μL, Reverseprimer (10 uM) 1 μL, DNA Template 2 μL, ddH_2O 8.75 μL, Q5 DNA Polymerase 0.25 μL. The amplification parameters were initial denaturation 98°C 2 min, followed by 25-30 cycles consisting of denaturation 98°C 15 s, annealing 55°C 30 s, extension 72°C 30 s, final extension 72°C 5 min, 10°C hold. Vazyme VAHTSTM DNA Clean Beads (Vazyme, Nanjing, China) were used to purify PCR amplicons, and the Quant-iT PicoGreen dsDNA Assay Kit was used to quantify them (Invitrogen, Carlsbad, CA, USA). Pair-end 250 bp sequencing was carried out at Shanghai Personal Biotechnology Co., Ltd. using the Illlumina NovaSeq platform and NovaSeq 6000 SP Reagent Kit (500 cycles).

Data analytics

Amplicons were pooled in equal amounts following the individual quantification step. Taxonomy was assigned to amplicon sequence variants (ASVs) using the classify-sklearn naive Bayes taxonomy classifier in feature-classifier plugin against the silva_132. The NCBI database SRA accession number for of the raw high-throughput sequencing data of leaf bacterium is PRJNA924105. The primer fragments of the sequences were first excised by calling qiime cutadapt trim-paired and the unmatched primer sequences were discarded; then DADA2 was called by qiime dada2 denoise–paired for quality control, denoising, splicing and chimera removal. The above steps were analyzed separately for each library (Callahan et al., 2016). After the denoising of all libraries was completed, the ASVs feature sequences and ASV tables were merged and the total number of denoised sequences (effective sequence volume) was 1,318,062 with an average of 73,225.67 per sample. After removing the chimeras, the total amount of high-quality sequences obtained was 1,029,576 with a mean value of 57,198.67 (49,640 - 63,956).

Venn diagram and histogram of sample ASVs numbers were made with jvenn which is a plug-in for the jQuery Javascript library (Bardou et al., 2014). In order to provide a more com-prehensive assessment of the alpha diversity of the microbial community, the Chao1 and Observed species indices were used to characterize richness (Chao, 1984), the Shannon and Simpson indices to characterize diversity and the Pielou's evenness index to characterize evenness (Shannon, 1948; Simpson, 1949; Pielou, 1966). Box line plots were created using QIIME2 (2019.4) and the ggplot2 package for the R package (v3.2.0) (Wickham, 2009) and the significance of the differences was verified by Kruskal-Wallis rank sum test and dunn'test as a *post hoc* test. Cluster analysis was performed using the uclust function of the R package (v3.2.0) stat package, using the UPGMA algorithm by default for the Bray–Curtis distance matrix (i.e., the clustering method is average), and visualized using the R package (v3.2.0) script ggtree package (Ramette, 2007). The QIIME2 (2019.4) "qiime taxa barplot" was called to visualize the compositional distribution of each sample at five taxonomic levels: phylum, class, order, family and genus, by counting the feature list after removing singleton. The heatmap was drawn using the pheatmap package in R (v3.2.0) (Gu and Hübschmann, 2022). One-way ANOVA was used to analyze the significant difference of leave chemical properties, and S-N-K q test was used to conduct post-test. Data of significant differences in leave chemical properties were processed by Excel (2019) and analyzed by IBM SPSS 26.0 (Chicago, USA). The linkages between leaf nutrient factors and phyllosphere bacterial community composition and diversity were performed by Redundancy analysis (RDA) *via* Canoco 5. Phylogenetic Investigation of Communities by Reconstruction of Unobserved States (PICRUSt2) took 16S rRNA gene sequences for metabolic pathway prediction in the MetaCyc functional database (https://metacyc.org/) (Douglas et al., 2020). The data were normalized using the sum of the abundances of the EC's for each sample in parts per million. The average abundance of the second level pathway was calculated using R based on the selected samples.

Results

Composition and structure of phyllosphere bacterial communities of different *Populus* spp.

Venn diagrams were produced using the ASV abundance table, as shown in Figure 1A. Six species of *Populus* spp. shared 283 ASVs. The number of ASVs was 3280, 1983, 2829, 2814, 2182 and 2426 for YA, YB, YC, YD, YE, and YF, respectively (Figures 1B, 1C). The number of ASVs specific to YA (1733) was the highest and YE (889) the lowest (Figure 1A).

The alpha diversity indices of six different species of *Populus* spp. were analyzed based on the Kruskal-Wallis algorithm and differences were found between them. Chao 1, Shannon, Observed_species, Pielou_e indices were significantly different between groups ($p < 0.05$), while Simpson index was not significantly different between groups ($p > 0.05$). YA had the highest Chao 1, Shannon, Simpson, Observed_species, Pielou_e indices. The lowest mean values of Chao1 and Observed_species indices were found in YB, and the lowest mean values of Shannon, Simpson, Pielou_e indices were found in YC (Figure 2).

Hierarchical clustering analysis of phyllosphere bacterial communities at the genus level using Bray-Curtis distance algorithm and average clustering was performed as in Figure 3. YB and YC were clustered into one category alone and the remaining four treatments were clustered into one category. YD was more similar to YE. The histogram on the right indicates that the microbial communities were not equally abundant at the genus level, and although the species composition of the treatments was similar, there were differences in abundance. The heatmap also confirmed this conclusion (Figure 4).

Statistical analysis of the sampled ASVs resulted in a table of the specific composition of phyllosphere bacteria in each sample for each taxonomic level. With this table, it was possible to calculate the composition of taxonomic units contained in each taxonomic level for each of the six samples. Statistically, high-throughput sequencing yielded a total of 31 phyla, 76 classes, 179 orders, 313 families, 683 genera and 940 species.

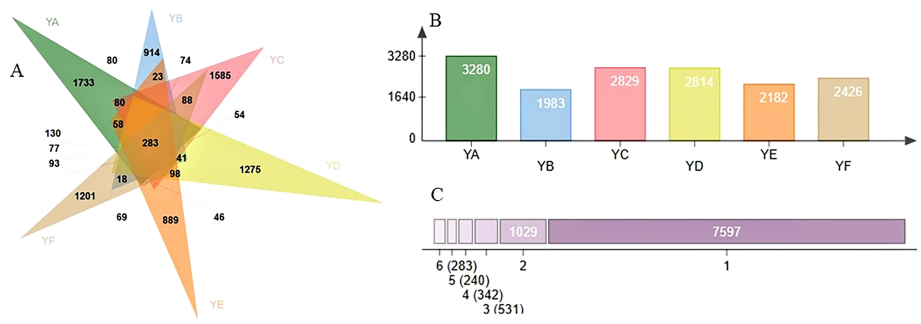

FIGURE 1
(A) venn diagram for different sample leaves; **(B)** number of ASVs per grouping; **(C)** number of ASVs, specific (1) or shared by 2,3, ..., 6. YA: *Populus* × euramaricana 'Bofeng 3 hao'; YB: P. deltoides 'Shanghaiguan' × P. deltides 'Harvard'; YC: P. nigra 'N46'; YD: P. nigra 'N102'; YE: P. × euramericana 'Guariento'; YF: P. alba × P. glandulosa '84k'.

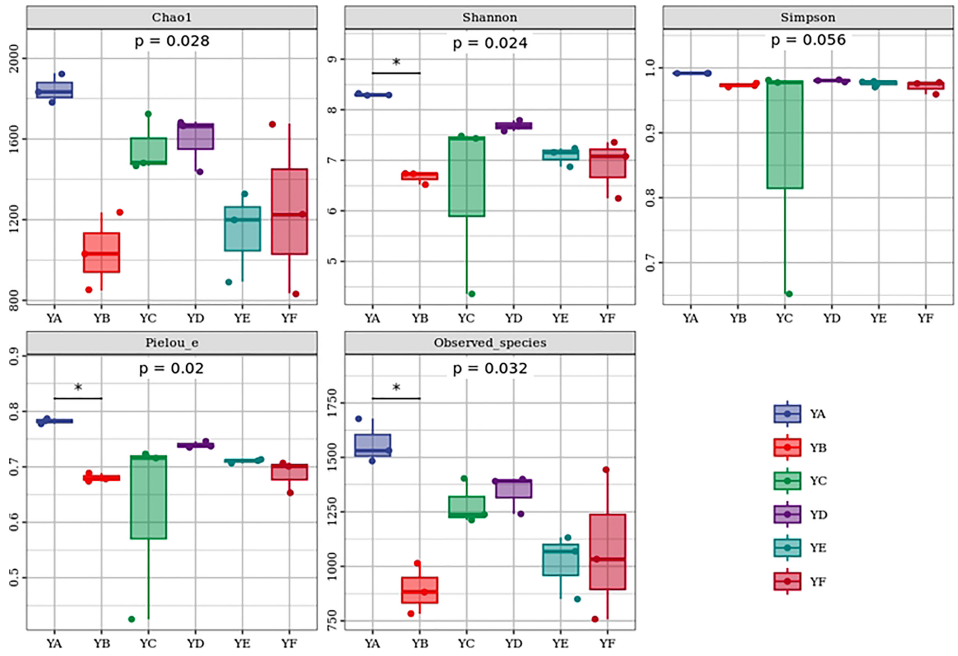

FIGURE 2
Box plot of alpha diversity of phyllosphere bacterial communities of different species of *Populus* spp.* indicated $p < 0.05$ by dunn'test as a post-hoc test. YA: *Populus* × *euramaricana* 'Bofeng 3 hao'; YB: *P.deltoides* 'Shanghaiguan' × *P. deltides* 'Harvard'; YC: *P.nigra* 'N46': YD: *P.nigra* 'N102'; YE: *P.* × *euramericana* 'Guariento'; YF: *P. alba* × *P.glandulosa* '84k'.

At the phylum level, the relative abundance of phyllosphere bacteria greater than 1% were Proteobacteria, Actinobacteria, Firmicutes, Bacteroidetes, Deinococcus-Thermus. Among them, Proteobacteria and Actinobacteria were the dominant phylum with relative abundance greater than 10%. The highest relative abundance content of Proteobacteria was found in YC (76.96%) and the lowest in YD (59.37%). Conversely, Actinobacteria had the highest relative abundance in YD (27.31%) and the lowest in YC (14.69%). Firmicutes had the significantly highest relative abundance in YB at 6.43%. Bacteroidetes had higher relative abundance in YD and YA at 6.20% and 5.24%, respectively (Figure 5A).

The top ten phyllosphere bacterial classes in relative abundance were Gammaproteobacteria, Alphaproteobacteria, Actinobacteria, Bacilli, Bacteroidia, Deinococci, Deltaproteobacteria, Saccharimonadia, Thermoleophilia, Acidimicrobiia. Gammaproteobacteria had the highest relative abundance among the six samples at 61.75%, while Alphaproteobacteria (14.98%) and Actinobacteria (14.12%) had the lowest relative abundance among the six samples. Alphaproteobacteria had the highest relative abundance in YF (49.33%) and Actinobacteria had the highest abundance in YD (26.97%) (Supplementary Figure 2A). At the order level, Enterobacteriales had the highest abundance in YC at 53.29%, while YA contained only 7.05%. Micrococcales varied little in

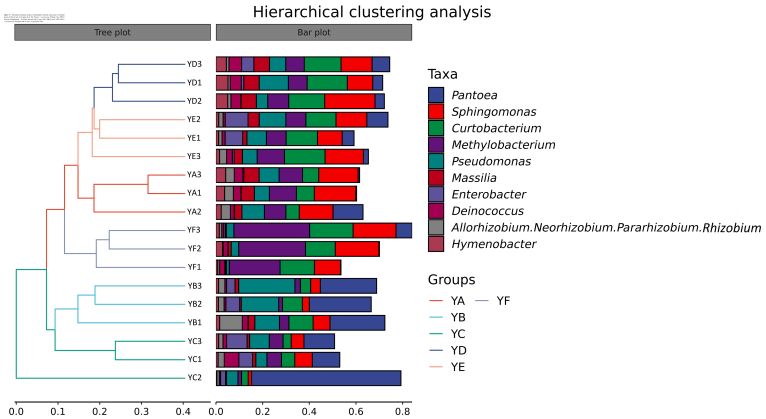

FIGURE 3
Hierarchical clustering analysis of phyllosphere bacterial communities of different species of *Populus* spp. at the genus level. YA: *Populus* x *euramaricana* 'Bofeng 3 hao'; YB: *P. deltoides* 'Shanghaiguan' *P. deltides* 'Harvard'; YC: *P. nigra* 'N46'; YD: *P. nigra 'N102'*; YE: *P.* x *euramericana* 'Guariento'; YF: *P. alba* × *P. glandulosa* '84k'.

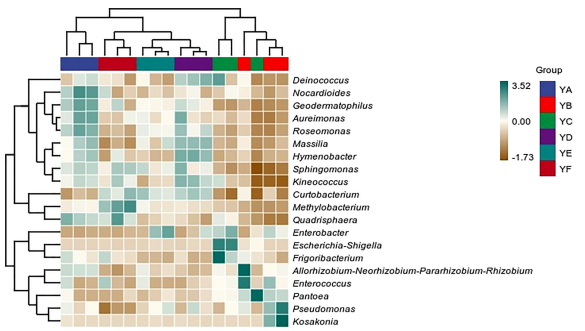

FIGURE 4
Heatmap of phyllosphere bacterial communities of different species of *Populus* spp. at the genus level. YA: *Populus* x *euramaricana* 'Bofeng 3 hao'; YB: *P. deltoides* 'Shanghaiguan' × *P. deltides* 'Harvard'; YC: *P. nigra* 'N46'; YD: *P. nigra* 'N102'; YE: *P.* x *euramericana* 'Guariento'; YF: *P. alba* × *P. glandulosa* '84k'.

abundance across the six *Populus* spp. leaves, ranging from 9.88% (YC) to 20.44% (YD). Rhizobiales had the highest abundance in YF at 30.63% and only 9.05% in YB (Supplementary Figure 2B). At the family level, the relative abundance of Enterobacteriaceae was as high as 53.29% in YC and less than 10% in both YA and YF. Microbacteriaceae had the highest abundance in YD (19.93%), Sphingomonadaceae had the highest abundance in YA (17.72%), and Beijerinckiaceae had the highest abundance in YF (28.04%) (Supplementary Figure 2C).

At the genus level, the genera ranked greater than 1% in relative abundance were *Pantoea*, *Sphingomonas*, *Curtobacterium*, *Methylobacterium*, *Pseudomonas*, *Massilia*, *Enterobacter*, *Deinococcus*, *Allorhizobium-Neorhizobium-Pararhizobium-Rhizobium*, *Hymenobacter*, *Escherichia-Shigella*, *Enterococcus*, *Kineococcus*, *Geodermatophilus*, *Aureimonas*, *Kosakonia*. *Pantoea* was the most abundant in YC with 29.62%, while in YF it was only 2.45%. the relative abundance of *Sphingomonas* in YA, YD, YE, YF was greater than 10%. *Curtobacterium* had the highest relative abundance in YD (16.12%) and *Methylobacterium* the highest in YF (27.62%). 2.55% of *Pseudomonas* was found in YF but 16.91% in YB (Figure 5B).

Variation in leaf nutrient indices among six *Populus* spp.

The six species of *Populus* spp. varied in their basal nutrient indexes in leaves. While the differences in soluble sugar and starch

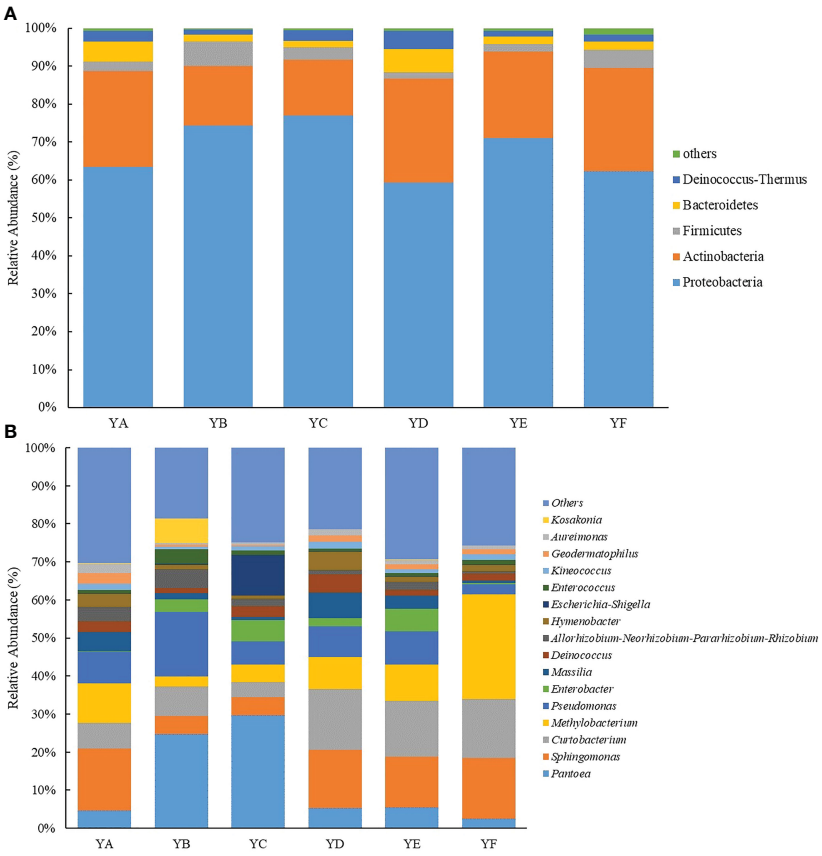

FIGURE 5
Analysis of the composition of phyllosphere bacterial communities in different *Populus* spp. at all levels of taxonomic units. **(A)** at the phylum level; **(B)** at the genus level; YA: *Populus* x *euramaricana* 'Bofeng 3 hao'; YB: *P. deltoides* 'Shanghaiguan' *P. deltides* 'Harvard'; YC: *P. nigra* 'N46'; YD: *P. nigra* 'N102'; YE: *P.* x *euramericana* 'Guariento: YF: *P. alba* × *P. glandulosa* '84k'.

content were not statistically significant ($p > 0.05$), there were significant differences in their carbon, nitrogen, phosphorus, and carbon/nitrogen ratios ($p < 0.05$). YC had the lowest carbon/nitrogen ratio (average value of 14.16), the highest N content (average value of 31.37 g/kg), and the highest phosphorus content (average value of 6.40 g/kg). The highest carbon/nitrogen ratio (mean value 17.79) and highest average carbon content (mean value 467.34 g/kg) were both found in the YF. YA had the least amount of soluble sugar, starch, phosphorus, nitrogen, and carbon (Table 1).

Effect of leaf nutrient factors on the composition and structure of phyllosphere bacterial communities

To better understand the relationship between phyllosphere bacterial communities diversity and leaf nutrient factors, Detrended correspondence analysis (DCA) was carried out on the alpha diversity and soil chemical properties of phyllosphere bacterial communities, and the result showed that the maximum gradient length = 0.10 < 3, indicating that the distribution of different species of poplar phyllosphere bacterial communities was closer to the linear model and that the redundancy analysis (RDA) could better explain the relationship between them. The RDA indicated that six leaf nutrient factors explained a total of 67.53% of the overall eigenvalues and had significant effects on phyllosphere bacterial community diversity. The eigenvalues of the first two sorting axes of the RDA explained 50.6% and 16.72% of the variation in phyllosphere bacterial communities' diversity, respectively (Figure 6). And only soluble sugar (p =0.004), and starch (p =0.046) among the six nutrient factors had a significant effect on phyllosphere bacterial community diversity, explaining 54.3%, and 17.6% of the variation in phyllosphere bacterial community diversity. Carbon/nitrogen was positively correlated with all five indices and the starch content was only positively correlated with the Simpson, Pielou_e and Shannon indices. The remaining leaf nutrient factors all had a negative effect on the alpha diversity index.

DCA of the relative abundance of phyllosphere bacterial communities at the phylum level and genus level greater than 1% with leaf nutrient factors showed that the maximum gradient length = 0.36 (phylum), 0.6 (genus), both less than 3. This indicates that RDA could better explain the relationship between them.

At the phylum level, RDA showed that the six leaf nutrient factors together explained 53.58% of the overall eigenvalues (Figure 7A). The eigenvalues from the first two ordination axes of RDA explained 39.72% and 7.52% of the variation in phyllosphere bacterial community's diversity, respectively. Only leaf nitrogen content had a significant effect on the phyllosphere bacterial clade, explaining 47.1% of the variation in community diversity (p = 0.008). At the genus level, the eigenvalues from the first two ordination axes of RDA explained 27.08% and 9.39% of the variation in phyllosphere bacterial community's diversity (Figure 7B). Only 48.8% of the eigenvalues are explained on the four axes. Leaf phosphorus content had a significant effect on the phyllosphere bacterial community diversity (p = 0.002).

Prediction of the functional potential of phyllosphere bacterial communities of different *Populus* spp.

The analysis of the bacterial community based on the MetaCyc database (Figure 8) showed that at the primary level, there were Biosymthesis, Degradation/Utilization/Assimilation, Detoxification, Generation of Precursor Metabolite and Energy, Glycan Pathways, Macromolecule Modification, and Metabolic Clusters. The highest relative abundance of bacteria was associated with Biosynthesis at 62.47%.

The top three metabolic functions studied at the secondary level were Cofactor, Prosthetic Group, Electron Carrier, and Vitamin Biosynthesis (15.03%), Amino Acid Biosynthesis (14.15%) and Nucleoside and Nucleotide Biosynthesis (12.29%). The flora also had metabolic functions, for example, Fatty Acid and Lipid Biosynthesis (8.19%), Carbohydrate Biosynthesis (5.00%), Fermentation (3.81%), TCA cycle (3.56%), Cell Structure Biosynthesis (3.13%), Nucleoside and Nucleotide Degradation (2.89%), Carbohydrate Degradation (2.74%), Secondary Metabolite Degradation (2.45%), Carboxylate Degradation (2.38%), Secondary Metabolite Biosynthesis (2.22%), C1 Compound Utilization and Assimilation (1.45%), Inorganic Nutrient Metabolism (1.45%),

TABLE 1 Variation in the chemical properties of the leaves of different species of *Populus* spp.

	Carbon/g kg^{-1}	Nitrogen/g kg^{-1}	Carbon/nitrogen	Phosphorus/g kg^{-1}	Soluble sugar/mg kg^{-1}	Starch/mg kg^{-1}
YA	439.26 ± 5.47 B	25.19 ± 0.97 C	17.51 ± 0.64 A	2.09 ± 0.16 C	15.72 ± 3.76 A	57.52 ± 4.61 A
YB	457.55 ± 9.45 AB	30.03 ± 1.46 AB	15.30 ± 0.45 BC	3.47 ± 0.41 B	21.93 ± 1.51 A	60.76 ± 2.16 A
YC	443.82 ± 0.94 B	31.37 ± 0.56 A	14.16 ± 0.27 C	6.40 ± 0.41 A	24.08 ± 5.53 A	74.13 ± 6.77 A
YD	442.33 ± 7.68 B	27.10 ± 0.33 BC	16.33 ± 0.20 AB	2.51 ± 0.02 C	22.91 ± 0.93 A	71.73 ± 1.94 A
YE	450.98 ± 3.71 AB	30.31 ± 0.26 AB	14.88 ± 0.08 BC	2.52 ± 0.06 C	26.27 ± 2.25 A	68.80 ± 6.75 A
YF	467.34 ± 1.75 A	26.46 ± 1.33 C	17.79 ± 0.87 A	2.10 ± 0.06 C	21.61 ± 2.89 A	68.44 ± 4.50 A
F	3.493	6.974	8.635	44.914	1.233	1.759
p	0.022	0.001	<0.001	<0.001	0.335	0.172

Data were average ± standard error. Different capital letters meant significant difference at 0.05 level. YA: *Populus* × euramaricana 'Bofeng 3 hao'; YB: P. deltoides 'Shanghaiguan' × P. deltides 'Harvard'; YC: P. nigra 'N46'; YD: P. nigra 'N102'; YE: P. × euramericana 'Guariento'; YF: P. alba × P. glandulosa '84k'.

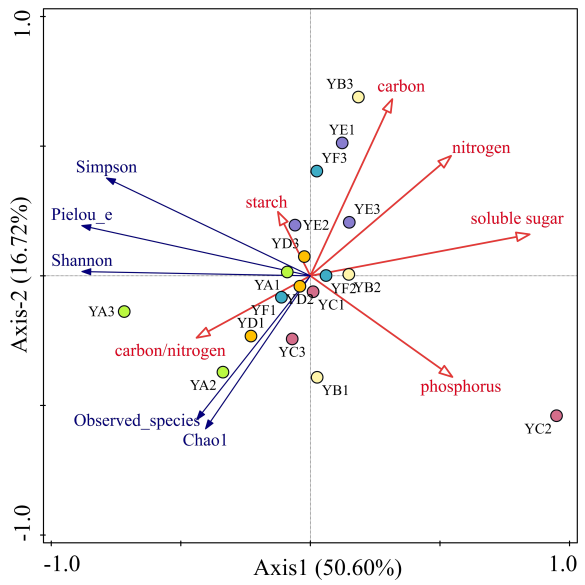

FIGURE 6
Redundancy analysis (RDA) of leaf nutrient factors and alpha diversity of phyllosphere bacterial communities. YA: *Populus* x *euramaricana* 'Bofeng 3 hao'; YB: *P. deltoides* 'Shanghaiguan' *P. deltides* 'Harvard'; YC: *P. nigra* 'N46'; YD: *P. nigra* 'N102'; YE: *P.* x *euramericana* 'Guariento'; YF: *P. alba P.*× *P. glandulosa* '84k'.

Glycolysis (1.40%), Aromatic Compound Degradation (1.40%), Amino Acid Degradation (1.37%), Pentose Phosphate Pathways (1.20%), Respiration (1.18%), Electron Transfer (1.18%), Aromatic Compound Biosynthesis (1.00%). Other than that, there were 38 metabolic functions with a relative abundance of less than 1%.

Discussions

The present study found differences in the composition and structure of the phyllosphere bacterial community of different *Populus* spp. under the same off-site conditions, which answers the first hypothesis presented in the previous section. A large proportion of the variation in the composition of phyllosphere microbial communities is explained by the hosts themselves (Laforest-Lapointe et al., 2016). Plant genotypes have a decisive influence on the composition of phyllosphere microbial communities (Whipps et al., 2008; Bálint et al., 2013; Bodenhausen et al., 2014). Current studies have shown that phyllosphere microbial community structure differs significantly between plants, that phyllosphere microbes of the same species vary with their geographical location, and that the community composition of phyllosphere microbes is distinctly host-specific (Finkel et al., 2012; Rastogi et al., 2012). Finkel et al. (2011) also found that geographical location, rather than tree species, was the main determinant of bacterial communities in the phyllosphere. The six *Populus* spp. in this study were all harvested from the same habitat and were similar in elevation, temperature, rainfall and sunlight, which may explain the differences in phyllosphere microbial community composition between them, but the alpha diversity indices were less significantly different (p<0.05).

A correlation heat map analysis of physicochemical properties and alpha diversity of the phyllosphere bacterial community and the top ten phyla and genera in relative abundance revealed that leaf carbon and soluble sugar content were the main and negative influences on the alpha diversity index. The bacterial composition of the phyllosphere was mainly influenced by leaf nitrogen content, carbon/nitrogen, at the phylum and genus level. Leaf phosphorus content also significantly influenced the relative abundance of phyllosphere bacterial genera. Previous studies have shown that the growth of interleaf bacteria is limited mainly by carbon and to a lesser extent by nitrogen (Delmotte et al., 2009; Kembel and Mueller, 2014), but in the present study the effect of leaf carbon content on bacteria was not significant. These essential nutrients are available resources for bacteria living on the leaf surface and thus influence the community structure of phyllosphere bacteria (Gong and Xin, 2021). Kembel et al. (2014) found that leaf nitrogen and

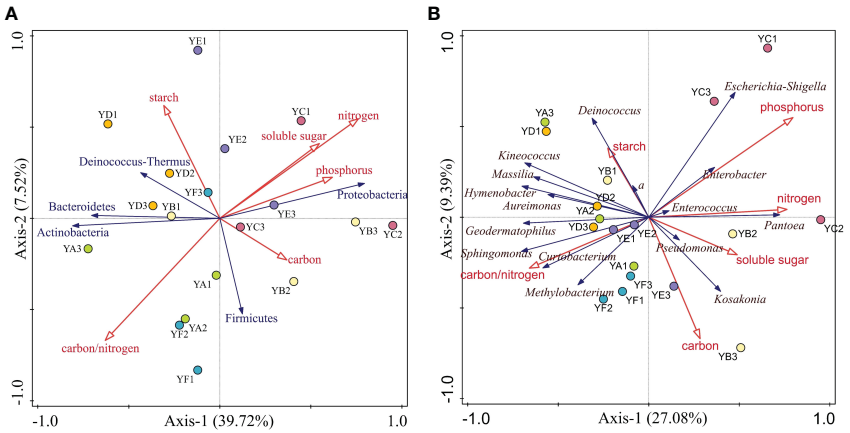

FIGURE 7
Redundancy analysis (RDA) of leaf nutrient factors and relative abundance > 1% of phyllosphere bacterial communities at the phylum **(A)** and genus **(B)** level. YA: *Populus* x *euramaricana* 'Bofeng 3 hao'; YB: *P. deltoides* 'Shanghaiguan' x *P. deltides* 'Harvard'; YC: *P. nigra* 'N46'; YD: *P. nigra* 'N102'; YE: *P.* x *euramericana* 'Guariento'; YF: *P. alba* × *P. glandulosa* '84k'.

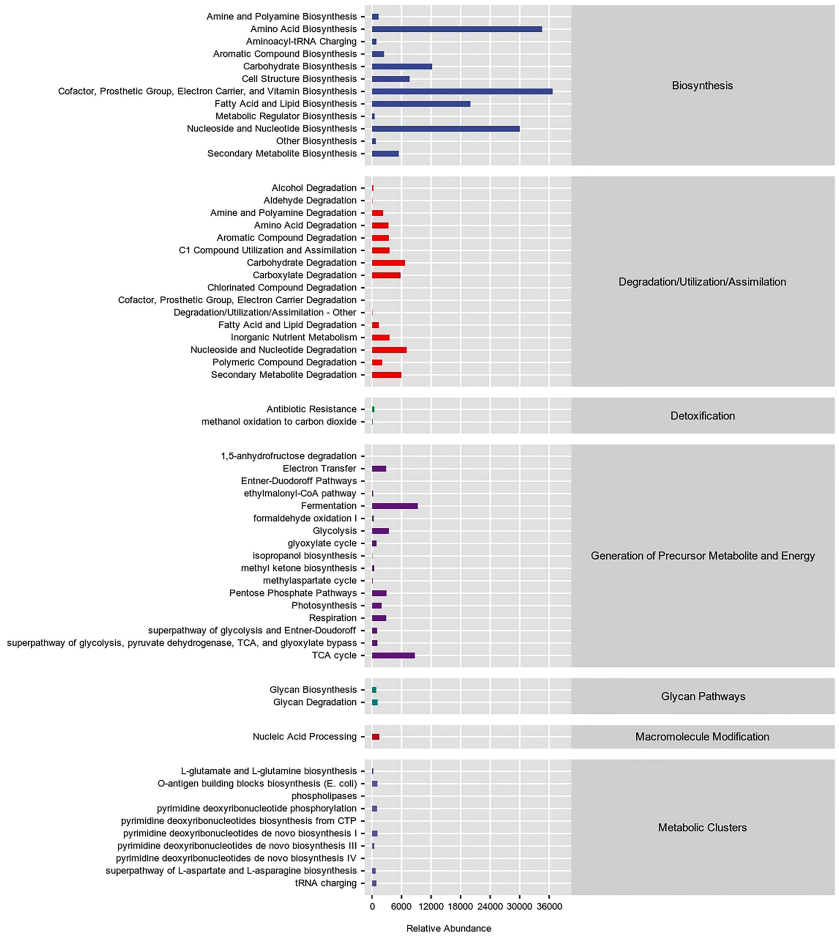

FIGURE 8
Predicting metabolic pathway statistics in interleaf bacterial communities based on the MetaCyc database.

phosphorus content effected the phyllosphere bacterial community. Yadav et al. (2005) demonstrated that leaf shape, marginal folds and stomata as well as leaf chemistry (nitrogen, phosphorus, soluble carbohydrates and water content) affect the community composition of phyllosphere microorganisms, resulting in different interleaf bacterial colonization. These previous studies all support the conclusions reached in this study.

The dominant taxa of phyllosphere bacteria are mainly Proteobacteria and Actinobacteria, which is consistent with the findings of other scholars (Delmotte et al., 2009; Rastogi et al., 2012). Additionally, there were also significant concentrations of the relatively abundant phyla Firmicutes, Bacteroidetes, Deinococcus-Thermus, Patescibacteria, Acidobacteria, Gemmatimonadetes, Chloroflexi, and FBP. Previous studies have shown that the bacterial community phylogenetic structure of the phyllosphere microbial community contains relatively few phyla, dominated by Proteobacteria, Actinobacteria, Firmicutes and Bacteroidetes, which generally dominate the bacterial community composition (Redford et al., 2010; Kembel et al., 2014; Kecskeméti et al., 2016; Grady et al., 2019). Furthermore, microflora belonging to the Proteobacteria phylum are rich in metabolic diversity and have a variety of functions in the interleaf bacterial community such as methylotrophy, nitrification, nitrogen fixation and non-oxygenic photosynthesis (Fürnkranz et al., 2008; Atamna-Ismaeel et al., 2012; Watanabe et al., 2016). Besides Proteobacteria, microorganisms of the Bacteroidetes and Actinobacteria all perform different ecological functions in the phyllosphere environment (Romero et al., 2016). A number of major bacterial genera, including *Methylobacterium*, *Pseudomonas*, *Bacillus*, *Massilia*, *Sphingomonas*, *Arthrobacter* and *Pantoea*, appear to constitute the core phyllosphere microbial taxa (Rausch et al., 2001; Lopez-Velasco et al., 2011; Knief et al., 2012; Rastogi et al., 2012). The relative abundance of the genera *Pantoea*, *Sphingomonas*, *Curtobacterium*, *Methylobacterium*, were found to be high in *Populus* spp. phyllosphere bacteria. The interactions of some phyllosphere microbial communities provide some protection to plants (Innerebner et al., 2011; Ottesen et al., 2015). For example, bioactive molecules produced by Pseudomonas strains (e.g., Coronatine and Syringolin A) can induce stomatal closure and thus affect the entry of pathogens into apoplast (Melotto et al., 2006; Hunter et al., 2010). The phyllosphere microbes are also able to

cycle carbon and nitrogen through the direct use of carbohydrates released by plants or secreted by arthropods, the interception of ammonium atmospheric pollutants by nitrifying bacteria and nitrogen fixation (Müller and Ruppel, 2014).

In summary, in our study it was found that different *Populus* spp. under the same stand conditions resulted in different phyllosphere bacterial communities. While bacterial community structure was mainly influenced by leaf carbon and soluble sugar content, leaf nitrogen, phosphorus and carbon/nitrogen were the main factors affecting the relative abundance of phyllosphere bacteria. This provides theoretical support for the study of the composition and structure of phyllosphere bacteria in woody plants and the factors influencing them.

Data availability statement

The datasets presented in this study can be found in online repositories. The names of the repository/repositories and accession number(s) can be found below: NCBI, accession number PRJNA924105.

Author contributions

CD and WenZ designed the research. JL, and WeiZ performed the research. JL, YL, ZY and WeiZ analyzed the data. WeiZ, JL, WenZ and CD wrote the manuscript. Project administration, XS and CD. Funding acquisition, XS and CD. All authors contributed to the article and approved the submitted version.

Funding

This work was supported by the National Key Research and Development Program of China (grant number 2021YFD2201205), and the Basic Research Fund of CAF (grant number CAFYBB2020SZ002).

Conflict of interest

The authors declare that the research was conducted in the absence of any commercial or financial relationships that could be construed as a potential conflict of interest.

Publisher's note

All claims expressed in this article are solely those of the authors and do not necessarily represent those of their affiliated organizations, or those of the publisher, the editors and the reviewers. Any product that may be evaluated in this article, or claim that may be made by its manufacturer, is not guaranteed or endorsed by the publisher.

Supplementary material

The Supplementary Material for this article can be found online at: https://www.frontiersin.org/articles/10.3389/fpls.2023.1143878/full#supplementary-material

References

Adams, P. D., and Kloepper, J. W. (2002). Effect of host genotype on indigenous bacterial endophytes of cotton (*Gossypium hirsutum* l.). *Plant Soil* 240 (1), 181–189. doi: 10.1023/A:1015840224564

Atamna-Ismaeel, N., Finkel, O., Glaser, F., von Mering, C., Vorholt, J. A., Koblížek, M., et al. (2012). Bacterial anoxygenic photosynthesis on plant leaf surfaces. *Env. Microbiol. Rep.* 4 (2), 209–216. doi: 10.1111/j.1758-2229.2011.00323.x

Bálint, M., Tiffin, P., Hallström, B., O'Hara, R. B., Olsin, M. S., Fankhauser, J. D., et al. (2013). Host genotype shapes the foliar fungal microbiome of balsam poplar (*Populus balsamifera*). *PloS One* 8 (1), e53987. doi: 10.1371/journal.pone.0053987

Bao, L., Cai, W., Cao, J., Zhang, X., Liu, J., Chen, H., et al. (2020). Microbial community overlap between the phyllosphere and rhizosphere of three plants from yongxing island, south China Sea. *Microbiologyopen* 9 (7), e1048. doi: 10.1002/mbo3.1048

Bardou, P., Mariette, J., Escudié, F., Djemiel, C., and Klopp, C. (2014). Jvenn: An interactive Venn diagram viewer. *BMC Bioinf.* 15, 293. doi: 10.1186/1471-2105-15-293

Beattie, G. A. (2011). Water relations in the interaction of foliar bacterial pathogens with plants. *Annu. Rev. Phytopathol.* 49 (1), 533–555. doi: 10.1146/annurev-phyto-073009-114436

Beckers, B., De Beeck, M. O., Thijs, S., Truyens, S., Weyens, N., Boerjan, W., et al. (2016). Performance of 16s rDNA primer pairs in the study of rhizosphere and endosphere bacterial microbiomes in metabarcoding studies. *Front. Microbiol.* 7. doi: 10.3389/fmicb.2016.00650

Beckers, B., De Beeck, M. O., Weyens, N., Boerjan, N., and Vangronsveld, J. (2017). Structural variability and niche differentiation in the rhizosphere and endosphere bacterial microbiome of field-grown poplar trees. *Microbiome* 5 (1), 25. doi: 10.1186/s40168-017-0241-2

Berlec, A. (2012). Novel techniques and findings in the study of plant microbiota: Search for plant probiotics. *Plant Sci.* 193–194, 96–102. doi: 10.1016/j.plantsci.2012.05.010

Bodenhausen, N., Bortfeld, M., Ackermann, M., and Vorholt, J. A. (2014). A synthetic community approach reveals plant genotypes affecting the phyllosphere microbiota. *PloS Genet.* 10, e1004283. doi: 10.1371/journal.pgen.1004283

Bodenhausen, N., Horton, M. W., and Joy, B. (2013). Bacterial communities associated with the leaves and the roots of arabidopsis thaliana. *PloS One* 8 (2), e56329. doi: 10.1371/journal.pone.0056329

Bradshaw, H. D., Ceulemans, R., Davis, J., and Stettler, R. (2000). Emerging model systems in plant biology: Poplar (Populus) as a model forest tree. *J. Plant Growth Regul.* 19, 306–313. doi: 10.1007/s003440000030

Bringel, F., and Couée, I. (2015). Pivotal roles of phyllosphere microorganisms at the interface between plant functioning and atmospheric trace gas dynamics. *Front. Microbiol.* 6. doi: 10.3389/fmicb.2015.00486

Brunner, A. M., Busov, V. B., and Strauss, S. H. (2004). Poplar genome sequence: Functional genomicsin an ecologically dominant plant species. *Trends Plant Sci.* 9, 49–56. doi: 10.1016/j.tplants.2003.11.006

Bunster, L., Fokkema, N. J., and Schippers, B. (1989). Effect of surface-active pseudomonas spp. on leaf wettability. *Appl. Environ. Microb.* 55, 1340–1345. doi: 10.1128/aem.55.6.1340-1345.1989

Callahan, B. J., Mcmurdie, P. J., Rosen, M. J., Han, A. W., Johnson, A. J., and Holmes, S. P. (2016). Dada2: high-resolution sample inference from illumina amplicon data. *Nat. Methods* 13, 581–583. doi: 10.1038/nmeth.3869

Chao, A. (1984). Nonparametric estimation of the number of classes in a population. *Scand. J. Stat.* 11, 265–270. doi: 10.2307/4615964

Claesson, M. J., O'Sullivan, O., Wang, Q., Nikkilä, J., Marchesi, J. R., Smidt, H., et al. (2009). Comparative analysis of pyrosequencing and a phylogenetic microarray for exploring microbial community structures in the human distal intestine. *PloS One* 4, e6669. doi: 10.1371/journal.pone.0006669

Correa, O. S., Romero, A. M., Montecchia, M. S., and Soria, M. A. (2007). Tomato genotype and azospirillum inoculation modulate the changes in bacterial communities associated with roots and leaves. *J. Appl. Microbiol.* 102 (3), 781–786. doi: 10.1111/j.1365-2672.2006.03122.x

Delmotte, N., Knief, C., Chaffron, S., Innerebner, G., Roschitzki, B., Schlapbach, R., et al. (2009). Community proteogenomics reveals insights into the physiology of phyllosphere bacteria. *Proc. Natl. Acad. Sci. U.S.A.* 106 (38), 16428–16433. doi: 10.1073/pnas.0905240106

Dickinson, C. H., Austin, B., and Goodfellow, M. (1975). Quantitative and qualitative studies of phylloplane bacteria from lolium perenne. *J. Gen. Appl. Microbiol.* 91 (1), 157. doi: 10.1099/00221287-91-1-157

Douglas, G. M., Maffei, V. J., Zaneveld, J. R., Yurgei, S. N., Brown, J. R., Taylor, C. M., et al. (2020). PICRUSt2 for prediction of metagenome functions. *Nat. Biotechnol.* 38, 685–688. doi: 10.1038/s41587-020-0548-6

Du, Y., Zhao, Q., Chen, L., Yao, X., Zhang, W., Zhang, B., et al. (2020). Effect of drought stress on sugar metabolism in leaves and roots of soybean seedlings. *Plant Physiol. Bioch* 146, 1–12. doi: 10.1016/j.plaphy.2019.11.003

Finkel, O. M., Burch, A. Y., Elad, T., Huse, S. M., Lindow, S. E., Post, A. F., et al. (2012). Distance-decay relationships partially determine diversity patterns of phyllosphere bacteria on tamarix trees across the sonoran desert. *Appl. Environ. Microbiol.* 78, 6187–6193. doi: 10.1128/AEM.00888-12

Finkel, O. M., Burch, A. Y., Lindow, S. E., Post, A. F., and Belkin, S. (2011). Geographical location determines the population structure in phyllosphere microbial communities of a salt-excreting desert tree. *Appl. Environ. Microbiol.* 77, 7647–7655. doi: 10.1128/AEM.05565-11

Fürnkranz, M., Wanek, W., Richter, A., Abell, G., Rasche, F., and Sessitsch, A. (2008). Nitrogen fixation by phyllosphere bacteria associated with higher plants and their colonizing epiphytes of a tropical lowland rainforest of Costa Rica. *ISME J.* 2 (5), 561–570. doi: 10.1038/ismej.2008.14

Gong, T., and Xin, X. (2021). Phyllosphere microbiota: Community dynamics and its interaction with plant hosts. *J. Integr. Plant Biol.* 63 (2), 297–304. doi: 10.1111/jipb.13060

Grady, K. L., Sorensen, J. W., Stopnisek, N., Guittar, J., and Shade, A. (2019). Assembly and seasonality of core phyllosphere microbiota on perennial biofuel crops. *Nat. Commun.* 10, 4135. doi: 10.1038/s41467-019-11974-4

Gu, Z., and Hübschmann, D. (2022). Make interactive complex heatmaps in r. *Bioinformatics* 38, 1460–1462. doi: 10.1093/bioinformatics/btab806

Hardoim, P. R., van Overbeek, L. S., Berg, G., Pirttilä, A. M., Compant, S., Campisano, A., et al. (2015). The hidden world within plants: Ecological and evolutionary considerations for defining functioning of microbial endophytes. *Microbiol. Mol. Biol. Rev.* 79 (3), 293–320. doi: 10.1128/MMBR.00050-14

Horton, M. W., Bodenhausen, N., Beilsmith, K., Meng, D., Muegge, B. D., Subramanian, S., et al. (2014). Genome-wide association study of arabidopsis thaliana leaf microbial community. *Nat. Commun.* 5, 5320. doi: 10.1038/ncomms6320

Hunter, P. J., Hand, P., Pink, D., Whipps, J. M., and Bending, G. D. (2010). Both leaf properties and microbe-microbe interactions influence within-species variation in bacterial population diversity and structure in the lettuce (Lactuca species) phyllosphere. *Appli Environ. Microbiol.* 76 (24), 8117–8125. doi: 10.1128/AEM.01321-10

Hunter, P. J., Pink, D. A. C., and Bending, G. D. (2015). Cultivar-level genotype differences influence diversity and composition of lettuce (*Lactuca* sp.) phyllosphere fungal communities. *Fungal Ecol.* 17, 183–186. doi: 10.1016/j.funeco.2015.05.007

Innerebner, G., Knief, C., and Vorholt, J. A. (2011). Protection of arabidopsis thaliana against leaf-pathogenic pseudomonas syringae by sphingomonas strains in a controlled model system. *Appl. Environ. Microbiol.* 77 (10), 3202–3210. doi: 10.1128/AEM.00133-11

Kecskeméti, E., Berkelmann-Löhnertz, B., and Reineke, A. (2016). Are epiphytic microbial communities in the carposphere of ripening grape clusters (*Vitis vinifera* l.) different between conventional, organic, and biodynamic grapes? *PloS One* 11, e0160852. doi: 10.1371/journal.pone.0160852

Kembel, S. W., and Mueller, R. C. (2014). Plant traits and taxonomy drive host associations in tropical phyllosphere fungal communities. *Botany* 92 (4), 159. doi: 10.1139/cjb-2013-0194

Kembel, S. W., O'Connor, T. K., Arnold, H. K., Hubbell, S. P., Wright, S. J., and Green, J. L. (2014). Relationships between phyllosphere bacterial communities and plant functional traits in a neotropical forest. *Proc. Natl. Acad. Sci. U.S.A.* 111 (38), 13715–13720. doi: 10.1073/pnas.1216057111

Kishore, G. K., Pande, S., and Podile, A. R. (2005). Biological control of late leaf spot of peanut (*Arachis hypogaea*) with chitinolytic bacteria. *Phytopathology* 95 (10), 1157. doi: 10.1094/PHYTO-95-1157

Knief, C., Delmotte, N., Chaffron, S., Stark, M., Innerebner, G., Wassmann, R., et al. (2012). Metaproteogenomic analysis of microbial communities in the phyllosphere and rhizosphere of rice. *ISME J.* 6, 1378–1390. doi: 10.1038/ismej.2011.192

Koskimäki, J. J., Pirttilä, A. M., Ihantola, E. L., Halonen, O., and Frank, A. C. (2015). The intracellular scots pine shoot symbiont methylobacterium extorquens DSM13060 aggregates around the host nucleus and encodes eukaryote-like proteins. *MBio* 6 (2), e00039-15. doi: 10.1128/mBio.00039-15

Laforest-Lapointe, I., Messier, C., and Kembel, S. W. (2016). Host species identity, site and time drive temperate tree phyllosphere bacterial community structure. *Microbiome* 4 (1), 27. doi: 10.1186/s40168-016-0174-1

Leveau, J. H. (2015). "Life of microbes on aerial plant parts," in *Principles of plant-microbe interactions* (Cham, Switzerland: Springer), 17–24.

Li, Q., Song, X., Chang, S., Peng, C., Xiao, W., Zhang, J., et al. (2019). Nitrogen depositions increase soil respiration and decrease temperature sensitivity in a moso bamboo forest. *Agr For. Meteorol* 268, 48–54. doi: 10.1016/j.agrformet.2019.01.012

Lindow, S. E., and Brandl, M. T. (2003). Microbiology of the phyllosphere. *Appl. Enviro Microbiol.* 69, 1875–1883. doi: 10.1128/AEM.69.4.1875-1883.2003

Lopez-Velasco, G., Welbaum, G. E., Boyer, R. R., Mane, S. P., and Ponder, M. A. (2011). Changes in spinach phylloepiphytic bacteria communities following minimal processing and refrigerated storage described using pyrosequencing of 16S rRNA amplicons. *J. Appl. Microbiol.* 110, 1203–1214. doi: 10.1111/j.1365-2672.2011.04969.x

Melotto, M., Underwood, W., Koczan, J., Nomura, K., and He, S. Y. (2006). Plant stomata function in innate immunity against bacterial invasion. *Cell* 126 (5), 969–980. doi: 10.1016/j.cell.2006.06.054

Miura, T., Sánchez, R., Castañeda, L. E., Godoy, K., and Barbosa, O. (2019). Shared and unique features of bacterial communities in native forest and vineyard phyllosphere. *Ecol. Evol.* 9, 3295–3305. doi: 10.1002/ece3.4949

Müller, T., and Ruppel, S. (2014). Progress in cultivation-independent phyllosphere microbiology. *FEMS Microbiol. Ecol.* 87 (1), 2–17. doi: 10.1111/1574-6941.12198

Ottesen, A. R., Gorham, S., Pettengill, J. B., Rideout, S., Evans, P., and Brown, E. (2015). The impact of systemic and copper pesticide applications on the phyllosphere microflora of tomatoes. *J. Sci. Food Agric.* 95 (5), 1116–1125. doi: 10.1002/jsfa.7010

Peñuelas, J., and Terradas, J. (2014). The foliar microbiome. *Trends Plant Sci.* 19 (5), 278–280. doi: 10.1016/j.tplants.2013.12.007

Pielou, E. C. (1966). The measurement of diversity in different types of biological collections. *J. Theor. Biol.* 13, 131–144. doi: 10.1016/0022-5193(66)90013-0

Ramette, A. (2007). Multivariate analyses in microbial ecology. *FEMS Microbiol. Ecol.* 62, 142–160. doi: 10.1111/j.1574-6941.2007.00375.x

Rasche, F., Trondl, R., Naglreiter, C., Reichenauer, T. G., and Sessitsch, A. (2006a). Chilling and cultivar type affect the diversity of bacterial endophytes colonizing sweet pepper (*Capsicum anuum* l.). *Can. J. Microbiol.* 52 (11), 1036–1045. doi: 10.1139/w06-059

Rasche, F., Velvis, H., Zachow, C., Berg, G., Van Elsas, J. D., and Sessitsch, A. (2006b). Impact of transgenic potatoes expressing antibacterial agents on bacterial endophytes is comparable with the effects of plant genotype, soil type and pathogen infection. *J. Appl. Ecol.* 43 (3), 555–566. doi: 10.1111/j.1365-2664.2006.01169.x

Rastogi, G., Sbodio, A., Tech, J. J., Suslow, T. V., Coaker, G. L., and Leveau, J. H. (2012). Leaf microbiota in an agroecosystem: Spatiotemporal variation in bacterial community composition on field-grown lettuce. *ISME J.* 6 (10), 1812–1822. doi: 10.1038/ismej.2012.32

Rausch, C., Daram, P., Brunner, S., Jansa, J., Laloi, M., Leggewie, G., et al. (2001). A phosphate transporter expressed in arbuscule-containing cells in potato. *Nature* 414, 462–470. doi: 10.1038/35106601

Redford, A. J., Bowers, R. M., Knight, R., Linhart, Y., and Fierer, N. (2010). The ecology of the phyllosphere: geographic and phylogenetic variability in the distribution of bacteria on tree leaves. *Environ. Microbiol.* 12 (11), 2885–2893. doi: 10.1111/j.1462-2920.2010.02258.x

Romero, F. M., Marina, M., and Pieckenstain, F. L. (2016). Novel components of leaf bacterial communities of field-grown tomato plants and their potential for plant growth promotion and biocontrol of tomato diseases. *Res. Microbiol.* 167 (3), 222–233. doi: 10.1016/j.resmic.2015.11.001

Ruinen, J. (1956). Occurrence of beijerinckia species in the 'Phyllosphere'. *Nature* 177, 220–221. doi: 10.1038/177220A0

Sessitsch, A., Reiter, B., Pfeifer, U., and Wilhelm, E. (2002). Cultivation-independent population analysis of bacterial endophytes in three potato varieties based on eubacterial and actinomycetes-specific PCR of 16S rRNA genes. *FEMS Microbiol. Ecol.* 39 (1), 23–32. doi: 10.1111/j.1574-6941.2002.tb00903.x

Shannon, C. E. (1948). A mathematical theory of communication. *Bell System Tech. J.* 27, 623–656. doi: 10.1002/j.1538-7305.1948.tb01338.x

Simpson, E. H. (1949). Measurement of diversity. *Nature* 163, 688. doi: 10.1136/thx.27.2.261

Taylor, G. (2002). *Populus*: arabidopsis for forestry. do we need a model tree? *Ann. Bot.* 90 (6), 681–689. doi: 10.1093/AOB/MCF255

Tkacz, A., Bestion, E., Bo, Z., Hortala, M., and Poole, P. S. (2020). Influence of plant fraction, soil, and plant species on microbiota: A multikingdom comparison. *mBio* 11 (1), e02785–19. doi: 10.1128/mBio.02785-19

Vacher, C., Hampe, A., Porté, A. J., Sauer, U., Compant, S., and Morris, C. E. (2017). The phyllosphere: Microbial jungle at the plant-climate interface. *Annu. Rev. Ecolog Evol. S* 47 (1), 1–24. doi: 10.1146/annurev-ecolsys-121415-032238

Vogel, M. A., Mason, O. U., and Miller, T. E. (2020). Host and environmental determinants of microbial community structure in the marine phyllosphere. *PloS One* 15, e0235441. doi: 10.1371/journal.pone.0235441

Vokou, D., Vareli, K., Zarali, E., Karamanoli, K., Constantinidou, H. I., Monokrousos, N., et al. (2012). Exploring biodiversity in the bacterial community of the mediterranean phyllosphere and its relationship with airborne bacteria. *Microbial Ecol.* 64 (3), 714–724. doi: 10.1007/s00248-012-0053-7

Vorholt, J. (2012). Microbial life in the phyllosphere. *Nat. Rev. Microbiol.* 10 (12), 828. doi: 10.1038/nrmicro2910

Watanabe, K., Kohzu, A., Suda, W., Yamamura, S., Takamatsu, T., Takenaka, A., et al. (2016). Microbial nitrification in throughfall of a Japanese cedar associated with archaea from the tree canopy. *Springerplus* 5 (1), 1596. doi: 10.1186/s40064-016-3286-y

Whipps, J. M., Hand, P., Pink, D., and Bending, G. D. (2008). Phyllosphere microbiology with special reference to diversity and plant genotype. *J. Appl. Microbiol.* 105, 1744–1755. doi: 10.1111/j.1365-2672.2008.03906.x

Wickham, H. (2009). *ggplot2: Elegant graphics for data analysis* (New York, NY: Springer).

Xu, N., Zhao, Q., Zhang, Z., Zhang, Q., Wang, Y., Qin, G., et al. (2022). Phyllosphere microorganisms: Sources, drivers, and their interactions with plant hosts. J. *Agric. Food Chem.* 70 (16), 4860–4870. doi: 10.1021/acs.jafc.2c01113

Yadav, R. K., Karamanoli, K., and Vokou, D. (2005). Bacterial colonization of the phyllosphere of mediterranean perennial species as influenced by leaf structural and chemical features. *Microb. Ecol.* 50 (2), 185–196. doi: 10.1007/s00248-004-0171-y

frontiers | Frontiers in Plant Science

TYPE Original Research
PUBLISHED 31 March 2023
DOI 10.3389/fpls.2023.1118363

OPEN ACCESS

EDITED BY
Daojun Yuan,
Huazhong Agricultural University, China

REVIEWED BY
Jia-Ming Song,
Guangxi University, China
Yiyong Zhao,
Guizhou University, China

*CORRESPONDENCE
Long Yang
lyang@sdau.edu.cn
Lu Wang
wanglu181716@163.com
Hongyan Du
dhy515@caf.ac.cn

†These authors have contributed equally to this work and share first authorship

‡This author is responsible for correspondence and material distributions

SPECIALTY SECTION
This article was submitted to Plant Bioinformatics, a section of the journal Frontiers in Plant Science

RECEIVED 08 December 2022
ACCEPTED 20 March 2023
PUBLISHED 31 March 2023

CITATION
Du Q, Wu Z, Liu P, Qing J, He F, Du L, Sun Z, Zhu L, Zheng H, Sun Z, Yang L, Wang L and Du H (2023) The chromosome-level genome of *Eucommia ulmoides* provides insights into sex differentiation and α-linolenic acid biosynthesis.
Front. Plant Sci. 14:1118363.
doi: 10.3389/fpls.2023.1118363

The chromosome-level genome of *Eucommia ulmoides* provides insights into sex differentiation and α-linolenic acid biosynthesis

Qingxin Du[1,2,3†], Zixian Wu[4†], Panfeng Liu[1,2,3†], Jun Qing[1,2,3], Feng He[1,2,3], Lanying Du[1,2,3], Zhiqiang Sun[1,2,3], Lili Zhu[5], Hongchu Zheng[6], Zongyi Sun[7], Long Yang[4*], Lu Wang[1,2,3*] and Hongyan Du[1,2,3*‡]

[1]Research Institute of Non-timber Forestry, Chinese Academy of Forestry, Zhengzhou, China, [2]Key Laboratory of Non-timber Forest Germplasm Enhancement and Utilization of National Forestry and Grassland Administration, Chinese Academy of Forestry, Zhengzhou, China, [3]Engineering Research Center of Eucommia ulmoides, State Forestry and Grassland Administration, Zhengzhou, China, [4]Agricultural Big-Data Research Center and College of Plant Protection, Shandong Agricultural University, Taian, China, [5]Academy of Chinese Medical Sciences, Henan University of Chinese Medicine, Zhengzhou, China, [6]Product Department, Henan Jinduzhong Agricultural Science and Technology Co., Ltd., Yanling, China, [7]Operation Department, Grandomics Biosciences Co., Ltd., Wuhan, China

Eucommia ulmoides Oliver is a typical dioecious plant endemic to China that has great medicinal and economic value. Here, we report a high-quality chromosome-level female genome of *E. ulmoides* obtained by PacBio and Hi-C technologies. The size of the female genome assembly was 1.01 Gb with 17 pseudochromosomes and 31,665 protein coding genes. In addition, Hi-C technology was used to reassemble the male genome released in 2018. The reassembled male genome was 1.24 Gb with the superscaffold N50 (48.30 Mb), which was increased 25.69 times, and the number of predicted genes increased by 11,266. Genome evolution analysis indicated that *E. ulmoides* has undergone two whole-genome duplication events before the divergence of female and male, including core eudicot γ whole-genome triplication event (γ-WGT) and a recent whole genome duplication (WGD) at approximately 27.3 million years ago (Mya). Based on transcriptome analysis, *EuAP3* and *EuAG* may be the key genes involved in regulating the sex differentiation of *E. ulmoides*. Pathway analysis showed that the high expression of ω-3 fatty acid desaturase coding gene *EU0103017* was an important reason for the high α-linolenic acid content in *E. ulmoides*. The genome of female and male *E. ulmoides* presented here is a valuable resource for the molecular biological study of sex differentiation of *E. ulmoides* and also will provide assistance for the breeding of superior varieties.

KEYWORDS

***Eucommia ulmoides* Oliver, genome, whole-genome duplication, MADS-box genes, sex differentiation, α-linolenic acid biosynthesis**

Introduction

There has been a wide range of uses for *Eucommia ulmoides* Oliver, such as medicinal and natural rubber extraction purposes. Because there has been a long history of application of this plant in China (Zhu and Sun, 2018), it has aroused the interest of many researchers. In 2018, the first draft reference genome of *E. ulmoides* (Male V1) was released based on next-generation sequencing, and consisted of a total genome length of 1.18 Gb genome with contig N50 that was 17.06 kb in length, and the assembled genome size was larger than the 1.1 Gb predicted by 17-mer analysis. A large number of superscaffolds were assembled from contigs, but none was completely anchored to the chromosomes (Wuyun et al., 2018).

It was realized that the accuracy and completeness of this genome assembly could be further refined. A new version of the genome was subsequently published in 2020, whereby the authors first obtained the *Eucommia* haploid plant through parthenogenesis, and then sequenced and assembled it. The genome size was 947.86 Mb, accounting for 92.93% of the estimated genome size (1.02 Gb). Contig N50 was 13.16 Mb, and scaffold N50 was 53.15 Mb in length, and long scaffolds were further anchored to 17 pseudochromosomes by Hi-C (Li et al., 2020). Although two versions of the *E. ulmoides* genome have been released, a high-quality female *E. ulmoides* genome has yet to be produced, which is necessary for the study of evolution and sex differentiation.

E. ulmoides is a dioecious perennial woody plant, with male and female inflorescences that greatly vary, and thus, the quantities of important compounds in male and female plant are different (Figure 1). The utilization value of *E. ulmoides* also varies with the sex of the plant (Wang et al., 2020). In flowering plants, the sex difference is mainly manifested as different flower organs, and therefore, genes related to flower development may participate in the process of sex differentiation (Barrett and Hough, 2012; Massonnet et al., 2020). As the key regulators of almost all aspects of plant reproductive development, MADS-box genes play a particularly prominent role in flowering time control, inflorescence structure, floral organ identity determination, and seed development. However, the floral induction and floral organ regulation genes and regulatory networks of *E. ulmoides* are still unclear.

Based on the studies of model plants *Arabidopsis thaliana* (Bowman et al., 1989) and *Antirrhinum majus* (Schwarz-Sommer et al., 1990), the genetic regulation mechanisms that govern flower organ development have been preliminarily explored, and the famous ABC model of flower organ development has been proposed (Coen and Meyerowitz, 1991; Soltis et al., 2007), which was later supplemented by the ABCDE model (Theissen, 2001; Causier et al., 2010). Except for the *AP2* gene, all the genes involved in the ABCDE model were MADS-box genes belonging to different functional categories (Hu et al., 2021). Therefore, the MADS-box gene family may play an important role in regulating the sexual differentiation of flowers, and a large number of MADS-box genes and their functions have been found and verified in plants such as *Arabidopsis* (Di Marzo et al., 2020), *Orchidaceae* (Teo et al., 2019), *Petunia* (Morel et al., 2019), *Oryza sativa* (Yin et al., 2019) and *Zea*

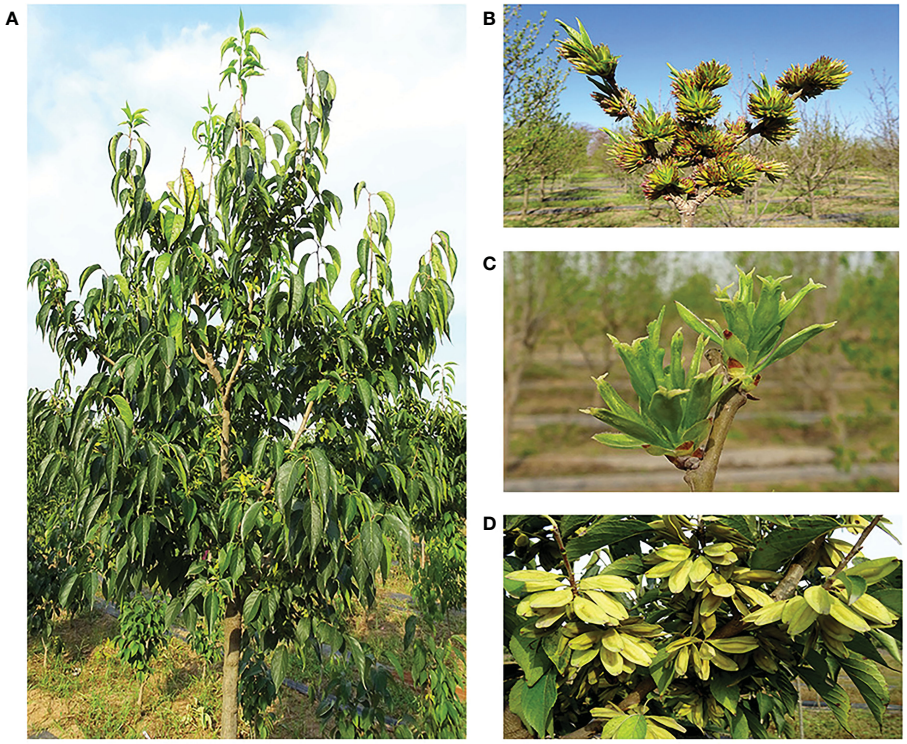

FIGURE 1
Morphological characteristic of *Eucommia ulmoides*. **(A)** Mature plant, **(B)** male inflorescence, **(C)** female inflorescence, **(D)** fruit.

mays (Abraham-Juárez et al., 2020). A previous study based on comparative transcriptome analysis of male and female *E. ulmoides* identified putative sex-associated genes (Wang and Zhang, 2017). Regrettably, only one gene with high homology to the *AP3* gene in *Arabidopsis* was detected, which was a B class organ identity gene. Although that study provides a reference for exploring the sex differentiation of *E. ulmoides*, there is currently a lack of information on the sex differentiation mechanism of *E. ulmoides*.

In plants, stearic acid is catalyzed by fatty acid desaturase to produce oleic acid and linoleic acid, and eventually α-linolenic acid (Li-Beisson et al., 2013), which is an essential fatty acid and is very important for human health (Kim et al., 2014). There has been prior study on α-linolenic in plants such as *Perilla frutescens* (Liao et al., 2018), *Plukenetia volubilis* (Hu et al., 2018), *Paeonia ostia* (Yu et al., 2021). *E. ulmoides* is a woody plant with a very high α-linolenic acid content, even more than 60% in its seed oil (Zhang et al., 2018), well above purslane which has the highest content of linolenic acid in green leafy vegetables (30.15%). Although the synthesis of α-linolenic acid in *E. ulmoides* has also been studied from the glycolytic pathway based on transcriptome analysis (Feng et al., 2016), the information in genes encoding key enzymes for linolenic acid synthesis and the mechanism of α-linolenic acid accumulation are still not clear.

In this study, we aimed to construct a female and male *E. ulmoides* genome and explore the molecular mechanism of sex differentiation and α-linolenic acid accumulation in *E. ulmoides*. Our results will provide essential resources for studies on *E. ulmoides* evolution and directional variety improvement, and also lay a foundation for the rapid identification of male and female plants, thus improving the utilization rate of *E. ulmoides*.

Materials and methods

Plant samples

Fresh leaves for genome sequencing were collected from a female *E. ulmoides* plant 'Huazhong No. 8', which was used to assemble the Female V1 genome. To observe the morphological structure of female and male flower bud development, flower buds were collected from female 'Huazhong No. 6' and the male 'Huazhong No. 11' during the entire development period. Samples were obtained every 5 days from the beginning of bud germination in late April to the end of September, once every 10 days from early October to January of the following year, and once every 3 days from February to early April of the following year, with 20 female and male flower buds being collected each time. The experimental materials for sex differentiation analysis were derived from the collected flower buds. Male and female flower buds at the floral organ induction stage (the inflorescence primordium formation stage), floral organ morphological differentiation initial stage (the pistil and stamen differentiation stage), and flower organ maturity stage were selected for transcriptome sequencing, with three biological repetitions for each sample. To analyze the expression of α-linolenic acid synthesis genes, four different tissues (stem, bark, leaf and fruit) of female 'Huazhong No. 8' were extracted. All plant samples were collected from the Yuanyang Experimental Base of Research Insitute of Non-timber Forestry, Chinese Academy of Forestry. Plant materials were immediately immersed in liquid nitrogen, transported to the laboratory, and then stored in a -80°C freezer for sequencing.

Morphological and structural observation of flower bud development

After collection, the materials were immediately immersed in FAA fixative solution (70% ethanol: glacial acetic acid: 38% formaldehyde =18:1:1), transported to the laboratory, and then stored in a -80° freezer. Materials preserved in FAA fixative solution were sliced using a conventional paraffin-sectioning method. Then the slices were observed and photographed using OLYMPUS optical microscope.

Sequencing and library construction

Total genomic DNA was extracted from fresh leaves using the QIAGEN® Genomic DNA extraction kit (Cat#13323, QIAGEN) for PacBio sequencing on a PacBio Sequel II instrument. For Hi-C library construction and sequencing, restriction endonucleases (HindIII/MboI) were used for chromatin digestion, and after biotin labeling, flat-end binding and DNA purification. Hi-C samples were prepared and sampled for DNA quality testing. The Hi-C fragment consisted of removed biotin that was fragmented by ultrasound, end-repaired, and after the addition of base A, the biotin-containing fragment was isolated and then sequenced to form the jointed product. Then, Polymerase Chain Reaction (PCR) conditions were tested, and DNA was amplified to obtain the library products (Kong and Zhang, 2019). An Illumina HiSeq X Ten sequencer was used for sequencing after the library quality control was confirmed.

RNA was extracted using a TRIzol kit (Invitrogen) according to the manufacturer's instructions. The RNA concentration was measured using a NanoDrop spectrophotometer, and RNA purity and integrity were determined by an Agilent 2100 Bioanalyzer and 1% agarose gel electrophoresis, respectively. After passing the quality inspection, a cDNA library was constructed according to the instructions accompanying the cDNA Library Construction Kit (NEB). Paired-end sequencing was performed on the cDNA library using the Illumina HiSeq X-10 platform, and 150 bp paired-end sequences were generated.

Genome assembly and evaluation

For the genome assembly of female *E. ulmoides* plant 'Huazhong No. 8', first, sub-sequences from PacBio sequencing were assembled using Falcon v2.0.5 (https://github.com/PacificBiosciences/FALCON/) with the parameter '–max diff 100 –max cov 100 –min cov 2 –min len 5000', the pure third-generation assembly software officially launched by PacBio. Then, Arrow (Chin

et al., 2013) was applied to align the third generation data to the preliminary assembly for correction with default parameters. After the initial genome assembly was completed, Pilon v1.22 (Walker et al., 2014) with the parameter '–mindepth 10 –changes –fix bases' was used for iterative polishing. The Hi-C data were aligned to the genome assembly *via* Juicer v1.5 software with the following parameter settings: -s DpnII -t 20 (Durand et al., 2016b). Finally, the draft genome of *E. ulmoides* was assembled onto chromosomes by 3D-DNA pipeline with the parameter '-m haploid -s 4 -c 17 -j 15' (Dudchenko et al., 2017). The contact matrix and heatmap of chromosomes were drawn with Juicebox (Durand et al., 2016a).

As for the male *E. ulmoides* tree (SNJ) genome reassembly, named Male V2 genome, we first downloaded the previous genome assembly data from the NCBI under accession number SRP095726. Next, the downloaded genome was refined using Hi-C data with the same method as that used for the female genome assembly. Benchmarking Universal Single-Copy Orthologs (BUSCO) v4.1.4 (https://busco.ezlab.org/) was used to assess the integrity and accuracy of the final genome assembly with the Eudicotyledons_odb10 database (Simão et al., 2015).

Genome annotation

TRF v4.07 (Benson, 1999) (tandem repeats finder) software (https://tandem.bu.edu/trf/trf.html) was applied to predict tandem repeats of the genome. Transposable elements (TEs) were identified by combining *de novo*-based and homology-based approaches. In the *de novo*-based approach, RepeatModeler v1.0.11 (Flynn et al., 2020) (http://www.repeatmasker.org/RepeatModeler/) and LTR-FINDER v1.05 (Xu and Wang, 2007) were used to build the repeat library (LTR length 100 to 5000 nt; length between two LTRs: 1000 to 20,000 nt), and then, RepeatMasker v4.0.7 (Tarailo-Graovac and Chen, 2009) (http://www.repeatmasker.org/) was used to identify and classify repeats under the parameter '-a -e ncbi -q -norna -nolow -div 30 -cutoff 225'. For the homology-based approach, the known repetitive sequences database Repbase (Bao et al., 2015) (https://www.girinst.org/repbase/) was searched by RepeatMasker to find homologous sequences in the *E. ulmoides* genome.

Gene prediction for the *E. ulmoides* genome was performed by integrating three different methods: *de novo* prediction, homology-based prediction and transcriptome-based prediction. *De novo* gene prediction was achieved using Augustus v3.3 (parameter: -strand=both -genemodel=partial -gff3=on -species= arabidopsis) (Stanke and Morgenstern, 2005) (http://bioinf.uni-greifswald.de/augustus/), SNAP (Korf, 2004) and GlimmerHMM v3.52 (Majoros et al., 2004). For the homology approach, BLASTP (Camacho et al., 2009) was used to map protein sequences onto the *E. ulmoides* genome, and GeneWise v2.4.1 (Birney et al., 2004) was used to align the homologous genome sequences with the matching proteins. RNA-seq sequences were mapped to the genome assembly using PASA v2.0.2 to identify putative exon regions and splice junctions. Finally, EVidenceModeler v1.1.1 (Haas et al., 2008) (https://evidencemodeler.github.io/) was employed to integrate the gene sets predicted by the three methods. For gene annotation, EggNOG-mapper v4.5 (Huerta-Cepas et al., 2017) software was employed with emapper DB 4.5.1 to obtain the Clusters of Orthologous Genes (COG), eggNOG, Gene Ontology (GO) and KEGG pathway information for each gene. HMMER v3.2.1 (Prakash et al., 2017) was applied to search the Pfam database (http://pfam.xfam.org/) and obtain the protein domains. Functional annotation of protein coding genes was performed using the UniProt database (https://www.uniprot.org/).

Four types of non-coding RNAs (ncRNAs), tRNA, rRNA, miRNA, and snRNA, were annotated in the *E. ulmoides* genome. TRNAscan-SE v1.4 (Lowe and Chan, 2016) (http://lowelab.ucsc.edu/tRNAscan-SE/)software was employed to identify the tRNAs with tRNAscn-SE -i -q and eukaryote parameters. rRNAs were detected using BLASTN alignment of rRNA sequences known related species. Other ncRNAs were predicted using INFERNAL v1.1 (Nawrocki et al., 2009) software with the parameter 'cmsearch –ga –incE 0.01 -E 10.0' to search the Rfam v12.0 (Nawrocki et al., 2015) database (http://rfam.xfam.org/).

Detection of WGD events

To identify whole genome duplication (WGD) events in *E. ulmoides*, BLASTP was used to perform a homology search using the female and male genome, and MCScanX v0.8 (Wang et al., 2012) (https://sourceforge.net/projects/mcscanx/) was employed to detect syntenic blocks. The collinearity analysis of male and female was conducted by JCVI v1.2.1. Ks (synonymous substitution) values for paralogous blocks were calculated by KaKs_Calculator v2.0 with the parameter '-i test.axt -m MA -c -o' (Wang et al., 2010), and a frequency distribution graph of the Ks values was drawn to identify WGD events in *E. ulmoides*. The WGD event time was estimated by the formula ks/2r, with a r value of 8.25 e-9.

MADS-box genes analysis

To identify MADS-box genes, HMMER v3.2.1 software with the SRF-TF domain (PF00319) and K-box (PF01486) were used to search against the *E. ulmoides* genome proteins (–cut_ga, E value<1×10^{-5}), which were obtained from Pfam. The search results containing MADS-box domain or K-box domain were retained, and incomplete functional domain sequences were removed. Using all Arabidopsis MADS-box genes as queries, the predicted *E. ulmoides* MADS genes were checked by BLASTP searches (E value<1×10^{-5}). The phylogenetic tree was then constructed using RAxML v8.2.12 with the GTRGAMMA substitution model and 1000 bootstraps on the CIPRES website (https://www.phylo.org/portal2/home.action). The phylogenetic tree was visualized using FigTree v1.4.4. The combination of genome annotation, homology search and MADS-box gene expression in male and female flower buds, enabled the ABCDE model genes to be identified. Using all female *E. ulmoides* MADS-box genes as queries, BLASTP was used to map protein sequences onto the male genome. For these protein sequences, the

phylogenetic tree was constructed through MEGA-X using the maximum likelihood method and the JTT matrix-based model with 1,000 bootstraps. Multiple sequence alignments were performed by CLUSTALW program and viewed in GeneDoc. The gene structure of these MADS-box genes was demonstrated by TBtools. The data of *Nymphaea colorata* was downloaded from BIG Data Center with the accession number GWHAAYW00000000. And the phylogenetic trees of genes related to sex differentiation in *E. ulmoides* and *N. colorata* were constructed using MEGA7 with the Neighbor Joining method.

Identification of α-linolenic acid biosynthesis and metabolism genes

The KEGG database (https://www.kegg.jp/kegg/kegg1.html) was queried to identify genes involved in α-linolenic acid synthesis and metabolism. First, known genes related to α-linolenic acid biosynthesis and metabolic pathways in KEGG were selected and their protein sequences were downloaded. The downloaded protein sequences were aligned with the *E. ulmoides* genome using the NCBI online comparison function BLASTP (https://blast.ncbi.nlm.nih.gov/Blast.cgi), and the annotation information was combined to predict genes involved in α-linolenic acid synthesis and metabolism.

Transcription analysis

FastQC v0.11.9 was used to estimate the quality of RNA sequences. To obtain clean sequences, Trimmomatic v0.36 was used to remove adapter sequences and low-quality sequences (with a base quality value less than 30 or greater than 5% unknown bases). To estimate the gene expression level, clean sequences from RNA-seq were mapped onto the final Female V1 genome assembly using Tophat2 v2.1.1 with the parameters: –b2-sensitive -N 2 -p 6 -g 10 –read-edit-dist 2 –read-mismatches 3 –read-gap-length 2 (Kim et al., 2013), and then fragments per kilobase per million (FPKM) of each gene was performed by Cufflinks v2.2.1 with the following parameter: -p 6 -g file.gff -u –library-type fr-unstranded (Trapnell et al., 2010) (http://cole-trapnell-lab.github.io/cufflinks/). Finally, the values of $\log_2$(FPKM +1)-that represented the gene expression level and the differentially expressed genes (DEGs) were identified using Cuffdiff v2.2.1, with a p-value (FDR) < 0.05 and |log2 (fold change)| > 1.

Results

Morphological and structural observation of female and male flower bud differentiation

With the growth and development of female and male flower buds of *E. ulmoides*, the cells of the flower bud meristem continued dividing, and the internal and external morphological structure gradually changed. The floral organ development of the female and male flower buds of *E. ulmoides* can be divided into four stages: inflorescence primordium formation, bract differentiation, pistil and stamen differentiation, and pistil and stamen morphological formation (Figure 2).

In the inflorescence primordium formation stage, the female and male flower buds exhibit similar morphological characteristics. The buds are young and green, approximately triangular, with white fluff on the surface (Figures 2A1, C1). The internal anatomical structure shows that the flower buds are apical and conical, with thick cytoplasm (Figures 2B1, D1).

In the bract differentiation stage, the female and male flower bud morphological characteristics remain relatively similar, and males and females cannot be accurately distinguished. The outer bracts of female and male flower buds gradually lignify into scales, and the color of the flower buds gradually changes from green to light brown (Figures 2A2, C2). The number of bracts increases, and the meristem at the bud apex widens and flattens (Figures 2B2, D2).

In the pistil and stamen differentiation stage, the internal structure of female and male flower buds showed obvious morphological differences. Round small protuberances form between the axils of the primordia of the female buds, namely the pistil primordia, and several stamen primordia that form between the axils of the male buds are clustered between the bracts. The male and female buds can be distinguished according to the sectioning results (Figures 2B3, D3).

In the pistil and stamen morphological formation stage, female flower buds grow faster longitudinally and are approximately conical in shape, while the stamens are approximately spherical (Figures 2A4, C4). A single pistil primordium is differentiated from the base to the center on both sides of the female flower bud, while the male flower bud is differentiated from several stamens to form a stamen cluster inside the bract (Figures 2B4, D4). The pistil shape is pinnate, with a central depression at the top that forms two protuberances, namely the pistil stigma. After the pistil completes its morphogenesis, and stamen pollen sac differentiates into the obvious endothecium, middle layer, and tapetum (Figures 2B5, D5). Then, the internal and external morphology of the flower bud does not change, and the bud enters the dormancy stage.

Genome assembly and assessment

A combined strategy of PacBio and Hi-C sequencing technologies was used to construct the high-quality female *E. ulmoides* genome assembly (Female V1). The PacBio long sequences were corrected and assembled into the preliminary genome assembly using FALCON. The obtained genome size was 957 Mb, which consisted of 2,662 contigs with contig N50 that was 1.3 Mb in length. Finally, with the assistance of 184.7 Gb of Hi-C sequences, the assembled contigs were anchored to 17 pseudochromosomes of 1.01 Gb with superscaffold N50 that was 51.89 Mb in length, and the GC content of the genome was 35.14% (Table 1). The interactions of contigs on pseudochromosomes were detected to adjust their order and direction in the Hi-C heat map, which also indicated the high quality of Female V1 genome

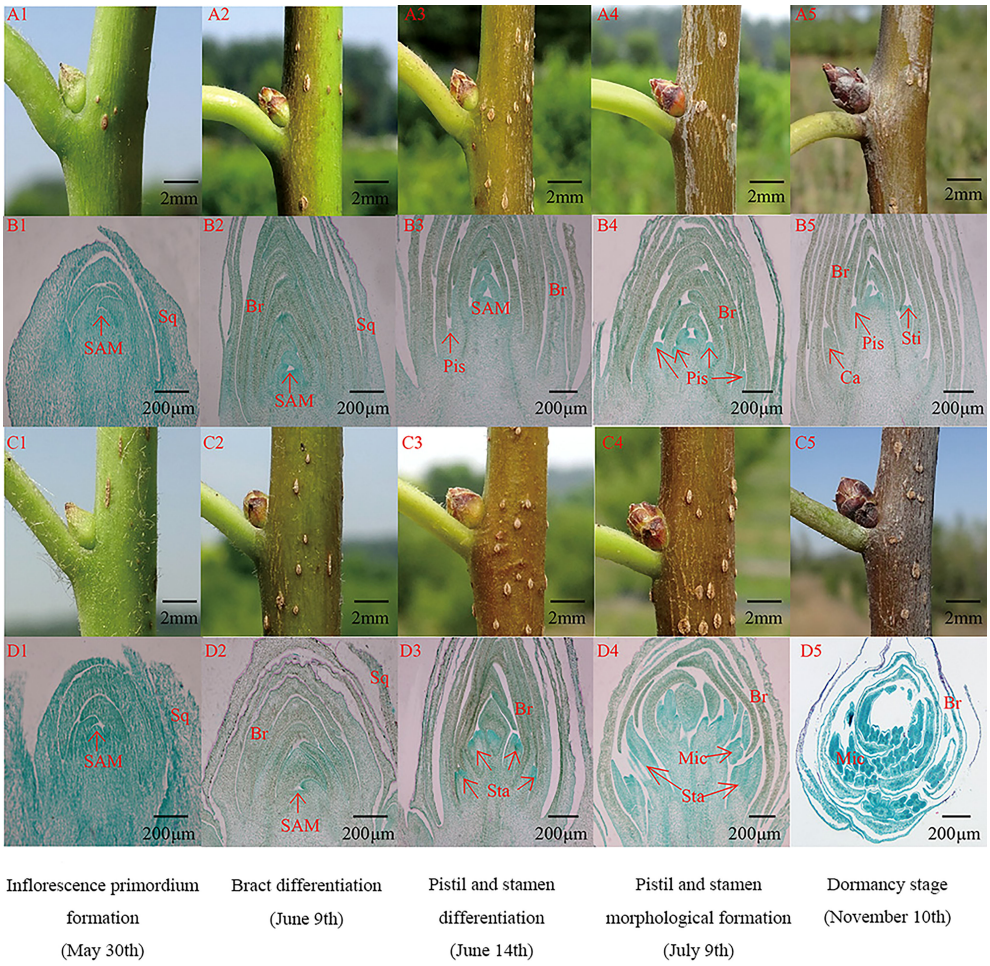

FIGURE 2
Internal anatomical structure and external morphological characteristics of male and female flower buds at different differentiation stages. Br, Bract; Ca, Carp; Mic, Microsporocyte; Pis, Pistil, SAM, Stem Apical Meristem; Sq, Squama; Sta, Stamen; Sti, Stigma. **(A1-A5)**: The external morphology structure of female flower bud; **(B1-B5)**: The anatomic structure of female flower bud; **(C1-C5)**: The external morphology structure of male flower bud; **(D1-D5)**: The anatomic structure of male flower bud.

TABLE 1 Summary of the *Eucommia ulmoides* genome.

Type	Female V1	Male V2	Male V1
Genome Size	1.01 Gb	1.24 Gb	1.18 Gb
Contig N50	1.33 Mb	17.06 Kb	17.06 Kb
Scaffold N50	5.31 Mb	1.03 Mb	1.03 Mb
SuperScaffold N50	51.89 Mb	48.30 Mb	1.88 Mb
GC content	35.14%	35.19%	–
Complete BUSCOs	93.2%	92.1%	90%
Protein coding genes	31,665	37,998	26,732
Mean gene length	6,273 bp	6,199 bp	–
Mean coding sequence length	1,086 bp	1,007 bp	1,001
Mean number of exons per gene	5.18	4.45	4.74
Mean exon length	209 bp	226 bp	211 bp
Total repetitive sequence	68.26%	62.25%	61.24%
Total non-coding RNAs	2,488	2,865	3,201

assembly (Supplementary Figures 1, 2). The Male V2 genome was re-constructed using Hi-C technology. The genome size of the new version (Male V2) was 1.24 Gb, with 23 superscaffolds and the superscaffold N50 that was 48.30 Mb long, and the GC content was 35.19% (Table 1). Genomic alignments of chromosomes and superscaffolds between Female V1 and Male V2 are showed in (Figure 3C).

To assess the quality of the two newly assembled genomes, BUSCO was carried out. Among the 2,121 plant-specific orthologs, 2,024 (95.4%) and 2,026 (95.5%) BUSCOs were identified in the Female V1 and Male V2 assembly respectively. In addition, 1,975 (93.2%, Female V1) and 1,954 (92.1%, Male V2) of the identified orthologs in the two genomes were considered to be complete, which were higher than the 90.0% completed genes identified in the Male V1 genome (Supplementary Figure 3 and Supplementary Table 1). The BUSCO results suggested that both genomes were assembled with high quality.

Genome annotation

The Female V1 and Male V2 genome consisted of 68.26% (688.75 Mb) and 62.25% (770.88 Mb) repeats, respectively (Table 1 and Figure 4). In both genomes, LTR (long terminal repeat) was the most abundant type of repetitive element, accounting for 40.15% (405.08 Mb) and 36.6% (453.30 Mb) of the genome size, respectively. Additionally, 59.05 Mb (5.85% of the Female V1 genome) and 64.56 Mb (5.21% of the Male V2 genome) DNA transposons were identified, which were the second highest repeated sequence in both genomes (Supplementary Table 2). The LTR-RT insertion time was estimated to provide a retrospective view of the expanded history of LTR-RTs in the two newly assembly *E. ulmoides* genomes. LTR-RTs gradually accumulated over 5 million years ago, and there was an insertion explosion approximately 2 million years ago in both genomes, with the Male V2 genome undergoing another peak at 0.15 Mya (Figure 3A).

A combination of ab initio prediction, RNA-seq, and homology-based search was used to predict the protein-coding genes in the *E. ulmoides* genome. Overall, 31,665 and 37,998 genes were predicted in the Female V1 and Male V2 genome, and the average protein-coding gene size was 6,273 bp and 6,199 bp respectively (Table 1). Among these predicted protein-coding genes, 24,049 (75.95%) genes from the Female V1 genome and 27,284 (71.8%) genes from the Male V2 genome were functionally annotated in the GO, KEGG, EggNOG, Pfam and UniProt databases (Supplementary Table 3). In addition, 2,488 and 2,910 noncoding RNAs were separately annotated in the two newly assembled genomes. The Female V1 genome contained 976 tRNAs, 178 rRNAs, 1,141 snRNAs and 193 miRNAs. Similarly, four types of noncoding RNAs were identified in the Male V2 genome, including 1,216 tRNAs, 214 rRNAs, 1,253 snRNAs and 182 miRNAs (Supplementary Figures 4, 5 and Supplementary Table 4).

Whole-genome duplication analysis

WGD analysis was performed by calculating synonymous substitutions per synonymous site (Ks) values in the two newly assembled genomes. The density distribution of Ks values exhibited two peaks both in Female V1 and Male V2, with Ks values of 0.45 and 2.29 (Figure 3B). After the early γ duplication event that affected

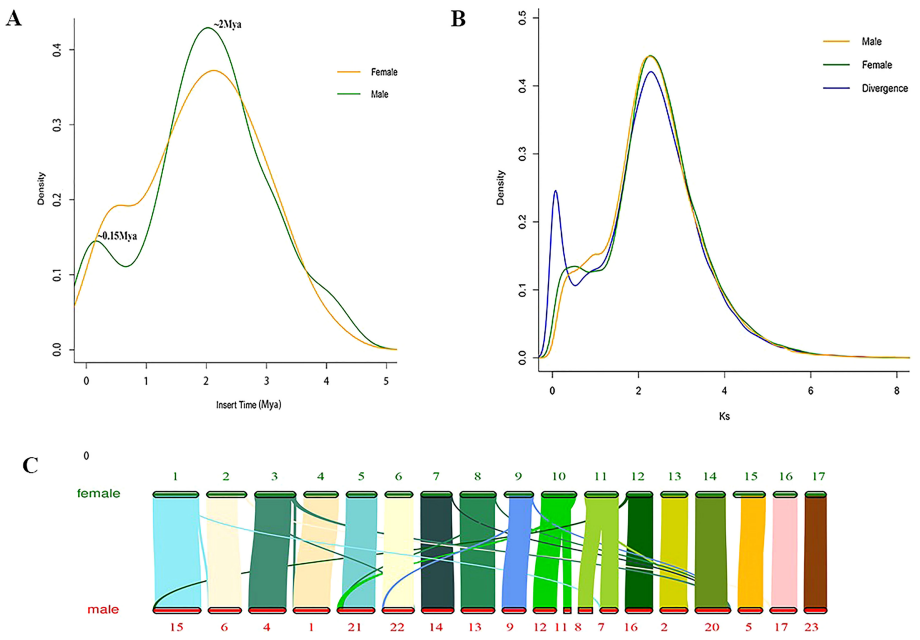

FIGURE 3
Genome evolutionary analysis. **(A)** Distribution of insertion times for LTR-RTs. **(B)** Ks value distribution in Female V1 and Male V2 genome. The divergence line represents Ks value distribution of syntenic blocks between male and female. **(C)** Genomic alignments of chromosomes and superscaffolds between Female V1 and Male V2.

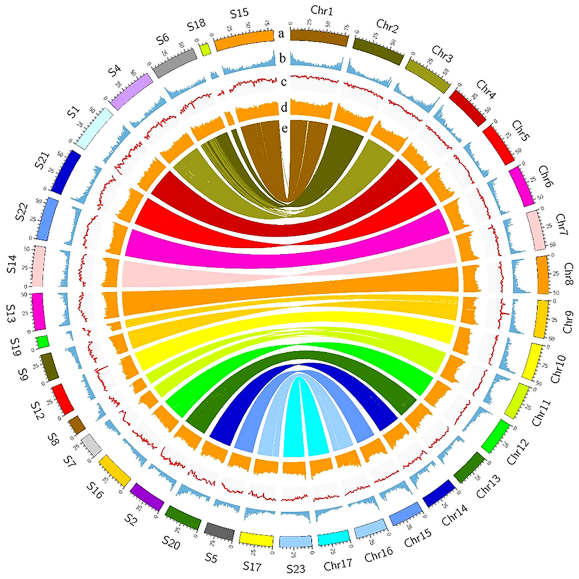

FIGURE 4
Landscape of Female V1 and Male V2 genome. The circle from outside to inside represents, **(A)** Chromosomes of Female V1 and Superscaffolds of Male V2, **(B)** gene density, **(C)** GC content, **(D)** repeat abundance, **(E)** synteny information. All distributions were drawn in a window size of 1 Mb.

eudicots, *E. ulmoides* experienced a more recent WGD event approximately 27.3 Mya. The collinearity analysis of male and female revealed a 1:1 synteny pattern (Supplementary Figure 6). The divergence time between female and male *E. ulmoides* was defined with a Ks peak value of 0.075 (Figure 3B).

MADS-box genes involved in sex differentiation

In the Female V1 and Male V2 genome, 76 and 81 MADS-box genes were separately identified, and further phylogenetic analysis of these genes was performed (Supplementary Figure 7). Based on the transcriptome analysis, 30 MADS-box genes of Female V1 were differentially expressed at different developmental stages of male and female flower buds. In addition, nine genes involved in the ABCDE model of floral development were identified in these MADS-box genes, which included three A-class genes (*EuAP1, EuFUL1, EuAGL6*), one B-class gene (*EuAP3*), one C-class gene (*EuAG*), two D-class genes (*EuSHP1, EuSHP2*), and two genes (*EuSEP1, EuSEP2*) that were associated with the E function (Supplementary Table 5). Nine MADS-box genes involved in the ABCDE model of floral development were identified in Male V2. We found high homology between male and female lineages (Supplementary Figure 8) and the gene structure and domain sequence of these genes were similar (Supplementary Figures 9, 10). In addition, we compared the obtained sex differentiation genes with the related sex differentiation genes in *Nymphaea colorata*, and the genes involved in sex differentiation in *E. ulmoides* and *N. colorata* showed high homology (Supplementary Figure 11).

The expression levels of the ABCDE genes at the floral organ maturity stage were higher than those in the floral organ induction stage and morphological differentiation initial stage. Except for the *EuFUL1* and *EuSHP2* genes, the other seven ABCDE genes were differentially expressed between the male and female flower buds. Seven ABCDE genes were differentially expressed during the floral organ maturity stage, with four differentially expressed genes in the floral organ morphological differentiation initial stage, and only one gene differentially expressed in the floral organ induction stage. The *EuAP3* gene was differentially expressed in three different

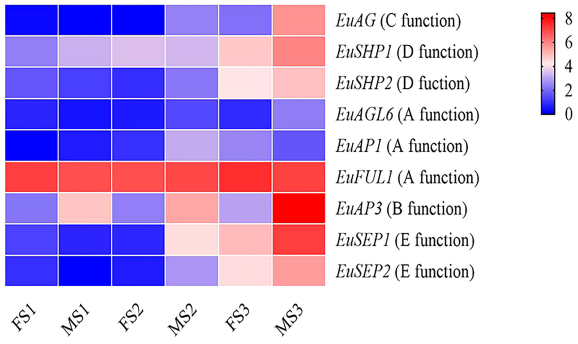

FIGURE 5
Heatmap of sex determination genes expression data in different stages of flower bud development in Female and male *E. ulmoides*. FS1: female floral organ induction stage flower bud, MS1: male floral organ induction stage flower bud, FS2: female floral organ morphological differentiation initial stage flower bud, MS2: and male floral organ morphological differentiation initial stage flower bud, FS3: female floral organ maturity stage flower bud, MS3: male floral organ maturity stage flower bud. Various color blocks represent the normalized gene expression levels of candidate genes involved in sex determination at different stages of flower bud development in Female and male *E. ulmoides*. The six boxes in one row of each heatmap (left to right) correspond to the expression levels in FS1, MS1, FS2, MS2, FS3, and MS3. Each row in the heatmap corresponds to one gene.

developmental stages of male and female flower buds (Figure 5 and Supplementary Figure 12).

Identification of the genes involved in α-linolenic acid synthesis

According to the functional annotation, 12 genes encoding key enzymes involved in the main synthesis and metabolic pathways of linolenic acid were identified in the Female V1 genome. Among them, six genes of four key enzymes related to the synthesis of α-linolenic acid were identified, including two acyl-ACP desaturase (FAB2) genes—*EU0119133* and *EU0120166*, which are homologues of SAD and perform the same function of converting stearoyl-ACP (C18:0-ACP) to oleoyl-ACP (C18:1-ACP) (Kazaz et al., 2020); one fatty acyl-ACP thioesterase A (FATA) gene—*EU0103200;* two omega-6 fatty acid desaturase (FAD2, FAD6) genes—*EU0105412* and *EU0128492;* and one omega-3 fatty acid desaturase (FAD7) gene—*EU0103017*. Six key enzyme genes for α-linolenic acid metabolism were also identified, including four lipoxygenase (LOX) genes—*EU0114412, EU0114414, EU0119724*, and *EU0119725*—and two alpha-dioxygenase (DOX) genes, *EU0107025, EU0131326* (Supplementary Table 6).

In addition, the expression levels of 12 identified key enzyme genes were compared between four parts of the fruit, stem, bark, and leaf. A heatmap of gene expression levels was also drawn (Figure 6). The expression levels of α-linolenic acid synthesis-related genes were higher in fruits and leaves than that in bark and stems. Overall, the expression levels of α-linolenic acid synthesis-related genes were much higher than those of metabolism-related genes. In particularly, the gene *EU0103017*—encoding FAD7, a key enzyme for linolenic acid synthesis—was highly expressed.

Discussion

E. ulmoides is an important economic plant because its bark, leaf, flower, fruit, and other tissues are rich in active secondary metabolites with important medicinal and economic value (Wang et al., 2019). High-quality *E. ulmoides* genomes have been useful for exploring the mechanisms of sex differentiation, synthesis and metabolism of important compounds. We assembled high-quality female and male genomes using PacBio and Hi-C technologies. There were 31,665 protein coding genes identified in Female V1 as compared to the 37,998 predicted genes in Male V2, and the repetitive sequence size in Female V1 was higher than that in Male V2. These results indicated that some differences in the genomes of male and female *E. ulmoides* were produced during the evolutionary process. Compared to previously published genomes (Wuyun et al., 2018) (Male V1), the quality of the reassembled version in this study (Male V2) was significantly increased. For example, superscaffold N50 was 25 times higher in Male V2 as compared to Male V1, and there were 1,266 new protein coding genes in addition to the 26,732 identified in Male V1. All these results indicated that there was greater accuracy and completeness in the Male V2 genome

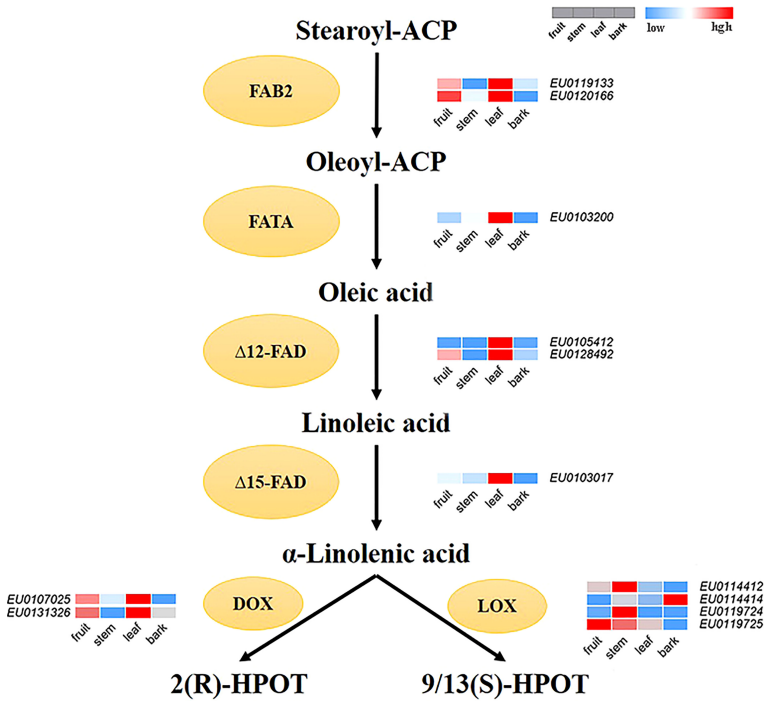

FIGURE 6
The reconstructed pathway of α-linolenic acid biosynthesis and metabolism in *E. ulmoides*. FAB2, Aacyl-ACP desaturase; FATA, acyl-ACP thioesterase; Δ12-FAD, omega-6 fatty acid desaturase; Δ15-FAD, omega-3 fatty acid desaturase; LOX, lipoxygenase; DOX, alpha-dioxygenase. Various color blocks represent the normalized gene expression levels of candidate genes related to α-linolenic acid biosynthesis and metabolism in *E. ulmoides*. The four boxes in one row of each heatmap (left to right) correspond to the expression levels in fruit, stem, leaf, and bark. Each row in the heatmap corresponds to one gene.

assembly as compared to the Male V1 genome. These two newly genomes provide a valuable resource for understanding sex differentiation and synthesis of important compounds in *E. ulmoides*, and they can be widely applied to genetics and genomics studies, such as the development of markers related to sex identification, detection of genes that synthesize important substances, and studies on the evolutionary history of *E. ulmoides*.

TEs is an important driving force to promote genome evolution, and the most important driving force is the accumulation of LTR-RTs (Sahebi et al., 2018; Lanciano and Cristofari, 2020). Further analysis showed that LTR-RTs erupted approximately 2 Mya, and cold tolerance may explain why *E. ulmoides* survived the Quaternary glaciation (Cros et al., 2020) approximately 2 Mya. Another insertion peak was identified in the Male V2 genome, this may be related to a greater number of repetitive sequences in the male genome. Whole genome duplication (WGD), also known as a paleopolyploidy event, provides abundant evolutionary materials for species and is considered as an important driving force for the formation and evolution of species (Soltis and Soltis, 2016; Clark and Donoghue, 2018). Most plants experience WGD, and many WGD events in angiosperms were detected during the Cretaceous-Tertiary period (145.5–65.5 Mya) (Vanneste et al., 2014). There is an obvious peak in the Ks distribution at the Ks value of 2.29375 in the two genomes, which indicated that males and females underwent a WGD event approximately 139 Mya (γ-WGT, 122–164 Mya) (Salse, 2016). Plants undergoing WGD events can enhance their environmental adaptability and stress resistance, thus promoting species evolution (del Pozo and Ramirez-Parra, 2015). Therefore, γ-WGT event may increase the adaptability of *E. ulmoides* to harsh environments, thus enabling *E. ulmoides* to resist the extinction event that occurred in the Cretaceous-Tertiary period. The peak at 0.45 in male genome is not as obvious as that in female, which might be the comparatively smaller continuity (Contig N50 17.06 kb) and lower quality of male genome than that of female genome. To detect whether there is a WGD event here, we have performed collinearity analysis. The 1:1 synteny pattern between male and female genomes also revealed that they have undergone the same number of WGD events. Besides, the divergence time between female and male *E. ulmoides* was identified with a Ks peak value of 0.075, while the recent WGD, specifically occurred in female, was with the Ks peak value of 0.45, which indicated that the recent WGD occurred before their differentiation.

There were nine MADS-box genes involved in the ABCDE mode in both female and male *E. ulmoides*, and their gene structure and domain sequence were conservative, suggesting their important role in floral development. During the development of male and female *E. ulmoides* flower buds, the greatest number of MADS-box differentially expressed genes was observed in the floral organ maturity stage, followed by the floral organ morphological differentiation initial stage, and the same was true for ABCDE genes. These results showed that the male and female flower buds of *E. ulmoides* were identical in the early developmental stage. However, with the development of female and male flower buds, the morphological differences gradually became obvious, and the differential genes increased. The ABCDE model of floral organ has been studied in *Nymphaea colorata* (Zhang et al., 2020), and the genes involved in floral organ in *E. ulmoides* and *N. colorata* showed high homology, which indicated that the genes related to flower development identified in *E. ulmoides* were reliable. In the ABCDE flower development model, B, C, and E genes jointly control stamen development (Hu et al., 2021). During the floral organ maturity stage of *E. ulmoides*, a large number of MADS-box family genes were differentially expressed in male and female flower buds. In particular, we observed that the B-class gene *EuAP3* was differentially expressed during the three stages of male and female flower bud development, and the expression level in male flower buds was significantly higher than that in female flower buds, which further supports the role of *EuAP3* in regulating stamen development. The expression of the C-class gene (*EuAG*) was also upregulated in male flower buds. This indicated that similar to the AG gene function in *Arabidopsis* and rice, the *EuAG* gene was involved in the development of stamens. *EuAP3* and *EuAG* are the key regulatory genes for stamen development and may be candidate genes for regulating sex differentiation.

E. ulmoides is rich in α-linolenic acid, which is synthesized from stearic acid under the catalysis of a series of fatty acid desaturases (Liu et al., 2020). First, stearoyl-ACP (C18:0-ACP) is catalyzed by enzyme FAB2 to produce oleoyl-ACP (C18:1-ACP), which is then converted to oleic acid (OA, C18:1) by the FATA enzyme. Oleic acid is desaturated by the enzyme fatty acid desaturase 2 (FAD2) and fatty acid desaturase 6 (FAD6) to generate linoleic acid (LA, C18:2). The fatty acid desaturase 7 (FAD7) enzyme catalyzes the synthesis of α-linolenic acid (ALA, C18:3) from LA in *E. ulmoides*. DOX and LOX are two key enzymes that catalyze the first step of α-linolenic acid metabolism, and they catalyze α-linolenic acid to produce 2 (R)-HPOT and 9/13(S)-HPOT, respectively (Gfeller et al., 2010; Shimada and Hara-Nishimura, 2015).

Transcriptome analysis results showed that the expression of synthesis-related genes was high, and there was very high expression of the genes encoding the key enzyme ω-3 fatty acid desaturase (FAD7), which is involved in α-linolenic acid synthesis and allows *Eucommia* to synthesize sufficient α-linolenic acid. The expression of metabolism-related genes was lower or they were not expressed, and thus, α-linolenic acid could be efficiently accumulated in *E. ulmoides*. These results may explain why the α-linolenic acid content in *E. ulmoides* is higher than that in other plants. In addition, the expression level of genes related to α-linolenic acid synthesis in fruit and leaf was higher than that in bark and stem. Although the expression of genes related to α-linolenic acid synthesis was higher in leaf (*EU0119133, EU0120166, EU0103017*), the expression of genes related to the downstream α-linolenic acid metabolic pathway was also higher in leaf (*EU0107025, EU0131326*). This allows the synthesis of α-linolenic acid in the leaf to be greatly metabolized, while the α-linolenic acid in the fruit can be accumulated, which explains why the α-linolenic acid is mainly distributed in the fruit of *E. ulmoides*.

In the current study, two high-quality *E. ulmoides* genomes are provided, which are helpful for evolutionary and genomics research. Using these genomic data, we identified WGD events and evaluated the LTR outbreak time to provide a basis for future studies on genomic evolution and stress resistance of *E. ulmoides*. MADS-box family genes were also identified, and the genes related to flower development in *E. ulmoides* were predicted according to the expression patterns of genes in male and female flower buds, and finally the key candidate genes that regulate sex differentiation were identified. In addition, the key

regulatory genes for α-linolenic acid synthesis and metabolism were identified, and the mechanism of α-linolenic acid accumulation was revealed. According to these genes, *E. ulmoides* can be improved by directed genetic modification. Overall, our research results not only provide valuable information for the evolutionary analysis of *E. ulmoides* but also advance our understanding of the molecular mechanism of sex differentiation and α-linolenic acid accumulation. This study will accelerate the breeding of superior varieties and enable us to more thoroughly explore and use the value inherent in *E. ulmoides*.

Data availability statement

The datasets presented in this study can be found in online repositories. The names of the repository/repositories and accession number(s) can be found below: https://www.ncbi.nlm.nih.gov/, PRJNA792509.

Author contributions

HD and LW conceived this study; QD, ZW, and PL worked on the data analysis and wrote the manuscript; JQ, FH, LD, ZhS LZ, and HZ contributed to the sample preparation; ZoS provided sequencing service; LY and LW revised the manuscript. All authors contributed to the article and approved the submitted version.

Funding

This work was supported by the Fundamental Research Funds for Central Public-interest Scientific Institution (CAFYBB2021MA009).

Acknowledgments

We sincerely thank each author who contributed to this study and thank Grandomics Biosciences Co., Ltd for providing sequencing service. We appreciate reviewers and editor for the insightful comments and valuable suggestions.

Conflict of interest

Author HZ is employed by Henan Jinduzhong Agricultural Science and Technology Co., Ltd., Henan, China. Author ZoS is employed by Grandomics Biosciences Co., Ltd., Wuhan, China.

The remaining authors declare that the research was conducted in the absence of any commercial or financial relationships that could be construed as a potential conflict of interest.

Publisher's note

Supplementary material

The Supplementary Material for this article can be found online at: https://www.frontiersin.org/articles/10.3389/fpls.2023.1118363/full#supplementary-material

References

Abraham-Juárez, M. J., Schrager-Lavelle, A., Man, J., Whipple, C., Handakumbura, P., Babbitt, C., et al. (2020). Evolutionary variation in MADS box dimerization affects floral development and protein abundance in maize. *Plant Cell* 32 (11), 3408–3424. doi: 10.1105/tpc.20.00300

Bao, W., Kojima, K. K., and Kohany, O. (2015). Repbase update, a database of repetitive elements in eukaryotic genomes. *Mob DNA* 6, 11. doi: 10.1186/s13100-015-0041-9

Barrett, S. C. H., and Hough, J. (2012). Sexual dimorphism in flowering plants. *J. Exp. Bot.* 64 (1), 67–82. doi: 10.1093/jxb/ers308

Benson, G. (1999). Tandem repeats finder: a program to analyze DNA sequences. *Nucleic Acids Res.* 27 (2), 573–580. doi: 10.1093/nar/27.2.573

Birney, E., Clamp, M., and Durbin, R. (2004). GeneWise and genomewise. *Genome Res.* 14 (5), 988–995. doi: 10.1101/gr.1865504

Bowman, J. L., Smyth, D. R., and Meyerowitz, E. M. (1989). Genes directing flower development in arabidopsis. *Plant Cell* 1 (1), 37–52. doi: 10.1105/tpc.1.1.37

Camacho, C., Coulouris, G., Avagyan, V., Ma, N., Papadopoulos, J., Bealer, K., et al. (2009). BLAST+: architecture and applications. *BMC Bioinf.* 10, 421. doi: 10.1186/1471-2105-10-421

Causier, B., Schwarz-Sommer, Z., and Davies, B. (2010). Floral organ identity: 20 years of ABCs. *Semin. Cell Dev. Biol.* 21 (1), 73–79. doi: 10.1016/j.semcdb.2009.10.005

Chin, C. S., Alexander, D. H., Marks, P., Klammer, A. A., Drake, J., Heiner, C., et al. (2013). Nonhybrid, finished microbial genome assemblies from long-read SMRT sequencing data. *Nat. Methods* 10 (6), 563–569. doi: 10.1038/nmeth.2474

Clark, J. W., and Donoghue, P. C. J. (2018). Whole-genome duplication and plant macroevolution. *Trends Plant Sci.* 23 (10), 933–945. doi: 10.1016/j.tplants.2018.07.006

Coen, E. S., and Meyerowitz, E. M. (1991). The war of the whorls: genetic interactions controlling flower development. *Nature* 353 (6339), 31–37. doi: 10.1038/353031a0

Cros, E., Chattopadhyay, B., Garg, K. M., Ng, N. S. R., Tomassi, S., Benedick, S., et al. (2020). Quaternary land bridges have not been universal conduits of gene flow. *Mol. Ecol.* 29 (14), 2692–2706. doi: 10.1111/mec.15509

del Pozo, J. C., and Ramirez-Parra, E. (2015). Whole genome duplications in plants: an overview from arabidopsis. *J. Exp. Bot.* 66 (22), 6991–7003. doi: 10.1093/jxb/erv432

Di Marzo, M., Roig-Villanova, I., Zanchetti, E., Caselli, F., Gregis, V., Bardetti, P., et al. (2020). MADS-box and bHLH transcription factors coordinate transmitting tract development in arabidopsis thaliana. *Front. Plant Sci.* 11. doi: 10.3389/fpls.2020.00526

Dudchenko, O., Batra, S. S., Omer, A. D., Nyquist, S. K., Hoeger, M., Durand, N. C., et al. (2017). *De novo* assembly of the aedes aegypti genome using Hi-c yields chromosome-length scaffolds. *Science* 356 (6333), 92–95. doi: 10.1126/science.aal3327

Durand, N. C., Robinson, J. T., Shamim, M. S., Machol, I., Mesirov, J. P., Lander, E. S., et al. (2016a). Juicebox provides a visualization system for Hi-c contact maps with unlimited zoom. *Cell Syst.* 3 (1), 99–101. doi: 10.1016/j.cels.2015.07.012

Durand, N. C., Shamim, M. S., Machol, I., Rao, S. S., Huntley, M. H., Lander, E. S., et al. (2016b). Juicer provides a one-click system for analyzing loop-resolution Hi-c experiments. *Cell Syst.* 3 (1), 95–98. doi: 10.1016/j.cels.2016.07.002

Feng, Y., Zhang, L., Fu, J., Li, F., Wang, L., Tan, X., et al. (2016). Characterization of glycolytic pathway genes using RNA-seq in developing kernels of eucommia ulmoides. *J. Agric. Food Chem.* 64 (18), 3712–3731. doi: 10.1021/acs.jafc.5b05918

Flynn, J. M., Hubley, R., Goubert, C., Rosen, J., Clark, A. G., Feschotte, C., et al. (2020). RepeatModeler2 for automated genomic discovery of transposable element families. *Proc. Natl. Acad. Sci. U.S.A.* 117 (17), 9451–9457. doi: 10.1073/pnas.1921046117

Gfeller, A., Dubugnon, L., Liechti, R., and Farmer, E. E. (2010). Jasmonate biochemical pathway. *Sci. Signal* 3 (109), cm3. doi: 10.1126/scisignal.3109cm3

Haas, B. J., Salzberg, S. L., Zhu, W., Pertea, M., Allen, J. E., Orvis, J., et al. (2008). Automated eukaryotic gene structure annotation using EVidenceModeler and the program to assemble spliced alignments. *Genome Biol.* 9 (1), R7. doi: 10.1186/gb-2008-9-1-r7

Hu, J., Chang, X., Zhang, Y., Yu, X., Qin, Y., Sun, Y., et al. (2021). The pineapple MADS-box gene family and the evolution of early monocot flower. *Sci. Rep.* 11 (1), 849. doi: 10.1038/s41598-020-79163-8

Hu, X. D., Pan, B. Z., Fu, Q., Niu, L., Chen, M. S., and Xu, Z. F. (2018). *De novo* transcriptome assembly of the eight major organs of sacha inchi (Plukenetia volubilis) and the identification of genes involved in α-linolenic acid metabolism. *BMC Genomics* 19 (1), 380. doi: 10.1186/s12864-018-4774-y

Huerta-Cepas, J., Forslund, K., Coelho, L. P., Szklarczyk, D., Jensen, L. J., von Mering, C., et al. (2017). Fast genome-wide functional annotation through orthology assignment by eggNOG-mapper. *Mol. Biol. Evol.* 34 (8), 2115–2122. doi: 10.1093/molbev/msx148

Kazaz, S., Barthole, G., Domergue, F., Ettaki, H., To, A., Vasselon, D., et al. (2020). Differential activation of partially redundant Δ9 stearoyl-ACP desaturase genes is critical for omega-9 monounsaturated fatty acid biosynthesis during seed development in arabidopsis. *Plant Cell* 32 (11), 3613–3637. doi: 10.1105/tpc.20.00554

Kim, K. B., Nam, Y. A., Kim, H. S., Hayes, A. W., and Lee, B. M. (2014). α-linolenic acid: nutraceutical, pharmacological and toxicological evaluation. *Food Chem. Toxicol.* 70, 163–178. doi: 10.1016/j.fct.2014.05.009

Kim, D., Pertea, G., Trapnell, C., Pimentel, H., Kelley, R., and Salzberg, S. L. (2013). TopHat2: accurate alignment of transcriptomes in the presence of insertions, deletions and gene fusions. *Genome Biol.* 14 (4), R36. doi: 10.1186/gb-2013-14-4-r36

Kong, S., and Zhang, Y. (2019). Deciphering Hi-c: from 3D genome to function. *Cell Biol. Toxicol.* 35 (1), 15–32. doi: 10.1007/s10565-018-09456-2

Korf, I. (2004). Gene finding in novel genomes. *BMC Bioinf.* 5, 59. doi: 10.1186/1471-2105-5-59

Lanciano, S., and Cristofari, G. (2020). Measuring and interpreting transposable element expression. *Nat. Rev. Genet.* 21 (12), 721–736. doi: 10.1038/s41576-020-0251-y

Li, Y., Wei, H., Yang, J., Du, K., Li, J., Zhang, Y., et al. (2020). High-quality *de novo* assembly of the eucommia ulmoides haploid genome provides new insights into evolution and rubber biosynthesis. *Hortic. Res.* 7 (1), 183. doi: 10.1038/s41438-020-00406-w

Liao, B., Hao, Y., Lu, J., Bai, H., Guan, L., and Zhang, T. (2018). Transcriptomic analysis of perilla frutescens seed to insight into the biosynthesis and metabolic of unsaturated fatty acids. *BMC Genomics* 19 (1), 213. doi: 10.1186/s12864-018-4595-z

Li-Beisson, Y., Shorrosh, B., Beisson, F., Andersson, M. X., Arondel, V., Bates, P. D., et al. (2013). Acyl-lipid metabolism. *Arabidopsis Book* 11, e0161. doi: 10.1199/tab.0161

Liu, K., Zhao, S., Wang, S., Wang, H., and Zhang, Z. (2020). Identification and analysis of the FAD gene family in walnuts (Juglans regia l.) based on transcriptome data. *BMC Genomics* 21 (1), 299. doi: 10.1186/s12864-020-6692-z

Lowe, T. M., and Chan, P. P. (2016). tRNAscan-SE on-line: integrating search and context for analysis of transfer RNA genes. *Nucleic Acids Res.* 44 (W1), W54–W57. doi: 10.1093/nar/gkw413

Majoros, W. H., Pertea, M., and Salzberg, S. L. (2004). TigrScan and GlimmerHMM: two open source ab initio eukaryotic gene-finders. *Bioinformatics* 20 (16), 2878–2879. doi: 10.1093/bioinformatics/bth315

Massonnet, M., Cochetel, N., Minio, A., Vondras, A. M., Lin, J., Muyle, A., et al. (2020). The genetic basis of sex determination in grapes. *Nat. Commun.* 11 (1), 2902. doi: 10.1038/s41467-020-16700-z

Morel, P., Chambrier, P., Boltz, V., Chamot, S., Rozier, F., Rodrigues Bento, S., et al. (2019). Divergent functional diversification patterns in the SEP/AGL6/AP1 MADS-box transcription factor superclade. *Plant Cell* 31 (12), 3033–3056. doi: 10.1105/tpc.19.00162

Nawrocki, E. P., Burge, S. W., Bateman, A., Daub, J., Eberhardt, R. Y., Eddy, S. R., et al. (2015). Rfam 12.0: updates to the RNA families database. *Nucleic Acids Res.* 43 (Database issue), D130–D137. doi: 10.1093/nar/gku1063

Nawrocki, E. P., Kolbe, D. L., and Eddy, S. R. (2009). Infernal 1.0: inference of RNA alignments. *Bioinformatics* 25 (10), 1335–1337. doi: 10.1093/bioinformatics/btp157

Prakash, A., Jeffryes, M., Bateman, A., and Finn, R. D. (2017). The HMMER web server for protein sequence similarity search. *Curr. Protoc. Bioinf.* 60, 3.15.1–3.15.23. doi: 10.1002/cpbi.40

Sahebi, M., Hanafi, M. M., van Wijnen, A. J., Rice, D., Rafii, M. Y., Azizi, P., et al. (2018). Contribution of transposable elements in the plant's genome. *Gene* 665, 155–166. doi: 10.1016/j.gene.2018.04.050

Salse, J. (2016). Ancestors of modern plant crops. *Curr. Opin. Plant Biol.* 30, 134–142. doi: 10.1016/j.pbi.2016.02.005

Schwarz-Sommer, Z., Huijser, P., Nacken, W., Saedler, H., and Sommer, H. (1990). Genetic control of flower development by homeotic genes in antirrhinum majus. *Science* 250 (4983), 931–936. doi: 10.1126/science.250.4983.931

Shimada, T. L., and Hara-Nishimura, I. (2015). Leaf oil bodies are subcellular factories producing antifungal oxylipins. *Curr. Opin. Plant Biol.* 25, 145–150. doi: 10.1016/j.pbi.2015.05.019

Simão, F. A., Waterhouse, R. M., Ioannidis, P., Kriventseva, E. V., and Zdobnov, E. M. (2015). BUSCO: assessing genome assembly and annotation completeness with single-copy orthologs. *Bioinformatics* 31 (19), 3210–3212. doi: 10.1093/bioinformatics/btv351

Soltis, D. E., Chanderbali, A. S., Kim, S., Buzgo, M., and Soltis, P. S. (2007). The ABC model and its applicability to basal angiosperms. *Ann. Bot.* 100 (2), 155–163. doi: 10.1093/aob/mcm117

Soltis, P. S., and Soltis, D. E. (2016). Ancient WGD events as drivers of key innovations in angiosperms. *Curr. Opin. Plant Biol.* 30, 159–165. doi: 10.1016/j.pbi.2016.03.015

Stanke, M., and Morgenstern, B. (2005). AUGUSTUS: a web server for gene prediction in eukaryotes that allows user-defined constraints. *Nucleic Acids Res.* 33 (Web Server issue), W465–W467. doi: 10.1093/nar/gki458

Tarailo-Graovac, M., and Chen, N. (2009). Using RepeatMasker to identify repetitive elements in genomic sequences. *Curr. Protoc. Bioinf.* 25, 4.10.1–4.10.14 doi: 10.1002/0471250953.bi0410s25

Teo, Z. W. N., Zhou, W., and Shen, L. (2019). Dissecting the function of MADS-box transcription factors in orchid reproductive development. *Front. Plant Sci.* 10. doi: 10.3389/fpls.2019.01474

Theissen, G. (2001). Development of floral organ identity: stories from the MADS house. *Curr. Opin. Plant Biol.* 4 (1), 75–85. doi: 10.1016/s1369-5266(00)00139-4

Trapnell, C., Williams, B. A., Pertea, G., Mortazavi, A., Kwan, G., van Baren, M. J., et al. (2010). Transcript assembly and quantification by RNA-seq reveals unannotated transcripts and isoform switching during cell differentiation. *Nat. Biotechnol.* 28 (5), 511–515. doi: 10.1038/nbt.1621

Vanneste, K., Baele, G., Maere, S., and Van de Peer, Y. (2014). Analysis of 41 plant genomes supports a wave of successful genome duplications in association with the Cretaceous-paleogene boundary. *Genome Res.* 24 (8), 1334–1347. doi: 10.1101/gr.168997.113

Walker, B. J., Abeel, T., Shea, T., Priest, M., Abouelliel, A., Sakthikumar, S., et al. (2014). Pilon: an integrated tool for comprehensive microbial variant detection and genome assembly improvement. *PloS One* 9 (11), e112963. doi: 10.1371/journal.pone.0112963

Wang, Y., Tang, H., Debarry, J. D., Tan, X., Li, J., Wang, X., et al. (2012). MCScanX: a toolkit for detection and evolutionary analysis of gene synteny and collinearity. *Nucleic Acids Res.* 40 (7), e49. doi: 10.1093/nar/gkr1293

Wang, C. Y., Tang, L., He, J. W., Li, J., and Wang, Y. Z. (2019). Ethnobotany, phytochemistry and pharmacological properties of eucommia ulmoides: A review. *Am. J. Chin. Med.* 47 (2), 259–300. doi: 10.1142/s0192415x19500137

Wang, W., Yang, G., Deng, X., Shao, F., Li, Y., Guo, W., et al. (2020). Molecular sex identification in the hardy rubber tree (Eucommia ulmoides Oliver) *via* ddRAD markers. *Int. J. Genomics* 2020, 2420976. doi: 10.1155/2020/2420976

Wang, W., and Zhang, X. (2017). Identification of the sex-biased gene expression and putative sex-associated genes in eucommia ulmoides Oliver using comparative transcriptome analyses. *Molecules* 22 (12), 2255. doi: 10.3390/molecules22122255

Wang, D., Zhang, Y., Zhang, Z., Zhu, J., and Yu, J. (2010). KaKs_Calculator 2.0: a toolkit incorporating gamma-series methods and sliding window strategies. *Genomics Proteomics Bioinf.* 8 (1), 77–80. doi: 10.1016/s1672-0229(10)60008-3

Wuyun, T. N., Wang, L., Liu, H., Wang, X., Zhang, L., Bennetzen, J. L., et al. (2018). The hardy rubber tree genome provides insights into the evolution of polyisoprene biosynthesis. *Mol. Plant* 11 (3), 429–442. doi: 10.1016/j.molp.2017.11.014

Xu, Z., and Wang, H. (2007). LTR_FINDER: an efficient tool for the prediction of full-length LTR retrotransposons. *Nucleic Acids Res.* 35 (Web Server issue), W265–W268. doi: 10.1093/nar/gkm286

Yin, X., Liu, X., Xu, B., Lu, P., Dong, T., Yang, D., et al. (2019). OsMADS18, a membrane-bound MADS-box transcription factor, modulates plant architecture and the abscisic acid response in rice. *J. Exp. Bot.* 70 (15), 3895–3909. doi: 10.1093/jxb/erz198

Yu, S. Y., Zhang, X., Huang, L. B., Lyu, Y. P., Zhang, Y., Yao, Z. J., et al. (2021). Transcriptomic analysis of α-linolenic acid content and biosynthesis in paeonia ostii fruits and seeds. *BMC Genomics* 22 (1), 297. doi: 10.1186/s12864-021-07594-2

Zhang, L., Chen, F., Zhang, X., Li, Z., Zhao, Y., Lohaus, R., et al. (2020). The water lily genome and the early evolution of flowering plants. *Nature* 577 (7788), 79–84. doi: 10.1038/s41586-019-1852-5

Zhang, Z. S., Liu, Y. L., and Che, L. M. (2018). Characterization of a new α-linolenic acid-rich oil: Eucommia ulmoides seed oil. *J. Food Sci.* 83 (3), 617–623. doi: 10.1111/1750-3841.14049

Zhu, M. Q., and Sun, R. C. (2018). Eucommia ulmoides Oliver: A potential feedstock for bioactive products. *J. Agric. Food Chem.* 66 (22), 5433–5438. doi: 10.1021/acs.jafc.8b01312

frontiers | Frontiers in Plant Science

TYPE Original Research
PUBLISHED 08 May 2023
DOI 10.3389/fpls.2023.1172857

OPEN ACCESS

EDITED BY
Long Yang,
Shandong Agricultural University, China

REVIEWED BY
Silvia Maribel Contreras Ramos,
CONACYT Centro de Investigación y Asistencia en Tecnología y Diseño del Estado de Jalisco (CIATEJ), Mexico
Louise Egerton-Warburton,
Chicago Botanic Garden, United States

*CORRESPONDENCE
Giovanna Visioli
giovanna.visioli@unipr.it
Laura Righetti
laura.righetti@wur.nl

†PRESENT ADDRESS
Marta Bertola,
Department of Sustainable Crop Production, University Cattolica del Sacro Cuore, Piacenza, Italy

RECEIVED 23 February 2023
ACCEPTED 06 April 2023
PUBLISHED 08 May 2023

CITATION
Bertola M, Righetti L, Gazza L, Ferrarini A, Fornasier F, Cirlini M, Lolli V, Galaverna G and Visioli G (2023) Perenniality, more than genotypes, shapes biological and chemical rhizosphere composition of perennial wheat lines.
Front. Plant Sci. 14:1172857.
doi: 10.3389/fpls.2023.1172857

Perenniality, more than genotypes, shapes biological and chemical rhizosphere composition of perennial wheat lines

Marta Bertola[1†], Laura Righetti[1,2,3*], Laura Gazza[4], Andrea Ferrarini[5], Flavio Fornasier[6], Martina Cirlini[1], Veronica Lolli[1], Gianni Galaverna[1] and Giovanna Visioli[7*]

[1]Department of Food and Drugs, University of Parma, Parma, Italy, [2]Wageningen Food Safety Research, Wageningen University and Research, Wageningen, Netherlands, [3]Laboratory of Organic Chemistry, Wageningen University, Wageningen, Netherlands, [4]Council for Agricultural Research and Economics, Research Centre for Engineering and Agro-Food Processing, Rome, Italy, [5]Department of Sustainable Crop Production, Università Cattolica del Sacro Cuore, Piacenza, Italy, [6]Council for Agricultural Research and Economics (CREA) Research Centre for Viticulture and Enology, Unit of Gorizia, Gorizia, Italy, [7]Department of Chemistry, Life Sciences and Environmental Sustainability, University of Parma, Parma, Italy

Perennial grains provide various ecosystem services compared to the annual counterparts thanks to their extensive root system and permanent soil cover. However, little is known about the evolution and diversification of perennial grains rhizosphere and its ecological functions over time. In this study, a suite of -OMICSs - metagenomics, enzymomics, metabolomics and lipidomics - was used to compare the rhizosphere environment of four perennial wheat lines at the first and fourth year of growth in comparison with an annual durum wheat cultivar and the parental species *Thinopyrum intermedium*. We hypothesized that wheat perenniality has a greater role in shaping the rhizobiome composition, biomass, diversity, and activity than plant genotypes because perenniality affects the quality and quantity of C input – mainly root exudates – hence modulating the plant-microbes crosstalk. In support of this hypothesis, the continuous supply of sugars in the rhizosphere along the years created a favorable environment for microbial growth which is reflected in a higher microbial biomass and enzymatic activity. Moreover, modification in the rhizosphere metabolome and lipidome over the years led to changes in the microbial community composition favoring the coexistence of more diverse microbial taxa, increasing plant tolerance to biotic and abiotic stresses. Despite the dominance of the perenniality effect, our data underlined that the OK72 line rhizobiome distinguished from the others by the increase in abundance of *Pseudomonas* spp., most of which are known as potential beneficial microorganisms, identifying this line as a suitable candidate for the study and selection of new perennial wheat lines.

KEYWORDS

perennial grains, rhizosphere environment, microbial biodiversity, metagenomics, soil metabolomics, soil enzymomics, soil lipidomics

1 Introduction

Nowadays, intense annual crop production is causing a global exacerbation of natural resources degradation and biodiversity loss (Veerman et al., 2020) which leads to remarkable adverse impacts on essential ecosystem services (Pimentel et al., 2012). In addition, conventional crops are threatened by climate change that strongly impacts agricultural yields (Veerman et al., 2020). Therefore, it is necessary to adopt sustainable agricultural practices that could either decrease the agricultural impacts on climate and at the same time enhance agriculture resilience. The cultivation of perennial grain cropping systems, mostly in marginal land, has been proposed as an innovative method to face climate changes and restore soil health (Glover et al., 2010; Audu et al., 2022b).

The advantages of perennial crops include a longer growing season, a permanent soil cover that doesn't require intensive soil tillage and seedling, and a deep and dense rooting system (DeHaan et al., 2005; Glover et al., 2010; Pimentel et al., 2012). These features are expected to reduce soil erosion, ensure more efficient use of nutrient and water, also in deep soil layers, and increase soil carbon (C) sequestration, providing fundamental advantages for climate change mitigation and adaptation (DeHaan et al., 2005; Sprunger et al., 2018). Permanent soil cover and reduced soil disturbance also support highly structured and complex food webs, thereby boosting functional biodiversity and conditions for soil diversity conservation (Rasche et al., 2017; Sprunger et al., 2019). Moreover, extensive root network and allocation of belowground carbon, in term of root exudates and root debris, have the potential to promote plant–microbial linkages with important implications for nutrient cycling and ecosystem functioning (Wardle David et al., 2004; Hargreaves and Hofmockel, 2014; Audu et al., 2022b). Indeed, the development of perennial root systems during the plant growth represents a continuous supply of C to soil that stimulates microbial biomass and activity and can shape microbial community composition over time (Culman et al., 2010; Hargreaves et al., 2015; Rasche et al., 2017; Audu et al., 2022a; Audu et al., 2022b).

Previous studies about conservative managed annual cropping system have demonstrated that C addition from organic residues application, use of cover crops, and adoption of conservation tillage, can increase microbial biomass and activity compared to conventional one (Ceja-Navarro et al., 2010; Finney et al., 2017; Ghaley et al., 2018). Likewise, perennial herbaceous cropping systems sustain greater and more complex biological communities (Culman et al., 2010), distinguished by higher microbial biomass (Allison et al., 2005; Culman et al., 2010; Liang et al., 2012), activity (Hargreaves and Hofmockel, 2014) and diversity (Allison et al., 2005; Mao et al., 2013). Moreover, long-term use of these practices can select microbes with different life strategies, resulting from changes in soil structure, increased microhabitat diversity and increased abundance and diversity of available C substrates (Mao et al., 2013; Hargreaves et al., 2015; Schmidt et al., 2018). Furthermore, these practices increase the relative abundance of fungi, mainly due to reduced soil disturbance and hyphal network preservation, which may promote soil organic matter (SOM) stabilization and overall ecosystem functioning (Liang et al., 2012; Finney et al., 2017).

Nevertheless, only few recent studies evaluated shifts of microbial communities under perennial grain crops cultivation (Sprunger et al., 2019; Audu et al., 2022a; Audu et al., 2022b). The authors highlighted that perennial grain often need to be fully established (i.e., > 3 years) before changes in microbial community structure are detectable (Sprunger et al., 2019). On the other hand, other authors showed that perennial wheat cultivation can improve microbial biomass and activity, as measured by enzymes activity and basal respiration, compared with cultivation of annual wheat (Audu et al., 2022a; Audu et al., 2022b).

Current tecnhnologies such as -Omics allow us to decipher the complex dynamics of soil microbial communities and their ecological functions. Indeed, -Omics techniques have recently allowed the characterization of the overall soil microbial genetic and functional diversity through high-throughput analysis of soil DNAs (genomics), RNAs (transcriptomics), proteins (proteomics), enzymes (enzymomics), metabolites (metabolomics) and more recently lipids (lipidomics) (Withers et al., 2020; Bertola et al., 2021). The advent of next generation sequencing (NGS) techniques, has hastened the identification of soil microorganism communities predicting also their potential functions by DNA and RNA shot gun sequencing, while enzymomics, proteomics, and more recently metabolomics, have allowed the investigation of soil microbial biological functions (Vogel et al., 2009; Baldrian, 2014; Withers et al., 2020; Macabuhay et al., 2022). In particular, soil metabolites can reflect interactions between microorganisms and plant roots since they determine microbial food webs, regulate soil chemistry, change microbial gene expression, and act as info-chemicals to mediate microbe-to-microbe interactions (Bais et al., 2006; Hu et al., 2018; Macabuhay et al., 2022). Sugars, amino acids and organic acids dominate the metabolite pool of root-associated soils and mediate plant-microbe and microbe-to-microbe interactions that govern the overall microbial community (Bais et al., 2006; Carvalhais et al., 2011; Canarini et al., 2019). Also, recent evidence revealed an important role of lipids in the cross-talk between roots and rhizosphere microbes (Macabuhay et al., 2022). Lipids are a diverse and ubiquitous group of compounds which play many key biological functions, mainly regulating the plasma membrane cellular processes and signaling mediation. Further, the relative diversity and abundance of lipids in soil have been used to investigate microbial communities' responses to a range of external stressors, hence providing useful insights to changes in microbial function (Brown et al., 2021).

To date, however, there has been no study that apply high-throughput molecular technologies to unravel the mechanisms that shape soil microbial communities under perennial grain crops. Indeed, there is a gap in understanding the plant-induced modulation of the rhizobiome associated with long-term cultivation of new perennial grain lines.

We hypothesized that wheat perenniality has a predominant role respect to plant genotype in shaping the microbial community composition, biomass, diversity, and activity by affecting the quality and quantity of C input – mainly root exudates – and modulating the plant-microbes crosstalk. Therefore, this study aims to examine the evolution of rhizobiome composition and activity of four perennial wheat lines derived from the cross-breeding between

common wheat cultivars and *Thinopyrum* spp. (Gazza et al., 2016; Baronti et al., 2022). These four genotypes have been selected from a wider group of nine wheat x wheatgrass derivatives with a relatively high post-harvest regrowth capacity and for their higher nutritional and technological quality (Gazza et al., 2016; Baronti et al., 2022). Rhizosphere microbial communities were evaluated on the first and fourth year of growth of the perennial wheat lines and compared with the rhizosphere microbial communities of an annual durum wheat cultivar and the parental species *Thinopyrum intermedium*. In particular, we analyzed: i) the variations in biochemical activity of a broad range of hydrolytic enzymes, ii) the 16S rDNA and ITS based bacterial and fungal community composition in the rhizospheres by NGS techniques and iii) the variation in primary metabolites and lipids associated to the root system by un-targeted mass spectrometry-based metabolomics and lipidomics. In addition, to get new insights into rhizobiome dynamics over time, we investigated the relationships between microbial communities' structure (key microbial phyla) and activity (measured as enzyme activity), and how this is modulated by primary metabolites and lipids.

2 Materials and methods

2.1 Site description

The field experiment was set up in Central Italy at "Montelibretti" experimental farm station (CREA-IT, Rome) (Lat 42°08'N; Long 12°44'E; 20 m a.s.l.) in the Tiber valley. The area is characterized by a sub-humid Mediterranean climate with annual rainfall of 902 mm and mean air temperature of 14.7°C (historical series 1973–2016). The soil is classified as Arenosol with a silty clay loam soil texture. The experimental field (30 m x 5 m) was placed in a flat and homogeneous area of the experimental farm. Prior to planting, the experimental site had hosted common and durum wheat. Four new perennial wheat genotypes (NPGs) selected by (Gazza et al., 2016) (CPI-147235a, CPI-147280b, 11955, OK7211542, hereafter 235a, 280b, 11955 and OK72, respectively), were sown in November 2017 (year 4) and November 2020 (year 1), while the annual durum wheat cv Ardente and the perennial parental species *Thinopyrum intermedium* (Tpi) were sown respectively in November 2020 (year 1) and November 2010 (year 11). The elementary plot consisted of eight rows, 17 cm apart, sown with 400 germinating kernels/m^2. Plots were fertilized only the first year at a rate of 150 kg/ha of N (commercial urea fertilizer) applied in three top-dressing: at sowing, at emergence and at tillering phases and no irrigation was used all the years of plant growth. Weeds between plots were mechanically controlled, while those within rows were removed by hand.

2.2 Rhizosphere sampling

Rhizosphere samples of perennial wheat genotypes (year 1 and 4), annual durum wheat cultivar Ardente and *Thinopyrum intermedium* were collected in June 2021. Three samples of bare soil (BS) were also collected nearby. Four plants per genotype (235A, 280B, 11955, OK72 and *Triticum durum*) and three plants for the *Thinopyrum intermedium* were excavated from the top 20 cm of soil to collect the rhizosphere with two different methods according to its proximity to roots. Hence, the coarse rhizosphere (RS1) was gently separated from roots, while the thin layer of the rhizosphere, closer to roots (rhizoplane) (RS2), was separated by using an appropriate buffer as described in (McPherson et al., 2018).

2.3 16S rDNA and ITS -based community analysis

DNA was extracted from BS and RS2 samples starting from 200 mg of soil using the NucleoSpin Soil Kit (Machery – Nagel) according with manufacturer's protocol and visualized by electrophoresis on 1% (w/v) agarose gels to test for DNA integrity and quantified with Nanodrop ND1000 (Thermo Fisher Scientific, Waltham; MA, USA). The DNA samples obtained were sent to a commercial provider (IGA-Technology, Udine; http://www.igatechnology.com/) for the 16S rRNA and ITS gene amplification and sequencing. Libraries were prepared by following Illumina 16S Metagenomic Sequencing Library Preparation protocol in two amplification steps: an initial PCR amplification using locus-specific PCR primers (16S-341F 5'-CCTACGGGNBGCASCAG -3' and 16S-805R 5'-GACTACNVGGGTATCTAATCC -3' for bacteria; ITS1F 5'-TCCGTAGGTGAACCTGCGG -3' and ITS4R 5'-TCCTCCGCTTATTGATATGC -3' for fungi) and a subsequent amplification that integrates relevant flow-cell binding domains and unique indices (NexteraXT Index Kit, FC-131-1001/FC-131-1002). Libraries were sequenced on a MiSeq instrument (Illumina) in paired end 300-bp mode read length and reads were de-multiplexed based on Illumina indexing system. Taxonomic assignment was done using the software Quantitative Insights into Microbial Ecology (QIIME) (Kuczynski et al., 2012). Raw sequences were processed using the QIIME pipelines and the USEARCH algorithm (version 8.1.1756, 32-bit) was applied for chimera filtering, grouping of replicate sequences, sorting sequences per decreasing abundance and OTU identification. The Operational Taxonomic Unit (OTU) were identified by adopting an "open-reference" algorithm where OTUs were built *de novo* with a clustering threshold set at 97%, with sequences that passed a pre-filter step for minimum identity of 90% with any sequence present in the reference database. OTUs in "open-reference" analysis were generated with a minimum of 2 sequenced fragments. The RDP classifier and Reference databases (GreenGene database (version 2013_8) for 16S rRNA gene and UNITEdatabase v.7.2 -UNITE community, 2017- for ITS gene) were used to assign taxonomy with a minimum confidence threshold of 0.50. For bacteria a total of 6,804,064 16S rDNA raw reads were generated, while for fungi a total of 6,698,310 ITS raw reads were sequenced, with an average number of reads per samples of 154,638 and 152,234 for bacteria and fungi respectively. After denoising and filtering they were reduced to 2,790,088 and 2,377,941 respectively (Supplementary

Datafiles S8, S9). All raw sequences have been uploaded to NCBI under Bioprojects PRJNA826315.

Alpha and beta diversity were both calculated on the total OTU matrices (see Supplementary Datasets S3, S4). To compare bacterial and fungal alpha diversity, Shannon Diversity and Simpson indices were estimated with the R vegan package. All indices were analyzed using a two-way ANOVA on generalized least squares model and means were compared with an adjusted Tukey's pairwise means comparison procedure using emmeans and multcomp packages in R. The beta diversity was evaluated through distance-based redundancy analysis (dbRDA) as described in (Ferrarini et al., 2021). Briefly, differences in OTU patterns among treatments were evaluated *via* a 2-way model (year x line) based on distance-based redundancy analysis (dbRDA). Contrasts between treatments analysed *via* one-way permutational multivariate analysis of variance using distance matrices (ADONIS) based on the Bray-Curtis matrix. Differences in relative abundances of the most representative genus (relative abundance > 0.3% for bacteria and > 0.03% for fungi) between samples were tested by two-way Analysis of Variance (ANOVA). All graphing was performed with the package ggplot2 in R.

2.4 Soil enzymes activities and microbial biomass

Enzyme activity analysis (EAA) was performed on rhizosphere (RS1) samples. The assay based on the procedure of (Cowie et al., 2013) tested 17 hydrolytic enzymes involved in the principal nutrient cycles, namely: arylsulfatase (aryS), α-glucosidase (alfaG), β-glucosidase (betaG), α-galactosidase (alfaGAL), β-galactosidase (betaGAL), arabinase (arabin), β-1,4-xylanase (xilo), β-D-glucuronidase (uroni), chitinase/N-acetyl-β-D-glucosaminidase (chit), tripsin-like protease (trip), leucine amino-peptidase (leu), acid- (acP) and alkaline- (alkP) phosphomonoesterase, phosphodiesterase (bisP), pyrophosphate-phosphodiesterase (piroP), inositol-P phosphatase (insitP) and butyric esterase (butir). All enzymatic activities (EA) were measured in triplicate using a heteromolecular exchange procedure (Cowie et al., 2013) and bead-beating to disrupt soil aggregates and microbial cells. Briefly, 0.4 g fresh weight of soil was transferred to 2 mL microcentrifuge tubes together with 1.4 mL of 3% lysozyme containing 0.4 mL of 100 µm glass beads and 0.4 mL of 800 µm ceramic beads. Bead-beating was carried out using a Retsch 400 mill at 30 strokes s−1 for 3 min, followed by centrifugation at 20,000g for 5 min at 10°C. The supernatant containing desorbed enzymes was dispensed into 384-well white microplates containing the appropriate buffers (aryS, acP, inositP, alfaG, betaG, alfaGAL, betaGAL, arabin, xilo, uroni, and chit in morpholine heptane sulfonic acid 100 mM, pH 6; trip, leu, bisP, butir and piroP, in Tri-hydroxymethyl aminomethane 100 mM, pH 7.5; alkP in Tri-hydroxymethyl-aminomethane 100 mM, pH 9.0) to determine the enzymatic activities by fluorometry using 4- methyl-umbelliferyl (MUF) and 4-amido-7 methyl-coumarine (AMC) fluorogenic substrates, with readings taken using a Synergy HT microplate reader (Bio-Tek, Winooski, Vermont, United States). All measurements were taken in triplicate and the activities were expressed as nanomoles of MUF (or AMC) min/g dry soil. Microbial biomass was determined using the double-stranded DNA (dsDNA) content as a proxy (Bragato et al., 2016). DNA was extracted as described by (Fornasier et al., 2014). Briefly, the bead-beating as well as the centrifugation procedure was the same as for the enzyme described above, but the extraction buffer was 0.12 M sodium phosphate, pH 7.8. After diluting the supernatant, the dsDNA was quantified using PicoGreen (Thermo Fisher Scientific, Milan, Italy).

Differences in EA patterns among treatments were evaluated by distance-based redundancy analysis (dbRDA) using the R:vegan package. Four steps were applied: (1) a Bray–Curtis dissimilarity (nonlinear) matrix was calculated on square root transformed data; (2) a principal coordinate analysis (PCoA) was calculated based on the distance matrix, from which the eigenvalues (obtained in the PCoA) were applied to a RDA with 999 permutations to obtain dbRDA axis coordinates for treatments to be plotted as multivariate centroids surrounded by 95% confidence interval ellipsoids; (3) one-way permutational multivariate analysis of variance using distance matrices (ADONIS) based on the Bray-Curtis matrix was conducted for all 999 permutations on all pairwise contrasts tested for differences among treatments; (4) a similarity percentage (SIMPER) was used toidentify among all the enzymes measured the ones that contributes cumulatively less than 90% to dissimilarity in all contrasts. The following cut-off criterion was applied to allow the identification of the enzymes to use in the dbRDA: 90% cumulative contribution to dissimilarity in at least 70% of total number of contrasts.

Analysis of Variance (ANOVA) was performed on dsDNA data and means were compared with an adjusted Tukey's pairwise means comparison procedure using emmeans and multcomp packages in R.

2.5 Rhizosphere metabolomics and lipidomics

2.5.1 Sample extraction and mass spectrometry detection

Rhizosphere primary metabolites and lipids were extracted from RS1. Briefly, 0.5 g of lyophilized samples were aliquoted into 15-ml Falcon tubes together with 2 ml of 60% (vol/vol) methanol in Nanopure water. Samples were vortexed at maximum speed for 15 min at 4°C and subsequently 3.5 ml of ice-cold chloroform were added. Each sample was sonicated for 5 minute and allowed to cool on ice for 1 min. This latest step was carried out for 5 more times. The samples were allowed to completely cool at -80°C for 10 min, then centrifuged at 4500 g for 10 min at 4°C to separate the aqueous and the organic phase. For each sample 1 ml of the upper aqueous phase was dried down completely in a vacuum concentrator (Labconco, Kansas City, MO), and stored at -20°C until chemical derivatization before GC-MS analysis. In turn,1 ml of organic phase was dried down and reconstructed in 1 ml of ternary mix of acetonitrile/isopropanol/methanol before LC-HRMS untargeted lipidomics analysis.

2.5.2 Metabolomics: sample derivatization for GC/MS and data acquisition

The determination of simple sugars, polyalcohols, amino acids and organic acids of rhizosphere soil, was performed following the sample derivatization protocol described by (Swenson et al., 2015), with minor modifications (SI Appendix, Methods). Briefly, each dried sample residue was added to a mixture of 780 µl of dimetilformammide (DMF), containing 0.050 mg of internal standard phenyl-β-D-glucoside, and 20 µl of a solution containing 2 mg/mL of internal standard tetracosane (C24) in hexane. Then, each solution was added to 200 µl of N,O-bis (trimethylsilyl)trifluoroacetamide (BSTFA) with 1% of trimethylchlorosilane, shaken and incubated at 37°C for 30 min. In this way, all the analytes of interest were transformed in their corresponding trimethyl-silyl-ethers.

Aqueous standard solutions containing simple sugars, organic acids and amino acids were used for metabolite identification, based on comparison of analyte typical retention times and mass spectra. Specifically, for sugars and organic acids, solutions at a concentration of 1 mg/mL of each compound were prepared considering: arabinose, fructose, fucose, galactose, glucose, maltose, mannose, melibiose, myo-inositol, palatinose, ramnose, ribose, sorbitol, trehalose, and xylose (Sigma Aldrich) for simple sugars and polyols, and caffeic acid, cinnamic acid cumaric acid, galacturonic acid, gallic acid, glycolic acid, ferulic acid, lactic acid, malic acid, malonic acid, and sinapic acid (Sigma Aldrich) as organic acids. Concerning amino acids, a 1.25 mM solution was obtained by mixing (in a 1:1 ratio) a 2.5 mM Amino Acid Standard H solution (Thermo Fisher Scientific) and a 2.5 mM mixture of remaining amino acids (nor-leucine, tryptophan, asparagine, and glutamine, from Sigma Aldrich) to a final volume of 1 mL. From each standard mixtures, 100 µl were dried, and dissolved in a solution of 800 µl DMF and 200 µl BSTFA and incubated at 60°C for 1h for derivatization.

For each GC-MS analysis, derivatized samples (1 µl) were split injected (1:20 split ratio) into a Thermo Scientific Trace 1300 gas-chromatograph coupled to a Thermo Scientific ISQ mass spectrometer equipped with electronic impact (EI) source. The separation of analytes was achieved using a BP5MS (30 m × 0.25 mm × 0.25 µm, SGE Analytical Science, Milan, Italy) capillary column and helium as carrier gas. Injector and detector temperatures were kept at 280°C. The oven temperature was programmed from 60°C to 280°C at a 15°C/min thermal gradient, as follows: from 60°C for 0.2 min after injection, to 80°C at 15°C/min, hold for 0.2 min, to 280°C at 15°C/min and hold for 15 min, with a total run time of 30 min. Acquisition was performed in the full scan mode with a 40–500 m/z range. The GC-MS raw data files were collected with Xcalibur 2.2 SP1 w Foundation 2.0 SP1. Compound identification was based on comparison of retention times and mass spectra with those of pure standards or spectral information provided by NIST 14 GC-MS library (Supplementary Dataset S6). In addition, the derivatization mode applied lead to the detection of different isomers for some metabolites, especially in case of sugars, so both the obtained signals were reported and identified as different position isomers, when possible (Supplementary Dataset S6).

The quantification of each identified gas-chromatographic signal was performed by manually integrating its peak area and calculating with respect to the peak area of the selected internal standard (C24 for organic acids and polyalcohols, nor-leucine for amino acids, and phenyl-beta-D-glucoside for sugars). Finally, values were reported as relative percentage on total metabolites.

2.5.3 Lipidomics: UHPLC–TWIMS–QTOF analysis and data processing

The untargeted lipidomics workflow was performed as described previously (Pedrazzani et al., 2021) (SI Appendix, Methods). An ACQUITY I-Class UPLC separation system coupled to a Vion IMS QTOF mass spectrometer (Waters, Wilmslow, UK) equipped with an electrospray ionization (ESI) interface was employed for soil lipidomics. Samples were injected (2 µL) and chromatographically separated using a reversed-phase C18 BEH ACQUITY column (2.1 × 100 mm, 1.7 µm particle size) (Waters, Milford, MA, USA). Gradient elution was performed as previously reported (Pedrazzani et al., 2021) by using 5 mM ammonium formate in Milli-Q water/methanol (95:5, v/v) (solvent A) and 5 mM ammonium formate in isopropanol/methanol/Milli-Q water (65:30:5, v/v) (solvent B) both acidified with 0.1% formic acid. The following multistep elution gradient was used: 0.0 min (10% solvent B; 0.40 mL/min) to 1.0 min (50% solvent B; 0.40 mL/min), subsequently 1–5 min (80% solvent B; 0.40 mL/min), and 11.0 min (100% solvent B; 0.50 mL/min). After a 4.5 min isocratic step, the system was re-equilibrated to initial conditions for 2.5 min (10% solvent B; 0.4 mL/min). Samples were permanently kept at 10°C. Mass spectrometry data were collected in positive and negative electrospray mode over the mass range of m/z 100–1200. Source settings were maintained using a capillary voltage of 2.5 kV, a source temperature of 120°C, a desolvation temperature of 500°C, and a desolvation gas flow of 1000 L/h. A TOF analyzer was operated in sensitivity mode, and data were acquired using HDMSE, which is a data-independent approach (DIA) coupled with ion mobility. The optimized ion mobility settings included a nitrogen flow rate of 90 mL/min (3.2 mbar), a wave velocity of 650 m/s, and a wave height of 40 V. The device within the Vion was calibrated using a Major Mix IMS calibration kit (Waters, Wilmslow, UK) to allow for CCS values to be determined in nitrogen. The calibration covered the CCS range from 130 to 306 Å2. The TOF was also calibrated prior to data acquisition and covered the mass range from m/z 151 to 1013. TOF and CCS calibrations were performed for both positive- and negative-ion mode. Data acquisition was conducted using UNIFI 1.8 (Waters, Wilmslow, UK).

Data processing and compound identification were conducted using Progenesis QI Informatics (Nonlinear Dynamics, Newcastle, UK). Each UHPLC-MS run was imported as an ion-intensity map, including m/z (m/z range 100–1200) and retention time, that were then aligned in the retention-time direction (0–15 min). Isotope and adduct deconvolution were applied, to reduce the number of features detected. Features identification was performed against publicly available database including LIPID MAPS, Human Metabolome database (HMDB), and METLIN, as well as by fragmentation patterns, retention times, and CCS. CCS values

were searched against "MetCCS Predictor" database containing m/z and CCS values by selecting a ΔCCS of 5% for metabolite matching (Zhou et al., 2016). Based on the Metabolomics Standards Initiative (Summer et al., 2007), metabolites were annotated as level III (putatively characterized), level II (putatively identified compounds), and level I (identified compound). A mix of monoacylglycerol, diacylglycerols and triacylglycerols was run at the beginning, in the middle and at the end of the sample list to monitor system retention time, CCS and mass error stability.

2.5.4 Metabolomics and lipidomics multivariate modeling

Both metabolomics and lipidomics data matrices were independently subjected to unsupervised principal components analysis (PCA) with pareto scaling was performed to check the quality of the raw data. Afterwards, supervised models, including partial least-squares discriminant analysis (PLS-DA) were built and validated using SIMCA software (v. 16.0.2, Sartorius Stedim Data Analytics, Sweden). The variable influence in projection analysis (VIP) was further used to identify the compounds that had the highest discrimination potential (VIP value threshold > 1.2). Moreover, agglomerative hierarchical clustering analysis was applied to metabolite concentration data and soil samples. Similarity was determined by Euclidean distance for analysis of the differences in metabolite concentrations, and clustering was performed using Ward's linkage. The dendrograms were combined with a heatmap, generated based on z-scores of metabolite concentrations using the MetaboAnalyst platform (Chong and Xia, 2020).

The redundancy analysis (RDA) was employed to identify the relationship between bacterial and fungal community composition and metabolites and lipid accumulation in the perennial wheat rhizosphere. Data correlation between the composition of microbial communities, metabolites and lipids in the rhizosphere was evaluated by Spearman correlation coefficient ($p < 0.005$) (see Supplementary Dataset S10).

3 Results

3.1 DNA-based bacterial and fungal community composition and diversity

Multivariate analyses on the total OTU matrices showed significant effects of plant genotypes and perenniality in shaping both bacterial and fungal communities. Indeed, dbRDA analysis reported a significant interaction "genotype" × "year" for bacteria ($P = 0.019$) and fungi ($P = 0.02$), with single factors "genotype" and "year" ($P< 0.001$) for both bacteria and fungi. The dbRDA model explains a percentage of the total variance of 47.7% (bacteria) (Figure 1A), and 49% (fungi) (Figure 1B). ADONIS showed that the rhizosphere and the bare soil microbial communities were significantly separated from each other (Figures 1A, B), indicating a significant impact of plants roots on selecting and shaping the rhizosphere microbial community. Moreover, for both bacteria and fungi, samples belonging to year 1 and year 4 were significantly different (p<0,005), together with the annual durum wheat and the parental species *Thinopyrum intermedium* respectively, suggesting a selection of the microbial community over the years. However, differences of microbial communities' composition among wheat genotypes were not significant.

Additionally, plant genotype had no significant effect on bacterial (Figures 2A, B) and fungal diversity (Figures 2C, D), while perenniality significantly increased the fungal evenness from the first to the fourth year of plant growth. Perenniality also increased the bacterial evenness even if not significantly. Phylogenetic analysis revealed a microbial composition and complexity with 20 phyla for bacteria (Figure S1A) and 6 phyla for fungi (Figure S1B). Among those, the most represented bacterial phyla were Proteobacteria (38%), followed by Bacteroidetes (12%), Actinobacteria (7%) and Verrucomicrobia (6%), while Ascomycota (33%), Basidiomycota (8%) and Zygomycota (6%) were the most abundant fungal phyla. A total of 458 bacterial genera and 331 fungal genera were also identified (see Supplementary Datasets S1,

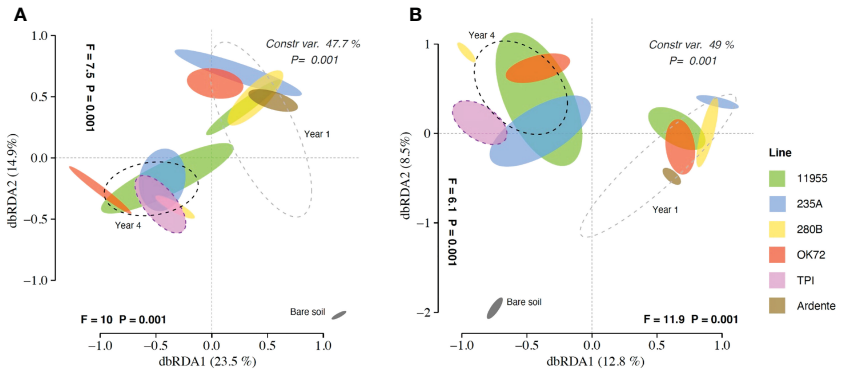

FIGURE 1
Distance-based redundancy analysis (dbRDA) plots showing shifts in bacterial **(A)** and fungal **(B)** community composition colonizing the rhizosphere of *Triticum durum* cv. Ardente, *Thinopyrum intermedium* (TPI) and four perennial wheat genotypes 235A, 280B, 11955, OK72 at the first and fourth year of growth.

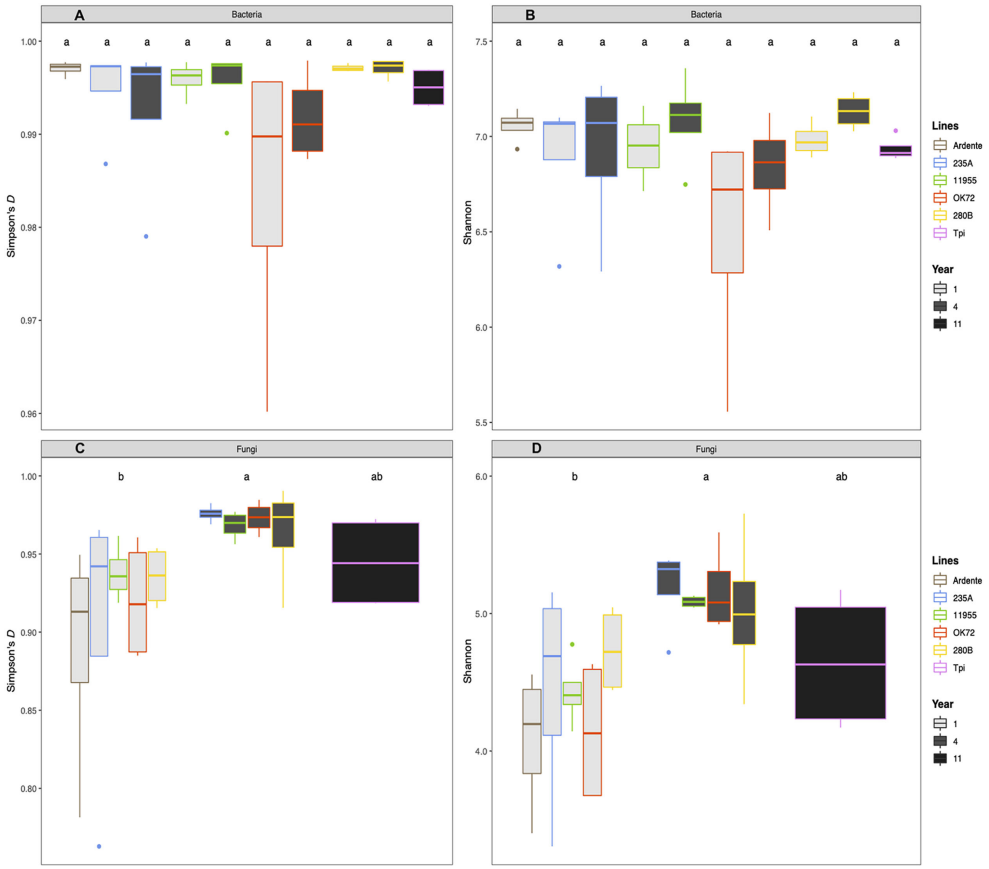

FIGURE 2
Mean values of Simpson's *(D)* and index Shannon Wiever for bacteria **(A, B)** and fungi **(C, D)** as affected by time of plant residence on soil (1,4 and 11 years) as well as plant species/genotypes (*Triticum durum* cv. Ardente, *Thinopyrum intermedium* (Tpi) and four perennial wheat genotypes 235A, 280B, 11955, OK72). Different letters denote statistically different (Tukey's test, P = 0.05) D-values among treatment.

S2). About 25 bacterial genera had relative abundance >0.3% while only 10 fungal genera had relative abundance >0.03%. across all samples. Of these bacteria, the genera *Niabella*, *Flavisolibacter*, *Kaistobacter* and *Opitutus*, were more abundant in association with the roots of durum wheat and NPGs at the first year of growth. On the other hand, the rhizospheres of *Thinopyrum intermedium* and NPGs at the fourth year of growth were richer in the genera *Gemmata*, *Haliangium* and *Steroidobacter*. It is noteworthy that *Pseudomonas* genus (Phylum Proteobacteria) was highly abundant (more than 15% of the relative abundance) in association with the OK72 genotype both at the 1st and 4th year, (SI Supplementary Mat Dataset S1). At the 4th year of cultivation, a greater abundance of fungi was detected, including the genera *Aspergillus*, *Chrysosporium* and *Fusarium*, among which plant pathogenic species occur (SI Supplementary Mat Dataset S2). Despite this, the higher fungal evenness at the 4th year might contain the overgrowth of these fungi, as indicated by their low relative abundance (<1.5%). Moreover, the bacterial genus *Bacillus* and the fungal genus *Mortierella* to which belong beneficial species, were widely present across all samples.

3.2 Enzymatic activities and microbial biomass

The dbRDA patterns of hydrolytic enzyme activity differed significantly among the treatment groups (P = 0.001) accounting for 61.1% of the total variance (Figure 3A). The factors "genotypes" and "years" caused separation along axes 1 (F = 1.3 and P = 0.991) accounting for 2.8% of the total variance and along axes 2 (F = 42.8 and P = 0.001) accounting for 86.6% of the total variance. ADONIS and dbRDA showed how enzyme profiles of *Thinopyrum intermedium*' and durum wheat's rhizospheres were clearly differentiated from each other as well as the enzyme profiles of OK72 and 235A genotypes at the 1st and 4th year of cultivation. On the contrary, the genotypes 11955 and 280B at the 1st and 4th year of cultivation were closer to each other. Species score plot (Figure 3B) showed that the higher activity (see Supplementary Mat Dataset S5) of alkaline (alkP) phosphomonoesterase, pyrophosphate-phosphodiesterase (piroP) and butyric esterase (butir) at the 4th year of NPGs cultivation and associated with *Thinopyrum intermedium* compared to NPGs at the 1st year and durum wheat, caused the

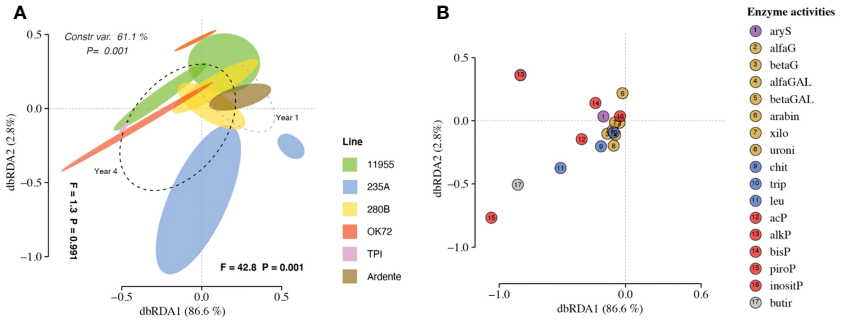

FIGURE 3
(A) Distance-based redundancy analysis (dbRDA) plot showing shifts in enzyme activities in the rhizosphere of *Triticum durum* cv. Ardente, *Thinopyrum intermedium* (TPI) and four perennial wheat genotypes 235A, 280B, 11955, OK72 at the first and fourth year of growth. Species scores corresponding to the dbRDA plots (coordinates for enzymes included in model) are reported in the scatter plots on the right **(B)**.

horizontal differentiation in the dbRDA plot. This indicate that over the years production of P-acquiring enzymes (alkP and piroP) and enzymes involved in organic matter degradation (butir) increase under perennial wheats growth.

Univariate analysis on microbial biomass revealed that *Thinopyrum intermedium* had the highest microbial biomass, while at the 4th year of cultivation it was similar among the NPGs (Figure 4). On the contrary, at the 1st year of NPGs cultivation, the microbial biomass associated with genotype 280B was significantly higher than that associated to 235A, and not for the other genotypes. No statistical differences can be claimed between Ardente and NPGs, but only for the comparison Ardente/Thinopyrum.

3.3 Metabolomics

Following the GC-MS untargeted analysis of soil samples, 33 metabolites were annotated, as summarized in (Supplementary Dataset 6). Mono- and disaccharides (glucose, fructose, sucrose, trehalose) and sugar alcohol (mannitol/ribitol) were the most abundant biochemical classes detected. Polyalcohol, organic acids and nucleobases were also annotated but their intensities were lower compared to the other classes. These primary metabolites can accumulate in soils from leaves litter, root exudates, but are also produced by different microorganisms (Withers et al., 2020).

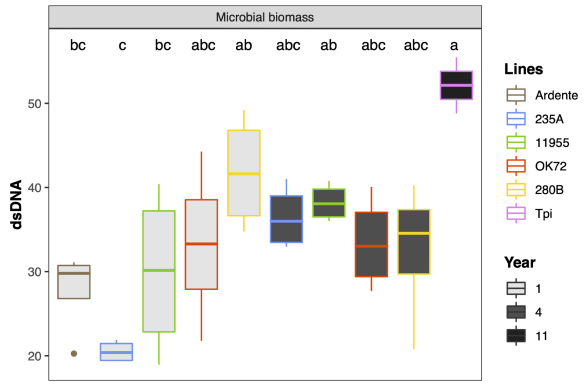

FIGURE 4
Mean values of microbial biomass as affected by time of plant residence on soil (1,4 and 11 years) and plant species/genotypes (*Triticum durum* cv. Ardente, *Thinopyrum intermedium* (Tpi) and four perennial wheat genotypes 235A, 280B, 11955, OK72). Different letters denote statistically different (Tukey's test, P =0.05) D-values among treatment.

At first, the PCA was employed to explore the data. The first 3 PCs describes 58% of the total variance. As show in Figure S2A, a trend to separate samples according to the year of plant residence on soil is reported for the first PC. No clustering according to the genotypes was observed (Figure S2B).

Afterwards, supervised PLS-DA (Figure S3) was performed and displayed a clear differentiation between two main groups, i) samples belonging to NPGs' rhizosphere collected at the 4th year of growth with *Thinopyrum intermedium* (11 years), and ii) samples belonging to NPGs' rhizosphere collected at the 1st year of growth with *Triticum durum* cv. Ardente. The spread of the samples in the score plot as well as the low prediction ability of the PLS-DA model (Q^2 0.179) is ascribable to the biological variability of the soil samples. Among the most significant metabolites responsible for this group separation, sugar alcohol, mono and disaccharides such as mannitol, glucose and maltose were accumulated in NPGs' rhizosphere collected at the 4th year and in *Thinopyrum intermedium* (11 years) (see heatmap in Figures 5A, S4). The opposite trend was observed for benzoic acid and glycerol, among other, whose intensities were significantly higher in soils collected at the 1st year and decreased over time (4 and 11 years). Therefore, our results confirmed the importance of plant permanence on soil in shaping plant-soil polar metabolites.

3.4 Lipidomics

A total of 163 lipids grouped within 15 biochemical classes and 33 sub-classes were annotated (see Supplementary Dataset S7) among the statistically significant (FDR ANOVA p-value < 0.01) features. Triacylglycerol (TG) were the most abundant species followed by diacylglycerols (DG), fatty acids (FA), ceramides, sterols and prenol lipids. The mixing of various lipid sources in soil, as for sugars, makes difficult to determine if their origin is from

plant or microorganism. Indeed, apart from glycolipid and sterols, the other lipid classes are common to most of the living organisms.

The sample clustering observed for lipids data (Figure S5) was in line with those observed for primary metabolites (Figure S3). TG and DG were accumulated in the rhizosphere collected at the 4th year of growth and from *Thinopyrum intermedium*, compared to soils collected after 1 year of growth and *Triticum durum* cv (see heat map in Figure 5B). Same tendency was reported for glycerophospholipids, including glycerophosphocholine (PCs), glycerophosphoserine (PSs) and glycerophosphoethanolamines (PEs). On the other hands, opposite trend was observed for sphingoid bases, prenol lipids and fatty acids. Our results revealed that both storage (i.e., TG) and signalling (i.e., sphingolipids, fatty acids) lipids play a role in modulating the plant-microbial interaction, being statistically significant differentially accumulated in the rhizosphere collected at different years of plant permanence on soil.

4 Discussions

A combination of -Omics techniques was applied to examine the rhizosphere environment of four new perennial wheat genotypes at the 1st and 4th year of cultivation in comparison to an annual durum wheat cultivar and the parental specie *Thinopyrum intermedium*. Our results showed that permanent soil cover and no-tillage, which characterize a perennial cropping system, have a predominant role in shaping perennial wheats rhizobiome and the rhizosphere environment. This is also confirmed by other studies where soil properties were the main factors structuring the rhizobiome (Schlatter et al., 2020; Simonin et al., 2020; Audu et al., 2022b), followed by crop management (Hargreaves and Hofmockel, 2014; Sprunger et al., 2019; Audu et al., 2022a), and crop genotypes (Brisson et al., 2019; Simonin et al., 2020; Ndour et al., 2021; Semchenko et al., 2021). In our study multivariate analysis on total bacterial and fungal OTUs, revealed a common rhizosphere microbial community composition between new perennial wheat genotypes at the 1st year from sowing and the annual durum wheat. After four years of plant development, the composition of the rhizobiome mutated, resulting more similar to that one of the parental specie *Thinopyrum intermedium*, suggesting that the continuous development of perennial root system along the years affected the microbial community. Moreover, NPGs rhizobiome didn't mutate after several years of plant establishment as shown by the similarity with *Thinopyrum intermedium* rhizosphere community, probably because with minor environmental disturbances the rhizosphere ecosystem saturates, becoming redundant (Yachi and Loreau, 1999). Despite the dominance of the perenniality effect, some differences in bacterial taxa were also observed by analyzing the 16S rDNA profiling between lines. In particular, *Pseudomonas* genus (phylum Proteobacteria) relative abundance was significantly higher in OK72 comparing to the other lines, regardless of the cultivation year (Figures 6, S1A). *Pseudomonas* strains are known to be able to control plant pathogens (Sah et al., 2021) and to respond well to the presence of root exudates by upregulating genes involved in the catabolism of myo-inositol (Mavrodi et al., 2021) which had been reported as an essential trait for the colonization of *Arabidopsis*

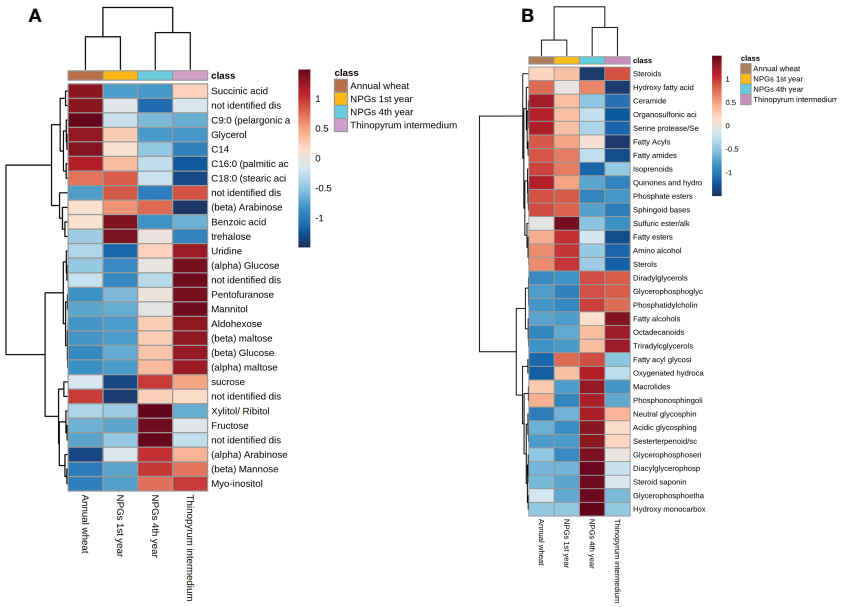

FIGURE 5
Hierarchical clustering analysis and heat map visualization obtained using annotated **(A)** metabolites and **(B)** lipids grouped in biochemical classes (distance: Euclidean; clustering algorithm: Ward).

thaliana roots (Cole et al., 2017). These enzymes release phosphorus (P) from myo-inositol P making it available for uptake by plants. *Pseudomonas* is also able to solubilize phosphorous from inorganic source, which is confirmed in our study by the positive correlation ($p<0.0001$) with myo-inositol and phosphorous acquiring enzymes (alkP, piroP and inositP) (See Figure 6, where is referenced the phylum, and Supplementary Dataset S10).

The presence of potential plant beneficial microbes involved in plant defense (Qiu et al., 2012; Liu et al., 2018; Lin et al., 2021) both at the 1st and 4th year of growth such as, *Flavisolibacter*, *Kaistobacter*, *Haliangium, Bacillus and Pseudomonas*, might be of particular interest since these perennial wheat derivatives never showed powdery mildew and rusts (*Puccinia* spp.) disease symptoms during our experiment as well as in other field experiments (Pogna et al., 2014). This is noteworthy since perennial grains are generally considered susceptible to diseases (Cox et al., 2005). Indeed, typical cultural practices effective at reducing soil- and residue-borne pathogens, such as annual crop rotations, delayed fall planting, and tillage, are not feasible in perennial systems. Moreover, the higher fungal evenness detected on NPGs after four years might be also involved in the phenomenon of the general soil-borne disease suppressiveness, controlling the spread of pathogenic (Mazzola, 2002). Indeed, when many different species are present, they can fulfil a variety of different ecological niches within a given ecosystem, thus competing with potential plant pathogen. This result is confirmed also by the lipid analysis. Indeed, phytosphingosines are significantly accumulated in the rhizosphere after one and four years most likely as root exudates. These compounds have been recently demonstrated to be produced by plants following plant-pathogen interaction as a resistance strategy (Glenz et al., 2022).

However, the prolonged absence of significant soil disturbances, as in the case of *Thinopyrum intermedium* which is resident in the same soil for 11 years, led to fungal evenness reduction, which could jeopardize the resistance to biotic stresses. Indeed, according to the insurance hypothesis, biodiversity insures ecosystems against declines in their functioning because many species provide greater guarantees that some will maintain functioning even if others fail (Yachi and Loreau, 1999). Moreover, *Thinopyrum intermedium* reported the highest microbial biomass due to the reduced environmental disturbance and the constant supply of carbon from above- and belowground plant biomass as well as root exudates (Allison et al., 2005; Culman et al., 2010; Liang et al., 2012; Xia et al., 2019). Further, significant differences among plant genotypes (280B and 235A) at the first year of growth were detected for microbial biomass. Based on a previous study, these differences might be caused by a dissimilar development strategy of the roots' apparatus of the lines which showed variability in agronomic and eco-physiological performance in two subsequent years of cultivation (Baronti et al., 2022). However, the progressive reduction of differences in microbial biomass between genotypes after four years, might be the consequence of the vertical root development and the continuous deposition of aboveground plant litter on soil. Moreover, plant litter accumulation, root turnover and the continuous production of root exudates for many years had boosted the activity of all the enzymes considered in this study and significantly the enzymes involved in organic matter decomposition (butir) (Hargreaves and Hofmockel, 2014) and of phosphorous acquiring enzymes (alkP and piroP) (See Figure 6). Butyrate esterase is generally related to microbial biomass content (Kähkönen et al., 1999; Trivedi et al., 2016), while changes in microbial community structure and diversity over the years are not reflected, with the same extent, to an improvement of the

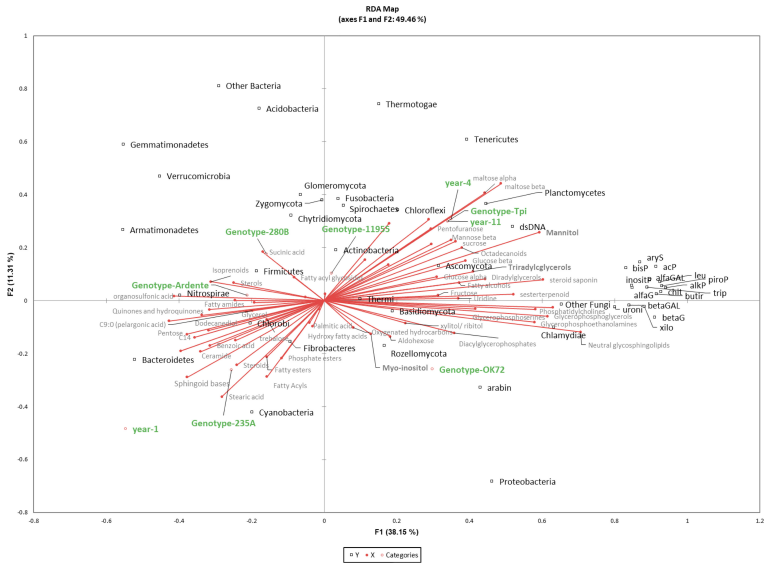

FIGURE 6
Redundancy analysis (RDA) of 16S rDNA, enzyme activity, metabolites and lipids in different species/genotypes (annual wheat-Ardente, NPGS- 280B, -235A, -11955, -OK72 and *T. intermedium*) and year of soil permanence (1_{st}, 4_{th}, 11_{th}). The model accounted for 46% of the total inertia, with a global p-value < 0.0001. Squares (black) represent bacteria and fungi with their taxonomic affiliation; circles represent year and genotypes (green); metabolites and lipids are in grey palette.

functional diversity. This indicate that decomposition of organic matter is not related to the microbial diversity since most microorganisms can carry out this function (Nannipieri et al., 2003). Moreover, the increase of rhizodeposit quantity, but with small changes in their composition is not sufficient to change soil functionality, because there is no need to change enzyme pattern when the substrate is very similar.

Furthermore, perennial wheats root development along the years modifies the chemical properties of the rhizosphere environment. In our study, the abundance of rhizosphere metabolites is consistent with other research (Liu et al., 2020; Iannucci et al., 2021), where the most abundant are usually sugars, followed by polyalcohols, organic acids, and amino acids. They are involved in a variety of functions including the modulation of nutrient availabilities, mainly by means of soil acidification (Carvalhais et al., 2011), and in plant–microbe interactions (Bais et al., 2006; Liu et al., 2020; Bi et al., 2021). Indeed, sugars, independent of origins (roots, bacteria, fungi) improve soil structure by affecting aggregates formation and water retention, contributing to C stabilization and creating a favorable environment for both root development and microbial growth (Gunina and Kuzyakov, 2015). However, sugars are the energy source for all the living organisms, making challenging the identification of their origin in soil. Indeed, it is estimated that only 20% of the carbohydrates in soils are exudated from plant, while the remaining 80% originates from the secondary source, which are microorganisms and their residue (Gunina and Kuzyakov, 2015). The higher content of hexose, including glucose, in the rhizosphere collected at the 11th year may be the result of the repetitive and thus, cumulative accumulation both as root exudate (originated from cellulose decomposition) and microorganism synthesis. Indeed, its trend 11th year > 4th year >1st year is consistent with the continuous development of perennial root system along the years, which, in turn, affects the microbial biomass as highlighted by the RDA analysis in Figure 6. Moreover, we observed a positive correlation ($p<0.01$) between glucose and betaG enzyme activity which is further correlated with Proteobacteria and Actinobacteria ($p<0.01$) (see Supplementary Dataset S10). These are the main bacterial phyla, while Ascomycota is the only dominant fungal phylum that exhibit high betaG enzyme activity, as recently reported (Zeng et al., 2022).

Together with glucose, maltose, and mannitol, significantly accumulated in the rhizosphere along the years (see Figures 6, S4). These metabolites are commonly associated with osmotic regulation (Brown et al., 2021), suggesting that along the years both plants and microorganisms are led to maintain a favorable environment for their growth. Interestingly, mannitol is synthesized in numerous plant species, but not in common wheat (*Triticum aestivum*) (Abebe et al., 2003). Therefore, its accumulation has to be mediated by fungal and bacteria metabolism (Patel and Williamson, 2016). We observed the same trend for TGs, that can be accumulated in soil mainly as root exudates. They are a major energy deposit for most of eukaryotic organisms, including fungi, yeast, plants and animals but occurrence in bacteria is limited to the actinomycetes taxa (Alvarez and Steinbchel, 2002). Their accumulation in the rhizosphere collected at the 4th and 11th year may result from i) a higher excretion from the continuous development of perennial root system, as well as ii) from a lower degradation rate occurring in the soil but also iii) due to the higher presence of actinomycetes in the rhizosphere (positive correlation $p < 0.001$). Indeed, TGs in soil undergo β-oxidation with the formation of FAs (Hita et al., 1996), which in our study were found to be accumulated in the annual wheat and NPGs after one years. Fatty acids are essential molecules that play crucial roles in plant-plant, plant-microbe and plant-environment interactions (Macabuhay et al., 2022). Furthermore, some studies have revealed that fatty acids and their derivatives directly inhibit the growth of plant pathogens within the rhizosphere, and improve the surrounding environment of plant rhizosphere to reduce the occurrence of crop diseases and promote crop growth (Upchurch, 2008; Raffaele et al., 2009). In our study, wheat perenniality has led to an increase in abundance of complex lipids, glycerolipids and the glycerophospholipids. These are involved in many regulatory processes such as cell signaling and intracellular trafficking (Macabuhay et al., 2022). In addition, the higher amount of glycerophospholipids and glycerolipids in the microbial plasma membrane can be an adaptive trait for the well-established and selected microbial community of NPGs rhizosphere after 4 years. In particular, phosphatidil ethanolammine showed to be significantly more abundant in the 4th year NPGs respect to the annual wheat line. Moreover, the increase in glycerophospholipids reduces microbes membrane permeability and increases resistance against antimicrobial compounds allowing the establishment of coexistence between different microbial species rather than their eradication (Molina-Santiago et al., 2021). Furthermore, they are released as exudates of plant roots and their role in directly influencing growth of plant interacting microorganisms has been only recently investigated (Glenz et al., 2022; Zeng and Yao, 2022). In addition, the increased level of hydrophobic components of organic matter can enhance soil aggregate stability and C stabilization (Goh, 2004). However, the study of the soil lipidome is a new frontier of research and very few studies were conducted so far (Tinoco et al., 2018; Wilson et al., 2021). Even though the role of lipid in rhizodeposition and plant-microbe signaling (Bi et al., 2021) as well as microbes-to-plant signaling (Macabuhay et al., 2022) is undoubtedly relevant, the interpretation of these data remain challenging due to the lack of knowledge.

In conclusion, in this study, we demonstrate that the long permanence of perennial wheat lines on soil (see Figure 7) remarkably modifies the quality and quantity of root exudates, shaping the rhizosphere microbial community composition and favoring the growth of microorganisms as indicated by their higher biomass and activity. Moreover, these modifications point to the existence of a less stressful environment which favor the plant-microbiome crosstalk, thus improving plant resilience to biotic and abiotic stresses. Despite the dominance of the perenniality effect, OK72 distinguished from the other lines not only for its better agronomic features and nutritional quality, as previously shown

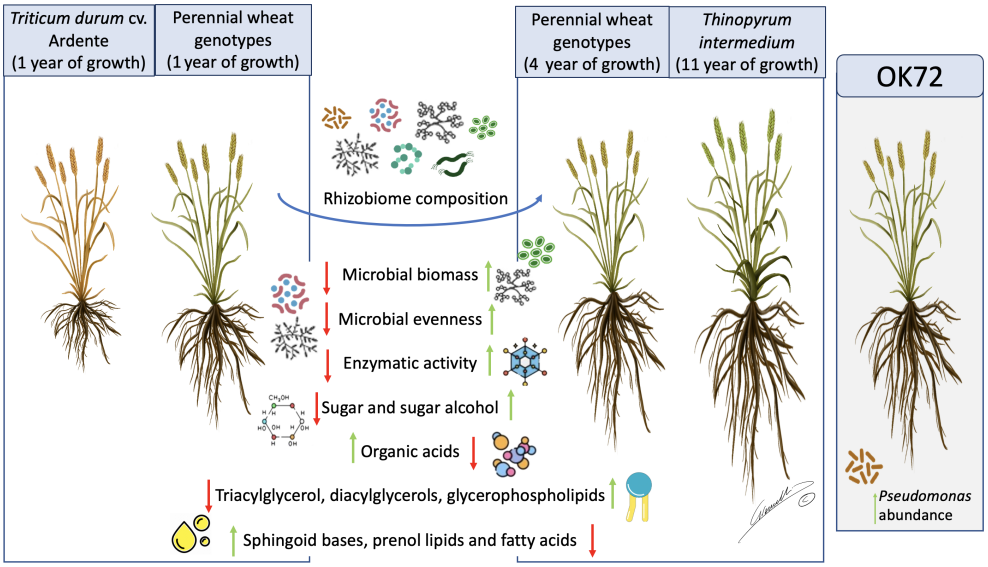

FIGURE 7
Schematic representation of the results obtained in this work. Green arrows represent increasing in abundance while red arrows represent decreasing in abundance in the different samples analyzed. OK72 line was highlighted as promising genotype for selection of new perennial wheat lines. Image by Gianluigi Giannelli (University of Parma).

(Gazza et al., 2016; Baronti et al., 2022) but also for the increase of potential beneficial microorganisms such as *Pseudomonas* spp., thus resulting a suitable candidate for the study and selection of new perennial wheat lines (Figure 7).

Data availability statement

The data of 16S rDNA and ITS sequences presented in the study are deposited in the NCBI database at the following link https://www.ncbi.nlm.nih.gov/sra/PRJNA826315.

Author contributions

GV, MB, and LR planned and designed the research, MB performed the experiments, FF performed soil enzymatic activities, LG conducted fieldwork, MB, GV, AF, LR, MC, VL analysed data. GV, LR supervise the work. GG funded the research, MB, GV, LR wrote the manuscript, all the authors revise the manuscript. All authors contributed to the article and approved the submitted version.

Funding

This study is part of the project CHANGE-UP - Innovative agroecological APProaches to achieving resilience to climate CHANGE in Mediterranean countries, funded by MUR (DD n. 16787, 19/11/2021) within the PRIMA EU Section 2 – Multi-topic 2020 (Partnership for Research and Innovation in the Mediterranean Area) CALL 2020.

Acknowledgments

The authors acknowledged Dr. Pierino Cacciatori from CREA, Research Centre for Engineering and Agro-Food Processing, Rome for field management and Dr. Enrico Martani from Davines Group-Rodale Institute European Regenerative Organic Center (EROC) for in field roots and rhizosphere sampling.

Conflict of interest

The authors declare that the research was conducted in the absence of any commercial or financial relationships that could be construed as a potential conflict of interest.

Publisher's note

Supplementary material

The Supplementary Material for this article can be found online at: https://www.frontiersin.org/articles/10.3389/fpls.2023.1172857/full#supplementary-material

References

Abebe, T., Guenzi, A. C., Martin, B., and Cushman, J. C. (2003). Tolerance of mannitol-accumulating transgenic wheat to water stress and salinity. *Plant Physiol.* 131, 1748–1755. doi: 10.1104/pp.102.003616

Allison, V. J., Miller, R. M., Jastrow, J. D., Matamala, R., and Zak, D. R. (2005). Changes in soil microbial community structure in a tallgrass prairie chronosequence. *Soil Sci. Soc Am. J.* 69, 1412–1421. doi: 10.2136/sssaj2004.0252

Alvarez, H. M., and Steinbchel, A. (2002). Triacylglycerols in prokaryotic microorganisms. *Appl. Microbiol. Biotechnol.* 60, 367–376. doi: 10.1007/s00253-002-1135-0

Audu, V., Rasche, F., Dimitrova Mårtensson, L.-M., and Emmerling, C. (2022a). Perennial cereal grain cultivation: implication on soil organic matter and related soil microbial parameters. *Appl. Soil Ecol.* 174, 104414. doi: 10.1016/j.apsoil.2022.104414

Audu, V., Ruf, T., Vogt-Kaute, W., and Emmerling, C. (2022b). Changes in microbial biomass and activity support ecological intensification of marginal land through cultivation of perennial wheat in organic agriculture. *Biol. Agric. Hortic.* 38 (3):202–215. doi: 10.1080/01448765.2022.2040589

Bais, H. P., Weir, T. L., Perry, L. G., Gilroy, S., and Vivanco, J. M. (2006). The role of root exudates in rhizosphere interactions with plants and other organisms. *Annu. Rev. Plant Biol.* 57, 233–266. doi: 10.1146/annurev.arplant.57.032905.105159

Baldrian, P. (2014). Distribution of extracellular enzymes in soils: spatial heterogeneity and determining factors at various scales. *Soil Sci. Soc Am. J.* 78, 11–18. doi: 10.2136/sssaj2013.04.0155dgs

Baronti, S., Galassi, E., Ugolini, F., Miglietta, F., Genesio, L., Vaccari, F. P., et al. (2022). Agronomic and ecophysiological evaluation of an early establishment of perennial wheat lines in central Italy. *Genet. Resour. Crop Evol.* 69, 619–633. doi: 10.1007/s10722-021-01248-8

Bertola, M., Ferrarini, A., and Visioli, G. (2021). Improvement of soil microbial diversity through sustainable agricultural practices and its evaluation by -omics approaches: a perspective for the environment, food quality and human safety. *Microorganisms* 9, 1400. doi: 10.3390/microorganisms9071400

Bi, B., Wang, K., Zhang, H., Wang, Y., Fei, H., Pan, R., et al. (2021). Plants use rhizosphere metabolites to regulate soil microbial diversity. *Land Degrad. Dev.* 32, 5267–5280. doi: 10.1002/ldr.4107

Bragato, G., Fornasier, F., and Brus, D. J. (2016). Characterization of soil fertility and soil biodiversity with dsDNA as a covariate in a regression estimator for mean microbial biomass C: Soil dsDNA as a covariate for microbial biomass C. *Eur. J. Soil Sci.* 67, 827–834. doi: 10.1111/ejss.12387

Brisson, V. L., Schmidt, J. E., Northen, T. R., Vogel, J. P., and Gaudin, A. C. M. (2019). Impacts of maize domestication and breeding on rhizosphere microbial community recruitment from a nutrient depleted agricultural soil. *Sci. Rep.* 9, 15611. doi: 10.1038/s41598-019-52148-y

Brown, R. W., Chadwick, D. R., Zang, H., and Jones, D. L. (2021). Use of metabolomics to quantify changes in soil microbial function in response to fertiliser nitrogen supply and extreme drought. *Soil Biol. Biochem.* 160, 108351. doi: 10.1016/j.soilbio.2021.108351

Canarini, A., Kaiser, C., Merchant, A., Richter, A., and Wanek, W. (2019). Root exudation of primary metabolites: mechanisms and their roles in plant responses to environmental stimuli. *Front. Plant Sci.* 10. doi: 10.3389/fpls.2019.00157

Carvalhais, L. C., Dennis, P. G., Fedoseyenko, D., Hajirezaei, M., Borriss, R., and von Wirén, N. (2011). Root exudation of sugars, amino acids, and organic acids by maize as affected by nitrogen, phosphorus, potassium, and iron deficiency. *J. Plant Nutr. Soil Sci.* 174, 3–11. doi: 10.1002/jpln.201000085

Ceja-Navarro, J. A., Rivera-Orduña, F. N., Patiño-Zúñiga, L., Vila-Sanjurjo, A., Crossa, J., Govaerts, B., et al. (2010). Phylogenetic and multivariate analyses to determine the effects of different tillage and residue management practices on soil bacterial communities. *Appl. Environ. Microbiol.* 76, 3685–3691. doi: 10.1128/AEM.02726-09

Chong, J., and Xia, J. (2020). "Using MetaboAnalyst 4.0 for metabolomics data analysis, interpretation, and integration with other omics data," in *Computational methods and data analysis for metabolomics*. Ed. S. Li (New York, NY: Springer US), 337–360. doi: 10.1007/978-1-0716-0239-3_17

Cole, B. J., Feltcher, M. E., Waters, R. J., Wetmore, K. M., Mucyn, T. S., Ryan, E. M., et al. (2017). Genome-wide identification of bacterial plant colonization genes. *PloS Biol.* 15, e2002860. doi: 10.1371/journal.pbio.2002860

Cowie, A. L., Lonergan, V. E., Rabbi, S. M. F., Fornasier, F., Macdonald, C., Harden, S., et al. (2013). Impact of carbon farming practices on soil carbon in northern new south Wales. *Soil Res.* 51, 707. doi: 10.1071/SR13043

Cox, C. M., Garrett, K. A., and Bockus, W. W. (2005). Meeting the challenge of disease management in perennial grain cropping systems. *Renew. Agric. Food Syst.* 20, 15–24. doi: 10.1079/RAF200495

Culman, S. W., DuPont, S. T., Glover, J. D., Buckley, D. H., Fick, G. W., Ferris, H., et al. (2010). Long-term impacts of high-input annual cropping and unfertilized perennial grass production on soil properties and belowground food webs in Kansas, USA. *Agric. Ecosyst. Environ.* 137, 13–24. doi: 10.1016/j.agee.2009.11.008

DeHaan, L. R., Van Tassel, D. L., and Cox, T. S. (2005). Perennial grain crops: a synthesis of ecology and plant breeding. *Renew. Agric. Food Syst.* 20, 5–14. doi: 10.1079/RAF200496

Ferrarini, A., Fracasso, A., Spini, G., Fornasier, F., Taskin, E., Fontanella, M. C., et al. (2021). Bioaugmented phytoremediation of metal-contaminated soils and sediments by hemp and giant reed. *Front. Microbiol.* 12. doi: 10.3389/fmicb.2021.645893

Finney, D. M., Buyer, J. S., and Kaye, J. P. (2017). Living cover crops have immediate impacts on soil microbial community structure and function. *J. Soil Water Conserv.* 72, 361–373. doi: 10.2489/jswc.72.4.361

Fornasier, F., Ascher, J., Ceccherini, M. T., Tomat, E., and Pietramellara, G. (2014). A simplified rapid, low-cost and versatile DNA-based assessment of soil microbial biomass. *Ecol. Indic.* 45, 75–82. doi: 10.1016/j.ecolind.2014.03.028

Gazza, L., Galassi, E., Ciccoritti, R., Cacciatori, P., and Pogna, N. E. (2016). Qualitative traits of perennial wheat lines derived from different thinopyrum species. *Genet. Resour. Crop Evol.* 63, 209–219. doi: 10.1007/s10722-015-0240-8

Ghaley, B., Rusu, T., Sandén, T., Spiegel, H., Menta, C., Visioli, G., et al. (2018). Assessment of benefits of conservation agriculture on soil functions in arable production systems in Europe. *Sustainability* 10, 794. doi: 10.3390/su10030794

Glenz, R., Kaiping, A., Göpfert, D., Weber, H., Lambour, B., Sylvester, M., et al. (2022). The major plant sphingolipid long chain base phytosphingosine inhibits growth of bacterial and fungal plant pathogens. *Sci. Rep.* 12, 1081. doi: 10.1038/s41598-022-05083-4

Glover, J. D., Reganold, J. P., Bell, L. W., Borevitz, J., Brummer, E. C., Buckler, E. S., et al. (2010). Increased food and ecosystem security *via* perennial grains. *Science* 328, 1638–1639. doi: 10.1126/science.1188761

Goh, K. M. (2004). Carbon sequestration and stabilization in soils: implications for soil productivity and climate change. *Soil Sci. Plant Nutr.* 50, 467–476. doi: 10.1080/00380768.2004.10408502

Gunina, A., and Kuzyakov, Y. (2015). Sugars in soil and sweets for microorganisms: review of origin, content, composition and fate. *Soil Biol. Biochem.* 90, 87–100. doi: 10.1016/j.soilbio.2015.07.021

Hargreaves, S. K., and Hofmockel, K. S. (2014). Physiological shifts in the microbial community drive changes in enzyme activity in a perennial agroecosystem. *Biogeochemistry* 117, 67–79. doi: 10.1007/s10533-013-9893-6

Hargreaves, S. K., Williams, R. J., and Hofmockel, K. S. (2015). Environmental filtering of microbial communities in agricultural soil shifts with crop growth. *PloS One* 10, e0134345. doi: 10.1371/journal.pone.0134345

Hita, C., Parlanti, E., Jambu, P., Joffre, J., and Amblès, A. (1996). Triglyceride degradation in soil. *Proc. 17th Int. Meet. Org. Geochem.* 25, 19–28. doi: 10.1016/S0146-6380(96)00107-6

Hu, L., Robert, C. A. M., Cadot, S., Zhang, X., Ye, M., Li, B., et al. (2018). Root exudate metabolites drive plant-soil feedbacks on growth and defense by shaping the rhizosphere microbiota. *Nat. Commun.* 9, 2738. doi: 10.1038/s41467-018-05122-7

Iannucci, A., Canfora, L., Nigro, F., De Vita, P., and Beleggia, R. (2021). Relationships between root morphology, root exudate compounds and rhizosphere microbial community in durum wheat. *Appl. Soil Ecol.* 158, 103781. doi: 10.1016/j.apsoil.2020.103781

Kähkönen, M. A., Liukkonen, M., Wittmann, C., Suominen, K. P., and Salkinoja-Salonen, M. S. (1999). Integrative assessment of sediment quality history in pulp mill recipient area in Finland. *Water Sci. Technol.* 40, 139–146. doi: 10.1016/S0273-1223(99)00711-8

Kuczynski, J., Stombaugh, J., Walters, W. A., González, A., Caporaso, J. G., and Knight, R. (2012). Using QIIME to analyze 16S rRNA gene sequences from microbial communities. *Curr. Protoc. Microbiol.* 27, 1E.5.1–1E.5.20. doi: 10.1002/9780471729259.mc01e05s27

Liang, C., Jesus, E., da, C., Duncan, D. S., Jackson, R. D., Tiedje, J. M., et al. (2012). Soil microbial communities under model biofuel cropping systems in southern Wisconsin, USA: impact of crop species and soil properties. *Appl. Soil Ecol.* 54, 24–31. doi: 10.1016/j.apsoil.2011.11.015

Lin, H., Liu, C., Li, B., and Dong, Y. (2021). Trifolium repens l. regulated phytoremediation of heavy metal contaminated soil by promoting soil enzyme activities and beneficial rhizosphere associated microorganisms. *J. Hazard. Mater.* 402, 123829. doi: 10.1016/j.jhazmat.2020.123829

Liu, K., Ding, X., and Wang, J. (2020). Soil metabolome correlates with bacterial diversity and co-occurrence patterns in root-associated soils on the Tibetan plateau. *Sci. Total Environ.* 735, 139572. doi: 10.1016/j.scitotenv.2020.139572

Liu, C., Lin, H., Dong, Y., Li, B., and Liu, Y. (2018). Investigation on microbial community in remediation of lead-contaminated soil by trifolium repensL. *Ecotoxicol. Environ. Saf.* 165, 52–60. doi: 10.1016/j.ecoenv.2018.08.054

Macabuhay, A., Arsova, B., Walker, R., Johnson, A., Watt, M., and Roessner, U. (2022). Modulators or facilitators? roles of lipids in plant root–microbe interactions. *Trends Plant Sci.* 27, 180–190. doi: 10.1016/j.tplants.2021.08.004

Mao, Y., Yannarell, A. C., Davis, S. C., and Mackie, R. I. (2013). Impact of different bioenergy crops on n-cycling bacterial and archaeal communities in soil: impact of

bioenergy crops on soil n-cycling archaea and bacteria. *Environ. Microbiol.* 15, 928–942. doi: 10.1111/j.1462-2920.2012.02844.x

Mavrodi, O. V., McWilliams, J. R., Peter, J. O., Berim, A., Hassan, K. A., Elbourne, L. D. H., et al. (2021). Root exudates alter the expression of diverse metabolic, transport, regulatory, and stress response genes in rhizosphere pseudomonas. *Front. Microbiol.* 12. doi: 10.3389/fmicb.2021.651282

Mazzola, M. (2002). Mechanisms of natural soil suppressiveness to soilborne diseases. *Antonie Van Leeuwenhoek* 81, 557–564. doi: 10.1023/A:1020557523557

McPherson, M. R., Wang, P., Marsh, E. L., Mitchell, R. B., and Schachtman, D. P. (2018). Isolation and analysis of microbial communities in soil, rhizosphere, and roots in perennial grass experiments. *J. Vis. Exp.* 57932(137):e57932. doi: 10.3791/57932

Molina-Santiago, C., Vela-Corcía, D., Petras, D., Díaz-Martínez, L., Pérez-Lorente, A. I., Sopeña-Torres, S., et al. (2021). Chemical interplay and complementary adaptative strategies toggle bacterial antagonism and co-existence. *Cell Rep.* 36, 109449. doi: 10.1016/j.celrep.2021.109449

Nannipieri, P., Ascher, J., Ceccherini, M. T., Landi, L., Pietramellara, G., and Renella, G. (2003). Microbial diversity and soil functions. *Eur. J. Soil Sci.* 54(4):655–670. doi: 10.1046/j.1351-0754.2003.0556.x

Ndour, P. M. S., Barry, C. M., Tine, D., de la Fuente Cantó, C., Gueye, M., Barakat, M., et al. (2021). Pearl millet genotype impacts microbial diversity and enzymatic activities in relation to root-adhering soil aggregation. *Plant Soil* 464, 109–129. doi: 10.1007/s11104-021-04917-w

Patel, T. K., and Williamson, J. D. (2016). Mannitol in plants, fungi, and plant–fungal interactions. *Trends Plant Sci.* 21, 486–497. doi: 10.1016/j.tplants.2016.01.006

Pedrazzani, C., Vanara, F., Bhandari, D. R., Bruni, R., Spengler, B., Blandino, M., et al. (2021). 5-n-Alkylresorcinol profiles in different cultivars of einkorn, emmer, spelt, common wheat, and tritordeum. *J. Agric. Food Chem.* 69, 14092–14102. doi: 10.1021/acs.jafc.1c05451

Pimentel, D., Cerasale, D., Stanley, R. C., Perlman, R., Newman, E. M., Brent, L. C., et al. (2012). Annual vs. perennial grain production. *Agric. Ecosyst. Environ.* 161, 1–9. doi: 10.1016/j.agee.2012.05.025

Pogna, N. E., Galassi, E., Ciccoritti, R., Cacciatori, P., Gazza, L., and Bozzini, A. (2014). "Evaluation of nine perennial wheat derivativesgrown in Italy," in *Perennial crops for food security–proceedings of the FAO expert workshop*. Eds. C. Batello, L. Wade, S. Cox, N. Pogna, A. Bozzini and J. Choptiany (Rome, Italy: FAO), 54–71.

Qiu, M., Zhang, R., Xue, C., Zhang, S., Li, S., Zhang, N., et al. (2012). Application of bio-organic fertilizer can control fusarium wilt of cucumber plants by regulating microbial community of rhizosphere soil. *Biol. Fertil. Soils* 48, 807–816. doi: 10.1007/s00374-012-0675-4

Raffaele, S., Leger, A., and Roby, D. (2009). Very long chain fatty acid and lipid signaling in the response of plants to pathogens. *Plant Signal. Behav.* 4, 94–99. doi: 10.4161/psb.4.2.7580

Rasche, F., Blagodatskaya, E., Emmerling, C., Belz, R., Musyoki, M. K., Zimmermann, J., et al. (2017). A preview of perennial grain agriculture: knowledge gain from biotic interactions in natural and agricultural ecosystems. *Ecosphere* 8, e02048. doi: 10.1002/ecs2.2048

Sah, S., Krishnani, S., and Singh, R. (2021). Pseudomonas mediated nutritional and growth promotional activities for sustainable food security. *Curr. Res. Microb. Sci.* 2, 100084. doi: 10.1016/j.crmicr.2021.100084

Schlatter, D. C., Yin, C., Hulbert, S., and Paulitz, T. C. (2020). Core rhizosphere microbiomes of dryland wheat are influenced by location and land use history. *Appl. Environ. Microbiol.* 86, e02135–e02119. doi: 10.1128/AEM.02135-19

Schmidt, R., Gravuer, K., Bossange, A. V., Mitchell, J., and Scow, K. (2018). Long-term use of cover crops and no-till shift soil microbial community life strategies in agricultural soil. *PloS One* 13, e0192953. doi: 10.1371/journal.pone.0192953

Semchenko, M., Xue, P., and Leigh, T. (2021). Functional diversity and identity of plant genotypes regulate rhizodeposition and soil microbial activity. *New Phytol.* 232, 776–787. doi: 10.1111/nph.17604

Simonin, M., Dasilva, C., Terzi, V., Ngonkeu, E. L. M., Diouf, D., Kane, A., et al. (2020). Influence of plant genotype and soil on the wheat rhizosphere microbiome: evidences for a core microbiome across eight African and European soils. *FEMS Microbiol. Ecol.* 96, fiaa067. doi: 10.1093/femsec/fiaa067

Sprunger, C. D., Culman, S. W., Peralta, A. L., DuPont, S. T., Lennon, J. T., and Snapp, S. S. (2019). Perennial grain crop roots and nitrogen management shape soil food webs and soil carbon dynamics. *Soil Biol. Biochem.* 137, 107573. doi: 10.1016/j.soilbio.2019.107573

Sprunger, C. D., Culman, S. W., Robertson, G. P., and Snapp, S. S. (2018). How does nitrogen and perenniality influence belowground biomass and nitrogen use efficiency in small grain cereals? *Crop Sci.* 58, 2110–2120. doi: 10.2135/cropsci2018.02.0123

Summer, L. W., Amberg, A., Barrett, D., Beale, M. H., Beger, R., Daykin, C. A., et al. (2007). Proposed minimum reporting standards for chemical analysis. *Metabolomics* 3 (3), 211–221.

Swenson, T. L., Jenkins, S., Bowen, B. P., and Northen, T. R. (2015). Untargeted soil metabolomics methods for analysis of extractable organic matter. *Soil Biol. Biochem.* 80, 189–198. doi: 10.1016/j.soilbio.2014.10.007

Tinoco, P., Almendros, G., and Sanz, J. (2018). Soil perturbation in Mediterranean ecosystems reflected by differences in free-lipid biomarker assemblages. *J. Agric. Food Chem.* 66, 9895–9906. doi: 10.1021/acs.jafc.8b01483

Trivedi, P., Delgado-Baquerizo, M., Trivedi, C., Hu, H., Anderson, I. C., Jeffries, T. C., et al. (2016). Microbial regulation of the soil carbon cycle: evidence from gene–enzyme relationships. *ISME J.* 10, 2593–2604. doi: 10.1038/ismej.2016.65

Upchurch, R. G. (2008). Fatty acid unsaturation, mobilization, and regulation in the response of plants to stress. *Biotechnol. Lett.* 30, 967–977. doi: 10.1007/s10529-008-9639-z

Veerman, C., Pinto Correia, T., Bastioli, C., Biro, B., Bouma, J., Cienciala, E., et al. (2020). Caring for soil is caring for life : ensure 75% of soils are healthy by 2030 for healthy food, people, nature and climate : interim report of the mission board for soil health and food. *Eur. Comm.* doi: 10.2777/918775

Vogel, T. M., Hirsch, P. R., Simonet, P., Jansson, J. K., Tiedje, J. M., van Elsas, J. D., et al. (2009). Advantages of the metagenomic approach for soil exploration: reply from Vogel. *Nat. Rev. Microbiol.* 7, 756–757. doi: 10.1038/nrmicro2119-c3

Wardle David, A., Bardgett Richard, D., Klironomos John, N., Heikki, Setälä, van der Putten Wim, H., and Wall Diana, H. (2004). Ecological linkages between aboveground and belowground biota. *Science* 304, 1629–1633. doi: 10.1126/science.1094875

Wilson, R. M., Tfaily, M. M., Kolton, M., Johnston, E. R., Petro, C., Zalman, C. A., et al. (2021). Soil metabolome response to whole-ecosystem warming at the spruce and peatland responses under changing environments experiment. *Proc. Natl. Acad. Sci.* 118, e2004192118. doi: 10.1073/pnas.2004192118

Withers, E., Hill, P. W., Chadwick, D. R., and Jones, D. L. (2020). Use of untargeted metabolomics for assessing soil quality and microbial function. *Soil Biol. Biochem.* 143, 107758. doi: 10.1016/j.soilbio.2020.107758

Xia, Y., Sahib, M. R., Amna, A., Opiyo, S. O., Zhao, Z., and Gao, Y. G. (2019). Culturable endophytic fungal communities associated with plants in organic and conventional farming systems and their effects on plant growth. *Sci. Rep.* 9, 1669. doi: 10.1038/s41598-018-38230-x

Yachi, S., and Loreau, M. (1999). Biodiversity and ecosystem productivity in a fluctuating environment: the insurance hypothesis. *Proc. Natl. Acad. Sci.* 96, 1463–1468. doi: 10.1073/pnas.96.4.1463

Zeng, Q., Mei, T., Wang, M., and Tan, W. (2022). Intensive citrus plantations suppress the microbial profiles of the β-glucosidase gene. *Agric. Ecosyst. Environ.* 323, 107687. doi: 10.1016/j.agee.2021.107687

Zeng, H.-Y., and Yao, N. (2022). Sphingolipids in plant immunity. *Phytopathol. Res.* 4, 20. doi: 10.1186/s42483-022-00125-1

Zhou, Z., Shen, X., Tu, J., and Zhu, Z. J. (2016). Large-scale prediction of collision cross-section values for metabolites in ion mobility-mass spectrometry. *Analytical Chemistry* 88(22), 11084–11091.

frontiers | Frontiers in Plant Science

TYPE Original Research
PUBLISHED 08 May 2023
DOI 10.3389/fpls.2023.1098042

OPEN ACCESS

EDITED BY
Xuewen Wang,
University of North Texas Health Science Center, United States

REVIEWED BY
Damaris Desgarennes,
Instituto de Ecología (INECOL), Mexico
Irina Kravchenko,
Winogradsky Institute of Microbiology (RAS), Russia

*CORRESPONDENCE
Dongkui Chen
chendongkui2018@gxaas.net
Shaolong Wei
weishaolong@gxaas.net
Zelin Qin
hqchun1288@163.com

†These authors have contributed equally to this work and share first authorship

RECEIVED 14 November 2022
ACCEPTED 03 April 2023
PUBLISHED 08 May 2023

CITATION
Huang Q, Wang N, Liu J, Liao H, Zeng Z, Hu C, Wei C, Tan S, Liu F, Li G, Huang H, Chen D, Wei S and Qin Z (2023) Soil bacterial communities associated with marbled fruit in *Citrus reticulata* Blanco 'Orah'. *Front. Plant Sci.* 14:1098042. doi: 10.3389/fpls.2023.1098042

Soil bacterial communities associated with marbled fruit in *Citrus reticulata* Blanco 'Orah'

Qichun Huang[1,2†], Nina Wang[1†], Jimin Liu[3,4†], Huihong Liao[1], Zhikang Zeng[5], Chengxiao Hu[2], Chizhang Wei[1], Songyue Tan[1], Fuping Liu[1], Guoguo Li[1], Hongming Huang[1], Dongkui Chen[1*], Shaolong Wei[6*] and Zelin Qin[5*]

[1]Horticulture Research Institute, Guangxi Academy of Agricultural Sciences, Nanning, China, [2]College of Resources and Environment, Huazhong Agricultural University, Wuhan, China, [3]Institute of Plant Protection, Guangxi Academy of Agricultural Sciences, Nanning, China, [4]College of Plant Science and Technology, Huazhong Agricultural University, Wuhan, China, [5]Institute of Agricultural Science and Technology Information, Guangxi Academy of Agricultural Sciences, Nanning, China, [6]Guangxi Academy of Agricultural Sciences, Nanning, China

Citrus reticulata Blanco 'Orah' is grown throughout southern China and provides enormous economic value. However, the agricultural industry has suffered substantial losses during recent years due to marbled fruit disease. The present study focuses on the soil bacterial communities associated with marbled fruit in 'Orah'. The agronomic traits and microbiomes of plants with normal and marbled fruit from three different orchards were compared. No significant differences were found in agronomic traits between the groups, except for higher fruit yields and higher quality of fruits in normal fruit group. Additionally, a total of 2,106,050 16S rRNA gene sequences were generated *via* the NovoSeq 6000. The alpha diversity index (including the Shannon and Simpson indices), Bray–Curtis similarity, and principal component analyses indicated no significant differences in microbiome diversity between normal and marbled fruit groups. For the healthy 'Orah', the most abundant associated phyla were Bacteroidetes, Firmicutes, and Proteobacteria. In comparison, Burkholderiaceae and Acidobacteria were the most abundant taxa with the marbled fruit group. In addition, the family Xanthomonadaceae and the genus *Candidatus Nitrosotalea* were prevalent with this group. Analysis using the Kyoto Encyclopedia of Genes and Genomes pathways showed that several pathways related to metabolism significantly differed between the groups. Thus, the present study provides valuable information regarding soil bacterial communities associated with marbled fruit in 'Orah'.

KEYWORDS

orah, marbled fruit, 16S rRNA sequencing, soil bacterial communities, pathways

1 Introduction

Soil health is a vital factor for plants and provides for a central living ecosystem and crop yields (Lehmann et al., 2020). Soil health can be affected by climate, mineral composition, organic content, and biotic factors (Turmel et al., 2015; Lal, 2016). Recent studies have shown that soil microbiota influence plant growth and yields (Bulgarelli et al., 2013; Khodakovskaya et al., 2013; Tkacz and Poole, 2015). Microbiota are complex systems of microbial communities that provide important proteins, such as enzymatic resources, for plant roots (Gianfreda and Rao, 2008). The rapid development of next-generation high-throughput sequencing and bioinformatic technologies has revealed new information about the function of microbiota. The connections between plants and the soil microbiota around their roots are critical for nutrient absorption, metabolism, and growth (Hacquard et al., 2015; Chialva et al., 2022).

Citrus reticulata Blanco 'Orah' is a small, fruiting citrus tree that was bred by Spiegel-Roy and Vardi (Usman and Fatima, 2018; Qin et al., 2022). To date, this variety has been planted throughout southern China and has produced substantial income for farmers and high-quality fruits for consumers (He et al., 2022). Although 'Orah' orchards have been expanding rapidly in recent years, the plants suffer from several diseases, such as marbled fruit (Liu et al., 2020b). Marbled fruit occurs in several citrus varieties and results in shrunken and light-weight fruit. Boron deficiency and citrus yellow vein clearing virus can also lead to marbled fruit (Liu et al., 2019). Furthermore, grafting, scions, seedlings, and indirect contact by tools can spread the disease, causing large financial losses. Therefore, understanding the pathogeny of this disease would improve the production of 'Orah'.

Identification of soil-based probiotics provides potential therapies for plant diseases (Wu et al., 2020). For example, irrigation of plant roots with *Bacillus subtilis* has been found to alleviate wilt disease in watermelon (*Citrullus lanatus*) (Ge et al., 2021). *Bacillus amyloliquefaciens* inhibits pathogenic bacteria, including *Gymnosporangium asiaticum*, *Phytophtora parasitica*, and *Pythium helicoides* (Asari et al., 2016; Ngalimat et al., 2021). Furthermore, investigation of soil microbiomes from the roots of diseased plants may identify possible pathogens, thereby aiding in providing precise and specific therapies for marbled fruit disease. Unfortunately, data on the microbiome remains scarce, resulting in a lack of key evidence regarding the pathogeny of marbled fruit disease in 'Orah'.

Nevertheless, this is among the most concerning diseases in 'Orah'. The current treatment strategies include increasing nutrition by fertilizing, replenishing the beneficial microbiome, sod-culture, and hormonal control (Qin et al., 2022). These therapies provide clear effects against marbled fruit disease; however, they still have several defects. First, these therapies are concerned with the whole environment of the plants rather than the inhibition of a specific pathogen. Additionally, these therapies are complicated to use. Thus, more details are required regarding the pathogenesis of marbled fruit disease in 'Orah'. In the present study, we compared normal, healthy fruits (NF) and marbled fruits (MF) from three different orchards. The plant and fruit morphologies of the NF and MF groups were examined. In addition, the soil microbiomes from the roots of these groups were evaluated *via* 16S rRNA gene sequencing using a next-generation approach. Finally, we analyzed the differences in diversity, taxa, and functions of the microbiome between NF and MF. This information will will provide potential information of marble fruit disease for 'Orah'.

2 Materials and methods

2.1 Field experiments and sampling

The tested 'Orah' trees were growing in three different orchards in Wuming, Naning, China, specifically Guangxi Jiacai Ecological Agriculture Co., Ltd (Wuming, Nanning, China; named JC), Guangxi Nanning Wanjin Agriculture Co., Ltd (Wuming, Nanning, China; named WJ), and Xiaoleima village (Wuming, Nanning, China; named XLM). The plants were sampled from 2019–2021. All the trees were four years old and randomly selected in the present study. The plants were managed following standardized fertilization and management techniques as described by (Huang et al., 2022). All the samples and tested groups was blind to the investigators in the study. Twenty individuals from each group were included in the study. The soil samples were collected from the root of the tree in 20 cm depth. For each group, 100 g soil samples from 5 trees were collected and 3 replications were performed. We used 0.5 g soil from each sample for DNA extraction. For analysis of agronomic traits, 10 fruits from each tree were used for the present study. The soil samples were talking about the soil around the plant roots.

2.2 Measurements of plant and fruit quality

The plant height, stem diameter, leaf thickness, leaf length, leaf width, number of fruits, and percentage of NF were calculated following the methods of (He et al., 2022). Leaf chlorophyll content was determined as described by (Zhu et al., 2020) using a SPAD-502 chlorophyll meter (Konica Minolta Inc., Japan).

The histology of leaves and fruit peel from the NF and MF groups were observed *via* paraffin section as described by (Zhang et al., 2021). Briefly, the leaf and fruit peel tissues were cut into 2–3 mm sections and embedded in paraffin. The tissues were then cut into 5 μm slices. Subsequently, the slices were dewaxed using xylene and the tissues were stained using safranine and fast-green followed by neutral gum sealing. Finally, the sections were observed and photographed using a DM2500 optical microscope (Leica Microsystems, USA).

2.3 DNA extraction and sequencing

DNA was extracted from the samples using a TIANamp Soil DNA Kit (TIANGEN, China) according to the manufacturer's protocols. The quality of the DNA was measured using a 1% agarose gel and NanoDrop 2000 spectrophotometer (NanoDrop,

USA). The 16S rRNA genes from partial bacterial DNA fragments were amplified *via* touchdown polymerase chain reaction (PCR). The primers for amplification of the variable regions, which included V3-V4 of the 16S rRNA genes, were 341F: 5′-CCTAYGGGRBGCASCAG and 806R: 5′-GGACTACNN GGGTATCTAAT (Chialva et al., 2022). Three biological replicates of the groups were included in the study. For each sample, PCR was performed on three replicates in a reaction system with a total volume of 30 µL, composed of 15 µL of Phusion® High-Fidelity PCR Master Mix (New England Biolabs), 2.5 µL of each primer (10 µM), sterile water, and 10 µL of DNA (1 ng/µL). The reaction was performed as follows: initial denaturation at 98°C for 30 s, followed by 25 cycles (98°C for 10 s, 55°C for 30 s, and 72°C for 30 s), and a final extension at 72°C for 5 min. The products were purified using agarose gel and Agencourt Ampure XP beads (Beckman, USA) according to the manufacturer's instructions. The DNA samples were assayed using a PicoGreen dsDNA quantitation assay (Thermo Fisher, USA). Sequencing libraries were constructed using a TruSeq® DNA PCR-Free Sample Preparation Kit (Cat number: FC-121-3003, Illumina, USA) following the manufacturer's instructions, with the addition of index codes assayed using a Qubit@ 2.0 fluorometer (Cat number: Q33216, Thermo Fisher, USA) and Agilent Bioanalyzer 2100 (Cat number: 2100-1, Agilent, USA). Finally, the prepared DNA libraries were sequenced using an Illumina NovoSeq 6000 platform (Illumina, USA).

2.4 Bioinformatic analysis

The raw reads were first filtered to remove low-quality sequences, tags, and primers; subsequently, the non-bacterial ribosome sequences and chimeras were removed. The pair-end reads were assembled using FLASH v1.2.11 (Liu et al., 2021) and the assembled sequences were clustered into operational taxonomic units using the CD-HIT algorithm within the UCLUST program (USEARCH V11; https://www.drive5.com/usearch/). The alpha and beta diversity comparisons were performed using QIIME2 plugins. The similarity matrices were used Bray-Curtis distances and the s distances on square-root transformed abundance data were calculated using R packages "phyloseq", "dplyr" and "ggplot2" (Yin et al., 2013). Functional analysis utilizing the Kyoto Encyclopedia of Genes and Genomes (KEGG) pathways was performed using MicrobiomeAnalyst (https://www.microbiomeanalyst.ca/MicrobiomeAnalyst/home.xhtml).

2.5 Statistical analysis

The statistical analysis and plotting were performed using R project (V4.2.1). The alpha and beta diversities were normalized prior to analysis using the read counts. The Shannon diversity index was used to reflect the alpha diversity. The Bray–Curtis dissimilarity matrix and permutational analysis of variance were used to assess the beta diversity which were analyzed by PRIMER v. 6 (PRIMER-E, UK). For the different groups, a principal component analysis (PCA) graph was plotted to show the clustering of the bacteria.

3 Results

3.1 Plant and fruit quality of 'Orah'

First, the trees that produced normal and marbled fruit were compared (Figure 1A). The plant heights, tree trunk, leaf thicknesses, leaf lengths, leaf widths, and leaf chlorophyll contents showed no significant differences between the NF and MF from the three orchards ($p>0.05$, Table 1). The leaf histology did not differ between the NF and MF groups; however, the fruit peel contained more lignin in MF than that in NF (Figure 1B).

The MF contained more lignified cells than did the NF, which are shown stained red by Safranine in Figure 1A. However, the number of fruits produced did not significantly differ between the NF and MF groups ($p>0.05$, Figure 1C). The percentage of NF was significantly higher in the NF group than that in the MF group ($p<0.05$, Figure 1D).

3.2 Alpha and beta diversity analyses

The present study obtained a total of 2,106,050 16S rRNA gene sequences, including 1,754,017 sequences (83.28%) that represented a total of 7,889 effective operational taxonomic units (Supplementary Table S1), which were mostly assigned to 10 phyla (91.29–94.62%): Firmicutes, Chloroflexi, Proteobacteria, Bacteroidetes, Acidobacteria, Actinobacteria, Verrucomicrobia, Cyanobacteria, Thermotogae, and Thaumarchaeota (Supplementary Table 2).

We used the alpha diversity to calculate the Shannon and Simpson indices of the different genera. The Shannon index indicated no significant differences in the average diversity of the NF and MF groups at all orchards ($p>0.05$, Figure 2A). In addition, similar results were found when using the Simpson index to compare these groups ($p>0.05$, Figure 2B). To compare the overall divergence in the bacterial community compositions among the tested groups, the Bray-Curtis similarity and PCA were utilized (Figures 2C, D). Both analyses suggested that in the XLM, the NF and MF groups were highly similar to each other. However, in WJ and JC orchards, the NF and MF groups were most similar to the fruit same group from the other orchard.

3.3 Bacterial diversity in soil from roots of healthy 'Orah'

The 10 most abundant phyla associated with the NF groups are shown in Figure 3. For the three orchards, the predominant bacterial phylum was Bacteroidetes (24.08%), followed by Firmicutes (22.13%) and Proteobacteria (16.61%). Moreover, the most abundant bacterial phylum at XLM was Firmicutes (23.21%), whereas, at the other two orchards, Bacteroidetes was the most

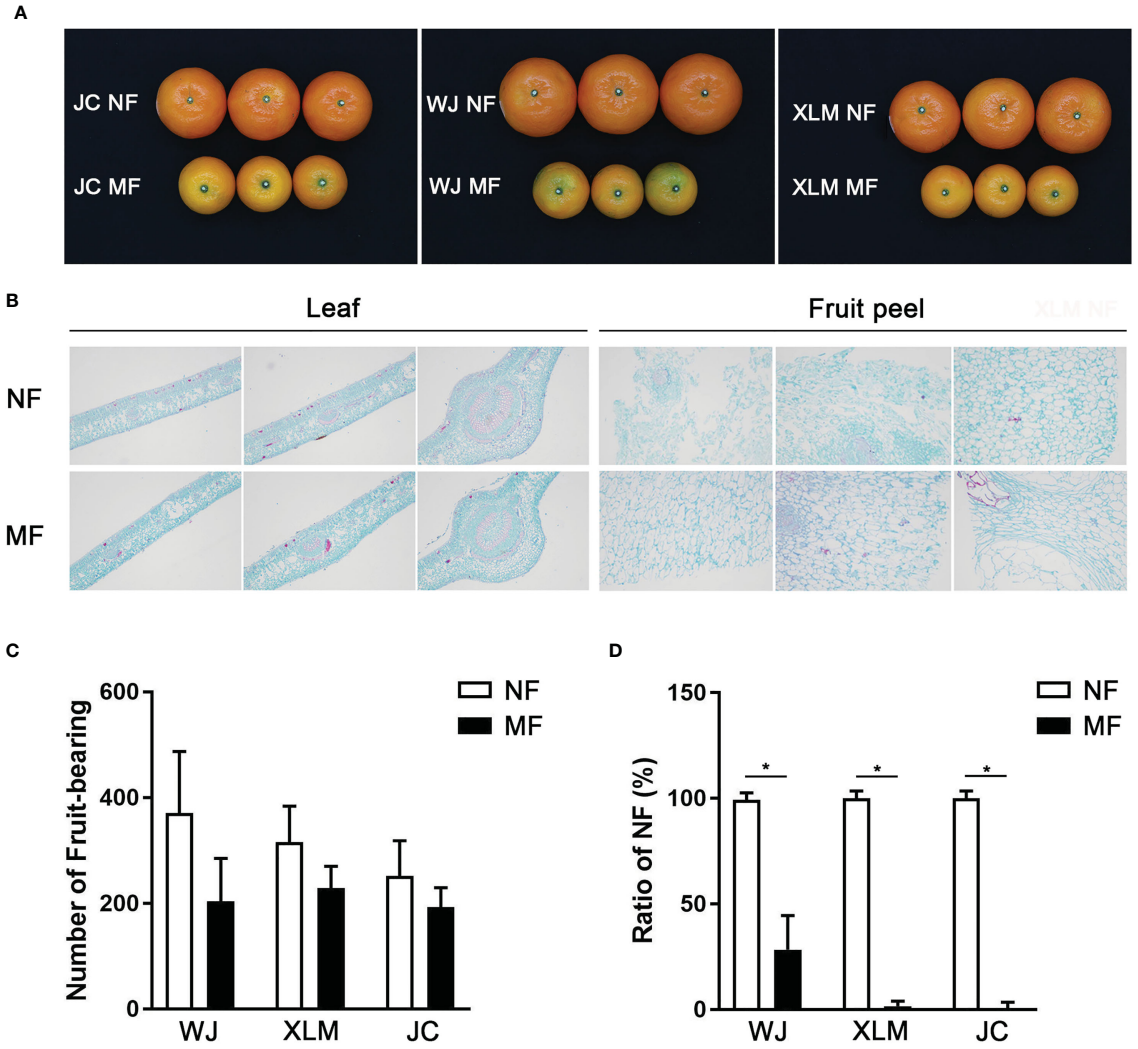

FIGURE 1
Comparisons of leaves and fruits between MF and NF groups. **(A)** The fruits in the MF and NF groups at the WJ, XLM, and JC orchards. **(B)** Histology of the leaves and fruit peel of MF and NF groups, which were analyzed *via* safranine and fast-green. **(C)** Statistical analysis of the number of fruits produced in the MF and NF groups at WJ, XLM, and JC. **(D)** Percentage of NF in the MF and NF groups at WJ, XLM, and JC. The asterisks show the significant differences between the two groups (P<0.05) by t-test.

TABLE 1 comparison of the NF and MF plants from three planting areas.

Groups	Plant height (cm)	Tree trunk (mm)	Leaf thickness (mm)	Leaf length (mm)	Leaf width (mm)	SPAD	Number of fruiting-bearing	Ratio of NF (%)
WJ NF	272.67±6.96aA	76.82±3.65abAB	0.35±0.03abA	9.34±0.48aA	4.82±0.37aA	79.26±1.56aA	371.00 ±116.29aA	99.48±3.25aA
XLM NF	218.00±16.35bB	65.49±7.62cBC	0.33±0.01abA	7.85±0.05bB	4.35±0.09abA	75.68 ±0.54abA	316.00 ±68.13abA	100.00±3.53aA
JC NF	204.67±7.30bB	62.59±2.38cC	0.31±0.01bA	8.15±0.33bAB	4.46±0.18abA	73.33±4.63bA	252.33 ±66.54abA	100.00±3.53aA
WJ MF	282±22.37aA	81.71±5.75aA	0.37±0.03aA	8.47±0.82abAB	4.25±0.30bA	74.49 ±1.12abA	203.67±81.44bA	28.39±16.20bB
XLM MF	226.33±2.11bB	65.36±0.65cBC	0.33±0abA	8.19±0.45bAB	4.51±0.04abA	75.55 ±2.20abA	229.00 ±41.54abA	1.69±2.41cC
JCJ MF	203.67±8.48bB	70.60 ±3.69bcABC	0.33±0.03abA	8.01±0.38bAB	4.43±0.36abA	75.91 ±3.46abA	193.00±36.79bA	0±3.53cC

The lowercase letters and uppercase letters after the values showed significant differences at $p < 0.05$ and $p < 0.01$, respectively.

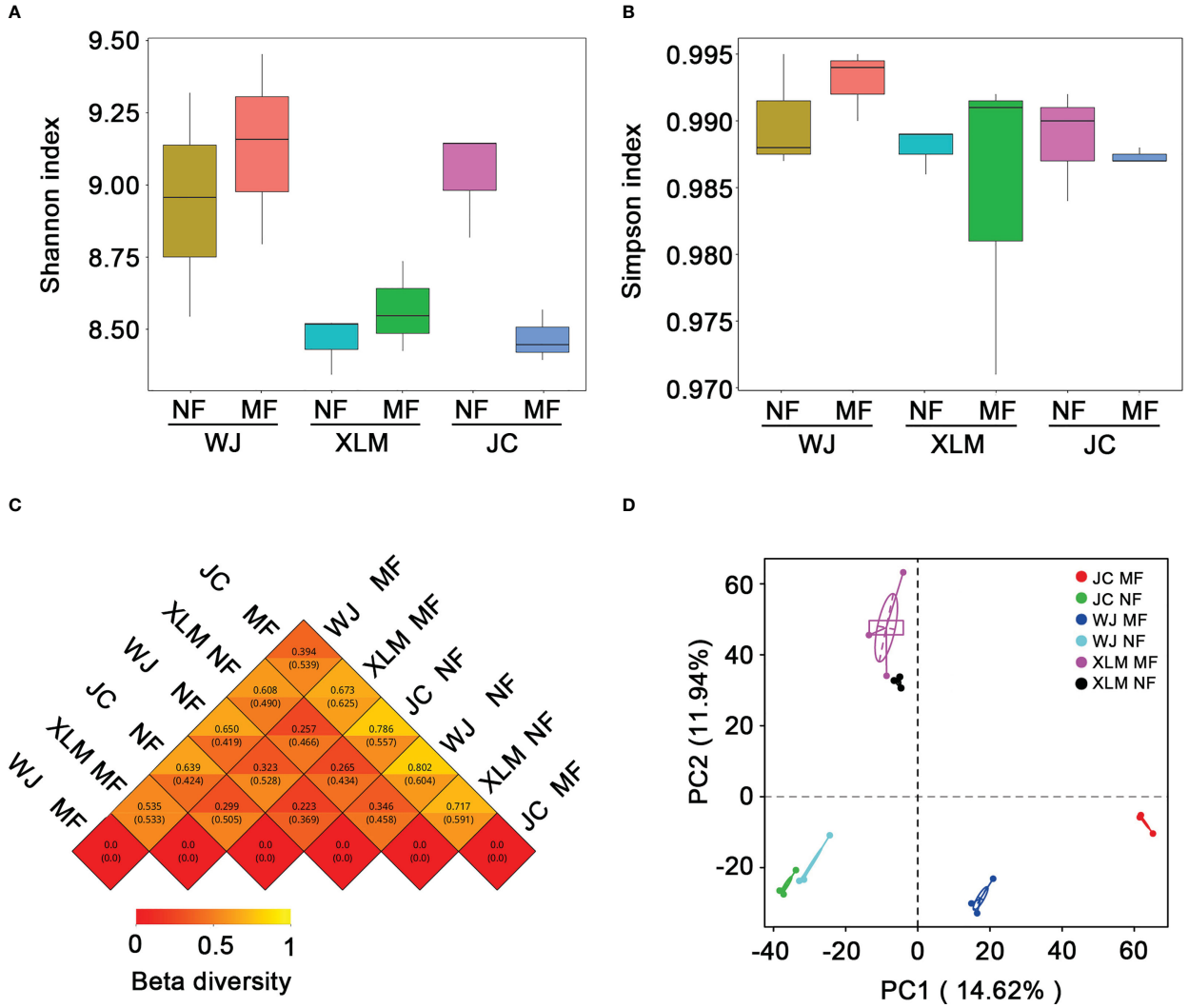

FIGURE 2
Alpha and beta diversity analyses of the samples from the MF and NF groups. **(A)** Shannon index and **(B)** Simpson index for alpha diversity of the samples in the MF and NF groups. **(C)** Correlations of beta diversity and **(D)** PCA among the groups in the present study.

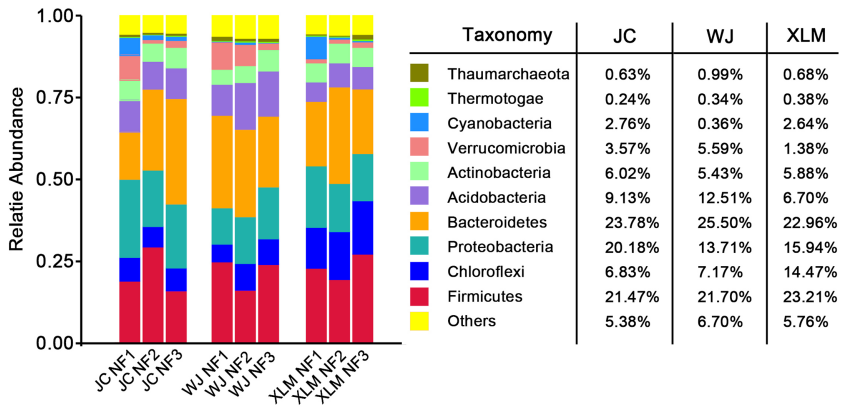

Taxonomy	JC	WJ	XLM
Thaumarchaeota	0.63%	0.99%	0.68%
Thermotogae	0.24%	0.34%	0.38%
Cyanobacteria	2.76%	0.36%	2.64%
Verrucomicrobia	3.57%	5.59%	1.38%
Actinobacteria	6.02%	5.43%	5.88%
Acidobacteria	9.13%	12.51%	6.70%
Bacteroidetes	23.78%	25.50%	22.96%
Proteobacteria	20.18%	13.71%	15.94%
Chloroflexi	6.83%	7.17%	14.47%
Firmicutes	21.47%	21.70%	23.21%
Others	5.38%	6.70%	5.76%

FIGURE 3
The 10 most abundant phyla of the NF group at JC, WJ and XLM.

abundant phylum (23.78% at JC and 25.50% at WJ). The top three phyla comprised 62.82% of the observed taxa in the three orchards. Only 5.95% of observed taxa were not among the top 10 phyla, which were Bacteroidetes, Firmicutes, Proteobacteria, Chloroflexi, Acidobacteria, Actinobacteria, Verrucomicrobia, Cyanobacteria, Thaumarchaeota, and Thermotogae (Figure 3).

3.4 Comparing of the microbiomes of NF and MF groups

To analyze the differences in the soil microbiome between the NF and MF groups, a linear discriminant analysis of effect size was conducted. The results show that Burkholderiaceae and Acidobacteria were abundant in the MF groups. These two bacterial taxa also showed significantly different abundances ($p<0.05$, Student's t-test; Figure 4). At the family level, Xanthomonadaceae was significantly more abundant in all the MF groups compared to that in the NF groups ($p<0.05$). SAGMCG-1 was significantly more abundant in the MF groups from JC and WJ than in the MF group from XLM ($p<0.05$, Figure 5A, Supplementary Table 3). At the genus level, *Candidatus Nitrosotalea* was overrepresented in all the MF groups compared to that in the NF groups ($p<0.05$, Figure 5B, Supplementary Table 4).

3.5 Function of prokaryotic communities in soil from roots of 'Orah'

KEGG analysis was performed to predict and investigate the functional profiles of the prokaryotic communities. The results showed that 21 pathways were significantly different between the NF and MF groups ($p<0.05$, Figure 6, Supplementary Table 5). Several metabolic pathways were significantly more enriched in the NF groups than those in the MF groups, such as tetracycline biosynthesis, glyoxylate and dicarboxylate metabolism, flavonoid biosynthesis, xylene degradation, limonene and pinene degradation, lysine degradation, metabolism of xenobiotics by cytochrome P450, and chloroalkane and chloroalkene degradation. The KEGG pathways for dioxin degradation, phosphonate and phosphinate metabolism, phosphotransferase system, linoleic acid metabolism, ethylbenzene degradation, prolyl 4-hydroxylase, and benzoate degradation were more enriched in the MF groups than those in the NF groups (Figure 6).

4 Discussion

In the present study, 'Orah' trees with healthy fruit and marbled fruit were sampled to reveal their differences in agronomic traits and soil microbiome in the root regions. To assess potential pathogenic microbes related to marbled fruit disease, PCA and clustering analyses were conducted to determine the diversity of the microbiome. Marbled fruit disease, which occurs due to multiple factors, such as pathogenic microbes, can be relieved by soil-based probiotic treatments (Vuong et al., 2017). Finding and utilizing beneficial microorganisms to improve the quality of citrus fruit is a worthwhile research task. Three different orchards were included in the present study to eliminate the effects of varied natural growth conditions. Moreover, the cultivation and management techniques were similar among these orchards, which approximated those of commercial production. However, under these conditions, 5–10% plants still developed this disease and knowledge on its occurrence from a microbiome view is limited. Therefore, this study investigated the differences in agronomic variables and soil microbiomes from the root regions of NF and MF groups of 'Orah'.

Many investors who bear the risks brought by MF disease desire to solve this issue. A previous study showed that approximately 57.14% of plants with MF also suffered from yellow vein disease and 100% were infected with the *Citrus tristeza* virus (Bettini et al., 2018). Furthermore, several diseases in citrus that occur due to microbial or viral infections affect fruit production. In America, a stubborn disease of citrus caused by *Spiroplasma citri* results in smaller, deformed fruits with lower yields (Mello et al., 2010). Citrus yellow vein clearing virus causes yellow vein disease in lemons, which leads to yellowing, bright veins, and leaf drop, resulting in a decrease in yield (Liu et al., 2020a). This virus can be spread by grafting, tools, seedlings, and scions (Zhen et al., 2015). Additionally, *Aphid leguminosae* and *Aphid spiraea* can spread this disease in lemons (Tannice and Eric, 2013; García et al., 2016). Some lemon trees are cut down once MF occurs. To date, specific treatments for MF disease are lacking. Furthermore, the pathogenesis of MF may result from a virus or other microbes. The common treatment strategies, such as hormonal treatment and additional fertilization, cannot cure the disease (Banyal and Sharma, 2015; García et al., 2016). Hence, developing new probiotics is important for this disease (Luang-In et al., 2020). Hence, the present study compared the agronomic characteristics of the leaves and fruits of plants with and without MF disease. The disease did not affect the leaf histology, but only lead to low fruit yields. PCA indicated that the difference in microbiomes was higher among the orchards than that between the NF and MF samples. Therefore, these results imply that MF disease affects fewer aspects than previously considered. Although the Shannon and Simpson indices were higher in the MF groups than those in the NF groups at WJ and XLM, no significant difference in the diversity of the soil microbiomes of NF and MF groups was found at JC. Previous studies showed that diversity indicators, such as the Shannon and Simpson indices, were affected by plant biostimulant treatment for endemic huanglongbing (also known as citrus greening disease) (Castellano-Hinojosa et al., 2021) and reared host plants (Meng et al., 2022). Surprisingly, the present results showed no significant differences in diversity between the soil from the roots of the NF and MF groups. We propose that the different conditions such as temperature, water and location among the orchards affected the results.

10.3389/fpls.2023.1098042

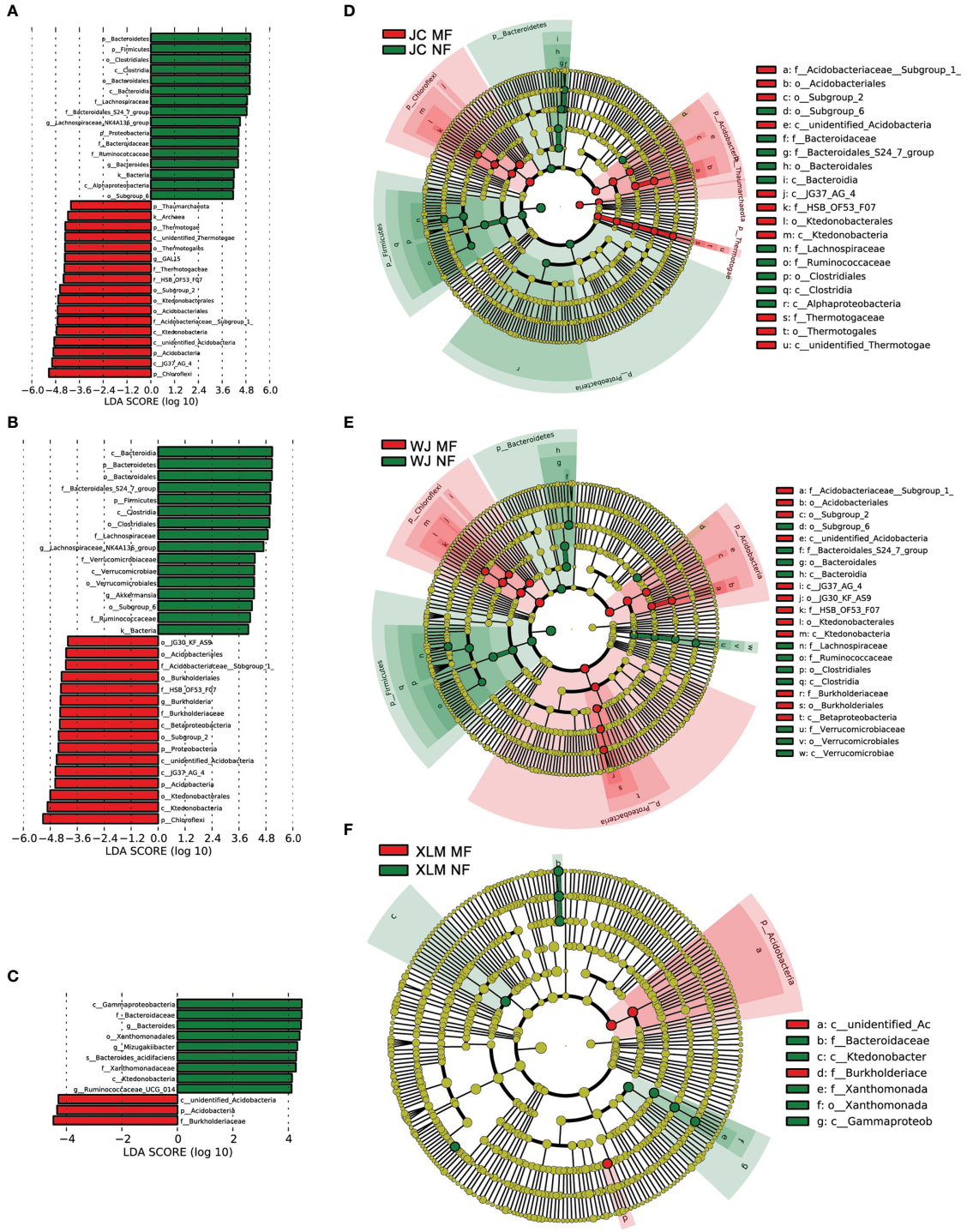

FIGURE 4
Differences in bacterial taxa abundances in the samples of the MF and NF groups. The forest plots show the linear discriminant analysis score (effect size), indicating the significant differences between the MF and NF groups from **(A)** JC, **(B)** WJ, and **(C)** XLM. The cladograms, which were generated using the linear discriminant analysis of effect size method, indicate the phylogenetic distribution of microbes in the MF and NF groups from **(D)** JC, **(E)** WJ, and **(F)** XLM.

The taxonomic analysis of healthy 'Orah' microbiomes showed that the predominant taxa in three orchards were Bacteroidetes, Firmicutes, and Proteobacteria; this is similar to previous studies. For example, in a study regarding the microbial profiles of affected intensive citrus orchards in Shuitianba town (31°4′ N, 110°41′ E), Zigui City, Hubei, China, the five predominant phyla were Acidobacteria, Bacteroidetes, Firmicutes, Gemmatimonadetes, and Actinobacteria (He et al., 2022). This similarity shows that the compositions of the microbiome are similar among various citrus orchards, and these predominant phyla dominate the microbial

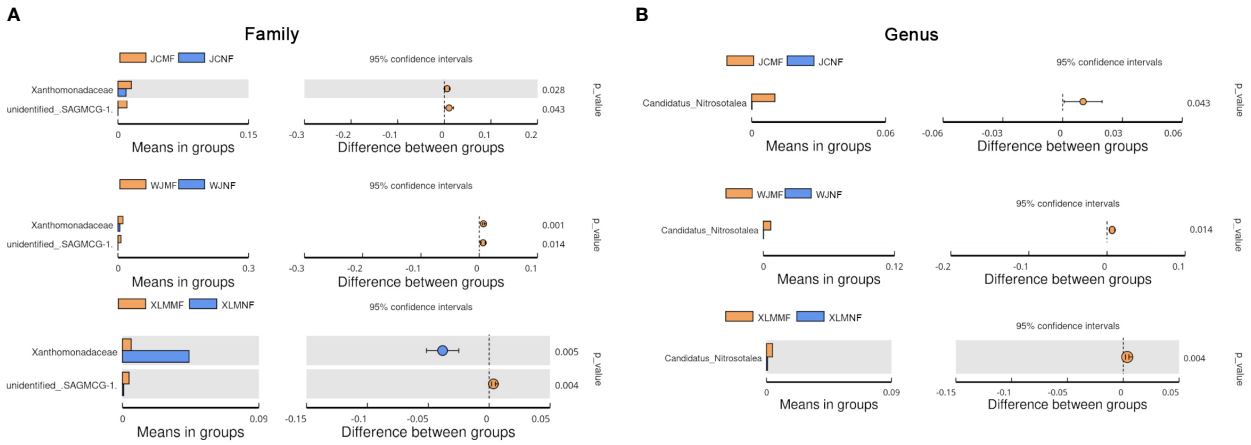

FIGURE 5
Extended error plots identifying significantly different taxa at the **(A)** family and **(B)** genus levels.

community. The microbiome analysis of NF and MF groups of 'Orah' suggested that Burkholderiaceae and Acidobacteria were the most abundant in MF groups. Burkholderiaceae includes several plant pathogens, including *Rhizobium* spp. and *Agrobacterium* spp. (Krimi et al., 2002; Deakin and Broughton, 2009). Moreover, at the family and genus levels, Xanthomonadaceae and *Candidatus Nitrosotalea*, respectively, were significantly more abundant in the MF groups and those in the NF groups. Within the Xanthomonadaceae family, genera such as *Xanthomonas* and *Stenotrophmonas* contain several species that are plant pathogens (Ryan et al., 2009). Members of the genus *Candidatus Nitrosotalea*, which includes *Candidatus Nitrosotalea devanaterra* and *Candidatus Nitrosotalea* sp. Nd2, have been found in acidic soils as ammonia-oxidizing archaea (Lehtovirta-Morley Laura et al., 2016). *Candidatus Nitrosotalea* spp. were also found in soil microbial community structures in the soil of rice-frog cultivation and high-quality grassland topsoils (Yi et al., 2019). The functions of these microbes are associated with nitrogen cycle. Nevertheless, the mechanism causing the high concentrations of these microbes in the soil around MF plants remains understudied. We propose that *Candidatus Nitrosotalea* has a novel function in MF that requires further investigation. Additionally, the present study found functional differences in several metabolic pathways in the prokaryotic soil communities between the NF and MF groups. The enriched pathways in the NF groups, including flavonoid biosynthesis and metabolism of xenobiotics by cytochrome P450, contributed to fruit yields, whereas the enriched pathways in the MF groups, such as linoleic acid metabolism, ethylbenzene degradation, prolyl 4-hydroxylase, and benzoate degradation were a possible reason for the low weight and quality of the fruit.

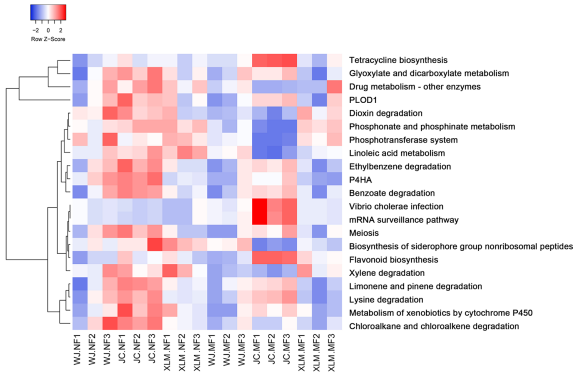

FIGURE 6
Heatmap of the KEGG analysis of the functional profiles of the prokaryotic communities.

5 Conclusion

The agronomic characteristics and soil microbiomes from the root areas were compared between NF and MF groups of 'Orah' trees. The plants showed no significant differences between groups; however, the fruits of the MF group were lower quality and lighter weight than those of the NF group. The microbiomes showed no significant differences between the two groups, which was inferred from the alpha and beta diversity analyses. The taxonomy of the microbiomes showed that Burkholderiaceae and Acidobacteria were predominant in the MF groups. At the family and genus levels, Xanthomonadaceae and *Candidatus Nitrosotalea*, respectively, were significantly more abundant in the MF groups than those in the NF groups. The functional analysis by KEGG pathways suggested that the most abundant differing pathways between both groups were those related to metabolism. Thus, these findings provide valuable information regarding the control of MF disease.

Data availability statement

The datasets presented in this study can be found in online repositories. The names of the repository/repositories and accession number(s) can be found in the article/Supplementary Material.

Author contributions

QH designed the study and wrote the manuscript. NW, JL, ZZ, CW, ST, FL, GL and HH performed the experiment and analyzed the data. HL performed the bioinformatic analysis. CH edited the manuscript. DC, SW and ZQ designed supervised the work the work. All authors contributed to the article and approved the submitted version.

Funding

This work was funded by Science and Technology Major Project of Guangxi (GuiKeAA20108003 GuiKeAA22036002), Science and Technology Major Project of Nanning (20212141, 20222065), Chinese Academy of Agricultural Sciences-Guangxi Academy of Agricultural Sciences Collaborative Innovation Project (CAAS-GXAASXTCX2019026-2), Guangxi Characteristic Crop Experimental Station, China (GuiTS202201), Science and Technology Project of Jiangnan District, Nanning (2020020102); Guinongke (2021YT051, 2022JM32), Citrus Huanglongbing Prevention and Control Engineering Technology Research Center of Guangxi.

Conflict of interest

The authors declare that the research was conducted in the absence of any commercial or financial relationships that could be construed as a potential conflict of interest.

Publisher's note

Supplementary material

The Supplementary Material for this article can be found online at: https://www.frontiersin.org/articles/10.3389/fpls.2023.1098042/full#supplementary-material

References

Asari, S., Matzén, S., Petersen, M. A., Bejai, S., and Meijer, J. (2016). Multiple effects of bacillus amyloliquefaciens volatile compounds: plant growth promotion and growth inhibition of phytopathogens. *FEMS Microbiol. Ecol.* 92, fiw070. doi: 10.1093/femsec/fiw070

Banyal, S. K., and Sharma, D. (2015). Effect of hormonal treatment and mulching on fruit drop and quality in mango. *J. Hortic. Sci.* 10, 102–109.

Bettini, B., Cavichioli, T., Cristofani-Yaly, M., Schinor, E., Azevedo, F., and Martins, A. (2018). "Performance and reaction to huanglongbing of'Tahiti'acid lime grafted on citrandarins," in *IV international symposium on citrus biotechnology 1230*, 101–108.

Bulgarelli, D., Schlaeppi, K., Spaepen, S., Van Themaat, E. V. L., and Schulze-Lefert, P. (2013). Structure and functions of the bacterial microbiota of plants. *Annu. Rev. Plant Biol.* 64, 807–838. doi: 10.1146/annurev-arplant-050312-120106

Castellano-Hinojosa, A., Meyering, B., Nuzzo, A., Strauss, S. L., and Albrecht, U. (2021). Effect of plant biostimulants on root and plant health and the rhizosphere microbiome of citrus trees in huanglongbing-endemic conditions. *Trees* 35, 1525–1539. doi: 10.1007/s00468-021-02133-8

Chialva, M., Lanfranco, L., and Bonfante, P. (2022). The plant microbiota: composition, functions, and engineering. *Curr. Opin. Biotechnol.* 73, 135–142. doi: 10.1016/j.copbio.2021.07.003

Deakin, W. J., and Broughton, W. J. (2009). Symbiotic use of pathogenic strategies: rhizobial protein secretion systems. *Nat. Rev. Microbiol.* 7, 312–320. doi: 10.1038/nrmicro2091

García, J. F., Olmo, M., and García, J. M. (2016). Decay incidence and quality of different citrus varieties after postharvest heat treatment at laboratory and industrial scale. *Postharvest Biol. Technol.* 118, 96–102. doi: 10.1016/j.postharvbio.2016.03.019

Ge, A.-H., Liang, Z.-H., Xiao, J.-L., Zhang, Y., Zeng, Q., Xiong, C., et al. (2021). Microbial assembly and association network in watermelon rhizosphere after soil fumigation for fusarium wilt control. *Agriculture Ecosyst. Environ.* 312, 107336. doi: 10.1016/j.agee.2021.107336

Gianfreda, L., and Rao, M. A. (2008). Interactions between xenobiotics and microbial and enzymatic soil activity. *Crit. Rev. Environ. Sci. Technol.* 38, 269–310. doi: 10.1080/10643380701413526

Hacquard, S., Garrido-Oter, R., González, A., Spaepen, S., Ackermann, G., Lebeis, S., et al. (2015). Microbiota and host nutrition across plant and animal kingdoms. *Cell Host Microbe* 17, 603–616. doi: 10.1016/j.chom.2015.04.009

He, Y., Li, W., Zhu, P., Wang, M., Qiu, J., Sun, H., et al. (2022). Comparison between the vegetative and fruit characteristics of 'Orah' (Citrus reticulata blanco) mandarin under different climatic conditions. *Scientia Hortic.* 300, 111064. doi: 10.1016/j.scienta.2022.111064

Huang, Q., Liu, J., Hu, C., Wang, N., Zhang, L., Mo, X., et al. (2022). Integrative analyses of transcriptome and carotenoids profiling revealed molecular insight into variations in fruits color of citrus reticulata blanco induced by transplantation. *Genomics* 114, 110291. doi: 10.1016/j.ygeno.2022.110291

Khodakovskaya, M. V., Kim, B.-S., Kim, J. N., Alimohammadi, M., Dervishi, E., Mustafa, T., et al. (2013). Carbon nanotubes as plant growth regulators: effects on tomato growth, reproductive system, and soil microbial community. *Small* 9, 115–123. doi: 10.1002/smll.201201225

Krimi, Z., Petit, A., Mougel, C., Dessaux, Y., and Nesme, X. (2002). Seasonal fluctuations and long-term persistence of pathogenic populations of agrobacterium spp. in soils. *Appl. Environ. Microbiol.* 68, 3358–3365. doi: 10.1128/AEM.68.7.3358-3365.2002

Lal, R. (2016). Soil health and carbon management. *Food Energy Secur.* 5, 212–222. doi: 10.1002/fes3.96

Lehmann, J., Bossio, D. A., Kögel-Knabner, I., and Rillig, M. C. (2020). The concept and future prospects of soil health. *Nat. Rev. Earth Environ.* 1, 544–553. doi: 10.1038/s43017-020-0080-8

Lehtovirta-Morley Laura, E., Sayavedra-Soto Luis, A., Gallois, N., Schouten, S., Stein Lisa, Y., Prosser James, I., et al. (2016). Identifying potential mechanisms enabling acidophily in the ammonia-oxidizing archaeon "Candidatus nitrosotalea devanaterra". *Appl. Environ. Microbiol.* 82, 2608–2619. doi: 10.1128/AEM.04031-15

Liu, C., Liu, H., Hurst, J., Timko, M. P., and Zhou, C. (2020a). Recent advances on citrus yellow vein clearing virus in citrus. *Hortic. Plant J.* 6, 216–222. doi: 10.1016/j.hpj.2020.05.001

Liu, F., Wang, X., Chen, D., Chen, X., Liao, H., Wang, N., et al. (2020b). Nested-PCR detection and investigation for *Candidatus* liberibacter asiaticus of orah. *J. South. Agric.* 5, 101–107. doi: 10.3969/j.issn.2095-1191.2020.01.013

Liu, Y., Wang, Y., Wang, Q., Zhang, Y., Shen, W., Li, R., et al. (2019). Development of a sensitive and reliable reverse transcription droplet digital PCR assay for the detection of citrus yellow vein clearing virus. *Arch. Virol.* 164, 691–697. doi: 10.1007/s00705-018-04123-7

Liu, Y., Xu, C., Sun, Y., Chen, X., Dong, W., Yang, X., et al. (2021). Method for quick DNA barcode reference library construction. *Ecol. Evol.* 11, 11627–11638. doi: 10.1002/ece3.7788

Luang-In, V., Katisart, T., Konsue, A., Nudmamud-Thanoi, S., Narbad, A., Saengha, W., et al. (2020). Psychobiotic effects of multi-strain probiotics originated from Thai fermented foods in a rat model. *Food Sci. Anim. Resour.* 40, 1014–1032. doi: 10.5851/kosfa.2020.e72

Mello, A. F. S., Yokomi, R. K., Melcher, U., Chen, J., Civerolo, E., Wayadande, A. C., et al. (2010). New perspectives on the epidemiology of citrus stubborn disease in California orchards. *Plant Health Prog.* 11, 37. doi: 10.1094/PHP-2010-0526-04-SY

Meng, L., Xia, C., Jin, Z., and Zhang, H. (2022). Investigation of gut bacterial communities of Asian citrus psyllid (Diaphorina citri) reared on different host plants. *Insects* 13, 694. doi: 10.3390/insects13080694

Ngalimat, M. S., Yahaya, R. S. R., Baharudin, M.-A., Yaminudin, S. M., Karim, M., Ahmad, S. A., et al. (2021). A review on the biotechnological applications of the operational group *bacillus amyloliquefaciens*. *Microorganisms* 9, 614. doi: 10.3390/microorganisms9030614

Qin, Z., Pan, J., Li, J., Sun, J., Khoo, H. E., and Dong, X. (2022). Effects of 1-methylcyclopropene and abscisic acid treatments on texture properties and microstructures of postharvest tangerine (Citrus reticulata cv. orah). *J. Food Process. Preservation* 46, e16633. doi: 10.1111/jfpp.16633

Ryan, R. P., Monchy, S., Cardinale, M., Taghavi, S., Crossman, L., Avison, M. B., et al. (2009). The versatility and adaptation of bacteria from the genus stenotrophomonas. *Nat. Rev. Microbiol.* 7, 514–525. doi: 10.1038/nrmicro2163

Tannice, A. H., and Eric, G. (2013). The aphids (Hemiptera: aphididae) of Jamaica, their hosts, predators, parasitoids and other associates. *Caribbean J. Sci.* 47, 305–324. doi: 10.18475/cjos.v47i3.a19

Tkacz, A., and Poole, P. (2015). Role of root microbiota in plant productivity. *J. Exp. Bot.* 66, 2167–2175. doi: 10.1093/jxb/erv157

Turmel, M.-S., Speratti, A., Baudron, F., Verhulst, N., and Govaerts, B. (2015). Crop residue management and soil health: a systems analysis. *Agric. Syst.* 134, 6–16. doi: 10.1016/j.agsy.2014.05.009

Usman, M., and Fatima, B. (2018). "Mandarin (Citrus reticulata blanco) breeding," in *Advances in plant breeding strategies: fruits*, vol. 3 . Eds. J. M. Al-Khayri, S. M. Jain and D. V. Johnson (Cham: Springer International Publishing), 465–533.

Vuong, H. E., Yano, J. M., Fung, T. C., and Hsiao, E. Y. (2017). The microbiome and host behavior. *Annu. Rev. Neurosci.* 40, 21–49. doi: 10.1146/annurev-neuro-072116-031347

Wu, Y., Qu, M., Pu, X., Lin, X., and Shu, B. (2020). Distinct microbial communities among different tissues of citrus tree *Citrus reticulata* cv. chachiensis. *Sci. Rep.* 10, 6068. doi: 10.1038/s41598-020-62991-z

Yi, X., Yi, K., Fang, K., Gao, H., Dai, W., and Cao, L. (2019). Microbial community structures and important associations between soil nutrients and the responses of specific taxa to rice-frog cultivation. *Front. Microbiol.* 10. doi: 10.3389/fmicb.2019.01752

Yin, D., Wang, N., Xia, F., Li, Q., and Wang, W. (2013). Impact of biocontrol agents pseudomonas fluorescens 2P24 and CPF10 on the bacterial community in the cucumber rhizosphere. *Eur. J. Soil Biol.* 59, 36–42. doi: 10.1016/j.ejsobi.2013.09.001

Zhang, M., Wang, A., Qin, M., Qin, X., Yang, S., Su, S., et al. (2021). Direct and indirect somatic embryogenesis induction in *Camellia oleifera* Abel. *Front. Plant Sci.* 12. doi: 10.3389/fpls.2021.644389

Zhen, S., Kurth, E. G., Peremyslov, V. V., Changyong, Z., and Dolja, V. V. (2015). Molecular characterization of a citrus yellow vein clearing virus strain from China. *Arch. Virol.* 160, 1811–1813. doi: 10.1007/s00705-015-2423-1

Zhu, Y., Luo, X., Nawaz, G., Yin, J., and Yang, J. (2020). Physiological and biochemical responses of four *cassava cultivars* to drought stress. *Sci. Rep.* 10, 6968. doi: 10.1038/s41598-020-63809-8

frontiers | Frontiers in Plant Science

TYPE Original Research
PUBLISHED 05 June 2023
DOI 10.3389/fpls.2023.1180061

OPEN ACCESS

EDITED BY
Long Yang,
Shandong Agricultural University, China

REVIEWED BY
Adijailton José de Souza,
University of São Paulo, Brazil
Germán Tortosa Muñoz,
Spanish National Research Council (CSIC), Spain

*CORRESPONDENCE
Valeria Ventorino
valeria.ventorino@unina.it

RECEIVED 05 March 2023
ACCEPTED 05 May 2023
PUBLISHED 05 June 2023

CITATION
Gugliucci W, Cirillo V, Maggio A, Romano I, Ventorino V and Pepe O (2023) Valorisation of hydrothermal liquefaction wastewater in agriculture: effects on tobacco plants and rhizosphere microbiota.
Front. Plant Sci. 14:1180061.
doi: 10.3389/fpls.2023.1180061

Valorisation of hydrothermal liquefaction wastewater in agriculture: effects on tobacco plants and rhizosphere microbiota

Wanda Gugliucci[1], Valerio Cirillo[2], Albino Maggio[2], Ida Romano[1], Valeria Ventorino[1,3]* and Olimpia Pepe[1,3]

[1]Department of Agricultural Sciences, Division of Microbiology, University of Naples Federico II, Naples, Italy, [2]Department of Agricultural Sciences, Division of Plant Biology and Crop Science, University of Naples Federico II, Naples, Italy, [3]Task Force on Microbiome Studies, University of Naples Federico II, Naples, Italy

Industrial wastewater obtained from hydrothermal liquefaction (HTL-WW) of food wastes for biofuels production could represent a source of crop nutrients since it is characterized by a high amount of organic and inorganic compounds. In the present work, the potential use of HTL-WW as irrigation water for industrial crops was investigated. The composition of the HTL-WW was rich in nitrogen, phosphorus, and potassium with high level of organic carbon. A pot experiment with *Nicotiana tabacum* L. plants was conducted using diluted wastewater to reduce the concentration of some chemical elements below the official accepted threshold values. Plants were grown in the greenhouse under controlled conditions for 21 days and irrigated with diluted HTL-WW every 24 hours. Soils and plants were sampled every seven days to evaluate, over time, the effect of wastewater irrigation both on soil microbial populations, through high-throughput sequencing, and plant growth parameters, through the measurement of different biometric indices. Metagenomic results highlighted that, in the HTL-WW treated rhizosphere, the microbial populations shifted *via* their mechanisms of adaptation to the new environmental conditions, establishing a new balance among bacterial and fungal communities. Identification of microbial taxa occurring in the rhizosphere of tobacco plants during the experiment highlighted that the HTL-WW application improved the growth of Micrococcaceae, Nocardiaceae and Nectriaceae, which included key species for denitrification, organic compounds degradation and plant growth promotion. As a result, irrigation with HTL-WW improved the overall performance of tobacco plants which showed higher leaf greenness and increased number of flowers compared to irrigated control plants. Overall, these results demonstrate the potential feasibility of using of HTL-WW in irrigated agriculture.

KEYWORDS

HTL wastewater, microbiota, high-throughput sequencing, microbial community, biodiversity, *Nicotiana tabacum L.*

1 Introduction

The competition for fresh water among industry, agriculture, and public utilities is increasing due to population growth and climate change (Zucchinelli et al., 2021). On average, 40% of total water abstraction in Europe is used for industry and energy production, 15% for public water supply and 44% for agriculture. Agriculture is therefore the major user of freshwater. At the same time, agriculture is the most affected sector by water scarcity, especially in Mediterranean countries due to an aggravation of semi-arid and arid climatic conditions (Sofroniou and Bishop, 2014). In this scenario, the key to ensure water security is "water reuse", also commonly known as water recycling or water reclamation. Reclaimed water for irrigation includes different sources such as municipal and industrial wastewater, stormwater, agriculture runoff and return flows (EPA, 2021). About 380 billion m^3 of water can be recovered from the annual volumes of wastewater produced. Water recovery is expected to reach 470 billion m^3 by 2030 and 574 billion m^3 by 2050 (United Nations Educational, Scientific and Cultural Organization – UNESCO, 2021). The use of wastewater in agriculture offers several benefits including the availability of extra sources to cope with water scarcity; the possibility of reserving better-quality water for human consumption; the recovery of the nutrients contained in wastewater; replenishment of soil organic matter; reduction of wastewater release into the surrounding area; limiting/avoiding marine intrusion in coastal areas and overexploitation of fresh water (Ungureanu et al., 2020). Wastewater recycling not only offers an alternative source for crop irrigation, but also the opportunity to recover fertilizing elements, such as nitrogen (N), phosphorous (P), potassium (K), organic matter, minerals, and micronutrients. Nevertheless, according to Petousi et al. (2019), in Europe only the 2.4% accounting for 700 Mm^3/year of wastewater is reused and mostly in Spain. Until 2020, the major barriers preventing a wider spreading of this practice in EU were the limited awareness of potential benefits among stakeholders, and the lack of a supportive and coherent framework for water reuse. According to Directive 91/271/EEC - Article 12, "*treated wastewater must be reused whenever appropriate and disposal routes must minimize any adverse effects on the environment*". However, the document does not specify the minimum quality requirements for wastewater reuse (Petousi et al., 2019). Recently, the EU commission approved a new regulation on minimum requirements for water reuse in agricultural irrigation (EU 2020/741) that will be applied starting from 26 June 2023. This will eventually encourage and facilitate water reuse across Europe.

In Italy, the agricultural use of wastewater is currently regulated by Ministerial Decree no.185/2003 (limits for heavy metals in mg/L: Al 13, As 0.02, Ban 10, Be 0.1, B 1, Cd 0.005, Co 0.05, Cr 0.1, Fe 22, Mn 0.22, Hg 0.001, Ni 0.2, Pb 0.1, Cu 1, Se 0.01, Ti 0.001, V 0.1, Zn 0.5, Sn 3; limits for macro and micronutrients: BOD, 20 mg O_2/L; COD, 100 mg O_2/L; Total Nitrogen, 15 mg N/L; Ammonia Nitrogen, 5 mg NH_4/L; Total Phosphorous, 2 mg P/L; Sulphates, 500 mg SO_4/L; Chlorides, 100 mg Cl/L), which regards only the municipal and agro-industrial effluents. Most research on testing the use of wastewater in agriculture refers to treated municipal wastewater, olive mill wastewater, sewage sludges and digestates (Food and Agriculture Organization – FAO, 2022). However, there are additional industrial processes which deliver, as side products, high levels of liquid wastes that could be recovered and valorised for agricultural uses. In particular, the hydrothermal liquefaction (HTL) is a high-performance and eco-sustainable thermochemical technology to produce bioenergy from organic biomass and wastes. According to UNEP Food Waste Index report, 2021 (UNEP Food Waste Index report, 2021), a total of around 931 million tonnes of food waste from households, food service and retail were produced worldwide in 2019. In undeveloped countries more than 90% of the waste is openly dumped, burned, or landfilled without landfill gas collection systems, resulting in high GHG emissions. The available technologies for organic waste disposal and management include landfilling, incineration, composting, and anaerobic digestion. Hydrothermal liquefaction is an additional option, especially suitable for feedstock with high moisture content, such as the sorted organic fraction of household waste. Typically, HTL is carried out in the absence of oxygen, at temperature ranging between 250 and 350°C, under autogenic pressure (50–200 bar) and 15–90 minutes reaction times. The main steps of this reaction are: (i) depolymerization of macromolecules to form water soluble monomers, (ii) dehydration, decarboxylation, and deamination to degrade the different monomers, (iii) recombination of the reactive fragments to form a water insoluble bio-oil, (iv) further polymerization at prolonged reaction time to form hydro-char. At the end of this process, four main outputs are produced: the water insoluble bio-oil, the water phase containing organic and inorganic components, the gaseous phase, mainly constituted by CO_2 and the solid residues consisting in hydro-char and ash (Gu et al., 2019). The bio-oil, which can be used directly as low sulphur fuel or further refined to produce high-performance biofuels. Depending on the moisture content of the starting feedstock, the process generates also up to 95% of hydrothermal liquid wastewater (HTL-WW) with high concentrations of organic and inorganic compounds/elements. Therefore, the valorisation of this liquid co-product is a crucial step in hydrothermal liquefaction development since its discharge into civil wastewater treatment plants requires high extra-costs, making this process no longer economic viable (Posmanik et al., 2017). Moreover, HTL-WW may have some interesting properties as irrigation water, since it is rich in plant macro and micronutrients as well as organic carbon. The HTL-WW does not contain pathogens, pesticides and emerging contaminants including analgesics, antihypertensive drugs favouring its reuse in different areas (Jaramillo and Restrepo, 2017). Nevertheless, the presence of organic and inorganic matter in wastewaters could affect the soil physic-chemical properties including the electrical conductivity (EC), hydrophobicity, heavy-metal concentrations, pH as well as organic carbon content, humus, nitrogen, phosphate, and potassium levels and should be adequately monitored (Muamar et al., 2014). Moreover, wastewater applications are expected to alter the soil microbiota, because it is particularly sensitive to human-induced perturbations or environmental stress compared to higher organisms due to their close relations with the surroundings and because of higher surface area to volume ratio (Karimi et al., 2017). Investigating the soil microbiota composition and the interactions

with plant systems could provide useful information on both crops and soils productivity and health status (Ventorino et al., 2018a). In this context, the aim of this study was to assess the feasibility of the use of HTL-WW as irrigation water in agriculture using *Nicotiana tabacum* L. as a model plant since this species is easy to grow and does not have problems in terms of pathogens, allowing to reduce the interactions with other environmental constraints and have a cleaner assessment of the effects of HTL-WW on plant growth. Moreover, the impact of HTL-WW on root-associated microbiota was also determined and described by evaluating diversity and richness variations of bacterial and fungal communities. To the best of our knowledge, this is the first work reporting the use of wastewater deriving from hydrothermal liquefaction for crop irrigation purpose.

2 Material and methods

2.1 HTL-WW analysis

The HTL-WW used in this study was provided by the Eni Renewable Energy and Material Science Research Center (Novara, Italy). Two samples were taken from the Waste to Fuel HTL pilot plant in Eni Gela Refinery (Caltanissetta, Italy) at different time. For each sample, two 1 L aliquots were taken from two different storage tanks and were analysed to quantify their chemical composition. The HTL-WW was, on average, acidic with a pH value of 4.75 and Chemical Oxygen Demand (COD) and Total Organic Carbon (TOC) of 57250 and 22433.5 mg/L, respectively. It contained considerable amounts of total nitrogen (TN) (1845.75 mg/L) including ammonia (710 mg/L) and nitrates (9.8 mg/L), phosphate (24.45 mg/L), sulphate (23.7 mg/L) and potassium (3130 mg/L). The concentrations of macronutrients were: 50 mg/L of Ca, 25 mg/L of Mg, 23.5 mg/L of S. The heavy metals concentration (mg/kg) was composed by 0.3 of Cu, 8 of Fe, 2.9 of Zn, 0.1 of Ni, 6 of Al, 0.4 of Cr and 0.1 of Mo. The electrical conductivity reached 12.9 mS/cm, directly related to the high concentrations of Na^+ and Cl^-, 2990 and 1784 mg/L, respectively.

The HTL-WW was diluted 1:10 with tap water to reduce the values of some parameters below the threshold limits reported in the Ministerial Decree n.185/2003, which regulates the agricultural use of wastewater (Table 1).

TABLE 1 Comparison between the main parameters of HTL-WW from the *waste to fuel* process and the legislative limits (DM 2003/185) for wastewater use in agriculture.

	HTL-WW	Diluted HTL-WW (1:10)	Italian thresholds (DM183/2003)
pH	5	5	5-9.5
TSS	29.5 mg/L	2.95 mg/L	10 mg/L
COD	57250 mg/L	5725 mg/L	100 mg/L
NH_3	710 mg/L	71 mg/L	2 mg/L
E.C.	12900 mS/cm	1290 mS/cm	3000 mS/cm

TSS, Total Suspended Solids; COD, Chemical Oxygen Demand; NH_3, ammonia; E.C., Electrical Conductivity.

2.2 Experimental design and plant growth conditions

The tobacco experiment was set up in a greenhouse located at the experimental station of the University of Naples Federico II, Southern Italy (lat. 43°31'N, long. 14°58′E; alt. 60 m above sea level) with *Nicotiana tabacum* L. plants. The germination of tobacco seeds was carried out in peats under controlled conditions (T 28°C, 16 h light/8h, Ur ~ 60%) until the appearance of the 3rd-4th true leaf. Plants were transplanted in 19 cm Ø plastic pots and drip irrigated with nutrient solutions (N-P-K 20:20:20). At 60 Days-After-Sowing (DAS), when plants were at the 4-5 true leaves, half of the plants were irrigated with HTL-WW diluted in water at a ratio of 1:10, while control plants were irrigated with tap water. Irrigation was performed for 21 days.

2.3 Soil and rhizosphere sampling

Soil samples were collected after irrigation with HTL-WW from each pot at the beginning of the experiment (T0) and at 7 (T7), 14 (T14 and 21 (T21) days. For the microbiological analysis tobacco rhizosphere were sampled according to Romano et al. (2020a). The soil chemical parameters were analysed before and after treatment. In particular, after soil drying (65°C) were determined the pH-H_2O (1:2.5 soil:water solution ratio – pH meter GLP 22, Crison, Barcelona, Spain); electrical conductivity (E.C.) (1:5 soil:water solution ratio—Conductimeter basic 30, Crison, Barcelona, Spain); total nitrogen (N) concentration, assessed after acid digestion with sulfuric acid (96%) in the presence of potassium sulphate and a low concentration of copper by the Kjeldahl method (Kjeldahl, 1883); total carbon (TC), measured according to the Walkley–Black method and reported as soil organic matter (SOM% = C% × 1.726); phosphorus (P_2O_5) content, following the Olsen method and finally the ammonium acetate method was adopted for exchangeable potassium (K_2O) measurement.

2.4 Microbiological analysis

Microbiological analysis was performed on fresh soil samples. For molecular analysis, total genomic DNA was extracted from tobacco rhizosphere using a FastDNA SPIN Kit for Soil (MP Biomedicals, Illkirch Cedex, France) according to the manufacturer's instructions.

2.4.1 High-throughput sequencing

Synthetic oligonucleotide primers S-D-Bact-0341F50 (5′-CCTACGGGNGGCWGCAG-3′) and S-D-Bact-0785R50 (5′-GACTACHVGGGTATCTAATCC-3′) (Klindworth et al., 2013)

and the primers EMP.ITS1 (5′-CTTGGTCATTTAG AGGAAGTAA-3′) and EMP.ITS2 (5′-GCTGCGTTCTT CATCGATGC-3′) (Bokulich and Mills, 2013) were used to evaluate bacterial and fungal diversity, respectively, by amplicon-based metagenomic sequencing. PCR conditions for V3-V4 region consisted of 25 cycles (95°C for 30 s, 55°C for 30 s and 72°C for 30 s) plus one additional cycle at 72°C for 10 min as a final chain elongation. PCR conditions for ITS1-ITS2 region consisted of 35 cycles (94°C for 30 s, 52°C for 30 s and 68°C for 30 s) plus one additional cycle at 68°C for 7 min as a final chain elongation. Agencourt AMPure beads (Beckman Coulter, Milan, IT) were used to purify PCR products; whereas, quantification was performed by AF2200 Plate Reader (Eppendorf, Milan, IT). Equimolar pools were obtained, and sequencing was carried out on an Illumina MiSeq platform, yielding to 2× 250 bp, paired end reads.

2.4.2 Bioinformatics and data analysis

After sequencing, QIIME 2 software was used to analyse fastq files (Bolyen et al., 2019). Sequence adapters and primers were trimmed by using cut adapter, whereas DADA2 algorithm (Callahan et al., 2016) was used to trim low quality reads, to remove chimeric sequences, and joined sequences shorter than 250 bp by using the DADA2 denoise paired plugin of QIIME2. DADA2 produced amplicon sequence variants (ASVs), which were rarefied at the lowest number sequences/sample and used for taxonomic assignment using the QIIME feature-classifier plugin against Greengenes and UNITE database for the bacterial and fungal microbiota, respectively. The taxa abundances were recalculated after the exclusion of chloroplast, mitochondria contaminants and singleton ASVs.

Alpha diversity metrics (Shannon index, Faith's PD index and Observed_OTUs) was computed by QIIME2 and the pairwise Kruskal-Wallis' test was used for significant differences. Beta diversity was also calculated and plotted by QIIME 2 for the Weighted UniFrac (Lozupone et al., 2006).

Bar-plots were generated using R packages phyloseq 1.38.0 (McMurdie and Holmes, 2013) and ggplot2 3.4.2. Furthermore, the metabolic function was predicted by Tax4Fun analysis through Kyoto Encyclopedia of Genes and Genomes (KEGG) database (Wang et al., 2019). Analysis mainly focused on the differences of predicted abundances of genes involved in nitrogen fixation, 1-aminocyclopropane-1-carboxylate (ACC) deaminase, aminopeptidase, and glucanase activities across treated with HTL-WW and untreated samples. Heatmaps were generated in R using the package Pheatmap 1.0.12 (Kolde, 2019).

2.5 Biometric and physiological measurements

At 7, 14 21 days after HTL-WW treatment (DAT), three plants per treatments have been sampled for shoot biomass determination. At the same time points, SPAD index was measured with a MINOLTA chlorophyll meter (SPAD 502-Plus). The flower biomass was measured at the end of the experiment (after 21 days).

Data were analysed by test-t for pairwise comparison of means (at $P < 0.05$) using SPSS 19.0 statistical software package (SPSS Inc., Cary, NC, United States).

3 Results

3.1 Phenotypic and physiological evaluation of *Nicotiana tabacum L* plants

The impact of HTL-WW irrigation on *Nicotiana tabacum* L. plants was evaluated by phenotypic observations and biometric measurements carried out every seven days. Phenotype differences between treated and untreated plants increased with the time of growth. After 14 and 21 days, plants treated with HTL-WW showed a more intense tissue pigmentation (Figure 1) and higher SPAD values (T14 + 13.6% and T21 + 46.8%) (Table 2). Despite the greener/healthier appearance of wastewater treated plants, no significant differences were found in the fresh weight of the shoot

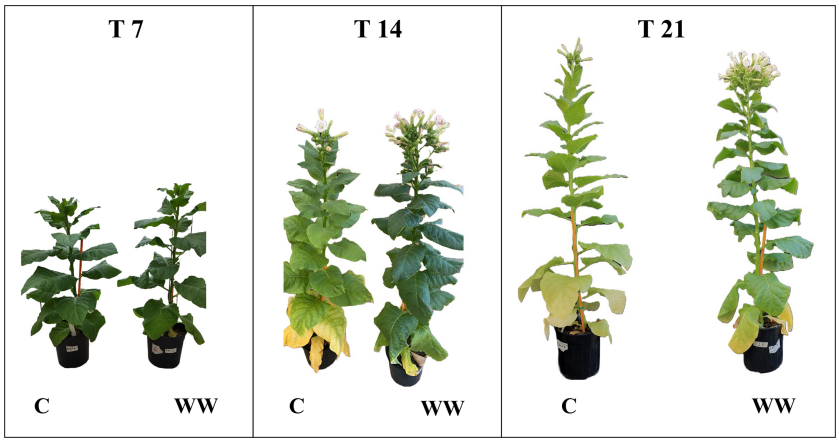

FIGURE 1
Nicotiana tabacum L. plants treated (WT) and untreated (C) with HTL-WW deriving from *Waste to Fuel* industrial process after 7 (T7), 14 (T14) and 21 (T21) days of growth.

10.3389/fpls.2023.1180061

TABLE 2 SPAD index of *Nicotiana tabacum* treated (HTL-WW) and untreated (C) with HTL-WW after 7 (T7), 14 (T14) and 21 (T21) days of growth.

	SPAD		
Treatment	T7	T14	T21
Control	43.3 ± 0.95	37.2 ± 0.68	31.4 ± 0.56
HTL-WW	42.9 ± 0.85	41.9 ± 0.75	46.1 ± 0.95
Test-t	*ns*	***	***

Test-t ($p<0.05$) was performed to identify significant differences between the treatments (ns, not significant; *** = $p<0.001$).

biomass between treated (HTL-WW) and untreated (C) plants (Table 3). The flower biomass at the end of the experiment (T21) was significantly higher (T-test: 0.007; $P<0.05$) in plants irrigated with HTL-WW (34.05 ± 14 g) compared to untreated plants (6.25 ± 2.67 g) (Figure 2). The main chemical properties of the soils collected from the tobacco's pots before (T0) HTL-WW treatment were total nitrogen (TN) 0.18%, electrical conductivity (EC) 420.0 µS/cm, organic matter (OM) 6.07%, phosphate (P_2O_5) 223.514 ppm, potassium (K_2O) 994.8 ppm and pH 7.3, remaining constant after the experiment.

3.2 Alpha and beta diversity of microbial community

The microbial diversity was characterized by partial 16S rRNA gene and ITS region (ITS1, 5.8S and ITS2) sequencing obtained from DNA directly extracted from rhizosphere samples of *Nicotiana tabacum* L. plants irrigated with HTL-WW (WW) or with tap water (C). In total, 652,845 and 49,184 high quality reads were analysed for prokaryotes and eukaryotes, respectively. The alpha-diversity was determined by calculating the Shannon diversity index, Faith's Phylogenetic Diversity index and Observed OTUs based on OTUs of 99% identity.

As shown in Figure 3, no significant differences ($p > 0.05$) in bacterial and fungal diversity were found between HTL-WW treated (WW) and untreated (C) tobacco rhizosphere, as revealed by the Shannon (Figures 3A, D), Faith's Phylogenetic Diversity indices (Figures 3B, E) and Observed OTUs (Figures 3C, F).

The PCoA of the weighted UniFrac community distance showed a marked difference between the microbiota of HTL-WW treated and untreated rhizosphere samples, highlighting that the use of industrial wastewater exerts selection pressure on the soil microbiota, especially for the bacterial communities (Figure 4). In fact, the sample of treated rhizosphere grouped separately on the right side of the chart in Figure 4A compared to untreated rhizosphere highlighting a separation of the samples based on irrigation treatment. It was interesting to note how the tobacco rhizosphere irrigated with HTL-WW at the beginning of the experiment (WW_T0) grouped with the control samples irrigated with tap water. However, the samples irrigated with the wastewater gradually separated over time from the control rhizosphere (Figure 4A).

A similar trend was observed for the fungal community structure, although the distribution of the samples was less marked (Figure 4B). In fact, the rhizosphere of the treated plants at the beginning of the experiment (WW_T0) was more grouped with the control samples irrigated with tap water; while samples irrigated with wastewater over time slightly separated among them (Figure 4B).

TABLE 3 Fresh biomass accumulation (shoot FW) of *Nicotiana tabacum* treated (HTL-WW) and untreated (C) with HTL-WW after 7 (T7), 14 (T14) and 21 (T21) days of growth.

		Shoot FW (g)	
Treatment	T7	T14	T21
Control	145.3 ± 13.39	183.5 ± 6.51	222.8 ± 22.36
HTL-WW	139.2 ± 6.11	230.0 ± 17.61	246.7 ± 23.22
Test-t	*ns*	*ns*	*ns*

Test-t ($p<0.05$) was performed to identify significant differences between the treatments (ns, not significant).

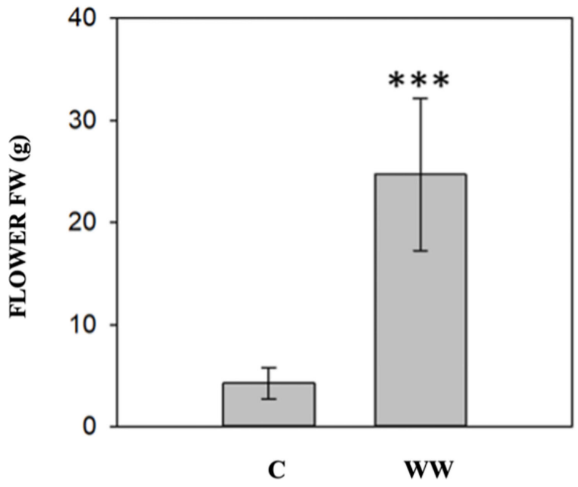

FIGURE 2
Flower fresh weight (FW) of *Nicotiana tabacum* irrigated with tap water (C) and with HTL-WW (WW) at the end of the experiment (21 days). Test-t ($p<0.05$) was performed to identify significant differences between the treatments (*** = $p<0.001$).

3.3 Microbial taxonomic composition

To evaluate any alteration in the microbial communities' structure after the HTL-WW irrigation treatment, the relative abundances of bacterial and fungal taxa were determined at phyla and family level.

3.3.1 Bacteria

In total, fifteen different bacterial phyla were detected in the soil samples with a relative abundance > 0.1%. Proteobacteria and Actinobacteria were the taxa which heavily dominated the bacterial composition of tobacco rhizosphere. These phyla together accounted for approximately from 63% to 90% of the total bacterial biodiversity in

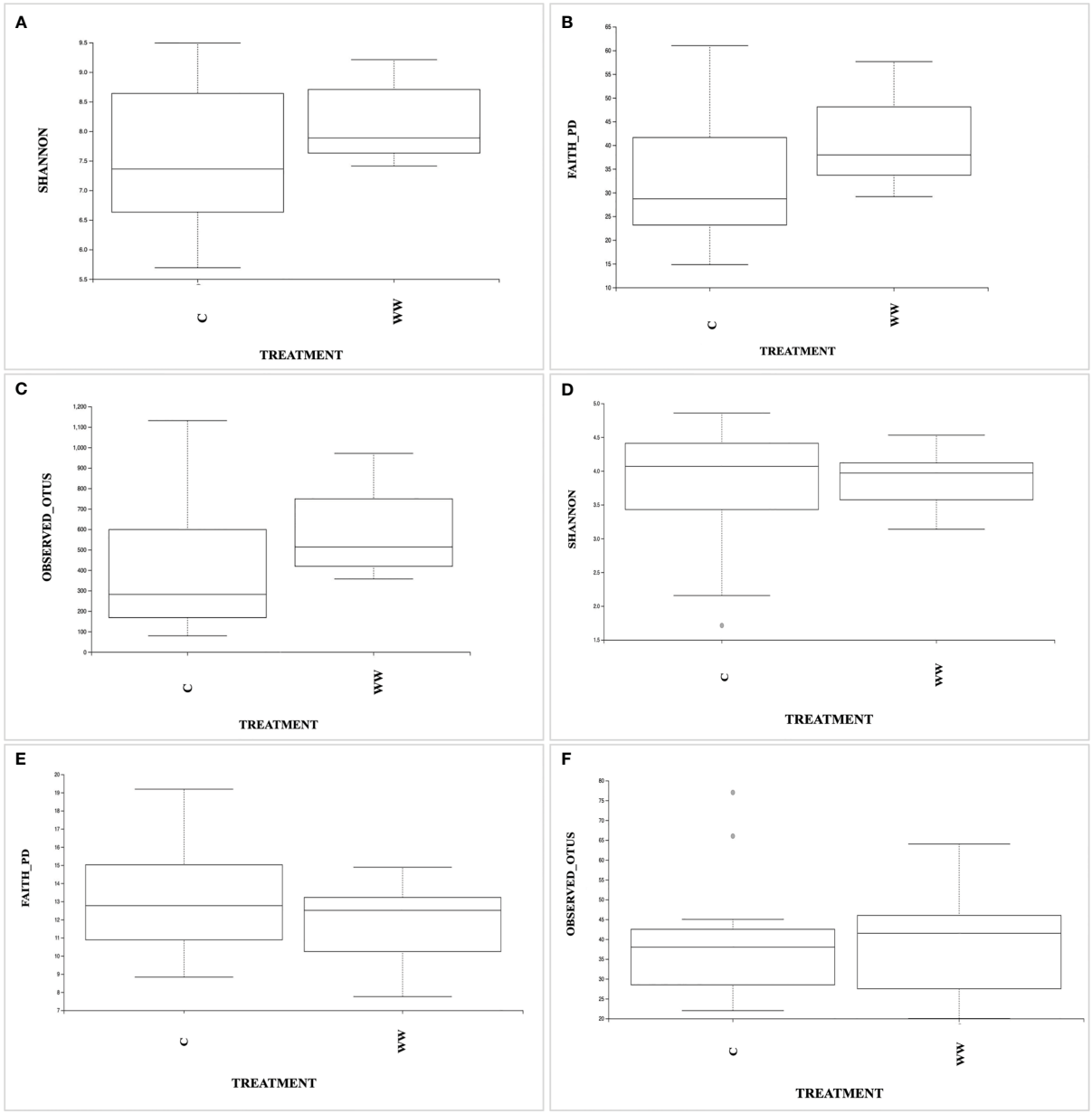

FIGURE 3
The box plots showing Shannon diversity, Faith's Philogenetic Diversity, and Observed OTUs indices based on prokaryotic **(A–C)** and eukaryotic **(D–F)** communities in the rhizosphere samples irrigated with HTL-WW (WW) and tap water (C).

the rhizosphere of plants treated and untreated with HTL-WW. Additionally, Acidobacteria, Armatimonadetes, Bacteroidetes, Chlorobi, Choroflexi, Cyanobacteria, Firmicutes, Gemmatimonadetes, Nitrospirae, Planctomycetes, and Verrucomicrobia, along with candidate phylum OD1 and TM7 showed a relative abundance > 0.1% in at least one sample (Figure 5A).

The relative frequency of Proteobacteria was enough uniform in function of the experimental sampling time in both treated and untreated plants, whereas Actinobacteria showed a different trend. In particular, the concentration of this phylum was constant in the rhizosphere of control plants irrigated with tap water (range of relative abundance: 31-34%), with a peak at day 14 (43%). Conversely, in the rhizosphere of tobacco plants treated with HTL-WW a constant increase was observed over time, from about 34% at the beginning of the experiment (WW_T0) to 48% after 21 days of treatment (WW_T21) (Figure 5A). The other abundant phyla showed a different trend between the samples treated and untreated with wastewater. In fact, while Chloroflexi exhibited a similar relative abundance in all the samples, Acidobacteria, Gemmatimonadetes and Planctomycetes were mainly present in the rhizosphere of the control plants irrigated with tap water; while Firmicutes, Bacteroidetes and the candidate phylum TM7 showed a higher relative abundance in the rhizosphere of plants irrigated with HTL-WW (Figure 5A).

The microbial diversity was also analysed at a deeper taxonomic level. In particular, the analysis of the sequences at family level,

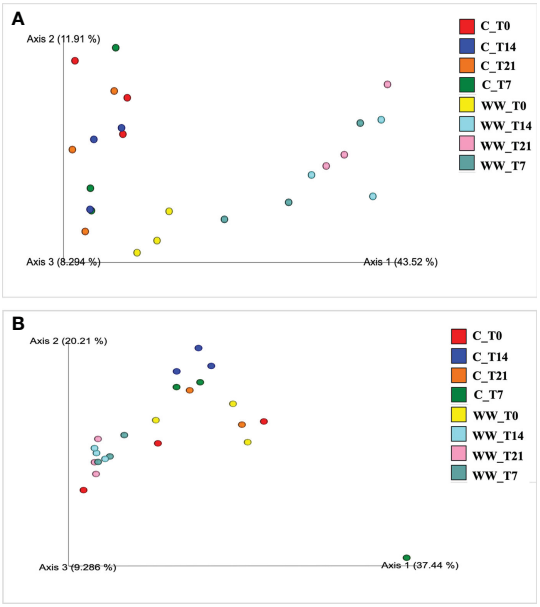

FIGURE 4
Principal Coordinates Analysis (PCoA) of weighted UniFrac distances of prokaryotic **(A)** and eukaryotic **(B)** communities of tobacco rhizosphere. WW_T0, plants irrigated with HTL-WW at time 0; WW_T7, plants irrigated with HTL-WW after 7 days; WW_T14, plants irrigated with HTL-WW after 14 days; WW_T21, plants irrigated with HTL-WW after 21 days; C_T0, plants irrigated with tap water at time 0; C_T7, plants irrigated with tap water after 7 days; C_T14, plants irrigated with tap water after 14 days; C_T21, plants irrigated with tap water after 21 days.

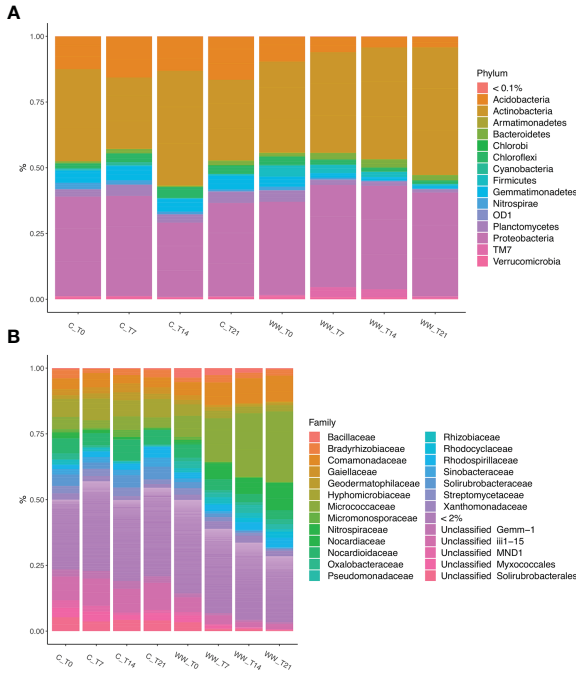

FIGURE 5
Relative abundance of bacterial phyla **(A)** and families **(B)** in the rhizosphere of *Nicotiana tabacum* L. plants treated (WW) and untreated (C) with HTL-WW. Only phyla with an abundance > 0.1% or families with an abundance > 2% in at least one sample are shown in the legend. WW_T0, plants irrigated with HTL-WW at time 0; WW_T7, plants irrigated with HTL-WW after 7 days; WW_T14, plants irrigated with HTL-WW after 14 days; WW_T21, plants irrigated with HTL-WW after 21 days; C_T0, plants irrigated with tap water at time 0; C_T7, plants irrigated with tap water after 7 days; C_T14, plants irrigated with tap water after 14 days; C_T21, plants irrigated with tap water after 21 days.

considering only those with an abundance > 2% in at least one sample, allow to identify 20 bacterial families and 5 unclassified taxa (Figure 5B). These taxa showed a different relative abundance depending on the time and on the type of water used for irrigation (HTL-WW or tap water). Micrococcaceae and Nocardiaceae were most abundant in the wastewater treated (WW) rhizosphere. In detail, the relative abundance of Micrococcaceae was on average about 4% in the control samples (C), while in the treated rhizospheres there was a constant increase from 8% at the beginning of the experiment (WW_T0) up to 27% after 21 days of irrigation (WW_T21; Figure 5B). Nocardiaceae was almost totally absent in the rhizosphere of control plants, while it showed a relative abundance of at least 4% in the rhizosphere of plants treated with HTL-WW, especially at the end of the experiment after 21 days of irrigation (WW_T21) constituting about 13-14% of the total bacterial biodiversity (Figure 5B). Bacillaceae and Pseudomonaceae exhibited different behaviour. In fact, although these two families were present mainly in the rhizosphere of plants treated with wastewater, they decreased over time from 3-6% at the beginning of the experiment (WW_T0) to about 0.8-0.2% at day 21 (WW_T21; Figure 5B). Although Comamonadaceae was recovered in all samples, its relative abundance increased over time in the wastewater treated rhizosphere. Differently, Solirubrobacteraceae, Gaiellaceae and Sinobacteraceae were more abundant in the rhizosphere of control plants, and they decreased over time in the rhizosphere of HTL-WW treated plants (Figure 5B).

3.3.2 Fungi

The phylum-level taxonomic analysis of the fungal community showed that Ascomycota and Basidiomycota dominated in all samples (WW and C), accounting for > 90% of the total biodiversity in each sample (Figure 6A), followed by Chytridiomycota and Mortierellomycota. Ascomycota and Basidiomycota exhibited different pattern in the treated and untreated rhizosphere. In fact, while Ascomycota was mainly present in the rhizosphere of HTL-WW treated plants, Basidiomycota showed a greater relative abundance in the rhizosphere of control plants irrigate with tap water (Figure 6A).

The analysis of the relative abundance of fungal families present in the tobacco rhizosphere samples with an abundance >1% in at least one sample, allowed to identify 11 fungal families (Aspergillaceae, Bionectriaceae, Chaetomiaceae Diatrypaceae, Entolomataceae, Hypocreaceae, Microascaceae, Mortierellaceae, Nectriaceae, Sporormiaceae and Trichocomaceae) which accounted for >70% of the total biodiversity, together with taxa belonging to different families without taxonomic assignment or identified only at higher taxonomic level such as Onygenales_fam_Incertae_sedis, Saccharomycetales_incertae_sedis, and unclassified Agaricomycetes, Hypocreales and Sordariomycetes (Figure 6B). As observed for the bacterial community, the fungal taxa were differentially present

10.3389/fpls.2023.1180061

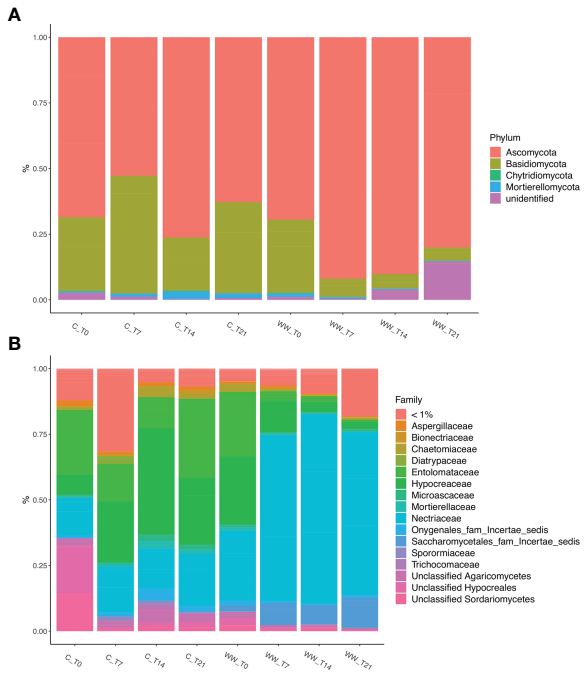

FIGURE 6
Relative abundance of fungal phyla **(A)** and families **(B)** in the rhizosphere of *Nicotiana tabacum* L. plants treated (WW) and untreated **(C)** with HTL-WW. Only families with an abundance > 1% in at least one sample are shown in the legend. WW_T0, plants irrigated with HTL-WW at time 0; WW_T7, plants irrigated with HTL-WW after 7 days; WW_T14, plants irrigated with HTL-WW after 14 days; WW_T21, plants irrigated with HTL-WW after 21 days; C_T0, plants irrigated with tap water at time 0; C_T7, plants irrigated with tap water after 7 days; C_T14, plants irrigated with tap water after 14 days; C_T21, plants irrigated with tap water after 21 days.

depending on the time and type of water used for irrigation. In particular, the family Nectriaceae, belonging to the Ascomycota phylum, was more abundant in the HTL-WW treated rhizosphere (WW) and increased over time. In detail, the relative abundance of Nectriaceae was on average <25% in the control samples (C), while in the treated rhizosphere there was a constant increase from about 25% at the beginning of the experiment (WW_T0) to about 53% after 21 days of irrigation (WW_T21; Figure 6B). On the contrary, Entolomataceae, belonging to *Basidiomycota* phylum, was more abundant in control samples, although in treated rhizo-soils was present at the beginning of experiment (WW_T0) and gradually decreased until it disappeared at day 21 (Figure 6B).

3.4 Functional prediction analysis

Functional profiles were predicted based on the 16S rRNA gene sequencing data to assess differences between HTL-WW treated and non-treated tobacco rhizosphere. Although this analysis allowed us to analyse over 6000 functional genes, predicted abundances of some interesting enzyme-encoding genes associated with plant growth-promoting traits and soil fertility were reported (Figures 7, 8). In detail, analysis focused on functional genes involved in nitrogen fixation as well as 1-aminocyclopropane-1-carboxylic acid (ACC) deaminase, aminopeptidase, and glucanase activities.

Functional profiles of the bacterial communities were clustered into two major groups clearly associated to the wastewater treatment (Figures 7, 8). Cluster 1 included samples treated with HTL-WW after 7, 14, and 21 days (WW_T7, WW_T14, and WW_T21, respectively); whereas cluster 2 grouped untreated samples (C_T0, C_T7, C_T14, and C_T21) as well as treated samples at the beginning of the experiment (WW_T0). Several predicted functions, including endoglucanase (EC:3.2.1.4), leucyl aminopeptidase (EC:3.4.11.1), aminopeptidase N (EC:3.4.11.2), Xaa-Pro aminopeptidase (EC:3.4.11.9), methionyl aminopeptidase (EC:3.4.11.18), D-aminopeptidase (EC:3.4.11.19) (Figure 7), as well as nitrogen fixation proteins *Nif*B and *Nif*U, the nitrogen fixation regulation protein CRP/FNR family transcriptional regulator and ACC-deaminase (EC:3.5.99.7) (Figure 8), seems to play a discriminating role in the overall system. In particular, from day 7 until the end of the experiment, predicted abundances of genes for aminopeptidase N (EC:3.4.11.2) and endoglucanase (EC:3.2.1.4) increased in the samples treated with HTL-WW (Figure 7). In contrast, untreated samples show higher levels of D-aminopeptidase (EC:3.4.11.19) and leucyl aminopeptidase (EC:3.4.11.1) (Figure 7).

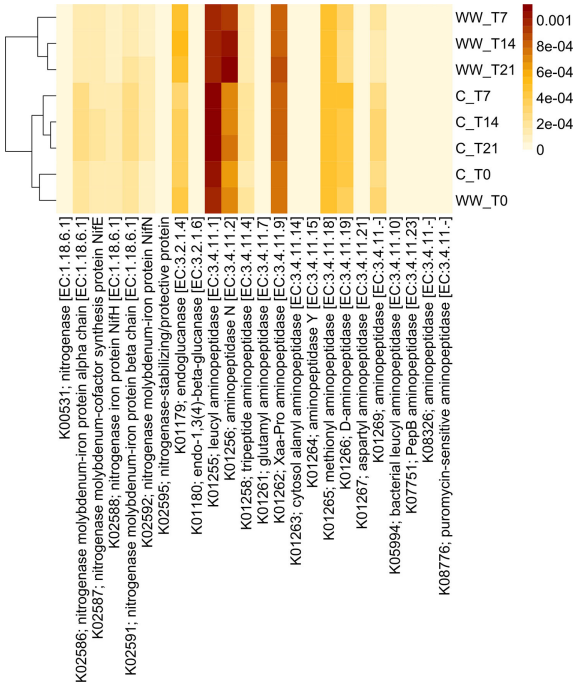

FIGURE 7
Predicted abundances of enzyme-encoding aminopeptidase, nitrogenase and glucanase genes. The colour code refers to gene abundance, with high predicted abundances (brown) and low predicted abundances (light yellow). WW_T0, plants irrigated with HTL-WW at time 0; WW_T7, plants irrigated with HTL-WW after 7 days; WW_T14, plants irrigated with HTL-WW after 14 days; WW_T21, plants irrigated with HTL-WW after 21 days; C_T0, plants irrigated with tap water at time 0; C_T7, plants irrigated with tap water after 7 days; C_T14, plants irrigated with tap water after 14 days; C_T21, plants irrigated with tap water after 21 days.

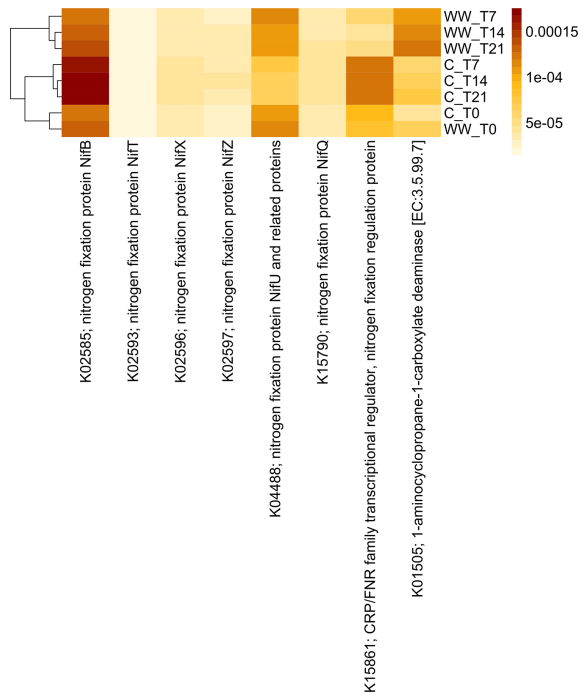

FIGURE 8
Predicted abundances of enzyme-encoding genes involved in the nitrogen fixation and ACC deaminase genes. The colour code refers to gene abundance, with high predicted abundances (brown) and low predicted abundances (light yellow). WW_T0, plants irrigated with HTL-WW at time 0; WW_T7, plants irrigated with HTL-WW after 7 days; WW_T14, plants irrigated with HTL-WW after 14 days; WW_T21, plants irrigated with HTL-WW after 21 days; C_T0, plants irrigated with tap water at time 0; C_T7, plants irrigated with tap water after 7 days; C_T14, plants irrigated with tap water after 14 days; C_T21, plants irrigated with tap water after 21 days.

However, predicted abundances of some enzyme-encoding nitrogenase genes showed that although *Nif*B and the nitrogen-fixing transcriptional regulator of the CRP/FNR family were present in all rhizosphere samples, their predicted abundance increased in untreated samples from 7 to 21 days (C_T7, CT14 and C_T21; Figure 8). Whereas the nitrogen fixation protein *Nif*U remained constant in HTL-WW treated rhizosphere (WW_T0, WW_T7, WW_T14 and WW_T21) and decreased over time in the control samples (C_T7, CT14 and C_T21; Figure 8). Finally, the predicted abundance of ACC-deaminase increased in all tobacco rhizosphere samples, especially in HTL-WW treated samples (WW_T7, WW_T14 and WW_T21; Figure 8).

4 Discussion

The use of wastewater is gaining increasing interest to meet agricultural irrigation needs and to face the increase of population growth and climate change. Although it was reported that wastewater may deliver nutrients and organic matter to the soil (Ungureanu et al., 2020), its composition could have an impact on the microbial communities that contribute to the soil biological fertility, with variable consequences on plant growth and development. In this context, the potential use of hydrothermal liquefaction wastewater (HTL-WW) for irrigation of agricultural crops was explored.

HTL-WW irrigation improved plant chlorophyll content and increased the flower biomass in tobacco plants (Figure 2 and Table 2). These results can be respectively associated with high levels of nitrogen, phosphorus, and potassium as well as macro-nutrients such as sulphates, calcium and magnesium contained in the HTL-WW (Table 1) since it is reported their involvement in flowering of different plants (Patel et al., 2006; Erel et al., 2008; Ye et al., 2019) and in chlorophyll content (Wang et al., 2021; Zhang et al., 2021). The tobacco plants treated with HTL-WW have not shown symptoms of heavy metals stress confirming that the concentrations of heavy metals were under harmful levels and anyhow below the official admitted thresholds. The impact of this wastewater on autochthonous microbiota of bulk-soil and rhizosphere was assessed over time using metagenomic approach and bioinformatic tools.

High-throughput sequencing was used to obtain an assessment of the effect of the HTL-WW treatment on resident soil microbial community in the rhizosphere of tobacco. Beta diversity analysis of rhizosphere-associated microbiota demonstrated a shift in the microbial structure especially for bacterial community. In fact, the PCoA exhibited two distinct groups based on water treatments. This behaviour could be due to the different adaptation mechanisms used by several microbial groups to survive and grow under these environmental conditions resulting in a new balance among microbial populations. However, this effect could be temporary. As reported by Frenk et al. (2013) initial variations observed in the soil microbial structure following municipal wastewater irrigation disappeared after three years of treatment suggesting that autochthonous microbiota shown a natural resilience to anthropogenic soil perturbations.

A highly complex bacterial community was also found in the tobacco rhizosphere treated with HTL-WW, in which among the most frequently occurring bacteria were those belonging to Proteobacteria and Actinobacteria. These phyla have been previously reported as dominant populations in the rhizosphere of crops grown in hydroponics and natural environments (Bulgarelli et al., 2013; Sheridan et al., 2017). Several members belonging to the phylum Proteobacteria possess specific genes involved in plant growth-promotion activities (PGP) and can contribute, both by direct and indirect mechanisms, to the development of plants of agricultural interest (Ventorino et al., 2007; Ventorino et al., 2014; Romano et al., 2020b). Although our data did not show significant growth improvements, an increased SPAD levels and flowers number upon treatment with HTL-WW were consistent with possible beneficial effects of Proteobacteria on the overall plant performance. While the relative abundance of Proteobacteria was enough uniform over time in both treated and untreated rhizosphere, the Actinobacteria showed a different trend. In details, the abundance of this phylum remained constant in untreated rhizosphere, whereas it increased over time in HTL-WW treated plants. Members belonging to phylum Actinobacteria are able to synthetize specific hydrolytic enzymes for efficiently decomposition of a wide variety of recalcitrant organic materials

as well as to assimilate inorganic nitrogen (Ventorino et al., 2013; Pennacchio et al., 2018; Ventorino et al., 2019). In addition, this microbial group included species that can synthesize plant growth promoting substances and increase nutrient availability and uptake to/by plants as well as exert suppressive effects vs. plant soil-borne pathogens (Chouyia et al., 2020; Fagnano et al., 2020; Di Mola et al., 2021; Chouyia et al., 2022). Once again, the abundance of these bacterial populations was consistent with the high biological fertility potential of treated rhizosphere as demonstrated by a generally enhanced plant performance. Among Actinobacteria, Micrococcaceae and Nocardiaceae were the more abundant bacterial families in the rhizosphere of tobacco HTL-WW treated plants. Micrococcaceae is a well-known stress-tolerant bacterial taxon which has a bioremediation potential as production of bioactive compounds (Caradonia et al., 2019), degradation of phenanthrene, cellobiose and glucose (Li et al., 2019), tolerance to drought and salinity stress (Munoz-Ucros et al., 2021) as well as to heavy metals (Xi et al., 2021). Micrococcaceae is also studied for its plant growth promoting activities such as synthesis of the 1-aminocyclopropane-1-carboxylic acid (ACC) deaminase, indole-3-acetic acid (IAA) and siderophores as well as phosphorus solubilisation even in arid environments (Yang et al., 2019). The high abundance of this taxon in the treated tobacco rhizosphere could be due to the excess of different nitrogen compounds introduced to the soil through HTL-WW or some organic acids (Xi et al., 2021). The use of N by Micrococcaceae, and most likely other bacteria and/or fungi, could explain the missing growth effects on plants treated with HTL-WW, since only a part of its N content was available for plant growth. Moreover, since many species belonging to the Micrococcaceae family are halotolerant, their abundance could have increased because of them ability to tolerate high level of Na^+ and Cl^- present in HTL-WW (Mishra et al., 2018). An increased population of halotolerant bacteria, including also Comamonadaceae family belonging to the Proteobacteria phylum, in the rhizosphere may have had protective effects on plants, a concentration that would be harmful for tobacco and other plants, did not show any stress symptoms. Protective effects of stress tolerant bacteria on plant growth have been documented in tomato and spinach rhizosphere (Ibekwe et al., 2017; Van Oosten et al., 2018).

Nocardiaceae, together Bacillaceae and Pseudomonaceae, are the bacterial taxa present only in the treated rhizosphere. The most abundant family was Nocardiaceae, which play an important ecological role in nature in the recycling of organic matter and recovery oil-contaminated environments as biosurfactant producers. This taxon has also a great potential for plant growth-promotion potential and biocontrol of different plant diseases (Yang et al., 2019). Nocardiaceae are recently detected in the rhizosphere of different crops as well as in activated sludge, wastewater, digestate and hydrocarbon polluted soils (Ali et al., 2021).

Bacillaceae and Pseudomonaceae were also present mainly in the rhizosphere of plants treated with HTL-WW, although their abundance decreased over time. Members belonging to these bacterial families include many rhizobacteria which are able to promote plant growth through various mechanisms, including phosphate solubilization and synthesis of phytohormones (Shrivastava et al., 2018), as well as to exert a biocontrol action against various soil borne plant pathogens (Beneduzi et al., 2012). Furthermore, many species belonging to the Bacillaceae family could degrade cellulose, hemicellulose, pectin, and lignin (Di Pasqua et al., 2014), suggesting their possible involvement in the degradation and mineralization of organic and humic compounds in the soil.

According to Lüneberg et al. (2019) Ascomycota and Basidiomycota dominated in most agricultural soil. These phyla constituted the key primary decomposers of soil organic matter, and they are among drivers in regulating the ecosystem functions. Most members belonging to these phyla are saprotrophic fungi that participated in critical processes, such as the decomposition and mineralization of recalcitrant and labile compounds as well as xenobiotic substances (Yang et al., 2022). Ascomycota, previously described as sensitive to high nitrogen, phosphorous and carbon inputs (Chen et al., 2017), did not seem to be affected by the higher nutrient levels of HTL-WW vs. control water. Within this phylum, Nectriaceae was the most abundant family in treated samples. This result was consistent with those of Lüneberg et al. (2019), who also reported this fungal taxon as the most abundant in a field irrigated with untreated wastewater. The Nectriaceae family has also a key role in the nitrogen bioremediation (Cheng et al., 2020) in N-rich environments, such as the soil irrigated with HTL-WW. The fungal families selected only in treated tobacco rhizosphere were Saccharomycetales-incertae-sedis and Trichocomaceae, belonged to phyla of Ascomycota and Basidiomycota respectively. Furthermore, Saccharomycetales-incertae-sedis and Trichocomaceae are both involved in bioremediation of heavy metals, especially cadmium, lead, chromium, nickel, copper, and manganese (Malikula et al., 2022). Thus, as mentioned before, these fungal families may have protected the plants by degrading the heavy metals introduced with HTL-WW.

The study of the potential bacterial activities is fundamental to establish new agricultural practices as the use of HTL-WW for irrigation purposes. In this context, differences in bacterial functioning between HTL-WW treated and non-treated tobacco rhizosphere were investigated based on predicted abundances of enzyme-encoding genes involved in plant growth promotion, soil fertility and suppression disease such as nitrogen fixation, ACC deaminase, aminopeptidase, and glucanase (Hong and Meng, 2003; Fiorentino et al., 2016; Norman et al., 2020; Orozco-Mosqueda et al., 2020; Romano et al., 2020b). The clustering of predicted functions demonstrated that potential gene abundances were strongly affected by water treatment since two major clusters were observed clearly associated to the HTL-WW treatment. Shift in microbial community structure was also previously observed when different wastewaters, as household, industrial, or olive mill, were used for plant irrigation (Zhao et al., 2014; Giagnoni et al., 2016; Krause et al., 2020). Changes in the rhizosphere microbial community could be due to modifications of root exudates resulting from the high amount of nutrients and the different nitrogen forms introduced by wastewater as well as by the C/N ratio. The shift in microbial community structure could also be attributed to the high availability and quality of the carbon sources supplied by wastewater irrigation. Indeed, following the use of carbon-rich wastewater as HTL-WW, the presence of easily degradable carbon compounds could stimulate the growth of copiotrophic as well as of cellulolytic microorganisms

(Marschner et al., 2003), as also confirmed by the increasing of predicted abundance of endoglucanases following wastewater treatment. In addition, bacterial endoglucanases confer a competitive advantage against soil-borne plant pathogens and therefore, their presence could be considered as a mechanism to improve plant resistance to biotic stress (Hong and Meng, 2003). HTL-WW irrigation increased also the predicted abundance of ACC-deaminase; an enzyme produced by some plant growth-promoting microbes to alleviate negative effects due to ethylene production. Synthesis of ACC deaminase could also improve plant tolerance to several abiotic or biotic stress, such as drought, salinity, and high temperature (del Carmen Orozco-Mosqueda et al., 2020; Romano et al., 2020b).

The predicted abundances of genes encoding aminopeptidase N and nitrogen fixation protein NifU increased or remained constant in HTL-WW treated samples. These predicted bacterial functions could help to increase soil fertility and enhance plant growth, since aminopeptidases producing bacteria can degrade proteins from soil organic matter increasing amino acid availability in the near-cell environment (Norman et al., 2020), as well as nitrogen-fixers can supply plants with this essential nutrient and improving soil fertility (Fiorentino et al., 2016).

5 Conclusion

Although the use of industrial wastewater to satisfy crop water requirements could have several economic and environmental advantages, the response of the soil microbiota to different wastewater sources must be ascertain on a case-by-case basis, since this may critically affect the overall soil biological fertility. This work improves the knowledge about the responses of indigenous microbial populations to anthropogenic activities, particularly related to the potential ecological risks of using untreated industrial wastewater derived from hydrothermal liquefaction process (HTL-WW) for irrigation purposes and the capacity of natural ecosystems to develop an adapted microbiota, ultimately leading to the establishment of a new microbial community affecting the soil fertility properties.

Based on the results obtained in this study, the wastewater from the hydrothermal liquefaction of organic wastes could be an important source of irrigation water which could contribute to reduce the increasing pressure on freshwater resources. However, further specific investigations will be necessary to assess the long-term impact of this untreated industrial wastewater on soil biological fertility and possible critical effects on the biogeochemical cycles of relevant soil nutrients.

Data availability statement

The datasets presented in this study can be found in online repositories. The names of the repository/repositories and accession number(s) can be found below: https://www.ncbi.nlm.nih.gov/, PRJNA939137.

Author contributions

WG carried out the experiments and drafted the manuscript. VC performed agronomic analyses and analysed the results for the part. AM reviewed and edited the manuscript. IR performed functional prediction analysis and drafted the manuscript for this part. VV reviewed and edited the manuscript, conceived the concepts of the study and participated in its design. OP reviewed the manuscript and contributed to its conceiving. All authors have read and approved the final manuscript.

Funding

WG was supported by a PhD fellowship from ENI S.p.A. provided within the PhD program on Sustainable Agricultural and Forestry Systems and Food Security of the University of Naples Federico II. The funder was not involved in the study design, collection and interpretation of data, the writing of this article or the decision to submit it for publication.

Acknowledgments

We would like to thank Dr. Bianchi Daniele (Eni S.p.A.) for editorial assistance and comments regarding hydrothermal liquefaction (HTL) technology.

Conflict of interest

The authors declare that the research was conducted in the absence of any commercial or financial relationships that could be construed as a potential conflict of interest.

Publisher's note

References

Ali, M., Walait, S., Farhan Ul Haque, M., and Mukhtar, S. (2021). Antimicrobial activity of bacteria associated with the rhizosphere and phyllosphere of *Avena fatua* and *Brachiaria reptans*. *Environ. Sci. pollut. Res.* 28, 68846–68861. doi: 10.1007/s11356-021-15436-7

Beneduzi, A., Ambrosini, A., and Passaglia, L. M. (2012). Plant growth-promoting rhizobacteria (PGPR): their potential as antagonists and biocontrol agents. *Genet. Mol. Biol.* 35, 1044–1051. doi: 10.1590/s1415-47572012000600020

Bokulich, N. A., and Mills, D. A. (2013). Improved selection of internal transcribed spacer specific primers enables quantitative, ultra-high-throughput profiling of fungal communities. *Appl. Environ. Microbiol.* 79, 2519–2526. doi: 10.1128/AEM.03870-12

Bolyen, E., Rideout, J. R., Dillon, M. R., Bokulich, N. A., Abnet, C. C., Al-Ghalith, G. A., et al. (2019). Reproducible, interactive, scalable and extensible microbiome data science using QIIME 2. *Nat. Biotechnol.* 37, 852–857. doi: 10.1038/s41587-019-0209-9

Bulgarelli, D., Schlaeppi, K., Spaepen, S., Van Themaat, E. V. L., and Schulze-Lefert, P. (2013). Structure and functions of the bacterial microbiota of plants. *Annu. Rev. Plant Biol.* 64, 807–838. doi: 10.1146/annurev-arplant-050312-120106

Callahan, B. J., McMurdie, P. J., Rosen, M. J., Han, A. W., Johnson, A. J. A., and Holmes, S. P. (2016). DADA2: high-resolution sample inference from illumina amplicon data. *Nat. Methods* 13, 581–583. doi: 10.1038/nmeth.3869

Caradonia, F., Battaglia, V., Righi, L., Pascali, G., and La Torre, A. (2019). Plant biostimulant regulatory framework: prospects in Europe and current situation at international level. J. *Plant Growth Regul.* 38, 438–448. doi: 10.1007/s00344-018-9853-4

Chen, Y. L., Xu, T. L., Veresoglou, S. D., Hu, H. W., Hao, Z. P., Hu, Y. J., et al. (2017). Plant diversity represents the prevalent determinant of soil fungal community structure across temperate grasslands in northern China. *Soil Biol. Biochem.* 110, 12–21. doi: 10.1016/j.soilbio.2017.02.015

Cheng, H., Xu, A., Kumar Awasthi, M., Kong, D., Chen, J., Wang, Y., et al. (2020). Aerobic denitrification performance and nitrate removal pathway analysis of a novel fungus *Fusarium solani* RADF-77. *Bioresour. Technol.* 295, 122250. doi: 10.1016/j.biortech.2019.122250

Chouyia, F. E., Romano, I., Fechtali, T., Fagnano, M., Fiorentino, N., Visconti, D., et al. (2020). P-solubilizing *Streptomyces roseocinereus* MS1B15 with multiple plant growth-promoting traits enhance barley development and regulate rhizosphere microbial population. *Front. Plant Sci.* 11. doi: 10.3389/fpls.2020.01137

Chouyia, F. E., Ventorino, V., and Pepe, O. (2022). Diversity, mechanisms and beneficial features of phosphate-solubilizing *Streptomyces* in sustainable agriculture: a review. *Front. Plant Sci.* 13. doi: 10.3389/fpls.2022.1035358

Di Mola, I., Ventorino, V., Cozzolino, E., Ottaiano, L., Romano, I., Duri, L. G., et al. (2021). Biodegradable mulching vs traditional polyethylene film for sustainable solarization: chemical properties and microbial community response to soil management. *Appl. Soil Ecol.* 163, 103921. doi: 10.1016/j.apsoil.2021.103921

Di Pasqua, R., Ventorino, V., Aliberti, A., Robertiello, A., Faraco, V., Viscardi, S., et al. (2014). Influence of different lignocellulose sources on endo-1, 4-β-glucanase gene expression and enzymatic activity of *Bacillus amyloliquefaciens* B31C. *BioResources* 9, 1303–1310. doi: 10.15376/biores.9.1.1303-1310

EPA – United States Environmental Protection Agency (2021). Available at: https://www.epa.gov/waterreuse/basic-information-about-water-reuse#basics (Latest accession: August 19, 2022).

Erel, R., Dag, A., Ben-Gal, A., Schwartz, A., and Yermiyahu, U. (2008). Flowering and fruit set of olive trees in response to nitrogen, phosphorus, and potassium. *J. Am. Soc Hortic. Sci.* 133, 639–647. doi: 10.21273/JASHS.133.5.639

Fagnano, M., Agrelli, D., Pascale, A., Adamo, P., Fiorentino, N., Rocco, C., et al. (2020). Copper accumulation in agricultural soils: risks for the food chain and soil microbial populations. *Sci. Total Environ.* 734, 139434. doi: 10.1016/j.scitotenv.2020.139434

Fiorentino, N., Ventorino, V., Bertora, C., Pepe, O., Moschetti, G., Grignani, C., et al. (2016). Changes in soil mineral n content and abundances of bacterial communities involved in n reactions under laboratory conditions as predictors of soil n availability to maize under field conditions. *Biol. Fertil. Soils* 52, 523–537. doi: 10.1007/s00374-016-1095-7

Food and Agriculture Organization – FAO (2022) *Wastewater treatment and reuse in agriculture*. Available at: https://www.fao.org/land-water/water/water-management/wastewater/en/ (Accessed November 27, 2022).

Frenk, S., Hadar, Y., and Minz, D. (2013). Resilience of soil bacterial community to irrigation with water of different qualities under Mediterranean climate. *Environ. Microbiol* 16, 559–569. doi: 10.1111/1462-2920.12183

Giagnoni, L., Pastorelli, R., Mocali, S., Arenella, M., Nannipieri, P., and Renella, G. (2016). Availability of different nitrogen forms changes the microbial communities and enzyme activities in the rhizosphere of maize lines with different nitrogen use efficiency. *Appl. Soil Ecol.* 98, 30–38. doi: 10.1016/j.apsoil.2015.09.004

Gu, Y., Zhang, X., Deal, B., and Han, L. (2019). Biological systems for treatment and valorization of wastewater generated from hydrothermal liquefaction of biomass and systems thinking: a review. *Bioresour. Technol.* 278, 329–345. doi: 10.1016/j.biortech.2019.01.127

Hong, T. Y., and Meng, M. (2003). Biochemical characterization and antifungal activity of an endo-1,3-β-glucanase of paenibacillus sp. isolated from garden soil. *Appl. Microbiol. Biotechnol.* 61, 472–478. doi: 10.1007/s00253-003-1249-z

Ibekwe, A. M., Ors, S., Ferreira, J., Liu, X., and Suarez, D. (2017). Seasonal induced changes in spinach rhizosphere microbial community structure with varying salinity and drought. *Sci. Total Environ.* 579, 1485–1495. doi: 10.1016/j.scitotenv.2016.11.151

Jaramillo, M., and Restrepo, I. (2017). Wastewater reuse in agriculture: a review about its limitations and benefits. *Sustainability* 9, 1734. doi: 10.3390/su9101734

Karimi, B., Maron, P., Chemidlin-Prevost Boure, N., Bernard, N., Gilbert, D., and Ranjard, L. (2017). Microbial diversity and ecological networks as indicators of environmental quality. *Environ. Chem. Lett.* 15, 265–281. doi: 10.1007/s10311-017-0614-6

Kjeldahl, C. (1883). A new method for the determination of nitrogen in organic matter. *J. Anal. Chem.* 22, 366–382. doi: 10.1007/BF01338151

Klindworth, A., Pruesse, E., Schweer, T., Peplies, J., Quast, C., Horn, M., et al. (2013). Evaluation of general 16S ribosomal RNA gene PCR primers for classical and next-generation sequencing-based diversity studies. *Nucleic Acids Res.* 41, e1. doi: 10.1093/nar/gks808

Kolde, R. (2019). *Pheatmap: pretty heatmaps* (R package version 1.0.12). Available at: https://CRAN.R-project.org/package=pheatmap.

Krause, S., Dohrmann, A., Gillor, O., Christensen, B., Merbach, I., and Tebbe, C. (2020). Soil properties and habitats determine the response of bacterial communities to agricultural wastewater irrigation. *Pedosphere* 30, 146–158. doi: 10.1016/S1002-0160(19)60821-0

Li, J., Luo, C., Zhang, D., Cai, X., Jiang, L., Zhao, X., et al. (2019). Diversity of the active phenanthrene degraders in PAH-polluted soil is shaped by ryegrass rhizosphere and root exudates. *Soil Biol Biochem* 128, 100–110. doi: 10.1016/j.soilbio.2018.10.008

Lozupone, C., Hamady, M., and Knight, R. (2006). UniFrac–an online tool for comparing microbial community diversity in a phylogenetic context. *BMC Bioinf.* 7, 1–14. doi: 10.1038/nmeth.3869

Lüneberg, K., Schneider, D., Brinkmann, N., Siebe, C., and Daniel, R. (2019). Land use change and water quality use for irrigation alters drylands soil fungal community in the mezquital valley, Mexico. *Front. Microbiol.* 10. doi: 10.3389/fmicb.2019.01220

Malikula, R., Kaonga, C., Mapoma, H., Thulu, F., and Chiipa, P. (2022). Heavy metals and nutrients loads in water, soil, and crops irrigated with effluent from WWTPs in Blantyre city, Malawi. *Water* 14, 121. doi: 10.3390/w14010121

Marschner, P., Kandeler, E., and Marschner, B. (2003). Structure and function of the soil microbial community in a long-term fertilizer experiment. *Soil Biol. Biochem.* 35, 453–461. doi: 10.1016/S0038-0717(02)00297-3

McMurdie, P. J., and Holmes, S. (2013). Phyloseq: an r package for reproducible interactive analysis and graphics of microbiome census data. *PloS One* 8, e61217. doi: 10.1371/journal.pone.0061217

Mishra, A., Jha, G., and Thakur, I. S. (2018). Draft genome sequence of zhihengliuella sp. strain ISTPL4, a psychrotolerant and halotolerant bacterium isolated from pangong lake, India. *Genome Announc.* 6, e01533–e01517. doi: 10.1128/genomeA.01533-17

Muamar, A., Tijane, M. H., Shawqi, E., El Housni, A., Zouahri, A., and Bouksaim, M. (2014). Assessment of the impact of wastewater use on soil properties. *J. Mater. Environ. Sci.* 5, 747–752.

Munoz-Ucros, J., Wilhelm, R. C., Buckley, D. H., and Bauerle, T. L. (2021). Drought legacy in rhizosphere bacterial communities alters subsequent plant performance. *Plant Soil* 471, 443–461. doi: 10.1007/s11104-021-05227-x

Norman, J. S., Smercina, D. N., Hileman, J. T., Tiemann, L. K., and Friesen, M. L. (2020). Soil aminopeptidase induction is unaffected by inorganic nitrogen availability. *Soil Biol. Biochem.* 149, 107952. doi: 10.1016/j.soilbio.2020.107952

Orozco-Mosqueda, M. D. C., Glick, B. R., and Santoyo, G. (2020). ACC deaminase in plant growth-promoting bacteria (PGPB): an efficient mechanism to counter salt stress in crops. *Microbiol. Res.* 235, 126439. doi: 10.1016/j.micres.2020.126439

Patel, M. M., Parmar, P. B., and Parmar, B. R. (2006). Effect of nitrogen, phosphorus and spacing on growth and flowering in tuberose (*Polianthes tuberosa* linn.) cultivar single. *J. Ornam. Hortic.* 9, 286–289.

Pennacchio, A., Ventorino, V., Cimini, D., Pepe, O., Schiraldi, C., Inverso, M., et al. (2018). Isolation of new cellulase and xylanase producing strains and application to lignocellulosic biomasses hydrolysis and succinic acid production. *Bioresour. Technol.* 259, 325–333. doi: 10.1016/j.biortech.2018.03.027

Petousi, I., Daskalakis, G., Fountoulakis, M., Lydakis, D., Fletcher, L., Stentiford, E., et al. (2019). Effects of treated wastewater irrigation on the establishment of young grapevines. *Sci. Total Environ.* 658, 485–492. doi: 10.1016/j.scitotenv.2018.12.065

Posmanik, R., Labatut, R. A., Kim, A. H., Usack, J. G., Tester, J. W., and Angenent, L. T. (2017). Coupling hydrothermal liquefaction and anaerobic digestion for energy valorization from model biomass feedstocks. *Bioresour. Technol.* 233, 134–143. doi: 10.1016/j.biortech.2017.02.095

Romano, I., Ventorino, V., Ambrosino, P., Testa, A., Chouyia, F. E., and Pepe, O. (2020b). Development and application of low-cost and eco-sustainable bio-stimulant containing a new plant growth-promoting strain *Kosakonia pseudosacchari* TL13. *Front. Microbiol.* 11. doi: 10.3389/fmicb.2020.02044

Romano, I., Ventorino, V., and Pepe, O. (2020a). Effectiveness of plant beneficial microbes: overview of the methodological approaches for the assessment of root colonization and persistence. *Front. Plant Sci.* 11. doi: 10.3389/fpls.2020.00006

Sheridan, C., Depuydt, P., De Ro, M., Petit, C., Van Gysegem, E., Delaere, P., et al. (2017). Microbial community dynamics and response to plant growth-promoting microorganisms in the rhizosphere of four common food crops cultivated in hydroponics. *Microb. Ecol.* 73, 378–393. doi: 10.1007/s00248-016-0855-0

Shrivastava, M., Srivastava, P.C., and D'Souza, S.F. (2018). "Phosphate-solubilizing microbes: Diversity and phosphates solubilization mechanism", in: Role of Rhizospheric Microbes in Soil, ed. V. Meena, V.. (Singapore: Springer), 136–165. doi: 10.1007/978-981-13-0044-8_5

Sofroniou, A., and Bishop, S. (2014). Water scarcity in Cyprus: a review and call for integrated policy. *Water* 6, 2898–2928. doi: 10.3390/w6102898

UNEP Food Waste Index report (2021). Available at: https://www.unep.org/resources/report/unep-food-waste-index-report-2021 (Accessed February 27, 2023).

Ungureanu, N., Vlăduț, V., and Voicu, G. (2020). Water scarcity and wastewater reuse in crop irrigation. *Sustainability* 12, 9055. doi: 10.3390/su12219055

United Nations Educational, Scientific and Cultural Organization – UNESCO (2021) *The united nations world water development report 2021*. Available at: https://unesdoc.unesco.org/ark:/48223/pf0000375751 (Accessed March 2, 2022).

Van Oosten, M. J., Di Stasio, E., Cirillo, V., Silletti, S., Ventorino, V., Pepe, O., et al. (2018). Root inoculation with *Azotobacter chroococcum* 76A enhances tomato plants adaptation to salt stress under low n conditions. *BMC Plant Biol.* 18, 1–12. doi: 10.1186/s12870-018-1411-5

Ventorino, V., Chiurazzi, M., Aponte, M., Pepe, O., and Moschetti, G. (2007). Genetic diversity of a natural population of *Rhizobium leguminosarum* bv. *viciae* nodulating plants of *Vicia faba* in the vesuvian area. *Curr. Microbiol.* 55, 512–517. doi: 10.1007/s00284-007-9024-5

Ventorino, V., Parillo, R., Testa, A., Aliberti, A., and Pepe, O. (2013). Chestnut biomass biodegradation for sustainable agriculture. *BioResources* 8, 4647–4658. doi: 10.15376/biores.8.3.4647-4658

Ventorino, V., Pascale, A., Adamo, P., Rocco, C., Fiorentino, N., Mori, M., et al. (2018). Comparative assessment of autochthonous bacterial and fungal communities and microbial biomarkers of polluted agricultural soils of the Terra dei fuochi. *Sci. Rep.* 8, 14281. doi: 10.1038/s41598-018-32688-5

Ventorino, V., Pascale, A., Fagnano, M., Adamo, P., Faraco, V., Rocco, C., et al. (2019). Soil tillage and compost amendment promote bioremediation and biofertility of polluted area. *J. Clean. Prod.* 239, 118087. doi: 10.1016/j.jclepro.2019.118087

Ventorino, V., Sannino, F., Piccolo, A., Cafaro, V., Carotenuto, R., and Pepe, O. (2014). *Methylobacterium populi* VP2: plant growth-promoting bacterium isolated from a highly polluted environment for polycyclic aromatic hydrocarbon (PAH) biodegradation. *Sci. World J.* 2014, 931793. doi: 10.1155/2014/931793

Wang, N., Fu, F., Wang, H., Wang, P., He, S., Shao, H., et al. (2021). Effects of irrigation and nitrogen on chlorophyll content, dry matter and nitrogen accumulation in sugar beet (*Beta vulgaris* l.). *Sci. Rep.* 11, 16651. doi: 10.1038/s41598-021-95792-z

Wang, X.-B., Hsu, C.-M., Dubeux, J. C. B.Jr., Mackowiak, C., Blount, A., Han, X.-G., et al. (2019). Effects of rhizoma peanut cultivars (*Arachis glabrata* benth.) on the soil bacterial diversity and predicted function in nitrogen fixation. *Ecol. Evol.* 9, 12676–12687. doi: 10.1002/ece3.5735

Xi, B., Yu, H., Li, Y., Dang, Q., Tan, W., Wang, Y., et al. (2021). Insights into the effects of heavy metal pressure driven by long-term treated wastewater irrigation on bacterial communities and nitrogen-transforming genes along vertical soil profiles. *J. Hazard. Mater.* 403, 123853. doi: 10.1016/j.jhazmat.2020.123853

Yang, R., Liu, G., Chen, T., Li, S., An, L., Zhang, G., et al. (2019). Characterization of the genome of a *Nocardia* strain isolated from soils in the qinghai-Tibetan plateau that specifically degrades crude oil and of this biodegradation. *Genomics* 111, 356–366. doi: 10.1016/j.ygeno.2018.02.010

Yang, S., Wu, H., Wang, Z., Semenov, M. V., Ye, J., Yin, L., et al. (2022). Linkages between the temperature sensitivity of soil respiration and microbial life strategy are dependent on sampling season. *Soil Biol. Biochem.* 172, 108758. doi: 10.1016/j.soilbio.2022.108758

Ye, T., Li, Y., Zhang, J., Hou, W., Zhou, W., Lu, J., et al. (2019). Nitrogen, phosphorus, and potassium fertilization affects the flowering time of rice (*Oryza sativa* l.). *Glob. Ecol. Conserv.* 20, e00753. doi: 10.1016/j.gecco.2019.e00753

Zhang, H., Zhao, Q., Wang, Z., Wang, L., Li, X., Fan, Z., et al. (2021). Effects of nitrogen fertilizer on photosynthetic characteristics, biomass, and yield of wheat under different shading conditions. *Agronomy* 11, 1989. doi: 10.3390/agronomy11101989

Zhao, S., Liu, D., Ling, N., Chen, F., Fang, W., and Shen, Q. (2014). Bio-organic fertilizer application significantly reduces the *Fusarium oxysporum* population and alters the composition of fungi communities of watermelon *Fusarium* wilt rhizosphere soil. *Biol. Fertil. Soils* 50, 765–774. doi: 10.1007/s00374-014-0898-7

Zucchinelli, M., Spinelli, R., Corrado, S., and Lamastra, L. (2021). Evaluation of the influence on water consumption and water scarcity of different healthy diet scenarios. *J. Environ. Manage.* 291, 112687. doi: 10.1016/j.jenvman.2021.112687

frontiers | Frontiers in Plant Science

TYPE Original Research
PUBLISHED 04 August 2023
DOI 10.3389/fpls.2023.1223720

OPEN ACCESS

EDITED BY
Long Yang,
Shandong Agricultural University, China

REVIEWED BY
Yangwenke Liao,
Nanjing Forestry University, China
Mohamed Mannaa,
Cairo University, Egypt

*CORRESPONDENCE
Shilin Chen
slchen@icmm.ac.cn
Zhixiang Liu
zhixiangliu88@cdutcm.edu.cn

RECEIVED 16 May 2023
ACCEPTED 18 July 2023
PUBLISHED 04 August 2023

CITATION
Liu C, Yu J, Ying J, Zhang K, Hu Z, Liu Z and Chen S (2023) Integrated metagenomics and metabolomics analysis reveals changes in the microbiome and metabolites in the rhizosphere soil of *Fritillaria unibracteata*.
Front. Plant Sci. 14:1223720.
doi: 10.3389/fpls.2023.1223720

Integrated metagenomics and metabolomics analysis reveals changes in the microbiome and metabolites in the rhizosphere soil of *Fritillaria unibracteata*

Chengcheng Liu[1,2], Jingsheng Yu[2,3], Jizhe Ying[1], Kai Zhang[1], Zhigang Hu[1], Zhixiang Liu[2]* and Shilin Chen[1,2,3]*

[1]College of Pharmacy, Hubei University of Chinese Medicine, Wuhan, China, [2]Institute of Herbgenomics, Chengdu University of Traditional Chinese Medicine, Chengdu, China, [3]Institute of Chinese Materia Medica, China Academy of Chinese Medical Sciences, Beijing, China

Fritillaria unibracteata (FU) is a renowned herb in China that requires strict growth conditions in its cultivation process. During this process, the soil microorganisms and their metabolites may directly affect the growth and development of FU, for example, the pathogen infection and sipeimine production. However, few systematic studies have reported the changes in the microbiome and metabolites during FU cultivation thus far. In this work, we simultaneously used metagenomics and metabolomics technology to monitor the changes in microbial communities and metabolites in the rhizosphere of FU during its cultivation for one, two, and three years. Moreover, the interaction between microorganisms and metabolites was investigated by co-occurrence network analysis. The results showed that the microbial composition between the three cultivation-year groups was significantly different (2020-2022). The dominant genera changed from *Pseudomonas* and *Botrytis* in CC1 to *Mycolicibacterium* and *Pseudogymnoascus* in CC3. The relative abundances of beneficial microorganisms decreased, while the relative abundances of harmful microorganisms showed an increasing trend. The metabolomics results showed that significant changes of the of metabolite composition were observed in the rhizosphere soil, and the relative abundances of some beneficial metabolites showed a decreasing trend. In this study, we discussed the changes in the microbiome and metabolites during the three-year cultivation of FU and revealed the relationship between microorganisms and metabolites. This work provides a reference for the efficient and sustainable cultivation of FU.

KEYWORDS

***Fritillaria unibracteata*, rhizosphere soil, metagenomics, cooccurrence analysis, metabolomics**

1 Introduction

Fritillaria is a famous medicinal genus of Liliaceae, which includes more than 150 species (Protopopova et al., 2023). Fritillariae Cirrhosae Bulbus, the dried bulb of some *Fritillaria* plants, including *Fritillaria unibracteata* (FU), has been listed as a herbal medicine in the Chinese Pharmacopoeia (2020). It shows satisfactory therapeutic effects for the treatment of cough, bronchitis, and pneumonia and has a potential role in COVID-19 treatment (Niu et al., 2021). As one of the most important medicinal plant resources of Fritillaria Cirrhosae Bulbus (Chuan Beimu in Chinese), the quality of FU has received wide attention. The growth of FU requires multiple environmental factors, including altitude, temperature, and humidity, which causes its low yield. The harsh growth environment of FU forces growers to engage in continuous cropping. However, the pests and diseases have seriously affected the production and quality of FU (He et al., 2022). After two years of cultivation, Yan et al. (2022) observed that the production of *F. thunbergii* was reduced by more than half. He et al. (2022) also indicated that the quality of *F. taipaiensis* after three years of cultivation was affected by various factors, including the accumulation of diseases, growth damage, and quality degradation. Although various scientists have proposed distinct opinions, a conclusion has been accepted regarding which microorganisms and metabolites have remarkable effects on the quality of *Fritillaria* during its cultivation.

Microorganisms are widely distributed on Earth, and make great contribution to global biomass (Banerjee and van der Heijden, 2022). As the material support for terrestrial ecosystems, soil exhibits the most microbial community diversity and complexity (Dubey et al., 2019). Rhizosphere serves as the direct interface for energy and material exchange between plant and soil, and is also the primary habitat for microorganisms (Bardgett and van der Putten, 2014). Soil microorganisms colonized plant roots through mutualism or symbiosis to form complex rhizosphere microbial communities, thus influencing plant nutrient uptake and health (Philippot et al., 2013). The rhizosphere microbiome, also known as the "second genome" of plants, has a series of beneficial functions during plant growth and development, including nutrient acquisition, pathogen resistance, and stress tolerance (Sharma et al., 2020). It has been reported that many medicinal plants could recruit specific microorganisms through root exudates to resist biotic or abiotic stress as well as assisting the production of secondary metabolites, such as *Salvia milliorrhiza*, *Cannabis sativa*, *Panax notaginseng* (Yue et al., 2019; Li et al., 2020a; Vujanovic et al., 2020). These studies demonstrated that rhizosphere microbiomes made great contributions to medicinal plants. In addition, the rhizosphere microbiome can also affect the chemical composition and secretion of roots through systematic signaling mechanisms, thereby the metabolic composition of the rhizosphere soil of plants (Korenblum et al., 2020). The soil metabolites were mainly consisted of plant root secretions and small molecules released by soil microorganisms, such as sugars, amino acids, organic acids, phenolic compounds and other secondary metabolites (Cheng et al., 2022). For example, continuous cropping, fertilizer, and pesticide application significantly altered the metabolic composition of plant rhizosphere soil soils (Ge et al., 2022; He et al., 2022; Xu et al., 2023). Therefore, it is essential and important to reveal the changes in rhizosphere soil microorganisms and metabolites during plant growth and development for guiding plant production.

In this work, we used metagenomics and metabolomics technology through the Illumina MiSeq platform combined with the LC–MS/MS detection method to monitor the changes in microbial community structure and metabolites in the rhizosphere soil of FU during its three-year cultivation process. Furthermore, the differences in soil microbial communities and metabolites between three cultivation-year groups were compared. The interaction between microorganisms and metabolites was analyzed. This study revealed the rhizosphere soil microbial structure and metabolites of FU for the first time, providing a reference for standard settings in its practical cultivation.

2 Materials and methods

2.1 Location of the experiment and collection of soil samples from the rhizosphere

The rhizosphere soil samples of FU were collected from the Lv Lin Chuan BeiMu cultivation base (28°55′ N, 102°10′ E) in Mianning County, Sichuan Province, China. The cultivation area has a subtropical climate with an altitude of up to 2800 meters (m), an annual rainfall of 1095 millimeters (mm), an annual mean air temperature of 13.8°C and an annual evaporation of 1857 mm. The soil in the experimental area is dark brown loam. The 1000-seed weight of FU was approximately 1.2 grams (g), and the seeds were sown in March 2020, 2021 and 2022. The land was in a natural fallow state before sowing, and the FU was not transplanted after sowing. After mixing 5 g of seeds with 5 kilograms of humus, the seeds were sown per square meter in the test field and finally covered with approximately 1.5 centimeters (cm) of humus. Throughout the entire growth process of FU, no fertilizers or insecticides were used, and all plots were managed in the same way. The rhizosphere soil samples of FU for three consecutive years (years one, two, and three) were sampled on October 18 and 2022 and numbered CC1, CC2 and CC3, respectively (Table 1). Each treatment consisted of three replicates. Each replicate contained 10 samples and sampling was performed using the "Z" pattern. The specific sampling method was as follows: approximately 2-3 cm of surface soil was removed with a sampling shovel to expose the *Fritillaria* bulb, and the rhizosphere soil within 0.2 cm of the bulb was carefully scooped, filtered through a 100-mesh screen, and placed in a Ziplock bag. The samples were then shipped to the laboratory in ice boxes, immersed in liquid nitrogen for at least 5 minutes, and stored at -80°C.

TABLE 1 Detailed information for *Fritillaria unibracteata* rhizosphere soil sample.

Sampling information								
Host Latin name	Cultivation year	Group	Sample id	Planting date	Sampling date	Elevation	Sampling temperature	SAMN number
Fritillaria unibracteata	one	CC1	CC1a	Mar-2020	Oct. 18, 2022	2800 meters	4°C	SAMN34413994
Fritillaria unibracteata	one		CC1b	Mar-2020	Oct. 18, 2022	2800 meters	4°C	SAMN34413995
Fritillaria unibracteata	one		CC1c	Mar-2020	Oct. 18, 2022	2800 meters	4°C	SAMN34413996
Fritillaria unibracteata	two	CC2	CC2a	Mar-2021	Oct. 18, 2022	2800 meters	4°C	SAMN34413997
Fritillaria unibracteata	two		CC2b	Mar-2021	Oct. 18, 2022	2800 meters	4°C	SAMN34413998
Fritillaria unibracteata	two		CC2c	Mar-2021	Oct. 18, 2022	2800 meters	4°C	SAMN34413999
Fritillaria unibracteata	three	CC3	CC3a	Mar-2022	Oct. 18, 2022	2800 meters	4°C	SAMN34414000
Fritillaria unibracteata	three		CC3b	Mar-2022	Oct. 18, 2022	2800 meters	4°C	SAMN34414001
Fritillaria unibracteata	three		CC3c	Mar-2022	Oct. 18, 2022	2800 meters	4°C	SAMN34414002

2.2 Determination of the physicochemical properties of the rhizosphere soil

The measurement of pH, organic matter (OM), dissolved organic carbon (DOC), cation exchange capacity (CEC), total nitrogen (TN), nitrate nitrogen (NO3-N), ammonium nitrogen (NH4-N), total phosphorus (TP), total potassium (TK), available phosphorus (AP), and available potassium (AK) in rhizosphere soils was performed as described by (Song et al., 2020).

2.3 Soil metabolome analysis

One gram of soil sample was accurately weighed and placed in a 2 ml centrifuge tube, and then 1 milliliter of aqueous methanol solution (80%, V/V, Macklin) was accurately pipetted. Then, the centrifuge tube containing the sample was placed in an ice-water mixture for 10 minutes and vortexed for 5 minutes to completely dissolve the soil sample. After dissolving, it was placed in a high-speed centrifuge at 12000 rpm, centrifuged at 4°C for 15 minutes. The supernatant was carefully aspirated and centrifuged again for 30 minutes. The supernatant was gently aspirated again, freeze dried and stored at -80°C for subsequent use. Prior to injection, the lyophilized samples were resuspended in 200 microliters of methanol, and the instruments used for LC–MS/MS analysis were a Vanquish Neo UHPLC system (Thermo Scientific) and Q Active HF-X (Thermo Scientific). The chromatographic column was a Hypseril Gold (100 × 2.1 mm, 1.9 μm, Thermo Fisher) column, and the chromatographic conditions were as follows: flow rate of 0.2 ml per minute and linear gradient elution for 12 minutes. The eluent consisted of methanol (B), an aqueous 0.1% formic acid solution (positive ion mode) and ammonium acetate at pH 9.0.

2.4 DNA extraction, library construction, and metagenomic sequencing

The extraction of DNA from 0.5 g of soil was performed using the DP336-02 TIANamp Soil DNA Kit (Omega Biotek, Inc., Norcross, GA, USA) according to the manufacturer's instructions. The concentration of soil DNA was determined using a NanoDrop 2000-UV spectrophotometer (Thermo Scientific, Waltham, MA, USA), and the quality of the DNA was examined using 1% agarose gels. A library was prepared using the NEB Next® Ultra™ DNA Library Prep Kit for Illumina (NEB, USA). Qualified DNA samples were randomly fragmented into 350 bp fragments using a Covaris (Covaris S2 System, Massachusetts,USA) ultrasonic fragmentation instrument. A complete library was constructed by terminus repair, polyA tailing, sequence linking, purification, PCR amplification and other steps. Finally, the AMPure XP system was used to purify the PCR products, an Agilent 2100 was used to determine the insert size of the library, and real-time PCR was used for quantitative analysis of the library concentration. The indexed coding samples were clustered on the cBot Cluster Generation System using the Illumina PE Cluster Kit (Illumina, USA) according to the manufacturer's instructions. After clustering, the DNA library was sequenced on the Illumina NoVaseq 6000 platform, and 150 bp paired-end reads were generated.

2.5 Statistical analysis

This experiment investigated the metabolome of the sample by LC–MS/MS. The specific procedure was as follows: (1) The original data obtained were converted to mzXML format (xcms input file format) using Proteowizard software (v3.0.8789). (2) The R (v3.1.3) XCMS package was used to perform peak identification, peak filtering, and peak alignment. (3) The mass to charge ratio (m/z), retention time, and intensity data matrix were obtained. Finally, the precursor molecules were obtained in positive and negative ion modes, and the data were exported for further analysis.

Macrogenomic analysis was performed based on sequencing reads. The original sequencing data were preprocessed using Kneaddata software to ensure data availability. The number of sequences of the species present in the sample were determined using Kraken2 and a custom microbial nucleic acid database.

Bracken was used to predict the actual relative abundance of species in the sample. The quality control and host-removed sequences were compared with the DIAMOND-based protein database UniRef using HUMAnN2 software. Based on the correspondence between UniRef ID and various databases, annotation information and relative abundance tables were obtained for each functional database.

SPSS 20.0 (IBM) was used for analysis of variance (ANOVA), and R version 4.2.2 was used for data visualization. Microbial alpha diversity was achieved using the vegan and picante packages, co-correlation analysis between microorganisms and metabolites was performed using the Igraph package and psych package. Procrustes analysis and principal coordinate analysis (PCoA) analysis were performed using the vegan package, and cluster heatmap analysis was performed using the ComplexHeatmap package. Linear discriminant analysis effect size (LEfSe) analysis was performed at https://www.bioincloud.tech. Microbial function prediction was conducted using FAPROTAX 1.2.6 software.

3 Result

3.1 Physicochemical properties of rhizosphere soil

The physicochemical properties of the rhizosphere soil during the three-year cultivation period of FU are shown in Supplementary Table 1. There was no significant difference in the contents of TK, AK, NH_4-N and DOC among the CC1, CC2 and CC3 groups. During the three years of cultivation, the pH level of the FU rhizosphere soil increased in CC2 and then decreased in CC3. Similar change trend was also observed for TN and TP, but the CC3 group was still significantly higher than the CC1 group. Notably, the AP content showed a significant increasing trend from the CC1 to CC3 groups.

3.2 Microbial diversity in various CC samples

A total of 215,662,114 raw reads were derived from 9 samples after Illumina sequencing in this study. A total of 199,835,955 clean reads were obtained after quality control, and there was sufficient sequencing depth to reflect the microbiome structure in each sample (Supplementary Table 2). The Shannon index of the bacterial community did not change significantly between the CC1 and CC2 groups but decreased significantly (4.63-4.09) in the CC3 group. No significant differences were observed in the Chao1 index of the bacterial community among the CC1, CC2 and CC3 groups (Figures 1A, B; Supplementary Table 3). The Shannon (2.13-3.14) and Chao1 (4313-10607) indices of the fungal community increased significantly in the CC3 group (Figures 2A, B; Supplementary Table 4). These results showed that the α-diversity of the bacterial community decreased significantly during FU cultivation, and the fungal community diversity and richness increased significantly.

3.3 Composition of the bacterial community in various CC samples

From the phylum to the species level, metagenomic sequencing identified 40, 63, 143, 318, 977, and 3803 taxa, respectively. A total of 749, 673, and 776 genera were detected in CC1, CC2, and CC3, respectively (Figure 1C). Proteobacteria had the highest relative abundance among all phyla, followed by Actinobacteria, Bacteroidetes, Firmicutes, and Acidobacteria (Figure 3A). During cultivation, the relative abundance of Actinobacteria increased with cultivation time, while the relative abundance of Acidobacteria decreased. Interestingly, the relative abundance of Proteobacteria and Firmicutes showed a trend of first increasing and then decreasing during the cultivation process, while the relative abundance of Bacteroidetes showed an opposite trend (decreasing first and then increasing). Actinomycetia, Corynebacteriales, and Mycobacteriaceae were dominant at the class, order, and family levels. We further analyzed the bacterial community at the genus level to better understand the changes in bacterial abundance and composition during cultivation. *Mycolicibacterium*, *Pseudomonas*, *Afipia*, *Bradyrhizobium*, and *Nocardioides* were more abundant than other genera (Figure 3B). The cluster heatmap (Supplementary Figure 1) showed that the relative abundances of some bacterial genera, such as *Afipia*, *Mycolicibacterium*, *Deinococcus*, *Rhodanobacter* and *Nitrosospira*, were higher in the CC3 group than those in the other groups. The relative abundances of *Micromonospora*, *Sphingopyxis*, *Massilia*, *Nocardioides*, *Sphingomonas* and *Ralstonia* were higher in the CC2 group, and the relative abundances of *Methylocaldum*, *Thermobifida*, *Bradyrhizobium Saccharomonospora* and *Thermomonospora* were higher in the CC1 group. The beta diversity of the bacterial community in the CC1, CC2 and CC3 groups was analyzed by PCoA (Figure 1D). PC1 explained 60.81% of the variation, while PC2 explained 28.23%. The PCoA results revealed that the three groups could be distinguished, indicating that cultivation time affected the structure of the microbial community in the rhizosphere soil of FU. This result was also supported by Bray–Curtis clustering analysis (Supplementary Figure 2). Based on LEfSe analysis, the three groups showed significantly differences in the relative abundances of bacterial species (Figure 3C; Supplementary Figure 3). Twenty-eight biomarkers were enriched across the samples with LDA scores >4. Among these biomarkers, there were seven taxa in CC3, with *Mycolicibacterium gilvum*, a rarely reported bacterium in cultivation soil, being the largest contributor. There were 11 taxa in CC2, and the major contributors were Propionibacteriales, Burkholderiales, Nocardioidaceae, Sphingomonadaceae, and *Nocardioides*. There were ten taxa in CC1, and the major contributors were Proteobacteria and *Arenimonas daejeonensis*.

3.4 Composition of the fungal community in various CC samples

From the phylum to the species level, metagenomic sequencing identified 7, 24, 60, 119, 188, and 345 taxa. There were 110, 111 and

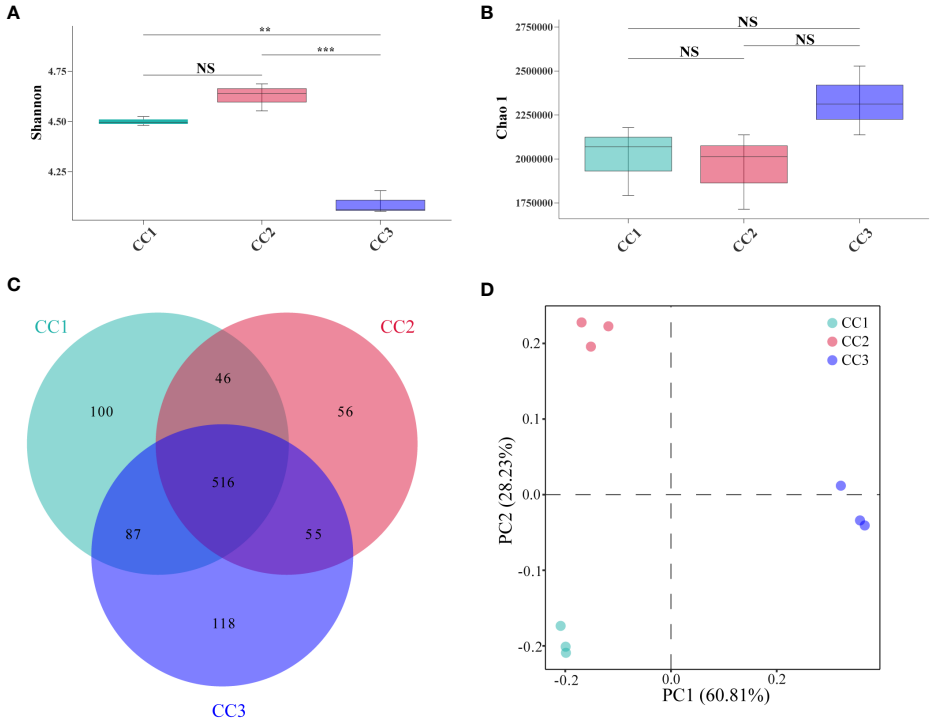

FIGURE 1
Shannon index **(A)** and Chao 1 index **(B)** of bacterial communities. Venn diagram of genera in different groups **(C)**. PCoA analysis of bacterial communities in three groups **(D)**. **Indicating very significant differences between groups, p<0.01; ***Indicating extreme significant differences between groups, p<0.001; NS indicates no significant difference between groups.

135 genera that were identified in CC1, CC2 and CC3, respectively (Figure 2C). This result indicated that cultivation increased the number of fungal genera in the rhizosphere soil of FU. The relative abundances of Ascomycota (64.02%), Mucoromycota (4.37%), and Basidiomycota (2.72%) were higher than those of other phyla. The relative abundance of Ascomycota significantly increased (13.6%-27.1%) with cultivation time, while the relative abundance of Mucoromycota decreased (Figure 4A). At the genus level, *Botrytis*, *Pseudogymnoascus*, *Cladosporium* and *Fusarium* were abundantly present in the FU samples (>2%) (Figure 4B; Supplementary Table 5). The relative abundances of these genera were higher in CC2 or CC3 than in CC1. Furthermore, the relative abundance of *Penicillium* increased significantly (2.1% - 9.9%) in CC3. The relative abundances of *Beauveria* and *Aspergillus* were higher in CC1 than in the other groups (Supplementary Figure 4). PCoA was performed based on soil fungal communities (Figure 2D). PC1 explained 45.61% of the variance, and PC2 explained 37.49% of the variance. Similar to the results of bacterial PCoA, the three groups were distinct (Supplementary Figure 2). The LEfSe analysis results showed that CC1 had the seven out of the 23 biomarkers with LDA>4, with two ubiquitous fungi, *Fusarium culmorum* and *Aspergillus fumigatus*. In addition, the beneficial fungal genus *Scedosporium* was also a biomarker of CC1. In CC2, only *Cladosporium cladosporioides* was a biomarker. There were 15 taxa in CC3, and the major contributors were Ascomycota and *Pseudogymnoascu* (Figure 4C; Supplementary Figure 3).

3.5 Potential functional pathways in FU rhizospheric soil microbes

As illustrated by the Venn diagram (Supplementary Figure 5), a total of 355 level 3 pathways were annotated in the KEGG database for all samples, of which 325, 341, and 325 pathways were detected in CC1, CC2, and CC3, respectively. Among them, there were 4, 24, and 3 unique pathways, respectively. The annotation results show that the dominant categories were Ribosome, Valine, leucine and isoleucine biosynthesis, Synthesis and degradation of ketone bodies, Lipoic acid metabolism, and Cell cycle - Caulobacter, representing 3.21%, 2.97%, 2.70%, 1.96%, and 1.91% of the total, respectively. Furthermore, among all categories, the relative abundances of genes related to the Citrate cycle (TCA cycle), Carbon fixation in photosynthetic organisms, Valine, leucine and isoleucine degradation increased during the three cultivation stages. However, the relative abundances of genes associated with Atrazine degradation, Steroid hormone biosynthesis, and Polycyclic aromatic hydrocarbon degradation decreased with the cultivation years (Supplementary Table 6). In the FAPROTAX database of microbial ecological function predictions, the annotated OTUs were assigned to 90 predicted functional groups (Supplementary Table 7). Nevertheless, in the ANOVA test, only 30 groups showed significant differences between the three compartments ($P < 0.05$). Therefore, the data were plotted as a functional heatmap (Figure 5). The results showed that the CC1 soil was enriched with the denitrification of nitrogen,

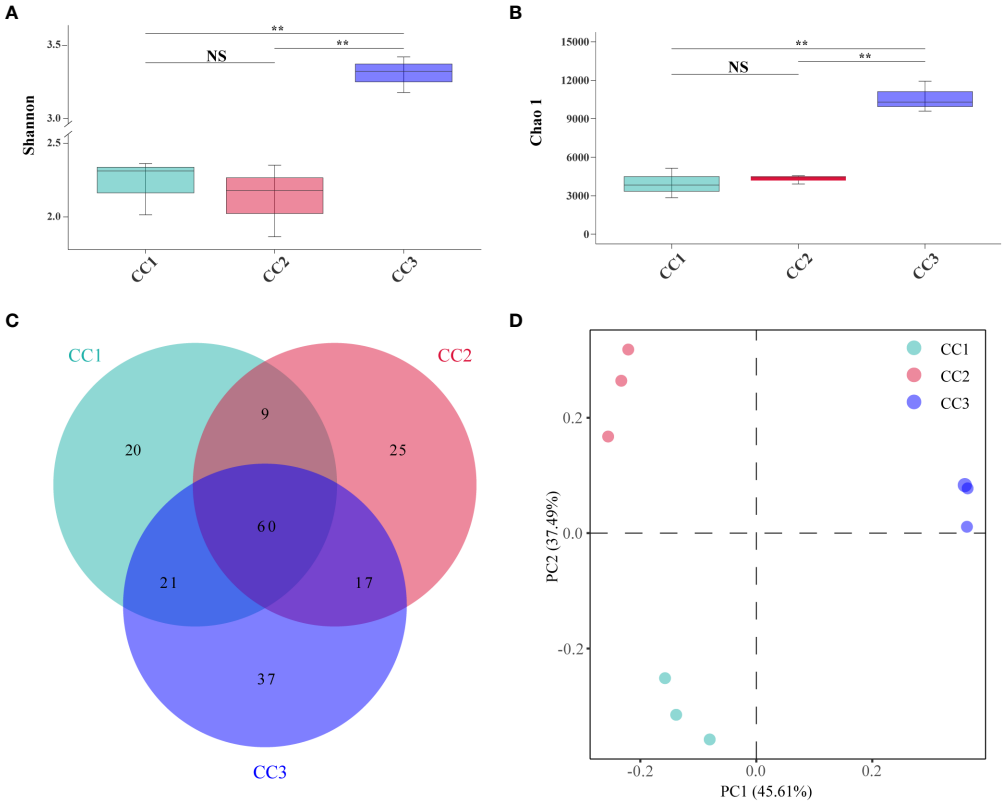

FIGURE 2
Shannon index **(A)** and Chao 1 index **(B)** of fungal communities. Venn diagram of genera in different groups **(C)**. PCoA analysis of fungal communities in three groups **(D)**. **Indicating very significant differences between groups, p<0.01; NS indicates no significant difference between groups.

methylotrophy, methylotrophy, and hydrocarbon degradation. CC2 was enriched with nitrogen respiration, nitrate respiration, and aromatic compound degradation. CC3 was enriched with nitrification, aerobic ammonia oxidation, and aromatic hydrocarbon degradation.

3.6 Analysis of nontargeted soil metabolites

In all rhizosphere soil samples, a total of 1087 compounds were detected. After annotation of br08001 in the KEGG database, 103 compounds with biological functions were obtained, among which the relative content of carbohydrates was the highest (44.16%), followed by nucleic acids (19.06%) and lipids (16.19%) (Figure 6A; Supplementary Table 8). With increasing years of cultivation, the relative content of carbohydrates in the rhizosphere soil decreased sharply, but the relative content of lipids, peptides, and steroids increased. According to the principal component analysis (Figure 6B), the CC1, CC2 and CC3 groups showed significant differences in the metabolite composition of the rhizosphere soil. PC1 accounted for 49.3% of the total variation, while PC2 accounted for 19.5%. Supplementary Figure 6 and Supplementary Table 9 list the top 20 compounds with the highest relative abundance that had biological functions. Although there was only one type of carbohydrate (sucrose), its relative abundance was indeed the highest at 29.59% and it was also one of the compounds with the most significant differences (Supplementary Table 10). This was followed by palmitic acid (19.43%), adenosine (9.97%), L-phenylalanine (8.68%) and prostaglandin J2 (2.09%). The metabolites with biological functions with the most significant differences among the three groups were screened to determine the metabolites that differed significantly among the groups, with VIP > 1 as the criterion. The top 10 metabolites with significant differences were prostaglandin E1, sucrose, cytidine, docosahexaenoic acid, palmitoleic acid, myristic acid, serotonin, L-hydroxyproline, oleic acid, and 2-deoxyuridine. The relative contents of sucrose, palmitoleic acid, myristic acid and oleic acid decreased with increasing cultivation time. The relative abundances of serotonin, L-hydroxyproline and 2-deoxyuridine increased with cultivation time. To elucidate the specific changes in soil metabolic processes, pathway enrichment analysis was performed. The metabolic pathway was the most significantly altered pathway in the rhizosphere soil, as shown in Figure 6C. Pyrimidine metabolism, unsaturated fatty acid biosynthesis, purine metabolism, fatty acid biosynthesis, and nitrogen metabolism were also significantly enriched.

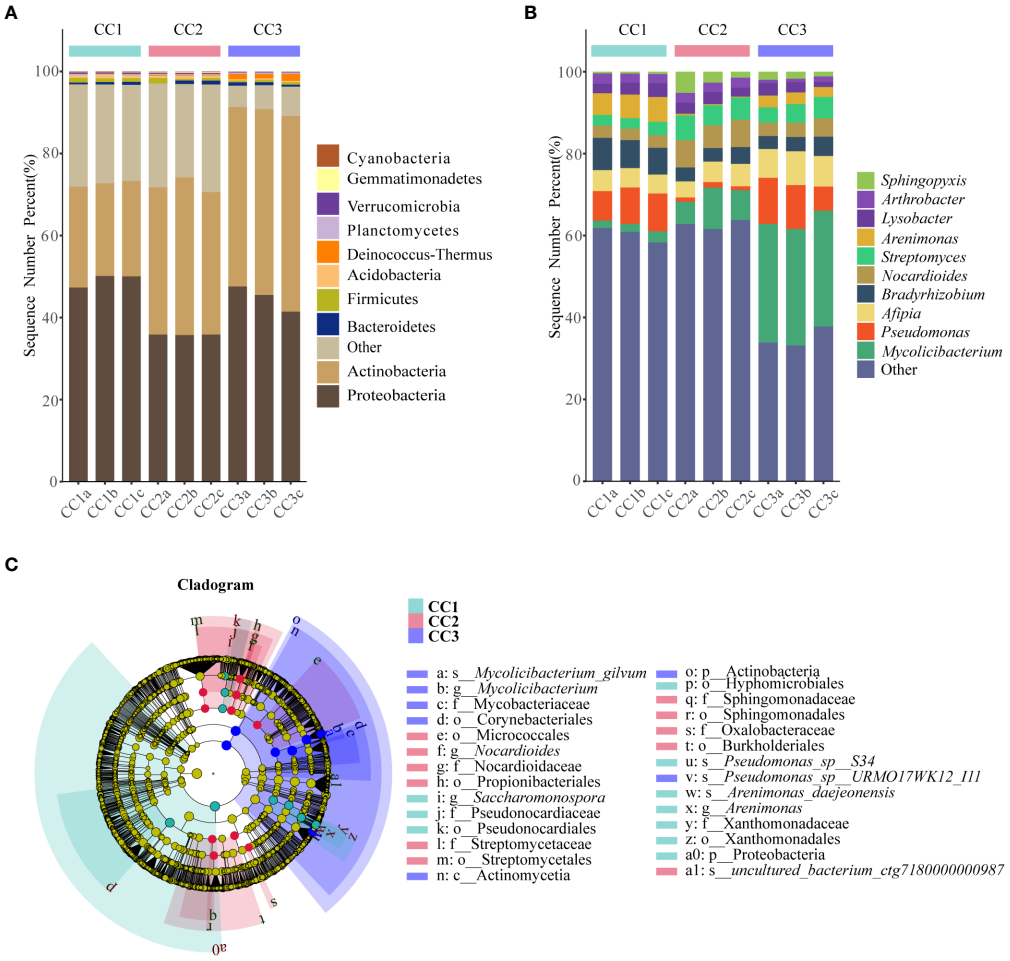

FIGURE 3
The composition of rhizosphere soil bacterial phylum **(A)** and genus **(B)** levels during FU cultivation (only Top10 is shown). Cladogram from LEfSe analysis showed changes in the abundance of bacterial at different taxonomic levels **(C)**.

3.7 Correlations between soil bacteria, fungi, and metabolism

To investigate the relationships among the bacterial groups, the fungal groups and the soil metabolites, the Bray–Curtis distance was used to perform the Procrustes analysis. The results showed that the correlation between bacterial groups and soil metabolites (Figure 7A, $M^2 = 0.02$, P=0.002) was higher than that between fungal groups and soil metabolites (Figure 7B, $M^2 = 0.05$, P=0.002). An interaction network (Figure 8) was constructed to further elucidate the relationships between differentially abundant metabolites and differentially abundant microbes in the rhizosphere. In general, the networks of metabolites or microorganisms were more positively correlated than negatively correlated. However, there was a more negative correlation between differential metabolites and differential microorganisms. For example, sucrose, palmitoleic acid and oleic acid have differential microbes. The varying sizes of soil microbial nodes indicated that these different microorganisms contributed differently to metabolism. Among the differential metabolites, L-hydroxyproline was positively correlated with the microbial genera with which it was significantly associated. The opposite was observed for myristic acid. Cytidine and docosahexaenoic acid were significantly correlated with only differentially abundant bacteria, not with differentially abundant fungi. Among the differentially abundant microbial genera, the greatest number of differentially abundant metabolites were significantly associated with the differentially abundant bacterial genus *Mycolicibacterium*, while *Saccharopolyspora* was not significantly associated with any differentially abundant metabolite. The greatest number of differentially abundant metabolites was significantly associated with the differentially abundant fungal genus *Fusarium*, while *Pochonia* and *Botrytis* were not significantly associated with any differential metabolites. Moreover, the correlation heat map analysis (Supplementary Figure 7) results showed that *Botrytis* had significant positive correlations (P<0.05) with Candidatus_*Rhabdochlamydia*, *Hymenobacter* and *Mucilaginibacter*, while it showed highly significant negative correlations (P<0.01) with *Arenimonas* and *Saccharomonospora*. *Lederbergia* and *Mycolicibacterium* showed positive correlations with almost all fungal genera. In contrast, *Saccharopolyspora* showed negative correlations with all fungal genera. We conducted a correlation heat map analysis between the microbial genus and the top 20 differential metabolites, in order to identify metabolites

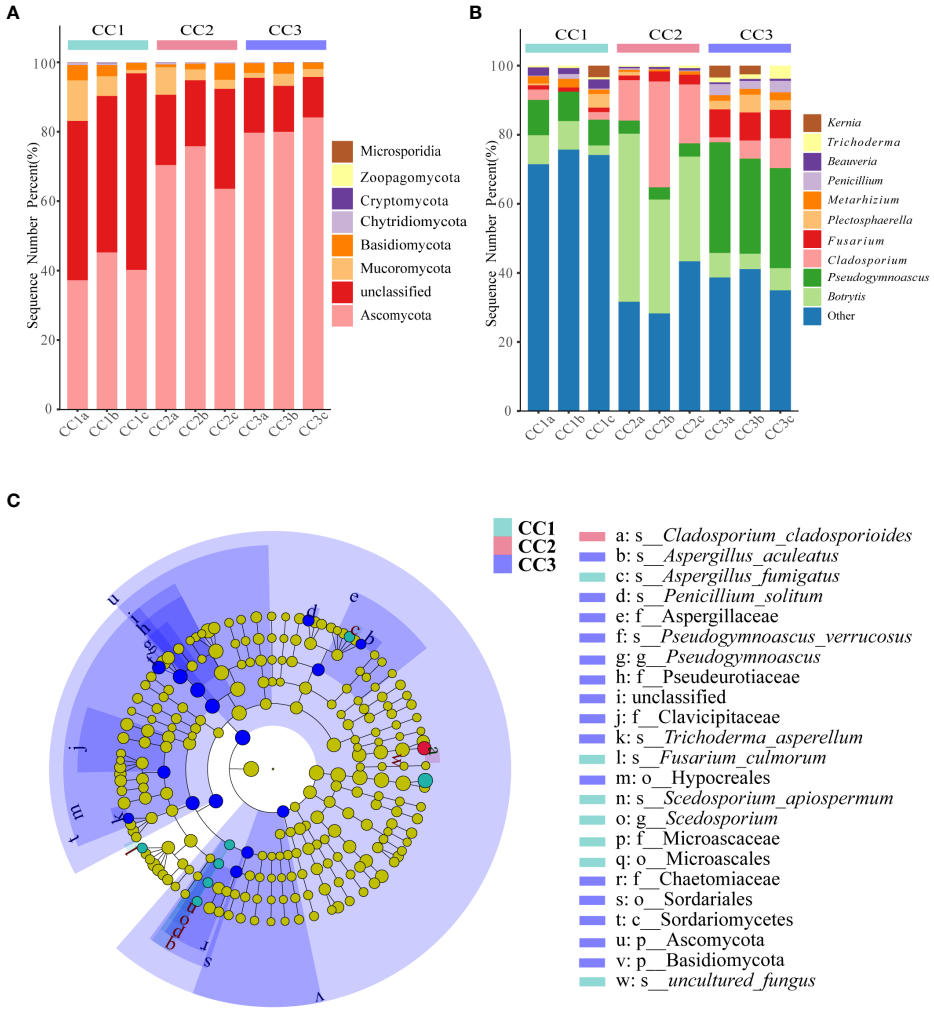

FIGURE 4
The composition of rhizosphere soil fungal phylum **(A)** and genus **(B)** levels during FU cultivation (only Top10 is shown). Cladogram from LEfSe analysis showed changes in the abundance of fungal at different taxonomic levels **(C)**.

specifically related to microorganisms (Supplementary Figure 8). Among the 30 bacterial genera with the highest degree of significant correlation with differential metabolites, all genera showed significant correlations with Prostaglandin J2, L-Glutamic acid, and Uridine, with a positive correlation exceeding a negative correlation. In addition, most bacterial counts are significantly correlated with 6-Deoxy-D-glucose, Sucrose, Adenine, and Guanine, with a positive correlation more than a negative correlation. For fungi, there is more negative correlation between fungi and metabolites than positive correlation. The metabolites most significantly associated with fungi are Prostaglandin J2 and 6-Deoxy-D-glucose, followed by L-Glutamic acid, Sucrose, and Uridine, which also have a significant correlation with the bacterial genus. From this, it can be seen that Prostaglandin J2, 6-Deoxy-D-glucose, L-Glutamic acid, Sucrose, and Uridine are specific metabolites highly associated with microorganisms during FU cultivation.

4 Discussion

4.1 Cultivation affects the structure of microbial communities and increases the relative abundance of pathogens

With the intensification of agricultural development, it is becoming increasingly common to grow the same crop continuously on the same cultivated land. Monocultures are considered likely to lead to pathogen accumulation and deterioration of soil conditions (Liu et al., 2018). Monocultures can also cause continuous cropping disorders, as observed for *Panax quinquefolius*, *Pinellia ternata*, and *Lilium lancifolium* (Dai et al., 2022; Li et al., 2022; Bi et al., 2023). The soil microbial communities and metabolites were considered non-ignorable factor that affected the plant growth and development in single cultivation

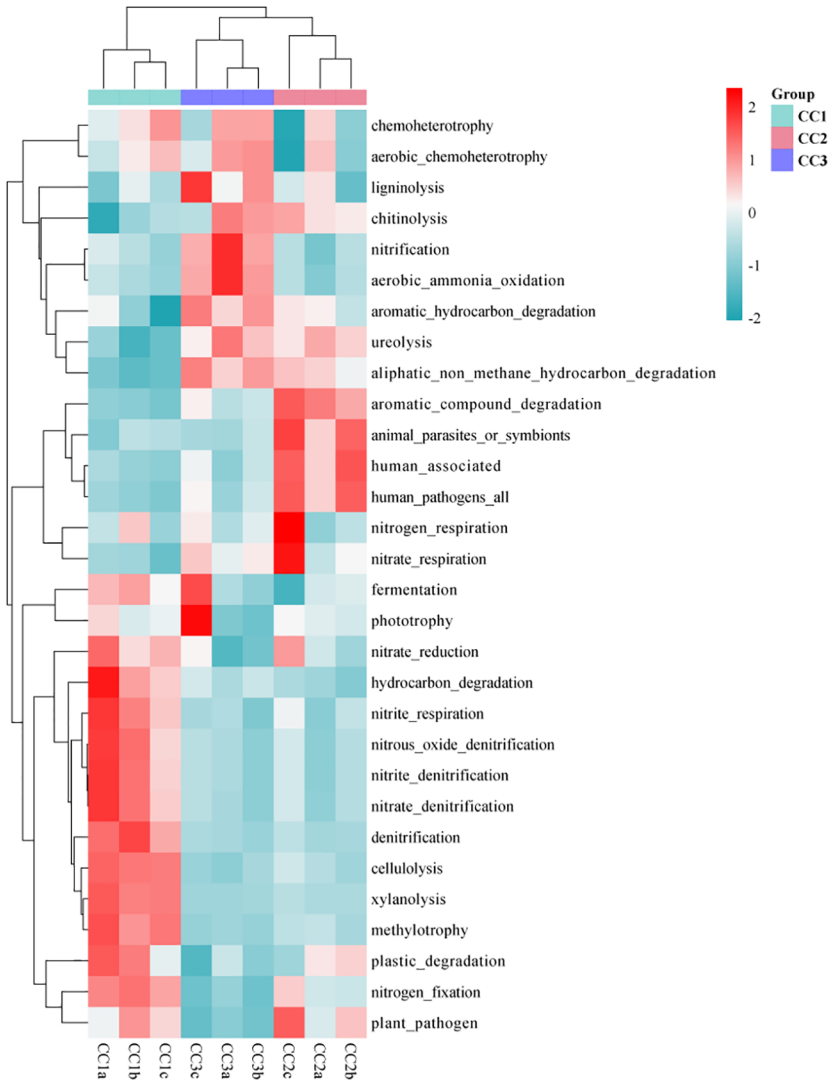

FIGURE 5
Functional heat map of microbial community in FAPROTAX database of three groups.

practices based on the previous studies (Lu et al., 2022; Zhang et al., 2022). On the one hand, rhizosphere microorganisms have the potential to assist host plants in taking up nutrients and resisting biotic/abiotic stress (Liu et al., 2020; Choi et al., 2021; Zhang et al., 2021). On the other hand, some harmful rhizosphere microorganisms can also cause adverse effects on plants, such as reduced resistance and reduced yield (Mansfield et al., 2012; Ullrich et al., 2019). Therefore, rhizosphere microorganisms play an important role in the growth and development of host plants. In this study, we applied metagenomics and metabolomics technologies to evaluate the effect of cultivation time on rhizosphere microorganisms and soil metabolites. The results showed that the alpha diversity indices of the bacterial community decreased significantly after three years of cultivation, while the alpha diversity indices of the fungal community increased significantly. This was similar to the study on continuous cultivation of ginseng conducted by Dong et al. (2018). Changing the "fungal type" was obvious, which would lead to deteriorating the soil microecological environment (Li et al., 2017). Additionally, the microbial community composition in this work was similar to that in previous reports. Proteobacteria was the most common phylum among all bacteria. During the three years of cultivation, the changes in the relative abundance of Proteobacteria showed a decreasing trend followed by an increasing trend. It was reported that these bacteria showed the ability to decompose organic matter and promote plant growth (Chaudhry et al., 2012). In addition, Actinomycetes play an important role in agriculture because they can indirectly assist plants in defending against pathogens and pests (Borah et al., 2022). Dai et al. (2018) indicated that most Actinomycetes were saprophytes, and the abundance of Actinobacteria increased in soils with long periods of intense production. Therefore, the reason for the increased relative abundance of Actinomycetes in this study might have occurred response to the increase in pathogens. To combat the accumulation of soil-borne pathogens associated with continuous crop disturbance, studies have shown that more biocontrol bacteria are

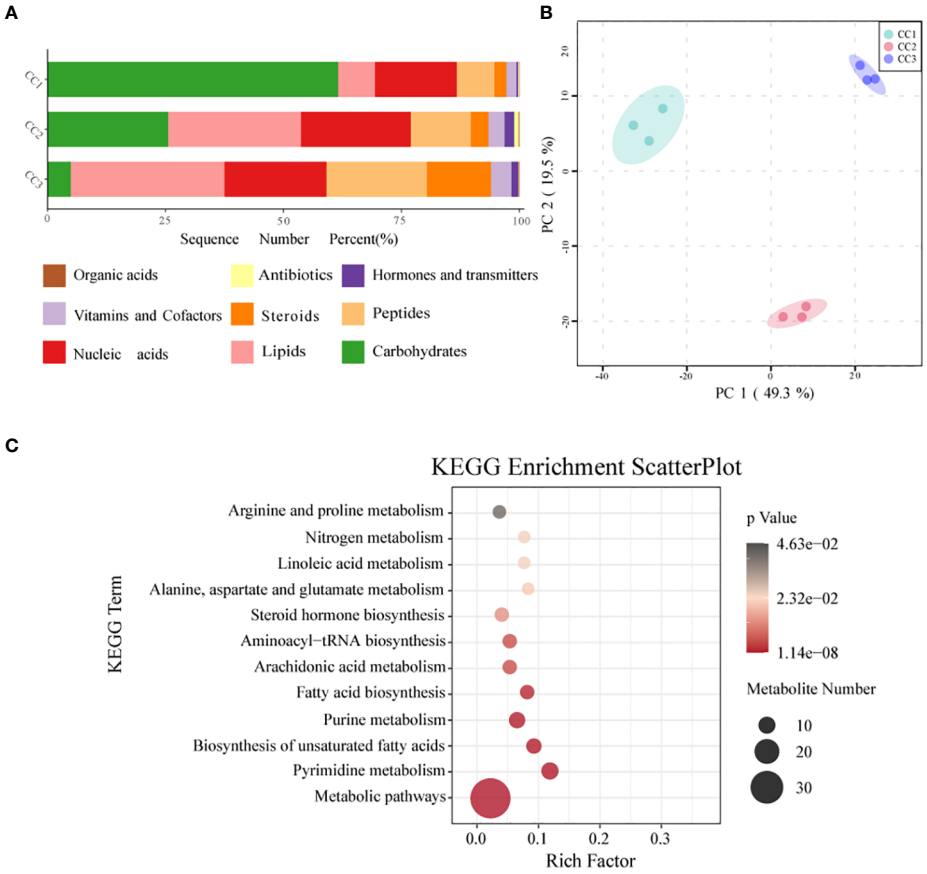

FIGURE 6
Metabonomics analysis of three groups. **(A)** Level of functional metabolite content **(B)** PCA analysis of metabolites in three groups. **(C)** KEGG pathway enrichment analysis of soil metabolic profiles. *P* <.05 indicated that the pathway was significantly enriched. The size of the bubbles and the "Numbers" legend in this image represents the amount of metabolites that are. Enriched. The size of the bubbles and the "numbers" legend in this image represents the amount of metabolites that are concentrated in this pathway.

needed to ensure plant health (Siegel-Hertz et al., 2018; Tariq et al., 2020). *Pseudomonas* species are important biocontrol bacteria of special interest for their ability to control a wide range of soil-borne plant diseases (Biessy and Filion, 2021). Interestingly, in our results, the relative abundance of *Pseudomonas* showed a decreasing trend followed by an increasing trend. However, the relative abundance of another important biotrophic fungal genus, *Streptomyces*, increased significantly with increasing years of cultivation. The relative abundance of the harmful bacterial genus *Nocardioides* gradually increased during the cultivation of FU. We speculate that *Streptomyces* may have an interactive relationship with *Nocardoides*, and *Pseudomonas* may be involved in the prevention and control of *Nocardoides* infection in the later stage. In this work, we observed that *Mycolicibacterium gilvum*, a bacterium rarely reported in cultivation soil, had a relative abundance that increased dramatically in the continuous cropping process of *FU*. This bacterial species might have the potential for application as a biocontrol agent in FU cultivation in the future. Among fungi, the relative abundance of Ascomycetes, which are sap-sucking fungi, increased. They display the ability to decay and decompose litter and are a major source of toxins that cause plant diseases. *Botrytis* species are known to cause disease in more than a thousand species of plants (Veloso and van Kan, 2018). The relative abundance of *Botrytis* in the rhizosphere soil increased significantly during the second year of FU cultivation, so the gray mold rot that *Botrytis* can induce during the second year of planting (Veloso and van Kan, 2018) should be considered. The relative abundance of other pathogenic fungal genera, *Pseudogymnoascus* and *Plectosphaerella*, increased significantly in the third year of cultivation. The relative abundance of *Fusarium*, a typical pathogenic genus, increased significantly in medicinal plant soils (Zhang et al., 2020). In summary, the structure of the microbial community in the cultivation soil of FU shifted from the bacterial type to the fungal type, and the relative abundance of the pathogens in the soil increased. Our research results can provide a reference for the efficient detection and identification of pathogenic bacteria.

4.2 Cultivation affects the composition of metabolites in FU rhizosphere soil

It is crucial to clarify how rhizosphere metabolism regulates soil-microbe–plant interactions, which could provide insight into the feedback mechanisms of different plants necessary for plant

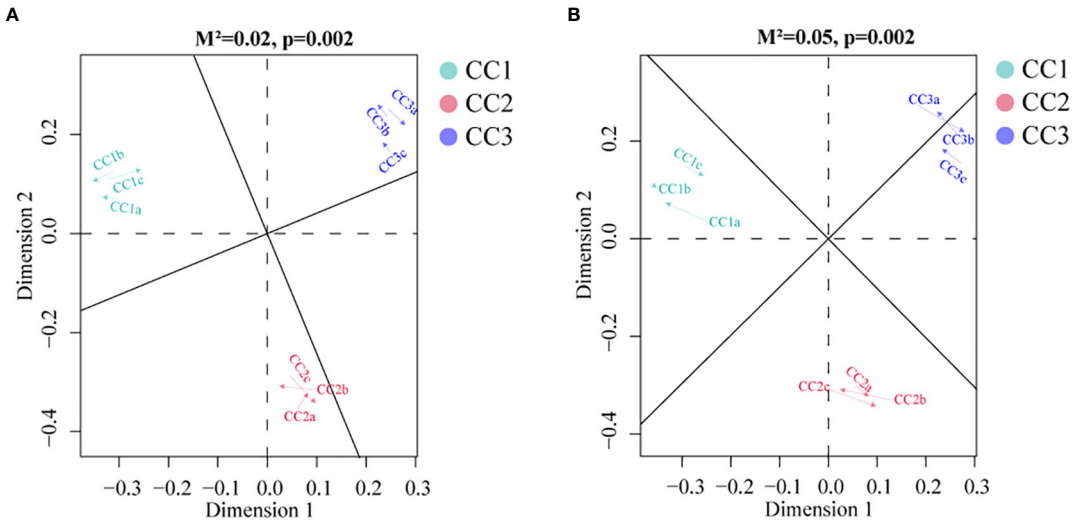

FIGURE 7
Procrustes analyses of metabolic profiles at bacterial **(A)** and fungal **(B)** taxa.

health and improved crop yields (Bi et al., 2021; Korenblum et al., 2022). The results of PCoA showed that the metabolic composition of the rhizosphere soil changed significantly during the cultivation of FU. According to the VIP and p values of OPLS-DA, significantly differently abundant metabolites were screened out. Sucrose was the most depleted metabolite. The bulbs of FU were mainly composed of carbohydrates such as starch, and sucrose conversion affects the storage of starch. This implied that a large amount of sucrose in the soil was consumed in the third year of FU cultivation to meet the needs of FU growth. In addition, green manure application significantly increased the levels of beneficial metabolites (such as sucrose) in peanut soil (Xu et al., 2023). Therefore, some organic fertilizers, such as green manure, should be applied in a timely manner during the cultivation of FU based on our study. Additionally, the relative abundances of some root secretions such as sucrose and glucose, which were considered as the nutrients and energy substances for microorganism, significantly reduced during FU cultivation (Figure 6; Supplementary Table 8). Based on the previous studies, the low level of these secretions might affect the growth and development of microorganisms that used sugars as a carbon source, such as *Thermobifida*, *Beauveria* and *Aspergillus* (Chen et al., 2006; Gultom et al., 2014; Zhou et al., 2014). Similarly, our results demonstrated that the relative abundances of these fungi were related with the sucrose and glucose level (Supplementary Figures 1, 4). In contrary, the relative abundances of two other important root secretions, nucleic and organic acids, increased during FU cultivation (Figure 6). Similar change trends were observed in the root secretions of Arabidopsis after pathogen infection (Yuan et al., 2018), suggesting that the risk of pathogen infection should be monitored during FU cultivation. As a result of the lack of phosphorus fertilizer, the abundance of organic acid abundance increased (Khorassani et al., 2011). In this study, the AP content in the rhizosphere soil continuously increased with FU cultivation, and correspondingly, the relative abundances of organic acid continued to decrease (Supplementary Table 1). The relative abundances of some microorganisms closely related to root exudates, such as *Arthrobacter*, *Bacillus*, *Azospirillum*, *Serratia*, and *Azotobacter*, exhibited a decreasing trend during FU cultivation. Previous studies have shown that they could assist plants to resist stress such as salt and alkali (Singh and Jha, 2016; Vives-Peris et al., 2020). This reminds us to provide a stable growth environment for FU in the later stage of cultivation. In recent years, much information has emerged about the antimicrobial potential of palmitoleic acid. Research has shown that palmitoleic acid derivatives exhibit high inhibitory activity against pathogens such as *Streptococcus mutans*, *Candida albicans*, *Fusobacterium nucleatum*, and *Porphyromonas gingivis* (Huang et al., 2010). Palmitoleic acid also inhibited spore germination of *Erysiphe polygoni*, a pathogen that causes powdery mildew (Wang et al., 2002). (Morgunov et al., 2017) reported that transgenic eggplants with high palmitoleic acid content also showed increased resistance to *Verticillium* wilt. According to our results, the relative abundance of palmitoleic acid decreased with the time of cultivation, so it is necessary to be vigilant for the diseases caused by these pathogens during the cultivation of FU. Furthermore, the relative abundances of other beneficial metabolites (myristic acid and oleic acid), which have been reported to have antibacterial and antifungal potential, also showed a decreasing trend (Liu et al., 2008; Kim et al., 2022). Serotonin is a potent antioxidant. In plants, phytoserotonin has been found to have many functions, including the regulation of plant growth and development, photosynthesis, reproduction, and responses to biotic and abiotic stresses (Raza et al., 2022). Thus, serotonin has been considered a biomarker for biotic or abiotic stress. The relative abundance of serotonin in the rhizosphere soil increased during FU cultivation, suggesting that FU might be affected by biotic or abiotic stress. Dar et al. (2016) reported that L-hydroxyproline plays an important role in regulating cell division, cell wall self-assembly, and cell elongation. During FU cultivation, the content of L-hydroxyproline in soil increased, especially in CC2

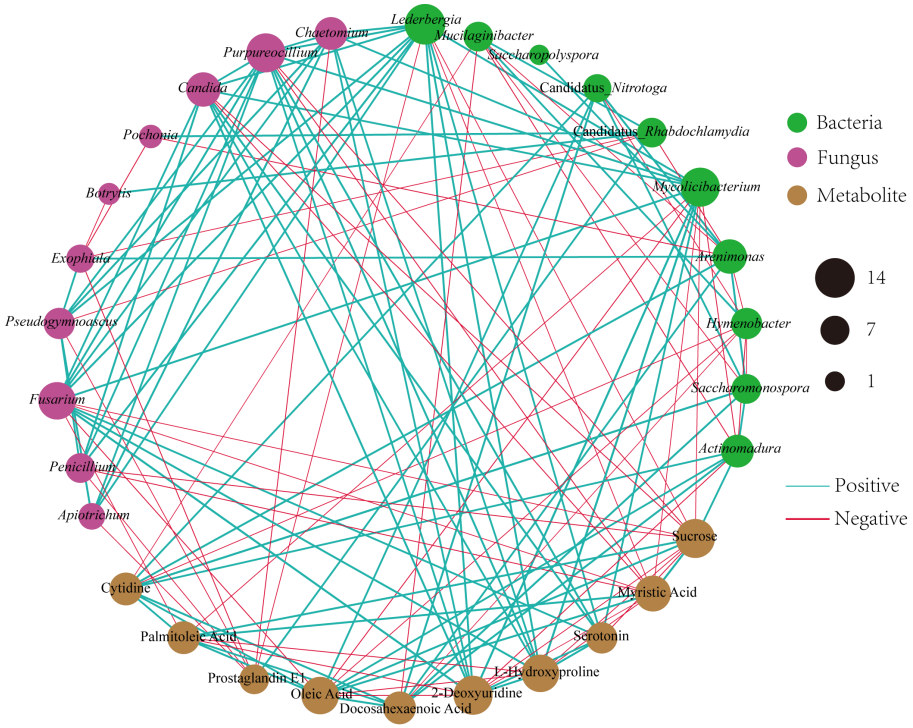

FIGURE 8
Different microbial genera and metabolites of Co-occurrence network. The red line shows a negative correlation, and the green line shows a positive correlation. The thicker the line, the stronger the correlation.

and CC3, and the FU bulbs are also in a rapid growth stage in the second and third years of cultivation. Overall, FU cultivation significantly affected the composition and structure of soil metabolites. This result can be applied to the screening of biomarkers of soil metabolites in rhizosphere soil during FU cultivation.

4.3 Correlations between soil metabolism and the microbial community

Effective communication of soil metabolism plays a crucial role in facilitating microorganism-plant interactions (Wang et al., 2019). Furthermore, microbial communities are important drivers of soil metabolism (Li et al., 2020b). Our study found that soil metabolites were more strongly related to bacterial communities than fungal communities (Figure 7), although differences in fungal community structure seemed more pronounced during cultivation (Figures 1, 2). We proposed that the metabolites of FU soil had a greater impact on the structure of the fungal community than on that of the bacterial community, while the bacteria played a more significant role in altering the rhizosphere metabolites. Co-occurrence network analysis showed a strong correlations among differentially abundant microorganisms and differentially abundant metabolites, suggesting that microorganisms may interact with metabolites or that metabolites may alter the relative abundance of microorganisms for stress adaptation. Half of the top 10 metabolites with the most significant differences were lipids. They are key compounds of the plasma membrane that promote plant adaptation to abiotic stresses (Wang et al., 2022). Our results demonstrated that these lipids had more negative correlations with differentially abundant microbes (Figure 8). Fatty acid biosynthesis and unsaturated fatty acid biosynthesis were significantly enriched among the KEGG pathway. These results implied that lipids affected the composition of microbes during the cultivation of FU. Sucrose was negatively correlated with all the related differentially abundant microorganisms except for *Actinomadura*. Most of these differentially abundant microbial genera were detrimental to plant growth. This implied that a low abundance of sucrose may favor the growth of these pathogenic microorganisms. In addition, the relative abundance of sucrose was positively correlated with that of the beneficial bacterial genus *Actinomadura*, and a low abundance of sucrose was not conducive to the growth of the beneficial bacterial genus *Actinomadura*. Although we have speculated on the relationship between some metabolites and microorganisms, the interactions between microorganisms have

not been thoroughly investigated, and more importantly, FU plants were not included in our analysis. In the future, we will combine these results with FU plants to provide better references for improving soil quality and for high-quality cultivation of FU.

5 Conclusion

In this study, metagenomics and metabolomics were integrated to reveal FU rhizosphere soil microorganisms and metabolites. The community structure of rhizosphere soil microorganisms was significantly altered during the three-year cultivation of FU, with a decreasing trend in bacterial community diversity and an increasing trend in fungal community diversity. Moreover, the relative abundances of beneficial microorganisms decreased, while the relative abundances of pathogenic microorganisms increased. Soil metabolome expression and metabolic processes were also significantly altered, with the most significant changes in some lipids and sucrose. Microbial community structure was also closely related to the distribution of metabolites in the soil. This study enhances our understanding of the ecological role of metabolites and microbes in FU cultivation.

Data availability statement

The original contributions presented in the study are publicly available. This data can be found here: https://www.ncbi.nlm.nih.gov/bioproject/PRJNA967213.

Author contributions

CL and ZL: experimental design. ZL and SC: Fund and resource acquisition. CL: Partial data processing and mapping for initial draft writing. JYu: Provide suggestions and modifications for article writing. JYi and KZ: Provide assistance in some data processing and drawing. ZH supervises this work and provides guidance for it. All authors contributed to the article and approved the submitted version.

Funding

This work was supported by the National Natural Science Foundation of China Youth Science Foundation Project:82003888.

Conflict of interest

The authors declare that the research was conducted in the absence of any commercial or financial relationships that could be construed as a potential conflict of interest.

Publisher's note

Supplementary material

The Supplementary Material for this article can be found online at: https://www.frontiersin.org/articles/10.3389/fpls.2023.1223720/full#supplementary-material

SUPPLEMENTARY FIGURE 1
Cluster heat map of the distribution of content between different groups for the top 30 bacterial genera in terms of relative content.

SUPPLEMENTARY FIGURE 2
Bray-Curtis-based UPGMA clustering maps for bacteria **(A)** and fungi **(B)**.

SUPPLEMENTARY FIGURE 3
LDA score map obtained from LEfSe analysis: bacterial community **(A)**, fungal community **(B)**.

SUPPLEMENTARY FIGURE 4
Cluster heat map of content distribution among different groups for the top 30 fungal genera in terms of relative content.

SUPPLEMENTARY FIGURE 5
Venn diagram of the number of KEGG level 3 pathways among different groups.

SUPPLEMENTARY FIGURE 6
The top 20 functional compounds with the highest relative content.

SUPPLEMENTARY FIGURE 7
Correlation heatmap between the top 10 differential genera of bacterial communities and the top 10 differential genera of fungal communities.

SUPPLEMENTARY FIGURE 8
Heat map of the correlation between microbial genera and the top 30 differential metabolites. bacteria **(A)** and fungi **(B)**.

References

Banerjee, S., and van der Heijden, M. G. A. (2022). Soil microbiomes and one health. *Nat. Rev. Microbiol.* 15, 6–20. doi: 10.1038/s41579-022-00779-w

Bardgett, R. D., and van der Putten, W. H. (2014). Belowground biodiversity and ecosystem functioning. *Nature* 515(7528), 505–511. doi: 10.1038/nature13855

Bi, B. Y., Wang, K., Zhang, H., Wang, Y., Fei, H. Y., Pan, R. P., et al. (2021). Plants use rhizosphere metabolites to regulate soil microbial diversity. *Land Degradation Dev.* 32(18), 5267–5280. doi: 10.1002/ldr.4107

Bi, Y. M., Zhang, X. M., Jiao, X. L., Li, J. F., Peng, N., Tian, G. L., et al. (2023). The relationship between shifts in the rhizosphere microbial community and root rot disease in a continuous cropping American ginseng system. *Front. Microbiol.* 14. doi: 10.3389/fmicb.2023.1097742

Biessy, A., and Filion, M. (2021). Phloroglucinol derivatives in plant-beneficial pseudomonas spp.: biosynthesis, regulation, and functions. *Metabolites* 11(3), 19. doi: 10.3390/metabo11030182

Borah, A., Hazarika, S. N., and Thakur, D. (2022). Potentiality of actinobacteria to combat against biotic and abiotic stresses in tea Camellia sinensis (L) O. Kuntze. *J. Appl. Microbiol.* 133(4), 2314–2330. doi: 10.1111/jam.15734

Chaudhry, V., Rehman, A., Mishra, A., Chauhan, P. S., and Nautiyal, C. S. (2012). Changes in bacterial community structure of agricultural land due to long-term organic and chemical amendments. *Microbial Ecol.* 64(2), 450–460. doi: 10.1007/s00248-012-0025-y

Chen, S., Jian, C., Zhaozhe, H., and Guocheng, D. (2006). Optimization of fermentation conditions for cutinase production with a mutant of thermobifida fusca WSH03-11. *J. Food Sci. Biotechnol.* 05), 44–48.

Cheng, H. Y., Yuan, M. S., Tang, L., Shen, Y. F., Yu, Q., and Li, S. Q. (2022). Integrated microbiology and metabolomics analysis reveal responses of soil microorganisms and metabolic functions to phosphorus fertilizer on semiarid farm. *Sci. Total Environ.* 817, 14. doi: 10.1016/j.scitotenv.2021.152878

Choi, K., Khan, R., and Lee, S. W. (2021). Dissection of plant microbiota and plant-microbiome interactions. *J. Microbiol.* 59(3), 281–291. doi: 10.1007/s12275-021-0619-5

Dai, L. L., Singh, S. K., Gong, H., Tang, Y. Y., Peng, Z. G., Zhang, J., et al. (2022). Rhizospheric microbial consortium of Lilium lancifolium Thunb. causes lily root rot under continuous cropping system. *Front. Microbiol.* 13. doi: 10.3389/fmicb.2022.981615

Dai, Z. M., Su, W. Q., Chen, H. H., Barberan, A., Zhao, H. C., Yu, M. J., et al. (2018). Long-term nitrogen fertilization decreases bacterial diversity and favors the growth of Actinobacteria and Proteobacteria in agro-ecosystems across the globe. *Global Change Biol.* 24(8), 3452–3461. doi: 10.1111/gcb.14163

Dar, M. I., Naikoo, M. I., Rehman, F., Naushin, F., Khan, F. A., Iqbal, N., et al. (2016). "*Osmolytes and plants acclimation to changing environment: emerging omics technologies*," in *"Proline accumulation in plants: roles in stress tolerance and plant development,"*(New Delhi: Springer India: Springer New Delhi), 155–166.

Dong, L. L., Xu, J., Zhang, L. J., Cheng, R. Y., Wei, G. F., Su, H., et al. (2018). Rhizospheric microbial communities are driven by Panax ginseng at different growth stages and biocontrol bacteria alleviates replanting mortality. *Acta Pharm. Sin. B* 8(2), 272–282. doi: 10.1016/j.apsb.2017.12.011

Dubey, A., Malla, M. A., Khan, F., Chowdhary, K., Yadav, S., Kumar, A., et al. (2019). Soil microbiome: a key player for conservation of soil health under changing climate. *Biodiversity Conserv.* 28(8-9), 2405–2429. doi: 10.1007/s10531-019-01760-5

Ge, A.-H., Liang, Z.-H., Han, L.-L., Xiao, J.-L., Zhang, Y., Zeng, Q., et al. (2022). Rootstock rescues watermelon from Fusarium wilt disease by shaping protective root-associated microbiomes and metabolites in continuous cropping soils. *Plant Soil* 479 (1), 423–442. doi: 10.1007/s11104-022-05532-z

Gultom, S. O., Zamalloa, C., and Hu, B. (2014). Microalgae Harvest through Fungal Pelletization-Co-Culture of Chlorella vulgaris and Aspergillus niger. *Energies* 7(7), 4417–4429. doi: 10.3390/en7074417

He, Y., Zhu, Z. D., Zhou, Z. H., Lu, T., Kumar, A., and Xia, Z. C. (2022). Foliar application of lambda-cyhalothrin modulates root exudate profile and the rhizosphere bacteria community of dioecious Populus cathayana. *Environ. pollut.* 313, 9. doi: 10.1016/j.envpol.2022.120123

Huang, C. B., George, B., and Ebersole, J. L. (2010). Antimicrobial activity of n-6, n-7 and n-9 fatty acids and their esters for oral microorganisms. *Arch. Oral. Biol.* 55(8), 555–560. doi: 10.1016/j.archoralbio.2010.05.009

Khorassani, R., Hettwer, U., Ratzinger, A., Steingrobe, B., Karlovsky, P., Claassen, N., et al. (2011). Citramalic acid and salicylic acid in sugar beet root exudates solubilize soil phosphorus. *BMC Plant Biol.* 11, 121. doi: 10.1186/1471-2229-11-121

Kim, Y. G., Lee, J. H., Park, S., Kim, S., and Lee, J. (2022). Inhibition of polymicrobial biofilm formation by saw palmetto oil, lauric acid and myristic acid. *Microbial Biotechnol.* 15(2), 590–602. doi: 10.1111/1751-7915.13864

Korenblum, E., Dong, Y., Szymanski, J., Panda, S., Jozwiak, A., Massalha, H., et al. (2020). Rhizosphere microbiome mediates systemic root metabolite exudation by root-to-root signaling. *Proc. Natl. Acad. Sci. U.S.A.* 117(7), 3874–3883. doi: 10.1073/pnas.1912130117

Korenblum, E., Massalha, H., and Aharoni, A. (2022). Plant-microbe interactions in the rhizosphere *via* a circular metabolic economy. *Plant Cell* 34(9), 3168–3182. doi: 10.1093/plcell/koac163

Li, Z. T., Alami, M. M., Tang, H. M., Zhao, J. S., Nie, Z. N., Hu, J. L., et al. (2022). Applications of Streptomyces jingyangensis T. and Bacillus mucilaginosus A. improve soil health and mitigate the continuous cropping obstacles for Pinellia ternata (Thunb.) Breit. *Ind. Crops Products* 180, 12. doi: 10.1016/j.indcrop.2022.114691

Li, M., Chen, Z., Qian, J., Wei, F., Zhang, G., Wang, Y., et al. (2020a). Composition and function of rhizosphere microbiome of Panax notoginseng with discrepant yields. *Chin. Med.* 15, 85. doi: 10.1186/s13020-020-00364-4

Li, T. Z., Liu, T. T., Zheng, C. Y., Kang, C. S., Yang, Z. C., Yao, X. T., et al. (2017). Changes in soil bacterial community structure as a result of incorporation of Brassica plants compared with continuous planting eggplant and chemical disinfection in greenhouses. *PloS One* 12(3), 17. doi: 10.1371/journal.pone.0173923

Li, X. N., Song, Y., Bian, Y. R., Gu, C. G., Yang, X. L., Wang, F., et al. (2020b). Insights into the mechanisms underlying efficient Rhizodegradation of PAHs in biochar-amended soil: From microbial communities to soil metabolomics. *Environ. Int.* 144, 10. doi: 10.1016/j.envint.2020.105995

Liu, H. W., Brettell, L. E., Qiu, Z. G., and Singh, B. K. (2020). Microbiome-mediated stress resistance in plants. *Trends Plant Sci.* 25(8), 733–743. doi: 10.1016/j.tplants.2020.03.014

Liu, C. L. C., Kuchma, O., and Krutovsky, K. V. (2018). Mixed-species versus monocultures in plantation forestry: Development, benefits, ecosystem services and perspectives for the future. *Global Ecol. Conserv.* 15, 13. doi: 10.1016/j.gecco.2018.e00419

Liu, S., Ruan, W., Li, J., Xu, H., Wang, J., Gao, Y., et al. (2008). Biological control of phytopathogenic fungi by fatty acids. *Mycopathologia* 166(2), 93–102. doi: 10.1007/s11046-008-9124-1

Lu, S., He, Y. H., Chen, Y. Q., Chen, L. J., Wang, Z. Y., Yuan, J., et al. (2022). Co-analysis of rhizosphere metabolomics and bacterial community structures to unfold soil ecosystem health in Camellia oleifera land under long-term cultivation. *Appl. Soil Ecol.* 171, 8. doi: 10.1016/j.apsoil.2021.104336

Mansfield, J., Genin, S., Magori, S., Citovsky, V., Sriariyanum, M., Ronald, P., et al. (2012). Top 10 plant pathogenic bacteria in molecular plant pathology. *Mol. Plant Pathol.* 13(6), 614–629. doi: 10.1111/j.1364-3703.2012.00804.x

Morgunov, I. G., Kamzolova, S. V., Dedyukhina, E. G., Chistyakova, T. I., Lunina, J. N., Mironov, A. A., et al. (2017). Application of organic acids for plant protection against phytopathogens. *Appl. Microbiol. Biotechnol.* 101(3), 921–932. doi: 10.1007/s00253-016-8067-6

Niu, Y., Stevens, M., and Sun, H. (2021). Commercial harvesting has driven the evolution of camouflage in an alpine plant. *Curr. Biol.* 31(2), 446–44+. doi: 10.1016/j.cub.2020.10.078

Philippot, L., Raaijmakers, J. M., Lemanceau, P., and van der Putten, W. H. (2013). Going back to the roots: the microbial ecology of the rhizosphere. *Nat. Rev. Microbiol.* 11(11), 789–799. doi: 10.1038/nrmicro3109

Protopopova, M., Sandanov, D., Pavlichenko, V., Selyutina, I., and Stepanov, N. (2023). The Curious Case of Fritillaria sonnikovae (Liliaceae) in South Siberia: New Insights into Its Origin and Phylogeny. *Diversity* 15(2), 193. doi: 10.3390/d15020193

Raza, A., Salehi, H., Rahman, M. A., Zahid, Z., Madadkar Haghjou, M., Najafi-Kakavand, S., et al. (2022). Plant hormones and neurotransmitter interactions mediate antioxidant defenses under induced oxidative stress in plants. *Front. Plant Sci.* 13. doi: 10.3389/fpls.2022.961872

Sharma, M., Sudheer, S., Usmani, Z., Rani, R., and Gupta, P. (2020). Deciphering the omics of plant-microbe interaction: perspectives and new insights. *Curr. Genomics* 21 (5), 343–362. doi: 10.2174/1389202921999200515140420

Siegel-Hertz, K., Edel-Hermann, V., Chapelle, E., Terrat, S., Raaijmakers, J. M., and Steinberg, C. (2018). Comparative microbiome analysis of a fusarium wilt suppressive soil and a fusarium wilt conducive soil from the chateaurenard region. *Front. Microbiol.* 9. doi: 10.3389/fmicb.2018.00568

Singh, R. P., and Jha, P. N. (2016). The Multifarious PGPR Serratia marcescens CDP-13 Augments Induced Systemic Resistance and Enhanced Salinity Tolerance of Wheat (Triticum aestivum L.). *PLoS One* 11 (6), e0155026. doi: 10.1371/journal.pone.0155026

Song, Y., Li, X., Yao, S., Yang, X., and Jiang, X. (2020). Correlations between soil metabolomics and bacterial community structures in the pepper rhizosphere under plastic greenhouse cultivation. *Sci. Total Environ.* 728, 138439. doi: 10.1016/j.scitotenv.2020.138439

Tariq, M., Khan, A., Asif, M., Khan, F., Ansari, T., Shariq, M., et al. (2020). Biological control: a sustainable and practical approach for plant disease management. *Acta Agriculturae Scandinavica Section B-Soil Plant Sci.* 70(6), 507–524. doi: 10.1080/09064710.2020.1784262

Ullrich, C. I., Aloni, R., Saeed, M. E. M., Ullrich, W., and Efferth, T. (2019). Comparison between tumors in plants and human beings: Mechanisms of tumor development and therapy with secondary plant metabolites. *Phytomedicine* 64, 26. doi: 10.1016/j.phymed.2019.153081

Veloso, J., and van Kan, J. A. L. (2018). Many shades of grey in botrytis-host plant interactions. *Trends Plant Sci.* 23(7), 613–622. doi: 10.1016/j.tplants.2018.03.016

Vives-Peris, V., de Ollas, C., Gómez-Cadenas, A., and Pérez-Clemente, R. M. (2020). Root exudates: from plant to rhizosphere and beyond. *Plant Cell Rep.* 39 (1), 3–17. doi: 10.1007/s00299-019-02447-5

Vujanovic, V., Korber, D. R., Vujanovic, S., Vujanovic, J., and Jabaji, S. (2020). Scientific prospects for cannabis-microbiome research to ensure quality and safety of products. *Microorganisms* 8(2), 15. doi: 10.3390/microorganisms8020290

Wang, T., Duan, Y., Liu, G. D., Shang, X. W., Liu, L. F., Zhang, K. X., et al. (2022). Tea plantation intercropping green manure enhances soil functional microbial abundance and multifunctionality resistance to drying-rewetting cycles. *Sci. Total Environ.* 810, 8. doi: 10.1016/j.scitotenv.2021.151282

Wang, Y. T., Ren, W. J., Li, Y., Xu, Y. F., Teng, Y., Christie, P., et al. (2019). Nontargeted metabolomic analysis to unravel the impact of di (2-ethylhexyl) phthalate stress on root exudates of alfalfa (Medicago sativa). *Sci. Total Environ.* 646, 212–219. doi: 10.1016/j.scitotenv.2018.07.247

Wang, C., Xing, J., Chin, C. K., and Peters, J. S. (2002). Fatty acids with certain structural characteristics are potent inhibitors of germination and inducers of cell death of powdery mildew spores. *Physiol. Mol. Plant Pathol.* 61, 151–161. doi: 10.1006/pmpp.2002.0429

Xu, Y., Ding, H., Zhang, G. C., Li, Z. L., Guo, Q., Feng, H., et al. (2023). Green manure increases peanut production by shaping the rhizosphere bacterial community and regulating soil metabolites under continuous peanut production systems. *BMC Plant Biol.* 23(1), 15. doi: 10.1186/s12870-023-04079-0

Yan, Z.-Q., Wang, C.-Y., and Wu, G.-Q. (2022). The Influence of Different Cultivation Modes on the Yield and Quality of Fritillaria thunbergii and the Key Cultivation Points of Fritillaria thunbergii. *Shanghai Vegetables* 29–30+90.

Yuan, J., Zhao, J., Wen, T., Zhao, M. L., Li, R., Goossens, P., et al. (2018). Root exudates drive the soil-borne legacy of aboveground pathogen infection. *Microbiome* 6, 12. doi: 10.1186/s40168-018-0537-x

Yue, W., Hao, Y. B. W., Ju, Y. C. Z., Meng, Z., and Ruyi, Y. (2019). Variation in microbial community structure in the rhizosphere soil of Salvia miltiorrhiza Bunge under three cropping modes. *Acta Ecologica Sin.* 39(13), 4832–4843.

Zhang, J. N., Cook, J., Nearing, J. T., Zhang, J. Z., Raudonis, R., Glick, B. R., et al. (2021). Harnessing the plant microbiome to promote the growth of agricultural crops. *Microbiological Res.* 245, 14. doi: 10.1016/j.micres.2020.126690

Zhang, J. G., Fan, S. H., Qin, J., Dai, J. C., Zhao, F. J., Gao, L. Q., et al. (2020). Changes in the microbiome in the soil of an american ginseng continuous plantation. *Front. Plant Sci.* 11. doi: 10.3389/fpls.2020.572199

Zhang, J. X., Zhou, D. P., Yuan, X. Q., Xu, Y. H., Chen, C. B., and Zhao, L. (2022). Soil microbiome and metabolome analysis reveals beneficial effects of ginseng-celandine rotation on the rhizosphere soil of ginseng-used fields. *Rhizosphere* 23, 9. doi: 10.1016/j.rhisph.2022.100559

Zhou, H., Luan, H., Wang, H., Dong, K., and Miao, L. (2014). Optimization of the fermentation medium of an antitumor endophytic fungus Aspergillus oryzae YX- 5 isolated from Ginkgo biloba. *Microbiol. China* 41(07), 1358–1367. doi: 10.13344/j.microbiol.china.130545

frontiers | Frontiers in Plant Science

TYPE Original Research
PUBLISHED 21 December 2023
DOI 10.3389/fpls.2023.1248476

OPEN ACCESS

EDITED BY
Long Yang,
Shandong Agricultural University, China

REVIEWED BY
Qijie Guan,
University of Mississippi, United States
Ajay Madhusudan Sorty,
Aarhus University, Denmark
Manoj Kumar Solanki,
University of Silesia in Katowice, Poland

*CORRESPONDENCE
Liangzhi Li
205601006@csu.edu.cn
Huaqun Yin
yinhuaqun_cs@sina.com

RECEIVED 27 June 2023
ACCEPTED 03 November 2023
PUBLISHED 21 December 2023

CITATION
Wang Z, Peng D, Fu C, Luo X, Guo S, Li L and Yin H (2023) Pan-metagenome reveals the abiotic stress resistome of cigar tobacco phyllosphere microbiome. *Front. Plant Sci.* 14:1248476. doi: 10.3389/fpls.2023.1248476

Pan-metagenome reveals the abiotic stress resistome of cigar tobacco phyllosphere microbiome

Zhenhua Wang[1], Deyuan Peng[1], Changwu Fu[1], Xianxue Luo[1], Shijie Guo[1], Liangzhi Li[2,3]* and Huaqun Yin[2,3]*

[1]Zhangjiajie Tobacco Company of Hunan Province, Zhangjiajie, China, [2]School of Minerals Processing and Bioengineering, Central South University, Changsha, China, [3]Key Laboratory of Biometallurgy of Ministry of Education, Central South University, Changsha, China

The important role of microbial associations in mediating plant protection and responses to abiotic stresses has been widely recognized. However, there have been limited studies on the functional profile of the phyllosphere microbiota from tobacco (*Nicotiana tabacum*), hindering our understanding of the mechanisms underlying stress resilience in this representative and easy-to-cultivate model species from the solanaceous family. To address this knowledge gap, our study employed shotgun metagenomic sequencing for the first time to analyze the genetic catalog and identify putative plant growth promoting bacteria (PGPB) candidates that confer abiotic stress resilience throughout the growth period of cigar tobacco in the phyllosphere. We identified abundant genes from specific bacterial lineages, particularly *Pseudomonas*, within the cigar tobacco phyllospheric microbiome. These genes were found to confer resilience against a wide range of stressors, including osmotic and drought stress, heavy metal toxicity, temperature perturbation, organic pollutants, oxidative stress, and UV light damage. In addition, we conducted a virome mining analysis on the metagenome to explore the potential roles of viruses in driving microbial adaptation to environmental stresses. Our results identified a total of 3,320 scaffolds predicted to be viral from the cigar tobacco phyllosphere metagenome, with various phages infecting *Pseudomonas, Burkholderia, Enterobacteria, Ralstonia*, and related viruses. Within the virome, we also annotated genes associated with abiotic stress resilience, such as alkaline phosphatase D (*phoD*) for nutrient solubilization and glutamate-5-semialdehyde dehydrogenase (*proA*) for osmolyte synthesis. These findings shed light on the unexplored roles of viruses in facilitating and transferring abiotic stress resilience in the phyllospheric microbiome through beneficial interactions with their hosts. The findings from this study have important implications for agricultural practices, as they offer potential strategies for harnessing the capabilities of the phyllosphere microbiome to enhance stress tolerance in crop plants.

KEYWORDS

phyllosphere, abiotic stress resistance, metagenome, virus, auxiliary metabolic gene

Introduction

The phyllosphere, also known as the phylloplane, refers to the aerial foliage surface where microbes thrive. It serves as a protective barrier against various biotic and abiotic stresses, including temperature changes, ultraviolet (UV) radiation, drying out, and nutrient deficiency (Zhang et al., 2022). Traditionally, the phyllosphere was thought to be inhospitable to microbes, but subsequent research has shown that it harbors a diverse array of microbial taxa that have adapted to these challenging conditions (Vorholt, 2012). Microbial communities in the phyllosphere rely on specific resilience mechanisms to withstand external stresses. These mechanisms incorporate various strategies, such as pigment production to protect against intense UV radiation, the secretion of extracellular polysaccharides (EPS) or biosurfactants to facilitate surface attachment and prevent desiccation, and the production of chemical compounds to compete for resources (Heredia-Ponce et al., 2021; Bashir et al., 2022). The assembly of phyllosphere microbiota is influenced by a combination of intrinsic factors, like plant genotype, age, and species, as well as biotic and abiotic environmental factors, including climate, geographical location, and properties (Shakir et al., 2021). Among the phyllosphere-associated ecosystem, bacterial species are the most abundant members, with an estimated density of 10^6 to 10^7 bacterial cells per square centimeter. These bacteria can play beneficial, pathogenic, or antagonistic roles in the phyllosphere (Lindow and Brandl, 2003).

The phyllospheric microbiota engages in complex, dynamic, and multipartite interactions that significantly contribute to plant health and productivity (Lindow and Brandl, 2003). These interactions between plants and associated microbial communities are important drivers of terrestrial ecosystems (van der Putten et al., 2013). Moreover, the phyllosphere microbiota exhibits diverse functional roles, including one-carbon conversion (Knief et al., 2012), fixation of nitrogen, nitrification (Fürnkranz et al., 2008), modulation of plant metal transporters (Zhou et al., 2020) and bioremediation of aerial hydrocarbon pollutant (Ali et al., 2012; Franzetti et al., 2020).

Microbial colonization on plant surfaces has also been shown to promote plant growth through various mechanisms. These include increased antioxidant defense enzyme activity (Mastouri et al., 2012), production of volatile organic compounds (VOCs)/phytohormones to regulate plant communication and development (Taghavi et al., 2009; Liu and Zhang, 2015), protection against foliar pathogens (Innerebner et al., 2011), decomposition of toxic substances (Vorholt, 2012) and enhancement of stress tolerance (Márquez et al., 2007; Patel et al., 2017). For instance, rice seedlings inoculated with specific phyllosphere bacterial strains have demonstrated improved survival under drought stress, along with enhanced nutrient availability, exopolysaccharide levels, phytohormones, soluble sugars, chlorophyll, and total protein (Arun et al., 2020). Similarly, inoculation with the rice phyllosphere bacteria *Bacillus megaterium* strain PB50 has been found to enhance the drought tolerance of *Oryza sativa* (rice) pots (Devarajan et al., 2021). These beneficial effects on plant growth have been reported in various other studies as well (Enya et al., 2007; Batool et al., 2016; Fu et al., 2016).

While the beneficial properties of phyllosphere microbes are known, much remains to be explored regarding their genetic repertoire (Meyer and Leveau, 2012). Additionally, the mutualistic aspects of plant-microbe interactions, such as stress tolerance and plant defense, in the phyllosphere require further in-depth study.

In addition to bacteria, abundant viruses, including bacteriophages (phages), have been discovered on the phyllosphere. These viruses can infect and replicate within bacteria that reside on the phyllosphere, impacting the composition and diversity of the associated bacterial communities. Phages can also exert selective pressure on bacterial populations, leading to the elimination or reduction of specific bacterial populations (Forero-Junco et al., 2022). Furthermore, the prevalence of certain phages can vary across environments and plant species, influencing the composition of associated bacterial communities. Interestingly, beneficial effects of viral infections in host plants have been documented, as certain plant virus strains enhance the abiotic stress resistance of their hosts. For example, cucumber mosaic virus (CMV) strain Fny, bromo mosaic virus (BMV) strain Russian, tobacco mosaic virus (TMV) U1 strain, and tobacco rattle virus (TRV) have been found to enhance the heat, cold, or drought resistance of their plant hosts (Xu P. et al., 2008; Roossinck, 2013; Westwood et al., 2013). Thus, the role of viruses in the phyllosphere and their impact on plant-microbe interactions warrant further investigation.

Tobacco (*Nicotiana tabacum*) is a leafy, annually-grown solanaceous crop of significant economic importance, cultivated worldwide for thousands of years. China is one of the major tobacco producers, accounting for 39.06% of global tobacco production (http://www.fao.org/faostat/en/#data/QC). This highlights the agricultural significance of tobacco and its role in the global market. Moreover, tobacco with broad environmental adaptability serves as a valuable model plant for studying various physiological processes and plant-pathogen interactions. Researchers often turn to tobacco as a model due to its well-established experimental systems and the ease of manipulation in laboratory settings (Dai et al., 2022). Tobacco is typically grown during the summer and harvested at the end of August. Being exposed to excessive solar/ultraviolet radiation, diurnal temperature fluctuations, and occasional heavy rainfall during growth, tobacco leaves offer a unique opportunity to investigate microbial communities under strong abiotic stresses. Consequently, the phyllosphere of solanaceous crops, such as tobacco, serves as a suitable model system for investigating the dynamics of microbial populations and their interactions in the face of environmental challenges. This is due to the significant environmental heterogeneity and intricate ecological interactions that occur on the surfaces of leaves (Meyer and Leveau, 2012; Xing et al., 2022).

Methods for studying the structure and biodiversity of the plant phyllospheric microbiome have evolved significantly in recent years. These methods enable researchers to gain insights into the complex microbial communities that inhabit the phyllosphere of solanaceous crops like tobacco. Early studies were limited to

culture-dependent methods, but the introduction of denaturing gradient gel electrophoresis (DGGE) by Yang et al. revolutionized the field (Yang et al., 2001). However, traditional culture methods are time-consuming and have low throughput, often leading to an underestimation of microbial population sizes and biodiversity (Dai et al., 2022). Recent advancements in low-cost high-throughput (Knight et al., 2018) and next-generation sequencing technologies (Soucy et al., 2015) have overcome these limitations, enabling researchers to explore microbial communities in greater detail and with higher resolution.

High-throughput sequencing methods, such as targeted sequencing of phylogenetic markers like 16S rRNA for bacteria and ITS for fungi, have been successfully applied in the study of the tobacco foliage microbiome (Chen et al., 2020; Huang et al., 2021; Zheng et al., 2022). While in-silico predictions based on phylogenetic marker genes like the 16S rRNA gene can provide valuable insights into microbial diversity and community composition, there are several limitations such as the lack of functional information, limited resolution and bias towards abundant taxa (Pan et al., 2023).

More advanced metagenomic and metaproteomic shotgun sequencing approaches have allowed for faster and more accurate characterization of taxonomic and functional profiles of microbiomes at the species level, encompassing multiple domains such as bacteria and fungi. These approaches have been applied to various plant phyllospheric microbiomes, including those of sugarcane (Khoiri et al., 2021), brick tea (Wang et al., 2021) and neotropical forest (Lajoie et al., 2020).

However, metagenomic studies of the tobacco phyllospheric microbiome are limited, and functional characterization is primarily based on in-silico predictions using marker genes like the 16S rRNA gene. This limitation hinders our understanding of microbial functions and their adaptation to the tobacco phyllosphere, as well as the factors influencing microbiome dynamics over time and space. Thus, for enhancing plant health and growth and manage disease outbreaks, there is a need for further research to gain a more accurate and in-depth understanding of the tobacco microbial community and its functional repertoire, particularly in relation to abiotic stress responses.

In this study, we conducted pan-metagenomic investigations of the phyllosphere (leaf-epiphytic) microbiome of cigar tobacco from Hunan province, China. This region has a long history of tobacco production and is also affected by bacterial wildfire disease. To capture temporal dynamics, our investigations were performed throughout the tobacco growth season. Using genome assembly and annotation, we characterized the taxonomic and functional profiles of the cigar tobacco phyllospheric microbiome. Specifically, we focused on the "resistome," which encompasses the complete set of genes or genetic elements involved in conferring resistance to various abiotic stresses, such as temperature, drought, salinity, and chemical pollutants. This pan-metagenomic approach allowed us to comprehensively analyze the cigar tobacco phyllospheric microbiome and gain valuable insights into its functional potential in relation to stress resistance.

Furthermore, our study also identified viral sequences within the metagenome scaffolds. This finding highlights the role of viruses as horizontal gene transfer (HGT) agents in facilitating the transfer of metabolic and stress resistance genes among the phyllospheric microbiota. HGT refers to the transfer of genes between organisms that do not have a direct parent-offspring relationship, contrasting with vertical gene transfer that occurs through reproduction. In the context of microbial communities, HGT enables the exchange of genetic material, including genes or DNA fragments, between different microorganisms (Huang, 2013; Daubin and Szöllősi, 2016).

Results and discussion

Pan-metagenome analyses and taxonomic composition

A total of 444,193 protein-coding genes were annotated from all three groups of metagenomes representing phyllosphere (leaf-epiphytic) microbiota from cigar tobacco. This diversity greatly exceeds the previously reported 4,587 metagenomic orthologous genes from tropical tree phyllosphere communities (Lajoie et al., 2020), emphasizing the exceptional richness and genetic potential of the cigar tobacco phyllospheric microbiota. It suggests that the phyllospheric microbiota associated with cigar tobacco harbors a vast repertoire of genetic elements, which likely contributes to its ability to adapt, interact with the host plant, and engage in various functional processes. This extensive genetic diversity in the metagenomes is indicative of the vast microbial species richness and functional capacity present in the phyllosphere of cigar tobacco.

Among these genes, 47,189 gene families were found to be shared by all groups of metagenome samples in this study. These gene families are significantly enriched in gene ontology (GO) terms such as aromatic compound catabolic process (GO:0019439), conjugation (GO:0000746), viral genome integration into host DNA (GO:0044826), and antibiotic biosynthetic process (GO:0017000) (Figure 1A). The number of unique gene families shows an increasing trend from group I (samples collected in June; 458), to group II (samples collected in July; 1,002), and group III (samples collected in August; 1,814), indicating an increasing diversity of metagenomic genes over time.

In our study, the core gene set primarily consists of gene families that are annotated as clusters of orthologous groups (COG) categories, including post-translational modification [O], translation, ribosomal structure, and biogenesis [J], energy production and conversion [C], carbohydrate transport and metabolism [G], amino acid transport and metabolism [E], and nucleotide transport and metabolism [F] (Figure 1B).

The enrichment of these COG categories suggests important functional roles within the core gene set. Post-translational modification [O] may be involved in protein folding, stability, and enzymatic activity regulation, which could impact the adaptation and survival of the phyllospheric microbiota on plant surfaces. Translation, ribosomal structure, and biogenesis [J] are

10.3389/fpls.2023.1248476

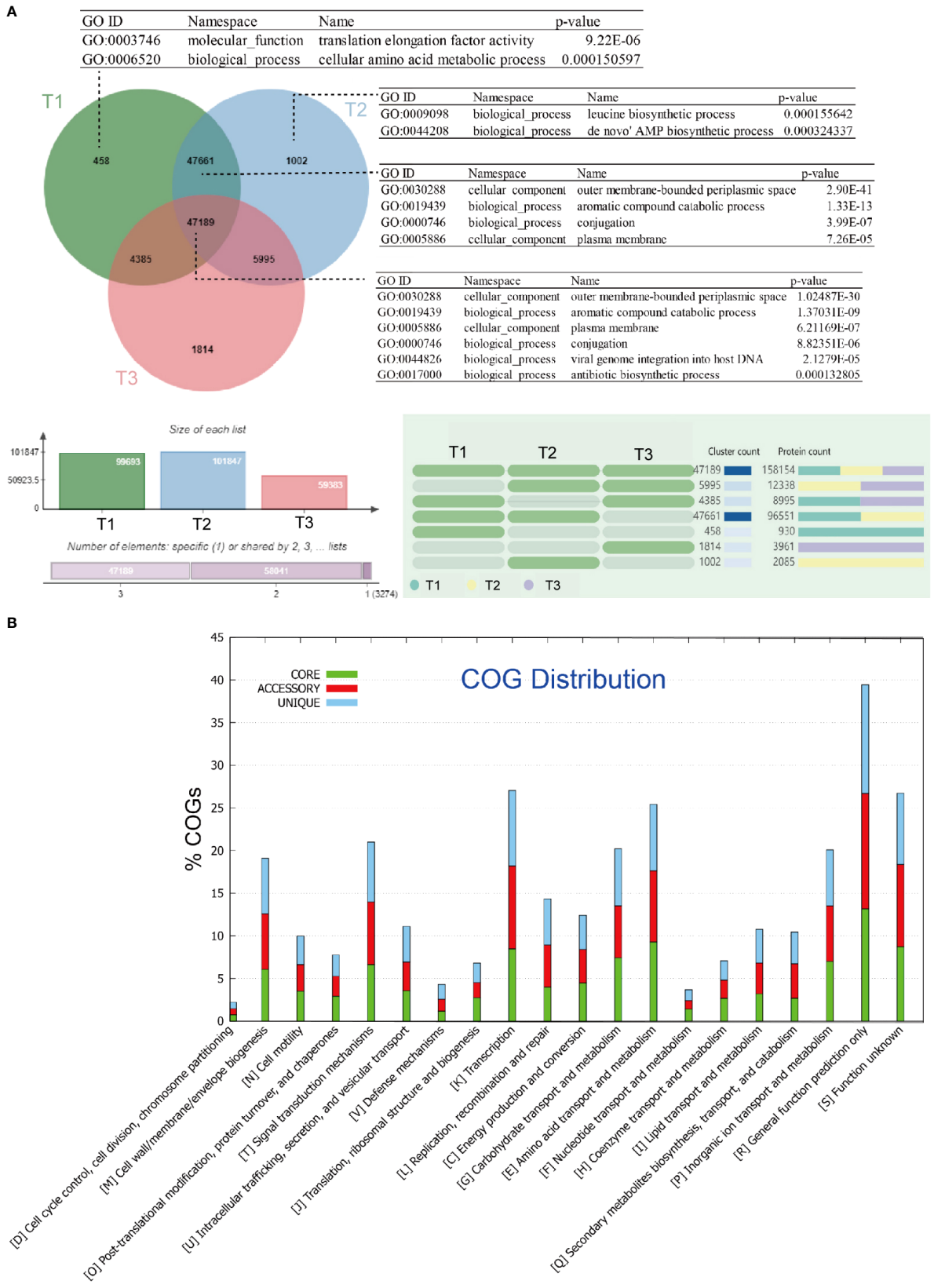

FIGURE 1
Clustering and comparative metagenomic analyses of three group of samples: **(A)** Venn diagram showing the number of genes shared by all strains (i.e., the core genome), the number of genes shared by partial strains (i.e., the accessory genome), and the number of strain-specific genes (i.e., the unique gene) in the tested strains. The gene ontology (GO) categories were determined using OrthoVenn, and the hypergeometric test with a *p*-value < 0.05 was applied to find enriched GO in the clusters; **(B)** Bar chart showing functional proportions (based on COG categories) of different parts of the pan-metagenome (i.e., core, accessory, unique).

essential for protein synthesis, suggesting that the core gene set is enriched in genes involved in protein production and regulation.

Energy production and conversion [C] indicate the presence of genes related to energy metabolism, suggesting that the core gene set includes functional traits associated with energy utilization and adaptation in the phyllosphere. Carbohydrate transport and metabolism [G] and amino acid transport and metabolism [E] categories imply that the core gene set contributes to the utilization of carbon and nitrogen sources available on plant surfaces. Additionally, nucleotide transport and metabolism [F] imply that the core gene set may possess genetic capabilities related to DNA and RNA metabolism.

Overall, the enrichment of these specific COG categories in the core gene set suggests that the phyllospheric microbiota has developed functional capabilities to interact with the plant environment, including protein regulation, energy metabolism, resource utilization, and genetic processes. These functional implications are crucial for microbial adaptation and survival on leaf surfaces.

The Kyoto Encyclopedia of Genes and Genomes (KEGG) annotation further reveals enrichment of categories related to the metabolism of cofactors and vitamins in the core gene set (see Figure S1 at https://doi.org/10.6084/m9.figshare.21257361.v1). On the other hand, enriched GO terms in the unique gene families of group I include translation elongation factor activity (GO:0003746), and correspondingly, in group II include leucine biosynthetic process (GO:0009098), *de novo*' AMP biosynthetic process (GO:0044208); while in the shared gene families of group I and group II, aromatic compound catabolic process (GO:0019439), conjugation (GO:0000746), are again significantly enriched.

Model extrapolation revealed an "open" pan-metagenome fitted into a power-law regression function [$Ps\ (n) = 57974.6n^{0.4196}$] with a calculated exponent γ falling in the range between 0 and 1, while the core metagenome was fitted into an exponential regression [$Fc\ (n) = 86462.6e^{-0.414371n}$]. This indicates that our sampling of microbial taxa from cigar tobacco phyllosphere is still unsaturated.

In the cigar tobacco phyllosphere, bacteria were found to be the most abundant microbial colonizers, comprising approximately 99.9% of the total community, followed by viral communities at around 0.04%. Among the bacterial taxa, the phylum Proteobacteria dominated, accounting for about 98.1% of the community, with the phylum Firmicutes representing a minor proportion of around 0.05%.

Within Proteobacteria, the class Gammaproteobacteria was the most abundant, representing approximately 91% of the community, followed by the class Alphaproteobacteria at around 8%. Among the orders of Gammaproteobacteria, Enterobacterales and Pseudomonadales were the dominant groups, making up around 58% and 41% of the Gammaproteobacteria community, respectively.

Interestingly, the study revealed variations in the abundance of Enterobacterales and the wildfire disease pathogen *Pseudomonas syringae* among different sampling time points (T1, T2, and T3). The T3 group, corresponding to late August, exhibited a higher abundance of Enterobacterales (~76%) and *Pseudomonas syringae* (~2%) compared to the T1 group (~53% and ~0.07%) and T2 group (~54% and ~0.10%) (see Figure S2 at https://doi.org/10.6084/m9.figshare.21257361.v1 and Supplemented data at https://doi.org/10.6084/m9.figshare.21257256.v1).

The taxonomic analysis of the cigar tobacco phyllospheric microbiome revealed a dominance of bacteria, particularly those belonging to the Proteobacteria phylum. Among these, the bacterial wildfire disease pathogen *P. syringae* were found to be highly abundant, especially during late August (T3 group). This observation aligns with previous studies based on 16S rRNA amplicon analysis, which indicated a correlation between the abundance of these bacteria and the development of bacterial wildfire disease in tobacco (Wang et al., 2022).

These findings shed light on the potential dynamics and composition of the microbial community in the phyllosphere and their potential roles in cigar tobacco health and disease development. They further support the study's goal of understanding microbial interactions and their ecological significance in the phyllosphere environment.

Furthermore, the differential abundance of specific bacterial groups and pathogens at different sampling time points may provide valuable insights into the identification of microbial signatures associated with disease progression. This information can aid in the development of effective management strategies to improve cigar tobacco health and mitigate the impact of diseases.

Abiotic stress resistome in cigar tobacco phyllosphere

Osmotic and drought stress resilience

Osmotic and drought stress impose significant pressure on the nutrient uptake and cellular physiology of both plant-associated microbes and their hosts (Bashir et al., 2014; Hanin et al., 2016). To combat osmotic stress, microbes and plants employ three major mechanisms: maintaining cellular ion homeostasis, enhancing cell barriers, and utilizing compatible solute protectants such as trehalose, proline, betaine, and sarcosine (Behr et al., 2015). Plant-microbial interactions play a crucial role in osmotic adjustment, as they facilitate the secretion of metabolites that help maintain osmotic balance (Shaffique et al., 2022). Exopolysaccharides (EPSs) are hydrophilic macromolecules composed of long-chain polymers with repeating sugar units (Ilyas et al., 2020; Nadeem et al., 2021), and they form protective biofilms that enhance water retention in the microbe-sheath and regulate the distribution of carbon sources to mitigate the effects of aridity and dehydration caused by abiotic stress (Xu J. et al., 2008; Naseem et al., 2018).

In our analysis, we identified gene orthogroups related to osmotic stress resistance in the metagenome of the tested tobacco phyllosphere. Details of these gene orthogroups can be found in Table S1 at https://doi.org/10.6084/m9.figshare.21257352.v1 and are illustrated in Figure 2A. These genes play crucial roles in various mechanisms that contribute to osmotic stress resistance:

a. Universal stress regulators, such as osmotically inducible lipoprotein (*osmBE*), universal stress protein (*uspABCEG*), biofilm regulator (*bssRS*), biofilm protein (*tabA*), help microorganisms adapt to osmotic stress by coordinating cellular responses.

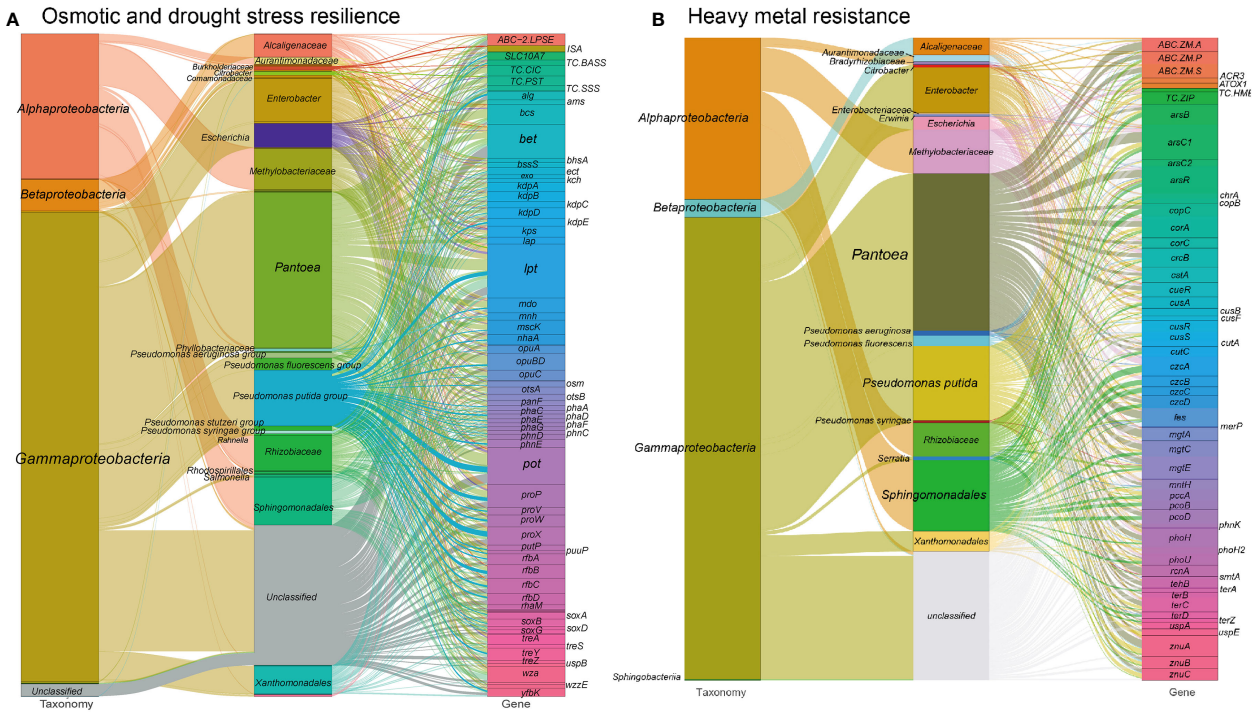

FIGURE 2
Sankey diagram showing the taxonomic and functional profiles of genes conferring abiotic stress resilience in the cigar tobacco phyllospheric microbiome: **(A)** Osmotic and drought stress resilience; **(B)** Heavy metal resistance. Details for gene abbreviations can be found in Table S1 at https://doi.org/10.6084/m9.figshare.21257352.v1.

b. Ion transporters, including voltage-gated potassium channel (*trkA*), potassium-dependent mechanosensitive channel (*kefABCFG*), potassium-transporting ATPase (*kdpABCDE*), multicomponent K^+:H^+ antiporter (*phaACDEFG*), multicomponent Na^+:H^+ antiporter (*nhaAB*, *mnhABCDEG*), sodium channel (VGSC), sodium/proline symporter (*putP*), sodium/bile acid symporter (SLC10A7, TC.BASS), solute:Na^+ symporter (TC.SSS) and chloride channel (*yfbK*, TC.CIC), play a vital role in maintaining cellular homeostasis under osmotic stress.
c. Biosynthesis/export proteins involved in enhancing the cell barrier, including the production of lipopolysaccharide (LPS) precursor rhamnose (dTDP-l-rhamnose synthase: *rfbABCD* (Parakkottil et al., 2010), L-rhamnose mutarotase and transporter (*rhaMPQST*), cellulose synthase (*bcsBC*), and capsular polysaccharide or lipopolysaccharide biosynthesis/export protein (*kpsTS, etc.*);
d. Biosynthesis and transport proteins involved in the synthesis of protectant sugars, such as ectoine (*ectABCD*), succinoglycan (*exoFHIQXY*), glycine betaine (*betABCLT, BHMT, CMO*), amylovoran (*amsFL*), alginate (*algEFIJKX*), trehalose (*treASXYZ, otsAB*), glucans (*mdoCG*), sarcosine (*soxABDG*) as well as osmoprotectant transport system (*opuABDC*), and glycine proline/betaine transporter (*proPVWX*). These sugars act as osmoprotectants, helping to maintain cellular integrity and functionality.

These osmotic stress resistance genes are primarily encoded by specific bacterial groups in the metagenome. Gammaproteobacteria, such as *Enterobacter* (6.5%), *Pseudomonas* (13.3%), *Pantoea* (23.4%), and Alphaproteobacteria including *Rhizobiaceae* (5.3%), *Methylobacteriaceae* (6.2%), and *Sphingomonadales* (7.2%), play a significant role in encoding these proteins. Specially, *Sphingomonadales* (16.0%) and *Pantoea* (20.5%) are the primary contributors to the encoding of lipopolysaccharide biosynthesis/export proteins. *Methylobacteriaceae* (11.8%) and *Pantoea* (18.5%) are predominantly involved in encoding ion transporters. Besides, *Pseudomonas* (14.3%), *Pantoea* (18.2%) and *Sphingomonadales* (9.3%) are the major contributors to the synthesis of compatible solutes. Among these taxa, *Enterobacter* may contribute to nutrient cycling by participating in the breakdown of organic matter and nutrient solubilization, indirectly benefiting the plants. Most *Pseudomonas* species produce plant growth-promoting substances, including IAA, siderophores, and volatile organic compounds, which can enhance plant growth and trigger defense mechanisms against pathogens. *Pantoea* spp. have been reported as nitrogen-fixing bacteria, having the ability to convert atmospheric nitrogen into plant-usable forms (Singh et al., 2020).

Microorganisms indirectly mitigate osmotic pressure in plant cells by accelerating trehalose biosynthesis, maintaining osmolyte concentrations, and stabilizing turgor pressure (Kahraman et al., 2019; Shaffique et al., 2022). The application of osmotic-stress-resilient microbiota to plants can induce the secretion of organic acids and mineral solubilization, thereby increasing nutrient availability, metabolic rate, and sustaining osmoregulation in

plant cells (Chen and Jiang, 2010; Shaffique et al., 2022). Plant-growth-promoting bacteria (PGPB) contribute to osmotic adjustment by generating a low water potential gradient in the cytosol, maintaining turgor pressure, osmotic adjustment, and improving stress tolerance in plant cells (Shaffique et al., 2022).

Furthermore, compatible solutes produced by the microbiome protect both the microbiome itself and the plant host against drought, heat, or cold stress (Bashir et al., 2014; Hanin et al., 2016). The biosynthesis of osmoprotectants and the production of EPS enriched in the tested metagenome may reflect adaptations of microbial inhabitants by enhancing attachment to surfaces and offering resistance to environmental pressures and plant defenses (Rastogi et al., 2013). In a recent study by de Sousa et al. (de Sousa et al., 2022), it was demonstrated that Pseudomonas spp. rely on increased synthesis of exopolysaccharides (EPSs) to cope with osmotic stress and protect cells from desiccation in the phyllosphere. This finding supports our previous study, where we identified an enrichment of *Pseudomonas* spp. (LDA = 5.29) during the T3 period, which coincided with the predicted enrichment of genes associated with osmoprotectant biosynthesis (Wang et al., 2022). This suggests a correlation between the abundance of Pseudomonas spp. and the presence of osmoprotectant biosynthesis genes, particularly during periods of intense sun exposure and drought stress such as the T3 period.

Similarly, the increased production of EPSs under osmotic stress was reported in rhizobacteria *Pseudomonas aeruginosa* and *Bacillus endophyticus* (Ghosh et al., 2019). Finally, the accumulation of compatible solutes (glycine-betaine and ectoine) in the biocontrol agent *Pantoea* spp. serves as an osmotic stress adaptation (Teixidó et al., 2005).

These findings have practical implications and can contribute to various applications. For example, the knowledge gained from studying these osmotic stress-related proteins could lead to the development of microbial-based strategies for enhancing crop resilience. Understanding the mechanisms underlying osmotic stress resistance may also help improve plant adaptation to challenging environments. Ultimately, these advancements could reduce the reliance on traditional chemical stressors in agriculture and promote more sustainable practices.

Heavy metal resistance

Heavy metal contamination can have detrimental effects on plant health and the microbial communities associated with both the rhizosphere and phyllosphere. However, it is worth noting that the phyllospheric surface can act as an important reservoir for toxic element pollutants, providing significant insight into the complex interactions between plants and heavy metals (Sánchez-López et al., 2018). Furthermore, the presence of metal-resistant plant growth-promoting bacteria (PGPB) in plant spheres has been shown to enhance plant tolerance against heavy metal stress (Mishra et al., 2017; Zhou et al., 2020).

In our analysis of the metagenome from the cigar tobacco phyllosphere, a diverse range of 948 gene families were predicted to confer resistance against various heavy metals (Figure 2B and see Table S1 at https://doi.org/10.6084/m9.figshare.21257352.v1). These gene families mainly consist of metal ion transport proteins that facilitate the efflux of cytosolic toxic metal ions and metal reductases that convert metal ions to less toxic forms. Examples of these genes include those associated with arsenate/arsenite, chromate, copper,

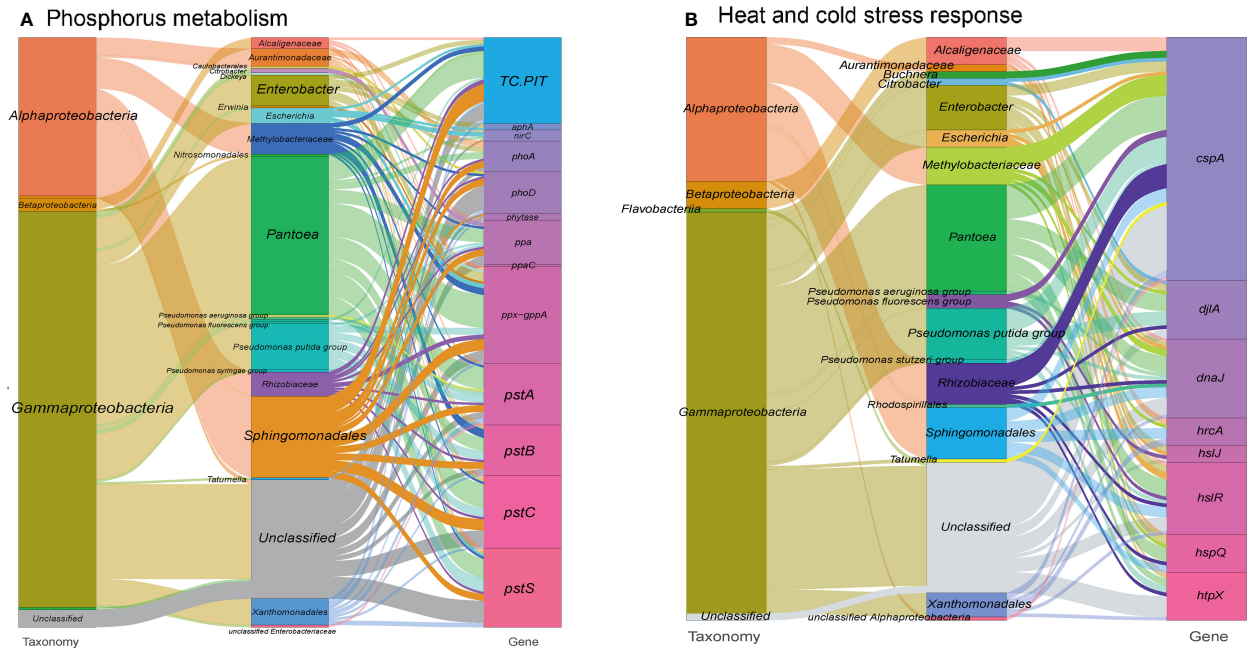

FIGURE 3
Sankey diagram showing the taxonomic and functional profiles of genes conferring abiotic stress resilience in the cigar tobacco phyllospheric microbiome: **(A)** Phosphorus metabolism; **(B)** Heat and cold stress response. Details for gene abbreviations can be found in Table S1 at https://doi.org/10.6084/m9.figshare.21257352.v1.

fluoride, nickel/cobalt, mercuric, manganese, tungstate, zinc/manganese, and tellurite resistance. Notably, the metal resistance gene orthogroups in our metagenome were predominantly encoded by *Pantoea* (~23.3%), *Pseudomonas* (~13.1%), Sphingomonadales (~10.3%), and Methylobacteriaceae (~6.5%) (Table S1). For instance, Methylobacteriaceae exclusively encoded the HME family heavy-metal exporter (TC.HME), while *Pseudomonas* predominantly encoded thioredoxin arsenate reductase (*arsC2*), ZIP family zinc transporter (TC.ZIP), zinc transport system (*znuABC*), and periplasmic copper chaperone A (*pccA*) genes. Moreover, Sphingomonadales and Methylobacteriaceae, along with *Pantoea*, played a significant role in encoding the resistance nodulation cell division (RND)-type cobalt-zinc-cadmium efflux pump (*czcABCD*) genes.

Consistent with previous studies, *Pantoea* spp. and *Pseudomonas* spp. have demonstrated potential for the bioremediation of metal-contaminated soils (Patel et al., 2016; Audu et al., 2020), while Sphingomonadales have been found inhabiting areas contaminated with high levels of metals and organic pollutants (Girardot et al., 2020). Additionally, it has been shown that the endophytic *Sphingomonas* sp. LK11 exhibits phytotoxic mitigation of Cr(VI) in soybean plants (Bilal et al., 2018).

In addition to metal resistance genes, we also detected phosphatase and phosphorus uptake-related genes (313 gene orthogroups) in the metagenome (Figure 3A and see Table S1 at https://doi.org/10.6084/m9.figshare.21257352.v1). These genes may facilitate the solubilization of phosphorus, increasing its availability in the extracellular space, which is an essential nutrient for the plant host (Thapa et al., 2017). Consequently, this process might also contribute to the immobilization of toxic metal ions (Bechtaoui et al., 2021). In the other hand, a range of genes involved in biosynthesis of siderophore, which are high-affinity systems for the uptake of iron from the environment, were annotated in the metagenome. These siderophores contribute to plant nutrition and protection against phytopathogens (Scavino and Pedraza, 2013) (see Figure S3 at https://doi.org/10.6084/m9.figshare.21257361.v1 and Table S1 at https://doi.org/10.6084/m9.figshare.21257352.v1).

Overall, our findings provide comprehensive insights into the diverse repertoire of heavy metal resistance genes and their potential bacterial sources within the tobacco phyllosphere. These findings not only enhance our understanding of metal-microbe-plant interactions but also have implications for the development of strategies for phytoremediation and improving plant resilience to heavy metal stress.

Heat and cold stress response

Large fluctuations in environmental temperature, resulting from solar radiation overexposure and changing global climate patterns, can impose significant abiotic stress on the phyllosphere of plants, leading to heat and cold stresses. To cope with these challenges, gene expansions have been observed in heat/cold shock factor gene families during adaptive evolution (Wang et al., 2018; Li et al., 2021). In our study, we identified a specific set of gene orthogroups (171 gene entries) associated with the heat/cold shock response in the metagenome of the tobacco phyllosphere (Figure 3B and see Table S1 at https://doi.org/10.6084/m9.figshare.21257352.v1).

Among these gene orthogroups, 71 encode cold shock proteins (cspA), primarily originating from bacterial taxa such as *Pantoea*, *Pseudomonas*, and Rhizobiaceae. Additionally, 99 gene orthogroups encode heat shock proteins, predominantly found in taxa like *Enterobacter*, Sphingomonadales, and *Pseudomonas*. These proteins function as transcription factors and molecular chaperones, working collaboratively to maintain cellular protein homeostasis (Andrási et al., 2021). For example, the heat shock protein DnaJ has been reported to protect Rubisco activity during heat stress (Wang et al., 2015). Similarly, the cold shock protein CspA promotes the proper folding of RNA molecules (Rennella et al., 2017). Furthermore, we detected 34 gene entries encoding chitinases, mainly derived from *Pseudomonas*, which have been shown to participate in cold and osmotic stress responses (Cao et al., 2019), and accordingly, we have detected 34 gene entries encoding chitinases, mainly from *Pseudomonas* (23.7%) (see Table S1 at https://doi.org/10.6084/m9.figshare.21257352.v1).

These findings demonstrate the presence of a diverse repertoire of heat and cold stress response genes in the tobacco phyllosphere metagenome, originating from various bacterial taxa. It highlights the importance of these genes in enabling plants to withstand and adapt to fluctuating temperature conditions.

Organic pollutant resistance

Organic pollution resulting from human activities, such as the excessive use of herbicides and improper management of chemical waste, poses a significant threat to plant life. Among the various impacts of organic pollutants, phyllosphere microbes are particularly vulnerable to particulate matter, pesticides, and herbicides, which are commonly found in heavily polluted areas. For instance, a study by Chen et al. (Chen et al., 2021) investigated the effects of a broad-spectrum fungicide on bacterial communities in tobacco phyllosphere, revealing substantial differences in both core and rare taxa. Furthermore, the introduction of organic pollutant-degrading microbes to plants has been shown to mitigate the detrimental effects of organic pollutants on plants and facilitate the removal of air pollutants (Sun et al., 2015; Rajtor and Piotrowska-Seget, 2016; Franzetti et al., 2020).

In our study, we identified a total of 1,309 gene families associated with xenobiotic biodegradation and metabolism (Figure 4A and see Table S1 at https://doi.org/10.6084/m9.figshare.21257352.v1). These gene families encompass antimicrobial resistance genes, multidrug efflux systems, beta-lactam resistance genes, as well as genes involved in the degradation of benzoate, aminobenzoate, caprolactam, chloroalkanes, chloroalkenes, dioxins, fluorobenzoate, furfural, and nitrotoluene. Additionally, four orthogroups were annotated as cytochrome P450, which is a broad-substrate-specificity oxygenase capable of catalyzing various detoxification reactions such as hydroxylation, dealkylation, sulfurization, epoxidation, and reduction (Lin et al., 2022).

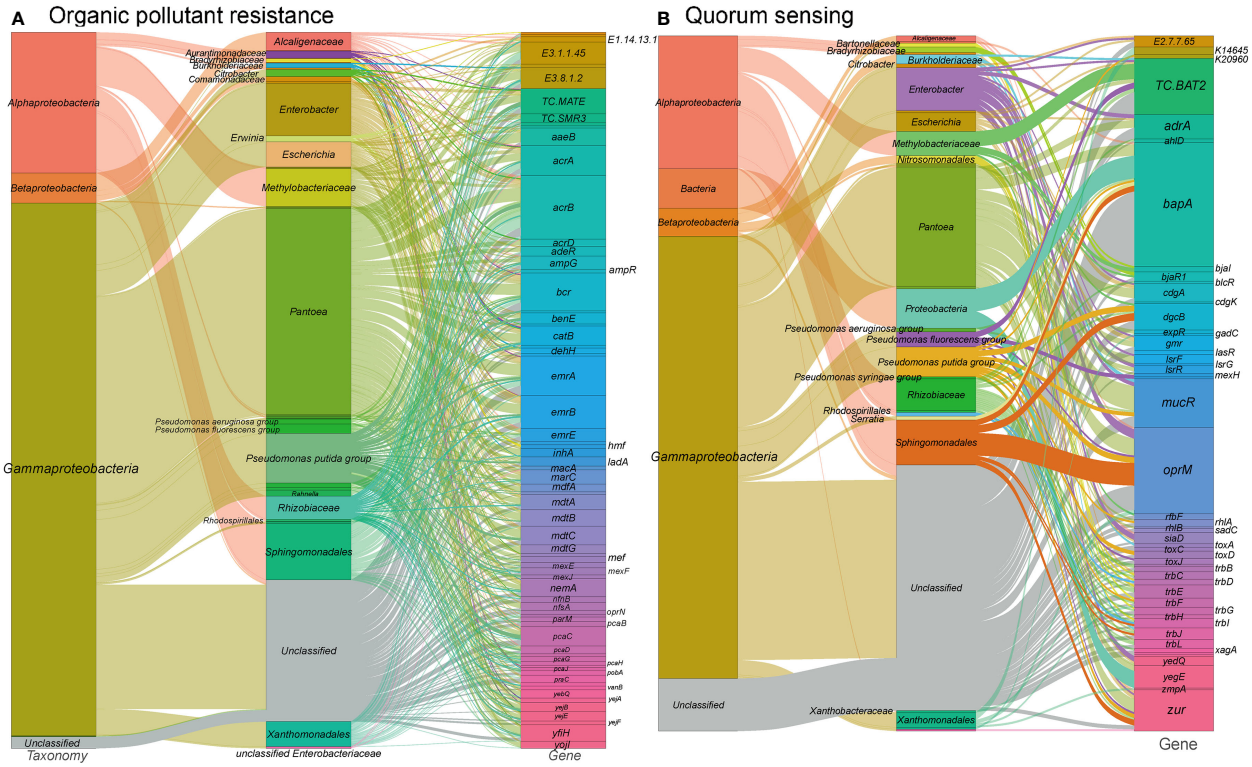

FIGURE 4
Sankey diagram depicting the taxonomic and functional profiles of genes conferring abiotic stress resilience in the metagenome of cigar tobacco phyllospheric microbiome: **(A)** Organic pollutant resistance; **(B)** Quorum sensing. Details for gene abbreviations can be found in Table S1 at https://doi.org/10.6084/m9.figshare.21257352.v1.

The majority of genes associated with xenobiotic biodegradation and metabolism pathways in our metagenome were found to be encoded by Pantoea, Sphingomonadales, Pseudomonas, and Methylobacteriaceae. Consistent with previous findings (Chen et al., 2021), taxa such as *Pantoea*, *Sphingomonas*, and *Pseudomonas* were dominant in the tobacco phyllosphere samples exposed to a 50% pesticide concentration. Moreover, studies have demonstrated the abilities of *Sphingomonas* species to degrade various organic pollutants, including phenol (Gong et al., 2016), bisphenol (Fujiwara et al., 2016), phenanthrene (Liu et al., 2016), nicotine, astaxanthin and chlorogenic acid (Ma et al., 2016), triclocarban (Mulla et al., 2016), γ-hexachlorocyclohexane (Tabata et al., 2013), nonylphenol polyethoxylates (Bai et al., 2016), hexachlorocyclohexane isomers (Kumari et al., 2002), plasticizers (Kera et al., 2016), and dioxin (Miller et al., 2010).

These findings highlight the potential of phyllosphere microbes, particularly those belonging to taxa such as *Pantoea* and *Sphingomonas*, to play a crucial role in the degradation of organic pollutants and the maintenance of plant health in polluted environments.

Quorum sensing

Quorum sensing (QS) is a crucial mechanism of microbial communication in the phyllosphere, allowing for coordinated phenotypic and behavioral responses through diffusible signal molecules, including biofilm formation, virulence, and pathogenicity (Lv et al., 2012). In our metagenome analysis, we identified a significant number of genes (381 gene orthogroups) associated with quorum sensing (Figure 4B and see Table S1 at https://doi.org/10.6084/m9.figshare.21257352.v1). These genes include N-acyl homoserine lactone hydrolase, acyl-homoserine lactone synthase, acyl-homoserine-lactone acylase, diguanylate cyclase, LsrR operon transcriptional repressor, and LuxR family transcriptional regulator that bind to homoserine lactones and activate respective operon genes. These genes are predominantly found in Gammaproteobacteria such as *Enterobacter*, *Escherichia*, as well as Alphaproteobacteria including Rhizobiaceae, Methylobacteriaceae, and Sphingomonadales. Specifically, acyl-homoserine lactone synthases are mainly encoded by Methylobacteriaceae and *Pantoea*, while diguanylate cyclases are primarily encoded by *Enterobacter* and *Pantoea*. Diguanylate cyclases are responsible for catalyzing the synthesis of cyclic di-GMP, a critical signaling molecule in quorum sensing, which is known to regulate biofilm formation and decrease motility (Antoniani et al., 2010). The predominant presence of diguanylate cyclase genes in *Enterobacter* and *Pantoea* aligns with previous studies highlighting their involvement in these processes (Bible et al., 2021; Wang et al., 2021).

The identification of genes related to quorum sensing in the tobacco phyllosphere microbiome suggests its potential importance in regulating various microbial behaviors and phenotypes. These findings provide valuable insights into the communication and coordination among phyllosphere microorganisms.

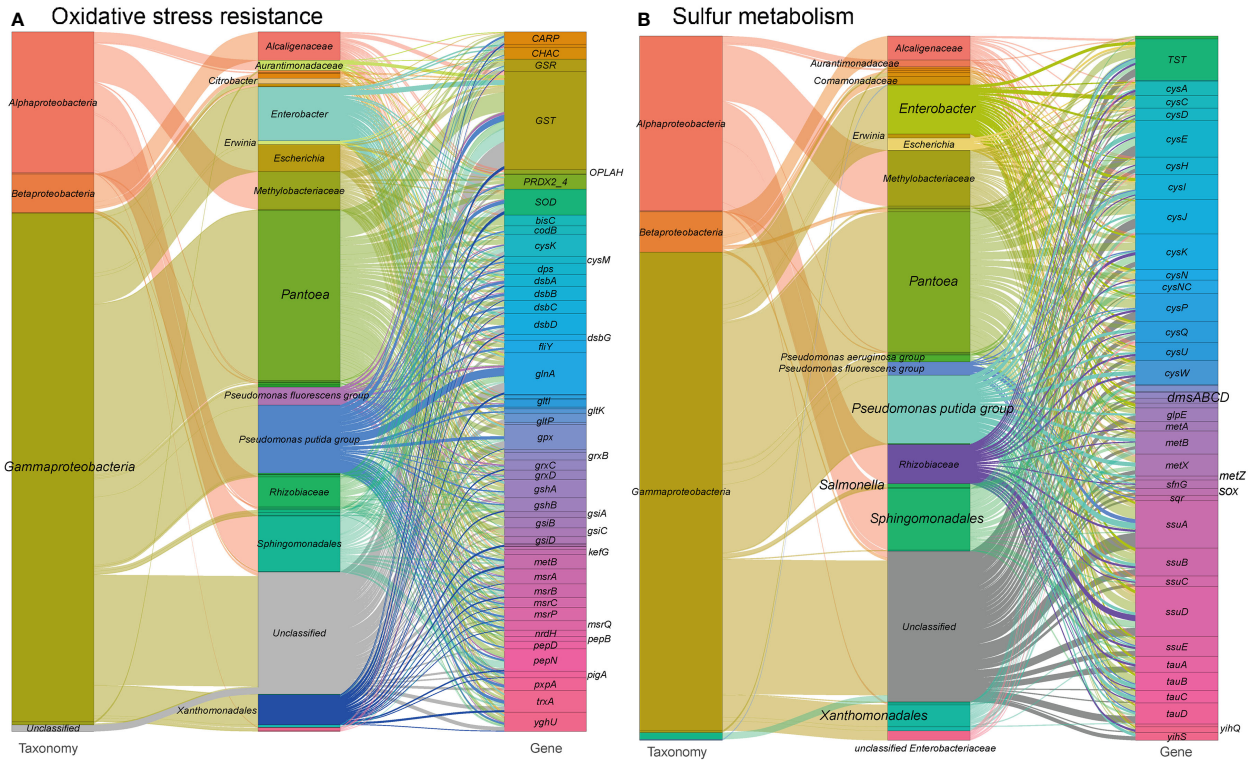

FIGURE 5
Sankey diagram depicting the taxonomic and functional profiles of genes conferring abiotic stress resilience in the metagenome of cigar tobacco phyllospheric microbiome: **(A)** Oxidative stress resistance; **(B)** Sulfur metabolism. Details for gene abbreviations can be found in Table S1 at https://doi.org/10.6084/m9.figshare.21257352.v1.

Oxidative stress resistance and sulfur metabolism

Oxidative stress occurs as a result of the excessive production of reactive oxygen species (ROS), which can cause damage to various cellular biomolecules and disrupt redox regulation. Various abiotic stresses such as drought (Niu et al., 2021), osmotic pressure (Cai-Hong et al., 2005), toxic metal stress (Schützendübel and Polle, 2002) contribute to the development of oxidative stress. However, the introduction of microbes to plants, whether naturally present or through exogenous inoculation, can enhance tolerance to oxidative stress by inducing the synthesis and secretion of antioxidants (Ilyas et al., 2021). Plant growth-promoting bacteria (PGPB) are particularly important in mitigating oxidative stress through the utilization of microbial antioxidant enzymes, which effectively scavenge ROS and maintain a balance between ROS production and removal mechanisms through plant-microbial interactions (Shaffique et al., 2022).

As illustrated in our findings, the phyllosphere microorganisms in tobacco harbor a substantial number of genes related to the canonical antioxidant systems (Gill and Tuteja, 2010; Hasanuzzaman et al., 2019) (see Figure 5A and Table S1 at https://doi.org/10.6084/m9.figshare.21257352.v1). These genes encode proteins involved in thiol:disulfide interchange, antioxidant enzymes, amino acid transporters, glutathione biosynthesis, glutaredoxins, ion transporters, and other components of the antioxidant defense system. Gammaproteobacteria, including *Enterobacter, Escherichia, Pseudomonas*, and Alphaproteobacteria, including Rhizobiaceae, Methylobacteriaceae, and Sphingomonadales, are the major contributors of these genes. Notably, *Pseudomonas* encodes a significant proportion of heme oxygenase and Fe-Mn superoxide dismutase (SOD), which are crucial components of the antioxidant defense system. We also detected genes encoding components of the oxidative electron transfer chain, such as cytochrome oxidase, that are likely involved in oxidative stress and acid stress tolerance (de la Garza-García et al., 2021). Additionally, we found genes encoding isocitrate dehydrogenase, which may contribute to a supply of reductant NADPH for defending against oxidative stress (Komatsu et al., 2014).

Sulfur metabolism (Figure 5B and see Table S1 at https://doi.org/10.6084/m9.figshare.21257352.v1) is closely related to the biosynthesis of antioxidant molecules, such as cystathionine. Genes involved in the inorganic sulfur metabolism pathway, including the *cysACDEHIJKNPQUW* operon and the bifunctional enzyme *cysNC*, are mainly encoded by *Enterobacter* in the metagenome. Other sulfur metabolism genes encode enzymes and transporters related to sulfur oxidation, cystathionine synthesis, taurine metabolism, sulfide oxidation, thiosulfate metabolism, and organic sulfur metabolism. Many of these genes are predominantly encoded by Sphingomonadales, *Pseudomonas*, and Rhizobiaceae, with specific functions such as the metabolism of sulfoquinovose and sulfoquinovosidase (Sharma et al., 2021). The sulfur metabolism

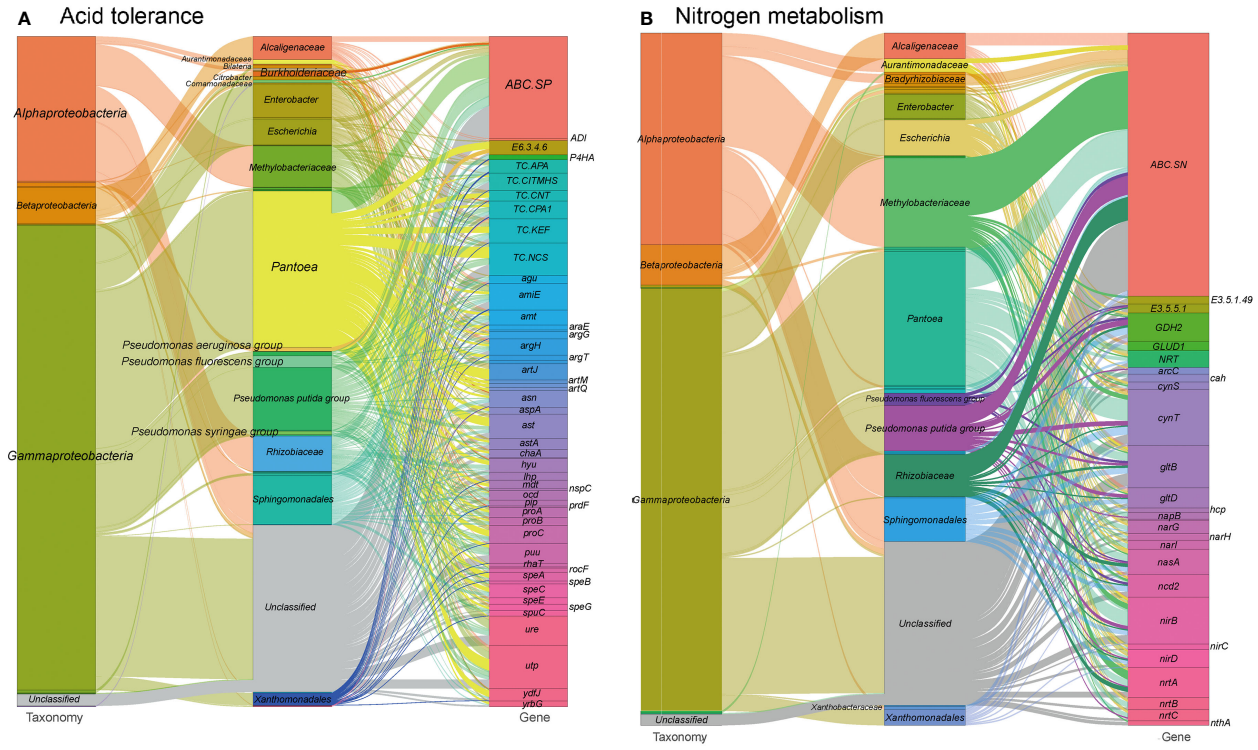

FIGURE 6
Sankey diagram that illustrates the taxonomic and functional profiles of genes conferring abiotic stress resilience in the cigar tobacco phyllospheric microbiome: **(A)** Acid resistance; **(B)** Nitrogen metabolism. Details for gene abbreviations can be found in Table S1 at https://doi.org/10.6084/m9.figshare.21257352.v1.

pathways in the metagenome are mainly encoded by *Pantoea*, *Pseudomonas*, and Methylobacteriaceae.

Overall, our findings suggest that the phyllosphere microbiome in tobacco possesses a diverse array of genes involved in antioxidant systems and sulfur metabolism, which contribute to oxidative stress protection and the modulation of redox regulation. These microbial functions are likely to play a crucial role in enhancing the plant's ability to cope with oxidative stress.

Acid tolerance and nitrogen metabolism

Environmental pH perturbation is a significant factor affecting both plants and their associated microbiota, as it can disrupt cellular homeostasis and physiology (Zhou et al., 2022). The southwestern regions of China have experienced high levels of acid rain, which may have had an impact on foliar ecology (Zhang et al., 2021). In our study, we identified 1,373 gene entries related to acid stress resistance in the tested metagenomes (see Table S1 at https://doi.org/10.6084/m9.figshare.21257352.v1). These genes are mainly encoded by *Pantoea* (22.0%), *Pseudomonas* (12.6%), *Sphingomonadales* (6.9%) and *Methylobacteriaceae* (6.0%) (Figure 6A). These genes encode proteins involved in acid stress chaperoning, transport systems for basic amino acids, spermidine, putrescine, urea, ammonium, and protons, as well as enzymes for arginine metabolism and urease production. These proteins play roles in pH regulation by neutralizing protons with basic products like arginine and polyamines (Stincone et al., 2011). Additionally, the ion/proton transporters related to osmotic pressure tolerance mentioned earlier could also contribute to adaptive responses to pH perturbation (Liang et al., 2020).

Furthermore, we identified 622 gene orthogroups involved in nitrogen metabolism (Figure 6B and see Table S1 at https://doi.org/10.6084/m9.figshare.21257352.v1). These gene orthogroups include genes encoding transporters (ABC.SN/NitT), enzymes (formamidase, nitrilase etc.), and other nitrogen metabolism-related proteins. These genes might also play a role in modulating pH homeostasis through the production of basic substrates, such as ammonium, and promoting nitrogen source utilization in the phyllosphere microbiome and the plant host. Nitrogen metabolism pathways in the metagenomes are primarily encoded by *Pantoea* (19.3%), *Pseudomonas* (9.0%) and *Methylobacteriaceae* (12.8%). Specially, glutamate dehydrogenase (GDH2) is mainly encoded by *Sphingomonadales* (26.0%), and *Pseudomonas* (26.0%), whereas nitronate monooxygenase (*ncd2*) is mainly encoded by *Sphingomonadales* (20.0%) and ferredoxin-nitrite reductase (*nirA*) is mainly encoded by *Methylobacteriaceae* (75.0%).

These findings suggest that the phyllosphere microbiome possesses genetic resources for adapting to acid stress and modulating pH homeostasis through mechanisms such as proton neutralization and nitrogen metabolism. However, further investigations are needed to understand the specific roles of these genes and their interactions in the context of environmental pH perturbation.

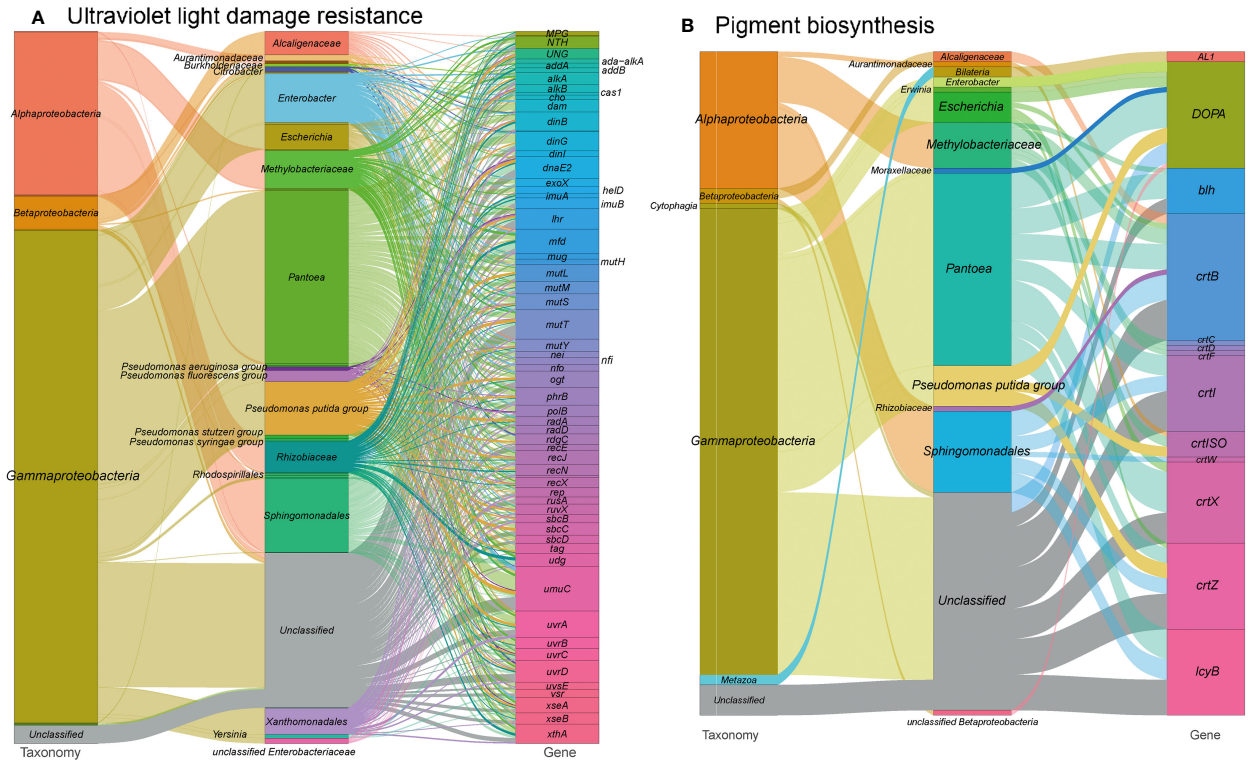

FIGURE 7
Sankey diagram that illustrates the taxonomic and functional profiles of genes conferring abiotic stress resilience in the cigar tobacco phyllospheric microbiome: **(A)** Ultraviolet light damage resistance; **(B)** Pigment biosynthesis. Details for gene abbreviations can be found in Table S1 at https://doi.org/10.6084/m9.figshare.21257352.v1.

Ultraviolet light damage resistance

DNA can undergo damage from various abiotic factors, such as ultraviolet (UV) light radiation resulting from prolonged sun exposure. This exposure can induce oxidative damage and cross-links between DNA and proteins or DNA strands. The accumulation of such damages can ultimately lead to genomic instability and cell death (Tuteja et al., 2009).

In our analysis of the functional profile of the tobacco microbiome, we observed a complete set of DNA repair machinery, consisting of 1,210 gene orthogroups (Figure 7A and see Table S1 at https://doi.org/10.6084/m9.figshare.21257352.v1). These genes are essential for protecting DNA from disruption caused by harmful radiation. They encode proteins involved in nucleotide excision repair (*mfd, uvrABCD*), base excision repair (*ada-alkA, alkA, xthA etc.*), DNA repair and recombination (*addAB, alkB, cas1, etc.*), and finally, mismatch repair (*dam, exoX, mutH, etc.*). Overall, the DNA repair metabolism pathways in our metagenome are mainly encoded by *Pantoea* (22.0%), *Pseudomonas* (12.6%), *Sphingomonadales* (6.9%) and *Methylobacteriaceae* (6.0%). This supports the notion that these microorganisms play a crucial role in protecting DNA from damage caused by harmful radiation. These findings are consistent with our previous study, which showed the enrichment of *Pseudomonas* (LDA = 5.29) and *Sphingomonas* (LDA = 4.19) during T3, a time period characterized by severe sun exposure (Wang et al., 2022).

Furthermore, we identified 132 gene orthogroups related with the production of pigments that absorb radiation (Figure 7B and see Table S1 at https://doi.org/10.6084/m9.figshare.21257352.v1), such as carotenoid biosynthesis (AL1, *crtBCDFIWXZ, crtISO, etc.*) and betalain biosynthesis (DOPA). Carotenoid biosynthesis is also linked to the production of phytohormones, such as gibberellins and abscisic acid, which help plants cope with abiotic stresses (Qin et al., 2007; Alagoz et al., 2018). Additionally, we annotated the microbial enzyme aminocyclopropane-1-carboxylic acid (ACC) deaminase, which reduces ethylene levels in host plants and contributes to plant tolerance against abiotic stresses (Ali et al., 2014; Glick and Nascimento, 2021).

Moreover, we found 33 gene orthogroups encoding sporulation proteins (*spoVR, spoVFA, spoIVCA*) and spore photoproduct lyase (*spmBE*), which are involved in abiotic stress tolerance and repair of UV-induced DNA damage in germinating bacterial spores (Table S1 at https://doi.org/10.6084/m9.figshare.21257352.v1) (Nicholson et al., 1997). Methylobacteriaceae, a family of Alpharoteobacteria, predominantly encoded these proteins, potentially explaining their abundance on the plant's phyllosphere and their tolerance to harmful UV irradiation (Yoshida et al., 2017).

In conclusion, the presence of DNA repair machinery, pigment-producing pathways, and stress-tolerance proteins in the tobacco phyllosphere microbiome suggests a microbial contribution to the plants' defense against abiotic stresses, including UV radiation. However, further research is needed to establish the specific mechanisms and interactions underlying these processes.

Viral sequence mining from metagenome

Viruses have been found to play a role in shaping bacterial communities. However, limited research has been conducted on the diversity and abundance of phyllosphere viral communities and their interactions with other microorganisms (Morella et al., 2018). Recently, there has been a growing focus on mining virome information using culture-independent metagenome or metatranscriptome technologies (Forero-Junco et al., 2022; Lauber and Seitz, 2022; Lee and Jeong, 2022). Understanding the virome in plant-associated environments can provide valuable insights into their potential influence on microbial adaptation to various stresses (Xu P. et al., 2008).

In this study, the researchers examined a total of 3,320 putative viral scaffolds from the metagenome of the cigar tobacco phyllosphere, divided into T1 (1,141), T2 (1,418), and T3 (761) groups, indicating that the viromes are diverse and dynamic. Out of these examined scaffolds, 2,616 were predicted to be confidential viral genomes (Table S2A at https://doi.org/10.6084/m9.figshare.21257382.v1). The average length of the predicted viral genomes was 2.45 kbp, with the longest being 76,944 bp and the smallest being 1,000 bp. The viral scaffolds contained an average of 4.18 ± 3.40 genes. The quality of the viral genomes varied, with only 0.2% classified as "complete," 0.3% as "high quality," 0.5% as "medium quality," 43.7% as "low quality," and 55.0% as "not determined" according to CheckV (Nayfach et al., 2021). Out of the predicted viral genomes, 36 were found to be lysogenic based on the presence of proviral sequences. However, it is important to note that bioinformatics prediction often underestimates the number of lysogenic viruses and fails to distinguish between pseudolysogens and lytic viruses (Roux et al., 2015). The tobacco phyllosphere viral genomes were clustered using vConTACT2 (Bin Jang et al., 2019) along with 2,616 known prokaryotic viruses (Figure 3A). The tobacco phyllosphere viral genomes were found to be closely related to phages that infect *Pseudomonas* (15.0%), *Burkholderia* (6.4%), *Enterobacteria* (8.4%), *Salmonella* (15.9%), *Escherichia* (14.8%), *Klebsiella* (9.9%), and *Ralstonia* (3.1%) at a taxonomic level higher than genus. It is worth noting that many of these taxa were found to be dominant lineages inhabiting the tobacco phyllosphere such as *Pseudomonas*, as mentioned earlier, and *Ralstonia* spp. is known as a significant tobacco pathogen causing severe bacterial wilt disease (Tao et al., 2022). Furthermore, the sampling site of this study is consistently affected by wildfire disease. It is known that viruses infecting the same type of host often exchange genes or DNA fragments, leading to the formation of strong genotypic clusters (Szymczak et al., 2019). Among the remaining viral populations, 1,400 nodes were classified as unclassified viruses that shared minimal genes with both the database and each other. This highlights the unexplored diversity of the tobacco phyllosphere virome (Figure 8A).

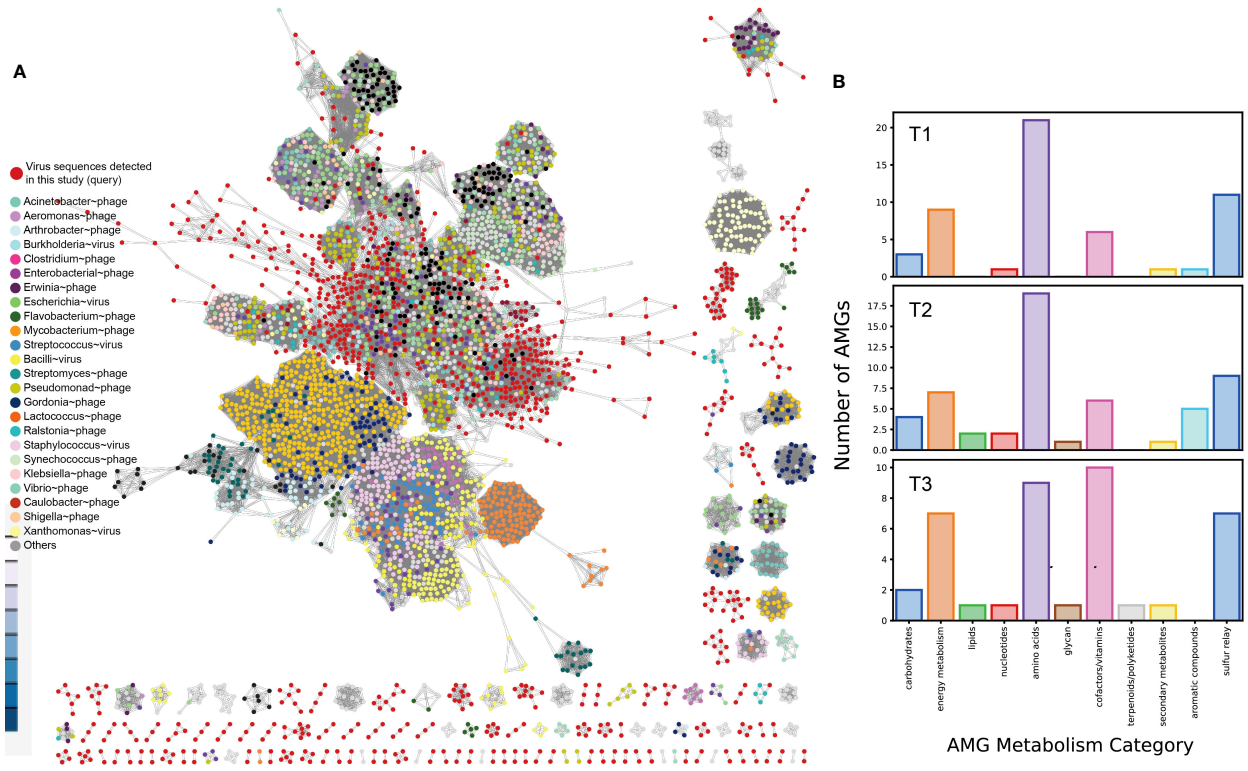

FIGURE 8
Clustering of detected viral genomes from cigar tobacco phyllosphere metagenome with reference viral genomes based on shared genes. **(A)** vConTACT2 output network. The network was visualized using Cytoscape v3.8.0 (https://cytoscape.org). Queried viruses are colored in red, and reference viruses are color coded based on the host they were annotated to infect; **(B)** Relative abundance of functional categories of identified viral genes per sample.

Upon closer examination of the genes present in the tobacco phyllosphere virome, a fascinating virus-host interaction is revealed. This interaction seems to maintain a delicate balance between viral predation and host stress resilience, which contributes to the sustainability of the phyllosphere ecosystem. The virome in the tobacco phyllosphere contains a diverse range of genes that potentially confer metabolic functions and resistance to abiotic stresses in the environment.

Through the analysis of the 3,320 viral scaffolds, a total of 15,908 proteins were identified and annotated, as shown in Table S2B at https://doi.org/10.6084/m9.figshare.21257382.v1. Approximately 53% of these proteins were assigned to sequences in the queried databases (KEGG/VOG/Pfam), while around 46.4% were categorized as "uncharacterized" or "hypothetical" proteins. Among the identified proteins, the most prevalent categories were cofactor and vitamin metabolism, amino acid metabolism, energy metabolism, and the sulfur relay system (Figure 8B). Notably, many genes within the viral populations appear to be involved in abiotic stress resistance (Table 1).

For example, the virome assembled from the metagenome of the T3 sample contained an alkaline phosphatase D (*phoD*), which may contribute to the solubilization of inorganic insoluble

TABLE 1 Auxiliary metabolic genes (AMGs) identified and annotated in viral scaffolds.

AMG KO	AMG count	AMG KO name	KEGG category
T1			
K01186	1	NEU1; sialidase-1 [EC:3.2.1.18]	00600 Sphingolipid metabolism
K01737	1	queD, ptpS, PTS; 6-pyruvoyltetrahydropterin/6-carboxytetrahydropterin synthase [EC:4.2.3.12 4.1.2.50]	00790 Folate biosynthesis
K00558	15	DNMT1, dcm; DNA (cytosine-5)-methyltransferase 1 [EC:2.1.1.37]	00270 Cysteine and methionine metabolism
K01179	1	E3.2.1.4; endoglucanase [EC:3.2.1.4]	00500 Starch and sucrose metabolism
K00390	6	cysH; phosphoadenosine phosphosulfate reductase [EC:1.8.4.8 1.8.4.10]	00920 Sulfur metabolism
K00147	1	proA; glutamate-5-semialdehyde dehydrogenase [EC:1.2.1.41]	00330 Arginine and proline metabolism
K01784	1	galE, GALE; UDP-glucose 4-epimerase [EC:5.1.3.2]	00052 Galactose metabolism
K10026	1	queE; 7-carboxy-7-deazaguanine synthase [EC:4.3.99.3]	00790 Folate biosynthesis
K21140	9	mec; [CysO sulfur-carrier protein]-S-L-cysteine hydrolase [EC:3.13.1.6]	04122 Sulfur relay system
K00121	1	frmA, ADH5, adhC; S-(hydroxymethyl)glutathione dehydrogenase/alcohol dehydrogenase [EC:1.1.1.284 1.1.1.1]	00010 Glycolysis/Gluconeogenesis
K01495	1	GCH1, folE; GTP cyclohydrolase IA [EC:3.5.4.16]	00790 Folate biosynthesis
K01939	1	purA, ADSS; adenylosuccinate synthase [EC:6.3.4.4]	00230 Purine metabolism
K01607	1	pcaC; 4-carboxymuconolactone decarboxylase [EC:4.1.1.44]	00362 Benzoate degradation
K16066	1	ydfG; 3-hydroxy acid dehydrogenase/malonic semialdehyde reductase [EC:1.1.1.381 1.1.1.-]	00240 Pyrimidine metabolism
K06920	2	queC; 7-cyano-7-deazaguanine synthase [EC:6.3.4.20]	00790 Folate biosynthesis
T2			
K00558	17	DNMT1, dcm; DNA (cytosine-5)-methyltransferase 1 [EC:2.1.1.37]	00270 Cysteine and methionine metabolism
K00147	1	proA; glutamate-5-semialdehyde dehydrogenase [EC:1.2.1.41]	00330 Arginine and proline metabolism
K00390	7	cysH; phosphoadenosine phosphosulfate reductase [EC:1.8.4.8 1.8.4.10]	00920 Sulfur metabolism
K01179	1	E3.2.1.4; endoglucanase [EC:3.2.1.4]	00500 Starch and sucrose metabolism
K00287	1	DHFR, folA; dihydrofolate reductase [EC:1.5.1.3]	00790 Folate biosynthesis
K01737	1	queD, ptpS, PTS; 6-pyruvoyltetrahydropterin/6-carboxytetrahydropterin synthase [EC:4.2.3.12 4.1.2.50]	00790 Folate biosynthesis
K16066	1	ydfG; 3-hydroxy acid dehydrogenase/malonic semialdehyde reductase [EC:1.1.1.381 1.1.1.-]	00240 Pyrimidine metabolism
K21140	11	mec; [CysO sulfur-carrier protein]-S-L-cysteine hydrolase [EC:3.13.1.6]	04122 Sulfur relay system
K01607	1	pcaC; 4-carboxymuconolactone decarboxylase [EC:4.1.1.44]	00362 Benzoate degradation

(Continued)

TABLE 1 Continued

AMG KO	AMG count	AMG KO name	KEGG category
K15634	2	gpmB; probable phosphoglycerate mutase [EC:5.4.2.12]	00010 Glycolysis/Gluconeogenesis
K06920	1	queC; 7-cyano-7-deazaguanine synthase [EC:6.3.4.20]	00790 Folate biosynthesis
K10026	1	queE; 7-carboxy-7-deazaguanine synthase [EC:4.3.99.3]	00790 Folate biosynthesis
K01495	1	GCH1, folE; GTP cyclohydrolase IA [EC:3.5.4.16]	00790 Folate biosynthesis
T3			
K21140	7	mec; [CysO sulfur-carrier protein]-S-L-cysteine hydrolase [EC:3.13.1.6]	04122 Sulfur relay system
K00558	8	DNMT1, dcm; DNA (cytosine-5)-methyltransferase 1 [EC:2.1.1.37]	00270 Cysteine and methionine metabolism
K01626	1	E2.5.1.54, aroF, aroG, aroH; 3-deoxy-7-phosphoheptulonate synthase [EC:2.5.1.54]	00400 Phenylalanine, tyrosine and tryptophan biosynthesis
K00059	1	fabG, OAR1; 3-oxoacyl-[acyl-carrier protein] reductase [EC:1.1.1.100]	00061 Fatty acid biosynthesis
K00737	1	MGAT3; beta-1,4-mannosyl-glycoprotein beta-1,4-N-acetylglucosaminyltransferase [EC:2.4.1.144]	00510 N-Glycan biosynthesis
K08289	1	purT; phosphoribosylglycinamide formyltransferase 2 [EC:2.1.2.2]	00230 Purine metabolism
K13315	1	eryBII, tylCII, tylC1, calS12, atmS12; NDP-hexose C3-ketoreductase/dTDP-4-oxo-2-deoxy-alpha-D-pentos-2-ene 2,3-reductase [EC:1.1.1.-]	00523 Polyketide sugar unit biosynthesis
K01737	1	queD, ptpS, PTS; 6-pyruvoyltetrahydropterin/6-carboxytetrahydropterin synthase [EC:4.2.3.12 4.1.2.50]	00790 Folate biosynthesis
K06211	1	nadR; HTH-type transcriptional regulator, transcriptional repressor of NAD biosynthesis genes [EC:2.7.7.1 2.7.1.22]	00760 Nicotinate and nicotinamide metabolism
K01113	1	phoD; alkaline phosphatase D [EC:3.1.3.1]	00790 Folate biosynthesis
K10026	1	queE; 7-carboxy-7-deazaguanine synthase [EC:4.3.99.3]	00790 Folate biosynthesis
K00390	7	cysH; phosphoadenosine phosphosulfate reductase [EC:1.8.4.8 1.8.4.10]	00920 Sulfur metabolism
K00287	1	DHFR, folA; dihydrofolate reductase [EC:1.5.1.3]	00790 Folate biosynthesis
K06920	1	queC; 7-cyano-7-deazaguanine synthase [EC:6.3.4.20]	00790 Folate biosynthesis
K01625	1	eda; 2-dehydro-3-deoxyphosphogluconate aldolase/(4S)-4-hydroxy-2-oxoglutarate aldolase [EC:4.1.2.14 4.1.3.42]	00030 Pentose phosphate pathway
K01495	1	GCH1, folE; GTP cyclohydrolase IA [EC:3.5.4.16]	00790 Folate biosynthesis

phosphorus, thereby enhancing environmental phosphorus availability (Thapa et al., 2017). Additionally, a glutamate-5-semialdehyde dehydrogenase (*proA*) was identified, which is involved in the synthesis of the osmolyte proline. Furthermore, numerous viruses carry genes related to cysteine and methionine metabolism, which are closely linked to oxidative stress resistance. These include genes such as phosphoadenosine phosphosulfate reductase (*cysH*, 20 entries), DNA (cytosine-5)-methyltransferase (*dcm*, 40 entries). It is noteworthy that these relatively abundant genes may confer benefits to viral populations, considering their detection in multiple samples, despite the presumably high maintenance cost associated with the presence of such genes in viral genomes. Moreover, the viral sequences also contain genes associated with the metabolism of protectant sugars, such as endoglucanase, NDP-hexose ketoreductase (*eryBII*), UDP-glucose 4-epimerase (*galE*), beta-1,4-N-acetylglucosaminyltransferase (MGAT3), which may contribute to the breakdown of complex polysaccharides abundant on plant surfaces (Xu et al., 2008). Additionally, genes involved in the degradation of organic pollutants, such as 4-carboxymuconolactone decarboxylase (*pcaC*), were also found.

Genes related to stress resilience and auxiliary metabolic functions were identified across all samples, with the highest abundance observed in the T2 group and the highest diversity in the T3 group (Figure 8A). It is proposed that these viruses may serve as vectors for horizontal gene transfer (HGT) and deliver stress resilience genes to their host counterparts. The emergence and mechanism of HGT events ("Why does lateral transfer occur in so many species and how?") is recommended as a still-pending and significant scientific question by the editorial of the journal Science in the article "So much more to know" (American Association for the Advancement of Science, 2005), and viruses could be instrumental in this process. Notably, (pseudo)lysogenic viruses carrying tolerance genes may enhance microbial survival on the plant phyllosphere by taking refuge in the host cytoplasm or genome. This mutualistic interaction aligns with similar proposals

in previous studies, such as marine cyanophages carrying photosystem genes (Sullivan et al., 2006) and mangrove soil viruses carrying carbohydrate-active enzymes (Jin et al., 2019). Viruses may also facilitate the formation and dispersal of microbial biofilms, providing them shelter in harsh environments (Rice et al., 2009; McDougald et al., 2011; Secor et al., 2015). Biofilms have even been observed in hot desert soil, where temperate viruses are suggested to be positively selected (Zablocki et al., 2016; Lebre et al., 2017).

The phyllosphere microbiota faces hostile abiotic conditions, such as high UV radiation, which can pose challenges for viruses (Iriarte et al., 2007). These conditions may have led to the selection of phages that are adapted to such pressures. Similarly, in the tobacco phyllosphere, viruses carrying stress resilience genes may improve their survival and reproduction by integrating their DNA into a bacterial host genome and aiding the host in thriving under abiotic stresses. However, it is worth noting that most of the identified viruses in the tobacco phyllosphere were predicted to be lytic, meaning they undergo a lytic cycle when environmental conditions are more favorable, such as during rainfall. The high ratio of lytic to lysogenic phages may be a result of the low microbial densities on the plant phyllosphere, which is consistent with the "kill-the-winner" dynamics, leading to a higher prevalence of lytic phages (Knowles et al., 2016). This finding is consistent with a previous report on the wheat phyllosphere (Forero-Junco et al., 2022). Nonetheless, experimental validation of a host-virus model specific to the tobacco phyllosphere is essential to confirm these hypotheses and determine the extent to which virus-mediated resilience genes contribute to enhancing microbial fitness under abiotic stresses.

Conclusions

In conclusion, our study utilized shotgun metagenomic sequencing to investigate the functional profile of the phyllosphere microbiota in tobacco plants and identify potential plant growth promoting bacteria (PGPB) that confer abiotic stress resilience. Our findings reveal the importance of microbial associations in mediating plant protection and responses to various stressors.

We observed that abundant genes from bacterial lineages, particularly *Pseudomonas*, within the cigar tobacco phyllospheric microbiome contribute to resilience against osmotic and drought stress, heavy metal toxicity, temperature perturbation, organic pollutants, oxidative stress resistance, and UV light damage. This highlights the crucial role of bacteria in enhancing stress tolerance in the phyllosphere.

Furthermore, our virome mining analysis unveiled the presence of viruses within the phyllosphere microbiome, including phages infecting *Pseudomonas, Burkholderia, Enterobacteria, Ralstonia*, and other related viruses. We identified genes associated with abiotic stress resilience in the virome, such as alkaline phosphatase D (*phoD*) and glutamate-5-semialdehyde dehydrogenase (*proA*), which contribute to nutrient solubilization and osmolyte synthesis, respectively.

These novel findings underscore the unexplored roles of viruses in facilitating and transferring abiotic stress resilience in the phyllospheric microbiome through beneficial virus-host interactions. By expanding our understanding of the taxonomic and functional profiles of abiotic stress resilience in the phyllosphere, this study provides valuable insights for the selection of PGPB candidates from the tobacco phyllosphere to enhance stress tolerance in plants.

Overall, our research enhances our knowledge on the intricate relationships between microorganisms and plants, advancing our understanding of the mechanisms underlying abiotic stress resilience. These findings have important implications for agricultural practices, as they can contribute to the development of strategies to enhance stress tolerance in crop plants by harnessing the potential of the phyllosphere microbiome.

Materials and methods

Sample collection

Samples of cigar tobacco (*Nicotiana tabacum* L.) leaves were collected from Yongding County, Zhangjiajie City, Hunan Province, China (29.13° N, 110.48° E) in June (T1), July (T2), and August (T3) of 2021. This sampling region is continuingly affected by bacterial wildfire disease. For each replicate, 5–7 middle leaves from a 90 m^2 plot area were randomly selected. This area was affected by bacterial wildfire disease. The leaf samples were stored in sterile plastic bags, transported to the laboratory, and stored at 4°C for subsequent foliar microbial DNA extractions. A total of over 120 leaves from thirty cigar tobacco plants were used in this study, representing the three time points (T1, T2, and T3) in three biological duplicates.

DNA extraction and shotgun metagenomic sequencing

In the DNA extraction and shotgun metagenomic sequencing procedures, leaf samples were collected from various parts of the leaf surface (excluding the main and branch veins) using a sterile puncher. A total of 15 grams of leaf samples were collected. The collected leaf samples were transferred into a 250-mL conical flask containing 200 mL of 0.1% Tween-80 bacterial phosphate buffer at pH 7.0. The flask was shaken for 30 minutes at 170 rpm and 25°C. This shaking step was performed to remove the epiphytic microbes from the leaf surface. After shaking, the bacterial suspension was collected by centrifugation at 10,000 rpm for 15 minutes at 4°C. The sediment obtained from the centrifugation was washed three times with sterile water. Finally, the sediment was resuspended with 1 mL of sterile water for DNA extraction purposes. Genomic DNA extraction was performed using the Plant Genomic DNA Kit following the manufacturer's protocol. The extracted DNA's quality was checked using a 1.0% agarose gel, and the DNA concentrations were measured using a NanoDrop 1000 spectrophotometer. To ensure replicability and reliability, three

types of samples were prepared corresponding to the three time points (T1, T2, and T3), and each time point had three replicates.

For shotgun metagenomic sequencing, the extracted DNA samples were fragmented using ultrasound into approximately 350 bp fragments. These fragments were used to construct sequencing libraries using the NEBNext® Ultra™ DNA Library Prep Kit for Illumina. The libraries were sequenced using the Illumina NovaSeq 6000 Sequencer. The combined datasets of the three groups of leaf samples contained a total of 54.8 Gbp of raw reads.

Shotgun metagenomic assembly and annotation

For the shotgun metagenomic data, the raw reads were trimmed with the sliding window approach to generate the QC (Quality Control) reads with Trimmomatic (Bolger et al., 2014). Contamination of reads originating from the host plant was aligned to the nuclear genome of *Nicotiana tabacum* TN90 (GCA_000715135.1) using Bowtie 2 (Langmead and Salzberg, 2012). After that, the concordantly mapped reads were removed to preserve the clean reads. To obtain the microbial reads and their taxonomic annotations, the clean reads were aligned using Kraken 2 (Wood et al., 2019), and the reads that could not be aligned to bacteria, fungi, archaea or virus were filtered out. The microbial reads from all the samples were pooled together for *de novo* assembly with MEGAHIT (Li et al., 2015) (-k-min 21, –k-max 191, –min-contig-len 500). For the assembled contigs, ORF (Open Reading Frame) were predicted with Prodigal (Hyatt et al., 2010) in metagenomics mode (–meta). This was followed by protein sequence clustering and analysis and through software BPGA v.1.0 by default procedures. The size of the pan-metagenome was extrapolated by implementing an power law regression function, $P_s = \kappa n^{\gamma}$, using a built-in program of the BPGA pipeline (Chaudhari et al., 2016), in which P_s represents the total number of non-orthologous gene families within its pan-metagenome, n represents the number of tested metagenomes, and both κ and γ are free parameters. An exponent γ of <0 suggests the pan-metagenome is "closed," where the size of the pan-metagenome reaches a constant value as extra metagenomes are added. Conversely, the species is predicted to harbor an open pan-metagenome for γ values between 0 and 1. In addition, the size of the core genome was extrapolated by fitting into an exponential decay function, $F_c = \kappa_c \exp(-n/\tau_c)$, with a built-in program of the BPGA pipeline (Chaudhari et al., 2016), where F_c is the number of core gene families, κ_c, and τ_c are free parameters.

For gene annotation, was used to annotate with eggNOG-mapper v.2.0 (Huerta-Cepas et al., 2019) searching with Diamond method (Buchfink et al., 2015) against multiple databases, including COG database (https://www.ncbi.nlm.nih.gov/research/cog/) and KEGG database (Aramaki et al., 2020) (–evalue 0.001 –score 60 –pident 40 –query_cover 20 –subject_cover 20). The orthogroup clustering and gene ontology (GO) categories were performed using OrthoVenn v.2.0 (Xu et al., 2019), and the hypergeometric test with a p-value < 0.05 was applied to find enriched GO in the clusters.

Prediction and analysis of viral scaffolds from metagenome

VIBRANT v1.2.1 (Kieft et al., 2020) with default settings was used for viral signal prediction across the assembled metagenomes and scaffolds length of ≥1,000 bp. CheckV v0.6.0 (Nayfach et al., 2021) was used for completeness and quality estimation. A viral contig was determined as lytic or lysogenic by VIBRANT v1.2.1 (Kieft et al., 2020) (-virome mode -l 5000). VIBRANT uses HMM profiles from three different databases: Kyoto Encyclopedia of Genes and Genomes (KEGG) KoFam (March 2019 release) (Aramaki et al., 2020), Pfam (v32) (El-Gebali et al., 2019), and Virus Orthologous Groups (VOG) (release 94, http://vogdb.org/). VIBRANT-predicted viral scaffolds with qualities of medium, high, and complete were annotated with KEGG, Pfam, and VOG HMMs (hmmsearch (v3.1), e-value < 1e−5) (Eddy, 1998). To identify viral contigs that were grouped with viral RefSeq genomes across the samples, output from vConTACT2 (v.0.9.8) (Bin Jang et al., 2019) for each sample was merged together to create a condensed network, visualized in Cytoscape v3.8.0 (https://cytoscape.org).

Data availability statement

The datasets presented in this study can be found in online repositories. The names of the repository/repositories and accession number(s) can be found in the article/Supplementary Material.

Author contributions

LL and HY conceived and designed the research. ZW, DP, CF, XL, SG and LL analyzed the data. LL wrote the manuscript. All authors contributed to the article and approved the submitted version.

Funding

The author(s) declare financial support was received for the research, authorship, and/or publication of this article. This research was supported by the key project of Science and Technology of Hunan Branch of China National Tobacco Corporation (HN2021KJ05, HKF202200143 [202201], H202201040560003 [202104]), the key research and development program of Hunan Province (grants no. 2020WK2022, 2022SK2076), Fundamental Research Funds for the Central Universities of Central South University (no. 2022ZZTS0420) and Hunan International Scientific and Technological Cooperation Base of Environmental Microbiome and Application (No. 2018WK4019). The funders were not involved in the study design,

collection, analysis, interpretation of data, the writing of this article, or the decision to submit it for publication.

Acknowledgments

We are grateful for resources from the High-Performance Computing Center of Central South University.

Conflict of interest

Author ZW, DP, CF, XL, and SG are employed by Zhangjiajie Tobacco Company of Hunan Province.

The remaining authors declare that the research was conducted in the absence of any commercial or financial relationships that could be constructed as a potential conflict of interest.

Publisher's note

All claims expressed in this article are solely those of the authors and do not necessarily represent those of their affiliated organizations, or those of the publisher, the editors and the reviewers. Any product that may be evaluated in this article, or claim that may be made by its manufacturer, is not guaranteed or endorsed by the publisher.

References

Alagoz, Y., Nayak, P., Dhami, N., and Cazzonelli, C. I. (2018). Cis-carotene biosynthesis, evolution and regulation in plants: the emergence of novel signaling metabolites. *Arch. Biochem. Biophys.* 654, 172–184. doi: 10.1016/j.abb.2018.07.014

Ali, N., Sorkhoh, N., Salamah, S., Eliyas, M., and Radwan, S. (2012). The potential of epiphytic hydrocarbon-utilizing bacteria on legume leaves for attenuation of atmospheric hydrocarbon pollutants. *J. Environ. Manage.* 93, 113–120. doi: 10.1016/j.jenvman.2011.08.014

Ali, S., Charles, T. C., and Glick, B. R. (2014). Amelioration of high salinity stress damage by plant growth-promoting bacterial endophytes that contain acc deaminase. *Plant Physiol. Biochem.* 80, 160–167. doi: 10.1016/j.plaphy.2014.04.003

American Association for the Advancement of Science. (2005). So much more to know. *Science* 309, 78–102. doi: 10.1126/science.309.5731.78b

Andrási, N., Pettkó-Szandtner, A., and Szabados, L. (2021). Diversity of plant heat shock factors: regulation, interactions, and functions. *J. Exp. Bot.* 72, 1558–1575. doi: 10.1093/jxb/eraa576

Antoniani, D., Bocci, P., Maciag, A., Raffaelli, N., and Landini, P. (2010). Monitoring of diguanylate cyclase activity and of cyclic-di-gmp biosynthesis by whole-cell assays suitable for high-throughput screening of biofilm inhibitors. *Appl. Microbiol. Biotechnol.* 85, 1095–1104. doi: 10.1007/s00253-009-2199-x

Aramaki, T., Blanc-Mathieu, R., Endo, H., Ohkubo, K., Kanehisa, M., Goto, S., et al. (2020). Kofamkoala: kegg ortholog assignment based on profile hmm and adaptive score threshold. *Bioinformatics* 36, 2251–2252. doi: 10.1093/bioinformatics/btz859

Arun, K. D., Sabarinathan, K. G., Gomathy, M., Kannan, R., and Balachandar, D. (2020). Mitigation of drought stress in rice crop with plant growth-promoting abiotic stress-tolerant rice phyllosphere bacteria. *J. Basic Microbiol.* 60, 768–786. doi: 10.1002/jobm.202000011

Audu, K. E., Adeniji, S. E., and Obidah, J. S. (2020). Bioremediation of toxic metals in mining site of zamfara metropolis using resident bacteria (pantoea agglomerans): a optimization approach. *Heliyon* 6, e4704. doi: 10.1016/j.heliyon.2020.e04704

Bai, N., Wang, S., Abuduaini, R., Zhu, X., and Zhao, Y. (2016). Isolation and characterization of sphingomonas sp. Y2 capable of high-efficiency degradation of nonylphenol polyethoxylates in wastewater. *Environ. Sci. pollut. Res.* 23, 12019–12029. doi: 10.1007/s11356-016-6413-y

Bashir, A., Hoffmann, T., Smits, S. H., and Bremer, E. (2014). Dimethylglycine provides salt and temperature stress protection to bacillus subtilis. *Appl. Environ. Microbiol.* 80, 2773–2785. doi: 10.1128/AEM.00078-14

Bashir, I., War, A. F., Rafiq, I., Reshi, Z. A., Rashid, I., and Shouche, Y. S. (2022). Phyllosphere microbiome: diversity and functions. *Microbiol. Res.* 254, 126888. doi: 10.1016/j.micres.2021.126888

Batool, F., Rehman, Y., and Hasnain, S. (2016). Phylloplane associated plant bacteria of commercially superior wheat varieties exhibit superior plant growth promoting abilities. *Front. Life Sci.* 9, 313–322. doi: 10.1080/21553769.2016.1256842

Bechtaoui, N., Rabiu, M. K., Raklami, A., Oufdou, K., Hafidi, M., and Jemo, M. (2021). Phosphate-dependent regulation of growth and stresses management in plants. *Front. Plant Sci.* 12. doi: 10.3389/fpls.2021.679916

Behr, M., Legay, S., Hausman, J. F., and Guerriero, G. (2015). Analysis of cell wall-related genes in organs of medicago sativa l. Under different abiotic stresses. *Int. J. Mol. Sci.* 16, 16104–16124. doi: 10.3390/ijms160716104

Bible, A. N., Chang, M., and Morrell-Falvey, J. L. (2021). Identification of a diguanylate cyclase expressed in the presence of plants and its application for discovering candidate gene products involved in plant colonization by pantoea sp. Yr343. *PloS One* 16, e248607. doi: 10.1371/journal.pone.0248607

Bilal, S., Khan, A. L., Shahzad, R., Kim, Y. H., Imran, M., et al. (2018). Mechanisms of cr(vi) resistance by endophytic sphingomonas sp. Lk11 and its cr(vi) phytotoxic mitigating effects in soybean (glycine max l.). *Ecotox. Environ. Safe.* 164, 648–658. doi: 10.1016/j.ecoenv.2018.08.043

Bin Jang, H., Bolduc, B., Zablocki, O., Kuhn, J. H., Roux, S., Adriaenssens, E. M., et al. (2019). Taxonomic assignment of uncultivated prokaryotic virus genomes is enabled by gene-sharing networks. *Nat. Biotechnol.* 37, 632–639. doi: 10.1038/s41587-019-0100-8

Bolger, A. M., Lohse, M., and Usadel, B. (2014). Trimmomatic: a flexible trimmer for illumina sequence data. *Bioinformatics* 30, 2114–2120. doi: 10.1093/bioinformatics/btu170

Buchfink, B., Xie, C., and Huson, D. H. (2015). Fast and sensitive protein alignment using diamond. *Nat. Methods* 12, 59–60. doi: 10.1038/nmeth.3176

Cai-Hong, P., Su-Jun, Z., Zhi-Zhong, G., and Bao-Shan, W. (2005). Nacl treatment markedly enhances h2o2-scavenging system in leaves of halophyte suaeda salsa. *Physiol. Plant* 125, 490–499. doi: 10.1111/j.1399-3054.2005.00585.x

Cao, S., Wang, Y., Li, Z., Shi, W., Gao, F., Zhou, Y., et al (2019). Genome-wide identification and expression analyses of the chitinases under cold and osmotic stress in ammopiptanthus nanus. *Genes* 10. doi: 10.3390/genes10060472

Chen, H., and Jiang, J. (2010). Osmotic adjustment and plant adaptation to environmental changes related to drought and salinity. *Environ. Rev.* 18, 309–319. doi: 10.1139/A10-014

Chen, Q. L., Cai, L., Wang, H. C., Cai, L. T., Goodwin, P., Ma, J., et al. (2020). Fungal composition and diversity of the tobacco leaf phyllosphere during curing of leaves. *Front. Microbiol.* 11. doi: 10.3389/fmicb.2020.554051

Chen, X., Wicaksono, W. A., Berg, G., and Cernava, T. (2021). Bacterial communities in the plant phyllosphere harbour distinct responders to a broad-spectrum pesticide. *Sci. Total Environ.* 751, 141799. doi: 10.1016/j.scitotenv.2020.141799

Dai, Y. F., Wu, X. M., Wang, H. C., Li, W. H., Cai, L. T., Li, J. X., et al. (2022). Spatio-temporal variation in the phyllospheric microbial biodiversity of alternaria alternata-infected tobacco foliage. *Front. Microbiol.* 13. doi: 10.3389/fmicb.2022.920109

Daubin, V., and Szöllősi, G. J. (2016). Horizontal gene transfer and the history of life. *Cold Spring Harbor Perspect. Biol.* 8, a18036. doi: 10.1101/cshperspect.a018036

de la Garza-García, J. A., Ouahrani-Bettache, S., Lyonnais, S., Ornelas-Eusebio, E., Freddi, L., Al Dahouk, S., et al. (2021). Comparative genome-wide transcriptome analysis of brucella suis and brucella microti under acid stress at ph 4.5: cold shock protein cspa and dps are associated with acid resistance of b. Microti. *Front. Microbiol.* 12. doi: 10.3389/fmicb.2021.794535

de Sousa, L. P., Cipriano, M. A. P., da Silva, M. J., Patrício, F. R. A., Freitas, S. D. S., Carazzolle, M. F., et al. (2022). Functional genomics analysis of a phyllospheric pseudomonas spp with potential for biological control against coffee rust. *BMC Microbiol.* 22, 222. doi: 10.1186/s12866-022-02637-4

Devarajan, A. K., Muthukrishanan, G., Truu, J., Truu, M., Ostonen, I., Kizhaeral, S. S., et al. (2021). The foliar application of rice phyllosphere bacteria induces drought-stress tolerance in oryza sativa (l.). *Plants-Basel* 10. doi: 10.3390/plants10020387

Eddy, S. R. (1998). Profile hidden markov models. *Bioinformatics* 14, 755–763. doi: 10.1093/bioinformatics/14.9.755

El-Gebali, S., Mistry, J., Bateman, A., Eddy, S. R., Luciani, A., Potter, S. C., et al. (2019). The pfam protein families database in 2019. *Nucleic Acids Res.* 47, D427–D432. doi: 10.1093/nar/gky995

Enya, J., Shinohara, H., Yoshida, S., Tsukiboshi, T., Negishi, H., Suyama, K., et al. (2007). Culturable leaf-associated bacteria on tomato plants and their potential as biological control agents. *Microb. Ecol.* 53, 524–536. doi: 10.1007/s00248-006-9085-1

Forero-Junco, L. M., Alanin, K. W. S., Djurhuus, A. M., Kot, W., Gobbi, A., and Hansen, L. H. (2022). Bacteriophages roam the wheat phyllosphere *Viruses-Basel* 14. doi: 10.3390/v14020244

Franzetti, A., Gandolfi, I., Bestetti, G., Padoa, S. E., Canedoli, C., Brambilla, D., et al. (2020). Plant-microorganisms interaction promotes removal of air pollutants in milan (Italy) urban area. *J. Hazard. Mater.* 384, 121021. doi: 10.1016/j.jhazmat.2019.121021

Fu, S. F., Sun, P. F., Lu, H. Y., Wei, J. Y., Xiao, H. S., Fang, W. T., et al. (2016). Plant growth-promoting traits of yeasts isolated from the phyllosphere and rhizosphere of drosera spatulata lab. *Fungal Biol.* 120, 433–448. doi: 10.1016/j.funbio.2015.12.006

Fujiwara, H., Soda, S., Fujita, M., and Ike, M. (2016). Kinetics of bisphenol a degradation by sphingomonas paucimobilis fj-4. *J. Biosci. Bioeng.* 122, 341–344. doi: 10.1016/j.jbiosc.2016.02.015

Fürnkranz, M., Wanek, W., Richter, A., Abell, G., Rasche, F., and Sessitsch, A. (2008). Nitrogen fixation by phyllosphere bacteria associated with higher plants and their colonizing epiphytes of a tropical lowland rainforest of Costa Rica. *Isme J.* 2, 561–570. doi: 10.1038/ismej.2008.14

Ghosh, D., Gupta, A., and Mohapatra, S. (2019). A comparative analysis of exopolysaccharide and phytohormone secretions by four drought-tolerant rhizobacterial strains and their impact on osmotic-stress mitigation in arabidopsis thaliana. *World J. Microbiol. Biotechnol.* 35, 90. doi: 10.1007/s11274-019-2659-0

Gill, S. S., and Tuteja, N. (2010). Reactive oxygen species and antioxidant machinery in abiotic stress tolerance in crop plants. *Plant Physiol. Biochem.* 48, 909–930. doi: 10.1016/j.plaphy.2010.08.016

Girardot, F., Allégra, S., Pfendler, S., Conord, C., Rey, C., Gillet, B., et al. (2020). Bacterial diversity on an abandoned, industrial wasteland contaminated by polychlorinated biphenyls, dioxins, furans and trace metals. *Sci. Total Environ.* 748, 141242. doi: 10.1016/j.scitotenv.2020.141242

Glick, B. R., and Nascimento, F. X. (2021). Pseudomonas 1-aminocyclopropane-1-carboxylate (acc) deaminase and its role in beneficial plant-microbe interactions. *Microorganisms* 9. doi: 10.3390/microorganisms9122467

Gong, B., Wu, P., Huang, Z., Li, Y., Dang, Z., Ruan, B., et al. (2016). Enhanced degradation of phenol by sphingomonas sp. Gy2b with resistance towards suboptimal environment through adsorption on kaolinite. *Chemosphere* 148, 388–394. doi: 10.1016/j.chemosphere.2016.01.003

Hanin, M., Ebel, C., Ngom, M., Laplaze, L., and Masmoudi, K. (2016). New insights on plant salt tolerance mechanisms and their potential use for breeding. *Front. Plant Sci.* 7. doi: 10.3389/fpls.2016.01787

Hasanuzzaman, M., Bhuyan, M. H. M. B., Anee, T. I., Parvin, K., Nahar, K., Mahmud, J. A., et al. (2019). Regulation of ascorbate-glutathione pathway in mitigating oxidative damage in plants under abiotic stress. *Antioxidants* 8. doi: 10.3390/antiox8090384

Heredia-Ponce, Z., de Vicente, A., Cazorla, F. M., and Gutiérrez-Barranquero, J. A. (2021). Beyond the wall: exopolysaccharides in the biofilm lifestyle of pathogenic and beneficial plant-associated pseudomonas. *Microorganisms* 9. doi: 10.3390/microorganisms9020445

Huang, J. (2013). Horizontal gene transfer in eukaryotes: the weak-link model. *Bioessays* 35, 868–875. doi: 10.1002/bies.201300007

Huang, Y., Wang, H. C., Cai, L. T., Li, W., Pan, D., Xiang, L., et al. (2021). Phyllospheric microbial composition and diversity of the tobacco leaves infected by didymella segeticola. *Front. Microbiol.* 12. doi: 10.3389/fmicb.2021.699699

Huerta-Cepas, J., Szklarczyk, D., Heller, D., Hernández-Plaza, A., Forslund, S. K., Cook, H., et al. (2019). Eggnog 5.0: a hierarchical, functionally and phylogenetically annotated orthology resource based on 5090 organisms and 2502 viruses. *Nucleic Acids Res.* 47, D309–D314. doi: 10.1093/nar/gky1085

Hyatt, D., Chen, G. L., Locascio, P. F., Land, M. L., Larimer, F. W., and Hauser, L. J. (2010). Prodigal: prokaryotic gene recognition and translation initiation site identification. *BMC Bioinf.* 11, 119. doi: 10.1186/1471-2105-11-119

Ilyas, N., Mumtaz, K., Akhtar, N., Yasmin, H., Sayyed, R. Z., Khan, W., et al. (2020). Exopolysaccharides producing bacteria for the amelioration of drought stress in wheat. *Sustainability* 12, 8876. doi: 10.3390/su12218876

Ilyas, M., Nisar, M., Khan, N., Hazrat, A., Khan, A. H., Hayat, K., et al. (2021). Drought tolerance strategies in plants: a mechanistic approach. *J. Plant Growth Regul.* 40, 926–944. doi: 10.1007/s00344-020-10174-5

Innerebner, G., Knief, C., and Vorholt, J. A. (2011). Protection of arabidopsis thaliana against leaf-pathogenic pseudomonas syringae by sphingomonas strains in a controlled model system. *Appl. Environ. Microbiol.* 77, 3202–3210. doi: 10.1128/AEM.00133-11

Iriarte, F. B., Balogh, B., Momol, M. T., Smith, L. M., Wilson, M., and Jones, J. B. (2007). Factors affecting survival of bacteriophage on tomato leaf surfaces. *Appl. Environ. Microbiol.* 73 (6), 1704–1711. doi: 10.1128/AEM.02118-06

Jin, M., Guo, X., Zhang, R., Qu, W., Gao, B., and Zeng, R. (2019). Diversities and potential biogeochemical impacts of mangrove soil viruses. *Microbiome* 7 (1), 58. doi: 10.1186/s40168-019-0675-9

Kahraman, M., Sevim, G., and Bor, M. (2019). *The role of proline, glycinebetaine, and trehalose in stress-responsive gene expression*. Eds. M. A. Hossain, V. Kumar, D. J. Burritt, M. Fujita and P. S. A. Mäkelä (Cham: Springer International Publishing), 241–256.

Kera, Y., Abe, K., Kasai, D., Fukuda, M., and Takahashi, S. (2016). Draft genome sequences of sphingobium sp. Strain tcm1 and sphingomonas sp. Strain tdk1, haloalkyl phosphate flame retardant- and plasticizer-degrading bacteria. *Genome Announc.* 4. doi: 10.1128/genomeA.00668-16

Khoiri, A. N., Cheevadhanarak, S., Jirakkakul, J., Dulsawat, S., Prommeenate, P., Tachaleat, A., et al. (2021). Comparative metagenomics reveals microbial signatures of sugarcane phyllosphere in organic management. *Front. Microbiol.* 12, 623799. doi: 10.3389/fmicb.2021.623799

Kieft, K., Zhou, Z., and Anantharaman, K. (2020). Vibrant: automated recovery, annotation and curation of microbial viruses, and evaluation of viral community function from genomic sequences. *Microbiome* 8, 90. doi: 10.1186/s40168-020-00867-0

Knief, C., Delmotte, N., Chaffron, S., Stark, M., Innerebner, G., Wassmann, R., et al. (2012). Metaproteogenomic analysis of microbial communities in the phyllosphere and rhizosphere of rice. *Isme J.* 6 (7), 1378–1390. doi: 10.1038/ismej.2011.192

Knight, R., Vrbanac, A., Taylor, B. C., Aksenov, A., Callewaert, C., Debelius, J., et al. (2018). Best practices for analysing microbiomes. *Nat. Rev. Microbiol.* 16 (7), 410–422. doi: 10.1038/s41579-018-0029-9

Knowles, B., Silveira, C. B., Bailey, B. A., Barott, K., Cantu, V. A., Cobián-Güemes, A. G., et al. (2016). Lytic to temperate switching of viral communities. *Nature* 531, 466–470. doi: 10.1038/nature17193

Komatsu, S., Kamal, A. H., and Hossain, Z. (2014). Wheat proteomics: proteome modulation and abiotic stress acclimation. *Front. Plant Sci.* 5. doi: 10.3389/fpls.2014.00684

Kumari, R., Subudhi, S., Suar, M., Dhingra, G., Raina, V., Dogra, C., et al. (2002). Cloning and characterization of lin genes responsible for the degradation of hexachlorocyclohexane isomers by sphingomonas paucimobilis strain b90. *Appl. Environ. Microbiol.* 68 (12), 6021–6028. doi: 10.1128/AEM.68.12.6021-6028.2002

Lajoie, G., Maglione, R., and Kembel, S. W. (2020). Adaptive matching between phyllosphere bacteria and their tree hosts in a neotropical forest. *Microbiome* 8, 70. doi: 10.1186/s40168-020-00844-7

Langmead, B., and Salzberg, S. L. (2012). Fast gapped-read alignment with bowtie 2. *Nat. Methods* 9, 357–359. doi: 10.1038/nmeth.1923

Lauber, C., and Seitz, S. (2022). Opportunities and challenges of data-driven virus discovery. *Biomolecules* 12. doi: 10.3390/biom12081073

Lebre, P. H., De Maayer, P., and Cowan, D. A. (2017). Xerotolerant bacteria: surviving through a dry spell. *Nat. Rev. Microbiol.* 15, 285–296. doi: 10.1038/nrmicro.2017.16

Lee, H. J., and Jeong, R. D. (2022). Metatranscriptomic analysis of plant viruses in imported pear and kiwifruit pollen. *Plant Pathol. J.* 38, 220–228. doi: 10.5423/PPJ.OA.03.2022.0047

Li, X. T., Feng, X. Y., Zeng, Z., Liu, Y., and Shao, Z. Q. (2021). Comparative analysis of hsf genes from secale cereale and its triticeae relatives reveal ancient and recent gene expansions. *Front. Genet.* 12. doi: 10.3389/fgene.2021.801218

Li, D., Liu, C. M., Luo, R., Sadakane, K., and Lam, T. W. (2015). Megahit: an ultra-fast single-node solution for large and complex metagenomics assembly via succinct de bruijn graph. *Bioinformatics* 31, 1674–1676. doi: 10.1093/bioinformatics/btv033

Liang, C., Ma, Y., and Li, L. (2020). Comparison of plasma membrane h(+)-atpase response to acid rain stress between rice and soybean. *Environ. Sci. Pollut. Res.* 27, 6389–6400. doi: 10.1007/s11356-019-07285-2

Lin, S., Wei, J., Yang, B., Zhang, M., and Zhuo, R. (2022). Bioremediation of organic pollutants by white rot fungal cytochrome p450: the role and mechanism of cyp450 in biodegradation. *Chemosphere* 301, 134776. doi: 10.1016/j.chemosphere.2022.134776

Lindow, S. E., and Brandl, M. T. (2003). Microbiology of the phyllosphere. *Appl. Environ. Microbiol.* 69, 1875–1883. doi: 10.1128/AEM.69.4.1875-1883.2003

Liu, S., Guo, C., Liang, X., Wu, F., and Dang, Z. (2016). Nonionic surfactants induced changes in cell characteristics and phenanthrene degradation ability of sphingomonas sp. Gy2b. *Ecotox. Environ. Safe.* 129, 210–218. doi: 10.1016/j.ecoenv.2016.03.035

Liu, X. M., and Zhang, H. (2015). The effects of bacterial volatile emissions on plant abiotic stress tolerance. *Front. Plant Sci.* 6. doi: 10.3389/fpls.2015.00774

Lv, D., Ma, A., Bai, Z., Zhuang, X., and Zhuang, G. (2012). Response of leaf-associated bacterial communities to primary acyl-homoserine lactone in the tobacco phyllosphere. *Res. Microbiol.* 163, 119–124. doi: 10.1016/j.resmic.2011.11.001

Ma, Y., Wang, X., Nie, X., Zhang, Z., Yang, Z., Nie, C., et al. (2016). Microbial degradation of chlorogenic acid by a sphingomonas sp. Strain. *Appl. Biochem. Biotechnol.* 179 (8), 1381–1392. doi: 10.1007/s12010-016-2071-2

Márquez, L. M., Redman, R. S., Rodriguez, R. J., and Roossinck, M. J. (2007). A virus in a fungus in a plant: three-way symbiosis required for thermal tolerance. *Science* 315, 513–515. doi: 10.1126/science.1136237

Mastouri, F., Björkman, T., and Harman, G. E. (2012). Trichoderma harzianum enhances antioxidant defense of tomato seedlings and resistance to water deficit. *Mol. Plant-Microbe Interact.* 25, 1264–1271. doi: 10.1094/MPMI-09-11-0240

McDougald, D., Rice, S. A., Barraud, N., Steinberg, P. D., and Kjelleberg, S. (2011). Should we stay or should we go: mechanisms and ecological consequences for biofilm dispersal. *Nat. Rev. Microbiol.* 10, 39–50. doi: 10.1038/nrmicro2695

Meyer, K. M., and Leveau, J. H. (2012). Microbiology of the phyllosphere: a playground for testing ecological concepts. *Oecologia* 168, 621–629. doi: 10.1007/s00442-011-2138-2

Miller, T. R., Delcher, A. L., Salzberg, S. L., Saunders, E., Detter, J. C., and Halden, R. U. (2010). Genome sequence of the dioxin-mineralizing bacterium sphingomonas wittichii rw1. *J. Bacteriol.* 192 (22), 6101–6102. doi: 10.1128/JB.01030-10

Mishra, J., Singh, R., and Arora, N. K. (2017). Alleviation of heavy metal stress in plants and remediation of soil by rhizosphere microorganisms. *Front. Microbiol.* 8. doi: 10.3389/fmicb.2017.01706

Morella, N. M., Gomez, A. L., Wang, G., Leung, M. S., and Koskella, B. (2018). The impact of bacteriophages on phyllosphere bacterial abundance and composition. *Mol. Ecol.* 27, 2025–2038. doi: 10.1111/mec.14542

Mulla, S. I., Wang, H., Sun, Q., Hu, A., and Yu, C. P. (2016). Characterization of triclosan metabolism in sphingomonas sp. Strain yl-jm2c. *Sci. Rep.* 6, 21965. doi: 10.1038/srep21965

Nadeem, S. M., Ahmad, M., Tufail, M. A., Asghar, H. N., Nazli, F., and Zahir, Z. A. (2021). Appraising the potential of eps-producing rhizobacteria with acc-deaminase activity to improve growth and physiology of maize under drought stress. *Physiol. Plant* 172 (2), 463–476. doi: 10.1111/ppl.13212

Naseem, H., Ahsan, M., Shahid, M. A., and Khan, N. (2018). Exopolysaccharides producing rhizobacteria and their role in plant growth and drought tolerance. *J. Basic Microbiol.* 58, 1009–1022. doi: 10.1002/jobm.201800309

Nayfach, S., Camargo, A. P., Schulz, F., Eloe-Fadrosh, E., Roux, S., and Kyrpides, N. C. (2021). Checkv assesses the quality and completeness of metagenome-assembled viral genomes. *Nat. Biotechnol.* 39 (5), 578–585. doi: 10.1038/s41587-020-00774-7

Nicholson, W. L., Chooback, L., and Fajardo-Cavazos, P. (1997). Analysis of spore photoproduct lyase operon (splab) function using targeted deletion-insertion mutations spanning the bacillus subtilis operons ptshi and splab. *Mol. Gen. Genet.* 255, 587–594. doi: 10.1007/s004380050532

Niu, T., Zhang, T., Qiao, Y., Wen, P., Zhai, G., Liu, E., et al. (2021). Glycinebetaine mitigates drought stress-induced oxidative damage in pears. *PloS One* 16 (11), e251389. doi: 10.1371/journal.pone.0251389

Pan, P., Gu, Y., Sun, D., Wu, Q. L., and Zhou, N. (2023). Microbial diversity biased estimation caused by intragenomic heterogeneity and interspecific conservation of 16s rrna genes. *Appl. Environ. Microbiol.* 89, e2108–e2122. doi: 10.1128/aem.02108-22

Parakkottil, C. M., Duncan, G. A., Armirotti, A., Abergel, C., Gurnon, J. R., Van Etten, J. L., et al. (2010). Identification of an l-rhamnose synthetic pathway in two nucleocytoplasmic large dna viruses. *J. Virol.* 84 (17), 8829–8838. doi: 10.1128/JVI.00770-10

Patel, S., Jinal, H. N., and Amaresan, N. (2017). Isolation and characterization of drought resistance bacteria for plant growth promoting properties and their effect on chilli (capsicum annuum) seedling under salt stress. *Biocatal. Agric. Biotechnol.* 12, 85–89. doi: 10.1016/j.bcab.2017.09.002

Patel, P. R., Shaikh, S. S., and Sayyed, R. Z. (2016). Dynamism of pgpr in bioremediation and plant growth promotion in heavy metal contaminated soil. *Indian J. Exp. Biol.* 54, 286–290.

Qin, G., Gu, H., Ma, L., Peng, Y., Deng, X. W., Chen, Z., et al. (2007). Disruption of phytoene desaturase gene results in albino and dwarf phenotypes in arabidopsis by impairing chlorophyll, carotenoid, and gibberellin biosynthesis. *Cell Res.* 17 (5), 471–482. doi: 10.1038/cr.2007.40

Rajtor, M., and Piotrowska-Seget, Z. (2016). Prospects for arbuscular mycorrhizal fungi (amf) to assist in phytoremediation of soil hydrocarbon contaminants. *Chemosphere* 162, 105–116. doi: 10.1016/j.chemosphere.2016.07.071

Rastogi, G., Coaker, G. L., and Leveau, J. H. (2013). New insights into the structure and function of phyllosphere microbiota through high-throughput molecular approaches. *FEMS Microbiol. Lett.* 348, 1–10. doi: 10.1111/1574-6968.12225

Rennella, E., Sára, T., Juen, M., Wunderlich, C., Imbert, L., Solyom, Z., et al. (2017). Rna binding and chaperone activity of the e. Coli cold-shock protein cspa. *Nucleic Acids Res.* 45 (7), 4255–4268. doi: 10.1093/nar/gkx044

Rice, S. A., Tan, C. H., Mikkelsen, P. J., Kung, V., Woo, J., Tay, M., et al. (2009). The biofilm life cycle and virulence of pseudomonas aeruginosa are dependent on a filamentous prophage. *Isme J.* 3 (3), 271–282. doi: 10.1038/ismej.2008.109

Roossinck, M. J. (2013). Plant virus ecology. *PloS Pathog.* 9, e1003304. doi: 10.1371/journal.ppat.1003304

Roux, S., Enault, F., Hurwitz, B. L., and Sullivan, M. B. (2015). Virsorter: mining viral signal from microbial genomic data. *Peerj* 3, e985. doi: 10.7717/peerj.985

Sánchez-López, A. S., González-Chávez, M., Solís-Domínguez, F. A., Carrillo-González, R., and Rosas-Saito, G. H. (2018). Leaf epiphytic bacteria of plants colonizing mine residues: possible exploitation for remediation of air pollutants. *Front. Microbiol.* 9. doi: 10.3389/fmicb.2018.03028

Scavino, A. F., and Pedraza, R. O. (2013). *The role of siderophores in plant growth-promoting bacteria*. Eds. D. K. Maheshwari, M. Saraf and A. Aeron (Berlin, Heidelberg: Springer Berlin Heidelberg), 265–285.

Schützendübel, A., and Polle, A. (2002). Plant responses to abiotic stresses: heavy metal-induced oxidative stress and protection by mycorrhization. *J. Exp. Bot.* 53, 1351–1365.

Secor, P. R., Sweere, J. M., Michaels, L. A., Malkovskiy, A. V., Lazzareschi, D., Katznelson, E., et al. (2015). Filamentous bacteriophage promote biofilm assembly and function. *Cell Host Microbe* 18 (5), 549–559. doi: 10.1016/j.chom.2015.10.013

Shaffique, S., Khan, M. A., Imran, M., Kang, S. M., Park, Y. S., Wani, S. H., et al. (2022). Research progress in the field of microbial mitigation of drought stress in plants. *Front. Plant Sci.* 13, 870626. doi: 10.3389/fpls.2022.870626

Shakir, S., Zaidi, S. S., de Vries, F. T., and Mansoor, S. (2021). Plant genetic networks shaping phyllosphere microbial community. *Trends Genet.* 37, 306–316. doi: 10.1016/j.tig.2020.09.010

Sharma, M., Abayakoon, P., Epa, R., Jin, Y., Lingford, J. P., Shimada, T., et al. (2021). Molecular basis of sulfosugar selectivity in sulfoglycolysis. *ACS Cent. Sci.* 7 (3), 476–487. doi: 10.1021/acscentsci.0c01285

Singh, P., Singh, R. K., Li, H. B., Guo, D. J., Sharma, A., Lakshmanan, P., et al. (2020). Diazotrophic bacteria pantoea dispersa and enterobacter asburiae promote sugarcane growth by inducing nitrogen uptake and defense-related gene expression. *Front. Microbiol.* 11, 600417. doi: 10.3389/fmicb.2020.600417

Soucy, S. M., Huang, J., and Gogarten, J. P. (2015). Horizontal gene transfer: building the web of life. *Nat. Rev. Genet.* 16, 472–482. doi: 10.1038/nrg3962

Stincone, A., Daudi, N., Rahman, A. S., Antczak, P., Henderson, I., Cole, J., et al. (2011). A systems biology approach sheds new light on escherichia coli acid resistance. *Nucleic Acids Res.* 39 (17), 7512–7528. doi: 10.1093/nar/gkr338

Sullivan, M. B., Lindell, D., Lee, J. A., Thompson, L. R., Bielawski, J. P., and Chisholm, S. W. (2006). Prevalence and evolution of core photosystem ii genes in marine cyanobacterial viruses and their hosts. *Plos. Biol.* 4 (8), e234. doi: 10.1371/journal.pbio.0040234

Sun, K., Liu, J., Gao, Y., Sheng, Y., Kang, F., and Waigi, M. G. (2015). Inoculating plants with the endophytic bacterium pseudomonas sp. Ph6-gfp to reduce phenanthrene contamination. *Environ. Sci. Pollut. Res.* 22 (24), 19529–19537. doi: 10.1007/s11356-015-5128-9

Szymczak, P., Rau, M. H., Monteiro, J. M., Pinho, M. G., Filipe, S. R., Vogensen, F. K., et al. (2019). A comparative genomics approach for identifying host-range determinants in streptococcus thermophilus bacteriophages. *Sci. Rep.* 9 (1), 7991. doi: 10.1038/s41598-019-44481-z

Tabata, M., Ohtsubo, Y., Ohhata, S., Tsuda, M., and Nagata, Y. (2013). Complete genome sequence of the γ-hexachlorocyclohexane-degrading bacterium sphingomonas sp. Strain mm-1. *Genome Announc.* 1. doi: 10.1128/genomeA.00247-13

Taghavi, S., Garafola, C., Monchy, S., Newman, L., Hoffman, A., Weyens, N., et al. (2009). Genome survey and characterization of endophytic bacteria exhibiting a beneficial effect on growth and development of poplar trees. *Appl. Environ. Microbiol.* 75, 748–757. doi: 10.1128/AEM.02239-08

Tao, J., Yu, S., Jin, J., Lu, P., Yang, Z., Xu, Y., et al. (2022). The wilt pathogen induces different variations of root-associated microbiomes of plant. *Front. Plant Sci.* 13, 1023837. doi: 10.3389/fpls.2022.1023837

Teixidó, N., Cañamás, T. P., Usall, J., Torres, R., Magan, N., and Viñas, I. (2005). Accumulation of the compatible solutes, glycine-betaine and ectoine, in osmotic stress adaptation and heat shock cross-protection in the biocontrol agent pantoea agglomerans cpa-2. *Lett. Appl. Microbiol.* 41 (3), 248–252. doi: 10.1111/j.1472-765X.2005.01757.x

Thapa, S., Prasanna, R., Ranjan, K., Velmourougane, K., and Ramakrishnan, B. (2017). Nutrients and host attributes modulate the abundance and functional traits of phyllosphere microbiome in rice. *Microbiol. Res.* 204, 55–64. doi: 10.1016/j.micres.2017.07.007

Tuteja, N., Ahmad, P., Panda, B. B., and Tuteja, R. (2009). Genotoxic stress in plants: shedding light on dna damage, repair and dna repair helicases. *Mutat. Res. Rev. Mutat. Res.* 681, 134–149. doi: 10.1016/j.mrrev.2008.06.004

van der Putten, W. H., Bardgett, R. D., Bever, J. D., Bezemer, T. M., Casper, B. B., Fukami, T., et al. (2013). Plant–soil feedbacks: the past, the present and future challenges. *J. Ecol.* 101, 265–276. doi: 10.1111/1365-2745.12054

Vorholt, J. A. (2012). Microbial life in the phyllosphere. *Nat. Rev. Microbiol.* 10, 828–840. doi: 10.1038/nrmicro2910

Wang, X., Du, G., Chen, H., Zeng, X., Liu, B., Guo, C., et al. (2021). Comparative metagenomics reveals microbial communities and their associated functions in two types of fuzhuan brick tea. *Front. Microbiol.* 12, 705681. doi: 10.3389/fmicb.2021.705681

Wang, Z., Fu, C., Tian, J., Wang, W., Peng, D., Dai, X., et al. (2022). Responses of the bacterial community of tobacco phyllosphere to summer climate and wildfire disease. *Front. Plant Sci.* 13, 1050967. doi: 10.3389/fpls.2022.1050967

Wang, G., Kong, F., Zhang, S., Meng, X., Wang, Y., Meng, Q., et al. (2015). A tomato chloroplast-targeted dnaj protein protects rubisco activity under heat stress. *J. Exp. Bot.* 66 (11), 3027–3040. doi: 10.1093/jxb/erv102

Wang, X., Shi, X., Chen, S., Ma, C., and Xu, S. (2018). Evolutionary origin, gradual accumulation and functional divergence of heat shock factor gene family with plant evolution. *Front. Plant Sci.* 9. doi: 10.3389/fpls.2018.00071

Westwood, J. H., McCann, L., Naish, M., Dixon, H., Murphy, A. M., Stancombe, M. A., et al. (2013). A viral rna silencing suppressor interferes with abscisic acid-mediated signalling and induces drought tolerance in arabidopsis thaliana. *Mol. Plant Pathol.* 14 (2), 158–170. doi: 10.1111/j.1364-3703.2012.00840.x

Wood, D. E., Lu, J., and Langmead, B. (2019). Improved metagenomic analysis with kraken 2. *Genome Biol.* 20, 257. doi: 10.1186/s13059-019-1891-0

Xing, L., Zhi, Q., Hu, X., Liu, L., Xu, H., Zhou, T., et al. (2022). Influence of association network properties and ecological assembly of the foliar fugal community on crop quality. *Front. Microbiol.* 13, 783923. doi: 10.3389/fmicb.2022.783923

Xu, P., Chen, F., Mannas, J. P., Feldman, T., Sumner, L. W., et al. (2008). Virus infection improves drought tolerance. *New Phytol.* 180, 911–921. doi: 10.1111/j.1469-8137.2008.02627.x

Xu, L., Dong, Z., Fang, L., Luo, Y., Wei, Z., Guo, H., et al. (2019). Orthovenn2: a web server for whole-genome comparison and annotation of orthologous clusters across multiple species. *Nucleic Acids Res.* 47 (W1), W52–W58. doi: 10.1093/nar/gkz333

Xu, J., Tan, L., Lamport, D. T., Showalter, A. M., and Kieliszewski, M. J. (2008). The o-hyp glycosylation code in tobacco and arabidopsis and a proposed role of hyp-glycans in secretion. *Phytochemistry* 69 (8), 1631–1640. doi: 10.1016/j.phytochem.2008.02.006

Yang, C. H., Crowley, D. E., Borneman, J., and Keen, N. T. (2001). Microbial phyllosphere populations are more complex than previously realized. *Proc. Natl. Acad. Sci. U. S. A.* 98, 3889–3894. doi: 10.1073/pnas.051633898

Yoshida, S., Hiradate, S., Koitabashi, M., Kamo, T., and Tsushima, S. (2017). Phyllosphere methylobacterium bacteria contain uva-absorbing compounds. *J. Photochem. Photobiol. B Biol.* 167, 168–175. doi: 10.1016/j.jphotobiol.2016.12.019

Zablocki, O., Adriaenssens, E. M., and Cowan, D. (2016). Diversity and ecology of viruses in hyperarid desert soils. *Appl. Environ. Microbiol.* 82, 770–777. doi: 10.1128/AEM.02651-15

Zhang, Y., Yu, T., Ma, W., Dayananda, B., Iwasaki, K., and Li, J. (2021). Morphological, physiological and photophysiological responses of critically endangered acer catalpifolium to acid stress. *Plants-Basel* 10 (9), 1958. doi: 10.3390/plants10091958

Zhang, H., Zhu, J., Gong, Z., and Zhu, J. (2022). Abiotic stress responses in plants. *Nat. Rev. Genet.* 23, 104–119. doi: 10.1038/s41576-021-00413-0

Zheng, Y., Wang, J., Zhao, W., Cai, X., Xu, Y., Chen, X., et al. (2022). Effect of bacterial wilt on fungal community composition in rhizosphere soil of tobaccos in tropical yunnan. *Plant Pathol. J.* 38 (3), 203–211. doi: 10.5423/PPJ.OA.03.2022.0035

Zhou, Y., Fan, Y., Lu, G., Zhang, A., Zhao, T., Sun, G., et al. (2022). Assessment of soil quality for guided fertilization in 7 barley agro-ecological areas of China. *PloS One* 17 (1), e261638. doi: 10.1371/journal.pone.0261638

Zhou, J., Li, P., Meng, D., Gu, Y., Zheng, Z., Yin, H., et al. (2020). Isolation, characterization and inoculation of cd tolerant rice endophytes and their impacts on rice under cd contaminated environment. *Environ. Pollut.* 260, 113990. doi: 10.1016/j.envpol.2020.113990

frontiers | Frontiers in Plant Science

TYPE Original Research
PUBLISHED 18 January 2024
DOI 10.3389/fpls.2023.1238896

OPEN ACCESS

EDITED BY
Andrea Genre,
University of Turin, Italy

REVIEWED BY
Prakash Babu Adhikari,
Nagoya University, Japan
Rubee Devi,
Eternal University, India

*CORRESPONDENCE
Zhengjun Xu
mywildrice@aliyun.com
Chao Zhang
jychaozhang@163.com

†These authors have contributed equally to this work and share first authorship

RECEIVED 12 June 2023
ACCEPTED 27 December 2023
PUBLISHED 18 January 2024

CITATION
Zhang L, Tao S, Zhang Y, Yang Y, Peng F, Liao H, Mao C, Wan X, Wu Y, Xu Z and Zhang C (2024) Study on the effect of compound cultivation on the growth feature and active ingredients content of *Salvia miltiorrhiza*. *Front. Plant Sci.* 14:1238896. doi: 10.3389/fpls.2023.1238896

Study on the effect of compound cultivation on the growth feature and active ingredients content of *Salvia miltiorrhiza*

Luyi Zhang[1,2†], Shan Tao[1†], Yifan Zhang[2], Yanmei Yang[2], Fang Peng[1], Hailang Liao[1], Changqing Mao[1], Xiufu Wan[3], Yu Wu[1], Zhengjun Xu[2*] and Chao Zhang[1*]

[1]Industial Crop Research Institute, Sichuan Academy of Agricultural Sciences, Chengdu, Sichuan, China, [2]Crop Ecophysiology and Cultivation Key Laboratory of Sichuan Province, Sichuan Agricultural University, Chengdu, Sichuan, China, [3]State Key Laboratory of Dao-di Herbs, China Academy of Chinese Medical Sciences, Beijing, China

We investigated the effects of the complex cultivation of *Salvia miltiorrhiza* on microbial communities, secretions, yield, and active ingredients, and the mechanism of action between microbial communities, secretions, and *S. miltiorrhiza* growth and development. Neither maize nor soybean was suitable to grow with *S. miltiorrhiza*, but sesame significantly increased salvinone content, the active ingredient of *S. miltiorrhiza*, and Tanshinone IIA, Tanshinone I, and Cryptotanshinone increased by 27.06%, 22.76%, and 26.41%, respectively, which increased the abundance and number of microbial communities in *S. miltiorrhiza* roots. 16S rRNA results showed that the most abundant bacterial phyla were Proteobacteria and Acidobacteriota, and their number increased with compound planting of sesame and *S. miltiorrhiza*. *Salvia* inter-root secretions affected the microbial community and *Salvia* growth and development, and lipids and lipid-like molecules significantly reduced *Salvia* yield and active ingredients. Overall, different plant secretions can lead to differences in the natural environment and *Salvia* root growth and development, and the composite planting of sesame with *Salvia* can improve inter-root microbial communities, enhance *Salvia* quality, and make fuller use of land resources.

KEYWORDS

***Salvia miltiorrhiza*, 16S rRNA, complex cultivation, inter-root secretions, microbial community**

1 Introduction

Salvia miltiorrhiza Bge. is a perennial herb in the family Labiatae, whose roots and rhizomes contain active ingredients (tanshinones and tannins) with therapeutic effects on diseases such as cardiovascular diseases, diabetes, and liver diseases (Liu et al., 2020c; Jiang et al., 2022a). *S. miltiorrhiza* is a medicinal herb widely grown in bulk in Henan, Sichuan,

Shandong, and Shaanxi (Wang et al., 2019). However, as adoption of highly efficient monocultures can lead to a decrease in quality and yield, measures such as composite cultivation are needed to promote sustainable development (Liu et al., 2020a).

High-efficiency monocultures usually lead to disturbances in soil physicochemical properties, reduced microbial community diversity, and toxin accumulation (Xin-hui et al., 2015). Recently, compound cropping has become an important research direction to solve continuous crop challenges. Compound cropping can increase plant species diversity, improve soil physicochemical properties, and enhance microbial community abundance by growing two or more crops simultaneously (Tang et al., 2014; Maitra, 2019; Domeignoz-Horta et al., 2020; Tang et al., 2021). Compound cropping can, therefore, increase agroecosystem diversity and promote sustainable agriculture (Stomph et al., 2020). Studies have shown that complex planting can modify plant root natural environments (Wang et al., 2019), and stimulate the production of unique inter-root secretions (Casper and Castelli, 2007), which regulate plant growth and promote nutrient uptake, attract specific probiotic bacteria to form plant-soil feedbacks (PSF) (Neumann and Romheld, 2003; Bais et al., 2006), and influence microbial community formation (Sasse et al., 2018).

The beneficial effects of intercropping in complex cropping systems, such as those involving cereals and legumes, have been extensively researched (Hsiao et al., 2019). Scholars have found that maize inter-root secretions contribute to enhanced reciprocity with legumes and promote nitrogen fixation by legumes (Jiang et al., 2022b). Hu demonstrated that maize inter-root secretions promote flavonoids synthesis in faba beans (Hu et al., 2021). However, not all plant species are conducive to a good inter-root microecological environment. For example, the combination of maize and *S. miltiorrhiza* was detrimental to growth and yield of the latter (Deng et al., 2017). Therefore, it is crucial to investigate suitable plants for successful *Salvia* complex cultivation.

Lei et al. (2018) found that different plants have a significant effect on *S. miltiorrhiza* growth and development, with pepper showing the greatest improvement in yield and quality. *S. miltiorrhiza* dry weight increased by 12.52%, salvianolic acid B increased by 10.25%, and tanshinone compound content significantly increased by 58.91%. Similarly, Liu et al. (2018) investigated the intercropping effects of mint, perilla, and alfalfa with *S. miltiorrhiza*. They found that they produced the highest weight gain and increased content of *S. miltiorrhiza* active ingredients. Moreover, the content of lipid-soluble components cryptotanshinone, tanshinone I, and tanshinone IIA in *S. miltiorrhiza* significantly increased after intercropping treatment, with the highest tanshinone content of 1.08% in *S. miltiorrhiza* roots after *S. miltiorrhiza*–mint intercropping, which was 163.41% higher than after monocropping. However, there has been no suitable grain and oil crop identified for intercropping with *S. miltiorrhiza*, and little research has been conducted on the effects of different plants on *S. miltiorrhiza* inter-root microbial community structure and abundance. Further research is needed to explore suitable crops and the underlying mechanisms of action.

To address these shortcomings, we investigated the effects of three crop plants on *S. miltiorrhiza* inter-root microecology and growth and development. The study designed pot experiments using macrogenomics and metabolomics to analyze *S. miltiorrhiza* inter-root microecology and investigate its responses to different plant secretions, including changes in soil physicochemical properties, bacterial abundance, inter-root soil community composition, and metabolite production. To confirm our results, we conducted field plot experiments. We hypothesized that various plants would lead to different *Salvia* inter-root microbial populations and community structures, affect its root morphology, and alter its inter-root secretions.

2 Materials and methods

2.1 Experimental site

The experiments were conducted at the Industrial Crop Research Institute, Sichuan Academy of Agricultural Sciences, Qingbaijiang District, Chengdu City, Sichuan Province, China (30°42′N, 104°19′E), where average annual temperature was 18°C, and average annual precipitation was 558.1 mm (local weather bureau data). *Salvia* seedlings and maize, sesame, and soybean varieties were provided by the Institute of Economic Crop Breeding and Cultivation, Sichuan Academy of Agricultural Sciences. Basic Soil Properties: Potted Plants, pondus hydrogenii = 6.7, organic matter = 21.90 g/kg, available P = 43.76 mg/kg, available K = 115.50 mg/kg, total nitrogen = 1.48 g/kg; Field, potential of hydrogen = 6.0, organic matter = 19.78 g/kg, available P = 26.75 mg/kg, available K = 188.27 mg/kg, total nitrogen = 1.48 g/kg.

2.2 Pot experiments and field experiments

Pot experiments were set up in six planting combinations: maize + *Salvia* completely isolated (*Salvia*|Maize), maize + *Salvia* without isolation (*Salvia*Maize), soybean + *Salvia* completely isolated (*Salvia*|Soybean), soybean + *Salvia* without isolation (*Salvia*Soybean), sesame + *Salvia* completely isolated (*Salvia*|Sesame), and sesame + *Salvia* without isolation (*Salvia*Sesame). *S. miltiorrhiza* was propagated from fresh root segments (1.3–1.8 cm in diameter) selected from seedlings dug in January 2022, and transplanted to pots and the field after seedlings were raised in the greenhouse. The pot experiment used 0.4-m-high, 0.6-m-diameter breeding bags, including two isolation treatments and was conducted in a randomized design (Figure 1): ① plastic film isolation where the two crops were completely separated, with no inter-root intercropping; and ② without any isolation, where the two crops can communicate openly between the roots, with inter-root secretions interacting with each other, and where inter-root intercropping is obvious. Five replicates of each treatment were made.

The field experiments were conducted in a randomized design (Figure 2), including soybean monoculture (soybeanm, 0.25 m spacing), maize monoculture (maizem, 0.4 m spacing), sesame monoculture (sesamem, 0.25 m spacing), *Salvia* monoculture (*salvia*m, 0.25 m spacing), *Salvia*-maize intercrop (*Salvia* + maize), *Salvia*-soybean intercrop (*Salvia* + soybean), and *Salvia*-sesame intercrop (*Salvia* + sesame). The size of each experimental area was 3.6 × 5 m, and each treatment was replicated three times.

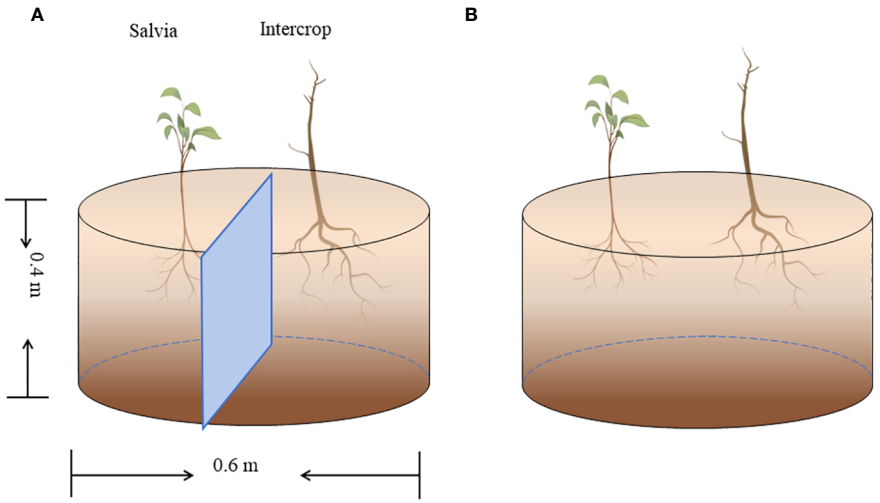

FIGURE 1
Pot experiment (*n* = 5). **(A)** Complete isolation of *Salvia* and other crops with plastic film, and **(B)** no isolation of *Salvia* and other crops.

2.3 Inter-root soil and general soil sampling

Soil samples were randomly taken from the field and pots at the time of sowing in March, and later mixed into composite samples that were naturally air-dried and stored in an oven for testing. Sampling was carried out in December 2022 on normal soil and inter-rhizosphere soil (soil close to plant roots and usually containing higher microbial populations than the surrounding normal soil) (Fierer, 2017). Inter-root soil (still attached to the roots) was shaken off gently and stored at −80°C for microbial community and inter-root metabolite analysis (Zhao et al., 2021). Simultaneously, soil around *S. miltiorrhiza* plants was collected, plant roots and stones were removed, and the soil was put into a self-sealing bag, and then it was dried and ground naturally, passed through a 60-mesh sieve and set aside for soil physical and chemical property testing.

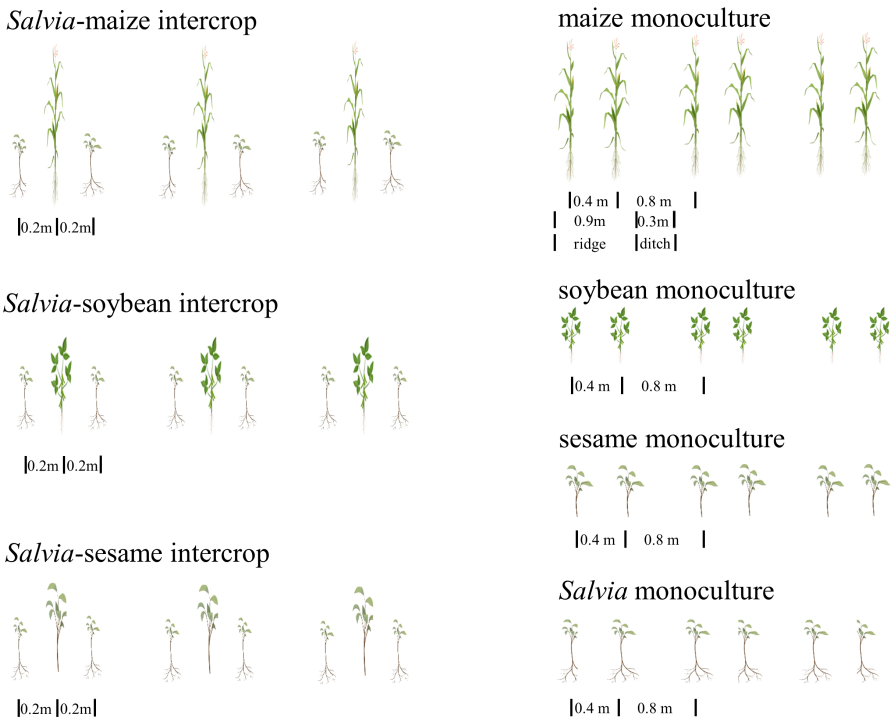

FIGURE 2
Layout of the fifield experiment (n = 3).

2.4 Determination of soil physical and chemical properties

Soil potential of hydrogen (pH) was determined by the point method (HJ 962-2018), where soil/water is mixed at 1/2.5 (w/v), stirred vigorously for 2 min, and left for 30 min, and then pH was measured with a pH meter (PHS-SE) (Pang et al., 2021). Soil organic matter (SOM) was determined using the Walkley–Black method, which oxidizes SOM by H_2SO_4 and $K_2Cr_2O_7$, followed by titration using $FeSO_4$ (Fu et al., 2015). Soil active phosphorus (available P) was measured by a spectrophotometer at 700 nm (NY/T 1121.7-2014) (Liu et al., 2018). Soil available potassium (available K) was determined by a flame photometer after extraction by 1 mol/L ammonium acetate (Saber et al., 1973). Soil total nitrogen was determined by the Kelvin digestion-constant distillation–titration method, followed by digestion using an automatic Kjeldahl nitrogen tester (Hennen K1100) (Wang et al., 2018).

2.5 Microbial community structure and diversity analysis

A Soil DNA Kit was used to isolate soil microbial DNA from 5-g soil samples. The V4 hypervariable region of the bacterial gene was amplified with PCR using primers F (ACTCCTACGGGAG GCAGCA) and R (GGACTACHVGGGTWTCTAAT). After PCR processing, sequencing was conducted using an Illumina NovaSeq 6000. The raw image data files were converted to raw Sequenced Reads by Base Calling analysis. Sequenced data were filtered for connectors and low-quality using FASTP and Trimmomatic for Raw Reads to obtain high-quality valid sequences (Berg et al., 2015). Finally, the sequences were clustered with USEARCH (Edgar, 2013) (version 10.0) at the 97% similarity level, and OTUs were filtered using 0.005% of the total number of sequences sequenced as a threshold (Bokulich et al., 2013).

2.6 Salvia inter-root metabolites

To analyze metabolites in inter-rhizosphere soil, a 50-mg sample was weighed and mixed with 1,000 µL of extraction solution containing internal standard. The mixture was then ground with steel beads and sonicated for 10 min in an ice water bath, followed by centrifugation, and the supernatant was carefully collected for testing. Metabolomics analysis was conducted using a liquid mass spectrometry system composed of a Waters Acquity I-Class PLUS UPLC tandem and a Waters Xevo G2-XS QTof high-resolution mass spectrometer (Acquity UPLC HSS T3, 1.8 µm 2.1*100 mm). Positive ionization mode: mobile phase A: 0.1% formic acid aqueous solution; mobile phase B: 0.1% formic acid acetonitrile; negative ionization mode: mobile phase A: 0.1% formic acid aqueous solution; mobile phase B: 0.1% formic acid acetonitrile. The Waters Xevo G2-XS QTof high-resolution mass spectrometer is capable of primary and secondary mass spectrometry data acquisition in MSe mode under acquisition software (MassLynx V4.2, Waters) control. In each data acquisition cycle, dual-channel data acquisition is possible for both low and high collision energies. Low collision energy was 2 V, the high collision energy range was 10–40 V, and scan frequency was 0.2 s for one mass spectral map. ESI ion source parameters were as follows: capillary voltage: 2,000 V (positive ion mode) or −1,500 V (negative ion mode); cone hole voltage: 30 V; ion source temperature: 150°C; desolvent gas temperature: 500°C; backblast gas flow rate: 50 L/h; desolvent gas flow rate: 800 L/h. Raw data collected by MassLynx V4.2 were processed by Progenesis QI software for peak extraction, alignment, and other data processing operations.

2.7 Salvia root morphology and active ingredients (tanshinones and tannins)

S. miltiorrhiza was harvested in December, its inter-root morphology was investigated, and its yield was measured. The number of branches, fresh weight, and dry weight of individual roots were also measured at harvest, along with root length (measured from the base of the stem) and diameter (the largest *S. miltiorrhiza* diameter) (Lei et al., 2018). After harvesting, the rhizome was dried, powdered, sieved (60 mesh), and stored to determine active ingredients. Intercrops were harvested in June and July.

S. miltiorrhiza active ingredients (tanshinones and tannins) were determined using high-performance liquid chromatography. Total tanshinones and tannic acid B were determined according to the Chinese Pharmacopoeia 2015 edition, wherein tanshinones (Tanshinone IIA, Cryptotanshinone, and Tanshinone I) shall not be<0.25% in total and tanshinolic acid B shall not be<3.0%. Chromatographic analysis was performed with high-performance liquid chromatography equipment (Agilent 1260 series, USA) on a ZORBAXSB-C18 (4:6 mm × 250 mm, 5 µm) column at a temperature of 20°C. For salvianolic acid B determination, the mobile phase consisted of acetonitrile (A) and 0.1% phosphoric acid aqueous solution (B) in gradient elution mode for 20 min at 90% A with a flow rate of 1.0 mL min^{-1} and an injection volume of 10 µL at a detection wavelength of 286 nm. The mobile phase was composed of acetonitrile (A) and 0.02% phosphoric acid aqueous solution (B): 0–6 min, 0%–61% A; 6–20 min, 61%–90% A; 20–20.5 min, 90%–61% A; 20.5–25 min, 61% A, with a flow rate of 0.8 mL min^{-1}, a sample volume of 10 µL, and a detection wavelength of 270 nm (Liu et al., 2020a).

2.8 Determination of field yield and land equivalent ratio

To measure land area efficiency when intercropping, Willey and Osiru (1972) introduced the land equivalent ratio (LER) concept, which reflects the yield of two crops as intercrops and as a monocrop, which can be used to evaluate the suitability of two crops for intercrop cultivation. It is:

$$LER = pLER_1 + pLER_2 = \frac{Y_1}{M_1} + \frac{Y_2}{M_2}$$

where *p*LER is a partial land equivalent ratio, Y_1 and Y_2 are the yields of seed 1 and seed 2 in interplanting, M_1 and M_2 are the yields of seed 1 and seed 2 in single crop, respectively.

2.9 Data analysis

All statistical analyses were performed using various packages in R version 3.3.0 (Vermeulen et al., 2013), including ANOVA tests for multiple comparisons of soil microbial diversity, soil properties, active ingredient content, and plant biomass. Root secretion aroma diversity and evenness indices were compared among the groups by unpaired *t*-tests. When $p< 0.05$, the means of the groups were considered significantly different using the least significant difference (LSD). Principal component analysis (PCA), redundancy analysis (RDA), and heatmaps were generated using the "ggplot2" package in the R platform. PCA regroups all the metabolites originally identified linearly to form a new set of variables to determine differences between the groups of samples. To determine the proportion of variation in community structure explained by environmental factors, microbial community compositional components were determined by RDA, followed by variance decomposition analysis (VPA). Heatmaps were used to compare correlations between species abundance (OTUs) and various indicators, including environmental factors, plant growth parameters, and root base secretions.

3 Results

3.1 Effect of different planting methods on *S. miltiorrhiza* growth and development

In commercial trade, *S. miltiorrhiza* yield, quality, and appearance are very important for *Salvia* growers to achieve profitability. The *S. miltiorrhiza* fresh weight index can represent its yield, while hydrophilic and lipophilic components as well as root length and diameter indicate its quality and appearance (Liu et al., 2020a). Inter-root secretions between different plants had a significant effect on *Salvia* morphology (Table 1), and *Salvia* dry weight in the *Salvia*Sesame treatment increased by 3.21% compared to that in *Salvia*|Sesame when the plants were compared with and without the isolated treatment. *S. miltiorrhiza* fresh weight, dry weight, and root diameter were significantly decreased by inter-root secretions from maize, and all *Salvia* growth indices were decreased in *Salvia*Soybean and *Salvia*Maize compared to *Salvia*Sesame. Overall, inter-root secretions from sesame had the least effect on *S. miltiorrhiza* root development. The combinations *Salvia*Maize and *Salvia*Maize significantly inhibited growth, as *Salvia* fresh weight, dry weight, and root diameter decreased by 46.29%, 46.77%, and 27.88%, respectively.

Active ingredient contents were compared under the six cultivation combinations (Figure 3). There were no significant differences in tanshinolic acid B. After *Salvia*Sesame treatment, *S. miltiorrhiza* tanshinones significantly increased, with the highest levels of Tanshinone IIA, Tanshinone I, and Cryptotanshinone, showing increases of 27.06%, 22.76%, and 26.41%, respectively, compared to *Salvia*|Sesame. Sesame and *Salvia* cultivation effectively increases accumulation of Tanshinone active ingredients.

3.2 Effect of different planting methods on soil properties

In the potted soil after each treatment group (*Salvia*|Soybean, *Salvia*Soybean, *Salvia*|Maize, *Salvia*Maize, *Salvia*|Sesame, and *Salvia*Sesame), there were no significant differences in acidity (Figure 4A), available P (Figure 4C), organic matter (Figure 4D), and total nitrogen (Figure 4E). The highest available K (Figure 4B) was found in *Salvia*Soybean (152.13 ± 13.69), which was significantly higher than available K in *Salvia*Sesame (122.94 ± 15.96), while there were no significant differences between plants with and without compartment treatments.

3.3 Effect of different planting methods on the *S. miltiorrhiza* inter-root bacterial community

Illumina detected a total of 1,121,526 clean reads generated from the 16S RNA gene in 18 samples, and a total of 8,654 OTUs

TABLE 1 Single plant yield and agronomic traits of *Salvia* Tanshinone under different cropping patterns (mean ± S.E., $n = 5$).

Treatments	Fresh weight (g)	Dry weight (g)	Number of branches	Root length (cm)	Root width (mm)
*Salvia*Maize	105.00 ± 25.16d	38.93 ± 9.51c	12.60 ± 3.21	24.50 ± 5.32a	9.70 ± 2.16c
Salvia|Maize	195.50 ± 5.26c	73.14 ± 8.92b	13.60 ± 5.08	32.25 ± 3.59a	13.45 ± 1.48b
*Salvia*Soybean	227.50 ± 9.57bc	79.19 ± 2.88b	16.20 ± 4.66	30.95 ± 4.73a	12.01 ± 1.65b
Salvia|Soybean	255.00 ± 62.45ab	92.55 ± 23.84ab	14.00 ± 8.60	37.37 ± 14.67a	13.55 ± 1.24ab
*Salvia*Sesame	288.50 ± 53.75a	107.55 ± 16.19a	18.20 ± 7.11a	30.50 ± 5.26a	13.70 ± 1.63a
Salvia|Sesame	297.50 ± 37.75a	104.20 ± 20.04a	13.80 ± 3.27a	37.75 ± 15.28a	13.97 ± 0.95a

maize + *Salvia* completely isolated (*Salvia*|Maize), maize + *Salvia* without isolation (*Salvia*Maize), soybean + *Salvia* completely isolated (*Salvia*|Soybean), soybean + *Salvia* without isolation (*Salvia*Soybean), sesame + *Salvia* completely isolated (*Salvia*|Sesame), and sesame + *Salvia* without isolation (*Salvia*Sesame). Standard errors (S.E.). Boxes with various lowercase letters indicate significant differences between various regimes based on the least significant difference (LSD) test ($p< 0.05$).

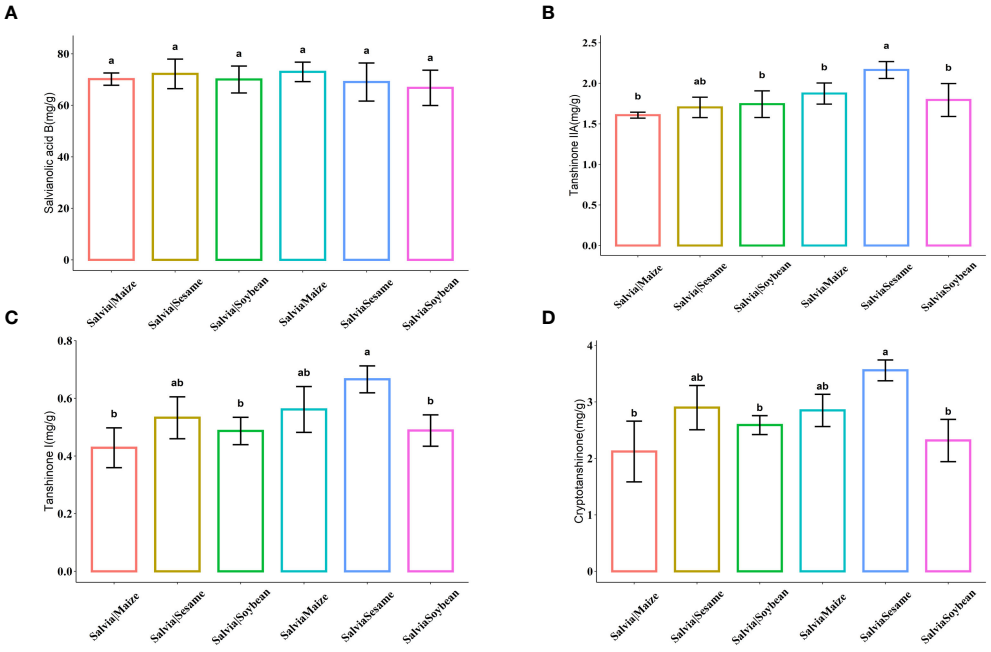

FIGURE 3
Histogram of active ingredient content of *Salvia* miltiorrhiza (n = 5). **(A)** Salvianolic acid B, **(B)** Tanshinone IIA, **(C)** Tanshinone I, and **(D)** Cryptotanshinone. Boxes with different lowercase letters indicate significant differences between various regimes based on the least significant difference (LSD) test (p< 0.05).

were identified in all samples. The Chao1 index (a measure of α-diversity) was significantly lower for *Salvia*Soybean and *Salvia*Maize than for *Salvia*Sesame, with *Salvia*Soybean having the lowest (275.67 ± 83.28c) number of species (Table 2). The Shannon and Simpson indices indicated that bacterial diversity and homogeneity were typically better for all treatments, with greater variation for *Salvia*Soybean.

Additionally, there were differences in bacterial community structure after the treatment in each group. The highest abundance at bacterial phylum level was found in Proteobacteria (26.41%–44.04%), Acidobacteriota (8.37%–26.88%), Gemmatimonadota (4.62%–17.40%), Actinobacteriota (3.78%–9.13%), and unclassified_Bacteria (2.28%–11.44%) (Figure 5A). Cyanobacteria and Fusobacteriota significantly increased in the *Salvia*Soybean

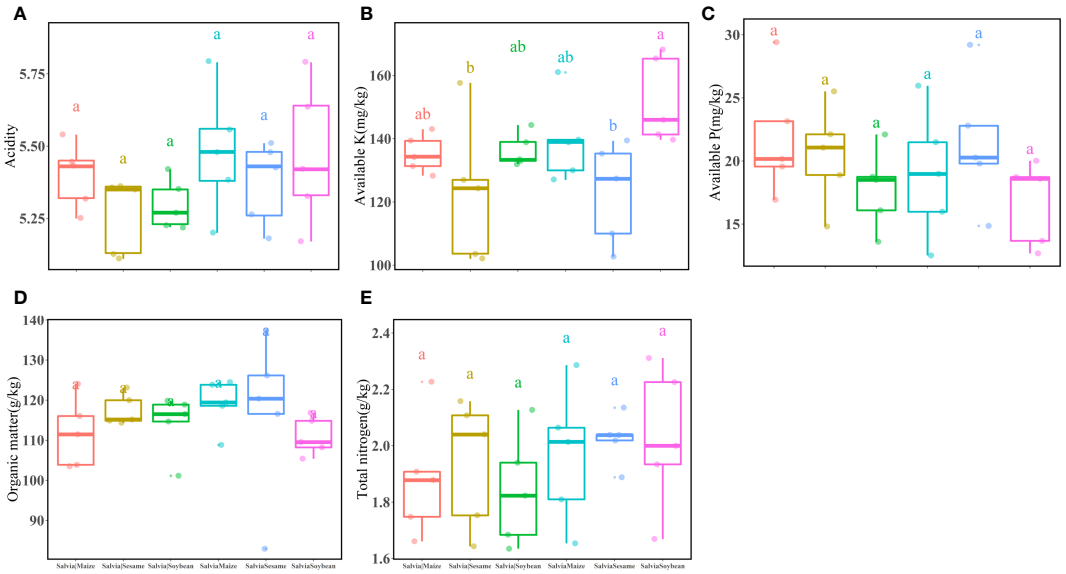

FIGURE 4
Inter-root soil factors under different cropping practices of *Salvia* and other crops (n = 3). **(A)** acidity, **(B)** available K, **(C)** available P, **(D)** organic matter, **(E)** total nitrogen. Boxes with different lowercase letters indicate significant differences between various regimes based on the LSD test (p< 0.05).

TABLE 2 Diversity indices of the inter-root microbial communities of *Salvia miltiorrhiza* under different cropping patterns (mean ± S.E., n = 3).

Treatments	ACE	Chao1	Simpson	Shannon
*Salvia*Maize	398.67 ± 28.57b	398.67 ± 28.57b	0.9930 ± 0.0010a	7.92 ± 0.22a
Salvia|Maize	532.71 ± 15.01a	532.67 ± 15.04a	0.9936 ± 0.0016a	8.21 ± 0.21a
*Salvia*Soybean	275.67 ± 83.28c	275.67 ± 83.28c	0.9420 ± 0.0317b	5.85 ± 1.01b
Salvia|Soybean	524.72 ± 39.22a	524.67 ± 39.31a	0.9925 ± 0.0012a	8.14 ± 0.07a
*Salvia*Sesame	580.67 ± 41.06a	580.67 ± 41.06a	0.9947 ± 0.0011a	8.46 ± 0.15a
Salvia|Sesame	571.38 ± 58.93a	571.33 ± 58.96a	0.9937 ± 0.0008a	8.36 ± 0.17a

This shows the richness (ACE, Chao1) and diversity (Simpson, Shannon) of the bacterial community. Standard errors (S.E.). Boxes with various lowercase letters indicate significant differences between various regimes based on the least significant difference (LSD) test (p< 0.05).

treatment, accounting for 29.11% and 4.34% of total community abundance, respectively, while both did not exceed 0.1% in any other treatment. *Salvia*Maize and *Salvia*Soybean bacterial community abundance and number showed a significant decrease compared to *Salvia*|Maize and *Salvia*|Soybean, while *Salvia*Sesame and *Salvia*|Sesame bacterial community structure did not. There was no significant difference in the structure of *Salvia*Sesame and *Salvia*|Sesame bacterial communities. An RDA was performed to accurately assess the relative effects of soil physicochemical properties (potential of hydrogen, organic matter, total nitrogen, available P, and available K) on the abundance and diversity of *S. miltiorrhiza* inter-rhizosphere bacterial communities. The first two RDA components explained 51.48% and 19.94% of the overall variation, respectively. Furthermore, potential of hydrogen, available P, available nitrogen, total nitrogen, and organic matter appeared to play a crucial role in building bacterial communities (Figure 5B). There was a negative correlation between organic matter and RDA1 (70.64%), a direct correlation between available P and RDA1 (59.13%), and a maximum contribution of 50.81% from total nitrogen to RDA2. This indicates that organic matter, available P, and total nitrogen remain the key environmental factors affecting *Salvia* inter-root microorganism abundance. The soil environmental factor and microbial communities correlation analysis

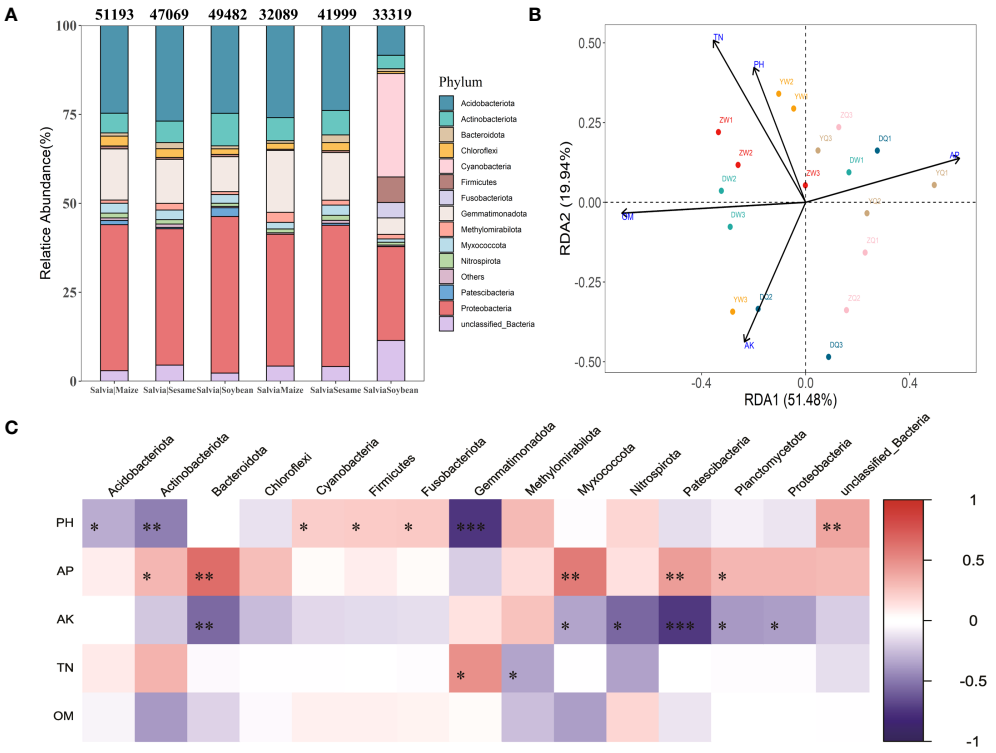

FIGURE 5
Distribution and composition of bacterial communities at the gate level under different cropping patterns (n = 3). **(A)** Relative abundance of staple microbial taxa on phylum level across all samples detected by 16S rRNA gene sequencing. The numbers above the bars indicate the number of microorganisms classified at the phylum level according to the sequence composition of feature. **(B)** Redundancy analysis of soil microbial communities and environmental parameters (RDA); arrows present the magnitude and direction of environmental factors associated with bacterial community structure. **(C)** Heatmap of soil environmental factors and phylum level bacterial correlations. Negative correlations and positive correlations are represented in blue and red. * indicates 0.01< $p \leq$ 0.05, ** indicates 0.001< $p \leq$ 0.01, *** indicates $p \leq$ 0.001.

revealed that the potential of hydrogen and Gemmatimonadota were significantly negatively correlated (r^2 = 0.74; p< 0.001), and available K and Patescibacteria were significantly negatively correlated (r^2 = 0.74; p< 0.001) (Figure 5C).

3.4 Effect of different planting methods on *S. miltiorrhiza* inter-root secretions

After analyzing the inter-root microbial community and agronomic trait indicators of *Salvia divinorum*, we found that sesame was the most promising plant to grow with it. The relationship between sesame and *S. miltiorrhiza* inter-root secretions was further analyzed by PCA, and there were similar metabolites between *Salvia*Sesame and *Salvia*|Sesame (Figure 6A). The *Salvia divinorum* inter-root microbial community was analyzed when the three crops were not isolated, and the lowest microbial community α-diversity was under *Salvia*Soybean treatment, while the highest microorganism abundance and number were found under *Salvia*Sesame treatment. This may be due to different crops resulting in different inter-root *S. miltiorrhiza* feedbacks. Analysis of *Salvia*Soybean and *Salvia*Sesame inter-root secretions revealed that 30 were significantly reduced in the *Salvia*Soybean treatment (p< 0.05 and VIP > 1.5) (Figure 6B), of which 18 belonged to the Human Metabolome Database (HMDB), with lipids and lipid-like compounds, nucleosides and analogs, organic acids and derivatives, organic oxides, and heterocyclic compounds accounting for 4.05%, 26.56%, 2.84%, 15.20%, and 8.27%, respectively. The two lowest p-value secretions screened, D-Sedoheptulose 7-phosphate and Nicotinamide-beta-riboside, both belong to the organic oxide class, and comparing the amounts of these two metabolites in *Salvia*Soybean and *Salvia*Sesame, the difference multiplicity (fold change) was −1.63746 and -2.02996 (Figure 6C), respectively. The correlation heatmap between *S. miltiorrhiza* yield, quality, and active ingredients showed that lipids were significantly and negatively correlated with yield (fresh weight and dry weight) and quality (Tanshinone IIA, Tanshinone I, and Cryptotanshinone) (Figure 7).

3.5 Relationships between microbial communities and *Salvia* root secretions, growth, and development

To accurately assess the effects of microbial communities on root secretions and *S. miltiorrhiza* growth and development, we investigated the relationships between the main secretions (lipids, nucleosides and analogs, organic acids and derivatives,

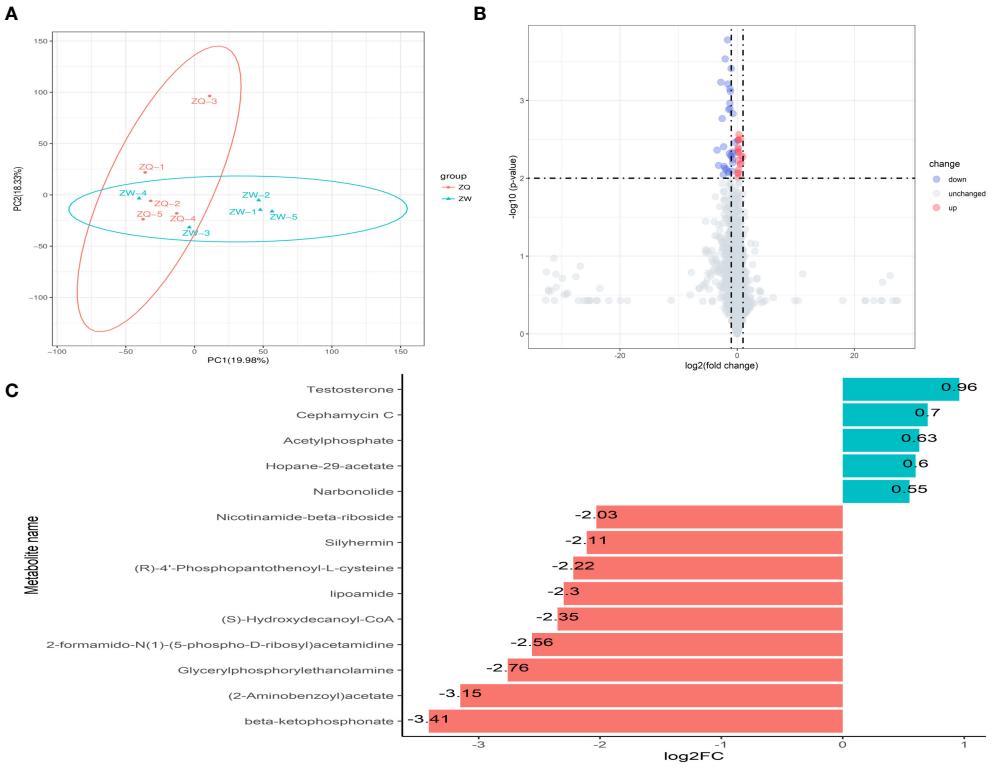

FIGURE 6
Analysis of inter-root secretion differences in *Salvia* (n = 3). **(A)** Principal component analysis (PCA) of inter-root secretion between *Salvia*|Sesame, and *Salvia*Sesame. **(B)** Volcano plot depicting inter-root secretions between *Salvia*Sesame and *Salvia*Soybean. **(C)** Fold change in the expression of inter-root metabolites of *Salvia miltiorrhiza* between *Salvia*Sesame and *Salvia*Soybean. **(B)** Each point in the graph represents a metabolite; the horizontal coordinate represents the log2 value of the fold difference of a metabolite between the two samples; the vertical coordinate represents the log10 value of the p-value. Red points represent upregulated differentially expressed metabolites, blue points represent downregulated differentially expressed metabolites, and gray points represent metabolites that were detected but did not meet the filtering parameters. **(C)** FC (fold change).

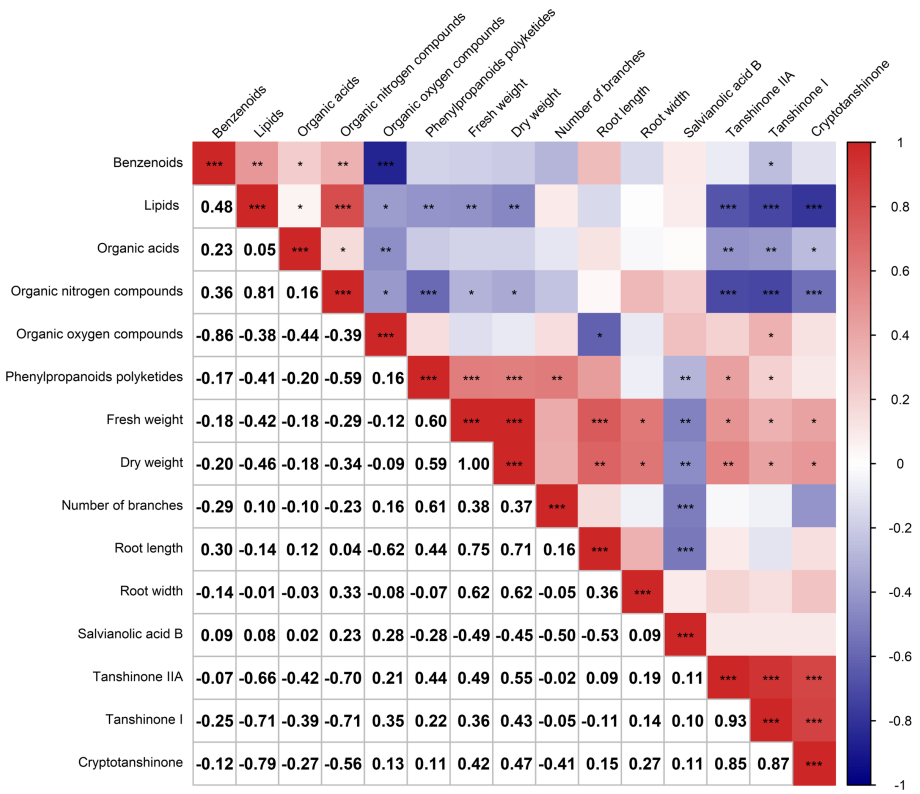

FIGURE 7
Correlation heatmap depicting the relationship between the six major root secretions and *Salvia miltiorrhiza* growth and development (n = 3). Negative correlations and positive correlations are represented in blue and red, respectively. * indicates 0.01< $p \leq$ 0.05, ** indicates 0.001< $p \leq$ 0.01, *** indicates $p \leq$ 0.001.

organic oxygen compounds, organoheterocyclic compounds, phenylpropanoids, and polyketides), *Salvia* basic growth and developmental indicators (fresh weight, dry weight, and number of nucleosides), *Salvia* active constituents (Salvianolic acid B, Tanshinone IIA, Tanshinone I, and Cryptotanshinone), and the main microbial communities. Lipids and lipid-like molecules and Bacteroidota, Chloroflexi, Nitrospirota, Planctomycetota, and Proteobacteria were significantly negatively correlated (p< 0.05) (Figure 8). Organic nitrogen compounds, root width, dry weight, and Patescibacteria all showed significant positive correlations (p< 0.05). Fresh weight, dry weight and Bacteroidota, Planctomycetota were significantly positively correlated with each other (p< 0.05). Interestingly, Bacteroidota, Planctomycetota, and Patescibacteria were all significantly positively correlated with each other (p< 0.05).

3.6 Field experiment yield and land equivalent ratio

Compound planting of different plants and *Salvia* led to differences in harvest yield and LERs. Averaging the data from three replications, *S. miltiorrhiza* yield after intercropping maize, soybean, and sesame was 9,817.20 ±322.20, 14,817.451,950.15, and 15,739.65 ±3,061.20 kg/hm^2, respectively, while monocropping maize, soybean, sesame, and *Salvia* yields were 17,385.001,967.7, 3,432.45 ±488.85, 1,800.15361.20, and 16,470.00 ±3,616.80 kg/hm^2, respectively. The lowest *Salvia* yield was after intercropping with maize, where it was reduced by 40.44%. *Salvia* yield was reduced by 10.11% and 4.52% when intercropped with soybean and sesame, respectively. The highest LER (1.82) was achieved with sesame and *Salvia* intercropping, with $pLER_1$ and $pLER_2$of 0.96 and 0.86, respectively, and the lowest LER of 1.36 for soybean and *Salvia* intercropping. Field experiments verified that sesame and *Salvia* are a good intercropping combination.

4 Discussion

Compound planting patterns can effectively improve yield and quality of many medicinal plants, such as *Salvia* and *Angelica*, which are affected by successive crop barriers (Zhang et al., 2013; Liu et al., 2020a; Maitra et al., 2021). Compared to monocropping, Liu et al. (2018) showed that intercropping cultivation significantly enhanced *Salvia* root fresh weight, dry weight, and lipid-soluble component content. We showed that the combined planting of maize and *Salvia* reduced *Salvia* yield, a result consistent with previous studies (Lei et al., 2018); however, sesame and *Salvia* intercropping significantly increased the tanninone content of *Salvia* roots, while individual plant fresh and dry weight, root diameter, and branch number all increased, as did the LER (1.82) in field experiments. Many studies have demonstrated that soil

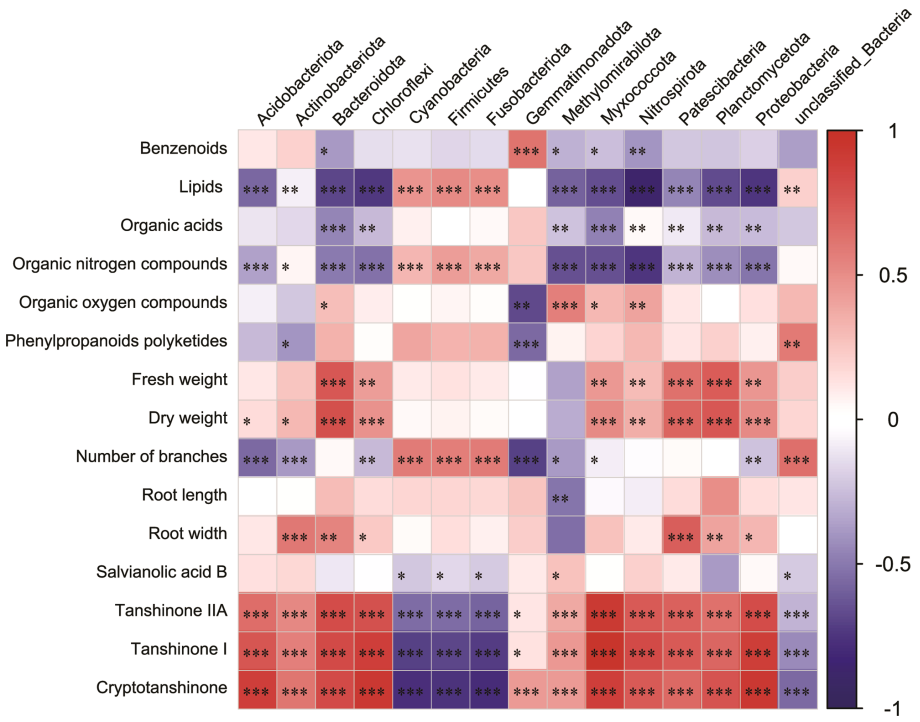

FIGURE 8
Correlation heatmap analysis of the association between the relative abundance of bacterial phyla and major inter-root secretions, and *Salvia miltiorrhiza* growth and development, including the relative richness (n = 3) of the top 15 microbial phyla. Negative correlations and positive correlations are represented by blue color and red color, respectively. Horizontal ordinate represents bacterial community abundance information, and vertical ordinate represents inter-root secretion and *Salvia miltiorrhiza* growth and development indicators. * indicates 0.01< $p \leq$ 0.05, ** indicates 0.001< $p \leq$ 0.01, *** indicates $p \leq$ 0.001.

factors are influenced by intercropping systems (Tang et al., 2020), e.g., hydrogen potential and available P significantly increased in both inter- and non-inter-rooted soils in the sugarcane–peanut intercropping system study group (Pang et al., 2021). In this study, there were no significant changes in potential of hydrogen, organic matter, available P, and total nitrogen, which may be due to the soil buffering effect, and/or the effects of plants on altering soil structure, which often takes several years to complete (Fierer, 2017).

Intercropping systems similarly cause changes in inter-root microbial community composition, which are mainly due to fertilization (Guo et al., 2020), crop type (Prommer et al., 2020), and changes associated with crop diversity, such as root secretions (Mommer et al., 2016) and soil environmental factors (Stefan et al., 2021). High-throughput sequencing of 16S rRNA is now an established approach (Bhakta et al., 2017) for deep exploration of soil microbial community composition and abundance. Li et al. (2022) found that Acidobacteriota and Proteobacteria were the dominant phyla in the maize intercropping system, and Proteobacteria relative abundance in the intercropped maize root soil increased significantly, primarily due to interspecific root interactions resulting in differences in bacterial community structure during intercropping. Meanwhile, Wang et al. (2019) showed that crop rotation and crop set could improve soil quality and inter-root bacterial diversity to some extent, and Symbiodinium relative abundance was higher in crop rotation and crop set than in continuous crop. In our experiment, Proteobacteria (26.41%–44.04%) and Acidobacteriota (8.37%–26.88%) were the dominant phyla, and interestingly, they (along with Salvia ketone content) were significantly and positively correlated with the fresh and dry weights of *Salvia* roots that were likewise positively correlated. Meanwhile, alpha diversity of the *S. miltiorrhiza* inter-root microbial community was highest in bacterial number and abundance when sesame and *S. miltiorrhiza* were grown in combination, while it was lowest when soybean and sesame were grown in combination. Thus, microbial community structure remains an important driver of *S. miltiorrhiza* root yield and quality.

The soil environment is the primary influencing factor in determining microbial community structure (Fierer, 2017). We found through RDA that soil environmental factors explained 51.48% and 19.94%, respectively, of the first two RDA components, which again confirmed previous studies. Available P, organic matter, and total nitrogen made the highest contribution, available P was the key factor affecting *S. miltiorrhiza* quality, and root Tanshinone IIA concentration was significantly and negatively correlated with soil effective phosphorus (Liang et al., 2021). Soil phosphorus content is also an important factor in soil bacterial community formation (Liu et al., 2020b). Additionally, total nitrogen is also considered the dominant factor in building microbial communities because it has key functions in cellular metabolic processes, such as energy metabolism, protein synthesis, and cell division (Rajan et al., 1991). Simultaneous analysis of soil

environmental factors and microbial communities found that potential of hydrogen was negatively correlated with Gemmatimonadota, which is consistent with the findings of Guo et al. (2017).

In addition to inter-root secretions being a key factor affecting inter-root microorganisms (Wang et al., 2022), root secretion-induced autotoxin accumulation is also widely recognized as an important contributor to crop succession disorders (Xu et al., 2015). The study revealed correlations between inter-root secretion and *Salvia* microbial communities as well as the *Salvia* growth and development index. It was observed that lipids and lipid-like molecules had a significant and negative correlation with *Salvia* yield (fresh weight and dry weight) and quality (Tanshinone IIA, Tanshinone I, and Cryptotanshinone). Additionally, lipids and lipid-like molecules and Bacteroidota, Chloroflexi, Nitrospirota, Planctomycetota, and Proteobacteria were also significantly negatively correlated. In previous studies, different inter-root secretions had different effects on shaping microbial community structure (Li and Wu, 2018; Zhao et al., 2021). Therefore, controlling lipids and lipid-like molecule contents in soil may be an important way to improve *Salvia* root yield and quality and play an active role in shaping *Salvia* inter-root microbial structure.

5 Conclusions

The present study demonstrates that the complex cultivation of sesame and *Salvia* is not only a viable agricultural practice but also an effective method for optimizing land resource utilization. When sesame and *Salvia* are planted together, they can significantly increase *Salvia* tanshinone content. Furthermore, the results of our 16S rRNA sequencing analysis indicate that the number and abundance of inter-root microbial communities in *Salvia* are significantly higher when sesame and *Salvia* are planted together, compared to when *Salvia* is planted with either soybean or maize. Soil factors and inter-root secretions play important roles in shaping the *Salvia* inter-root microbial community. In particular, inter-root secretions had a significant influence on *Salvia miltiorrhiza* yield and quality.

Data availability statement

The original contributions presented in the study are publicly available. This data can be found here: https://www.ncbi.nlm.nih.gov/bioproject under the accession number PRJNA992203.

Author contributions

LZ and CZ designed the experiment. LZ wrote the paper and CZ revised the manuscript. ST, YZ, YY, FP, HL, CM, XW, YW, and ZX contributed to experiments and the acquisition of data. All authors contributed to the article and approved the submitted version.

Funding

The author(s) declare financial support was received for the research, authorship, and/or publication of this article. This study was supported by the Chinese Materia Medica of China Agriculture Research System (CARS-21), the Ability establishment of sustainable use for valuable Chinese medicine resources (2060302), Discipline Construction Project of SAAS (2021XKJS105).

Conflict of interest

The authors declare that the research was conducted in the absence of any commercial or financial relationships that could be construed as a potential conflict of interest.

Publisher's note

References

Bais, H. P., Weir, T. L., Perry, L. G., Gilroy, S., and Vivanco, J. M. (2006). The role of root exudates in rhizosphere interactions with plants and other organisms. *Annu. Rev. Plant Biol.* 57, 233–266. doi: 10.1146/annurev.arplant.57.032905.105159

Berg, D., Yoon, K.-J., Will, B., Xiao, A., Kim, N.-S., Christian, K., et al. (2015). Tbr2-expressing intermediate progenitor cells in the adult mouse hippocampus are unipotent neuronal precursors with limited amplification capacity under homeostasis. *Front. Biol.* 10. doi: 10.1007/s11515-015-1364-0

Bhakta, J., Lahiri, S., Bhuiyna, F., Rokunuzzaaman, M., Ohonishi, K., Iwasaki, K., et al. (2017). Profiling of heavy metal(loid)-resistant bacterial community structure by metagenomic-DNA fingerprinting using PCR–DGGE for monitoring and bioremediation of contaminated environment. *Energy Ecol. Environ.* 3, 102–109. doi: 10.1007/s40974-017-0079-2

Bokulich, N. A., Subramanian, S., Faith, J. J., Gevers, D., Gordon, J. I., Knight, R., et al. (2013). Quality-filtering vastly improves diversity estimates from Illumina amplicon sequencing. *Nat. Methods* 10, 57–59. doi: 10.1038/nmeth.2276

Casper, B. B., and Castelli, J. P. (2007). Evaluating plant-soil feedback together with competition in a serpentine grassland. *Ecol. Lett.* 10, 394–400. doi: 10.1111/j.1461-0248.2007.01030.x

Deng, G., Li, X., Zhang, H., Ren, W., Zhang, J., Wang, X., et al. (2017). Effects of intercropping maize on growth of *salvia miltiorrhiza*. *J. Anhui Agric. Sci.* 45, 122–123. doi: 10.13989/j.cnki.0517-6611.2017.05.043

Domeignoz-Horta, L. A., Pold, G., Liu, X.-J. A., Frey, S. D., Melillo, J. M., and DeAngelis, K. M. (2020). Microbial diversity drives carbon use efficiency in a model soil. *Nat. Commun.* 11, 3684. doi: 10.1038/s41467-020-17502-z

Edgar, R. C. (2013). UPARSE: highly accurate OTU sequences from microbial amplicon reads. *Nat. Methods* 10, 996–998. doi: 10.1038/nmeth.2604

Fierer, N. (2017). Embracing the unknown: disentangling the complexities of the soil microbiome. *Nat. Rev. Microbiol.* 15, 579–590. doi: 10.1038/nrmicro.2017.87

Fu, M.-M., Huang, B., Jia, M.-M., Hu, W.-Y., Sun, W.-X., Weindorf, D. C., et al. (2015). Effect of intensive greenhouse vegetable cultivation on selenium availability in soil. *Pedosphere* 25, 343–350. doi: 10.1016/S1002-0160(15)30002-3

Guo, H., Nasir, M., Lv, J., Dai, Y., and Gao, J. (2017). Understanding the variation of microbial community in heavy metals contaminated soil using high throughput sequencing. *Ecotoxicol. Environ. Saf.* 144, 300–306. doi: 10.1016/j.ecoenv.2017.06.048

Guo, Z., Wan, S., Hua, K., Yin, Y., Chu, H., Wang, D., et al. (2020). Fertilization regime has a greater effect on soil microbial community structure than crop rotation and growth stage in an agroecosystem. *Appl. Soil Ecol.* 149, 103510. doi: 10.1016/j.apsoil.2020.103510

Hsiao, C.-J., Sassenrath, G., Zeglin, L., Hettiarachchi, G., and Rice, C. (2019). Temporal variation of soil microbial properties in a corn–wheat–soybean system. *Soil Sci. Soc. Am. J.* 83, 1696–1711. doi: 10.2136/sssaj2019.05.0160

Hu, H., Li, H., Hao, M., Ren, Y., Zhang, M., Liu, R., et al. (2021). Nitrogen fixation and crop productivity enhancements codriven by intercrop root exudates and key rhizosphere bacteria. *J. Appl. Ecol.* 58, 2243–2255. doi. 10.1111/1365-2664.13964

Jiang, J.-S., Gu, Q.-C., Feng, Z.-M., Yuan, X., Zhang, X., Zhang, P.-C., et al. (2022a). The phenolic acids from the plant of *Salvia miltiorrhiza*. *Fitoterapia* 159, 105180. doi: 10.1016/j.fitote.2022.105180

Jiang, Y., Khan, M. U., Lin, X., Lin, Z., Lin, S., and Lin, W. (2022b). Evaluation of maize/peanut intercropping effects on microbial assembly, root exudates and peanut nitrogen uptake. *Plant Physiol. Biochem.* 171, 75–83. doi: 10.1016/j.plaphy.2021.12.024

Lei, L., Guo, Q., Wang, C., Ma, Z., Cao, W., and An, J. (2018). Effects of compound planting on growth and quality of *Salvia miltiorrhiza*. *China J. Chin. Materia Med.* 43, 1818–1824. doi: 10.19540/j.cnki.cjcmm.20180307.011

Li, H., Luo, L., Tang, B., Guo, H., Cao, Z., Zeng, Q., et al. (2022). Dynamic changes of rhizosphere soil bacterial community and nutrients in cadmium polluted soils with soybean-corn intercropping. *BMC Microbiol.* 22, 57. doi: 10.1186/s12866-022-02468-3

Li, S., and Wu, F. (2018). Diversity and co-occurrence patterns of soil bacterial and fungal communities in seven intercropping systems. *Front. Microbiol.* 9, 1521. doi: 10.3389/fmicb.2018.01521

Liang, H., Kong, Y., Chen, W., Wang, X., Jia, Z., Dai, Y., et al. (2021). The quality of wild *Salvia miltiorrhiza* from Dao Di area in China and its correlation with soil parameters and climate factors. *Phytochem. Anal.* 32, 318–325. doi: 10.1002/pca.2978

Liu, H., Niu, M., Zhu, S., Zhang, F., Liu, Q., Liu, Y., et al. (2020a). Effect study of continuous monoculture on the quality of *salvia miltiorrhiza* bge roots. *BioMed. Res. Int.* 2020, 4284385. doi: 10.1155/2020/4284385

Liu, H., Wang, C., Xie, Y., Luo, Y., Sheng, M., Xu, F., et al. (2020b). Ecological responses of soil microbial abundance and diversity to cadmium and soil properties in farmland around an enterprise-intensive region. *J. Hazard Mater* 392, 122478. doi: 10.1016/j.jhazmat.2020.122478

Liu, H., Xu, F., Xie, Y., Wang, C., Zhang, A., Li, L., et al. (2018). Effect of modified coconut shell biochar on availability of heavy metals and biochemical characteristics of soil in multiple heavy metals contaminated soil. *Sci. Total Environ.* 645, 702–709. doi: 10.1016/j.scitotenv.2018.07.115

Liu, Q., Zhao, Y., Qi, Y., Zhang, Z., Hao, P., Pu, G., et al. (2020c). A comprehensive analytical platform for unraveling the effect of the cultivation area on the composition of *Salvia miltiorrhiza* Bunge. *Ind. Crops Prod.* 145, 111952. doi: 10.1016/j.indcrop.2019.111952

Liu, W., Zhou, B., Wan, X., Lu, H., Guo, L., Li, F., et al. (2018). Effect of efficient ecological intercropping patterns on the growth and active ingredient content of *Salvia miltiorrhiza*. *J. Chin. Medicinal Materials* 41, 1027–1030. doi: 10.13863/j.issn1001-4454.2018.05.003

Maitra, S. (2019). Potential of intercropping system in sustaining crop productivity. *Int. J. Agric. Environ. Biotechnol.* 12 (1), 39–45. doi: 10.30954/0974-1712.03.2019.7

Maitra, S., Hossain, A., Brestic, M., Skalicky, M., Ondrišík, P., Gitari, H., et al. (2021). Intercropping system-A low input agricultural strategy for food and environmental security. *Agronomy* 11, 343. doi: 10.3390/agronomy11020343

Mommer, L., Kirkegaard, J., and van Ruijven, J. (2016). Root-root interactions: towards A rhizosphere framework. *Trends Plant Sci.* 21, 209–217. doi: 10.1016/j.tplants.2016.01.009

Neumann, G., and Romheld, V. (2003). Root-induced changes in the availability of nutrients in the rhizosphere. *Cheminform* 34, 617–619. doi: 10.1002/chin.200304265

Pang, Z., Fallah, N., Weng, P., Zhou, Y., Tang, X., Tayyab, M., et al. (2021). Sugarcane-peanut intercropping system enhances bacteria abundance, diversity, and sugarcane parameters in rhizospheric and bulk soils. *Front. Microbiol.* 12, 815129. doi: 10.3389/fmicb.2021.815129

Prommer, J., Walker, T. W. N., Wanek, W., Braun, J., Zezula, D., Hu, Y., et al. (2020). Increased microbial growth, biomass, and turnover drive soil organic carbon accumulation at higher plant diversity. *Glob Chang Biol.* 26, 669–681. doi: 10.1111/gcb.14777

Rajan, S. S. S., Fox, R. L., Saunders, W. M. H., and Upsdell, M. (1991). Influence of pH, time and rate of application on phosphate rock dissolution and availability to pastures - I. Agronomic benefits. *Nutrient Cycling Agroecosystems* 28, 85–93. doi: 10.1007/bf01048860

Saber, M. S. M., Guirguis, M. A., and Zanati, M. R. (1973). Biological and chemical determination of available phosphorus in soil. *Zentralblatt für Bakteriologie, Parasitenkunde, Infektionskrankheiten und Hygiene. Zweite Naturwissenschaftliche Abteilung: Allgemeine Landwirtschaftliche und Technische Mikrobiologie* 128, 566–571. doi: 10.1016/S0044-4057(73)80078-4

Sasse, J., Martinoia, E., and Northen, T. (2018). Feed your friends: do plant exudates shape the root microbiome? *Trends Plant Sci.* 23, 25–41.

Stefan, L., Hartmann, M., Engbersen, N., Six, J., and Schöb, C. (2021). Positive effects of crop diversity on productivity driven by changes in soil microbial composition. *Front. Microbiol.* 12, 660749. doi: 10.3389/fmicb.2021.660749

Stomph, T., Dordas, C., Baranger, A., de Rijk, J., Dong, B., Evers, J., et al. (2020). "Chapter One - Designing intercrops for high yield, yield stability and efficient use of resources: Are there principles?" in *Advances in Agronomy*. Ed. D. L. Sparks (Academic Press), 1–50. doi: 10.1016/bs.agron.2019.10.002

Tang, X., Bernard, L., Brauman, A., Daufresne, T., Deleporte, P., Desclaux, D., et al. (2014). Increase in microbial biomass and phosphorus availability in the rhizosphere of intercropped cereal and legumes under field conditions. *Soil Biol. Biochem.* 75, 86–93. doi: 10.1016/j.soilbio.2014.04.001

Tang, X., Jiang, J., Huang, Z., Wu, H., Wang, J., He, L., et al. (2021). Sugarcane/peanut intercropping system improves the soil quality and increases the abundance of beneficial microbes. *J. Basic Microbiol.* 61, 165–176. doi: 10.1002/jobm.202000750

Tang, X., Zhong, R., Jiang, J., He, L., Huang, Z., Shi, G., et al. (2020). Cassava/peanut intercropping improves soil quality via rhizospheric microbes increased available nitrogen contents. *BMC Biotechnol.* 20, 13. doi: 10.1186/s12896-020-00606-1

Vermeulen, S. J., Heymans, M. W., Anema, J. R., Schellart, A. J. M., van Mechelen, W., and van der Beek, A. J. (2013). Economic evaluation of a participatory return-to-work intervention for temporary agency and unemployed workers sick-listed due to musculoskeletal disorders. *Scand. J. Work Environ. Health* 39, 46–56. doi: 10.5271/sjweh.3314

Wang, L., Rengel, Z., Zhang, K., Jin, K., Lyu, Y., Zhang, L., et al. (2022). Ensuring future food security and resource sustainability: insights into the rhizosphere. *iScience* 25, 104168. doi: 10.1016/j.isci.2022.104168

Wang, Q., Wang, C., Yu, W., Turak, A., Chen, D., Huang, Y., et al. (20181543). Effects of nitrogen and phosphorus inputs on soil bacterial abundance, diversity, and community composition in chinese fir plantations. *Front. Microbiol.* 9. doi: 10.3389/fmicb.2018.01543

Wang, Y., Yang, B., Wang, H., Yang, C., Zhang, J., Zhu, M., et al. (2019). Variation in microbial community structure in the rhizosphere soil of *Salvia miltiorrhiza* Bunge under three cropping modes. *Acta Ecologica Sin.* 39, 4832–4843. doi: 10.5846/stxb201805151071

Willey, R. W., and Osiru, D. S. O. (1972). Studies on mixtures of maize and beans (Phaseolus vulgaris) with particular reference to plant population. *J. Agric. Sci.* 79, 517–529. doi: 10.1017/S0021859600025909

Xin-hui, Z., Lang, D., Zhang, E., and Wang, Z. (2015). Effect of autotoxicity and soil microbes in continuous cropping soil on angelica sinensis seedling growth and rhizosphere soil microbial population. *Chin. Herbal Medicines* 7, 88–93. doi: 10.1016/S1674-6384(15)60025-9

Xu, Y., Wu, Y.-G., Chen, Y., Zhang, J.-F., Song, X.-Q., Zhu, G.-P., et al. (2015). Autotoxicity in Pogostemon cablin and their allelochemicals. *Rev. Bras. Farmacognosia* 25, 117–123. doi: 10.1016/j.bjp.2015.02.003

Zhang, X., Lang, D., Zhang, E., Bai, C., and Wang, H. (2013). Diurnal changes in photosynthesis and antioxidants of Angelica sinensis as influenced by cropping systems. *Photosynthetica* 51, 252–258. doi: 10.1007/s11099-013-0013-6

Zhao, M., Zhao, J., Yuan, J., Hale, L., Wen, T., Huang, Q., et al. (2021). Root exudates drive soil-microbe-nutrient feedbacks in response to plant growth. *Plant Cell Environ.* 44, 613–628. doi: 10.1111/pce.13928

Frontiers in
Plant Science

Cultivates the science of plant biology and its applications

The most cited plant science journal, which advances our understanding of plant biology for sustainable food security, functional ecosystems and human health.

Discover the latest Research Topics

See more →

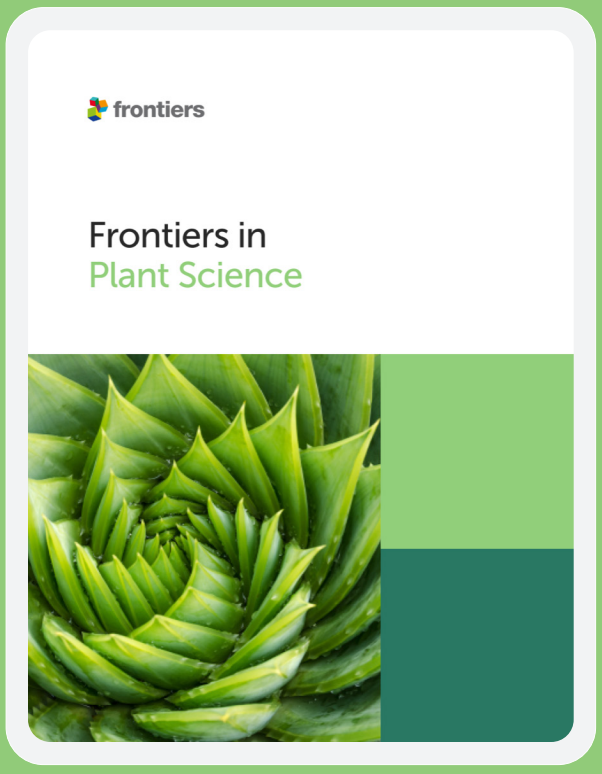

Frontiers

Avenue du Tribunal-Fédéral 34
1005 Lausanne, Switzerland
frontiersin.org

Contact us

+41 (0)21 510 17 00
frontiersin.org/about/contact